

AWARD NUMBER: W81XWH-16-1-0622

TITLE: Cellular Plasticity in the Diabetic Myocardium

PRINCIPAL INVESTIGATOR: Antonis Hatzopoulos

CONTRACTING ORGANIZATION: Vanderbilt University Medical Center, Nashville, TN

REPORT DATE: December 2020

TYPE OF REPORT: Final

PREPARED FOR: U.S. Army Medical Research and Materiel Command
Fort Detrick, Maryland 21702-5012

DISTRIBUTION STATEMENT: Approved for Public Release;
Distribution Unlimited

The views, opinions and/or findings contained in this report are those of the author(s) and should not be construed as an official Department of the Army position, policy or decision unless so designated by other documentation.

REPORT DOCUMENTATION PAGE

Form Approved
OMB No. 0704-0188

Public reporting burden for this collection of information is estimated to average 1 hour per response, including the time for reviewing instructions, searching existing data sources, gathering and maintaining the data needed, and completing and reviewing this collection of information. Send comments regarding this burden estimate or any other aspect of this collection of information, including suggestions for reducing this burden to Department of Defense, Washington Headquarters Services, Directorate for Information Operations and Reports (0704-0188), 1215 Jefferson Davis Highway, Suite 1204, Arlington, VA 22202-4302. Respondents should be aware that notwithstanding any other provision of law, no person shall be subject to any penalty for failing to comply with a collection of information if it does not display a currently valid OMB control number. **PLEASE DO NOT RETURN YOUR FORM TO THE ABOVE ADDRESS.**

1. REPORT DATE December 2020		2. REPORT TYPE Final		3. DATES COVERED 01Sep2016 – 31Aug2020		
4. TITLE AND SUBTITLE Cellular Plasticity in the Diabetic Myocardium				5a. CONTRACT NUMBER W81XWH-16-1-0622		
				5b. GRANT NUMBER PR151029P1		
				5c. PROGRAM ELEMENT NUMBER		
6. AUTHOR(S) Antonis Hatzopoulos E-Mail: antonis.hatzopoulos@vanderbilt.edu				5d. PROJECT NUMBER		
				5e. TASK NUMBER		
				5f. WORK UNIT NUMBER		
7. PERFORMING ORGANIZATION NAME(S) AND ADDRESS(ES) Vanderbilt University Medical Center 1161 21 ST Ave S D3300 MCN Nashville, TN 37232-0011				8. PERFORMING ORGANIZATION REPORT NUMBER		
9. SPONSORING / MONITORING AGENCY NAME(S) AND ADDRESS(ES) U.S. Army Medical Research and Materiel Command Fort Detrick, Maryland 21702-5012				10. SPONSOR/MONITOR'S ACRONYM(S)		
				11. SPONSOR/MONITOR'S REPORT NUMBER(S)		
12. DISTRIBUTION / AVAILABILITY STATEMENT Approved for Public Release; Distribution Unlimited						
13. SUPPLEMENTARY NOTES						
14. ABSTRACT Heart fibrosis and loss of blood vessels are prominent pathologic abnormalities in diabetics that lead to the development of heart failure. Moreover, reduced angiogenesis after a heart attack is responsible for defective myocardial repair in diabetic subjects. Although the negative impact of diabetes on the heart is widely appreciated, the cellular alterations and molecular signals involved in fibrosis and blood vessel loss in diabetes remain unknown. Applying genetic fate mapping tools, we have uncovered an unexpected plasticity and heterogeneity in reparative cells and identified common cellular links between angiogenesis and fibrosis. We investigate the role of these novel biological mechanisms in the pro-fibrotic and angiostatic effects of diabetes, focusing on the contribution of pericytes and endothelial cells in the cardiac tissue repair process.						
15. SUBJECT TERMS Diabetes, cardiomyopathy, heart failure, fibrosis, angiogenesis, vascular rarefaction, pericytes, endothelial cells, endothelial-to-mesenchymal transition, cellular plasticity, extracellular matrix, cell fate mapping, gene expression, signaling pathways						
16. SECURITY CLASSIFICATION OF:			17. LIMITATION OF ABSTRACT	18. NUMBER OF PAGES	19a. NAME OF RESPONSIBLE PERSON	
a. REPORT U Unclassified	b. ABSTRACT U Unclassified	c. THIS PAGE U Unclassified	UU Unclassified	275	USAMRMC	
					19b. TELEPHONE NUMBER (include area code)	

Table of Contents

	<u>Page</u>
1. Introduction.....	4
2. Keywords.....	4
3. Accomplishments.....	5
4. Impact.....	30
5. Changes/Problems.....	30
6. Products.....	30
7. Participants & Other Collaborating Organizations.....	35
8. Special Reporting Requirements.....	38
9. Appendices.....	38

USAMRMC Proposal Number PR151029

Title: "Cellular Plasticity in the Diabetic Myocardium"

DoD Award Number W81XWH-16-1-0621

Final Report from 09/01/2016 to 08/31/2020

1. Introduction

Heart tissue fibrosis and loss of blood vessels are prominent pathologic abnormalities in diabetics and lead to the development of heart failure. Moreover, reduced angiogenesis after a heart attack is responsible for defective myocardial repair in diabetic subjects. Although the negative impact of diabetes on heart function and repair is widely appreciated, the cellular alterations and molecular signals involved in fibrosis and blood vessel loss in diabetes remain unknown. Applying genetic fate mapping tools, we have uncovered an unexpected plasticity and heterogeneity in reparative cells and identified common cellular links between angiogenesis and fibrosis. We investigate the role of these novel biological mechanisms in the pro-fibrotic and angiostatic effects of diabetes, focusing on the contribution of pericytes and endothelial cells in the cardiac tissue repair process.

2. Keywords

Diabetes, cardiomyopathy, heart failure, fibrosis, angiogenesis, vascular rarefaction, pericytes, endothelial cells, endothelial-to-mesenchymal transition, cellular plasticity, extracellular matrix, lineage tracing, cell fate mapping, gene expression profiling, signaling pathways

3. Accomplishments

Major Scientific Goals of the Project

The project has the following three major goals:

- a) Determine the contribution of pericytes to the development of cardiac fibrosis in diabetic mice (AECOM);
- b) Evaluate the role of endothelial cells in the development of cardiac fibrosis in diabetic mice (VUMC);
- c) Identify sex-specific molecular pathways promoting fibrosis and causing blood vessel loss in diabetic hearts (AECOM & VUMC).

Scientific Accomplishments of the Project

a) Contribution of pericytes to cardiac fibrosis in diabetic hearts (Work performed at (AECOM)).

A1: Characterization of the db/db mouse as a model of diabetic cardiac fibrosis, associated with diastolic dysfunction.

We have characterized the db/db mouse as a model of cardiac fibrosis and diastolic dysfunction that recapitulates characteristics of human heart failure with preserved ejection fraction (HFpEF). This work was published in the American Journal of Physiology- Heart Circulatory Physiology (Alex et al AJP-Heart 2018). Moreover, we have systematically studied gender-specific responses in this model. Our experiments demonstrated that obese diabetic db/db mice in a C57Bl6J background exhibit cardiac remodeling, associated with modest ventricular dilation, accompanied by marked left ventricular hypertrophy, accompanied by modest elevations in systemic blood pressures in the absence of systolic dysfunction (Figure 1-3). Elevated left ventricular end-diastolic pressure (LVEDP) in db/db mice suggests significant diastolic dysfunction (Figure 4-5). Db/db mice exhibited increased deposition of collagen, in the absence of an increase in the density of interstitial cells (Figures 6-9). Fibrosis in diabetic hearts occurs in the absence of myofibroblast conversion (Figure 10). Hypertrophic changes, chamber dilation and diastolic dysfunction are more prominent in female animals (Figure 11-12). Thus, the db/db mouse model recapitulates features of HFpEF observed in human patient

populations and is particularly useful in understanding the pathogenesis of cardiac dysfunction associated with metabolic disease.

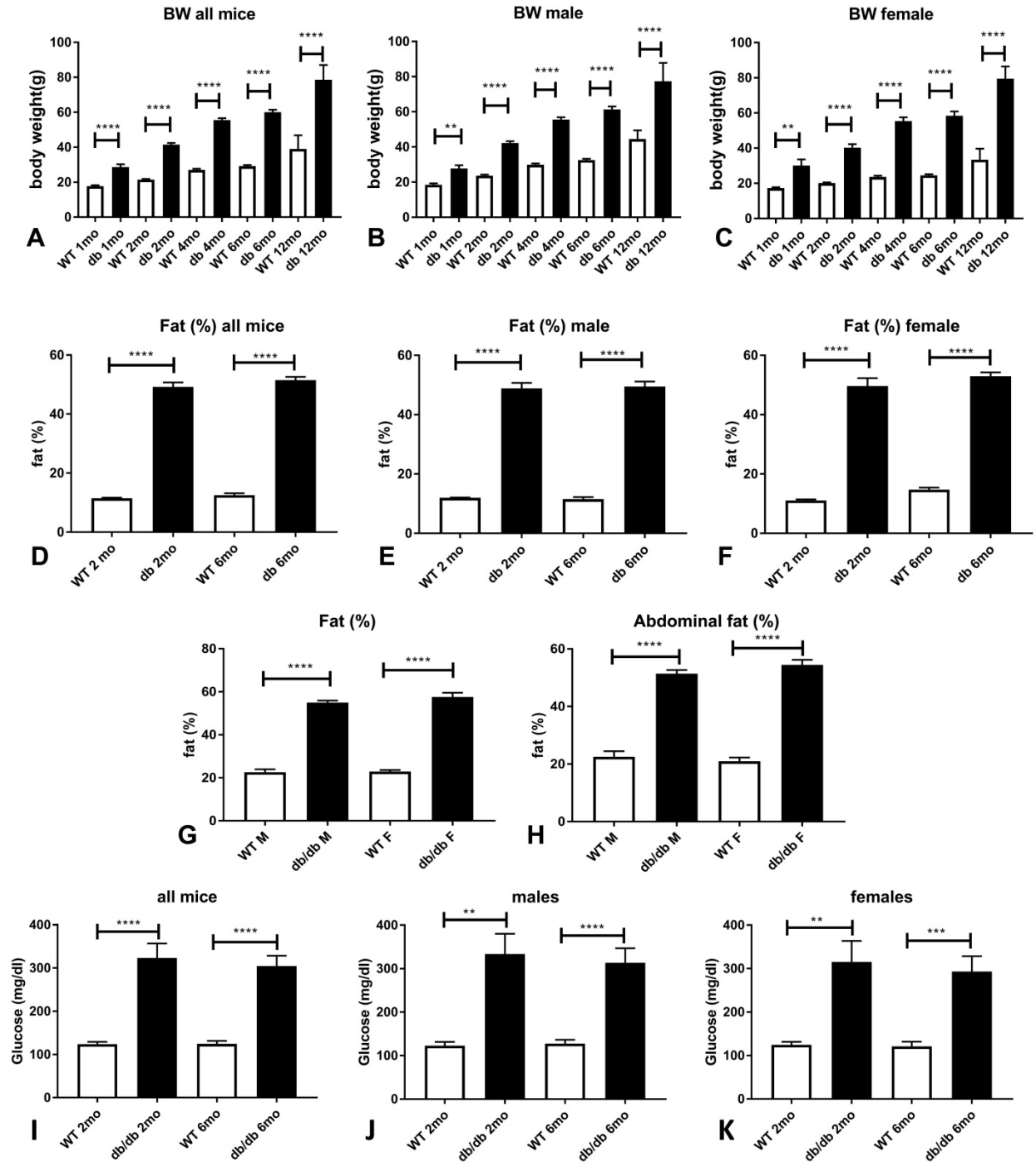


Figure 1: Both male and female db/db mice in a C57BL6J background exhibit severe obesity, increased adiposity and overt diabetes. A-C: Body weight (BW) was markedly higher in db/db mice when compared with age-matched WT controls. When compared with age-matched WT mice, female db/db mice had a more impressive increase in BW than male animals (female db/db mice: 2.38-fold higher BW than age-matched WT mice at 6 months of age and 2.37-fold higher at 12 months vs. male db/db mice: 1.88-fold at 6 months, and 1.74-fold at 12 months of age). D-F: MRI showed a marked increase in body fat content in both male and female db/db mice at 2 and 6 months of age. G-H DEXA performed at 4 months of age also showed that db/db mice had a marked increase in total (G) and abdominal fat content (H). Although there was significant variability, both male and female db/db animals exhibited a marked increase in fasting plasma glucose levels at 2 and 6 months of age. (* $p < 0.05$, ** $p < 0.01$, *** $p < 0.001$, **** $p < 0.0001$). Body weight sample size; WT mice: 1mo $n=37$, 2mo $n=63$, 4mo $n=58$, 6mo $n=91$, 12mo $n=22$; db/db mice: 1mo $n=11$, 2mo $n=35$, 4mo $n=45$, 6mo $n=68$, 12mo $n=24$. Male: WT 1mo $n=16$, 2mo $n=23$, 4mo $n=32$, 6mo $n=53$, 12mo $n=11$; db/db: 1mo $n=7$, 2mo $n=22$, 4mo $n=29$, 6mo $n=38$, 12mo $n=10$. Female: WT 1mo $n=21$, 2mo $n=40$, 4mo $n=31$, 6mo $n=38$, 12mo $n=11$, db/db: 1mo $n=4$, 2mo $n=13$, 4mo $n=16$, 6mo $n=30$, 12mo $n=14$. MRI fat content: $n=12-16$ /group; males $n=5-9$ /group; females $n=4-8$ /group. DEXA: $n=7-16$ /group. Fasting plasma glucose: $n=18-49$ /group, males: $n=9-27$ /group, females $n=9-22$ /group.

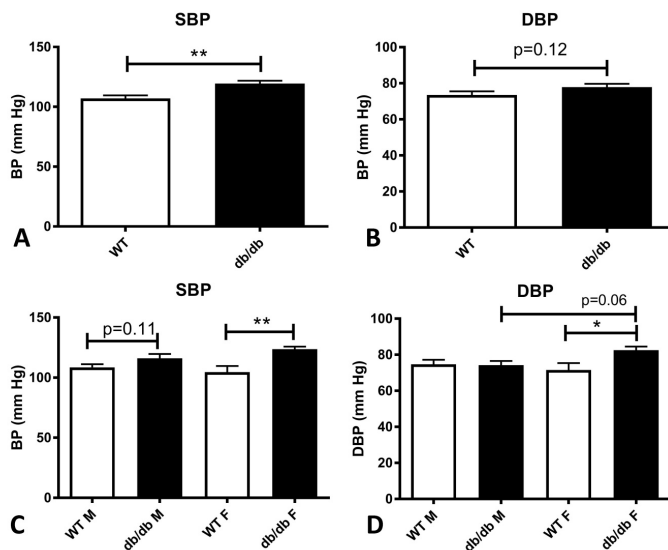


Figure 2: Female db/db mice have a modest, but significant elevation in systolic and diastolic blood pressure. A: At 4 months of age, obese diabetic db/db mice had a significant elevation in systolic blood pressure (SBP) and a trend towards higher diastolic blood pressure (DBP). Gender-specific analysis showed that male db/db mice had a trend towards increased SBP and no significant difference in DBP when compared with lean WT controls. Female db/db mice had significantly increased SBP and DBP, when compared with age-matched WT controls (* $p < 0.05$, ** $p < 0.01$, male mice: $n=10-11$ /group, female mice: $n=7-8$ /group, male+female: $n=18$ /group).

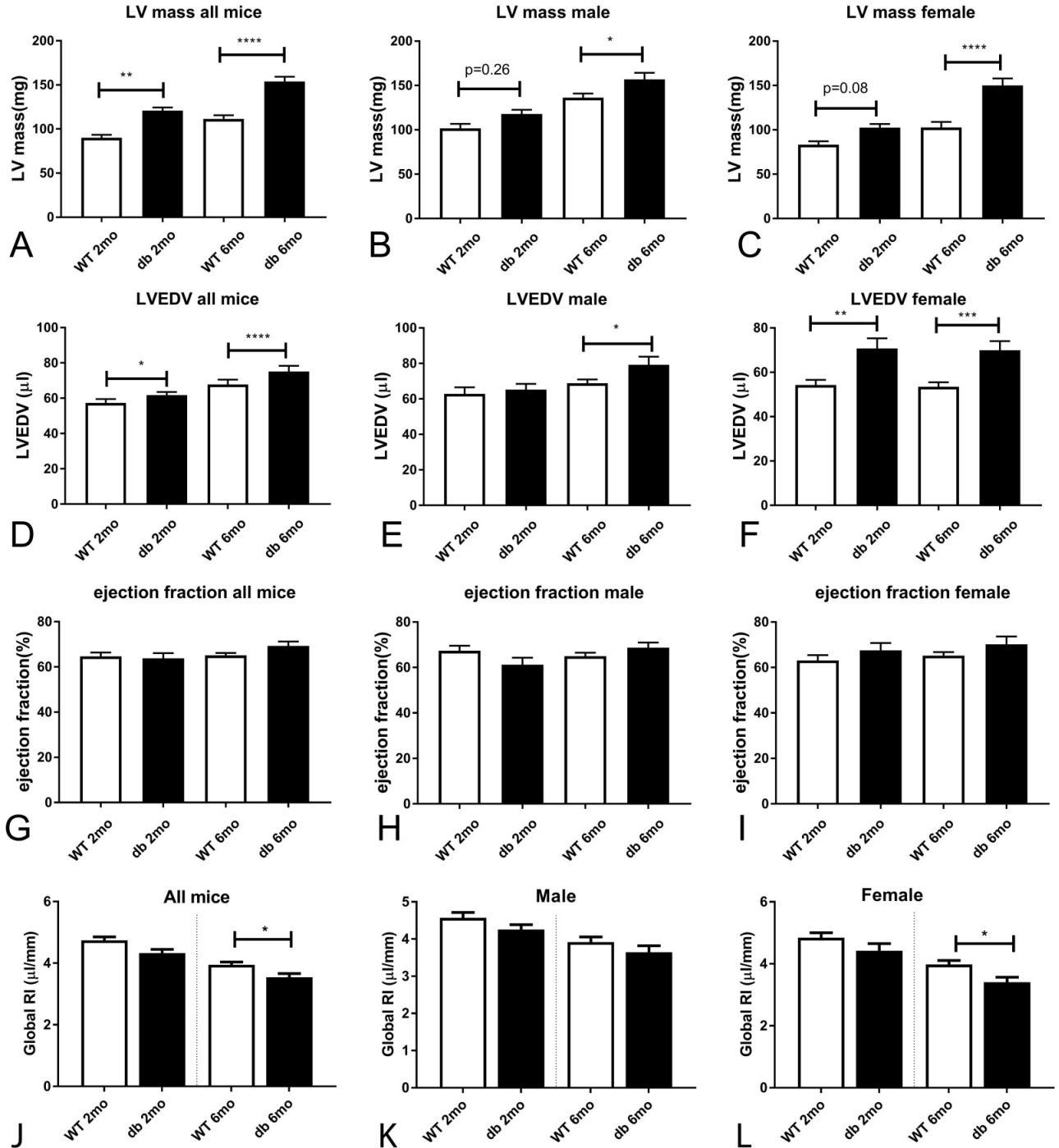


Figure 3: Obese diabetic db/db mice exhibit cardiac remodeling with preserved ejection fraction. A. When compared with lean WT animals, db/db mice had significantly higher LV mass at 2 and 6 months of age. B-C: Both male and female db/db mice had increased LV mass at 6 months of age. However, the increase in LV mass was exaggerated

in female db/db mice. At 6 months of age, male db/db mice had a 15.1% higher LV mass than age-matched WT animals, whereas female db/db animals at the same age exhibited a 46.4% increase. D: LVEDV was increased in db/db mice. E-F: Female mice had earlier ventricular dilation than male animals. G-I: Obese diabetic db/db mice and age-matched WT controls had comparable ejection fraction. J-L: The global remodeling index was assessed to compare maladaptive hypertrophic remodeling between groups. J: At 6 months of age, db/db mice had a lower remodeling index than corresponding lean WT controls. K-L: Female, but not male db/db mice had a significant reduction in the global remodeling index, indicating accentuated hypertrophic remodeling (* $p < 0.05$, ** $p < 0.01$, *** $p < 0.001$, **** $p < 0.0001$; male mice: $n=19-44$ /group, female mice: $n=12-37$ /group, male+female mice: $n=29-81$ /group).

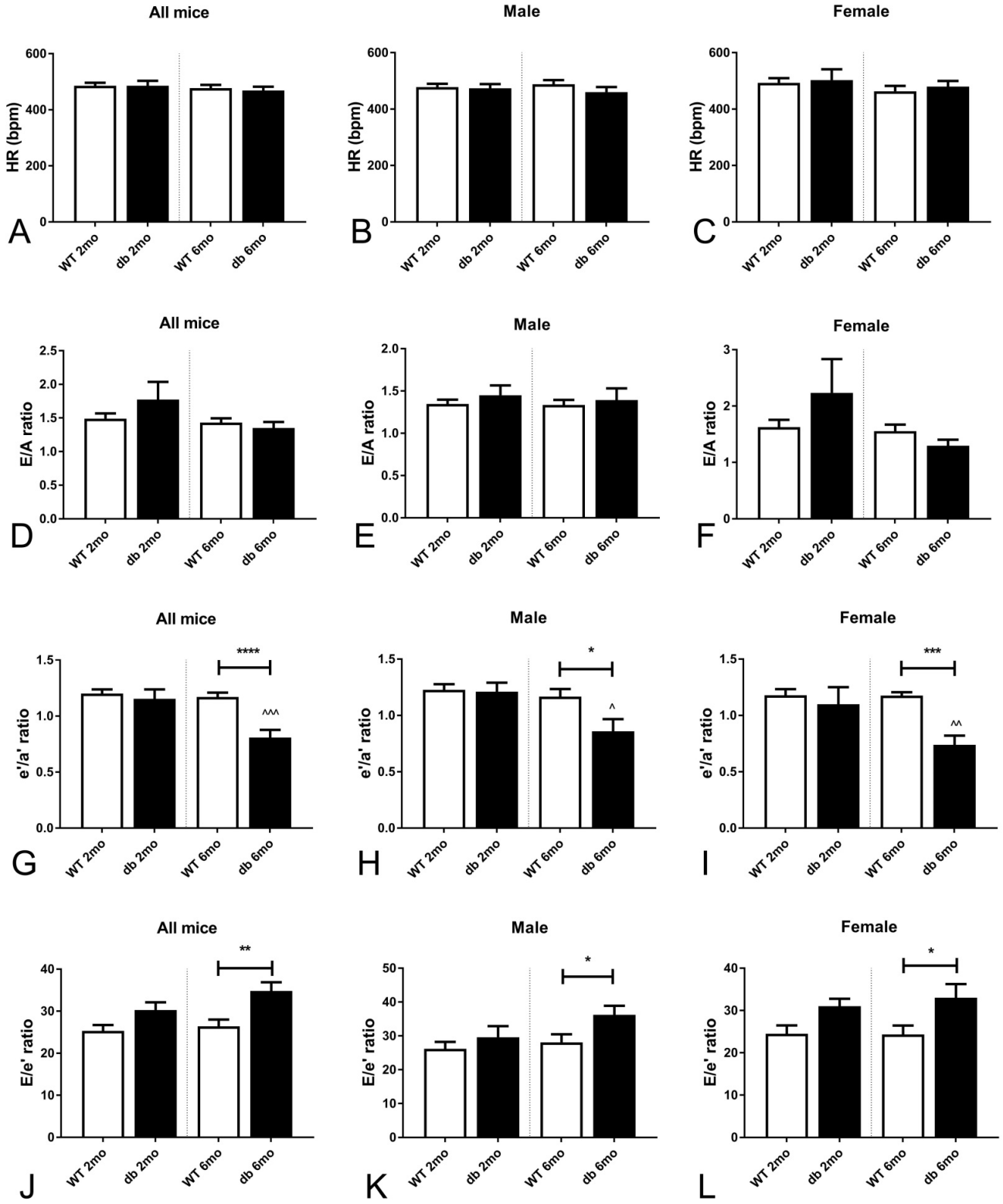


Figure 4: Tissue Doppler imaging suggests that db/db mice develop diastolic dysfunction. A-C: Both male and female db/db mice and age-matched WT controls had comparable heart rate. D-F: Mitral inflow Doppler showed no significant differences in the E/A ratio between groups. Tissue Doppler imaging showed that the E'/A' ratio was significantly reduced in both male and female db/db mice at 6 months of age. The E/E' ratio was significantly increased in both male and female db/db mice at 6 months of age. These findings suggest that db/db mice develop diastolic dysfunction. Tissue Doppler imaging may be more sensitive than mitral inflow Doppler in detecting changes in diastolic function in mice (*p<0.05, **p<0.01, ***p<0.001, ****p<0.0001; male mice 7-19/group, female mice: 7-16/group, male+female: 14-35/group).

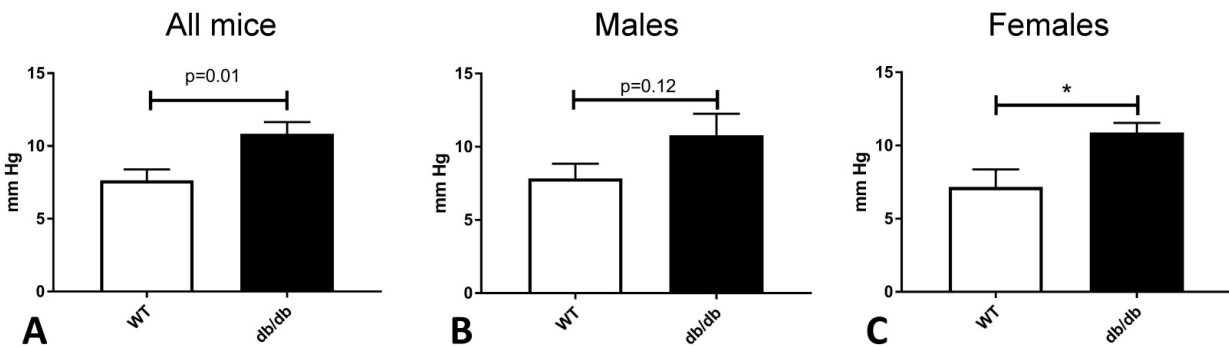


Figure 5: Obese diabetic db/db mice have significantly higher LVEDP than lean WT animals at 6 months of age. A: db/db mice had significantly higher LVEDP than age-matched lean WT mice. B-C: Gender-specific analysis showed that male db/db mice had a trend towards increased LVEDP (B), whereas female animals (C) had significantly higher LVEDP (*p<0.05; male mice: n=6-7/group; female mice: n=3-7/group; male+female mice: n=10-13/group).

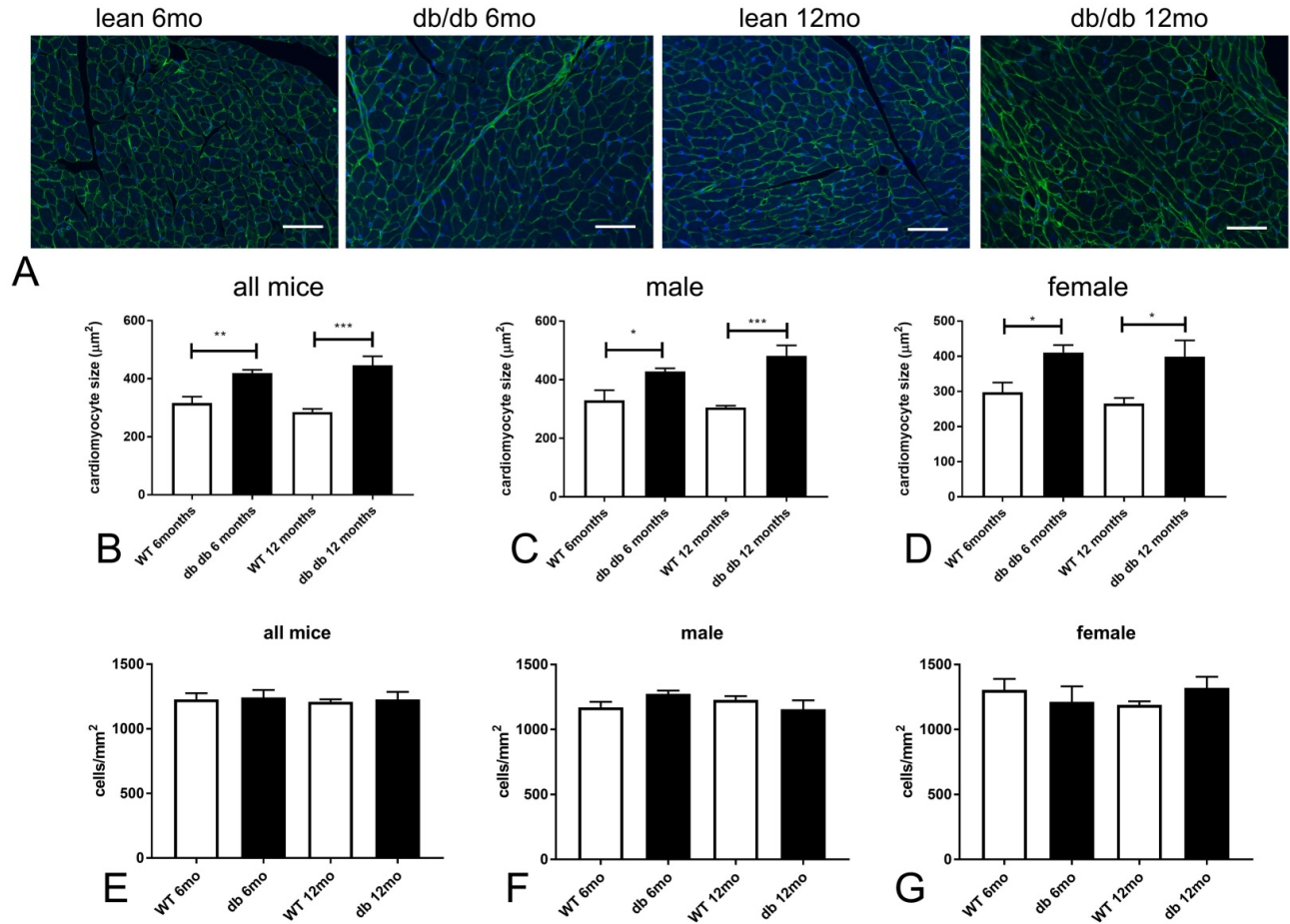


Figure 6: Obese diabetic db/db mice exhibit a marked increase in cardiomyocyte size without a significant increase in the density of interstitial cells. A: WGA lectin histochemistry was used to quantitatively assess cardiomyocyte size. DAPI staining was used for quantification of interstitial cell density. B-D: Both male and female db/db mice had a marked increase in cardiomyocyte size at 2 and 6 months of age. E-G: Interstitial cell density was comparable between groups (*p<0.05, **p<0.01, ***p<0.001, male mice: n=4/group, female mice: n=4/group, male+female: n=8/group). Scalebar=50µm.

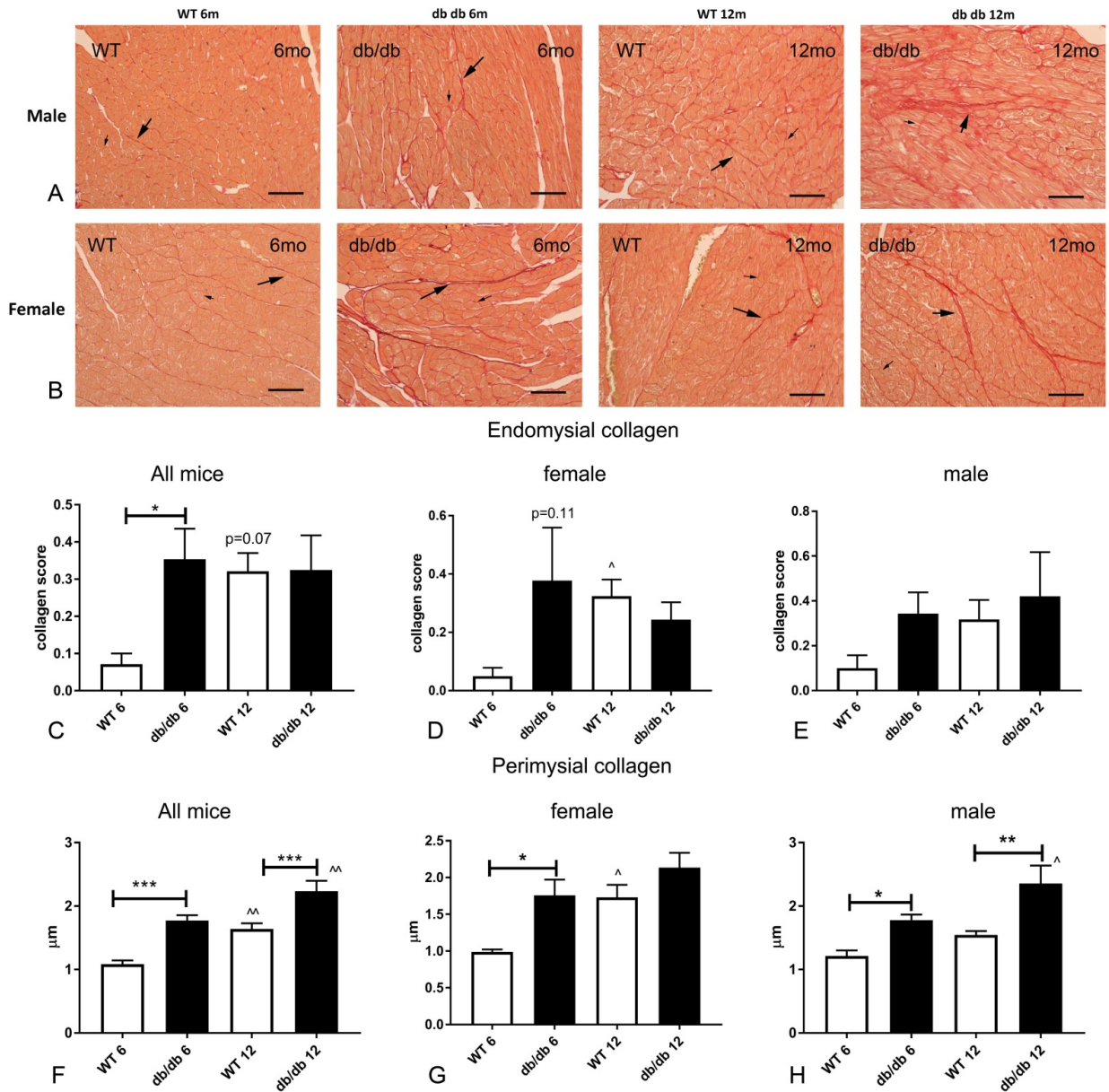


Figure 7: Obese diabetic db/db mice do not have replacement fibrosis, but exhibit thickening of the perimysial collagen network, and increased endomysial collagen. A-B: Picosirius red staining was used to identify perimysial collagen fibers that form the sheath that groups cardiomyocytes into bundles (long arrows) and endomysial collagen fibers surrounding each individual cardiomyocyte (short arrows). There was no evidence of replacement fibrosis in any of the db/db hearts. C-E: Semiquantitative analysis showed that db/db mice have accentuated endomysial collagen at 6 months of age. The increased endomysial collagen score in male or female mice did not reach statistical significance. F-H: Perimysial collagen thickness was markedly increased in db/db mice at 6 and 12 months of age. Both female and male mice had increased perimysial collagen thickness at 6 months

of age. (* $p < 0.05$, ** $p < 0.01$, *** $p < 0.001$; ^ $p < 0.05$, ^^ $p < 0.01$ vs. corresponding 6 month group; male mice: $n = 4/\text{group}$, female mice: $n = 4/\text{group}$, male+female: $n = 8/\text{group}$). Scalebar=50 μm .

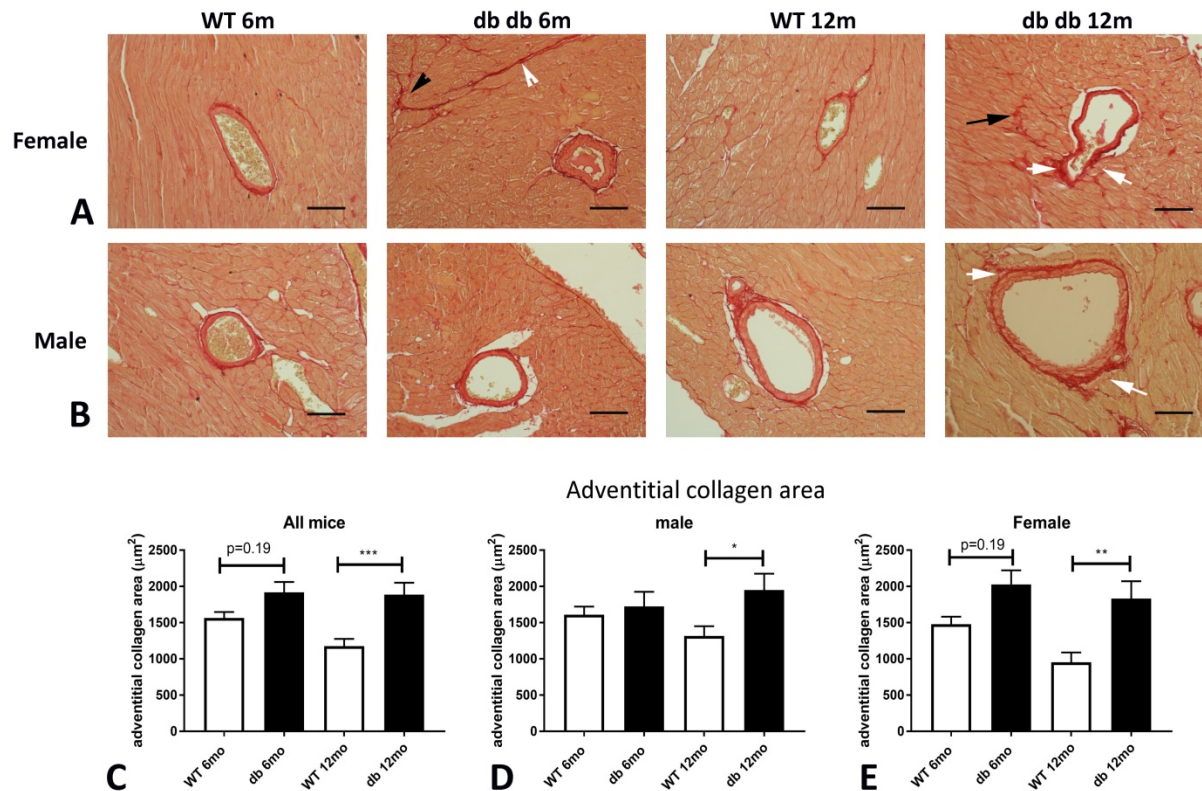


Figure 8: db/db mice exhibit expansion of the peri-adventitial collagen network in coronary arterioles. Periarteriolar collagen was identified using picosirius red staining in male and female WT and db/db mouse hearts (white arrows). Please note the increased perimysial thickness (arrowheads) and the accentuated deposition of endomysial collagen (black arrow) in db/db mouse hearts (quantified in Figure 7). Quantitative analysis showed that at 12 months of age, the periadventityial collagen area was higher in arterioles of db/db mice than in corresponding vessels of WT mouse hearts. Both male and female animals exhibited expansion of the periadventitial collagen area (* $p < 0.05$, ** $p < 0.01$, *** $p < 0.001$, male mice: $n = 19-45$ vessels/group, female mice: $n = 19-35$ vessels/group, male+female: $n = 50-70$ vessels/group). Scalebar=50 μm .

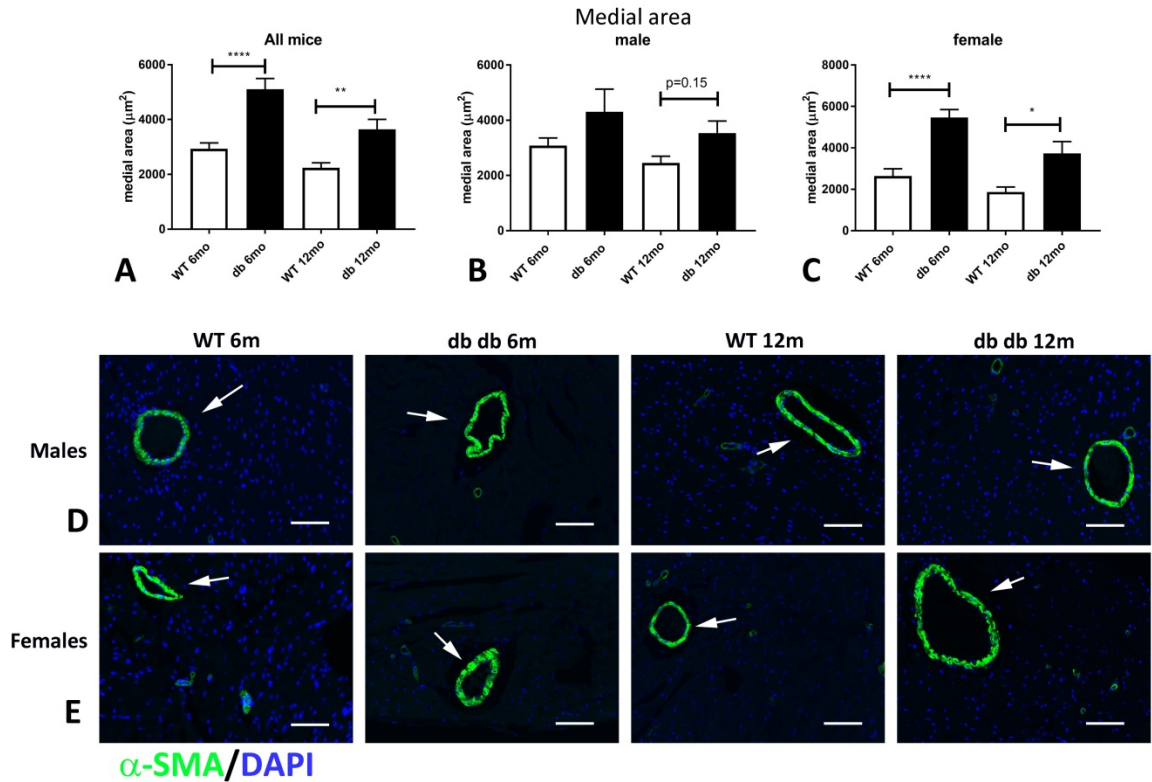


Figure 9: Female db/db mice show significant hypertrophy of the coronary arteriolar media. Quantitative analysis of the picosirius red-stained sections (shown in Figure 8) suggested that db/db mice had a significantly higher mean arteriolar area, when compared with WT mice at 6 and 12 months of age (A). Male mice had a trend towards increased arteriolar area at 12 months of age (B). Female mice had significantly higher arteriolar area at both 6 and 12 month timepoints (C). D-E: α -SMA immunofluorescence illustrates hypertrophy of the arteriolar media (arrows) in female db/db mice (* $p < 0.05$, ** $p < 0.01$, **** $p < 0.0001$, male mice: $n = 19-45$ vessels/group, female mice: $n = 19-35$ vessels/group, male+female: $n = 50-70$ vessels/group). Scalebar = $50\mu\text{m}$.

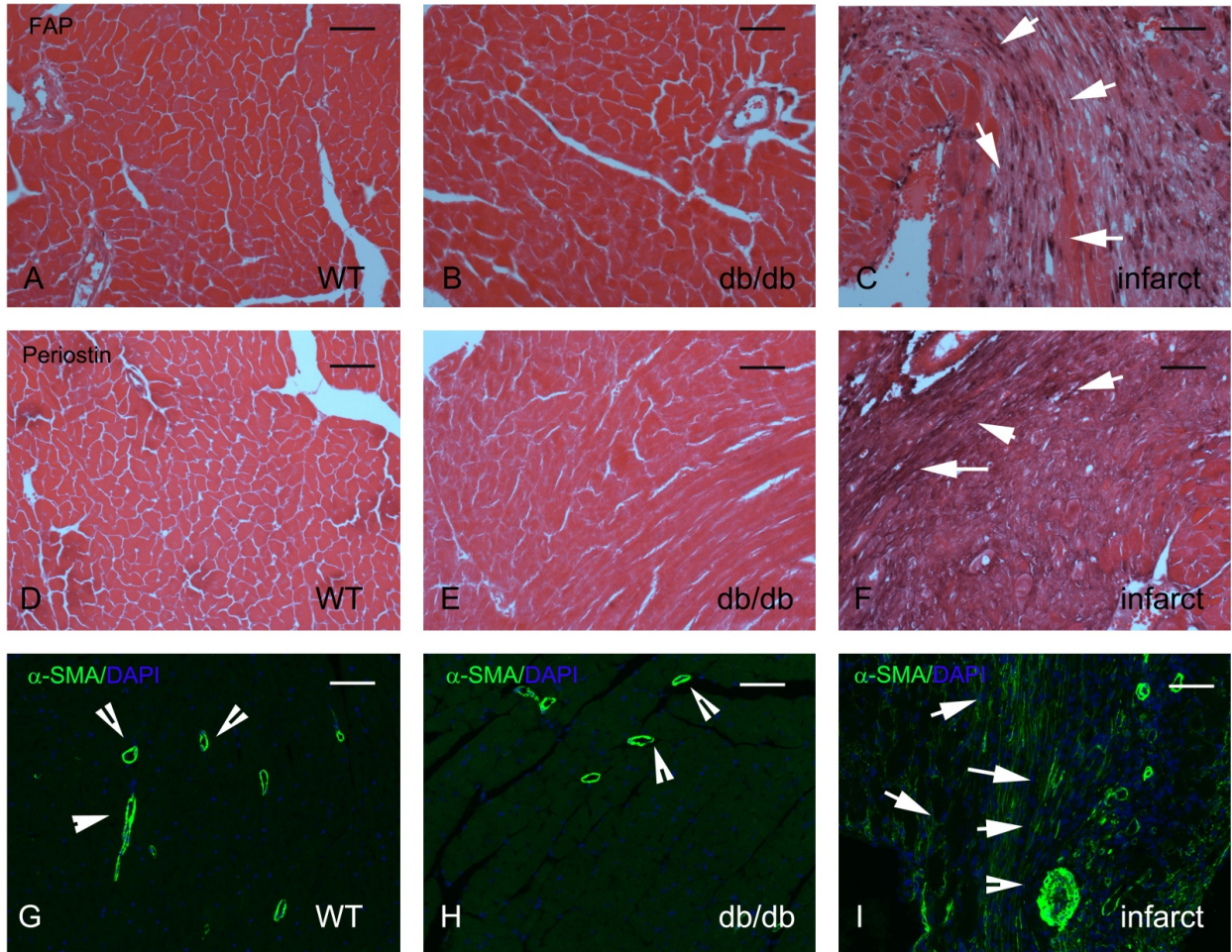


Figure 10: Increased collagen deposition in db/db hearts is not associated with myofibroblast conversion. A-C: Immunohistochemical staining for Fibroblast Activation Protein (FAP), a marker for activated fibroblasts, in lean WT (A), uninjured diabetic (B), and infarcted WT C57BL6J (C) mouse hearts. No FAP+ cells are noted in WT or diabetic myocardium. In contrast, abundant FAP+ fibroblasts infiltrate the infarcted myocardium 7 days after coronary occlusion (arrows – C). Counterstained with eosin. D-F: Periostin staining in lean WT (D), uninjured diabetic (E), and infarcted WT C57BL6J (F) mouse hearts. In injury sites and in fibrotic tissues, activated myofibroblasts typically exhibit periostin expression. Please note the complete absence of periostin immunoreactivity in db/db hearts (E). In contrast, infarcted hearts (F) exhibit periostin expression in activated myofibroblasts and in the surrounding extracellular matrix (arrows). G-I: α -SMA immunofluorescence was used to identify activated myofibroblasts as spindle-shaped immunoreactive cells located outside the vascular media. In uninjured WT (G) and db/db (H) hearts, α -SMA is exclusively localized in the arteriolar media (arrowheads). I: Please note the abundant α -SMA-expressing myofibroblasts in the infarcted myocardium (arrows). Images show sections from 6 month old-mice, representative of at least 4 different animals per group. Scalebar=50 μ m.

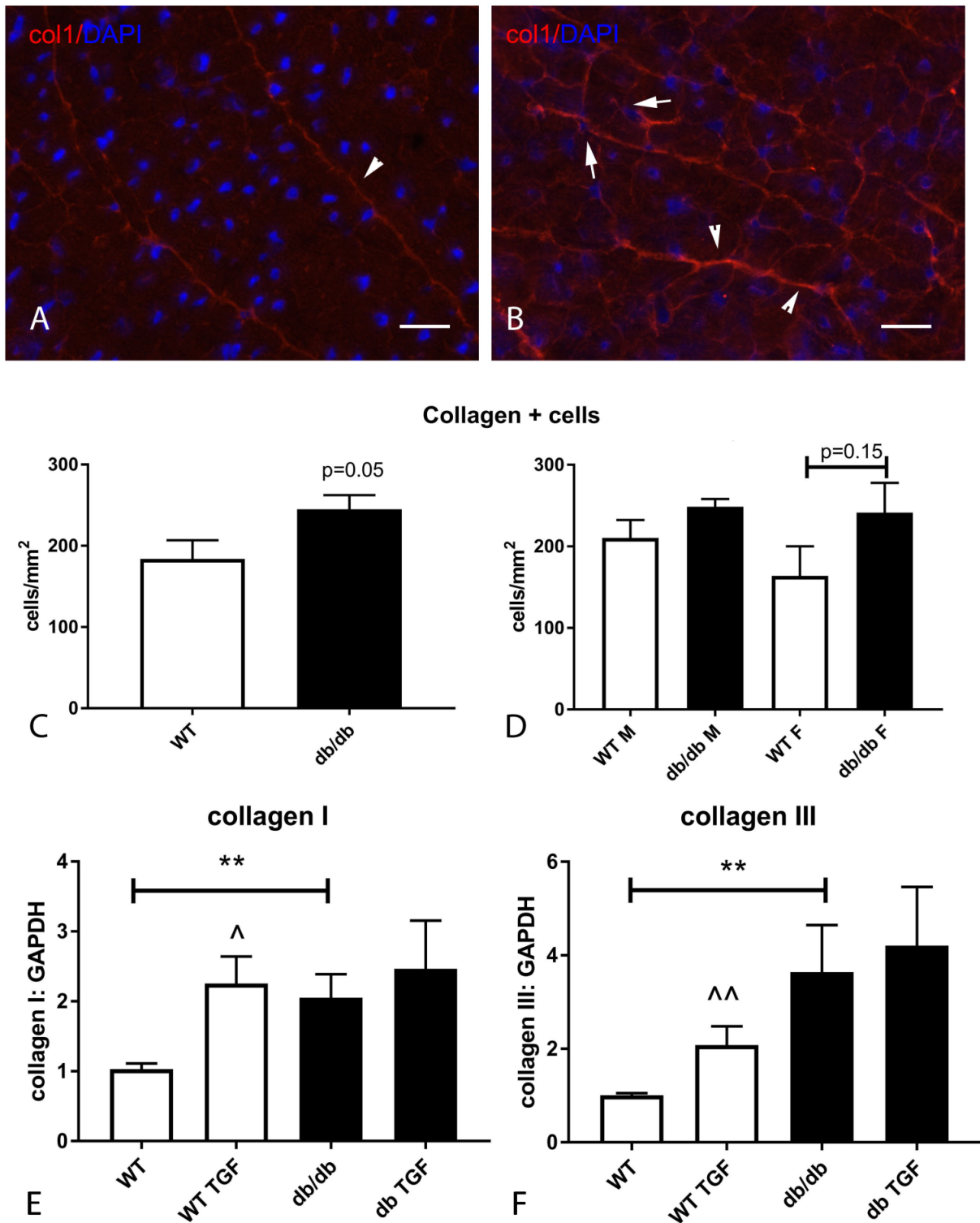


Figure 11: Fibroblasts in db/db hearts show increased collagen synthesis. A-B: Cryosections from 6 month-old lean WT and db/db mouse hearts were stained with an anti-collagen type I antibody. DAPI counterstaining was used to identify collagen I-expressing interstitial cells. C: db/db hearts had a higher density of collagen I-expressing interstitial

cells that did not reach statistical significance ($p=0.05$, $n=8/\text{group}$). Gender-specific analysis showed a trend towards higher density of collagen I-expressing cells in female db/db hearts ($n=4/\text{group}$). In vitro, cardiac fibroblasts harvested from 4 month-old db/db mice had a 2.0-3.0-fold increase in baseline collagen I and collagen III mRNA expression when compared with fibroblasts from WT hearts. Activated fibroblasts from db/db hearts were less responsive to TGF- β 1 stimulation. TGF- β 1 (10ng/ml) stimulation for 4h stimulated collagen I and III mRNA synthesis in WT cells, but did not significantly increase expression of collagens in db/db fibroblasts. (** $p<0.01$, ^ $p<0.05$, ^^ $p<0.01$ vs. corresponding unstimulated cells, $n=7-8/\text{group}$). Scalebar=25 μm .

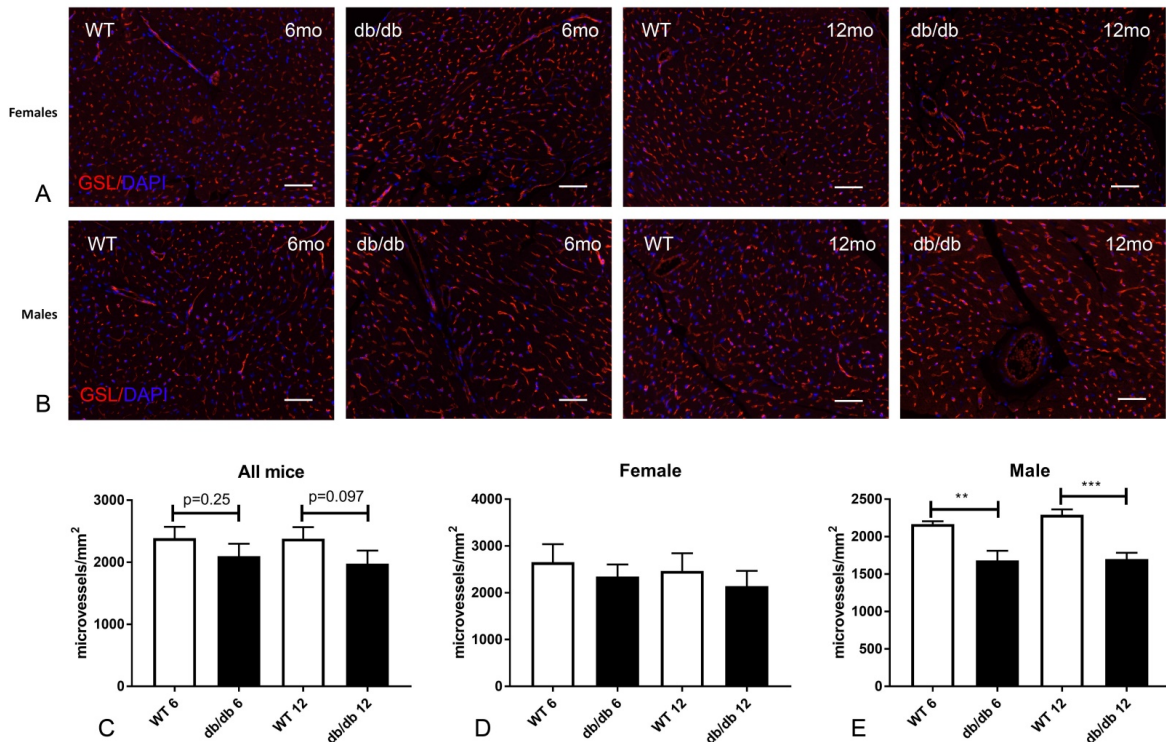


Figure 12: Male db/db mice have microvascular rarefaction. A-B: Microvascular density was assessed in db/db and lean WT mouse hearts using Griffonia Simplicifolia-I lectin staining. db/db mice had a trend towards reduced microvascular density at 6 and 12 months of age. Although female db/db mice had comparable microvascular density with age-matched WT controls, male animals exhibited a markedly lower microvascular density (** $p<0.01$, *** $p<0.001$; male mice: $n=4/\text{group}$, female mice: $n=4/\text{group}$, male+female: $n=8/\text{group}$). Scalebar=50 μm .

A2) Characterization of the cardiac pericytes.

Fibroblasts and pericytes are often considered related interstitial cell populations with common functional properties. In order to explore the distribution and function of pericytes in the myocardium, we have developed pericyte/fibroblast dual reporter mice

(NG2^{Dsred}/PDGFR α ^{GFP} mice). Using dual immunofluorescence and flow cytometry, we demonstrated that NG2+ perivascular cells (pericytes) and PDGFR α + fibroblasts are distinct populations in mouse hearts with minimal overlap (Figures 13, 14).

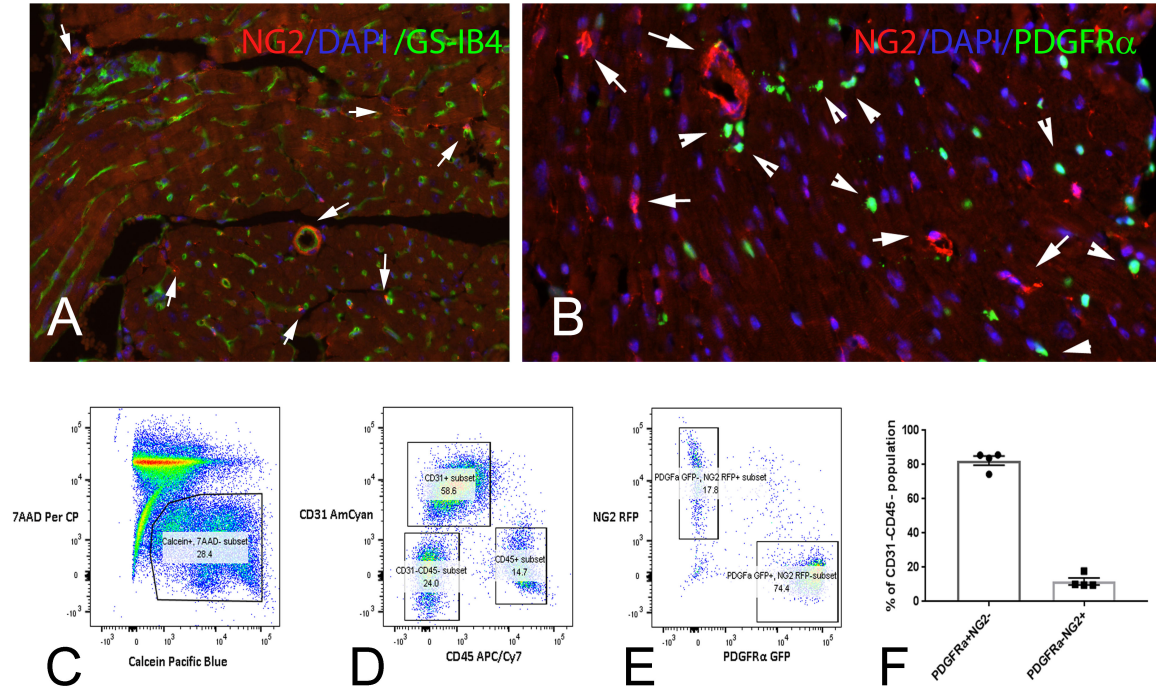


Figure 13: Fibroblasts and pericytes represent distinct populations of myocardial interstitial cells. A: NG2 is an established and reliable marker of pericytes in many tissues²⁹. Because anti-NG2 antibodies are suboptimal for immunohistochemical studies, we used NG2^{Dsred} pericyte reporter mice to identify pericytes in the mouse heart. Dual staining for Griffonia simplicifolia isolectin B4 (GS-IB4) and NG2 identifies abundant pericytes in the adult mouse heart as periendothelial cells (arrows). B. In order to examine possible overlap between pericyte and fibroblast populations, we generated NG2^{Dsred};PDGFR α ^{EGFP} pericyte/fibroblast dual reporter mice. In the adult mouse heart, NG2+ pericytes (arrows) and PDGFR α + fibroblasts (arrowheads) represent distinct interstitial cell populations without significant overlap. C-F. Flow cytometric analysis of interstitial cells from NG2^{Dsred};PDGFR α ^{EGFP} pericyte/fibroblast dual reporter mice. Viable (7AAD-), and metabolically active (calcein+) cells were gated, and the CD31-CD45- cell population (non-endothelial, non-hematopoietic cells) was subgated to identify NG2+ pericytes and PDGFR α + fibroblasts (E) F: The percentage of interstitial cells identified as NG2+ pericytes and PDGFR α + fibroblasts (n=4). Please note the significant population of pericytes along with a more abundant population of PDGFR α + fibroblasts.

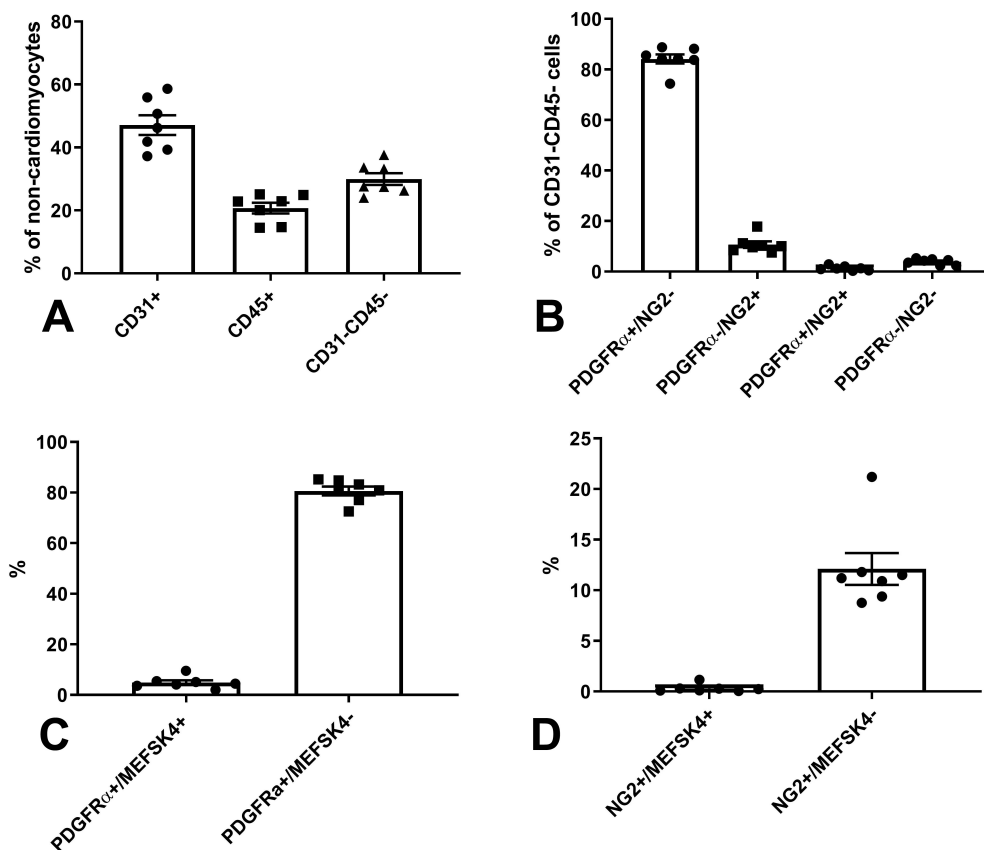


Figure 14: Flow cytometric characterization of interstitial cells in the mouse heart. A. CD31⁺ endothelial cells represent the most abundant population. Large populations of CD45⁺ hematopoietic cells, and of CD31⁻/CD45⁻ interstitial cells (pericytes and fibroblasts) are also identified. B. The majority of CD31⁻/CD45⁻ interstitial cells are PDGFR α ⁺/NG2⁻ fibroblasts. A significant population of PDGFR α ⁻/NG2⁺ pericytes is also identified. Double positive (NG2⁺/PDGFR α ⁺) and double negative (NG2⁻/PDGFR α ⁻) interstitial cells are very rare. C-D: The “fibroblast marker” MEFSK4 does not label the majority of PDGFR α ⁺ fibroblasts (C) and NG2⁺ pericytes (D) in the mouse heart.

A3. PDGFR α ⁺ fibroblasts express higher amounts of matrix genes in comparison to NG2⁺ pericytes.

In order to compare the transcriptomic profile of interstitial cell populations (fibroblasts and pericytes), we assessed gene expression in NG2⁺ pericytes and PDGFR α ⁺ fibroblasts sorted from mouse hearts. Preliminary analysis showed that fibroblasts had much higher expression levels of structural collagens (Figure 15)

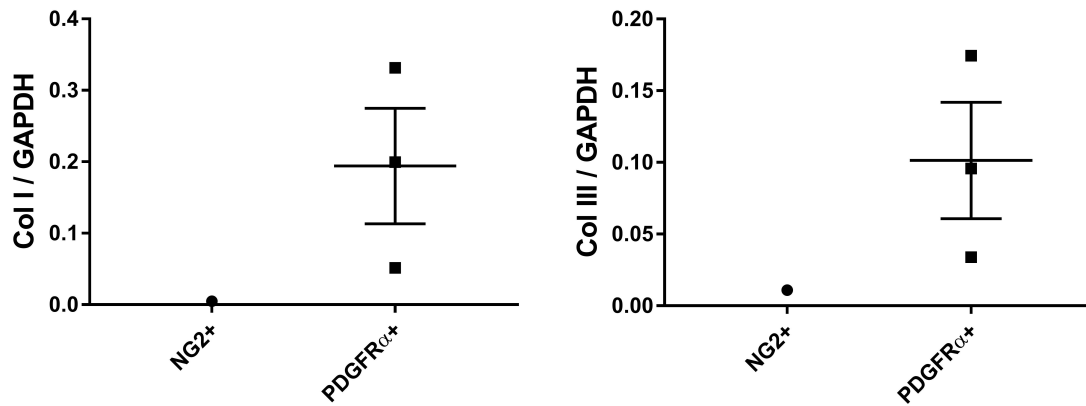


Figure 15: PDGFR α ⁺ fibroblasts sorted from fibroblast/pericyte dual reporter mice exhibit much higher expression of collagen I and collagen III mRNA, in comparison to NG2⁺ pericytes.

A3. Diabetes is associated with microvascular rarefaction. Effects on pericyte density and localization.

We developed diabetic pericyte reporter mice to compare microvascular density and pericyte numbers between db/db;NG2^{dsred} mice and lean wildtype NG2^{dsred} littermates. Microvascular density was significantly lower in obese diabetic mice (Figure 16). Vascular rarefaction was associated with a trend towards reduced density of perivascular NG2⁺ cells (pericytes).

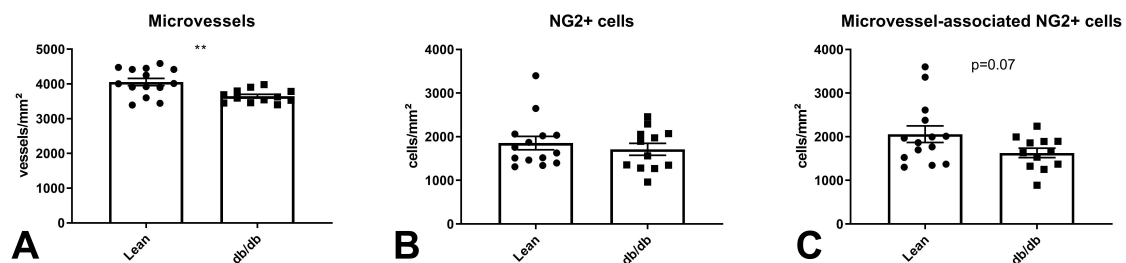


Figure 16: A. db/db mice have significantly lower microvascular density than lean wildtype littermates. Although the density of NG2⁺ cells was not significantly reduced (B), there was a trend towards reduced numbers of microvessel-associated NG2⁺ cells (C, pericytes). This finding may reflect loss of microvascular localization of NG2⁺ cells, due to acquisition of a fibroblast-like phenotype. This hypothesis will be tested using lineage tracing studies in inducible NG2-CreERT2 mice.

A4: Effects of high glucose on pericyte gene expression.

We examined the effects of 2 different concentrations of glucose on gene expression in human brain pericytes. The 17mM concentration simulates an environment of moderate hyperglycemia, whereas the very high concentration (25mM) recapitulates the effects of severe hyperglycemia. A PCR array was performed to examine the effects of high glucose on the transcriptomic profile of human brain pericytes. Moderately high glucose (17mM) increased synthesis of several fibrogenic genes (Figure 17), including α -smooth muscle actin (α -SMA)/*Acta2*, *colla2*, *col3a1*, *TGFb3*, *Tgbr1*, *Tsp1*, and *CCN2*. Very high glucose (25mM) induced a pro-inflammatory phenotype (Figure 18), increasing levels of *IL1a*, *TNFa*, and *MMP3*. Thus, in pericytes, moderate increases in glucose concentration promote expression of fibrosis-associated genes, while very high glucose may induce inflammatory activation.

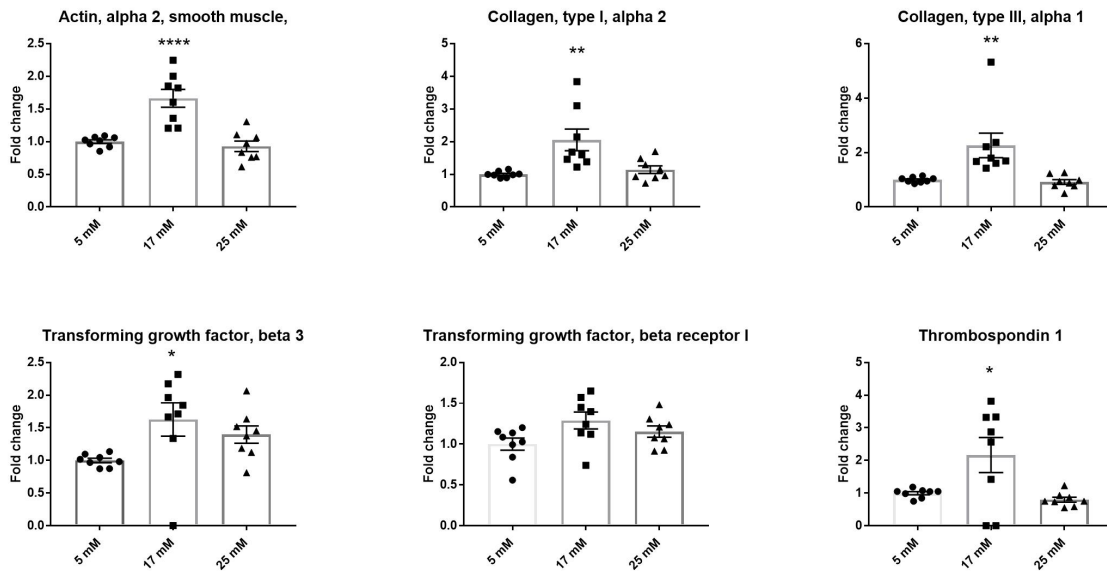


Figure 17: Effects of glucose on transcription of fibrosis-associated genes in human brain pericytes. Moderately high glucose concentration (17mM) induces expression of *Acta2*/ α -SMA, collagen genes, *Tgfb3*, *Tgbr1* and *Thbs1*/TSP-1 (* $p < 0.05$, ** $p < 0.001$, **** $p < 0.0001$, $n = 8$ /group).

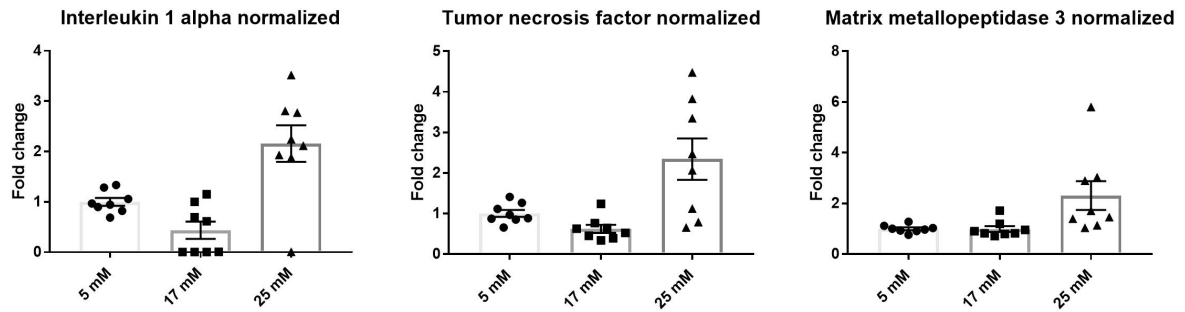


Figure 18: High glucose concentration (25mM) triggers acquisition of a pro-inflammatory profile in human brain pericytes, inducing synthesis of *Il1a*, *TNfa* and *MMP3* mRNA (* $p < 0.05$, $n = 8$).

b) The role of endothelial-to-mesenchymal transition in diabetic cardiomyopathy (Work performed at VUMC)

We are using Cre/Lox-based cell lineage tracing strategies to assess the contribution of endothelial cells to the generation of extracellular-matrix-producing cells in diabetic mouse hearts, thereby increasing interstitial fibrosis and leading to myocardial dysfunction. Specifically, we crossed the Tie1-Cre mice that express Cre recombinase in endothelial cells to the *R26RstopYFP* (*Rosa-YFP*) mice in order to generate double transgenic Tie1-Cre-YFP mice to uniquely label endothelial cells and their cellular derivatives. These mice were bred to each other and genotyped in order to generate Tie1-Cre-YFP mice that are homozygote for both the Cre recombinase and *R26RYFP* loci. Double homozygote Tie1-Cre-YFP mice were then crossed with *db/+* heterozygotes to generate *db/+* Tie1-Cre *Rosa-YFP* mice and non-diabetic Tie1-Cre *Rosa-YFP* siblings as controls. *db/+* heterozygotes were then crossed to each other to generate *db/db* Tie1-Cre *Rosa-YFP* mice and non-diabetic Tie1-Cre *Rosa-YFP* siblings as controls.

Twelve hearts representing healthy control and diabetic genotypes of both sexes, displaying typical echocardiography parameters of healthy and disease phenotypes, were processed to obtain 60 sections/per heart for immunofluorescence and other histological analyses. Cardiac tissue sections have been analyzed by immunohistological techniques to compare the effect of diabetes on cardiac inflammation, vascular density, vascular

rarefaction, fibrosis, endothelial-to-mesenchymal (EndMT) transition and Sca1⁺/CD31⁻ pericytes with properties of cardiac progenitor cells.

c) Molecular characterization of sex-specific DCM progression (Work performed collaboratively at VUMC and AECOM)

To determine molecular mechanisms linked to diabetic cardiomyopathy, we have isolated RNA samples from whole hearts and analyzed gene expression profiles using deep RNA sequencing. Because diabetic males and females display distinct histological and physiological abnormalities in the heart (Alex et al., 2018), we have isolated RNA samples from whole hearts of obese and diabetic *db/db* male and female mice at 3 distinct time points and established gene expression profiles by deep RNA sequencing.

Specifically, we have prepared RNA samples from whole hearts of 2, 6 and 12 month-old male and female obese *db/db* mice and age-matched lean siblings as controls, with three mice per group for a total of 36 samples. The hearts were isolated at AECOM and shipped to VUMC where RNA samples were prepared and submitted to the

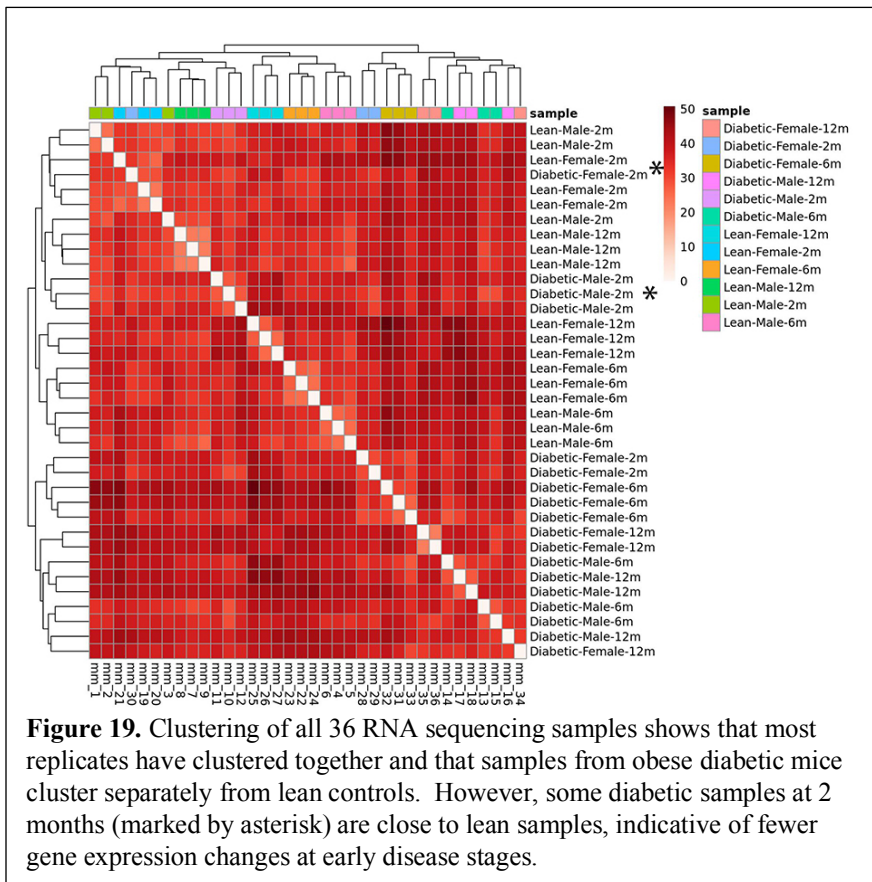


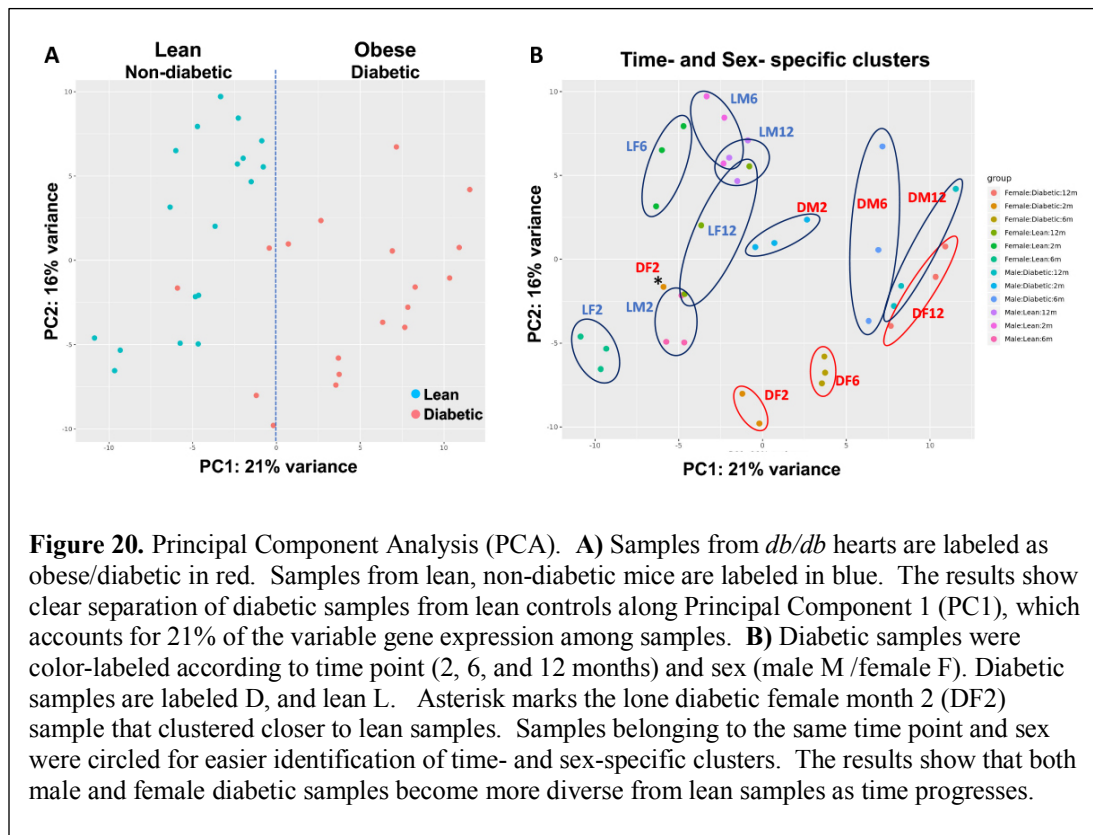
Figure 19. Clustering of all 36 RNA sequencing samples shows that most replicates have clustered together and that samples from obese diabetic mice cluster separately from lean controls. However, some diabetic samples at 2 months (marked by asterisk) are close to lean samples, indicative of fewer gene expression changes at early disease stages.

VANTAGE genomics Core at VUMC for quality control. All samples had RNA Integrity Numbers above the required threshold for further processing and were sequenced using the Illumina NovaSeq6000 on paired-end-150 flow cell runs at 32 million pass-filter

(PF) reads per sample. The RNA-seq data were then analyzed using Vanderbilt Technologies for Advanced Genomics Analysis and Research Design (VANGARD) resources. Aligning reads to mouse genome revealed excellent and uniform Mapping Quality, with low Zero Mapping Quality and high percentage of proper paired reads.

We subsequently performed clustering analysis using DESeq2. The results showed that replicate samples clustered together along disease status and time points and separately for male and female samples, providing a first indication that there are significant disease-stage- and sex- specific gene expression changes in diabetic hearts (Figure 19). Of note, month 2 samples aligned close to, or in some instances intercalated with lean samples, likely reflecting a variability in the early onset of disease phenotypes as also seen in Echo data of young *db/db* mice.

Principal Component Analysis (PCA) of the entire gene expression dataset shows clear separation of lean from diabetic samples in Principal Component (PC) 1, suggesting that there is a core group of genes that represent a universal, i.e., time- and sex-independent molecular signature of DCM (Figure 20A). Furthermore, diabetes-regulated



genes show clear time-dependent groups with distinct 2-, 6- and 12-month clusters (Figure 20B). We postulate that early gene expression changes at 2 months of age represent disease drivers, whereas changes at later points are characteristics of established DCM (6 months) or are consequences of the ensuing HF (12 months).

To identify the putative roles of dysregulated genes in diabetic hearts, we employed Ingenuity Pathway Analysis. The pathway analyses revealed that the majority of the universally dysregulated genes in diabetic hearts, independent of age and sex, relate to the following pathways and biological processes.

UNIVERSAL PATHWAYS OF DIABETIC CARDIOMYOPATHY

Cardiomyocyte Contractility

Cation homeostasis – transport

Calcium handling/Calcium channels

Gated channel activity

Calcium release from cytoplasmic reticulum/Sarcolemma

Cardiomyocyte development, contraction, conduction, polarization (hypertrophic response)

Contractile machinery, Z-disc, I-disc, filaments, etc.

Heart rate regulation

Metabolism

Fatty acid metabolism – lipid metabolism – lipid, fatty acid oxidation

Carbohydrate / Glucose Metabolism

Pyruvate metabolism

Insulin response

Downregulation of insulin receptor

ATP generation

Cellular respiration

NOS biosynthesis

Mitochondrial membrane

Oxidoreductase system

Inflammation/Fibrosis

Monocyte migration

Leukocyte chemotaxis

Cytokine secretion

MHC II downregulation

Drastic M1/M2 polarization

Suppression of IFN – signaling

ECM stiffening, reorganization
Laminins, Collagens

Vascular Dysfunction

Vasoconstriction

Suppression of Nppb, inhibitor of RAAS, promotor of vasorelaxation

SMC constriction

Endothelial development, migration

Vasculogenesis NOS-mediated signal transduction

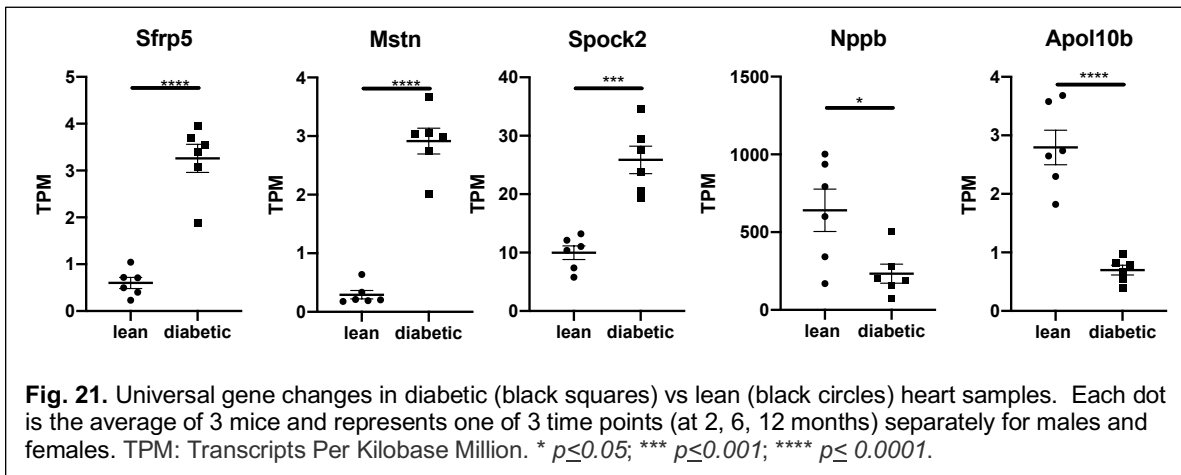
Neuropathy

Neuronal death

Axon growth, Synapses

Our results are in line with known characteristics of diabetic heart disease. However, a number of genes within each pathway have not been implicated in diabetic cardiomyopathy before, thus representing potential novel biomarkers and therapeutic targets that we will actively pursue in future studies.

Representative examples of genes that are universally expressed in diabetic hearts are shown in Figure 21.



Taken together, our discoveries have led to new testable hypotheses that we will explore in future approaches taking advantage of human disease databases and Electronic Health Records (EHR) such as BioVU, and mechanistic studies in animal models using available cell-specific knockout mice, CISPR/Cas9 technology to generate novel research tools, or suitable chemical agents.

Training opportunities and professional development

Cassandra Awgulewitsch is a graduate student in the Cell and Developmental Biology Training Program who worked on the project. Cassandra has received a fellowship from the NIH-sponsored T32 training grant “Program in Cardiovascular Mechanisms: Training in Investigation” (T32HL007411). Since joining our laboratory, she has published a first author review article on the role of endothelial cell plasticity in homeostasis and disease (Awgulewitsch et al., 2017), and co-authored a manuscript on the role of BMP signaling inhibition in cardiomyocyte differentiation (Bylund et al., *Stem Cells & Dev.*, 2017). The primary training of Cassandra is laboratory work under the direct supervision of Dr. Hatzopoulos. Cassandra has performed the breeding of Tie1-Cre-YFP mice to db/+ heterozygotes to generate diabetic and non-diabetic Tie1-Cre Rosa-YFP mice for lineage tracing experiments. She has also spearheaded the RNAseq data analyses. Her training includes daily informal interactions, weekly data review in face-to-face meetings (or Zoom meetings during the pandemic), and weekly laboratory meetings and journal clubs. She presented her work in the Research Exchange seminars at VU, and posters in the Cardiovascular Research Day, and Program in Developmental Biology Retreat at VU. She also attended the Basic Cardiovascular Sciences Scientific Sessions, July 29 - August 1, 2019 in Boston, MA.

David Wu is a MD/PhD student in the Human Genetics Training Program at Vanderbilt University School of Medicine. David has completed two years of Medical School and started his PhD thesis work in our laboratory in September 2017. After completion of his thesis, he will return for an additional two years to Vanderbilt School of Medicine to finish his medical degree. David has used the electronic medical records at VUMC that are also linked to genotyping data to search for novel associations between diabetic cardiomyopathy and genes of interest as emerge from the RNAseq studies. He has presented his research in the Cardiovascular Research Day, and the Human Genetics Retreat at VUMC.

An essential component of the training program of both students involved participation in Journal Clubs organized weekly by the Cell & Developmental Biology Department and the Human Genetics Institute throughout the academic year and Work-in-

Progress Cardiovascular Research Conference Series (CVRC). The CVRC meetings are formal seminars by graduate students, post-doctoral fellows, cardiology fellows and faculty, giving trainees an excellent opportunity to organize their findings, develop and defend hypotheses, and refine their communication skills. There were also numerous departmental seminars each week in the VUMC campus from prominent visiting investigators, closely related to the scientific interests of graduate students.

Cassandra and David also had the opportunity to take part in local annual scientific meetings such as the Graduate Student Research Symposium (GSRS), the Program in Developmental Biology retreat and the Cardiovascular Research Day at VUMC. These meetings brought nationally recognized scientists for seminars exposing trainees to the latest in contemporary research and giving students an opportunity to present their own work to a broader audience as posters, or short oral presentations. Finally, both students have supervised the work of junior investigators in the laboratory (e.g., rotating graduate students, undergraduates and research assistants), which helped develop their leadership and mentoring skills.

How were the results disseminated to communities of interest?

Most of the findings have been disseminated during presentations and discussions in work-in-progress meetings such as CVRC and teleconferences between the partnering institutions. Many of the findings outlined above resulted in several high-impact publications in top-quality journals. The concepts explored in this proposal have significantly contributed to development of our paradigm on the pathogenesis of diabetic fibrosis and diabetes-associated cardiomyopathy, and are discussed in a series of invited review manuscripts and editorials (please see “products”).

Future plans

Our RNAseq data have uncovered significant differences in gene activity in diabetic hearts between female and male mice. We will continue validation of the primary RNAseq data using histological, molecular and cellular techniques. We are

using bioinformatics tools to analyze in depth the assembled gene expression profiling data in order to identify genetic pathways activated or suppressed commonly or specifically in diabetic males as compared to diabetic females, thereby developing critical insights and novel hypotheses about sex-specific causes or effects of DCM. These analyses will likely yield new insights in the development of diabetic cardiomyopathy and may identify new targets to treat heart disease in diabetic patients. Moreover, efforts will focus on preparation of the large data sets for publication and dissemination to the scientific community.

4. Impact

HFpEF is a major cause of morbidity and mortality worldwide. There is currently no effective treatment for patients with HFpEF. Although cardiac fibrosis has been implicated in the pathogenesis of HFpEF, the cellular basis for fibrotic remodeling of the ventricle is poorly understood. Metabolic diseases (such as obesity and diabetes) are associated with an increased incidence of HFpEF; however, the pathophysiological mechanisms responsible for this association remain unknown. Our experiments have established a model of HFpEF due to metabolic disease that can be used to dissect cellular and molecular mechanisms. This is of outstanding significance for pathophysiologic dissection in vivo and the development of future therapeutic strategies to combat diabetic cardiomyopathy. Moreover, the importance of our studies extends beyond the cardiovascular field, as diabetes-associated tissue fibrosis has an impact on other organs (such as the kidney and the liver).

5. Changes/Problems

No changes or problems to report

6. Products

Publications:

NG Frangogiannis. The functional pluralism of fibroblasts in the infarcted myocardium. *Circ Res* 2016; 119: 1049-1051.

AV Shinde, C Humeres, and **NG Frangogiannis**. The role of α -smooth muscle actin in fibroblast-mediated matrix contraction and remodeling. *BBA Mol Bas Dis* 2017; 1863: 298-309.

NG Frangogiannis. The extracellular matrix in myocardial injury, repair and remodeling. *J Clin Invest* 2017; 127: 1600-1612.

W Hanif, L Alex, Y Su, AV Shinde, I Russo, N Li, and **NG Frangogiannis**. Left atrial remodeling, hypertrophy and fibrosis in mouse models of heart failure. *Cardiovasc Pathol* 2017;30:27-37.

AV Shinde, M Dobaczewski, JJ De Haan, A Saxena, KK Lee, Y Xia, W Chen, Y Su, W Hanif, IK Madahar, VM Paulino, G Melino and **NG Frangogiannis**. Tissue transglutaminase induction in the pressure-overloaded myocardium regulates cardiac remodeling. *Cardiovasc Res* 2017; 113:892-905.

NG Frangogiannis. Activation of the innate immune system in the pathogenesis of acute heart failure. *Eur Heart J Acute Cardiovasc Care* 2017 Apr1 (epub ahead of print).

NG Frangogiannis. Fibroblasts and the extracellular matrix in right ventricular disease. *Cardiovasc Res* 2017; 113: 12: 1453-1464.

Shinde AV and **NG Frangogiannis**. Mechanisms of fibroblast activation in the remodeling myocardium. *Curr Pathobiol Rep* 2017; 5:145-152.

AV Shinde, and **NG Frangogiannis**. Tissue transglutaminase in the pathogenesis of heart failure. *Cell Death Differentiation* 2018; 25(3): 453-456.

P Kong, A Shinde, Y Su, I Russo, B Chen, A Saxena, SJ Conway, JM Graff, and **NG Frangogiannis**. Opposing actions of fibroblast and cardiomyocyte Smad3 signaling in the infarcted myocardium. *Circulation* 2018 Feb 13;137(7):707-724.

ML Lindsey, R Bolli, JM Canty, XJ Du, **NG Frangogiannis**, S Frantz, RG Gourdie, JW Holmes, SP Jones, R Kloner, DJ Lefer, R Liao, E Murphy, P Ping, K Przyklenk, FA Recchia, L Schwartz Longacre, CM Ripplinger, JE Van Eyk, G Heusch. Guidelines for experimental models of myocardial ischemia and infarction. *Am J Physiol Heart Circ Physiol* 2018; 314:H812-838.

S Huang, and **NG Frangogiannis**. Anti-inflammatory therapies in myocardial infarction: failures, hopes and challenges. *Br J Pharmacol* 2018; 175:1377-1400.

L Alex and **NG Frangogiannis**. The cellular origin of activated fibroblasts in the infarcted and remodeling myocardium. *Circ Res* 2018 Feb 16;122(4):540-542.

NG Frangogiannis. Cell therapy for peripheral artery disease. *Curr Opin Pharmacol* 2018; Feb 13;39:27-34.

NG Frangogiannis. The inflammatory response in tissue repair. In *Inflammation: From molecular and cellular mechanisms to the clinic*. JM Cavaillon and M Synger (editors), 2018; 60: 1517-1538. Wiley DOI: 10.1002/9783527692156.ch6.

NG Frangogiannis. Cell biological mechanisms in regulation of the post-infarction inflammatory response. *Curr Opin Physiol* 2018; 1: 7-13.

NG Frangogiannis. Galectin-3 in the fibrotic response: cellular targets and molecular mechanisms. *Int J Cardiol* 2018; 258:226-227.

AV Shinde, Y Su, BA Palanski, K Fujikura, MJ Garcia, **and NG Frangogiannis.** Pharmacologic inhibition of the enzymatic effects of tissue transglutaminase reduces cardiac fibrosis and attenuates cardiomyocyte hypertrophy following pressure overload. *J Mol Cell Cardiol* 2018; 117: 36-48.

JA Kirk, **and NG Frangogiannis.** Galectin-3 in the pathogenesis of heart failure: a causative mediator, or simply a biomarker? *Am J Physiol Heart Circ Physiol* 2018; 314(6):H1256-1258.

B Chen, **and NG Frangogiannis.** The role of macrophages in nonischemic heart failure. *JACC BasicTransl Sci* 2018; 3(2):245-238.

NG Frangogiannis. Targeting mitochondrial calcium transport in myocardial infarction. *Hellenic J Cardiol* 2018; 59: 223-225.

L Alex, I Russo, V Holoborodko, **and NG Frangogiannis.** Characterization of a mouse model of obesity-related fibrotic cardiomyopathy that recapitulates features of human Heart Failure with Preserved Ejection Fraction. *Am J Physiol Heart Circ Physiol* 2018; 315:H934-949.

B Chen, S Huang **and NG Frangogiannis.** Aging, cardiac repair and Smad3. *Aging* 2018; 10:2230-2232.

NG Frangogiannis. Cardiac fibrosis: cell biological mechanisms, molecular pathways and therapeutic opportunities. *Mol Asp Med* 2019; 65:70-99.

NG Frangogiannis. Protean functions and phenotypic plasticity of regulatory T cells (Tregs) in chronic ischemic heart failure. *Circulation* 2019; 139:222-225.

B Chen, A Brickshawana, **and NG Frangogiannis.** The functional heterogeneity of resident cardiac macrophages in myocardial injury. CCR2+ cells promote inflammation, whereas CCR2- cells protect. *Circ Res* 2019; 124:183-185.

I Russo, M Cavalera, S Huang, Y Su, A Hanna, B Chen, AV Shinde, SJ Conway, JM Graff, **and NG Frangogiannis.** Protective effects of activated myofibroblasts in the

pressure-overloaded myocardium are mediated through Smad-dependent activation of a matrix-preserving program. *Circ Res* 2019; 124: 1214-1227.

I Andreadou, HA Cabrera-Fuentes, Y Devaux, **NG Frangogiannis**, S Frantz, T Guzik, E Liehn, CP da Gomes, R Schulz and DJ Hausenloy. Immune cells as targets for cardioprotection. New players and novel therapeutic opportunities. *Cardiovasc Res* 2019; 115:1117-1130.

S Huang, B Chen, Y Su, L Alex, C Humeres, AV Shinde, SJ Conway, **and NG Frangogiannis**. Distinct roles of myofibroblast-specific Smad2 and Smad3 signaling in repair and remodeling of the infarcted heart. *J Mol Cell Cardiol* 2019; 132:84-97.

NG Frangogiannis. Can myocardial fibrosis be reversed? *J Am Coll Cardiol* 2019; 73: 2283-2285.

B Chen, S Huang, Y Su, Y-J Wu, A Hanna, A Brickshawana, JM Graff, **and NG Frangogiannis**. Macrophage Smad3 protects the infarcted heart, stimulating phagocytosis and regulating inflammation. *Circ Res* 2019; 125: 55-70.

NG Frangogiannis. The extracellular matrix in ischemic and non-ischemic heart failure. *Circ Res* 2019; 125: 117-146.

A Hanna, **and NG Frangogiannis**. The cell biological basis for primary unloading in acute myocardial infarction. *Int J Cardiol* 2019; 293: 45-47.

NG Frangogiannis. How do endosomal Toll-like receptors (TLRs) sense and extend ischemic myocardial injury? *Cardiovasc Res* 2019; 115: 1687-1689.

L Alex **and NG Frangogiannis**. Pericytes in cardiac repair. *Vascular Biology* 2019; 1:H23-H31.

D Humeres **and NG Frangogiannis**. Fibroblasts in the infarcted, remodeling and failing heart. *JACC Basic Transl Res*. 2019; 4:449-467.

NG Frangogiannis. S100A8/A9 as a therapeutic target in myocardial infarction: cellular mechanisms, molecular interactions and translational challenges. *Eur Heart J* 2019; 40: 2724-2726.

A Hanna **and NG Frangogiannis**. The role of the TGF-beta superfamily in myocardial infarction. *Front Cardiovasc Med* 2019 18 Sep, <https://doi.org/10.3389/fcvm.2019.00140> (epub ahead of print).

NG Frangogiannis. Myocardial fibrosis in genetic cardiomyopathies: a cause of dysfunction or simply an epiphenomenon? *Trends Cardiovasc Med* 2019, Oct 5. pii: S1050-1738(19)30138-0. doi: 10.1016/j.tcm.2019.09.009. [Epub ahead of print].

NG Frangogiannis. Transforming Growth Factor (TGF)-beta in tissue fibrosis. *J Exp Med* 2020;217 (3): e20190103 <https://doi.org/10.1084/jem.20190103> (epub ahead of print).

S Huang, B Chen, C Humeres, L Alex, A Hanna, **and NG Frangogiannis.** The role of Smad2 and Smad3 in regulating homeostatic fibroblast functions in vitro and in vivo. *BBA Mol Cell Res* 2020; 1867(7):118703. doi: 10.1016/j.bbamcr.2020.118703.

NG Frangogiannis, JC Covacic. Extracellular matrix in Ischemic Heart Disease. Part 4/4: JACC Focus Seminar. *J Am Coll Cardiol* 2020 75(17):2219-2235.

B Chen **and NG Frangogiannis.** Chemokines in myocardial infarction. *J Cardiovasc Transl Res* 2020 May 15. doi: 10.1007/s12265-020-10006-7. Online ahead of print.

LE de Castro Bras **and NG Frangogiannis.** Extracellular matrix-derived peptides in tissue remodeling and fibrosis. *Matrix Biol* 2020; 91-92:176-187.

A Hanna, AV Shinde **and NG Frangogiannis.** Validation of diagnostic criteria and histopathological characterization of cardiac rupture in the mouse model of non-reperused myocardial infarction. *Am J Physiol Heart Circ Physiol.* 2020 Nov 1;319(5):H948-H964.

A Hanna **and NG Frangogiannis.** Inflammatory Cytokines and Chemokines as Therapeutic Targets in Heart Failure. *Cardiovasc Drugs Ther.* 2020 Dec;34(6):849-863.

NG Frangogiannis. COVID-19-associated myocardial injury: how overinterpretation of scientific findings can fuel media sensationalism and spread misinformation. *Eur Heart J* 2020 Oct 14;41(39):3836-3838.

NG Frangogiannis. Fact and fiction regarding fibroblast to endothelium conversion: semantics and substance of cellular identity. *Circulation* 2020 Oct 27;142(17):1663-1666.

NG Frangogiannis. Cardiac Fibrosis. *Cardiovasc Res* 2020 Nov 2;cvaa324 (online ahead of print).

A Hanna, C Humeres **and NG Frangogiannis.** The role of Smad signaling cascades in cardiac fibrosis. *Cell Signal* 2020 Nov 5;77:109826. doi: 10.1016/j.cellsig.2020.109826. (online ahead of print).

R Li **and NG Frangogiannis.** Chemokines and cardiac fibrosis. *Curr Opinion Physiol* 2021 Feb;19:80-91. doi: 10.1016/j.cophys.2020.10.004

Awgulewitsch C. P., L. T. Trinh **and A. K. Hatzopoulos.** The vascular wall: a plastic hub of activity in cardiovascular homeostasis and disease. *Current Cardiology Rep.*, 19: 51, 2017.

Bylund J. B., L. T. Trinh, C. P. Awgulewitsch, D. T. Paik, C. Jetter, R. Jha, J. Zhang, K. Nolan, C. Xu, T. B. Thompson, T. J. Kamp and **A. K. Hatzopoulos**. Coordinated proliferation and differentiation of human iPS cell-derived cardiac progenitor cells depends on BMP signaling regulation by GREMLIN 2. *Stem Cells Dev.*, 26: 678-693, 2017.

Schroer A. K., M. R. Bersi, C. R. Clark, Q. Zhang, L. H. Sanders, **A. K. Hatzopoulos**, T. L. Force, S. M. Majka, H. Lal and W. D. Merryman. Cadherin-11 blockade reduces inflammation-driven fibrotic remodeling and improves outcomes after myocardial infarction. *JCI Insight* 4:e131545, 2019.

Wu D. H. and **A. K. Hatzopoulos**. Bone morphogenetic protein signaling in inflammation. *Exp. Biol. Med. (Maywood)* 244: 147-156, 2019.

A. K. Hatzopoulos. Disease Models & Mechanisms in the age of Big Data. *Dis. Model Mech.*, 12: dmm041699. doi:10.1242/dmm.041699, 2019.

Summers M. E., B. W. Richmond, J. A. Kropski, S. A. Majka, J. A. Bastarache, **A. K. Hatzopoulos**, J. Bylund, M. Ghosh, I. Petrache, R. F. Foronjy, P. Geraghty and S. M. Majka. Balanced Wnt/Dickkopf1 signaling by mesenchymal vascular progenitor cells in the microvascular niche maintains distal lung structure and function. *Am. J. Physiol. Cell. Physiol.* in press, 2020.

Rauci F. J. Jr, A. P. Singh, J. Soslow, L. W. Markham, L. Zhong, W. Aljafar, N. Lessiohad, C. P. Awgulewitsch, P. Umbarkar, Q. Zhang, P. L. Cannon, M. Buchowski, J. T. Roland, E. J. Carrier, W. B. Burnette, **A. K. Hatzopoulos**, H. Lal and C. L. Galindo. The BDNF rs6265 Polymorphism is a Modifier of Cardiomyocyte Contractility and Dilated Cardiomyopathy. *Int. J. Mol. Sci.*, 21:7466, 2020.

7. Participants & Other Collaborating Organizations (VUMC)

Participants

Name:	<i>Antonis Hatzopoulos</i>
Project Role:	<i>PI</i>
Researcher Identifier (e.g. ORCID ID):	<i>0000-0001-5610-0017</i>
Nearest person month worked:	<i>5 per year</i>
Contribution to Project:	<i>Dr. Hatzopoulos designed experiments, supervised the experimental work and analyzed data.</i>

Funding Support:	<i>DoD W81XWH-16-1-0622, NIH R01HL122417, NIH R01HL138519, NIH R01GM114640</i>
------------------	--

Name:	<i>Milan Patel</i>
Project Role:	<i>RA I</i>
Researcher Identifier (e.g. ORCID ID):	<i>0000-0001-9752-1547</i>
Nearest person month worked:	<i>2</i>
Contribution to Project:	<i>Mr. Patel was involved in the breeding and genotyping of the diabetic db/db mice and immunohistological analyses of fibrosis and vascular density in diabetic mouse hearts.</i>
Funding Support:	<i>DoD W81XWH-16-1-0622, NIH R01HL138519</i>

Name:	<i>Awgulewitsch, Cassandra</i>
Project Role:	<i>Graduate Student</i>
Researcher Identifier (e.g. ORCID ID):	<i>0000-0002-4898-8578</i>
Nearest person month worked:	<i>12 per year</i>
Contribution to Project:	<i>Cassandra Awgulewitsch has generated diabetic Tie1Cre-YFP mice to lineage trace endothelial cells. She also had a major role in the generation and Bioinformatics analysis of RNAseq data from diabetic and control hearts, focusing on sex-specific differences in diabetic cardiomyopathy. In addition, she investigated the effects of high glucose on endothelial cells and induction of endothelial-to-mesenchymal transition.</i>
Funding Support:	<i>Ms. Awgulewitsch was supported by a T32 Training Program in "Cardiovascular Mechanisms: Training in Investigation" (HL007411) fellowship.</i>

Name:	<i>Wu, David</i>
Project Role:	<i>Graduate Student, MD/PhD program</i>
Researcher Identifier (e.g. ORCID ID):	<i>0000-0003-3452-0867</i>
Nearest person month worked:	<i>2 per year</i>
Contribution to Project:	<i>David Wu mined electronic medical records at VUMC for novel associations between diabetic cardiomyopathy and disease-causing genes identified in the RNAseq studies.</i>

Funding Support:	<i>DoD W81XWH-16-1-0622, NIH R01HL138519, NIH R01GM114640</i>
------------------	---

Name:	<i>Cannon-Stewart, Presley</i>
Project Role:	<i>RA III</i>
Researcher Identifier (e.g. ORCID ID):	<i>0000-0002-5832-1806</i>
Nearest person month worked:	<i>3 per year</i>
Contribution to Project:	<i>Presley Cannon-Stewart established cell isolation protocols from diabetic and lean hearts. Mrs. Cannon-Stewart participated in the generation of the Tie1-Cre-YFP mice. She isolated and performed quality controls on cardiac RNA samples from control and db/db mice that were analyzed by RNAseq in the VUMC Vantage Core.</i>
Funding Support:	<i>DoD W81XWH-16-1-0622, NIH R01HL138519</i>

Active other support of the PI (Antonis Hatzopoulos)

ACTIVE

1R01HL138519 (PI: Hatzopoulos) 07/01/2017-06/30/2021 5.00 calendar months
NIH/NHLBI
Functional heterogeneity of cardiac reparative cells after injury

COMPLETED

U01HL099997 (PI: Hatzopoulos) 09/01/2016-04/30/2018 0.60 calendar months
NIH/NHLBI
Functional heterogeneity in cardiac progenitor cells

U01 HL100398 (PI: Hatzopoulos) 9/30/2009-04/30/2017 5.40 calendar months
NIH/NHLBI
Optimizing Cardiovascular Stem Cells for Cardiac Repair and Regeneration

R01GM114640 (PI: Thompson) 04/01/2015-03/31/2019 1.20 calendar months
NIH/NIGMS
Structure-Function Investigation of DAN-mediated BMP Antagonism

5R01HL122417 (PI: Hemnes) 01/01/2015-12/31/2019 0.24 calendar months
NIH/NHLBI annually
Lipid Deposition in the Right Ventricle in Pulmonary Arterial Hypertension

PENDING

None

OVERLAP

None

Collaborating Organization

Albert Einstein College of Medicine (AECOM)

1300 Morris Park Ave.

Bronx, NY 10461

Collaborating PI: Dr. Nikolaos Frangogiannis

Collaboration as described above

8. Special Reporting Requirements

N/A

9. Appendices



Chemokines in cardiac fibrosis

Ruoshui Li, Nikolaos G Frangogiannis

The Wilf Family Cardiovascular Research Institute, Department of Medicine (Cardiology), Albert Einstein College of Medicine, Bronx NY

Abstract

Several members of the chemokine family are involved in regulation of fibrosis. This review manuscript discusses the role of the chemokines in the pathogenesis of myocardial fibrosis. The CC chemokine CCL2 exerts fibrogenic actions through recruitment and activation of monocytes and macrophages expressing its receptor, CCR2. Other CC chemokines may also contribute to fibrotic remodeling by recruiting subsets of fibrogenic macrophages. CXC chemokines containing the ELR motif may exert pro-fibrotic actions, through recruitment of activated neutrophils and subsequent formation of neutrophil extracellular traps (NETs), or via activation of fibrogenic monocytes. CXCL12 has also been suggested to exert fibrogenic actions through effects on fibroblasts and immune cells. In contrast, the CXCR3 ligand CXCL10 was found to reduce cardiac fibrosis, inhibiting fibroblast migration. Chemokines are critical links between inflammation and fibrosis in myocardial disease and may be promising therapeutic targets for patients with heart failure accompanied by prominent inflammation and fibrosis.

Keywords

chemokine; fibrosis; fibroblast; macrophage; heart failure; myocardial infarction; extracellular matrix

Introduction

Fibrotic remodeling is a common pathologic abnormality found in most myocardial diseases. The adult mammalian heart has negligible regenerative capacity; thus, following myocardial infarction the myocardium heals through formation of a collagen-based scar, resulting in reparative fibrosis. In many other pathophysiologic conditions, including pressure overload, metabolic disease and certain genetic cardiomyopathies, increased deposition of extracellular matrix proteins may occur in the absence of significant cardiomyocyte death, resulting in interstitial or perivascular fibrosis. Excessive deposition of

Nikolaos G Frangogiannis, MD, Albert Einstein College of Medicine, 1300 Morris Park Avenue Forchheimer G46B Bronx NY 10461, Tel: 718-430-3546, Fax: 718-430-8989, nikolaos.frangogiannis@einstein.yu.edu.

CONFLICT OF INTEREST STATEMENT:

The authors have no conflicts to disclose.

Publisher's Disclaimer: This is a PDF file of an unedited manuscript that has been accepted for publication. As a service to our customers we are providing this early version of the manuscript. The manuscript will undergo copyediting, typesetting, and review of the resulting proof before it is published in its final form. Please note that during the production process errors may be discovered which could affect the content, and all legal disclaimers that apply to the journal pertain.

fibrous tissue in the cardiac interstitium may promote both systolic and diastolic dysfunction. Moreover, fibrotic changes may play an important role in the pathogenesis of arrhythmias and conduction defects. Although, activated fibroblasts and myofibroblasts are the main cellular effectors of fibrosis, producing large amounts of extracellular matrix proteins, other cell types, including immune cells, vascular cells and cardiomyocytes may contribute to the fibrotic response, by secreting fibrogenic growth factors and matricellular proteins[1]. In many myocardial conditions, fibroblast activation is triggered by an inflammatory response, involving recruitment of fibrogenic leukocytes in the remodeling myocardium[2].

Chemokines are a family of chemotactic cytokines with a critical role in leukocyte trafficking in homeostasis and disease. Based on their structure, chemokines can be classified into four subfamilies (CC, CXC, CX3C and XC), depending on the number of aminoacids between their first two highly-conserved cysteine residues. In CC chemokines, the first two cysteines are adjacent, whereas CXC and CX3C chemokines have one and three non-conserved aminoacids respectively between the two cysteines (hence the CXC and CX3C designations). XC chemokines have only one cysteine residue near the N-terminus. This structural classification has important functional implications, determining which leukocyte populations are recruited by each subfamily. CC chemokines predominantly recruit mononuclear cells. In contrast, a subgroup of CXC chemokines that contain the ELR sequence (glutamic acid-leucine-arginine) immediately preceding the CXC motif, serve primarily as neutrophil chemoattractants. In injured and inflamed tissues, chemokines bind to glycosaminoglycans on the endothelial surface, or in the extracellular matrix and signal by interacting with G-protein-coupled seven-transmembrane chemokine receptors[3].

The pro-inflammatory actions of chemokines have been implicated in the pathogenesis of tissue fibrosis in the heart[4] and in other organs[5]. Although actions on immune cells are likely responsible for most of the effects of the chemokines in fibrosis, evidence suggests that certain members of the chemokine family may also exert direct actions on fibroblasts (Figure 1). This review manuscript summarizes recent progress in understanding the role of chemokines in myocardial fibrosis.

Immune cells in cardiac fibrosis

The idea that chronic inflammation may promote fibrotic tissue remodeling is not new [6]. Although activated fibroblasts and myofibroblasts are the central effector cells in tissue fibrosis [7],[8], serving as the main source of extracellular matrix proteins, their activation involves in many cases recruitment of immune cells that synthesize large amounts of fibrogenic growth factors, such as Transforming Growth Factor (TGF)- β [9]. Macrophages are recruited and activated following injury and secrete fibrogenic cytokines, growth factors and matricellular proteins [10]. Lymphocytes also infiltrate injured tissues and may stimulate fibrogenic cascades [11]. Mast cells accumulate and degranulate in many fibrotic conditions and may contribute to fibroblast activation by releasing their fibrogenic granular contents, including growth factors, matrix metalloproteinases and the mast cell-specific proteases tryptase and chymase [12],[13]. It has been suggested that certain leukocyte subsets may exhibit characteristics of fibroblast progenitors and may be directly involved in the

pathogenesis of fibrosis by converting to activated myofibroblasts [14],[15]. Although, in the injured heart, the contribution of circulating cells to the fibroblast population is likely to be limited [16],[17], there is no doubt that immune cell populations can play a critical role in cardiac fibrosis by secreting fibroblast-activating mediators [2]. Recruitment and activation of fibrogenic immune cells in injured and remodeling tissues, including the myocardium, is dependent on induction of chemokines [4]

Induction of chemokines in fibrotic hearts

Based on their patterns of expression, chemokines can be divided into homeostatic and inflammatory groups. Homeostatic chemokines are constitutively expressed and are implicated in cell homing in lymphoid organs. Inflammatory chemokines, on the other hand, show low levels of expression in normal tissues, and are markedly upregulated following injury regulating recruitment of leukocytes. Some members of the chemokine family (such as CXCL12/Stromal cell-Derived factor (SDF)-1 have both homeostatic and inflammatory roles, showing both constitutive expression, and induction in inflamed tissues. Fibrotic conditions are associated with induction of several inflammatory chemokines.

Injury rapidly upregulates chemokine expression in the myocardium, inducing a wide range of inflammatory CC and CXC chemokines, in cardiac endothelial cells, macrophages, fibroblasts and cardiomyocytes (Table 1) [18]. Increased chemokine levels have been consistently documented in experimental models of cardiac fibrosis [1],[19], and in patients with fibrotic cardiomyopathic conditions [20]. Several mechanisms have been implicated in activation of the chemokine system in injured and remodeling hearts. First, in myocardial diseases associated with cardiomyocyte death, necrotic cells release damage-associated molecular patterns (DAMPs), stimulating Toll-like receptor (TLR) signaling responses, and promoting downstream activation of the Nuclear Factor (NF)- κ B system and chemokine transcription [21]. Second, activation of the inflammasome results in release of active Interleukin (IL)-1 β , stimulating chemokine expression [22]. Third, injury-associated release and activation of proteases generates extracellular matrix fragments that induce chemokine expression in many different cell types. Fourth, mechanical stress may activate neurohumoral signals (such as angiotensin II), thus stimulating pro-inflammatory signaling, resulting in induction of chemokines [23]. Neurohumoral activation of calcium (Ca²⁺) / calmodulin (CaM)-dependent kinase II δ has been suggested to promote induction of CCL2 in pressure overload models [24],[25]. Fifth, oxidative stress has been extensively implicated in induction of the chemokine response following myocardial injury [26].

The role of the chemokines in cardiac fibrosis

CC chemokines

The CCL2/CCR2 axis—CCL2/monocyte chemoattractant protein (MCP)-1 is the best-studied member of the CC chemokine family in myocardial disease. CCL2 is markedly upregulated in experimental models of ischemic and non-ischemic cardiac fibrosis [27],[28], [29] and is overexpressed in myocardial samples from patients with heart failure [20]. Studies using genetic loss-of-function approaches or pharmacologic inhibition in mouse models support the notion that CCL2 and its main receptor CCR2 play a critical role in

myocardial fibrosis. In a mouse model of reperfused myocardial infarction, CCL2 disruption attenuated myofibroblast infiltration [30]. In a model of hypertensive fibrosis administration of an anti-CCL2 antibody reduced fibrotic remodeling [29]. In a model of ischemic non-infarctive cardiomyopathy induced through brief repetitive ischemia/reperfusion, CCL2 loss attenuated interstitial fibrosis and improved dysfunction [27]. Moreover, in models of diabetic cardiomyopathy, genetic and pharmacologic inhibition of CCR2 attenuated fibrosis [31].

Which cellular mechanisms mediate the fibrogenic actions of CCL2/CCR2? CCL2-mediated cardiac fibrosis is predominantly attributed to recruitment and activation of CCR2+ monocytes and macrophages, resulting in release of fibrogenic mediators, such as TGF- β and osteopontin, capable of activating cardiac fibroblasts [27],[30],[32],[33]. The mammalian heart contains a resident macrophage population, derived predominantly from yolk sac and fetal monocyte progenitors [34]. In normal hearts, these macrophages have the capability to self-renew; however, following infarction, the cardiac macrophage population markedly expands through recruitment of abundant CCR2+ monocytes [35],[36]. Thus, myocardial injury enriches the heart with a wide range of macrophage phenotypes with distinct functional properties. Some of these cells have been suggested to exert cardioprotective actions [35]; others may contribute to phagocytosis of dead cells and repair of the infarcted heart [37], whereas some subsets may exert pro-inflammatory [38], fibrogenic, or angiogenic actions. Much like remodeling mouse hearts, human failing hearts also contain CCR2+ and CCR2-negative macrophage subsets with distinct functional properties [39]. Single cell transcriptomic analysis may contribute to identification of specific fibroblast-activating macrophages in remodeling hearts.

Whether in addition to its effects on monocytes and macrophages, CCL2 induces cardiac fibrosis through actions on other cell types remains poorly documented. Lymphocytes have been implicated in the pathogenesis of cardiac fibrosis [40]; however, the potential involvement of CCL2 in their recruitment remains unknown. Although some studies have suggested that CCL2 may directly stimulate fibroblast activation [41], in mouse cardiac fibroblasts, CCL2 stimulation had no significant effects on profibrotic gene expression profile and proliferative activity [27].

The potential role of other CC chemokines in cardiac fibrosis—Induction of several other members of the CC chemokine subfamily (including CCL3, CCL4, CCL5, CCL12 and CCL24) has been reported in experimental models of cardiac fibrosis [42],[43],[44,45]. These chemokines may recruit distinct subpopulations of leukocytes, thus contributing to the pathogenesis of cardiac fibrosis. CCL5 and CCL3 may stimulate fibrosis through recruitment of monocytes and lymphocytes expressing the CCR5 receptor. In the ischemic myocardium, CCL5 was found to form heteromers with neutrophil-derived α -defensin, that bind to CCR5 mediating monocyte recruitment [46]. CCL5 neutralization in a model of myocardial infarction attenuated collagen deposition; however the effects on fibrotic remodeling were indirect, related to attenuated infarct size due to reduced inflammatory injury [47]. Other studies have suggested that CC chemokine-induced leukocyte infiltration may also play a role in suppression of post-infarction inflammation through recruitment of anti-inflammatory monocyte and lymphocyte subsets. In a model of

myocardial infarction, CCR5 was implicated in recruitment of regulatory T cells in the infarcted myocardium, suppressing inflammation and attenuating adverse matrix remodeling [48],[49]. Evidence suggesting direct effects of CCR5 ligands in non-infarctive cardiac fibrosis is lacking. In a model of hypertension induced through administration of desoxycorticosterone acetate (DOCA) and angiotensin II, global loss of CCR5 did not affect myocardial fibrosis [50].

CCL24 has been implicated in activation of fibrogenic pathways in the lung and skin [51]; however, its potential role in cardiac fibrosis remains unknown. As a potent eosinophil chemoattractant, CCL24 may be involved in the pathogenesis of fibrosis in eosinophilic myocarditis [52]. The marked induction of CCL24 in regenerating neonatal hearts [53] adds an intriguing layer of complexity to the possible actions of this CC chemokine in myocardial disease.

CXC chemokines in cardiac fibrosis

ELR+ CXC chemokines

ELR+ CXC chemokines act predominantly as neutrophil chemoattractants, signaling through the CXCR1 and CXCR2 receptors. CXCL8/Interleukin-8 is the prototypical ELR+ CXC chemokine in humans and acts as a potent neutrophil chemoattractant, binding CXCR1 with high affinity. In contrast, rodents lack a CXCL8 homologue, but have several ELR+ CXC chemokines with similar functional properties. In addition to their role in neutrophil recruitment, ELR+ CXC chemokines have also been suggested to play a role in angiogenesis [54] and fibrosis. Several recent investigations have demonstrated that disruption of CXCR2 signaling may attenuate cardiac fibrosis, presumably through attenuation of leukocyte infiltration. CXCL1 and CXCL2 are upregulated in spontaneously hypertensive rat hearts, and CXCR2 inhibition attenuates cardiac fibrosis, hypertrophy and dysfunction [55]. However, the fibrogenic and pro-hypertrophic actions of CXCR2 may be indirect, involving effects on blood pressure regulation. CXCL1, one of the CXCR2 ligands has been reported to contribute to the development of angiotensin-induced cardiac fibrosis [23]. The fibrogenic effects of CXCR2 ligands have been attributed to recruitment of fibrogenic monocyte subpopulations [23],[56]. Neutrophils, may also contribute to the fibrogenic actions of ELR+ CXC chemokines through secretion of proteases that generate fibrogenic matrix fragments, or through release of fibrogenic growth factors and cytokines. Neutrophils can also release their decondensed chromatin and form large extracellular DNA networks, called neutrophil extracellular traps (NETs). NETosis has been implicated in fibrogenic activation in the heart and other organs [57],[58],[59]. However, considering the short life span of neutrophils in the injured myocardium, their relative role as cellular effectors of fibrosis is unclear.

CXCR3 ligands: the role of CXCL10

The CXCR3 ligands (CXCL9, CXCL10 and CXCL11) are the best characterized group of ELR-negative CXC chemokines. These chemokines do not stimulate neutrophil chemotaxis, but have been implicated in recruitment of lymphocyte subsets. Moreover, CXCL10 has been suggested to exert direct actions on fibroblasts and endothelial cells that may have important implications in the regulation of cardiac fibrosis. Evidence in both large animal

models and rodents suggests that CXCL10/interferon- γ -inducible protein (IP)-10 is consistently induced following cardiac injury [60],[61]. Global loss-of-function studies in mice suggested that CXCL10 may exert anti-fibrotic actions. CXCL10-mediated inhibition of fibrosis may involve recruitment of anti-fibrotic leukocyte subpopulations, or direct deactivating effects on cardiac fibroblasts [60],[61]. In vitro experiments in cardiac fibroblasts showed that CXCL10 inhibits growth-factor-mediated fibroblast migration [61], through interactions with proteoglycans that were independent of CXCR3 [62].

CXCL4/platelet factor (PF)-4 has also been implicated in cardiac remodeling [63] through effects that may involve, at least in part, interactions with CXCR3 [64]. Exogenous infusion of CXCL4 perturbed repair of the infarcted heart, inhibiting macrophage phagocytosis and increasing MMP levels [63]. Unfortunately, very limited information is available on the role of endogenous CXCL4 in fibrotic remodeling of the heart. Pharmacologic inhibition experiments supported the notion that heterophilic interactions between CXCL4 and CCL5 may contribute to NET formation, accentuating ischemic inflammatory injury [65].

CXCL12/SDF-1

CXCL12/SDF-1 is a multifunctional ELR-negative chemokine with a critical role in cardiovascular development [66] and in angiogenesis [67,68]. CXCL12 is induced following myocardial injury, and has been suggested to play an important role in regulation of cardiomyocyte survival, inflammation and neovessel formation in healing infarcts [69],[70]. A growing body of evidence suggests that CXCL12 may be implicated in the pathogenesis of fibrosis in several different organs. Several studies have suggested that CXCL12 may exert fibrogenic actions through activation of its main receptor, CXCR4. CXCR4 inhibition attenuated cardiac fibrosis in a genetic model of murine cardiomyopathy due to cardiac-specific overexpression of the stress kinase MSt1 [71], and in models of diabetic fibrotic cardiomyopathy [72] and cardiorenal syndrome [73]. The cellular basis for the fibrogenic actions of CXCL12 remains poorly understood. CXCL12-induced fibrosis has been attributed to direct effects on fibroblast migration, to recruitment of fibroblast progenitors [74], or to activation of fibrogenic macrophages [75]. In vitro studies suggest direct activating effects of CXCL12 on fibroblasts. CXCL12 stimulation promotes proliferation and induces collagen synthesis in cardiac fibroblasts [76]. It has been suggested that CXCR4-mediated activation of a migratory phenotype in cardiac fibroblasts may not necessarily require CXCL12, but may also involve chemokine-independent interactions of the receptor with high-mobility group box-1 (HMGB1) [77], a DAMP released in the injured myocardium. On the other hand, some CXCL12 actions may be CXCR4-independent, involving the CXCR7 receptor. In a model of cardiac fibrosis induced through isoproterenol infusion, administration of a CXCR7 inhibitor attenuated cardiac fibrosis [78].

CX3CL1/Fractalkine

The CX3C chemokine CX3CL1/fractalkine is rapidly released following myocardial injury [79], and chemoattracts monocytes/macrophages expressing the CX3CR1 receptor. Considering the involvement of macrophages in tissue fibrosis, an important role for CX3CL1 in fibrotic remodeling has been suggested. However, in vivo studies investigating

the role of the CX3CL1/CX3CR1 axis in fibrosis have produced conflicting results. In a model of hepatic fibrosis CX3CL1/CX3CR1 signaling was found to inhibit macrophage-driven fibrogenesis [80]. In contrast, studies in models of renal fibrosis suggested pro-fibrotic actions of the CX3CL1/CX3CR1 axis [81]. Although CX3CR1+ macrophages are abundant in the infarcted and remodeling myocardium [82], the role of CX3CL1/CX3CR1 in cardiac fibrosis has not been systematically studied. In a model of viral myocarditis, global loss of CX3CR1 accentuated inflammation and increased fibrosis [83]; however, the cellular basis for these effects is unclear. In experimental models of heart failure induced through myocardial infarction or left ventricular pressure overload, CX3CL1 was found to promote dysfunction. These detrimental actions were attributed to effects on cardiomyocyte function and fibroblast phenotype [84]. Moreover, in a complex model of unilateral nephrectomy followed by angiotensin II infusion, loss of CX3CR1 did not affect myocardial fibrosis [85].

Chemokines as therapeutic targets in cardiac fibrosis

Considering their role in tissue inflammation and fibrosis, several members of the chemokine family are attractive therapeutic targets in human fibrotic conditions. Early phase clinical trials using therapeutic approaches neutralizing the CCL2/CCR2 axis, or dual CCR2/CCR5 inhibition have suggested beneficial effects in patients with fibrosis-associated conditions, such as diabetic nephropathy [86],[87], HIV-associated fibrogenic activation [88] and non-alcoholic steatohepatitis [89],[90] (Table 2). In contrast, a phase 2 trial using an anti-CCL2 neutralizing antibody in patients with idiopathic pulmonary fibrosis did not show protective effects. Clinical studies examining the effects of chemokine inhibition in patients with cardiac fibrotic conditions have not been performed. A large amount of experimental evidence suggests that some members of the chemokine family may be attractive therapeutic targets for patients with heart failure associated with prominent inflammatory and fibrotic changes. CCL2/CCR2, the best studied chemokine/chemokine receptor pair in myocardial disease, has been implicated in the pathogenesis of both ischemic and non-ischemic cardiomyopathy, and may be a promising target for therapeutic intervention. However, a lot of additional information is needed to support the case for chemokine-based therapeutics in heart failure. Although emerging evidence supports the notion that inflammation may play an important role in heart failure with preserved ejection fraction (HFpEF) [91],[92] and experimental studies suggest that macrophages may contribute to diastolic dysfunction [93], whether CCL2 or other CC chemokines are involved in disease progression remains unknown. The pathophysiologic heterogeneity of human HFpEF that cannot be recapitulated by any animal model is a major challenge for successful clinical translation. Therapeutic implementation of chemokine targeting approaches will require identification of heart failure patients with prominent chemokine responses that may be causally involved in progression of adverse remodeling.

Moreover, chemokine targeting in heart failure patients may carry significant risks, related to the need for prolonged inhibition of pathways involved in responses to injury and repair. Some members of the chemokine family, including CCL2, have also been implicated in arteriogenesis and may play a role in formation of collateral vessels in patients with chronic ischemic heart disease [94]. Other chemokines, such as CXCL12 have been suggested to exert pro-survival actions on cardiomyocytes [95], while recruiting angiogenic progenitors

and promoting angiogenesis [96]. Thus, in some cases the benefits of any anti-fibrotic effects of chemokine inhibition may be outweighed by the abrogation of important protective and reparative actions.

Design of therapeutic strategies targeting the chemokine system should also carefully consider and exploit the temporal and spatial patterns of chemokine induction and activity following myocardial injury (Figure 2). Following myocardial infarction, the rapid and intense upregulation of pro-inflammatory CC and CXC chemokines in the infarct plays an important role in reparative fibrosis by recruiting activated monocytes, activating phagocytic macrophages and promoting growth factors expression and release. As professional phagocytes clear the infarct from dead cells and matrix debris, the inflammatory response in the infarct zone is suppressed; this is a crucial event for cardiac repair. However, in large infarcts, extensive loss of contractile cardiomyocytes results in profound hemodynamic perturbations, chronic activation of neurohumoral pathways and a low-grade chemokine-driven inflammatory reaction in the non-infarcted remodeling myocardium [97],[98]. These inflammatory changes may play a major role in the pathogenesis of chronic post-infarction heart failure.

Conclusions:

Our understanding of the role of the chemokines in fibrotic remodeling of the heart remains limited. Future studies need to focus on identification of specific chemokine/chemokine receptor pairs that regulate recruitment of fibrogenic leukocytes in the injured myocardium, on dissection of leukocyte-derived mediators responsible for chemokine-driven fibrosis, and on the potential role of direct actions of chemokine family members on fibroblasts. Moreover, we need to expand our knowledge on the patterns of expression and potential role of chemokines in human cardiac fibrosis. Targeting fibrogenic immune cells may hold promise as a therapeutic strategy in subpopulations of heart failure patients exhibiting prominent fibrotic responses.

Acknowledgments

SOURCES OF FUNDING: Dr Frangogiannis' laboratory is supported by National Institutes of Health grants R01 HL76246, R01 HL85440, and R01 HL149407, and by U.S. Department of Defense grants PR151029 and PR181464.

References

* of special interest

** of outstanding interest

1. Frangogiannis NG: Cardiac fibrosis: Cell biological mechanisms, molecular pathways and therapeutic opportunities. *Mol Aspects Med* 2019, 65:70–99.
2. Okyere AD, Tilley DG: Leukocyte-Dependent Regulation of Cardiac Fibrosis. *Front Physiol* 2020, 11:301.
3. Griffith JW, Sokol CL, Luster AD: Chemokines and chemokine receptors: positioning cells for host defense and immunity. *Annu Rev Immunol* 2014, 32:659–702.
4. Dobaczewski M, Frangogiannis NG: Chemokines and cardiac fibrosis. *Front Biosci (Schol Ed)* 2009, 1:391–405.

5. Roh YS, Seki E: Chemokines and Chemokine Receptors in the Development of NAFLD. *Adv Exp Med Biol* 2018, 1061:45–53.
6. Frangogiannis NG: Chemokines in the ischemic myocardium: from inflammation to fibrosis. *Inflamm Res* 2004, 53:585–595.
7. Humeres C, Frangogiannis NG: Fibroblasts in the Infarcted, Remodeling, and Failing Heart. *JACC Basic Transl Sci* 2019, 4:449–467.
8. Pakshir P, Noskovicova N, Lodyga M, Son DO, Schuster R, Goodwin A, Karvonen H, Hinz B: The myofibroblast at a glance. *J Cell Sci* 2020, 133.
9. Frangogiannis NG: Transforming Growth Factor (TGF)-beta in tissue fibrosis. *J Exp Med* 2020, 217:e20190103. <https://doi.org/20190110.20191084/jem.20190103>.
10. Wynn TA, Vannella KM: Macrophages in Tissue Repair, Regeneration, and Fibrosis. *Immunity* 2016, 44:450–462.
11. Blanton RM, Carrillo-Salinas FJ, Alcaide P: T-cell recruitment to the heart: friendly guests or unwelcome visitors? *Am J Physiol Heart Circ Physiol* 2019, 317:H124–H140.
12. Levick SP, Melendez GC, Plante E, McLarty JL, Brower GL, Janicki JS: Cardiac mast cells: the centrepiece in adverse myocardial remodelling. *Cardiovasc Res* 2012, 89:12–19.
13. Frangogiannis NG, Perrard JL, Mendoza LH, Burns AR, Lindsey ML, Ballantyne CM, Michael LH, Smith CW, Entman ML: Stem cell factor induction is associated with mast cell accumulation after canine myocardial ischemia and reperfusion. *Circulation* 1998, 98:687–698.
14. Bucala R, Spiegel LA, Chesney J, Hogan M, Cerami A: Circulating fibrocytes define a new leukocyte subpopulation that mediates tissue repair. *Mol Med* 1994, 1:71–81.
15. Haider N, Bosca L, Zandbergen HR, Kovacic JC, Narula N, Gonzalez-Ramos S, Fernandez-Velasco M, Agrawal S, Paz-Garcia M, Gupta S, et al.: Transition of Macrophages to Fibroblast-Like Cells in Healing Myocardial Infarction. *J Am Coll Cardiol* 2019, 74:3124–3135.
16. Kanisicak O, Khalil H, Ivey MJ, Karch J, Maliken BD, Correll RN, Brody MJ, SC JL, Aronow BJ, Tallquist MD, et al.: Genetic lineage tracing defines myofibroblast origin and function in the injured heart. *Nat Commun* 2016, 7:12260.
17. Moore-Morris T, Cattaneo P, Guimaraes-Camboa N, Bogomolovas J, Cedenilla M, Banerjee I, Ricote M, Kisseleva T, Zhang L, Gu Y, et al.: Infarct Fibroblasts Do Not Derive From Bone Marrow Lineages. *Circ Res* 2018, 122:583–590.
18. Chen B, Frangogiannis NG: Chemokines in Myocardial Infarction. *J Cardiovasc Transl Res* 2020.
19. Dewald O, Frangogiannis NG, Zoerlein M, Duerr GD, Klemm C, Kneuferrmann P, Taffet G, Michael LH, Crapo JD, Welz A, et al.: Development of murine ischemic cardiomyopathy is associated with a transient inflammatory reaction and depends on reactive oxygen species. *Proc Natl Acad Sci U S A* 2003, 100:2700–2705.
20. Frangogiannis NG, Shimoni S, Chang SM, Ren G, Shan K, Aggeli C, Reardon MJ, Letsou GV, Espada R, Ramchandani M, et al.: Evidence for an active inflammatory process in the hibernating human myocardium. *Am J Pathol* 2002, 160:1425–1433.
21. Feng Y, Chen H, Cai J, Zou L, Yan D, Xu G, Li D, Chao W: Cardiac RNA induces inflammatory responses in cardiomyocytes and immune cells via Toll-like receptor 7 signaling. *J Biol Chem* 2015, 290:26688–26698.
22. Suetomi T, Miyamoto S, Brown JH: Inflammation in nonischemic heart disease: initiation by cardiomyocyte CaMKII and NLRP3 inflammasome signaling. *Am J Physiol Heart Circ Physiol* 2019, 317:H877–H890.
23. Wang L, Zhang YL, Lin QY, Liu Y, Guan XM, Ma XL, Cao HJ, Liu Y, Bai J, Xia YL, et al.: CXCL1-CXCR2 axis mediates angiotensin II-induced cardiac hypertrophy and remodelling through regulation of monocyte infiltration. *Eur Heart J* 2018, 39:1818–1831.
24. Suetomi T, Willeford A, Brand CS, Cho Y, Ross RS, Miyamoto S, Brown JH: Inflammation and NLRP3 Inflammasome Activation Initiated in Response to Pressure Overload by Ca(2+)/Calmodulin-Dependent Protein Kinase II delta Signaling in Cardiomyocytes Are Essential for Adverse Cardiac Remodeling. *Circulation* 2018, 138:2530–2544.
25. Willeford A, Suetomi T, Nickle A, Hoffman HM, Miyamoto S, Heller Brown J: CaMKIIdelta-mediated inflammatory gene expression and inflammasome activation in cardiomyocytes initiate inflammation and induce fibrosis. *JCI Insight* 2018, 3.

26. Stevenson MD, Canugovi C, Vendrov AE, Hayami T, Bowles DE, Krause KH, Madamanchi NR, Runge MS: NADPH Oxidase 4 Regulates Inflammation in Ischemic Heart Failure: Role of Soluble Epoxide Hydrolase. *Antioxid Redox Signal* 2019, 31:39–58.
27. Frangogiannis NG, Dewald O, Xia Y, Ren G, Haudek S, Leucker T, Kraemer D, Taffet G, Rollins BJ, Entman ML: Critical role of monocyte chemoattractant protein-1/CC chemokine ligand 2 in the pathogenesis of ischemic cardiomyopathy. *Circulation* 2007, 115:584–592.
28. Koyanagi M, Egashira K, Kitamoto S, Ni W, Shimokawa H, Takeya M, Yoshimura T, Takeshita A: Role of monocyte chemoattractant protein-1 in cardiovascular remodeling induced by chronic blockade of nitric oxide synthesis. *Circulation* 2000, 102:2243–2248.
29. Kuwahara F, Kai H, Tokuda K, Takeya M, Takeshita A, Egashira K, Imaizumi T: Hypertensive myocardial fibrosis and diastolic dysfunction: another model of inflammation? *Hypertension* 2004, 43:739–745.
30. Dewald O, Zymek P, Winkelmann K, Koerting A, Ren G, Abou-Khamis T, Michael LH, Rollins BJ, Entman ML, Frangogiannis NG: CCL2/Monocyte Chemoattractant Protein-1 regulates inflammatory responses critical to healing myocardial infarcts. *Circ Res* 2005, 96:881–889.
31. Tan X, Hu L, Shu Z, Chen L, Li X, Du M, Sun D, Mao X, Deng S, Huang K, et al.: Role of CCR2 in the Development of Streptozotocin-Treated Diabetic Cardiomyopathy. *Diabetes* 2019, 68:2063–2073.
32. Sakai N, Wada T, Furuichi K, Shimizu K, Kokubo S, Hara A, Yamahana J, Okumura T, Matsushima K, Yokoyama H, et al.: MCP-1/CCR2-dependent loop for fibrogenesis in human peripheral CD14-positive monocytes. *J Leukoc Biol* 2006, 79:555–563.
33. Patel B, Bansal SS, Ismahil MA, Hamid T, Rokosh G, Mack M, Prabhu SD: CCR2(+) Monocyte-Derived Infiltrating Macrophages Are Required for Adverse Cardiac Remodeling During Pressure Overload. *JACC Basic Transl Sci* 2018, 3:230–244.*This study suggests a critical role for CCR2+monocyte-derived macrophages in fibrosis and remodeling of the pressure-overloaded myocardium.
34. Epelman S, Lavine KJ, Beaudin AE, Sojka DK, Carrero JA, Calderon B, Brija T, Gautier EL, Ivanov S, Satpathy AT, et al.: Embryonic and Adult-Derived Resident Cardiac Macrophages Are Maintained through Distinct Mechanisms at Steady State and during Inflammation. *Immunity* 2014, 40:91–104.
35. Dick SA, Macklin JA, Nejat S, Momen A, Clemente-Casares X, Althagafi MG, Chen J, Kantores C, Hosseinzadeh S, Aronoff L, et al.: Self-renewing resident cardiac macrophages limit adverse remodeling following myocardial infarction. *Nat Immunol* 2019, 20:29–39.*A study documenting protective effects of the resident cardiac macrophage population following injury.
36. Heidt T, Courties G, Dutta P, Sager H, Sebas M, Iwamoto Y, Sun Y, Da Silva N, Panizzi P, van der Laan AM, et al.: Differential Contribution of Monocytes to Heart Macrophages in Steady-State and After Myocardial Infarction. *Circ Res* 2014.
37. Chen B, Huang S, Su Y, Wu YJ, Hanna A, Brickshawana A, Graff J, Frangogiannis NG: Macrophage Smad3 Protects the Infarcted Heart, Stimulating Phagocytosis and Regulating Inflammation. *Circ Res* 2019, 125:55–70.
38. Bajpai G, Bredemeyer A, Li W, Zaitsev K, Koenig AL, Lokshina I, Mohan J, Ivey B, Hsiao HM, Weinheimer C, et al.: Tissue Resident CCR2- and CCR2+ Cardiac Macrophages Differentially Orchestrate Monocyte Recruitment and Fate Specification Following Myocardial Injury. *Circ Res* 2019, 124:263–278.*A study suggesting distinct functional roles for CCR2+ and CCR2- resident cardiac macrophages following injury/
39. Bajpai G, Schneider C, Wong N, Bredemeyer A, Hulsmans M, Nahrendorf M, Epelman S, Kreisel D, Liu Y, Itoh A, et al.: The human heart contains distinct macrophage subsets with divergent origins and functions. *Nat Med* 2018, 24:1234–1245.**A seminal study identifying and characterizing CCR2+ and CCR2- macrophages in remodeling human hearts.
40. Nevers T, Salvador AM, Velazquez F, Ngwenyama N, Carrillo-Salinas FJ, Aronovitz M, Blanton RM, Alcaide P: Th1 effector T cells selectively orchestrate cardiac fibrosis in nonischemic heart failure. *J Exp Med* 2017, 214:3311–3329.
41. Kruglov EA, Nathanson RA, Nguyen T, Dranoff JA: Secretion of MCP-1/CCL2 by bile duct epithelia induces myofibroblastic transdifferentiation of portal fibroblasts. *Am J Physiol Gastrointest Liver Physiol* 2006, 290:G765–771.

42. Dewald O, Ren G, Duerr GD, Zoerlein M, Klemm C, Gersch C, Tincey S, Michael LH, Entman ML, Frangogiannis NG: Of mice and dogs: species-specific differences in the inflammatory response following myocardial infarction. *Am J Pathol* 2004, 164:665–677.
43. Lubos N, van der Gaag S, Gercek M, Kant S, Leube RE, Krusche CA: Inflammation shapes pathogenesis of murine arrhythmogenic cardiomyopathy. *Basic Res Cardiol* 2020, 115:42.
44. Ma Y, Chiao YA, Clark R, Flynn ER, Yabluchanskiy A, Ghasemi O, Zouein F, Lindsey ML, Jin YF: Deriving a cardiac ageing signature to reveal MMP-9-dependent inflammatory signalling in senescence. *Cardiovasc Res* 2015, 106:421–431.
45. Kaya Z, Goser S, Buss SJ, Leuschner F, Ottl R, Li J, Volkens M, Zittrich S, Pfitzer G, Rose NR, et al.: Identification of cardiac troponin I sequence motifs leading to heart failure by induction of myocardial inflammation and fibrosis. *Circulation* 2008, 118:2063–2072.
46. Alard JE, Ortega-Gomez A, Wichapong K, Bongiovanni D, Horckmans M, Megens RT, Leoni G, Ferraro B, Rossaint J, Paulin N, et al.: Recruitment of classical monocytes can be inhibited by disturbing heteromers of neutrophil HNP1 and platelet CCL5. *Sci Transl Med* 2015, 7:317ra196.
47. Montecucco F, Braunersreuther V, Lenglet S, Delattre BM, Pelli G, Buatois V, Guilhot F, Galan K, Vuilleumier N, Ferlin W, et al.: CC chemokine CCL5 plays a central role impacting infarct size and post-infarction heart failure in mice. *Eur Heart J* 2012, 33:1964–1974.
48. Dobaczewski M, Xia Y, Bujak M, Gonzalez-Quesada C, Frangogiannis NG: CCR5 signaling suppresses inflammation and reduces adverse remodeling of the infarcted heart, mediating recruitment of regulatory T cells. *Am J Pathol* 2010, 176:2177–2187.
49. Saxena A, Dobaczewski M, Rai V, Haque Z, Chen W, Li N, Frangogiannis NG: Regulatory T cells are recruited in the infarcted mouse myocardium and may modulate fibroblast phenotype and function. *Am J Physiol Heart Circ Physiol* 2014, 307:H1233–1242.
50. Krebs C, Fraune C, Schmidt-Haupt R, Turner JE, Panzer U, Quang MN, Tannapfel A, Velden J, Stahl RA, Wenzel UO: CCR5 deficiency does not reduce hypertensive end-organ damage in mice. *Am J Hypertens* 2012, 25:479–486.
51. Mor A, Segal Salto M, Katav A, Barashi N, Edelshtein V, Manetti M, Levi Y, George J, Matucci-Cerinic M: Blockade of CCL24 with a monoclonal antibody ameliorates experimental dermal and pulmonary fibrosis. *Ann Rheum Dis* 2019, 78:1260–1268.
52. Diny NL, Hou X, Barin JG, Chen G, Talor MV, Schaub J, Russell SD, Klingel K, Rose NR, Cihakova D: Macrophages and cardiac fibroblasts are the main producers of eotaxins and regulate eosinophil trafficking to the heart. *Eur J Immunol* 2016, 46:2749–2760.
53. Wang Z, Cui M, Shah AM, Ye W, Tan W, Min YL, Botten GA, Shelton JM, Liu N, Bassel-Duby R, et al.: Mechanistic basis of neonatal heart regeneration revealed by transcriptome and histone modification profiling. *Proc Natl Acad Sci U S A* 2019, 116:18455–18465.
54. Strieter RM, Polverini PJ, Kunkel SL, Arenberg DA, Burdick MD, Kasper J, Dzuiba J, Van Damme J, Walz A, Marriott D, et al.: The functional role of the ELR motif in CXC chemokine-mediated angiogenesis. *J Biol Chem* 1995, 270:27348–27357.
55. Zhang YL, Geng C, Yang J, Fang J, Yan X, Li PB, Zou LX, Chen C, Guo SB, Li HH, et al.: Chronic inhibition of chemokine receptor CXCR2 attenuates cardiac remodeling and dysfunction in spontaneously hypertensive rats. *Biochim Biophys Acta Mol Basis Dis* 2019, 1865:16551.
56. Zhang YL, Cao HJ, Han X, Teng F, Chen C, Yang J, Yan X, Li PB, Liu Y, Xia YL, et al.: Chemokine Receptor CXCR-2 Initiates Atrial Fibrillation by Triggering Monocyte Mobilization in Mice. *Hypertension* 2020, 76:381–392.
57. Martinod K, Witsch T, Erpenbeck L, Savchenko A, Hayashi H, Cherpokova D, Gallant M, Mauler M, Cifuni SM, Wagner DD: Peptidylarginine deiminase 4 promotes age-related organ fibrosis. *J Exp Med* 2017, 214:439–458.
58. Chrysanthopoulou A, Mitroulis I, Apostolidou E, Arelaki S, Mikroulis D, Konstantinidis T, Sivridis E, Koffa M, Giatromanolaki A, Boumpas DT, et al.: Neutrophil extracellular traps promote differentiation and function of fibroblasts. *J Pathol* 2014, 233:294–307.
59. Weckbach LT, Grabmaier U, Uhl A, Gess S, Boehm F, Zehrer A, Pick R, Salvermoser M, Czernak T, Pircher J, et al.: Midkine drives cardiac inflammation by promoting neutrophil trafficking and NETosis in myocarditis. *J Exp Med* 2019, 216:350–368.

60. Frangogiannis NG, Mendoza LH, Lewallen M, Michael LH, Smith CW, Entman ML: Induction and suppression of interferon-inducible protein 10 in reperfused myocardial infarcts may regulate angiogenesis. *FASEB J* 2001, 15:1428–1430.
61. Bujak M, Dobaczewski M, Gonzalez-Quesada C, Xia Y, Leucker T, Zymek P, Veeranna V, Tager AM, Luster AD, Frangogiannis NG: Induction of the CXC chemokine interferon-gamma-inducible protein 10 regulates the reparative response following myocardial infarction. *Circ Res* 2009, 105:973–983.
62. Saxena A, Bujak M, Frunza O, Dobaczewski M, Gonzalez-Quesada C, Lu B, Gerard C, Frangogiannis NG: CXCR3-independent actions of the CXC chemokine CXCL10 in the infarcted myocardium and in isolated cardiac fibroblasts are mediated through proteoglycans. *Cardiovasc Res* 2014, 103:217–227.
63. Lindsey ML, Jung M, Yabluchanskiy A, Cannon PL, Iyer RP, Flynn ER, DeLeon-Pennell KY, Valerio FM, Harrison CL, Ripplinger CM, et al.: Exogenous CXCL4 infusion inhibits macrophage phagocytosis by limiting CD36 signalling to enhance post-myocardial infarction cardiac dilation and mortality. *Cardiovasc Res* 2019, 115:395–408.
64. Mueller A, Meiser A, McDonagh EM, Fox JM, Petit SJ, Xanthou G, Williams TJ, Pease JE: CXCL4-induced migration of activated T lymphocytes is mediated by the chemokine receptor CXCR3. *J Leukoc Biol* 2008, 83:875–882.
65. Vajen T, Koenen RR, Werner I, Staudt M, Projahn D, Curaj A, Sonmez TT, Simsekylimaz S, Schumacher D, Mollmann J, et al.: Blocking CCL5-CXCL4 heteromerization preserves heart function after myocardial infarction by attenuating leukocyte recruitment and NETosis. *Sci Rep* 2018, 8:10647.
66. Nagasawa T, Hirota S, Tachibana K, Takakura N, Nishikawa S, Kitamura Y, Yoshida N, Kikutani H, Kishimoto T: Defects of B-cell lymphopoiesis and bone-marrow myelopoiesis in mice lacking the CXC chemokine PBSF/SDF-1. *Nature* 1996, 382:635–638.
67. Salvucci O, Yao L, Villalba S, Sajewicz A, Pittaluga S, Tosato G: Regulation of endothelial cell branching morphogenesis by endogenous chemokine stromal-derived factor-1. *Blood* 2002, 99:2703–2711.
68. Salcedo R, Wasserman K, Young HA, Grimm MC, Howard OM, Anver MR, Kleinman HK, Murphy WJ, Oppenheim JJ: Vascular endothelial growth factor and basic fibroblast growth factor induce expression of CXCR4 on human endothelial cells: In vivo neovascularization induced by stromal-derived factor-1alpha. *Am J Pathol* 1999, 154:1125–1135.
69. Doring Y, Pawig L, Weber C, Noels H: The CXCL12/CXCR4 chemokine ligand/receptor axis in cardiovascular disease. *Front Physiol* 2014, 5:212.
70. Penn MS, Pastore J, Miller T, Aras R: SDF-1 in myocardial repair. *Gene Ther* 2012, 19:583–587.
71. Chu PY, Joshi MS, Horlock D, Kiriazis H, Kaye DM: CXCR4 Antagonism Reduces Cardiac Fibrosis and Improves Cardiac Performance in Dilated Cardiomyopathy. *Front Pharmacol* 2019, 10:117.
72. Chu PY, Walder K, Horlock D, Williams D, Nelson E, Byrne M, Jandeleit-Dahm K, Zimmet P, Kaye DM: CXCR4 Antagonism Attenuates the Development of Diabetic Cardiac Fibrosis. *PLoS One* 2015, 10:e0133616.
73. Chu PY, Zatta A, Kiriazis H, Chin-Dusting J, Du XJ, Marshall T, Kaye DM: CXCR4 antagonism attenuates the cardiorenal consequences of mineralocorticoid excess. *Circ Heart Fail* 2011, 4:651–658.
74. Li X, Weng X, Shi H, Gao R, Wang P, Jia D, Zhang S, Dong Z, Sun X, Yang J, et al.: Acetaldehyde dehydrogenase 2 deficiency exacerbates cardiac fibrosis by promoting mobilization and homing of bone marrow fibroblast progenitor cells. *J Mol Cell Cardiol* 2019, 137:107–118.
75. Chu PY, Mariani J, Finch S, McMullen JR, Sadoshima J, Marshall T, Kaye DM: Bone marrow-derived cells contribute to fibrosis in the chronically failing heart. *Am J Pathol* 2010, 176:1735–1742.
76. Jackson EK, Zhang Y, Gillespie DD, Zhu X, Cheng D, Jackson TC: SDF-1alpha (Stromal Cell-Derived Factor 1alpha) Induces Cardiac Fibroblasts, Renal Microvascular Smooth Muscle Cells, and Glomerular Mesangial Cells to Proliferate, Cause Hypertrophy, and Produce Collagen. *J Am Heart Assoc* 2017, 6.

77. Di Maggio S, Milano G, De Marchis F, D'Ambrosio A, Bertolotti M, Palacios BS, Badi I, Sommariva E, Pompilio G, Capogrossi MC, et al.: Non-oxidizable HMGB1 induces cardiac fibroblasts migration via CXCR4 in a CXCL12-independent manner and worsens tissue remodeling after myocardial infarction. *Biochim Biophys Acta Mol Basis Dis* 2017, 1863:2693–2704.
78. Menhaji-Klotz E, Hesp KD, Londregan AT, Kalgutkar AS, Piotrowski DW, Boehm M, Song K, Ryder T, Beaumont K, Jones RM, et al.: Discovery of a Novel Small-Molecule Modulator of C-X-C Chemokine Receptor Type 7 as a Treatment for Cardiac Fibrosis. *J Med Chem* 2018, 61:3685–3696.
79. Boag SE, Das R, Shmeleva EV, Bagnall A, Egred M, Howard N, Bennaceur K, Zaman A, Keavney B, Spyridopoulos I: T lymphocytes and fractalkine contribute to myocardial ischemia/reperfusion injury in patients. *J Clin Invest* 2015, 125:3063–3076.
80. Karlmark KR, Zimmermann HW, Roderburg C, Gassler N, Wasmuth HE, Luedde T, Trautwein C, Tacke F: The fractalkine receptor CX(3)CR1 protects against liver fibrosis by controlling differentiation and survival of infiltrating hepatic monocytes. *Hepatology* 2010, 52:1769–1782.
81. Shimizu K, Furuichi K, Sakai N, Kitagawa K, Matsushima K, Mukaida N, Kaneko S, Wada T: Fractalkine and its receptor, CX3CR1, promote hypertensive interstitial fibrosis in the kidney. *Hypertens Res* 2011, 34:747–752.
82. Nahrendorf M, Swirski FK, Aikawa E, Stangenberg L, Wurdinger T, Figueiredo JL, Libby P, Weissleder R, Pittet MJ: The healing myocardium sequentially mobilizes two monocyte subsets with divergent and complementary functions. *J Exp Med* 2007, 204:3037–3047.
83. Muller I, Pappritz K, Savvatis K, Puhl K, Dong F, El-Shafeey M, Hamdani N, Hamann I, Noutsias M, Infante-Duarte C, et al.: CX3CR1 knockout aggravates Coxsackievirus B3-induced myocarditis. *PLoS One* 2017, 12:e0182643.
84. Xuan W, Liao Y, Chen B, Huang Q, Xu D, Liu Y, Bin J, Kitakaze M: Detrimental effect of fractalkine on myocardial ischaemia and heart failure. *Cardiovasc Res* 2011, 92:385–393.
85. Ahadzadeh E, Rosendahl A, Czesla D, Steffens P, Prussner L, Meyer-Schwesinger C, Wanner N, Paust HJ, Huber TB, Stahl RAK, et al.: The chemokine receptor CX3CR1 reduces renal injury in mice with angiotensin II-induced hypertension. *Am J Physiol Renal Physiol* 2018, 315:F1526–F1535.
86. de Zeeuw D, Bekker P, Henkel E, Hasslacher C, Gouni-Berthold I, Mehling H, Potarca A, Tesar V, Heerspink HJ, Schall TJ, et al.: The effect of CCR2 inhibitor CCX140-B on residual albuminuria in patients with type 2 diabetes and nephropathy: a randomised trial. *Lancet Diabetes Endocrinol* 2015, 3:687–696.
87. Menne J, Eulberg D, Beyer D, Baumann M, Saudek F, Valkusz Z, Wiecek A, Haller H, Emapticap Study G: C-C motif-ligand 2 inhibition with emapticap pegol (NOX-E36) in type 2 diabetic patients with albuminuria. *Nephrol Dial Transplant* 2017, 32:307–315.
88. Bowler S, Siriwardhana C, Mitchell BI, D'Antoni ML, Ogata-Arakaki D, Souza S, Yee R, Gangcuangco LMA, Chow DC, Ndhlovu LC, et al.: Cenicriviroc, a dual CCR2 and CCR5 antagonist leads to a reduction in plasma fibrotic biomarkers in persons living with HIV on antiretroviral therapy. *HIV Res Clin Pract* 2019, 20:123–129.
89. Friedman S, Sanyal A, Goodman Z, Lefebvre E, Gottwald M, Fischer L, Ratziu V: Efficacy and safety study of cenicriviroc for the treatment of non-alcoholic steatohepatitis in adult subjects with liver fibrosis: CENTAUR Phase 2b study design. *Contemp Clin Trials* 2016, 47:356–365.
90. Ratziu V, Sanyal A, Harrison SA, Wong VW, Francque S, Goodman Z, Aithal GP, Kowdley KV, Seyedkazemi S, Fischer L, et al.: Cenicriviroc Treatment for Adults with Nonalcoholic Steatohepatitis and Fibrosis: Final Analysis of the Phase 2b CENTAUR Study. *Hepatology* 2020, doi: [10.1002/hep.31108](https://doi.org/10.1002/hep.31108). Online ahead of print.
91. Schiattarella GG, Rodolico D, Hill JA: Metabolic Inflammation in Heart Failure with Preserved Ejection Fraction. *Cardiovasc Res* 2020.
92. Paulus WJ, Tschope C: A novel paradigm for heart failure with preserved ejection fraction: comorbidities drive myocardial dysfunction and remodeling through coronary microvascular endothelial inflammation. *J Am Coll Cardiol* 2013, 62:263–271.

93. Hulsmans M, Sager HB, Roh JD, Valero-Munoz M, Houstis NE, Iwamoto Y, Sun Y, Wilson RM, Wojtkiewicz G, Tricot B, et al.: Cardiac macrophages promote diastolic dysfunction. *J Exp Med* 2018, 215:423–440.*This study demonstrates an important role for cardiac macrophages in regulating diastolic function, thus supporting their potential involvement in the pathogenesis of HFpEF.
94. Hoefler IE, van Royen N, Buschmann IR, Piek JJ, Schaper W: Time course of arteriogenesis following femoral artery occlusion in the rabbit. *Cardiovasc Res* 2001, 49:609–617.
95. Saxena A, Fish JE, White MD, Yu S, Smyth JW, Shaw RM, DiMaio JM, Srivastava D: Stromal cell-derived factor-1alpha is cardioprotective after myocardial infarction. *Circulation* 2008, 117:2224–2231.
96. Kanki S, Segers VF, Wu W, Kakkar R, Gannon J, Sys SU, Sandrasagra A, Lee RT: Stromal cell-derived factor-1 retention and cardioprotection for ischemic myocardium. *Circ Heart Fail* 2011, 4:509–518.
97. Sager HB, Hulsmans M, Lavine KJ, Moreira MB, Heidt T, Courties G, Sun Y, Iwamoto Y, Tricot B, Khan OF, et al.: Proliferation and Recruitment Contribute to Myocardial Macrophage Expansion in Chronic Heart Failure. *Circ Res* 2016, 119:853–864.
98. Bansal SS, Ismahil MA, Goel M, Zhou G, Rokosh G, Hamid T, Prabhu SD: Dysfunctional and Proinflammatory Regulatory T-Lymphocytes Are Essential for Adverse Cardiac Remodeling in Ischemic Cardiomyopathy. *Circulation* 2019, 139:206–221.
99. Toyozaki T, Saito T, Shiraishi H, Tsukamoto Y, Takano H, Nagai T, Hiroshima K, Ohwada H, Ishiyama S, Hiroe M: Macrophage inflammatory protein-1alpha relates to the recruitment of inflammatory cells in myosin-induced autoimmune myocarditis in rats. *Lab Invest* 2001, 81:929–936.
100. Goser S, Ottl R, Brodner A, Dengler TJ, Torzewski J, Egashira K, Rose NR, Katus HA, Kaya Z: Critical role for monocyte chemoattractant protein-1 and macrophage inflammatory protein-1alpha in induction of experimental autoimmune myocarditis and effective anti-monocyte chemoattractant protein-1 gene therapy. *Circulation* 2005, 112:3400–3407.
101. Cook DN, Beck MA, Coffman TM, Kirby SL, Sheridan JF, Pragnell IB, Smithies O: Requirement of MIP-1 alpha for an inflammatory response to viral infection. *Science* 1995, 269:1583–1585.
102. Kukielka GL, Smith CW, LaRosa GJ, Manning AM, Mendoza LH, Daly TJ, Hughes BJ, Youker KA, Hawkins HK, Michael LH, et al.: Interleukin-8 gene induction in the myocardium after ischemia and reperfusion in vivo. *J Clin Invest* 1995, 95:89–103.
103. Ivey CL, Williams FM, Collins PD, Jose PJ, Williams TJ: Neutrophil chemoattractants generated in two phases during reperfusion of ischemic myocardium in the rabbit. Evidence for a role for C5a and interleukin-8. *J Clin Invest* 1995, 95:2720–2728.
104. Segret A, Rucker-Martin C, Pavoine C, Flavigny J, Deroubaix E, Chatel MA, Lombet A, Renaud JF: Structural localization and expression of CXCL12 and CXCR4 in rat heart and isolated cardiac myocytes. *J Histochem Cytochem* 2007, 55:141–150.
105. Ble A, Mosca M, Di Loreto G, Guglielmotti A, Biondi G, Bombardieri S, Remuzzi G, Ruggenenti P: Antiproteinuric effect of chemokine C-C motif ligand 2 inhibition in subjects with acute proliferative lupus nephritis. *Am J Nephrol* 2011, 34:367–372.
106. Raghu G, Martinez FJ, Brown KK, Costabel U, Cottin V, Wells AU, Lancaster L, Gibson KF, Haddad T, Agarwal P, et al.: CC-chemokine ligand 2 inhibition in idiopathic pulmonary fibrosis: a phase 2 trial of carlumab. *Eur Respir J* 2015, 46:1740–1750.
107. Sherman KE, Abdel-Hameed E, Rouster SD, Shata MTM, Blackard JT, Safaie P, Kroner B, Preiss L, Horn PS, Kottlilil S: Improvement in Hepatic Fibrosis Biomarkers Associated With Chemokine Receptor Inactivation Through Mutation or Therapeutic Blockade. *Clin Infect Dis* 2019, 68:1911–1918.

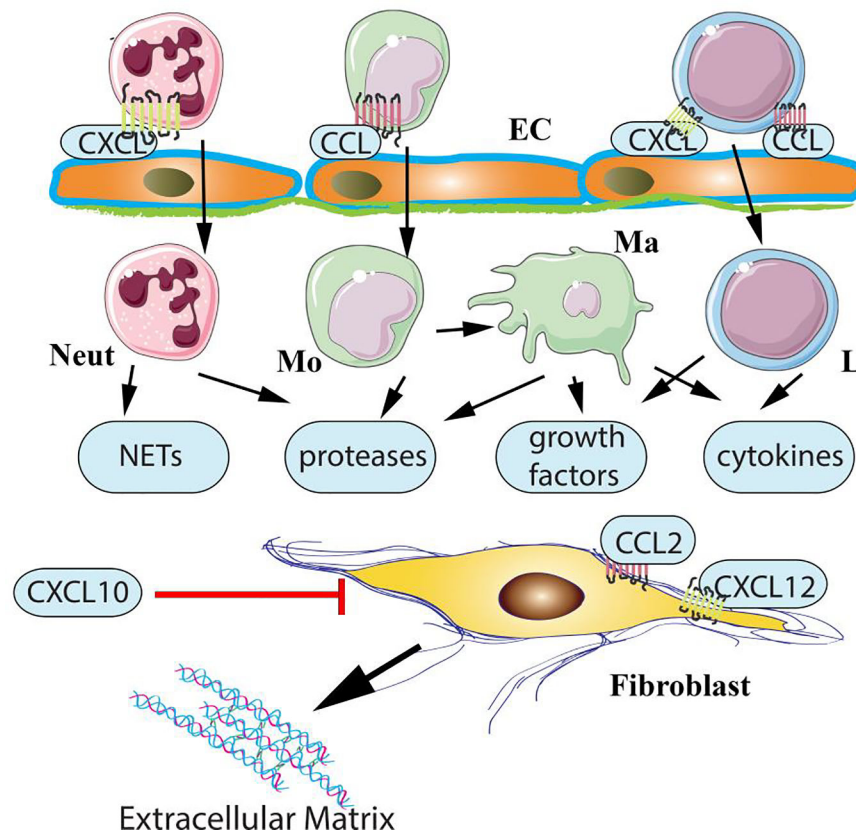


Figure 1: Chemokine actions in cardiac fibrosis.

Both CC (CCL) and CXC (CXCL) chemokines have been implicated in the pathogenesis of cardiac fibrosis. CC chemokines, such as CCL2, may promote fibrosis through recruitment of fibrogenic monocytes and activation of macrophages that produce growth factors and cytokines. CXC chemokines containing the ELR motif may promote fibrosis by recruiting neutrophils. Activated neutrophils may stimulate fibroblasts by generating neutrophil extracellular traps (NETs) or by secreting proteases and growth factors. Effects of ELR+ CXC chemokines on recruitment of fibrogenic mononuclear cells have also been suggested. Both CC and CXC chemokines may be involved in chemoattraction of lymphocytes with pro-fibrotic properties. Although the effects of chemokines in regulation of fibrosis are generally attributed to leukocyte recruitment, direct actions of some members of the family on fibroblasts cannot be excluded. The CXCR3 ligand CXCL10 exerts anti-fibrotic actions, inhibiting fibroblast migration through CXCR3-independent effects that may involve proteoglycans (Neut, neutrophil; Mo, monocyte; Ma, macrophage; L, lymphocyte; EC, endothelial cells).

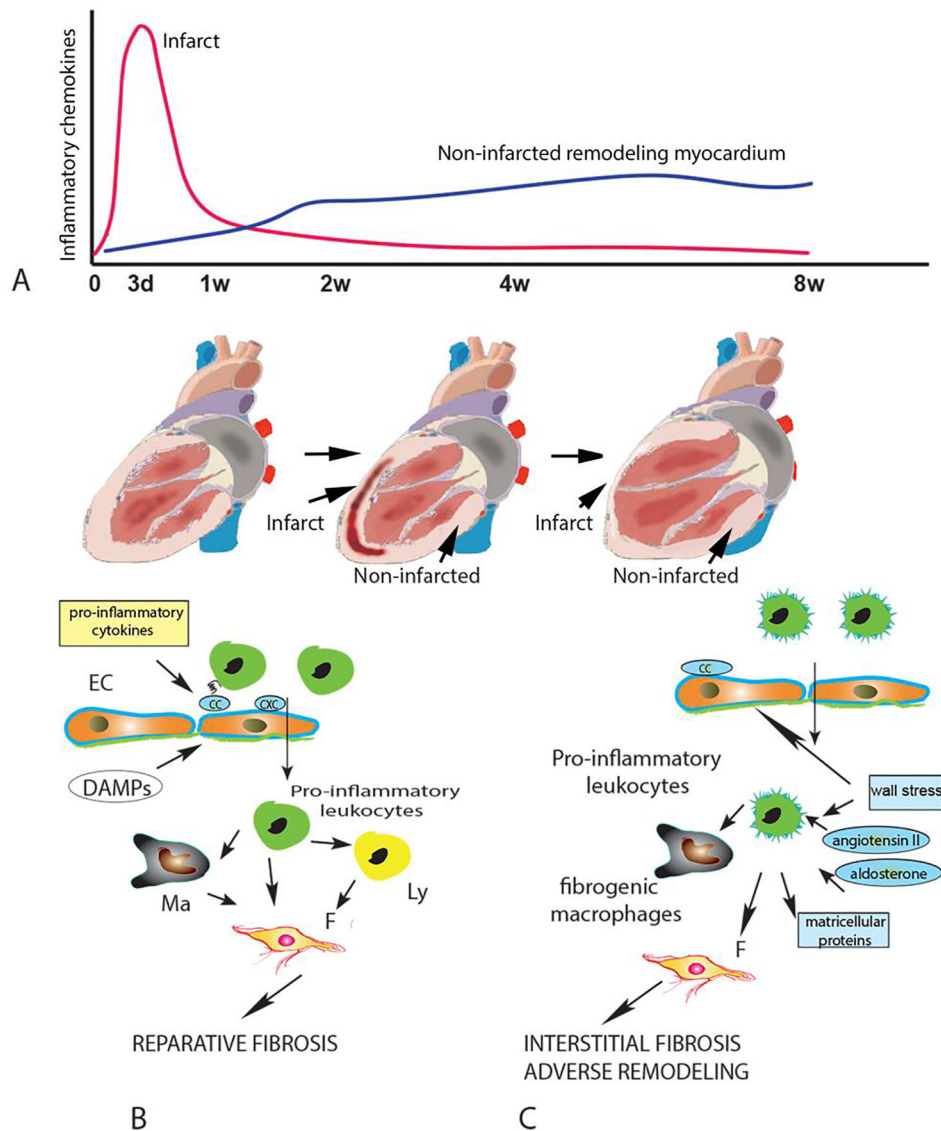


Figure 2: The spatiotemporal dynamics of chemokine actions in cardiac repair and post-infarction heart failure.

A. Following myocardial infarction, release of damage-associated molecular patterns (DAMPs) by dying cardiomyocytes and degraded extracellular matrix rapidly stimulates marked upregulation of pro-inflammatory CC and CXC chemokines in the infarct zone. As macrophages (Ma) clear the infarct from dead cells and matrix debris, the chemokine response is suppressed. However, in large infarcts, the profound hemodynamic perturbations caused by massive loss of contractile cardiomyocytes causes a low-grade chronic upregulation of pro-inflammatory chemokines in the non-infarcted myocardium. B. In the infarct, early induction of chemokines recruits pro-inflammatory leukocytes, resulting in expansion of phagocytic macrophages and fibroblast activation. The early chemokine response is important for reparative fibrosis. C. In the chronic remodeling phase, high intraventricular pressures increase wall stress and trigger neurohumoral activation, promoting low-level chemokine induction, followed by recruitment and activation of

fibrogenic monocytes and macrophages that may cause interstitial fibrosis, contributing to the pathogenesis of adverse remodeling and post-infarction heart failure. EC, endothelial cell; Ly, lymphocyte.

Author Manuscript

Author Manuscript

Author Manuscript

Author Manuscript

Table 1:

Chemokines in cardiac fibrosis

Chemokine	Chemokine receptors	Cellular source in models of cardiac fibrosis	Cellular targets and effects	References
CCL2	CCR2, CCR4	Macrophages, endothelial cells and fibroblasts have been reported as major sources of CCL2 in remodeling hearts. CCL2 upregulation in stressed and injured cardiomyocytes has also been demonstrated.	The fibrogenic actions of CCL2 likely involve recruitment of proinflammatory and fibrogenic CCR2+ monocytes and macrophages. May directly activate fibroblasts; however, the in vivo significance of such effects is unclear. Has been suggested to recruit fibroblast progenitors. May also promote arteriogenesis.	[27],[30],[32],[33],[24],[25]
CCL3	CCR1, CCR4, CCR5	In a model of myocarditis, macrophages and dendritic cells were the main source of CCL3.	May stimulate recruitment of pro-inflammatory leukocytes that may promote fibrosis. In myocarditis, CCL3 was found to play a critical role in virus-induced inflammation.	[99],[100],[101]
CCL4	CCR5, CCR8	CCL4 is upregulated in infarcted and remodeling hearts; however its cellular localization has not been systematically studied. Macrophages, endothelial cells and fibroblasts are likely cellular sources.	Although CCL4 is upregulated in injured and fibrotic hearts, its role in myocardial biology remains unknown.	[48]
CCL5	CCR5, CCR3, CCR1	Although many cell types (including macrophages, platelets, endothelial cells and fibroblasts) are known to produce CCL5, its cellular localization in fibrotic hearts has not been studied.	In a model of infarction, CCL5 was found to promote fibrosis, likely by accentuating inflammatory injury. May form heteromers with α -defensin, stimulating leukocyte recruitment. CCR5-mediated recruitment of anti-inflammatory leukocyte subsets has been suggested to restrain inflammation following infarction.	[47],[46],[48]
CCL24	CCR3	In myocarditis, macrophages were the main cellular source of CCL24. CCL24 levels were markedly increased in regenerating neonatal mouse hearts. However, its cellular localization has not been studied.	Although CCL24 has been implicated in fibrosis in other organs, whether it is involved in myocardial fibrosis is unknown. In eosinophilic myocarditis, CCL24 may promote fibrosis by recruiting eosinophils.	[53],[52]
CXCL8	CXCR1, CXCR2	Leukocytes, endothelial cells were found to be major sources of CXCL8 in infarcted and remodeling hearts. Fibroblasts and lymphocytes are also capable of secreting CXCL8.	May promote fibrosis by recruiting and activating neutrophils. Fibrogenic actions of CXCL8-activated neutrophils may involve formation of neutrophil extracellular traps (NETs). CXCL8 may also exert angiogenic actions.	[102],[103]
CXCL1 and other CXCR2 ligands	CXCR2	Macrophages, vascular cells, fibroblasts and mast cells can produce CXCR2 ligands.	CXCR2 ligands may promote fibrosis through recruitment of fibrogenic leukocyte subsets. CXCR2-mediated inflammation may indirectly promote fibrosis by increasing systemic blood pressure.	[23],[56],[55]
CXCL4	CXCR3	Platelets, macrophages	Although the involvement of CXCL4 in cardiac fibrosis has not been systematically studied, exogenous CXCL4 was found to increase MMP activity and to inhibit macrophage phagocytosis. CXCL4 may also be involved in lymphocyte recruitment.	[63], [65]
CXCL10	CXCR3, PG	Endothelial cells, leukocytes	CXCL10 exerts anti-fibrotic actions, inhibiting fibroblast migration and has also been suggested to have angiostatic properties. May also be involved in recruitment of lymphocytes.	[60],[61],[62]
CXCL12	CXCR4, CXCR7	Vascular cells, leukocytes, fibroblasts and cardiomyocytes	CXCL12 exerts a wide range of actions on all cell types involved in cardiac remodeling. Effects on inflammatory leukocyte recruitment, angiogenesis (through recruitment of progenitors), and cardiomyocyte survival have been reported. Fibrogenic actions may involve direct effects on	[71],[72],[73],[74],[75],[76],[77],[78],[104]

Chemokine	Chemokine receptors	Cellular source in models of cardiac fibrosis	Cellular targets and effects	References
			fibroblast migration, or activation of fibrogenic macrophages.	
CX3CL1	CX3CR1	Endothelial cells, macrophages	In a model of viral myocarditis, CX3CR1 was found to inhibit fibrosis; however, the cellular basis for these effects is unclear. In other tissues both fibrogenic and anti-fibrotic actions of CX3CL1 have been reported. Although macrophages are the most likely cellular targets of CX3CL1 in fibrotic and remodeling hearts, some experimental studies have suggested actions on many different cell types, including cardiomyocytes, fibroblasts and endothelial cells.	[83], [84]

Author Manuscript

Author Manuscript

Author Manuscript

Author Manuscript

Table 2:

Targeting the chemokines in human fibrosis-associated conditions

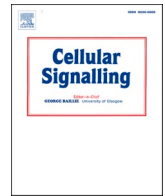
Condition	Anti-chemokine approach	Findings	Reference
Lupus nephritis	Inhibition of CCL2 (and other CC chemokines) through administration of bindarit	In a randomized double-blind clinical trial, treatment of acute lupus nephritis patients with bindarit reduced proteinuria. Fibrosis-related endpoints were not assessed.	[105]
Diabetic nephropathy (albuminuria)	Treatment with a CCR2 inhibitor (CCX140-B)	In a randomized double-blind placebo-controlled trial, CCR2 inhibition reduced proteinuria in patients with type 2 diabetes. Fibrosis-related endpoints were not assessed.	[86]
Diabetic nephropathy (albuminuria)	Treatment with emapticap pegol (NOX-E36), an L-aptamer that binds and inhibits CCL2.	In a phase IIa study, CCL2 inhibition was safe and well-tolerated and reduced the albumin to creatinine ratio. Fibrosis-related endpoints were not assessed.	[87]
Idiopathic pulmonary fibrosis (IPF)	Monoclonal anti-CCL2 neutralizing antibody (carlumab)	In a phase 2 trial, CCL2 inhibition did not affect forced vital capacity and the change in diffusing capacity in IPF patients.	[106]
HIV-infected patients	Oral CCR2/CCR5 antagonist (ceniciviroc)	In HIV-infected patients on stable antiretroviral therapy, ceniciviroc reduced plasma biomarkers of fibrosis	[88]
Hepatic fibrosis associated with HIV infection	Oral CCR2/CCR5 antagonist (ceniciviroc)	Ceniciviroc decreased the enhanced liver fibrosis index in HIV-infected patients.	[107]
Non-alcoholic steatohepatitis accompanied by liver fibrosis	Oral CCR2/CCR5 antagonist (ceniciviroc)	In a phase 2b randomized-controlled trial (CENTAUR) ceniciviroc was well tolerated and reduced fibrosis progression.	[89],[90]

Author Manuscript

Author Manuscript

Author Manuscript

Author Manuscript



Review

The role of Smad signaling cascades in cardiac fibrosis

Anis Hanna, Claudio Humeres, Nikolaos G. Frangogiannis*

The Wilf Family Cardiovascular Research Institute, Department of Medicine (Cardiology), Albert Einstein College of Medicine, Bronx, NY, USA

A B S T R A C T

Most myocardial pathologic conditions are associated with cardiac fibrosis, the expansion of the cardiac interstitium through deposition of extracellular matrix (ECM) proteins. Although replacement fibrosis plays a reparative role after myocardial infarction, excessive, unrestrained or dysregulated myocardial ECM deposition is associated with ventricular dysfunction, dysrhythmias and adverse prognosis in patients with heart failure. The members of the Transforming Growth Factor (TGF)- β superfamily are critical regulators of cardiac repair, remodeling and fibrosis. TGF- β s are released and activated in injured tissues, bind to their receptors and transduce signals in part through activation of cascades involving a family of intracellular effectors the receptor-activated Smads (R-Smads). This review manuscript summarizes our knowledge on the role of Smad signaling cascades in cardiac fibrosis. Smad3, the best-characterized member of the family plays a critical role in activation of a myofibroblast phenotype, stimulation of ECM synthesis, integrin expression and secretion of proteases and anti-proteases. In vivo, fibroblast Smad3 signaling is critically involved in scar organization and exerts matrix-preserving actions. Although Smad2 also regulates fibroblast function in vitro, its in vivo role in rodent models of cardiac fibrosis seems more limited. Very limited information is available on the potential involvement of the Smad1/5/8 cascade in cardiac fibrosis. Dissection of the cellular actions of Smads in cardiac fibrosis, and identification of patient subsets with overactive or dysregulated myocardial Smad-dependent fibrogenic responses are critical for design of successful therapeutic strategies in patients with fibrosis-associated heart failure.

1. Introduction

The term “cardiac fibrosis” describes the expansion of the cardiac interstitium due to net accumulation of extracellular matrix (ECM) proteins [1],[2]. Cardiac fibrosis is not a single disease entity, but rather a pathologic response that can be appropriate or inappropriate, depending on the context. For example, following myocardial infarction, massive loss of cardiomyocytes overwhelms the negligible regenerative capacity of the adult mammalian heart, and activates a fibrogenic response that ultimately results in scar formation. Despite the absence of contractile function, the collagen-based scar plays an important protective role, maintaining the structural integrity of the ventricle and preventing catastrophic mechanical complications, such as cardiac rupture [3],[4],[5],[6],[7]. Formation of scar following myocardial infarction is part of a reparative response and results in “replacement fibrosis”. In many other myocardial pathologic conditions, such as hypertensive heart disease, aortic stenosis, or diabetic cardiomyopathy, cardiac fibrosis develops insidiously in the absence of significant loss of cardiomyocytes and involves predominantly the interstitial and perivascular areas. These changes may contribute to the pathogenesis of heart failure by promoting both systolic and diastolic dysfunction and may be critically implicated in the development of heart failure with preserved ejection fraction (HFpEF) [8],[9].

The members of the TGF- β superfamily play a critical role in

regulation of cardiac fibrotic responses [10],[11]. In humans, the TGF- β superfamily is composed of 33 members. that can be subclassified into several subfamilies. The three TGF- β isoforms, TGF- β 1, β 2 and β 3 are the best studied members of the family in myocardial diseases [12]. The superfamily also includes the Growth differentiation factors (GDFs), the activins, the bone morphogenetic proteins (BMPs), the inhibins, the nodal and anti-Mullerian hormone proteins. Following myocardial injury, several members of the TGF- β superfamily are induced and/or activated and modulate the phenotype of both cardiomyocytes and non-cardiomyocytes [13],[14],[15],[16],[17]. The best characterized intracellular effectors of the TGF- β superfamily proteins are the Smads, a group of 8 structurally related proteins in humans with homologues that have been identified in both vertebrates and invertebrates. The founding member of the family is the product of the *Drosophila* gene *Mothers against decapentaplegic* (*Mad*), which was found to mediate signaling through the BMP homologue *decapentaplegic* (*Dpp*) [18]. In parallel, the *Sma* proteins were identified as *Mad* homologues in nematodes. Thus, the term “Smad”, (combining *Sma* and *Mad*) was coined to name the vertebrate members of this family [19]. From a functional perspective, the Smads are classified into 3 groups: a) the Receptor Activated Smads (R-Smads: Smad1, Smad2, Smad3, Smad5 and Smad8), responsible for TGF- β superfamily signaling, b) the common Smad (Co-Smad), Smad4, which binds to the R-Smads forming the signaling complex and c) the inhibitory Smads (I-Smads: Smad6 and Smad7), which are involved in

* Corresponding author at: Albert Einstein College of Medicine, 1300 Morris Park Avenue Forchheimer G46B, Bronx, NY 10461, USA.

E-mail address: nikolaos.frangogiannis@einstein.yu.edu (N.G. Frangogiannis).

negative regulation of R-Smad-mediated cascades [20].

Fibroblasts, immune cells, vascular cells and cardiomyocytes, the main cellular effectors of cardiac fibrosis are highly responsive to TGF- β s and activate Smad-dependent signaling cascades that play a critical role in regulation of the fibrogenic transcriptional program. This review manuscript discusses the role of Smad-dependent signaling cascades in cardiac fibrotic conditions.

2. The TGF- β signaling cascade: from the cell surface to the nucleus

The heart contains latent stores of TGF- β [21] that can be rapidly activated following injury [22] through interactions of the latent TGF- β complexes with proteases [23],[24], specialized matrix proteins (such as ED-A fibronectin and thrombospondin-1) [25],[26],[27] and cell surface integrins [28]. Moreover, in many fibrosis-associated myocardial conditions, infiltration with platelets capable of releasing large amounts of TGF- β from their granules [29], and de novo synthesis of TGF- β isoforms in cardiomyocytes, fibroblasts, immune cells and vascular cells [30],[17],[16], further increase the amounts of activatable TGF- β s in the site of injury. Several other members of the TGF- β superfamily are also upregulated in the injured and remodeling myocardium, including activins [31], BMPs [15] and GDFs [13].

All TGF- β superfamily members transduce signals through binding to characteristic combinations of type I and type II TGF- β receptors (T β Rs) [32]. Humans have 7 type I T β Rs, (also known as activin-like receptor kinase (ALK)1-7), and 5 type II T β Rs (T β RII, ActRII, ActRIIB, AMHRII and BMPRII) [33]. The three TGF- β isoforms (TGF- β 1, - β 2, and - β 3) act through a single type II receptor (T β RII) that may interact with ALK5 [34], or ALK1 (or both) depending on the cell type and the context [35], [36],[37],[38]. Some studies have suggested that ALK2 and ALK3 may

also mediate certain TGF- β -induced actions [39]. Other members of the superfamily use different TGF- β receptor combinations. Activins signal through ALK4, or ALK7 after binding to the ActRII or ActRIIB type II receptors. On the other hand, the members of the BMP family signal through a range of combinations, including one of the type I receptors ALK1 ALK2, ALK3 and ALK6 and one of the ActRII, ActRIIB and BMPRII type II receptors [40] [41].

Binding of a TGF- β superfamily member to its receptors triggers formation of a heterotetrameric complex, composed of two type I and two type II receptor molecules (Fig. 1). Subsequently, the phosphorylated type I receptor interacts with and phosphorylates members of the R-Smad family at the carboxyterminal Ser-Ser-X-Ser (SSXS) motif, activating a Smad-dependent (canonical) signaling cascade. Type I receptors have preferred Smad partners: ALK5, ALK4 and ALK7 phosphorylate Smad2 and Smad3, whereas ALK1, ALK2, ALK3 and ALK6 phosphorylate Smad1, Smad5 and Smad8 [42]. After phosphorylation by the type I receptor, the R-Smads dissociate from the receptor and form trimeric complexes with the common Smad, Smad4. These complexes can be either homomeric or heteromeric: one Smad4 molecule can bind to two molecules of the same R-Smad, or may form a mixed complex, composed of two different R-Smads (Smad2 and Smad3, or even Smad1 and Smad3). Subsequently, the R-Smad/Smad4 complex translocates to the nucleus, where it binds to Smad-binding elements or GC-rich sequences in the promoter regions of target genes, regulating their transcription [43].

The Smad cascades are modulated through the effects of accessory receptors (such as betaglycan and endoglin) [42], interactions with cytoplasmic proteins, and negative feedback pathways. Endoglin has been suggested to regulate the balance between Smad1/5 and Smad2/3 cascades in response to TGF- β s. It is predominantly expressed in endothelial cells and in activated fibroblasts, and negatively regulated ALK5-

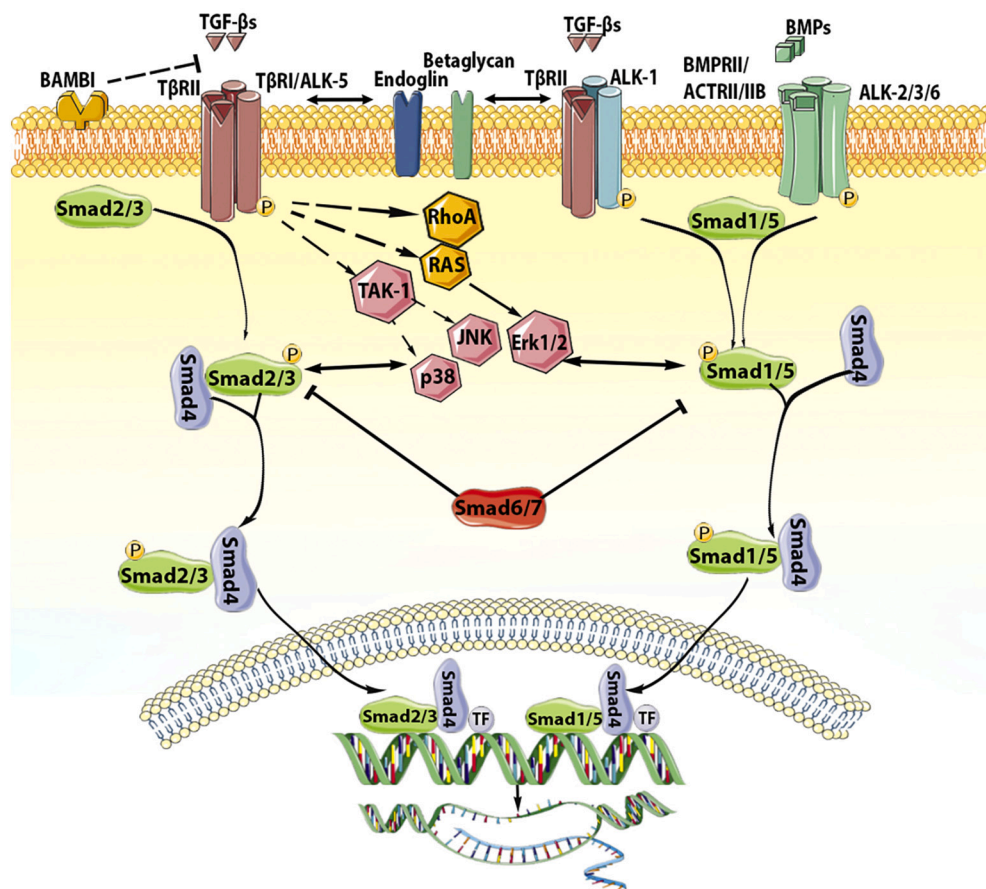


Fig. 1. Signaling cascades activated by the TGF- β superfamily. TGF- β superfamily ligands signal by binding to distinct combinations of two type II, and two type I receptors. TGF- β s bind T β RII inducing transphosphorylation of the type I receptor ALK5. Activated ALK5 phosphorylates the receptor-activated Smads (R-Smads) Smad2 and Smad3, which then form a heterotrimeric complex with the common Smad, Smad4, promoting the translocation of the Smad complex to the nucleus. Interactions between the Smad complex and transcriptional activators or repressors regulate transcription of target genes. In some cell types, TGF- β s may also act through another type I receptor, ALK1, stimulating Smad1/5/8 signaling. BMPs also bind to their specific type II receptors, subsequently activating type I receptors (ALK2, ALK3, ALK6) and phosphorylating Smad1/5. Smad1 and Smad5 then bind to Smad4 and translocate to the nucleus regulating transcription. In addition to the Smad-dependent signaling, TGF- β superfamily members may also signal through non-canonical Smad-independent cascades. The inhibitory Smads (Smad6 and Smad7) negatively regulate TGF- β superfamily cascades. Accessory receptors, such as endoglin and betaglycan, modulate TGF- β signaling. The cartoon was designed using Servier Medical Art (<https://smart.servier.com/>).

Table 1
In vitro effects of Smad signaling cascades in regulation of cardiac fibroblast phenotype

Species	Culture Condition	Smads manipulation	Role of Smad	Reference
Human	Collagen pads	Pharmacologic Smad3 inhibition with SIS3.	Smad3 mediates TGF- β 1-induced α -SMA and α 11 integrin expression.	[104]
Rat	Culture plates	Pharmacologic Smad3 inhibition with SIS3.	Smad3 mediates TGF- β 1-induced LOX expression.	[102]
Rat (neonatal)	Culture plates	Pharmacologic Smad3 inhibition with SIS3.	Smad3 mediates TGF β 1-induced cytoprotective and antiapoptotic effects in fibroblasts exposed to simulated ischemia/reperfusion	[106]
Rat (neonatal)	Culture plates	Pharmacologic Smad3 inhibition with SIS3.	Smad3 promotes cardiac myofibroblast conversion by mediating TGF- β 1-induced downregulation of FoxO3a.	[98]
Mouse	Culture plates	Smad2/Smad3 siRNA knockdown.	<ul style="list-style-type: none"> • Smad3 mediates baseline collagen I, collagen IV, fibronectin and TSP1 synthesis. • Smad2 mediates baseline collagen V, fibronectin, periostin and versican. • Smad3, but not Smad2, mediates α2 and α5 integrin expression. • Both Smad 2 and Smad3 stimulate α-SMA incorporation into stress fibers 	[109]
Mouse	Collagen pads/ Culture plates.	Smad2/Smad3 siRNA knockdown.	Smad3 mediates TGF- β 1-induced transcription of tissue transglutaminase.	[92]
Mouse	Collagen pads	Fibroblasts from global Smad3 null mice	Smad3 mediates TGF- β -induced collagen III and tenascin-C synthesis.	[103]
Mouse	Culture plates	Fibroblasts from global Smad3 null mice	Smad3 mediates TGF- β -induced TIMP1 upregulation and MMP3/MMP8 suppression, promoting a matrix-preserving phenotype.	[100]
Mouse	Collagen pads/ Culture plates	Fibroblasts from global Smad3 null mice.	<ul style="list-style-type: none"> • Smad3 accentuates contraction of fibroblast-populated lattices. • Smad3 mediates expression of Integrins α2, α5 and β3 in pad fibroblasts. • Smad3 mediates α-SMA synthesis only in plated fibroblasts. • Smad3 mediates anti-proliferative and promigratory effects of TGF-β. • Smad3 mediates contraction of fibroblast-populated lattices. • Smad3 stimulates CTGF and extracellular matrix gene synthesis. 	[93]
Mouse	Collagen pads/ Culture plates	Fibroblasts from global Smad3 null mice.	Smad3 mediates angiotensin II-induced upregulation of Collagen I, α -SMA, TNF- α , IL-1 β , and MCP-1.	[7]
Mouse	Culture plates	Fibroblasts from global Smad3 null mice.	Smad3 (but not Smad2) mediates TGF- β 1-induced fibroblast-populated pad contraction.	[94]
Mouse	Collagen pads/ Culture plates	Cre overexpression in fibroblasts from Smad2, Smad3 and Smad2/3 fl/fl mice to delete loxP-targeted Smads.	<ul style="list-style-type: none"> • Both Smad2 and Smad3 stimulate expression of extracellular matrix genes (<i>Col1a1</i>, <i>Col1a2</i>, <i>Col3a1</i>, <i>Fn1</i>, <i>Fbn1</i>, <i>Tnc</i>), matrix regulators (<i>Loxl2</i>, <i>Adam12</i>, <i>Adam30</i>, <i>Sparc</i>) and cell adhesion genes (<i>Itga2</i>, <i>Itga8</i>, <i>Itgb3</i>). 	[140]
Mouse	Collagen pads/ Culture plates	Cre overexpression in fibroblasts from Smad2, Smad3 and Smad2/3 fl/fl mice to delete loxP-targeted Smads.	<ul style="list-style-type: none"> • Both Smad2 and Smad3 stimulate expression of extracellular matrix genes (<i>Col1a1</i>, <i>Col1a2</i>, <i>Col3a1</i>, <i>Fn1</i>, <i>Fbn1</i>, <i>Tnc</i>), matrix regulators (<i>Loxl2</i>, <i>Adam12</i>, <i>Adam30</i>, <i>Sparc</i>) and cell adhesion genes (<i>Itga2</i>, <i>Itga8</i>, <i>Itgb3</i>). 	[101]

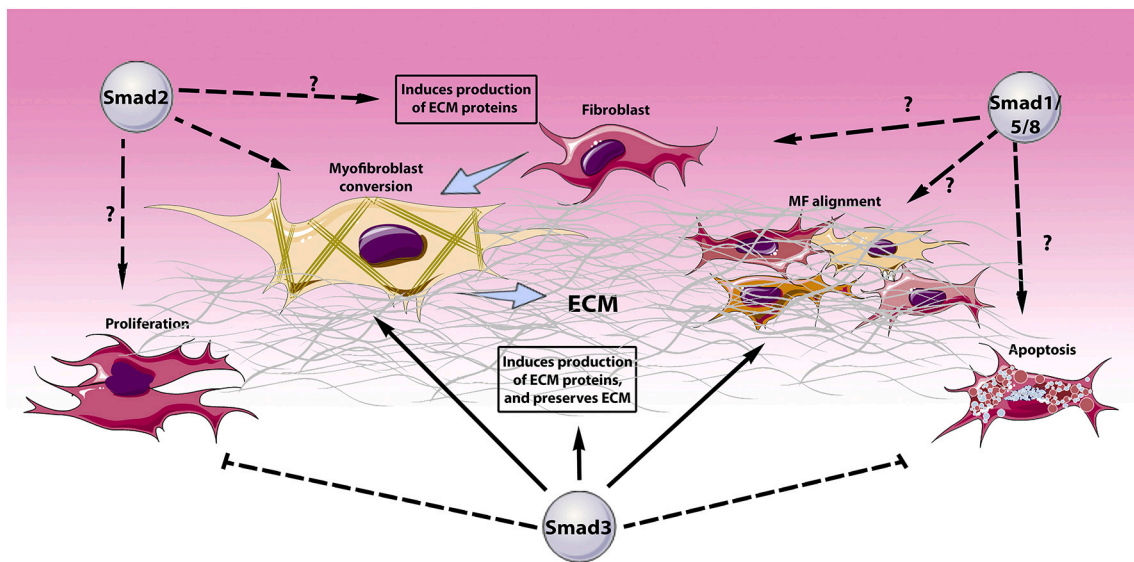


Fig. 2. Smad-mediated actions in cardiac fibroblasts.

The Smad proteins are key intracellular effectors of cascades involving TGF- β superfamily signaling. In cardiac fibroblasts, receptor-activated Smads regulate viability, proliferation, migration, transcriptional profile, phenotype and function. Smad3 activates fibroblast synthesis of extracellular matrix (ECM) proteins, while preserving the ECM by reducing protease-mediated matrix degradation. Smad3 also promotes the conversion of cardiac fibroblasts to myofibroblasts, and regulates myofibroblast alignment and formation of an organized scar by regulating integrin expression. Moreover, Smad3 tightly regulates cardiac fibroblast numbers by regulating proliferation and apoptosis. Smad2, has been reported to modulate fibroblast gene expression *in vitro*; however, its *in vivo* effects are more limited. The role of Smad1/5/8 in regulation of cardiac fibroblast phenotype is not known. The cartoon was designed using Servier Medical Art (<https://smart.servier.com/>).

Smad2/3 responses, while enhancing ALK1-Smad1/5/8 signaling [44], [45], [46]. Betaglycan, on the other hand can either activate or inhibit TGF- β signaling responses, depending on its expression levels, and on contextual factors [47], [48]. Several other transmembrane molecules (including CD44 and neuropilin-1) [49], [50] have been reported to act as non-selective co-receptors that may modulate TGF- β responses, while interacting with other growth factors and bioactive mediators.

Negative feedback mechanisms act to restrain overactive Smad signaling responses. At the receptor level, TGF- β -induced overexpression of the cell surface pseudo-receptor BAMBI (BMP and activin membrane-bound inhibitor) competes with T β RI for ligand binding [51], [52] and may suppress TGF- β /R-Smad responses [53]. The I-Smads Smad6 and Smad7 are induced following TGF- β stimulation and compete with R-smads for their binding to activated T β RI or Smad4, while also mediating T β RI degradation by recruitment of Smurf ubiquitin ligases [54]. Moreover, the nuclear co-repressors Ski and SnoN can bind to the translocated R-Smad/Smad4 complex promoting its degradation via Smurf2, or directly preventing transcription of Smad-target genes by recruiting histone deacetylases [55].

It should be emphasized that, in addition to Smad signaling cascades, TGF- β s also activate non-canonical signaling pathways, such as mitogen-activated protein kinase (MAPK), TGF- β -activated kinase 1 (TAK1), Rho GTPase, phosphatidylinositol3-kinase/AKT and focal adhesion kinases (FAK) [56] [57] [58]. These non-canonical pathways extensively interact with the Smad-mediated cascades and add additional layers of complexity to the biology of the TGF- β response [59], [60], [61]. Moreover, because these non-Smad cascades are also common downstream effector pathways for a wide range of mediators, dissection of their relative role in mediating effects of TGF- β superfamily members is challenging.

3. Can Smads be activated through mechanisms independent of TGF- β superfamily members?

Although the members of the TGF- β superfamily are considered the

main activators of Smad signaling, a growing body of evidence suggests that TGF- β -independent mechanisms may also contribute to Smad activation in certain cell types. In epithelial cell lines, viral infection has been suggested to activate Smads in a TGF- β -independent manner [62]. In macrophages, phagocytosis rapidly and consistently activated Smad3 in the absence of TGF- β secretion [30]. In NK cells, effects of Smad4 were found to be TGF- β -independent [63]. Experiments in renal mesangial cells suggested that advanced glycation end-products may activate R-Smads through a T β RRII-independent mechanism [64]. The significance of TGF- β -independent Smad signaling in cardiac fibrosis has not been documented. Although the fibrogenic actions of angiotensin II are associated with marked activation of Smad2 and Smad3, these effects are likely indirect and involve activation and induction of TGF- β [65], [66]. Thus, Smad activation in fibrotic cardiac conditions should be viewed as the result of induction and/or activation of TGF- β superfamily members.

4. The cellular basis of cardiac fibrosis

As the main matrix-producing cells, activated fibroblasts are the key cellular effectors of myocardial fibrosis, regardless of underlying etiology [67]. In many cardiac fibrotic conditions, fibroblasts convert to secretory myofibroblasts, expressing contractile proteins, such as α -smooth muscle actin (α -SMA), and producing large amounts of structural matrix proteins and fibrogenic matricellular macromolecules [68], [69], [70], [71]. Myofibroblasts contribute to the fibrotic response, not only by secreting matrix proteins, but also by producing proteases, such as matrix metalloproteinases (MMPs), and their inhibitors [72], [73], thus regulating matrix metabolism. Emerging evidence suggests that myofibroblast conversion is not required for fibrogenic activation. In a mouse model of type 2 diabetes, increased interstitial and perivascular collagen deposition was not associated with myofibroblast conversion [74]. Moreover, single cell transcriptomic analysis suggests that in remodeling hearts, high matrix gene synthesis in fibroblast subpopulations may occur in the absence of myofibroblast

transdifferentiation [75],[76]. Thus, alternative pathways of fibroblast activation may significantly contribute to cardiac fibrotic responses. The expansion and activation of fibroblasts and myofibroblasts in remodeling hearts may also involve several other cell types, including immune cells, cardiomyocytes and vascular cells. Macrophages and lymphocytes have been implicated in fibroblast activation through secretion of fibrogenic growth factors, cytokines and matricellular proteins [77], [78],[79],[80]. Mast cells may also contribute to fibrotic cardiac remodeling by releasing their fibrogenic granular contents [81],[82]. Under conditions of ischemic, mechanical or metabolic stress, cardiomyocytes are also capable of producing fibrogenic mediators and may contribute to fibroblast activation [83],[84]. Vascular endothelial cells can also produce bioactive mediators that stimulate fibroblasts. Several studies have suggested that endothelial cells may undergo endothelial-to-mesenchymal transition (EndMT) [85],[86],[87] thus directly participating in the myocardial fibrotic response. However, several publications using robust lineage tracing strategies in models of myocardial infarction and pressure overload have challenged the contribution of EndMT in cardiac fibrotic conditions [88],[89],[90].

The bulk of the experimental evidence suggests a major contribution of fibroblast Smad3 signaling in the cellular responses leading to myocardial fibrosis. In contrast, evidence supporting the role of other Smad proteins in fibroblast activation, and data on the potential involvement of Smad cascades in fibrogenic activation of other cell types

are limited.

5. Smad signaling cascades in fibroblasts

Activation of Smad2 and Smad3 has been extensively demonstrated in fibroblasts infiltrating fibrotic and remodeling hearts; in contrast, much less evidence is available on Smad1/5/8 activation [91],[17], [92]. In isolated cardiac fibroblasts TGF- β isoforms, but not BMPs, rapidly activate Smad2 and Smad3 signaling [91],[93]. In vitro, Smad3 is a central activating signal for cardiac fibroblasts that regulates several different functions (Table 1, Fig. 2) [10]. First, Smad3 induces myofibroblast conversion, increasing α -SMA expression and promoting its incorporation into stress fibers, the hallmark of myofibroblast transition [94],[95]. Smad3-mediated myofibroblast conversion involves direct effects on α -SMA transcription [94], [96], and may be accentuated by indirect actions, such as upregulation of fibronectin [7], a specialized matrix protein that stimulates acquisition of a myofibroblast phenotype [97] or downregulation of the transcription factor Forkhead box protein O3a (FoxO3a) [98], a signal that inhibits myofibroblast conversion [98,99]. Second, Smad3 stimulates the transcription of structural and matricellular extracellular matrix proteins, including type I and type III collagens, fibronectin, periostin and tenascin-C [7,94], [100], [101], and induces synthesis of matrix-crosslinking enzymes, such as lysyl-oxidase [102] and tissue transglutaminase [103]. Third, Smad3

Table 2
In vivo Effects of Smad Signaling in Cardiac Fibrosis

Model	Intervention	Role of Smad	Proposed Mechanism	Reference
Age-associated changes	Cardiomyocyte-specific Smad4 knockout mouse	Cardiomyocyte Smad4 protected the heart from age-associated hypertrophy and fibrosis.	Smad4-mediated protection of cardiomyocytes from injury, or suppression of fibrogenic signals.	[160]
Non-reperused MI	Myofibroblast-specific Smad2 or Smad3 loss.	Myofibroblast Smad3 a. Regulates organization of myofibroblast arrays. b. Mediates alignment of structural collagen fibers in the infarct Myofibroblast Smad2 does not play a major role in infarct healing.	Smad3-mediated integrin α 2 and α 5 activation.	[92]
Reperused MI	Global Smad3 null mice	Smad3 mediates cardiac collagen deposition in the infarct, the border zone and the remote remodeling.	Smad3-mediated synthesis of extracellular matrix genes and TIMPs.	[100]
Reperused MI	Global Smad3 null mice	Smad3 mediates deposition in the infarct, promotes myofibroblast conversion, but reduces myofibroblast proliferation. Myofibroblast Smad3:	Smad3-mediated anti-proliferative actions, α -SMA expression, induction of ECM proteins and CTGF.	[94]
Reperused and non-reperused MI	Myofibroblast-specific Smad3 loss	a. Prevents late cardiac rupture. b. Mediates formation and organization of well-aligned arrays of myofibroblasts.	Smad3-mediated activation of α 5 integrin-NOX2 axis.	[7]
Pressure overload (TAC)	Myofibroblast-specific Smad3 KO mice	Myofibroblast Smad3 preserves the extracellular matrix and attenuates collagen degradation	Smad3-mediated inhibition of collagenase (MMP3/8)-driven matrix degradation,	[93]
Pressure overload (TAC) Overexpression of a cardiomyocyte-specific, latency-resistant TGF- β mutant transgene.	Conditional Fibroblast and Myofibroblast-specific T β R1, T β R2, Smad2, Smad3 and Smad2/3 null mice.	Fibroblast Smad3, but not Smad2, mediates the fibrotic response in the pressure-overloaded heart and in a genetic model of cardiac TGF- β overactivation.	Smad3-mediated transcription of matrix genes.	[101]
Pressure overload (TAC).	Global Smad3 null mice	Smad3 mediates myocardial fibrosis	Smad3-mediated collagen synthesis.	[141]
Pressure overload	ALK5 inhibition using a small molecule inhibitor (SM16)	ALK5 mediates fibrosis and diastolic dysfunction.	Smad2/3-mediated expression of pro-fibrotic genes.	[142]
Angiotensin II infusion	Global Smad3 null mice	Smad 3 mediates angiotensin II-induced cardiac fibrosis.	Smad 3-mediated induction of TGF β 1, CTGF, collagen I/III and α -SMA.	[140]
db/db mouse	Obese diabetic db/db mice with partial or complete Smad3 loss.	Smad3 promotes fibrosis in obese diabetic mice.	Smad3-mediated suppression of MMP activity.	[133]
T. Cruzi infection	Pharmacological ALK5 inhibition with GW788388.	ALK5 mediates fibrosis.	Smad2/3-mediated matrix synthesis.	[165]

TAC, transverse aortic constriction; CTGF, connective tissue growth factor; ECM, extracellular matrix; MI, myocardial infarction; MMP, matrix metalloproteinase; NOX, NADPH Oxidase; SMA, smooth muscle actin; TIMP, Tissue inhibitor of metalloproteinases.

promotes a matrix-preserving phenotype characterized by suppressed synthesis and reduced activity of matrix metalloproteinase (MMP)-3 and MMP-8 and induction of anti-proteases, such as Tissue Inhibitor of Metalloproteinases (TIMP)-1 [93],[91]. Fourth, Smad3 stimulates fibroblast expression of α_2 , α_5 , β_3 and α_{11} integrins, facilitating interactions between the fibroblasts and the extracellular matrix; these interactions may be important for formation of an organized scar [7] [104]. Fifth, Smad3 may promote fibroblast migration and may enhance the capacity of fibroblasts to contract free-floating collagen lattices [94] (which is an indicator of fibroblast activation and is independent on myofibroblast conversion) [105]. Sixth, some studies have suggested that Smad3 may increase fibroblast viability under conditions of stress by exerting anti-apoptotic actions [106]. Finally, in addition to all these activating actions, Smad3 inhibits fibroblast proliferation, suggesting that Smad3-dependent myofibroblast activation is accompanied by tight regulation of the density of cardiac fibroblasts. The effects of Smad3 on cardiac fibroblasts are modulated through interactions with Smad-independent pathways [102],[7],[107], or through synergistic interactions with other fibrogenic transcription factors, such as scleraxis [108].

In vitro studies using isolated cardiac fibroblasts also suggest a significant role for Smad2 in activation of a fibrogenic transcriptional program (Fig. 2), albeit with less consistent effects on functional activity. siRNA knockdown experiments suggested that Smad2 enhances fibronectin, periostin and versican expression by unstimulated cardiac myofibroblasts [109]. Smad2 deletion experiments using Cre-expressing adenovirus transfection in Smad2 fl/fl cardiac fibroblasts suggested broad effects of Smad2 in TGF- β -induced extracellular matrix gene synthesis. Moreover, Smad2 knockdown was found to inhibit incorporation of α -SMA into myofibroblast stress fibers [92]. However, in contrast to the critical effects of Smad3, Smad2 did not mediate integrin synthesis in cardiac fibroblasts [92] and Smad2 loss did not affect fibroblast-mediated contraction of collagen lattices [96]. The distinct effects of Smad2 and Smad3 on fibroblast gene transcription and function may be due to distinct patterns of activation and nuclear translocation, or to different interactions with co-repressors and co-activators that may affect their transcriptional targets.

Very limited information is available regarding the role of the Smad1/5/8 pathway in cardiac fibroblast phenotype and function. Findings from studies examining the role of Smad1 signaling in fibroblast responses in other organs have produced conflicting results. In lung fibroblasts, Smad1 activation was found to be enhanced by the accessory receptor betaglycan and antagonized the stimulatory actions of ALK5/Smad3 signaling [110]. In contrast, in a mouse model of fibrosis due to forced expression of ALK5 that recapitulates features of scleroderma, activation of a fibrogenic program was surprisingly found to be dependent on Smad1 [111], and was attributed to a ALK5/ALK1/Smad1 axis. In cardiac fibroblasts, inhibition of matrix gene expression by BMP7 was attributed to activation of Smad1 signaling [112]. The significance of these observations in regulation of cardiac fibrotic responses in vivo is not known.

6. The inhibitory Smads as negative regulators of fibroblast function

The I-Smads, Smad6 and Smad7 lack the carboxyterminal SXS motif and cannot be phosphorylated upon binding to type 1 receptors, but act to inhibit signals transduced by TGF- β superfamily ligands through interactions with T β Rs or R-Smads [113]. Smad6 preferentially inhibits BMP responses, mediated through ALK3 and ALK6, whereas Smad7 inhibits both TGF- β and BMP-induced cascades [114]. Several molecular mechanisms have been proposed to explain the inhibitory effects of I-Smads on TGF- β superfamily signaling. First, I-Smads may directly associate with TGF- β receptors, inhibiting T β RI kinase activity, or simply interfering with R-Smad:T β RI binding [115],[116],[117]. Second, I-Smads may form a complex with the transmembrane pseudoreceptor

BAMBI, inhibiting T β R-driven R-Smad activation [52]. Third, I-Smads may interact with the Smurf1 and Smurf2 type E3 ligases promoting degradation of R-Smads [118],[119]. Fourth, I-Smads may interfere with formation of the R-Smad:Smad4 complex [120].

Whether Smad6 is involved in regulation of fibrosis has not been investigated. Smad7 on the other hand has been suggested to act as a negative regulatory signal that may inhibit myocardial fibrosis. In vitro, Smad7 synthesis is induced upon TGF- β stimulation and Smad7 overexpression in cardiac fibroblasts suppresses collagen synthesis [121], [122]. The in vivo role of Smad7 in regulation of cardiac fibrotic responses is supported predominantly through associative data. In models of ventricular remodeling, Smad7 induction may serve as a TGF- β -induced endogenous inhibitory signal that restrains fibrogenic activation [121],[123]. In contrast, in other pathologic conditions, such as atrial fibrillation, atrial fibrosis has been attributed to reduced Smad7 levels in response to neurohumoral activation [124]. Direct in vivo evidence documenting the role of endogenous Smad7 in regulation of fibroblast responses is lacking. Two published studies demonstrated increased cardiac fibrosis in a hypomorphic Smad7 mutant line in which exon 1 of the Smad7 gene was deleted (Smad7^{Δex1}) [125],[126]. Unfortunately, the significance of these findings is unclear, as these animals exhibit preserved Smad7 functions due to the presence of an intact MH2 domain, the key effector domain involved in Smad7 interactions with T β Rs and R-Smads [117],[127].

7. Smad activation in immune cells and endothelial cells may trigger fibrogenic responses

In addition to their effects on fibroblasts, Smad signaling may regulate phenotype and function of other cell types, thus contributing to their fibrogenic actions. In macrophages Smad3 plays an important role in activation of a phagocytic program, but also mediates the transition of macrophages to an anti-inflammatory phenotype in response to phagocytosis [30]. Phagocytic Smad3 null macrophages had impaired capacity to synthesize fibrogenic TGF- β s [30]. Whether this defect has an impact on the fibrogenic potential of macrophages has not been tested. In endothelial cells, Smad3 has been implicated in EndMT in a model of diabetic renal injury [128]. Whether Smad-dependent EndMT contributes to cardiac fibrosis has not been tested. However, this mechanism is unlikely considering the strong evidence from lineage tracing studies suggesting that the majority of activated fibroblasts in cardiac fibrotic conditions are not derived from endothelial cells [88], [89],[90],[129].

8. The role of Smad signaling cascades in homeostasis of the cardiac ECM network.

Smad cascades are critically involved in cardiac development [130]; however, their role in homeostasis of the adult heart is poorly understood. The adult mouse myocardium has high levels of constitutive Smad2 and Smad3 expression; however, baseline Smad2/3 phosphorylation is low [109]. In vivo studies showed that fibroblast-specific Smad3 (but not Smad2) loss modestly but significantly attenuated collagen levels in young adult mouse hearts, without affecting cardiac geometry or function [109]. These findings support the notion that fibroblast Smad3 signaling may play a role in maintaining the basal levels of collagen in the myocardium; however, this effect is not critical for preservation of function. Whether other Smad cascades are involved in homeostasis of the cardiac ECM network has not been investigated.

9. Smad signaling cascades in conditions associated with cardiac fibrosis (Table 2).

9.1. The role of Smad cascades in reparative fibrosis of the infarcted heart

Myocardial infarction results in sudden loss of up to a billion

cardiomyocytes, activating an inflammatory reaction that clears the infarct from dead cells and matrix debris and sets the stage for fibroblast-driven repair [131],[132]. Formation of a scar is critical for preservation of the structural integrity of the infarcted ventricle; however, excessive, unrestrained or expanded fibrosis may cause adverse remodeling, contributing to systolic and diastolic dysfunction and to the pathogenesis of heart failure. Induction and activation of TGF- β s in the infarcted myocardium is associated with activation of Smad2 and Smad3 in all cell types involved in cardiac repair, including border zone cardiomyocytes, infarct fibroblasts and macrophages [91],[92],[30]. The relative contribution of various members of the TGF- β superfamily in Smad2/3 activation remains unclear. The 3 TGF- β isoforms, the major activators of Smad2 and Smad3 cascades exhibit distinct patterns of induction following myocardial infarction with early upregulation of TGF- β 1 and TGF- β 2 and delayed increase in TGF- β 3 levels [16],[30]. Early studies using mice with global germline loss of Smad3 provided insights into the role of the pathway in fibrosis of the infarcted heart. Complete absence of Smad3 attenuated collagen deposition in the infarcted and remodeling myocardium, despite increased infiltration of the infarct with myofibroblasts [91],[94]. Based on in vitro studies, the effects of global Smad3 loss were attributed to alterations in fibroblast phenotype and function, leading to attenuated expression of structural collagens, tenascin-C and fibronectin, and reducing secretion of Connective Tissue Growth Factor (CTGF)/CCN2, a downstream mediator of TGF- β -induced fibrogenesis [94]. However, considering the broad effects of Smad3 on all cell types involved in cardiac repair and remodeling, and the effects of Smad3 signaling on baseline homeostasis [133], dissection of cellular mechanisms using the global loss-of-function model is challenging.

Investigations using cell-specific loss-of-function models have significantly enhanced our understanding of the role of Smad cascades in myocardial infarction. (Table 2). Studies using cardiomyocyte-specific knockouts suggested that cardiomyocyte Smad3 signaling is not implicated in cardiac homeostasis, but contributes to the pathogenesis of adverse remodeling and dysfunction following reperfused myocardial infarction [7]. The detrimental actions of cardiomyocyte Smad3 in post-infarction ventricular dysfunction were attributed to pro-apoptotic effects that may involve activation of oxidative pathways and to induction and activation of MMP2 that may accentuate matrix degradation, causing adverse dilative remodeling [7].

On the other hand, Smad3 loss in infarct myofibroblasts perturbed repair of the infarcted heart, increasing the incidence of catastrophic late rupture in the model of non-reperfused infarction, and accentuating adverse remodeling in the model of reperfused infarction. Impaired repair in the absence of myofibroblast Smad3 signaling was related to perturbed fibroblast:extracellular matrix interactions that resulted in formation of a disorganized scar [7]. Smad3 plays an important role in induction of fibroblast integrins, the cell surface proteins that link the cells to the extracellular matrix [7]. Smad3-mediated integrin synthesis in fibroblasts is critically involved in activation of an oxidative response, that promotes a reparative program. Moreover, integrin synthesis may be important for scar organization, contributing to myofibroblast alignment in the healing infarct [7], a process that may involve expression of polarity genes [134]. In contrast to the critical role of myofibroblast Smad3 in cardiac repair, Smad2 activation in myofibroblasts did not play a significant role in post-infarction repair [92]. Although both Smad2 and Smad3 are activated in infarct myofibroblasts, only Smad3 is involved in integrin upregulation [92].

The role of the Smad1/5/8 cascade in the pathogenesis of post-infarction fibrosis remains unknown. Smad1 activation in the infarcted ventricle may involve induction of both BMPs and TGF- β s. Cardiomyocyte Smad1 has been suggested to play a protective role following ischemic injury through effects that may involve activation of anti-apoptotic signals [135]. Whether these effects result in reduced fibrosis has not been tested. Moreover, direct effects of Smad1 signaling in fibroblast activation have not been explored.

9.2. Smad signaling in fibrotic remodeling of the pressure-overloaded heart

Myocardial activation of the Smad2/3 pathway has been reported in both adult and pediatric patients with heart failure [136]. Adult patients with dilated cardiomyopathy exhibited higher levels of myocardial Smad2/3 activity; this was associated with a more prominent fibrotic response [136]. Left ventricular pressure overload is the predominant pathophysiologic perturbation responsible for cardiac remodeling and fibrosis in patients with chronic hypertension or aortic stenosis. Studies in animal models of pressure overload induced through transverse aortic constriction or through neurohumoral activation showed robust myocardial activation of Smad2 Smad3 [137],[138] and Smad1 [139]. The molecular links between mechanical stress and activation of Smad signaling cascades remain poorly understood, but may involve angiotensin II-mediated actions and subsequent activation and induction of TGF- β s in the cardiac interstitium. Early studies using global loss-of-function approaches suggested that Smad3 mediates fibrosis and ventricular dysfunction in a model of angiotensin II infusion [140], and may promote fibrosis following pressure overload [141]. Moreover, ALK5 inhibition attenuated dysfunction and inhibited fibrosis in rodent models of left ventricular pressure overload; these protective actions were attributed to inhibition of Smad2/3 signaling [142],[143],[144]. However, considering the broad effects of Smad3 on all cells involved in cardiac remodeling and fibrosis (including cardiomyocytes, vascular cells, fibroblasts and immune cells), dissection of cell biological mechanisms responsible for the effects of R-Smads requires cell-specific interventions.

Experiments in fibroblast and myofibroblast-specific knockout mice have suggested an important role for Smad3 signaling in activation of fibroblasts in failing and remodeling hearts. These actions appear to have a major impact on cardiac function. Deletion of Smad3 (but not Smad2) from cardiac fibroblasts attenuated the cardiac fibrotic response to pressure overload. The fibrogenic actions of Smad3 were attributed to increased transcription of extracellular matrix genes, including type I and type III collagens, periostin, fibronectin, tenascin-C, and to upregulation of integrins [96]. In an independent study focusing on the role of fibroblast Smad3 in pressure overload-induced cardiac remodeling, early activation of Smad3 in myofibroblasts protected from systolic dysfunction by preserving the extracellular matrix through down-modulation of collagenases. The findings suggested that Smad3 signaling in activated myofibroblasts plays a crucial role in TGF- β -mediated suppression of the collagenases MMP3 and MMP8 and in upregulation of TIMP1, inhibiting fragmentation of the matrix under conditions of mechanical stress. In the absence of Smad3 in fibroblasts, increased MMP8-mediated proteolytic activity was associated with collagen denaturation and generation of pro-inflammatory matrix fragments that enhance inflammation, promote cardiomyocyte apoptosis and cause dysfunction. [93]. Thus, activated myofibroblasts may play an important protective role in the early stages of cardiac remodeling.

9.3. Smad signaling in fibrosis of the diabetic heart.

Diabetes, obesity and metabolic dysfunction are associated with an increased incidence of fibrosis that involves not only the myocardium [145],[146],[74] but also other organs, such as the liver and kidney [147]. Cardiac fibrosis may contribute to the pathogenesis of diastolic dysfunction and to the development of Heart Failure with Preserved Ejection Fraction (HFpEF), a common form of heart failure in diabetic and obese subjects [148]. Myocardial induction of TGF- β superfamily members and activation of Smad2 and Smad3 cascades have been consistently reported in animal models of type 1 and type 2 diabetes [149],[150],[133],[151]. In contrast, evidence of activation of the Smad1/5/8 cascade in the diabetic heart is lacking; however, Smad1 activation in the diabetic kidney has been implicated in mesangial

expansion [152]. Activation of the TGF- β /Smad2/3 axis in the diabetic myocardium may reflect, at least in part, the effects of hyperglycemia on expression of TGF- β receptors [153]. Moreover, diabetes-associated activation of the renin-angiotensin-aldosterone system (RAAS), oxidative stress, chronic stimulation of inflammatory cytokines and protein kinase C (PKC) activation may induce de novo synthesis of TGF- β , or activate latent stores, leading to stimulation of Smad2 and Smad3 signaling cascades [154],[155],[156].

Our knowledge on the role of Smad3 in diabetic cardiac fibrosis is derived from experiments using a global haploinsufficiency model. In the db/db mouse model of obesity-associated type 2 diabetes, Smad3 heterozygotes had attenuated fibrosis and improved diastolic function, associated with reduced collagen deposition and increased MMP activity. The reduction in interstitial collagen in animals with partial loss of Smad3 was associated with mild ventricular dilatation [133]. The findings are consistent with an important role for Smad3 in mediating fibrosis in diabetic hearts. However, considering the broad effects of Smad3 in all myocardial cells, whether these findings reflect Smad-dependent actions on fibroblast activity remains unknown. Moreover, the role of other R-Smads in diabetes-associated fibrosis is not known.

9.4. Smad signaling in aging-associated fibrosis

Senescence of the heart is associated with structural and morphological changes as hypertrophy and fibrosis that may lead to increased ventricular stiffness and impaired diastolic function [157]. Loss of one TGF- β 1 allele in TGF- β 1 heterozygous mice ameliorated age-associated myocardial fibrosis and reduced myocardial stiffness [158]. Whether aging-associated fibrosis is due to activation of Smad signaling pathways in fibroblasts remains unknown. Smad signaling in cardiomyocytes plays an important role in cardiac homeostasis in aging hearts [159]. Mice with cardiomyocyte-specific Smad4 loss exhibited increased hypertrophy associated with reduced cardiomyocyte survival and accentuated fibrosis as they aged [160],[159]. Fibrotic remodeling in the absence of cardiomyocyte Smad4 may be due to cell death and subsequent activation of a reparative program, or may reflect paracrine effects of stressed, or injured cardiomyocytes on interstitial fibroblasts.

Moreover, perturbed Smad signaling may explain the impaired reparative response of the senescent heart to injury. 24-month old mice exhibited increased post-infarction ventricular dilation, associated with markedly reduced deposition of collagen in the infarct zone [161]. The pathologic alterations noted in senescent mouse infarcts resembled the pathology of healing infarcts in mice with myofibroblast-specific Smad3 loss [7]. Moreover, fibroblasts harvested from senescent mouse hearts exhibit blunted Smad2 activation in response to TGF- β stimulation [161]. These observations support the intriguing hypothesis that the aging-associated impairment in repair following myocardial infarction may be related to attenuated TGF- β /Smad2/3 activation [162]. Perturbed Smad3 signaling in senescent fibroblasts may reflect a reduced reparative reserve that may be responsible for formation of a disorganized scar, composed of a fragmented matrix network. These age-associated alterations may reduce the tensile strength of the infarct, accentuating adverse remodeling and promoting post-infarction heart failure.

9.5. Smad signaling in myocarditis-induced cardiac fibrosis

Myocardial fibrosis is an important cellular mechanism responsible for development of dysfunction in patients with myocarditis who develop chronic dysfunction and cardiomyopathy. TGF- β s have been implicated in the pathogenesis of myofibroblast activation and fibrosis in models of autoimmune [163] and viral myocarditis [164]. However, evidence supporting the involvement of Smad signaling cascades in myocarditis-induced fibrosis is scarce. In a mouse model of chronic myocarditis due to Chagas disease, ALK5 inhibition was found to attenuate fibrosis [165]. The protective actions were attributed to

inhibition of Smad2/3 activity.

9.6. Smad signaling in valve fibrosis

Patients with mitral valve prolapse exhibit myxomatous degeneration of the valve, associated with activation of valve interstitial cells, matrix remodeling and valve fibrosis. In patients with mitral valve prolapse who underwent repair for severe mitral regurgitation, Smad2/3 activation was noted in fibrotic valve tissue and was associated with extracellular matrix deposition [166],[167]. Smad2/3 signaling was implicated in activation of a fibrogenic phenotype in valve interstitial cells [167]. In addition to fibrotic involvement of the mitral valve, patients with mitral valve prolapse also exhibit myocardial interstitial remodeling that is independent of the volume overload associated with severe mitral regurgitation [168]. These myocardial fibrotic changes may explain the high incidence of arrhythmias in patients with severe mitral valve prolapse. It is tempting to hypothesize that a common Smad-dependent mechanism may be involved in the pathogenesis of valvular and ventricular fibrosis in patients with malignant mitral valve prolapse. However, evidence supporting this notion is lacking.

10. Targeting Smads in cardiac fibrosis

TGF- β signaling pathways are critically involved in cardiac fibrosis, remodeling and dysfunction and represent promising therapeutic targets [12],[169],[170]. Targeting R-Smad signaling is feasible; however, the cell-specific and context-dependent actions of Smad cascades and our limited knowledge on the effects of key members of the Smad family hamper therapeutic translation, posing several major challenges. First, Smad3 activation plays distinct roles in various cell types that greatly affect outcome following myocardial injury. In the infarcted heart, fibroblast and macrophage Smad3 activation serves a reparative role, whereas cardiomyocyte Smad3 activation promotes dysfunction [7], [30]. Thus, development of effective therapeutics targeting the Smad3 cascade would require cell-specific interventions. Second, human patients with heart failure or myocardial infarction exhibit remarkable pathophysiologic heterogeneity. Following myocardial infarction, some patients may have excessive pro-inflammatory activation and defective matrix deposition, thus developing dilative ventricular remodeling and systolic dysfunction, while others have accentuated fibrotic responses and may develop diastolic dysfunction. Accentuated fibrosis may involve overactive Smad3 signaling; however effective therapeutic strategies would require identification of fibrosis-prone patients using biomarkers or imaging strategies [171]. Third, the effects of Smad3 inhibition in patients with heart failure may be dependent on the severity of fibrotic remodeling and the phenotype of fibrotic lesions. In chronic hypertensive heart failure, sustained or overactive Smad3 activation in interstitial cells is likely to be detrimental, promoting matrix deposition and accentuating diastolic dysfunction. However, in the early stages of hypertensive cardiac remodeling, Smad3-dependent activation of myofibroblasts may exert protective matrix-preserving actions that preserve the matrix that surrounds the cardiomyocytes and prevent release of pro-inflammatory matrikines [93]. Third, our current knowledge on the role of Smad cascades in myocardial disease is limited to evidence on the role of Smad3 in cardiomyocytes and fibroblasts. We currently have very limited information regarding the role of Smad3 in regulation of lymphocyte, dendritic cell and vascular cell function in the remodeling heart, and we know very little regarding the potential role of endogenous Smad2 and Smad1/5/8 cascades in myocardial disease. Fourth, considering the role of Smad signaling pathways in cardiac and vascular homeostasis and in tissue repair, chronic therapy to inhibit Smad3 or Smad4 may carry significant risks [133],[159].

11. Conclusions

Smad signaling cascades play a critical role in cardiac fibrotic

responses; however, our current understanding of their actions is not sufficient to design therapeutic interventions. Moreover, the context-dependent and cell-specific actions of receptor-activated Smads pose major challenges in therapeutic implementation. Extensive experimental work is needed to study the patterns and mechanisms of Smad activation in myocardial diseases and the role of specific members of the family in regulating phenotype and function of the cells involved in cardiac remodeling. Moreover, clinical investigations are needed to identify heart failure patient subpopulations with perturbed or over-active Smad responses in order to tailor therapeutic interventions.

Sources of Funding

Dr. Frangogiannis' laboratory is supported by NIH R01 grants HL76246, HL85440, and R01 HL149407 and by Department of Defense grants PR151029, PR151134, and PR181464. Dr. Humeres is supported by an American Heart Association post-doctoral award 19POST34450144.

Col, collagen; CTGF, connective tissue growth factor; Fbln, fibulin; Fn, fibronectin; IL, interleukin; Itg, integrin; MCP, monocyte chemo-attractant protein; MMP, matrix metalloproteinase; LOX, lysyl oxidase; SMA, smooth muscle actin; TIMP, Tissue inhibitor of metalloproteinases; Tnc, tenascin; TNF, tumor necrosis factor; TGF, transforming growth factor.

CRedit authorship contribution statement

Anis Hanna: Writing - review & editing. **Claudio Humeres:** Writing - review & editing. **Nikolaos G. Frangogiannis:** Writing - review & editing.

References

- [1] N.G. Frangogiannis, Cardiac fibrosis: Cell biological mechanisms, molecular pathways and therapeutic opportunities, *Mol Aspects Med* 65 (2019) 70–99.
- [2] B.C. Berk, K. Fujiwara, S. Lehoux, ECM remodeling in hypertensive heart disease, *J Clin Invest* 117 (2007) 568–575.
- [3] X.M. Gao, D.A. White, A.M. Dart, X.J. Du, Post-infarct cardiac rupture: recent insights on pathogenesis and therapeutic interventions, *Pharmacol Ther* 134 (2012) 156–179.
- [4] A. Hanna, A.V. Shinde, N.G. Frangogiannis, Validation of diagnostic criteria and histopathological characterization of cardiac rupture in the mouse model of nonreperfused myocardial infarction, *Am J Physiol Heart Circ Physiol* 319 (2020) H948–H964.
- [5] E. Forte, D.A. Skelly, M. Chen, S. Daigle, K.A. Morelli, O. Hon, V.M. Philip, M. W. Costa, N.A. Rosenthal, M.B. Furtado, Dynamic Interstitial Cell Response during Myocardial Infarction Predicts Resilience to Rupture in Genetically Diverse Mice, *Cell Rep* 30 (2020) 3149–3163, e3146.
- [6] S. Maruyama, K. Nakamura, K.N. Papanicolaou, S. Sano, I. Shimizu, Y. Asaumi, M.J. van den Hoff, N. Ouchi, F.A. Recchia, K. Walsh, Follistatin-like 1 promotes cardiac fibroblast activation and protects the heart from rupture, *EMBO Mol Med* 8 (2016) 949–966.
- [7] P. Kong, A.V. Shinde, Y. Su, I. Russo, B. Chen, A. Saxena, S.J. Conway, J.M. Graff, N.G. Frangogiannis, Opposing Actions of Fibroblast and Cardiomyocyte Smad3 Signaling in the Infarcted Myocardium, *Circulation* 137 (2018) 707–724.
- [8] S.F. Nagueh, Heart Failure with Preserved Ejection Fraction: Insights into Diagnosis and Pathophysiology, *Cardiovasc Res*, Jul 27;cvaa228. doi: 10.1093/cvr/cvaa228. Online ahead of print. (2020).
- [9] S.F. Mohammed, S. Hussain, S.A. Mirzoyev, W.D. Edwards, J.J. Maleszewski, M. M. Redfield, Coronary microvascular rarefaction and myocardial fibrosis in heart failure with preserved ejection fraction, *Circulation* 131 (2015) 550–559.
- [10] N.G. Frangogiannis, Transforming Growth Factor (TGF)-beta in tissue fibrosis, *J Exp Med* 217 (2020), e20190103 <https://doi.org/20190110.20191084/jem.20190103>.
- [11] M. Lodyga, B. Hinz, TGF-beta1 - A truly transforming growth factor in fibrosis and immunity, *Semin Cell Dev Biol* 101 (2020) 123–139.
- [12] A. Hanna, N.G. Frangogiannis, The Role of the TGF-beta Superfamily in Myocardial Infarction, *Front Cardiovasc Med* 6 (2019) 140.
- [13] T. Kempf, M. Eden, J. Strelau, M. Naguib, C. Willenbockel, J. Tongers, J. Heineke, D. Kotlarz, J. Xu, J.D. Molkentin, H.W. Niessen, H. Drexler, K.C. Wollert, The transforming growth factor-beta superfamily member growth-differentiation factor-15 protects the heart from ischemia/reperfusion injury, *Circ Res* 98 (2006) 351–360.
- [14] T. Kempf, A. Zarbock, C. Widera, S. Butz, A. Stadtman, J. Rossaint, M. Bolomini-Vittori, M. Korf-Klingebiel, L.C. Napp, B. Hansen, A. Kanwischer, U. Bavendiek, G. Beutel, M. Hapke, M.G. Sauer, C. Laudanna, N. Hogg, D. Vestweber, K. C. Wollert, GDF-15 is an inhibitor of leukocyte integrin activation required for survival after myocardial infarction in mice, *Nat Med* 17 (2011) 581–588.
- [15] L.N. Sanders, J.A. Schoenhard, M.A. Saleh, A. Mukherjee, S. Ryzhov, W. G. McMaster Jr., K. Nolan, R.J. Gumina, T.B. Thompson, M.A. Magnuson, D. G. Harrison, A.K. Hatzopoulos, BMP Antagonist Gremlin 2 Limits Inflammation After Myocardial Infarction, *Circ Res* 119 (2016) 434–449.
- [16] O. Dewald, G. Ren, G.D. Duerr, M. Zoerlein, C. Klemm, C. Gersch, S. Tincey, L. H. Michael, M.L. Entman, N.G. Frangogiannis, Of mice and dogs: species-specific differences in the inflammatory response following myocardial infarction, *Am J Pathol* 164 (2004) 665–677.
- [17] J. Hao, H. Ju, S. Zhao, A. Junaid, T. Scammell-La Fleur, I.M. Dixon, Elevation of expression of Smads 2, 3, and 4, decorin and TGF-beta in the chronic phase of myocardial infarct scar healing, *J Mol Cell Cardiol* 31 (1999) 667–678.
- [18] L.A. Raftery, V. Twombly, K. Wharton, W.M. Gelbart, Genetic screens to identify elements of the decapentaplegic signaling pathway in *Drosophila*, *Genetics* 139 (1995) 241–254.
- [19] M. Kretschmar, J. Massague, SMADs: mediators and regulators of TGF-beta signaling, *Curr Opin Genet Dev* 8 (1998) 103–111.
- [20] A. Hata, Y.G. Chen, TGF-beta Signaling from Receptors to Smads, *Cold Spring Harb Perspect Biol*, 8, 2016.
- [21] S. Ghosh, P.R. Brauer, Latent transforming growth factor-beta is present in the extracellular matrix of embryonic hearts in situ, *Dev Dyn* 205 (1996) 126–134.
- [22] J.P. Annes, J.S. Munger, D.B. Rifkin, Making sense of latent TGFbeta activation, *J Cell Sci* 116 (2003) 217–224.
- [23] Y. Yao, C. Hu, Q. Song, Y. Li, X. Da, Y. Yu, H. Li, I.M. Clark, Q. Chen, Q.K. Wang, ADAMTS16 Activates Latent TGF-beta, Accentuating Fibrosis and Dysfunction of the Pressure-overloaded Heart, *Cardiovasc Res*, 2019.
- [24] G. Taimor, K.D. Schluter, K. Frischkopf, M. Flesch, S. Rosenkranz, H.M. Piper, Autocrine regulation of TGF beta expression in adult cardiomyocytes, *J Mol Cell Cardiol* 31 (1999) 2127–2136.
- [25] F. Klingberg, G. Chau, M. Walraven, S. Boo, A. Koehler, M.L. Chow, A.L. Olsen, M. Im, M. Lodyga, R.G. Wells, E.S. White, B. Hinz, The fibronectin ED-A domain enhances recruitment of latent TGF-beta-binding protein-1 to the fibroblast matrix, *J Cell Sci*, 131, 2018.
- [26] Y. Zhou, M.H. Poczatek, K.H. Berecek, J.E. Murphy-Ullrich, Thrombospondin 1 mediates angiotensin II induction of TGF-beta activation by cardiac and renal cells under both high and low glucose conditions, *Biochem Biophys Res Commun* 339 (2006) 633–641.
- [27] N.G. Frangogiannis, G. Ren, O. Dewald, P. Zymek, S. Haudek, A. Koerting, K. Winkelmann, L.H. Michael, J. Lawler, M.L. Entman, The critical role of endogenous Thrombospondin (TSP)-1 in preventing expansion of healing myocardial infarcts, *Circulation* 111 (2005) 2935–2942.
- [28] V. Sarrazy, A. Koehler, M.L. Chow, E. Zimina, C.X. Li, H. Kato, C.A. Caldaroni, B. Hinz, Integrins alphavbeta5 and alphavbeta3 promote latent TGF-beta1 activation by human cardiac fibroblast contraction, *Cardiovasc Res* 102 (2014) 407–417.
- [29] A. Meyer, W. Wang, J.X. Qu, L. Croft, J.L. Degen, B.S. Coller, J. Ahamed, Platelet TGF-beta 1 contributions to plasma TGF-beta 1, cardiac fibrosis, and systolic dysfunction in a mouse model of pressure overload, *Blood* 119 (2012) 1064–1074.
- [30] B. Chen, S. Huang, Y. Su, Y.J. Wu, A. Hanna, A. Brickshawana, J. Graff, N. G. Frangogiannis, Macrophage Smad3 Protects the Infarcted Heart, Stimulating Phagocytosis and Regulating Inflammation, *Circ Res* 125 (2019) 55–70.
- [31] Y. Chen, C. Rothnie, D. Spring, E. Verrier, K. Venardos, D. Kaye, D.J. Phillips, M. P. Hedger, J.A. Smith, Regulation and actions of activin A and follistatin in myocardial ischaemia-reperfusion injury, *Cytokine* 69 (2014) 255–262.
- [32] J. Massague, How cells read TGF-beta signals, *Nat Rev Mol Cell Biol* 1 (2000) 169–178.
- [33] C.H. Heldin, A. Moustakas, Signaling Receptors for TGF-beta Family Members, *Cold Spring Harb Perspect Biol*, 8, 2016.
- [34] R.A. Rahimi, E.B. Leof, TGF-beta signaling: a tale of two responses, *J Cell Biochem* 102 (2007) 593–608.
- [35] O. Eickelberg, M. Centrella, M. Reiss, M. Kashgarian, R.G. Wells, Betaglycan inhibits TGF-beta signaling by preventing type I-type II receptor complex formation. Glycosaminoglycan modifications alter betaglycan function, *J Biol Chem* 277 (2002) 823–829.
- [36] M.J. Goumans, G. Valdimarsdottir, S. Itoh, A. Rosendahl, P. Sideras, P. ten Dijke, Balancing the activation state of the endothelium via two distinct TGF-beta type I receptors, *Embo J* 21 (2002) 1743–1753.
- [37] H. Zhang, L. Du, Y. Zhong, K.C. Flanders, J.D. Roberts Jr., Transforming growth factor-beta stimulates Smad1/5 signaling in pulmonary artery smooth muscle cells and fibroblasts of the newborn mouse through ALK1, *Am J Physiol Lung Cell Mol Physiol* 313 (2017) L615–L627.
- [38] D. Nurgazieva, A. Mickleby, K. Moganti, W. Ming, I. Ovsyi, A. Popova, Sachindra, K. Awad, N. Wang, K. Bieback, S. Goerd, J. Kzhyshkowska, A. Gratchev, TGF-beta1, but not bone morphogenetic proteins, activates Smad1/5 pathway in primary human macrophages and induces expression of proatherogenic genes, *J Immunol* 194 (2015) 709–718.
- [39] A.C. Daly, R.A. Randall, C.S. Hill, Transforming growth factor beta-induced Smad1/5 phosphorylation in epithelial cells is mediated by novel receptor complexes and is essential for anchorage-independent growth, *Mol Cell Biol* 28 (2008) 6889–6902.
- [40] X.H. Feng, R. Derynck, Specificity and versatility in tgf-beta signaling through Smads, *Annu Rev Cell Dev Biol* 21 (2005) 659–693.


- [41] K. Miyazono, S. Maeda, T. Imamura, BMP receptor signaling: transcriptional targets, regulation of signals, and signaling cross-talk, *Cytokine Growth Factor Rev* 16 (2005) 251–263.
- [42] C.H. Heldin, A. Moustakas, Signaling Receptors for TGF-beta Family Members, *Cold Spring Harb Perspect Biol*, 8, 2016.
- [43] Z. Xiao, R. Latek, H.F. Lodish, An extended bipartite nuclear localization signal in Smad4 is required for its nuclear import and transcriptional activity, *Oncogene* 22 (2003) 1057–1069.
- [44] F. Lebrin, M.J. Goumans, L. Jonker, R.L. Carvalho, G. Valdimarsdottir, M. Thorikay, C. Mummery, H.M. Arthur, P. ten Dijke, Endoglin promotes endothelial cell proliferation and TGF-beta/ALK1 signal transduction, *Embo J* 23 (2004) 4018–4028.
- [45] A. Leask, D.J. Abraham, D.R. Finlay, A. Holmes, D. Pennington, X. Shi-Wen, Y. Chen, K. Venstrom, X. Dou, M. Ponticos, C. Black, C. Bernabeu, J.K. Jackman, P.R. Findell, M.K. Connolly, Dysregulation of transforming growth factor beta signaling in scleroderma: overexpression of endoglin in cutaneous fibroblasts, *Arthritis Rheum* 46 (2002) 1857–1865.
- [46] A. Rodriguez-Pena, N. Eleno, A. Duwell, M. Arevalo, F. Perez-Barriocanal, O. Flores, N. Docherty, C. Bernabeu, M. Letarte, J.M. Lopez-Novoa, Endoglin upregulation during experimental renal interstitial fibrosis in mice, *Hypertension* 40 (2002) 713–720.
- [47] H.J. You, M.W. Bruinsma, T. How, J.H. Ostrander, G.C. Blobe, The type III TGF-beta receptor signals through both Smad3 and the p38 MAP kinase pathways to contribute to inhibition of cell proliferation, *Carcinogenesis* 28 (2007) 2491–2500.
- [48] K. Tazat, M. Hector-Greene, G.C. Blobe, Y.I. Henis, TbetaRIII independently binds type I and type II TGF-beta receptors to inhibit TGF-beta signaling, *Mol Biol Cell* 26 (2015) 3535–3545.
- [49] E. Villalobos, A. Criollo, G.G. Schiattarella, F. Altamirano, K.M. French, H.I. May, N. Jiang, N.U.N. Nguyen, D. Romero, J.C. Roa, L. Garcia, G. Diaz-Araya, E. Morselli, A. Ferdous, S.J. Conway, H.A. Sadek, T.G. Gillette, S. Lavandero, J. A. Hill, Fibroblast Primary Cilia Are Required for Cardiac Fibrosis, *Circulation* 139 (2019) 2342–2357.
- [50] P. Huebener, T. Abou-Khamis, P. Zymek, M. Bujak, X. Ying, K. Chatila, S. Haudek, G. Thakker, N.G. Frangogiannis, CD44 Is Critically Involved in Infarct Healing by Regulating the Inflammatory and Fibrotic Response, *J Immunol* 180 (2008) 2625–2633.
- [51] T. Sekiya, T. Oda, K. Matsuura, T. Akiyama, Transcriptional regulation of the TGF-beta pseudoreceptor BAMBI by TGF-beta signaling, *Biochem Biophys Res Commun* 320 (2004) 680–684.
- [52] X. Yan, Z. Lin, F. Chen, X. Zhao, H. Chen, Y. Ning, Y.G. Chen, Human BAMBI cooperates with Smad7 to inhibit transforming growth factor-beta signaling, *J Biol Chem* 284 (2009) 30097–30104.
- [53] A.V. Villar, R. Garcia, M. Llano, M. Cobo, D. Merino, A. Lantero, M. Tramullas, J. M. Hurler, M.A. Hurler, J.F. Nistal, BAMBI (BMP and activin membrane-bound inhibitor) protects the murine heart from pressure-overload biomechanical stress by restraining TGF-beta signaling, *Biochim Biophys Acta* 1832 (2013) 323–335.
- [54] K. Miyazawa, K. Miyazono, Regulation of TGF-beta Family Signaling by Inhibitory Smads, *Cold Spring Harb Perspect Biol*, 9, 2017.
- [55] K. Luo, Ski and SnoN: negative regulators of TGF-beta signaling, *Curr Opin Genet Dev* 14 (2004) 65–70.
- [56] M. Funaba, C.M. Zimmerman, L.S. Mathews, Modulation of Smad2-mediated signaling by extracellular signal-regulated kinase, *J Biol Chem* 277 (2002) 41361–41368.
- [57] S. Liu, S.W. Xu, L. Kennedy, D. Pala, Y. Chen, M. Eastwood, D.E. Carter, C. M. Black, D.J. Abraham, A. Leask, FAK is required for TGFbeta-induced JNK phosphorylation in fibroblasts: implications for acquisition of a matrix-remodeling phenotype, *Mol Biol Cell* 18 (2007) 2169–2178.
- [58] X. Shi-wen, S.K. Parapuram, D. Pala, Y. Chen, D.E. Carter, M. Eastwood, C. P. Denton, D.J. Abraham, A. Leask, Requirement of transforming growth factor beta-activated kinase 1 for transforming growth factor beta-induced alpha-smooth muscle actin expression and extracellular matrix contraction in fibroblasts, *Arthritis Rheum* 60 (2009) 234–241.
- [59] C. Hough, M. Radu, J.J. Dore, Tgf-beta induced Erk phosphorylation of smad linker region regulates smad signaling, *PLoS One* 7 (2012), e42513.
- [60] S.K. Leivonen, L. Hakkinen, D. Liu, V.M. Kahari, Smad3 and extracellular signal-regulated kinase 1/2 coordinately mediate transforming growth factor-beta-induced expression of connective tissue growth factor in human fibroblasts, *J Invest Dermatol* 124 (2005) 1162–1169.
- [61] D.M. Dolivo, S.A. Larson, T. Dominko, Crosstalk between mitogen-activated protein kinase inhibitors and transforming growth factor-beta signaling results in variable activation of human dermal fibroblasts, *Int J Mol Med* 43 (2019) 325–335.
- [62] A. Gowripalan, C.R. Abbott, C. McKenzie, W.S. Chan, G. Karupiah, L. Levy, T. P. Newsome, Cell-to-cell spread of vaccinia virus is promoted by TGF-beta-independent Smad4 signalling, *Cell Microbiol* 22 (2020), e13206.
- [63] Y. Wang, J. Chu, P. Yi, W. Dong, J. Saultz, Y. Wang, H. Wang, S. Scoville, J. Zhang, L.C. Wu, Y. Deng, X. He, B. Mundy-Bosse, A.G. Freud, L.S. Wang, M. A. Caligiuri, J. Yu, SMAD4 promotes TGF-beta-independent NK cell homeostasis and maturation and antitumor immunity, *J Clin Invest* 128 (2018) 5123–5136.
- [64] A.C. Chung, H. Zhang, Y.Z. Kong, J.J. Tan, X.R. Huang, J.B. Kopp, H.Y. Lan, Advanced glycation end-products induce tubular CTGF via TGF-beta-independent Smad3 signaling, *J Am Soc Nephrol* 21 (2010) 249–260.
- [65] J. Hao, B. Wang, S.C. Jones, D.S. Jassal, I.M. Dixon, Interaction between angiotensin II and Smad proteins in fibroblasts in failing heart and in vitro, *Am J Physiol Heart Circ Physiol* 279 (2000) H3020–H3030.
- [66] M. AlQudah, T.M. Hale, M.P. Czubyrt, Targeting the renin-angiotensin-aldosterone system in fibrosis, *Matrix Biol* 91–92 (2020) 92–108.
- [67] C. Humeres, N.G. Frangogiannis, Fibroblasts in the Infarcted, Remodeling, and Failing Heart, *JACC Basic Transl Sci* 4 (2019) 449–467.
- [68] J.P. Cleutjens, M.J. Verluyten, J.F. Smiths, M.J. Daemen, Collagen remodeling after myocardial infarction in the rat heart, *Am J Pathol* 147 (1995) 325–338.
- [69] N. Ashizawa, K. Graf, Y.S. Do, T. Nunohiro, C.M. Giachelli, W.P. Meehan, T. L. Tuan, W.A. Hsueh, Osteopontin is produced by rat cardiac fibroblasts and mediates A(II)-induced DNA synthesis and collagen gel contraction, *J Clin Invest* 98 (1996) 2218–2227.
- [70] I. Komatsubara, T. Murakami, S. Kusachi, K. Nakamura, S. Hirohata, J. Hayashi, S. Takemoto, C. Suezawa, Y. Ninomiya, Y. Shiratori, Spatially and temporally different expression of osteonectin and osteopontin in the infarct zone of experimentally induced myocardial infarction in rats, *Cardiovasc Pathol* 12 (2003) 186–194.
- [71] P. Pakshir, N. Noskovicova, M. Lodyga, D.O. Son, R. Schuster, A. Goodwin, H. Karvonen, B. Hinz, The myofibroblast at a glance, *J Cell Sci*, 133, 2020.
- [72] J.P. Cleutjens, J.C. Kandala, E. Guarda, R.V. Guntaka, K.T. Weber, Regulation of collagen degradation in the rat myocardium after infarction, *J Mol Cell Cardiol* 27 (1995) 1281–1292.
- [73] A.E. Awad, V. Kandalam, S. Chakrabarti, X. Wang, J.M. Penninger, S.T. Davidge, G.Y. Oudit, Z. Kassiri, Tumor necrosis factor induces matrix metalloproteinases in cardiomyocytes and cardiofibroblasts differentially via superoxide production in a PI3Kgamma-dependent manner, *Am J Physiol Cell Physiol* 298 (2010) C679–C692.
- [74] L. Alex, I. Russo, V. Holoborodko, N.G. Frangogiannis, Characterization of a mouse model of obesity-related fibrotic cardiomyopathy that recapitulates features of human heart failure with preserved ejection fraction, *Am J Physiol Heart Circ Physiol* 315 (2018) H934–H949.
- [75] N. Farbehi, R. Patrick, A. Dorison, M. Xaymardan, V. Janbandhu, K. Wystub-Lis, J.W. Ho, R.E. Nordon, R.P. Harvey, Single-cell expression profiling reveals dynamic flux of cardiac stromal, vascular and immune cells in health and injury, *Elife*, 8:e43882, 2019, <https://doi.org/10.7554/eLife.43882>.
- [76] M.A. McLellan, D.A. Skelly, M.S.I. Dona, G.T. Squiers, G.E. Farrugia, T.L. Gaynor, C.D. Cohen, R. Pandey, H. Diep, A. Vinh, N.A. Rosenthal, A.R. Pinto, High-Resolution Transcriptomic Profiling of the Heart During Chronic Stress Reveals Cellular Drivers of Cardiac Fibrosis and Hypertrophy, *Circulation*, doi: 10.1161/CIRCULATIONAHA.119.045115. Online ahead of print. (2020).
- [77] T. Nevers, A.M. Salvador, F. Velazquez, N. Ngwenyama, F.J. Carrillo-Salinas, M. Aronovitz, R.M. Blanton, P. Alcaide, Th1 effector T cells selectively orchestrate cardiac fibrosis in nonischemic heart failure, *J Exp Med* 214 (2017) 3311–3329.
- [78] A.D. Okyere, D.G. Tilley, Leukocyte-Dependent Regulation of Cardiac Fibrosis, *Front Physiol* 11 (2020) 301.
- [79] T. Nevers, A.M. Salvador, A. Grodecki-Pena, A. Knapp, F. Velazquez, M. Aronovitz, N.K. Kapur, R.H. Karas, R.M. Blanton, P. Alcaide, Left Ventricular T-Cell Recruitment Contributes to the Pathogenesis of Heart Failure, *Circ Heart Fail* 8 (2015) 776–787.
- [80] J. Hartupele, D.L. Mann, Role of inflammatory cells in fibroblast activation, *J Mol Cell Cardiol* 93 (2016) 143–148.
- [81] S.P. Levick, G.C. Melendez, E. Plante, J.L. McLarty, G.L. Brower, J.S. Janicki, Cardiac mast cells: the centrepiece in adverse myocardial remodelling, *Cardiovasc Res* 89 (2012) 12–19.
- [82] N.G. Frangogiannis, J.L. Perrard, L.H. Mendoza, A.R. Burns, M.L. Lindsey, C. M. Ballantyne, L.H. Michael, C.W. Smith, M.L. Entman, Stem cell factor induction is associated with mast cell accumulation after canine myocardial ischemia and reperfusion, *Circulation* 98 (1998) 687–698.
- [83] Q. Liu, L.J. Zhu, A.M. Waaga-Gasser, Y. Ding, M. Cao, S.J. Jadhav, S. Kirolos, P. S. Shekar, R.F. Padera, Y.C. Chang, X. Xu, E.M. Zeisberg, D.M. Charytan, L. L. Hsiao, The axis of local cardiac endogenous Klotho-TGF-beta1-Wnt signaling mediates cardiac fibrosis in human, *J Mol Cell Cardiol* 136 (2019) 113–124.
- [84] P. Flevaris, S.S. Khan, M. Eren, A.J.T. Scholdt, S.J. Shah, D.C. Lee, S. Gupta, A. D. Shapiro, P.W. Burridge, A.K. Ghosh, D.E. Vaughan, Plasminogen Activator Inhibitor Type I Controls Cardiomycocyte Transforming Growth Factor-beta and Cardiac Fibrosis, *Circulation* 136 (2017) 664–679.
- [85] E.M. Zeisberg, O. Tarnavski, M. Zeisberg, A.L. Dorfman, J.R. McMullen, E. Gustafsson, A. Chandraker, X. Yuan, W.T. Pu, A.B. Roberts, E.G. Neilson, M. H. Sayegh, S. Izumo, R. Kalluri, Endothelial-to-mesenchymal transition contributes to cardiac fibrosis, *Nat Med* 13 (2007) 952–961.
- [86] B. Widyantoro, N. Emoto, K. Nakayama, D.W. Anggrahini, S. Adiarto, N. Iwasa, K. Yagi, K. Miyagawa, Y. Rikitake, T. Suzuki, Y.Y. Kisanuki, M. Yanagisawa, K. Hirata, Endothelial cell-derived endothelin-1 promotes cardiac fibrosis in diabetic hearts through stimulation of endothelial-to-mesenchymal transition, *Circulation* 121 (2010) 2407–2418.
- [87] O. Aisagbonhi, M. Rai, S. Ryzhov, N. Atria, I. Feoktistov, A.K. Hatzopoulos, Experimental myocardial infarction triggers canonical Wnt signaling and endothelial-to-mesenchymal transition, *Dis Model Mech* 4 (2011) 469–483.
- [88] S.R. Ali, S. Ranjbarvaziri, M. Talkhabi, P. Zhao, A. Subat, A. Hojjat, P. Kamran, A. M. Muller, K.S. Volz, Z. Tang, K. Red-Horse, R. Ardehali, Developmental heterogeneity of cardiac fibroblasts does not predict pathological proliferation and activation, *Circ Res* 115 (2014) 625–635.
- [89] T. Moore-Morris, N. Guimaraes-Camboa, I. Banerjee, A.C. Zamboni, T. Kisseleva, A. Velayoudon, W.B. Stallcup, Y. Gu, N.D. Dalton, M. Cedenilla, R. Gomez-Amaro, B. Zhou, D.A. Brenner, K.L. Peterson, J. Chen, S.M. Evans, Resident fibroblast lineages mediate pressure overload-induced cardiac fibrosis, *J Clin Invest* 124 (2014) 2921–2934.

- [90] O. Kanisicak, H. Khalil, M.J. Ivey, J. Karch, B.D. Maliken, R.N. Correll, M. J. Brody, B.J. Aronow, M.D. Tallquist, J.D. Molkentin, Genetic lineage tracing defines myofibroblast origin and function in the injured heart, *Nat Commun* 7 (2016) 12260.
- [91] M. Bujak, G. Ren, H.J. Kweon, M. Dobaczewski, A. Reddy, G. Taffet, X.F. Wang, N.G. Frangogiannis, Essential Role of Smad3 in Infarct Healing and in the Pathogenesis of Cardiac Remodeling, *Circulation* 116 (2007) 2127–2138.
- [92] S. Huang, B. Chen, Y. Su, L. Alex, C. Humeres, A.V. Shinde, S.J. Conway, N. G. Frangogiannis, Distinct roles of myofibroblast-specific Smad2 and Smad3 signaling in repair and remodeling of the infarcted heart, *J Mol Cell Cardiol* 132 (2019) 84–97.
- [93] I. Russo, M. Cavalera, S. Huang, Y. Su, A. Hanna, B. Chen, A.V. Shinde, S. J. Conway, J. Graff, N.G. Frangogiannis, Protective Effects of Activated Myofibroblasts in the Pressure-Overloaded Myocardium Are Mediated Through Smad-Dependent Activation of a Matrix-Preserving Program, *Circ Res* 124 (2019) 1214–1227.
- [94] M. Dobaczewski, M. Bujak, N. Li, C. Gonzalez-Quesada, L.H. Mendoza, X.F. Wang, N.G. Frangogiannis, Smad3 signaling critically regulates fibroblast phenotype and function in healing myocardial infarction, *Circ Res* 107 (2010) 418–428.
- [95] J.G. Cogan, S.V. Subramanian, J.A. Polikandriotis, R.J. Kelm Jr., A.R. Strauch, Vascular smooth muscle alpha-actin gene transcription during myofibroblast differentiation requires Sp1/3 protein binding proximal to the MCAT enhancer, *J Biol Chem* 277 (2002) 36433–36442.
- [96] H. Khalil, O. Kanisicak, V. Prasad, R.N. Correll, X. Fu, T. Schips, R.J. Vagnozzi, R. Liu, T. Huynh, S.J. Lee, J. Karch, J.D. Molkentin, Fibroblast-specific TGF-beta-Smad2/3 signaling underlies cardiac fibrosis, *J Clin Invest* 127 (2017) 3770–3783.
- [97] G. Serini, M.L. Bochaton-Piallat, P. Ropraz, A. Geinoz, L. Borsi, L. Zardi, G. Gabbiani, The fibronectin domain ED-A is crucial for myofibroblastic phenotype induction by transforming growth factor-beta1, *J Cell Biol* 142 (1998) 873–881.
- [98] R. Vivar, C. Humeres, R. Anfossi, S. Bolivar, M. Catalan, J. Hill, S. Lavandero, G. Diaz-Araya, Role of FoxO3a as a negative regulator of the cardiac myofibroblast conversion induced by TGF-beta1, *Biochim Biophys Acta Mol Cell Res* 2020 (1867) 118695.
- [99] J.B. Koo, M.O. Nam, Y. Jung, J. Yoo, D.H. Kim, G. Kim, S.J. Shin, K.M. Lee, K. B. Hahm, J.W. Kim, S.P. Hong, K.J. Lee, J.H. Yoo, Anti-fibrogenic effect of PPAR-gamma agonists in human intestinal myofibroblasts, *BMC Gastroenterol* 17 (2017) 73.
- [100] M. Bujak, G. Ren, H.J. Kweon, M. Dobaczewski, A. Reddy, G. Taffet, X.F. Wang, N. G. Frangogiannis, Essential role of Smad3 in infarct healing and in the pathogenesis of cardiac remodeling, *Circulation* 116 (2007) 2127–2138.
- [101] H. Khalil, O. Kanisicak, V. Prasad, R.N. Correll, X. Fu, T. Schips, R.J. Vagnozzi, R. Liu, T. Huynh, S.J. Lee, J. Karch, J.D. Molkentin, Fibroblast-specific TGF-beta-Smad2/3 signaling underlies cardiac fibrosis, *J Clin Invest* 127 (2017) 3770–3783.
- [102] T.G. Voloshenyuk, E.S. Landesman, E. Khoutorova, A.D. Hart, J.D. Gardner, Induction of cardiac fibroblast lysyl oxidase by TGF-beta1 requires PI3K/Akt, Smad3, and MAPK signaling, *Cytokine* 55 (2011) 90–97.
- [103] A.V. Shinde, M. Dobaczewski, J.J. de Haan, A. Saxena, K.K. Lee, Y. Xia, W. Chen, Y. Su, W. Hanif, I. Kaur Madahar, V.M. Paulino, G. Melino, N.G. Frangogiannis, Tissue transglutaminase induction in the pressure-overloaded myocardium regulates matrix remodelling, *Cardiovasc Res* 113 (2017) 892–905.
- [104] I. Talior-Voldarsky, K.A. Connelly, P.D. Arora, D. Gullberg, C.A. McCulloch, alpha1 integrin stimulates myofibroblast differentiation in diabetic cardiomyopathy, *Cardiovasc Res* 96 (2012) 265–275.
- [105] A.V. Shinde, C. Humeres, N.G. Frangogiannis, The role of alpha-smooth muscle actin in fibroblast-mediated matrix contraction and remodeling, *Biochim Biophys Acta* 1863 (2017) 298–309.
- [106] R. Vivar, C. Humeres, P. Ayala, I. Olmedo, M. Catalan, L. Garcia, S. Lavandero, G. Diaz-Araya, TGF-beta1 prevents simulated ischemia/reperfusion-induced cardiac fibroblast apoptosis by activation of both canonical and non-canonical signaling pathways, *Biochim Biophys Acta* 1832 (2013) 754–762.
- [107] L. Li, D. Fan, C. Wang, J.Y. Wang, X.B. Cui, D. Wu, Y. Zhou, L.L. Wu, Angiotensin II increases periostin expression via Ras/p38 MAPK/CREB and ERK1/2/TGF-beta1 pathways in cardiac fibroblasts, *Cardiovasc Res* 91 (2011) 80–89.
- [108] R.A. Bagchi, M.P. Czubyrt, Synergistic roles of scleraxis and Smads in the regulation of collagen 1alpha2 gene expression, *Biochim Biophys Acta* 1823 (2012) 1936–1944.
- [109] S. Huang, B. Chen, C. Humeres, L. Alex, A. Hanna, N.G. Frangogiannis, The role of Smad2 and Smad3 in regulating homeostatic functions of fibroblasts in vitro and in adult mice, *Biochim Biophys Acta Mol Cell Res* 2020 (1867) 118703.
- [110] J.T. Schwartz, S. Becker, E. Sakkas, L.A. Wujak, G. Niess, J. Usemann, F. Reichenberger, S. Herold, I. Vadasz, K. Mayer, W. Seeger, R.E. Morty, Glucocorticoids recruit Tgfb3 and Smad1 to shift transforming growth factor-beta signaling from the Tgfb1/Smad2/3 axis to the Acvr1/Smad1 axis in lung fibroblasts, *J Biol Chem* 289 (2014) 3262–3275.
- [111] J. Pannu, S. Nakerakanti, E. Smith, P. ten Dijke, M. Trojanowska, Transforming growth factor-beta receptor type I-dependent fibrogenic gene program is mediated via activation of Smad1 and ERK1/2 pathways, *J Biol Chem* 282 (2007) 10405–10413.
- [112] X. Chen, J. Xu, B. Jiang, D. Liu, Bone Morphogenetic Protein-7 Antagonizes Myocardial Fibrosis Induced by Atrial Fibrillation by Restraining Transforming Growth Factor-beta (TGF-beta)/Smads Signaling, *Med Sci Monit* 22 (2016) 3457–3468.
- [113] K. Miyazawa, K. Miyazono, Regulation of TGF-beta Family Signaling by Inhibitory Smads, *Cold Spring Harb Perspect Biol*, 9, 2017.
- [114] A. Hanyu, Y. Ishidou, T. Ebisawa, T. Shimanuki, T. Imamura, K. Miyazono, The N domain of Smad7 is essential for specific inhibition of transforming growth factor-beta signaling, *J Cell Biol* 155 (2001) 1017–1027.
- [115] Y. Kamiya, K. Miyazono, K. Miyazawa, Smad7 inhibits transforming growth factor-beta family type I receptors through two distinct modes of interaction, *J Biol Chem* 285 (2010) 30804–30813.
- [116] K. Goto, Y. Kamiya, T. Imamura, K. Miyazono, K. Miyazawa, Selective inhibitory effects of Smad6 on bone morphogenetic protein type I receptors, *J Biol Chem* 282 (2007) 20603–20611.
- [117] T. Mochizuki, H. Miyazaki, T. Hara, T. Furuya, T. Imamura, T. Watabe, K. Miyazono, Roles for the MH2 domain of Smad7 in the specific inhibition of transforming growth factor-beta superfamily signaling, *J Biol Chem* 279 (2004) 31568–31574.
- [118] Y. Asano, H. Ihn, K. Yamane, M. Kubo, K. Tamaki, Impaired Smad7-Smurf-mediated negative regulation of TGF-beta signaling in scleroderma fibroblasts, *J Clin Invest* 113 (2004) 253–264.
- [119] G. Murakami, T. Watabe, K. Takaoka, K. Miyazono, T. Imamura, Cooperative inhibition of bone morphogenetic protein signaling by Smurf1 and inhibitory Smads, *Mol Biol Cell* 14 (2003) 2809–2817.
- [120] A. Hata, G. Lagna, J. Massague, A. Hemmati-Brivanlou, Smad6 inhibits BMP/Smad1 signaling by specifically competing with the Smad4 tumor suppressor, *Genes Dev* 12 (1998) 186–197.
- [121] B. Wang, J. Hao, S.C. Jones, M.S. Yee, J.C. Roth, I.M. Dixon, Decreased Smad 7 expression contributes to cardiac fibrosis in the infarcted rat heart, *Am J Physiol Heart Circ Physiol* 282 (2002) H1685–H1696.
- [122] B. Wang, A. Omar, T. Angelovska, V. Drobic, S.G. Rattan, S.C. Jones, I.M. Dixon, Regulation of collagen synthesis by inhibitory Smad7 in cardiac myofibroblasts, *Am J Physiol Heart Circ Physiol* 293 (2007) H1282–H1290.
- [123] H. Yu, G. Zhao, H. Li, X. Liu, S. Wang, Candesartan antagonizes pressure overload-evoked cardiac remodeling through Smad7 gene-dependent MMP-9 suppression, *Gene* 497 (2012) 301–306.
- [124] X. He, X. Gao, L. Peng, S. Wang, Y. Zhu, H. Ma, J. Lin, D.D. Duan, Atrial fibrillation induces myocardial fibrosis through angiotensin II type 1 receptor-specific Arkadia-mediated downregulation of Smad7, *Circ Res* 108 (2011) 164–175.
- [125] L.H. Wei, X.R. Huang, Y. Zhang, Y.Q. Li, H.Y. Chen, R. Heuchel, B.P. Yan, C. M. Yu, H.Y. Lan, Deficiency of Smad7 enhances cardiac remodeling induced by angiotensin II infusion in a mouse model of hypertension, *PLoS One* 8 (2013), e70195.
- [126] L.H. Wei, X.R. Huang, Y. Zhang, Y.Q. Li, H.Y. Chen, B.P. Yan, C.M. Yu, H.Y. Lan, Smad7 inhibits angiotensin II-induced hypertensive cardiac remodelling, *Cardiovasc Res* 99 (2013) 665–673.
- [127] R. Li, A. Rosendahl, G. Brodin, A.M. Cheng, A. Ahgren, C. Sundquist, S. Kulkarni, T. Pawson, C.H. Heldin, R.L. Heuchel, Deletion of exon 1 of SMAD7 in mice results in altered B cell responses, *J Immunol* 176 (2006) 6777–6784.
- [128] J. Li, X. Qu, J. Yao, G. Caruana, S.D. Ricardo, Y. Yamamoto, H. Yamamoto, J. F. Bertram, Blockade of endothelial-mesenchymal transition by a Smad3 inhibitor delays the early development of streptozotocin-induced diabetic nephropathy, *Diabetes* 59 (2010) 2612–2624.
- [129] P. Quijada, A. Misra, L.S. Velasquez, R.M. Burke, J.K. Lighthouse, D.M. Mickelsen, R.A. Dirx Jr., E.M. Small, Pre-existing fibroblasts of epicardial origin are the primary source of pathological fibrosis in cardiac ischemia and aging, *J Mol Cell Cardiol* 129 (2019) 92–104.
- [130] N. Dunker, K. Kriegelstein, Targeted mutations of transforming growth factor-beta genes reveal important roles in mouse development and adult homeostasis, *Eur J Biochem* 267 (2000) 6982–6988.
- [131] S.D. Prabhu, N.G. Frangogiannis, The Biological Basis for Cardiac Repair After Myocardial Infarction: From Inflammation to Fibrosis, *Circ Res* 119 (2016) 91–112.
- [132] A.V. Shinde, N.G. Frangogiannis, Fibroblasts in myocardial infarction: A role in inflammation and repair, *J Mol Cell Cardiol* 70C (2014) 74–82.
- [133] A. Biernacka, M. Cavalera, J. Wang, I. Russo, A. Shinde, P. Kong, C. Gonzalez-Quesada, V. Rai, M. Dobaczewski, D.W. Lee, X.F. Wang, N.G. Frangogiannis, Smad3 Signaling Promotes Fibrosis While Preserving Cardiac and Aortic Geometry in Obese Diabetic Mice, *Circ Heart Fail* 8 (2015) 788–798.
- [134] W.M. Blankesteyn, Y.P. Essers-Janssen, M.J. Verluyten, M.J. Daemen, J.F. Smits, A homologue of Drosophila tissue polarity gene frizzled is expressed in migrating myofibroblasts in the infarcted rat heart, *Nat Med* 3 (1997) 541–544.
- [135] M. Masaki, M. Izumi, Y. Oshima, Y. Nakaoka, T. Kuwada, R. Kimura, S. Sugiyama, K. Terai, M. Kitakaze, K. Yamauchi-Takahara, I. Kawase, H. Hirota, Smad1 protects cardiomyocytes from ischemia-reperfusion injury, *Circulation* 111 (2005) 2752–2759.
- [136] S. Jana, H. Zhang, G.D. Lopaschuk, D.H. Freed, C. Sergi, P.F. Kantor, G.Y. Oudit, Z. Kassiri, Disparate Remodeling of the Extracellular Matrix and Proteoglycans in Failing Pediatric Versus Adult Hearts, *J Am Heart Assoc* 7 (2018), e010427.
- [137] S. Yagi, K. Aihara, Y. Ikeda, Y. Sumitomo, S. Yoshida, T. Ise, T. Iwase, K. Ishikawa, H. Azuma, M. Akaike, T. Matsumoto, Pitavastatin, an HMG-CoA reductase inhibitor, exerts eNOS-independent protective actions against angiotensin II induced cardiovascular remodeling and renal insufficiency, *Circ Res* 102 (2008) 68–76.
- [138] P. Li, D. Wang, J. Lucas, S. Oparil, D. Xing, X. Cao, L. Novak, M.B. Renfrow, Y. F. Chen, Atrial natriuretic peptide inhibits transforming growth factor beta-induced Smad signaling and myofibroblast transformation in mouse cardiac fibroblasts, *Circ Res* 102 (2008) 185–192.

- [139] Y. Xia, K. Lee, N. Li, D. Corbett, L. Mendoza, N.G. Frangogiannis, Characterization of the inflammatory and fibrotic response in a mouse model of cardiac pressure overload, *Histochem Cell Biol* 131 (2009) 471–481.
- [140] X.R. Huang, A.C. Chung, F. Yang, W. Yue, C. Deng, C.P. Lau, H.F. Tse, H.Y. Lan, Smad3 mediates cardiac inflammation and fibrosis in angiotensin II-induced hypertensive cardiac remodeling, *Hypertension* 55 (2010) 1165–1171.
- [141] V. Divakaran, J. Adrogue, M. Ishiyama, M.L. Entman, S. Haudek, N. Sivasubramanian, D.L. Mann, Adaptive and maladaptive effects of SMAD3 signaling in the adult heart after hemodynamic pressure overloading, *Circ Heart Fail* 2 (2009) 633–642.
- [142] K.V. Engebretsen, K. Skardal, S. Bjornstad, H.S. Marstein, B. Skrbcic, I. Sjaastad, G. Christensen, J.L. Bjornstad, T. Tonnessen, Attenuated development of cardiac fibrosis in left ventricular pressure overload by SM16, an orally active inhibitor of ALK5, *J Mol Cell Cardiol* 76 (2014) 148–157.
- [143] S.M. Tan, Y. Zhang, K.A. Connelly, R.E. Gilbert, D.J. Kelly, Targeted inhibition of activin receptor-like kinase 5 signaling attenuates cardiac dysfunction following myocardial infarction, *Am J Physiol Heart Circ Physiol* 298 (2010) H1415–H1425.
- [144] J.L. Bjornstad, B. Skrbcic, H.S. Marstein, A. Hasic, I. Sjaastad, W.E. Louch, G. Florholmen, G. Christensen, T. Tonnessen, Inhibition of SMAD2 phosphorylation preserves cardiac function during pressure overload, *Cardiovasc Res* 93 (2012) 100–110.
- [145] I. Russo, N.G. Frangogiannis, Diabetes-associated cardiac fibrosis: Cellular effectors, molecular mechanisms and therapeutic opportunities, *J Mol Cell Cardiol* 90 (2016) 84–93.
- [146] M. Cavalera, J. Wang, N.G. Frangogiannis, Obesity, metabolic dysfunction, and cardiac fibrosis: pathophysiological pathways, molecular mechanisms, and therapeutic opportunities, *Transl Res* 164 (2014) 323–335.
- [147] K. Sharma, Obesity, oxidative stress, and fibrosis in chronic kidney disease, *Kidney Int Suppl* 4 (2011) 113–117.
- [148] M. Packer, D.W. Kitzman, Obesity-Related Heart Failure With a Preserved Ejection Fraction: The Mechanistic Rationale for Combining Inhibitors of Aldosterone, Nephilysin, and Sodium-Glucose Cotransporter-2, *JACC Heart Fail* 6 (2018) 633–639.
- [149] I. Talior-Volodarsky, K.A. Connelly, P.D. Arora, D. Gullberg, C.A. McCulloch, $\alpha 11$ integrin stimulates myofibroblast differentiation in diabetic cardiomyopathy, *Cardiovasc Res* 96 (2012) 265–275.
- [150] C. Gonzalez-Quesada, M. Cavalera, A. Biernacka, P. Kong, D.W. Lee, A. Saxena, O. Frunza, M. Dobaczewski, A. Shinde, N.G. Frangogiannis, Thrombospondin-1 induction in the diabetic myocardium stabilizes the cardiac matrix in addition to promoting vascular rarefaction through angiotensin-2 upregulation, *Circ Res* 113 (2013) 1331–1344.
- [151] S. Ares-Carrasco, B. Picatoste, A. Benito-Martin, I. Zubiri, A.B. Sanz, M. D. Sanchez-Nino, A. Ortiz, J. Egado, J. Tunon, O. Lorenzo, Myocardial fibrosis and apoptosis, but not inflammation, are present in long-term experimental diabetes, *Am J Physiol Heart Circ Physiol* 297 (2009) H2109–H2119.
- [152] T. Matsubara, M. Araki, H. Abe, O. Ueda, K. Jishage, A. Mima, C. Goto, T. Tominaga, M. Kinoshita, S. Kishi, K. Nagai, N. Iehara, N. Fukushima, T. Kita, H. Arai, T. Doi, Bone Morphogenetic Protein 4 and Smad1 Mediate Extracellular Matrix Production in the Development of Diabetic Nephropathy, *Diabetes* 64 (2015) 2978–2990.
- [153] L. Wu, R. Derynck, Essential role of TGF- β signaling in glucose-induced cell hypertrophy, *Dev Cell* 17 (2009) 35–48.
- [154] K.A. Connelly, D.J. Kelly, Y. Zhang, D.L. Prior, A. Advani, A.J. Cox, K. Thai, H. Krum, R.E. Gilbert, Inhibition of protein kinase C- β by ruboxistaurin preserves cardiac function and reduces extracellular matrix production in diabetic cardiomyopathy, *Circ Heart Fail* 2 (2009) 129–137.
- [155] C. Li, J. Zhang, M. Xue, X. Li, F. Han, X. Liu, L. Xu, Y. Lu, Y. Cheng, T. Li, X. Yu, B. Sun, L. Chen, SGLT2 inhibition with empagliflozin attenuates myocardial oxidative stress and fibrosis in diabetic mice heart, *Cardiovasc Diabetol* 18 (2019) 15.
- [156] G. Jia, J. Habibi, V.G. DeMarco, L.A. Martinez-Lemus, L. Ma, A.T. Whaley-Connell, A.R. Aroor, T.L. Domeier, Y. Zhu, G.A. Meininger, K.B. Mueller, I. Z. Jaffe, J.R. Sowers, Endothelial Mineralocorticoid Receptor Deletion Prevents Diet-Induced Cardiac Diastolic Dysfunction in Females, *Hypertension* 66 (2015) 1159–1167.
- [157] A. Biernacka, N.G. Frangogiannis, Aging and Cardiac Fibrosis, *Aging Dis* 2 (2011) 158–173.
- [158] W.W. Brooks, C.H. Conrad, Myocardial fibrosis in transforming growth factor beta (1) heterozygous mice, *J Mol Cell Cardiol* 32 (2000) 187–195.
- [159] P. Umbarkar, A.P. Singh, M. Gupte, V.K. Verma, C.L. Galindo, Y. Guo, Q. Zhang, J. W. McNamara, T. Force, H. Lal, Cardiomyocyte SMAD4-Dependent TGF- β Signaling is Essential to Maintain Adult Heart Homeostasis, *JACC Basic Transl Sci* 4 (2019) 41–53.
- [160] J. Wang, N. Xu, X. Feng, N. Hou, J. Zhang, X. Cheng, Y. Chen, Y. Zhang, X. Yang, Targeted disruption of Smad4 in cardiomyocytes results in cardiac hypertrophy and heart failure, *Circ Res* 97 (2005) 821–828.
- [161] M. Bujak, H.J. Kweon, K. Chatila, N. Li, G. Taffet, N.G. Frangogiannis, Aging-related defects are associated with adverse cardiac remodeling in a mouse model of reperfused myocardial infarction, *J Am Coll Cardiol* 51 (2008) 1384–1392.
- [162] B. Chen, S. Huang, N.G. Frangogiannis, Aging, cardiac repair and Smad3, *Aging (Albany NY)* 10 (2018) 2230–2232.
- [163] P. Blyszczuk, B. Muller-Edenborn, T. Valenta, E. Osto, M. Stellato, S. Behnke, K. Glatz, K. Basler, T.F. Luscher, O. Distler, U. Eriksson, G. Kania, Transforming growth factor- β -dependent Wnt secretion controls myofibroblast formation and myocardial fibrosis progression in experimental autoimmune myocarditis, *Eur Heart J* 38 (2017) 1413–1425.
- [164] P. Chen, Y. Xie, E. Shen, G.G. Li, Y. Yu, C.B. Zhang, Y. Yang, Y. Zou, J. Ge, R. Chen, H. Chen, Astragaloside IV attenuates myocardial fibrosis by inhibiting TGF- β 1 signaling in coxsackievirus B3-induced cardiomyopathy, *Eur J Pharmacol* 658 (2011) 168–174.
- [165] R.R. Ferreira, R.D.S. Abreu, G. Vilar-Pereira, W. Degraive, M. Meuser-Batista, N.V. C. Ferreira, O. da Cruz Moreira, N.L. da Silva Gomes, E. Mello de Souza, I. P. Ramos, S. Bailly, J.J. Feige, J. Lannes-Vieira, T.C. de Araújo-Jorge, M. C. Waghbi, TGF- β inhibitor therapy decreases fibrosis and stimulates cardiac improvement in a pre-clinical study of chronic Chagas' heart disease, *PLoS Negl Trop Dis* 13 (2019), e0007602.
- [166] A. Geirsson, M. Singh, R. Ali, H. Abbas, W. Li, J.A. Sanchez, S. Hashim, G. Tellides, Modulation of transforming growth factor- β signaling and extracellular matrix production in myxomatous mitral valves by angiotensin II receptor blockers, *Circulation* 126 (2012) S189–S197.
- [167] M.A. Hagler, T.M. Hadley, H. Zhang, K. Mehra, C.M. Roos, H.V. Schaff, R.M. Suri, J.D. Miller, TGF- β signalling and reactive oxygen species drive fibrosis and matrix remodelling in myxomatous mitral valves, *Cardiovasc Res* 99 (2013) 175–184.
- [168] D. Kitkungvan, F. Nabi, R.J. Kim, R.O. Bonow, M.A. Khan, J. Xu, S.H. Little, M. A. Quinones, G.M. Lawrie, W.A. Zoghbi, D.J. Shah, Myocardial Fibrosis in Patients With Primary Mitral Regurgitation With and Without Prolapse, *J Am Coll Cardiol* 72 (2018) 823–834.
- [169] N.G. Frangogiannis, Targeting the transforming growth factor (TGF)- β cascade in the remodeling heart: benefits and perils, *J Mol Cell Cardiol* 76 (2014) 169–171.
- [170] L.K. Huynh, C.J. Hipolito, P. Ten Dijke, A Perspective on the Development of TGF- β Inhibitors for Cancer Treatment, *Biomolecules*, 9, 2019.
- [171] N.G. Frangogiannis, The inflammatory response in myocardial injury, repair, and remodelling, *Nat Rev Cardiol* 11 (2014) 255–265.

RESEARCH ARTICLE | *Integrative Cardiovascular Physiology and Pathophysiology*

Validation of diagnostic criteria and histopathological characterization of cardiac rupture in the mouse model of nonreperfused myocardial infarction

 Anis Hanna, Arti V. Shinde, and Nikolaos G. Frangogiannis

Division of Cardiology, Department of Medicine, The Wilf Family Cardiovascular Research Institute, Albert Einstein College of Medicine, Bronx, New York

Submitted 4 May 2020; accepted in final form 30 August 2020

Hanna A, Shinde AV, Frangogiannis NG. Validation of diagnostic criteria and histopathological characterization of cardiac rupture in the mouse model of nonreperfused myocardial infarction. *Am J Physiol Heart Circ Physiol* 319: H948–H964, 2020. First published September 4, 2020; doi:10.1152/ajpheart.00318.2020.—In patients with myocardial infarction (MI), cardiac rupture is an uncommon but catastrophic complication. In the mouse model of nonreperfused MI, reported rupture rates are highly variable and depend not only on the genetic background and sex of animals but also on the method used for documentation of rupture. In most studies, diagnosis of cardiac rupture is based on visual inspection during autopsy; however, criteria are poorly defined. We performed systematic histopathological analysis of whole hearts from C57BL/6J mice dying after nonreperfused MI and evaluated the reliability of autopsy-based criteria in identification of rupture. Moreover, we compared the cell biological environment of the infarct between rupture-related and rupture-independent deaths. Histopathological analysis documented rupture in 50% of mice dying during the first week post-MI. Identification of a gross rupture site was highly specific but had low sensitivity; in contrast, hemothorax had high sensitivity but low specificity. Mice with rupture had lower myofibroblast infiltration, accentuated macrophage influx, and a trend toward reduced collagen content in the infarct. Male mice had increased mortality and higher incidence of rupture. However, infarct myeloid cells harvested from male and female mice at the peak of the incidence of rupture had comparable inflammatory gene expression. In conclusion, the reliability of autopsy in documentation of rupture in infarcted mice is dependent on the specific criteria used. Macrophage-driven inflammation and reduced activation of collagen-secreting reparative myofibroblasts may be involved in the pathogenesis of post-MI cardiac rupture.

NEW & NOTEWORTHY We show that cardiac rupture accounts for 50% of deaths in C57BL/6J mice undergoing nonreperfused myocardial infarction protocols. Overestimation of rupture events in published studies likely reflects the low specificity of hemothorax as a criterion for documentation of rupture. In contrast, identification of a gross rupture site has high specificity and low sensitivity. We also show that mice dying of rupture have increased macrophage influx and attenuated myofibroblast infiltration in the infarct. These findings are consistent with a role for perturbations in the balance between inflammatory and reparative responses in the pathogenesis of postinfarction cardiac rupture. We also report that the male predilection for rupture in infarcted mice is not associated with increased inflammatory activation of myeloid cells.

cardiac rupture; fibroblast; inflammation; macrophage; myocardial infarction

INTRODUCTION

Despite a steady reduction in mortality rates over the past three decades, acute myocardial infarction (MI) remains a deadly disease. In-hospital mortality for ST elevation MI (STEMI) is 4.6% for men and 7.4% for women (90). Patients with non-STEMI have a slightly lower in-hospital mortality than STEMI patients (3.9 and 4.8% for men and women, respectively) (90). In human MI patients, early death is most often due to dysrhythmias or acute pump failure leading to cardiogenic shock (47, 73). In the era of interventional reperfusion, mechanical complications of acute MI (such as left ventricular free wall rupture, ventricular septal rupture, or acute mitral regurgitation due to rupture of the papillary muscle) have become uncommon. The incidence of rupture has decreased from as high as 20% in the 1970s and 1980s to as low as 1–3% in the current era (28). However, the consequences of rupture remain catastrophic, as it may account for 5–20% of all in-hospital mortality after MI (28). It should be noted that the true incidence of free wall rupture may be underestimated, as many sudden pre-hospitalization deaths in MI patients may be due to rupture (41). Patients surviving acute MI remain at high risk for adverse remodeling of the ventricle, which is typically associated with development of chronic heart failure, increased incidence of arrhythmias, and increased late mortality.

Understanding the cellular mechanisms and molecular pathways involved in cardiac injury, repair, and remodeling is critical for the development of new therapeutic strategies for MI patients. Over the past 25 years, mouse models of MI have emerged as key tools for dissection of molecular mechanisms and for designing and testing therapeutic interventions (57, 66). Undoubtedly, the strength of the mouse model lies in the systematic analysis of functional, cell biological, molecular, and proteomic end points that, when coupled with relevant genetic or pharmacological interventions, can contribute to dissection of cellular responses and molecular networks. However, in clinical trials, mortality rate and incidence of adverse cardiac events represent the most important end points when the effects of various therapeutic approaches in acute MI are tested. Thus, acquisition of translationally relevant insights from mouse models requires systematic study of mortality end points and careful identification of the cause of death. Unfortunately, systematic pathological analysis of the cause of death in mice undergoing MI protocols is challenging and often impractical. It is widely believed that in mouse models of nonreperfused MI cardiac rupture is the predominant cause of

Correspondence: N. G. Frangogiannis (nikolaos.frangogiannis@einsteinmed.org).

death, typically occurring during the first week after coronary occlusion (60, 65). In most studies, rupture is assessed through visual inspection by identifying a blood clot around the heart and in the chest cavity (hemothorax) or a perforation site in the infarcted ventricular wall (27, 65, 71, 97).

Considering the obvious challenges in identifying a rupture site that is a few micrometers wide through visual inspection, we performed systematic histopathological analysis of the whole heart to identify structural causes of death in mice dying after nonreperfused MI. In contrast to the very high incidence of rupture reported in the majority of studies using gross pathologic criteria, only 50% of deaths during the first week post-MI could be attributed to histopathologically documented rupture. The reliability of visual inspection for identification of rupture was dependent on the specific criteria used: identification of a rupture site had high specificity but low sensitivity, whereas addition of hemothorax as a criterion markedly increased sensitivity but reduced specificity. Mice with rupture had lower cardiac myofibroblast infiltration and accentuated macrophage influx compared with animals with -non-rupture-related deaths. Male mice had increased mortality and higher incidence of rupture; however, this was not associated with consistent differences in inflammatory gene expression in myeloid cells.

METHODS

Mouse model of nonreperfused MI. Animal studies were approved by the Institutional Animal Care and Use Committee at Albert Einstein College of Medicine and conformed with the *Guide for the Care and Use of Laboratory Animals*, published by the National Institutes of Health. A model of nonreperfused myocardial infarction induced through coronary ligation was used, as previously described by our group (80). Female and male C57BL/6J mice (49 mice: 20 males and 29 females), 2–4 mo of age, were anesthetized using inhaled isoflurane (4% for induction, 2% for maintenance). For analgesia, buprenorphine (0.05–0.2 mg/kg sc) was administered at the time of surgery and ~12 h thereafter for 2 days. Additional doses of analgesics were given if the animals appeared to be experiencing pain (based on criteria such as immobility and failure to eat). Intraoperatively, heart rate, respiratory rate and electrocardiogram were continuously monitored, and the depth of anesthesia was assessed using the toe pinch method. The left anterior descending coronary artery was occluded. Mice were followed for 7 days. Dead mice underwent autopsy to determine the cause of death. Mice with rupture were identified through visual inspection. Criteria for rupture included visualization of a perforation site (rupture site, RS) and a thrombus or blood in the chest (hemothorax, Hem). Hearts were then harvested for histological analysis, fixed in zinc-formalin (Anatech, Ltd., Fisher Scientific) and embedded in paraffin.

Histological analysis. For histopathological analysis, murine hearts were fixed in zinc-formalin (Z-fix; Anatech, Battle Creek, MI), and embedded in paraffin. Infarcted hearts were sectioned from base to apex at 250- μ m intervals, thus reconstructing the whole heart, as previously described (10, 11, 40). Ten sections (5 μ m thick) were cut at each level. To determine the final infarct size, the first section at each partition was stained with hematoxylin and eosin (H&E). To identify the site of the rupture, sections from all levels were carefully examined.

Quantitative morphometry. Morphometric parameters were quantitatively assessed using Zen 2.6 Pro software (Zeiss Microscopy, White Plains, NY). The infarcted and noninfarcted areas were measured at each level, and the volume of the infarct and of the noninfarcted remodeling myocardium at each level was calculated as: infarct volume = infarct area \times 300 μ m (250 μ m + 10 sections \times 5

μ m = 300 μ m) and volume of noninfarcted myocardium = noninfarcted area \times 300 μ m. The total volume of the infarcted and noninfarcted myocardium was calculated as the sum of the volumes of each partition. Scar size was measured by dividing the volume of the infarct to the total volume of the left ventricle (left ventricular volume = infarct volume + volume of noninfarcted myocardium) and was expressed as a percentage.

To measure infarct thickness, maximum and minimum dimensions were measured from the endocardial to the epicardial surface of the transmural infarct wall at each level. The average minimum and average maximum wall thicknesses were then calculated. Similarly, maximum and minimum thickness of the noninfarcted segments was measured from all levels, and the average maximum and minimum thickness was calculated. Mean wall thickness of the infarct and of the noninfarcted area was the average of the maximum and minimum wall thickness.

Infarct length was calculated by measuring the length of the endocardial surface of the transmural infarct at each level, cutting through (excluding) the papillary muscles. The average length from all levels was reported as length of the infarct.

Immunohistochemistry. For histopathological analysis, murine hearts were fixed in zinc-formalin and embedded in paraffin. For comparisons of histological parameters between mice with and without rupture, only mice that died between 3 and 7 days after coronary occlusion were included; thus, one mouse that died in the absence of rupture 2 days after coronary occlusion was excluded (rupture group: 5.0 ± 0.53 days, $n = 7$; no rupture group: 5.16 ± 0.4 , $n = 6$). Picrosirius red staining was used to label the collagen fibers, as previously described (1). To identify myofibroblasts in the infarct, sections were stained with an anti- α -smooth muscle actin (α -SMA) antibody (1:100 dilution, Sigma, F3777), as previously described (80). Myofibroblasts were identified as spindle-shaped α -SMA-positive cells located outside the vascular media. Macrophages were stained using anti-Mac2 antibody (CL8942AP; Cedarlane, Burlington, ON, Canada) in 1:200 dilution, as previously described (25). Briefly, sections were deparaffinized, and heat-mediated antigen retrieval was performed for 25 min during incubation of the slides in citrate buffer, pH 6.0 (Sigma, C9999). Sections were then blocked with 10% serum of the species in which the secondary antibody was raised for 1 h and then incubated overnight at 4°C with the primary antibody. Sections were then washed and incubated with a fluorescently labeled secondary antibody for 1 h at room temperature. Autofluorescence quenching was performed using TrueBlack Lipofuscin Autofluorescence Quencher (23007; Biotium, Fremont, CA). Slides were mounted using Fluoro-Gel II with DAPI (17985; EMS, Hatfield, PA). Slides were then scanned using Zen 2.6 Pro software and the Zeiss Imager M2 microscope (Carl Zeiss Microscopy, White Plains, NY).

Machine learning-based quantitative analysis of myofibroblast density. Using default algorithms of the Intellesis Trainable Segmentation module of Zen 2.6 Pro software, an artificial intelligence (AI)-based model was trained on multiple fields of different regions of the myocardium to segment the images and identify myofibroblasts. Objects of interest were defined as the DAPI- α -SMA double-positive profiles, excluding vascular smooth muscle cells (VSMCs). The unstained myocardium (including VSMCs) was considered as background. By use of the Image Analysis module, specific settings were incorporated in the trained model to count the segmented objects. Automatic analysis of 10 fields from two different levels of the murine heart was performed using the trained model. Validation of the AI model was performed by manually counting myofibroblast density in 20 fields from four different mice with ImageJ software. There was an excellent correlation ($r = 0.98$) between the AI-based quantification and the myofibroblast density derived through manual counting (Fig. 1, A–C).

Machine learning-based quantitative analysis of macrophage density. Similarly, an AI-based model was trained to segment the images and identify macrophages. DAPI-Mac2 double-positive objects were identified as the objects of interest, while the unstained

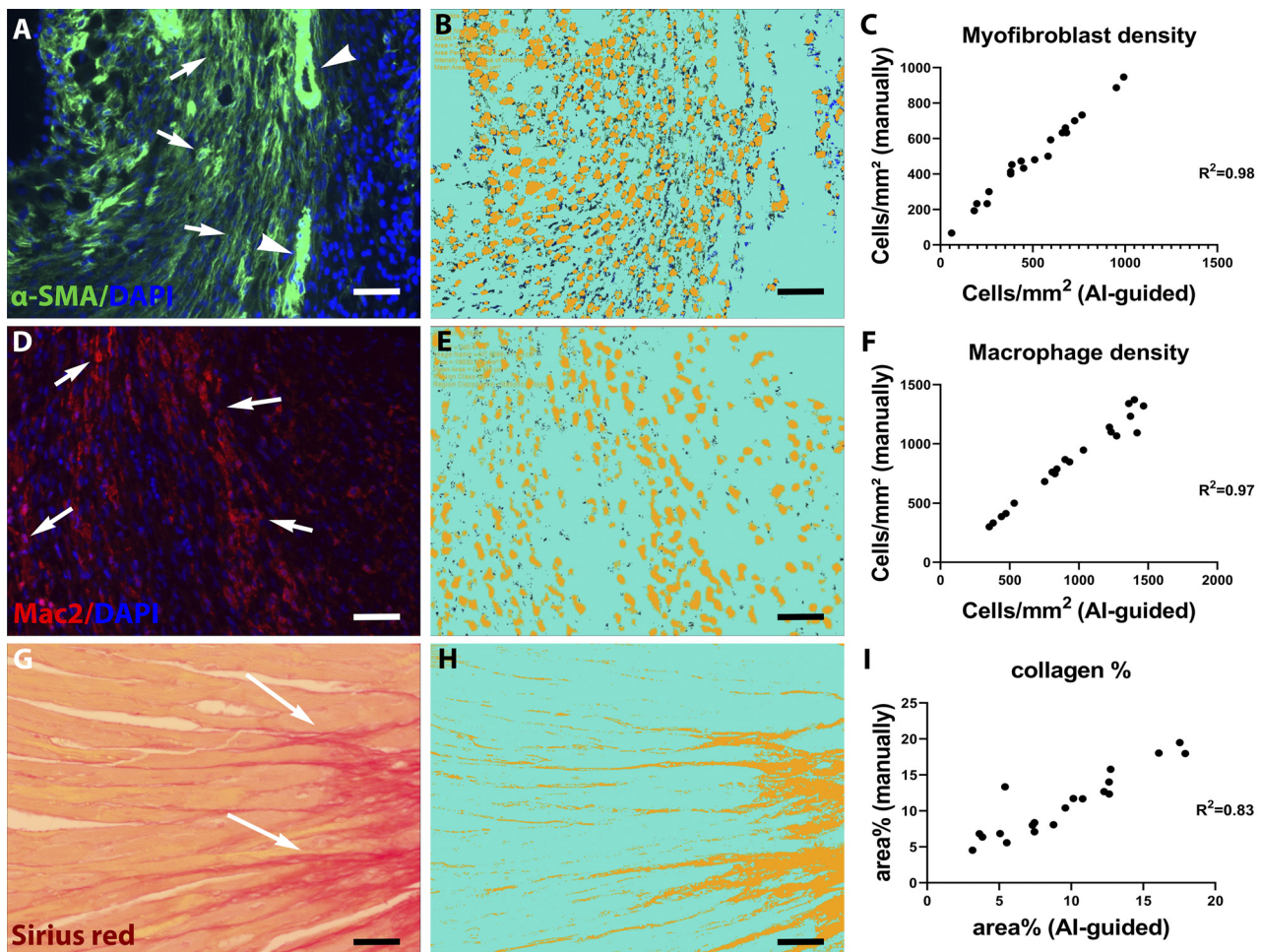


Fig. 1. Validation of artificial intelligence (AI)-based quantification protocols of myofibroblast density, macrophage density, and collagen content. *A–C*: α -smooth muscle actin (α -SMA) immunofluorescence was used to identify myofibroblasts as spindle-shaped immunoreactive cells located outside the vascular media (*A*, arrows). Arrowheads show vascular smooth muscle cells (VSMCs). The Intellesis Trainable Segmentation module of Zen 2.6 Pro software (Carl Zeiss Microscopy, New York, NY), an AI-based model, was trained on multiple fields of different regions of the myocardium to segment the images and identify myofibroblasts. Objects of interest were defined as the DAPI- α -SMA double-positive profiles, excluding VSMCs. *B*: unstained myocardium (including VSMCs) was considered the background. The trained AI-based model exhibited excellent correlation with manual measurement of myofibroblast density in the same fields ($r = 0.98$, $P < 0.0001$, $n = 20$). *D–F*: Mac2 immunofluorescence was used to identify macrophages (arrows). The AI-based quantification model was validated, showing excellent correlation with manual counts ($r = 0.97$, $P < 0.0001$, $n = 20$). *G–I*: Picrosirius red staining was used to label collagen fibers. The AI-based quantification model showed excellent correlation with manual quantification of collagen content ($r = 0.83$, $P < 0.0001$, $n = 20$). Scale bar, 20 μm .

myocardium was considered the background. By use of the Image Analysis module, specific settings were incorporated in the trained model to count the segmented objects. Automatic analysis of 10 fields from two different levels of the murine heart was performed using the trained model. Validation of the AI model was performed by manually counting macrophage densities in 20 fields from different mice with ImageJ software. There was an excellent correlation ($r = 0.97$) between the AI-based quantification and the manual counts (Fig. 1, *D–F*).

Machine learning-based quantitative analysis of collagen content. An AI-based model was trained on multiple fields of different regions of the myocardium to segment Picrosirius red-stained collagen fibers. Red fibrillar staining was considered the object of interest, while the unstained myocardium was considered the background. By use of the Image Analysis module, specific settings were incorporated in the trained model to count the segmented objects. Automatic analysis of 10 fields from two different levels of the murine heart was performed using the trained model. Validation of the AI model was performed by quantifying the collagen content in 20 fields from different mice with ImageJ software. There was an excellent correlation ($r = 0.83$) be-

tween the AI-based quantification and the measurements using the standard approach (Fig. 1, *G–I*).

Dual immunofluorescence for identification and quantification of M_1 and M_2 macrophages. Dual immunofluorescent staining was performed to identify M_1 and M_2 macrophages. Staining for inducible nitric oxide synthase (iNOS) using a rabbit anti-iNOS antibody (dilution 1:100; Abcam, Cambridge, MA) was used as an M_1 marker, whereas staining for arginase-1 (Arg1) using a rabbit anti-Arg1 antibody (dilution 1:100; Genetex, Irvine, CA) was used as an M_2 marker. Sections were deparaffinized, and heat-mediated antigen retrieval was performed for 25 min during incubation of the slides in citrate buffer, pH 6.0 (Sigma, C9999). Sections were then blocked with 10% serum for 1 h and then incubated overnight at 4°C with Mac2 antibody together with anti-iNOS or anti-Arg1 antibodies. Sections were then washed and incubated with fluorescently labeled secondary antibodies for 1 h at room temperature. Autofluorescence quenching was performed using TrueBlack Lipofuscin Autofluorescence Quencher (23007, Biotium). Slides were mounted using Fluoro-Gel II with DAPI (17985, EMS). Sections were then scanned using Zen 2.6 Pro software and the Zeiss Imager M_2 microscope. Mac2-

positive cells were identified as macrophages. $iNOS^+$ / $Mac2^+$ cells were manually counted using ImageJ software to assess the density of M_1 macrophages. Similarly, $Arg1^+$ / $Mac2^+$ cells were manually counted to assess the density of M_2 macrophages.

Isolation of infarct myeloid cells and mRNA extraction. Four male and four female C57BL/6J mice underwent 4-day coronary occlusion protocols to harvest myeloid cells. Myocardial tissue from individual mice was finely minced and placed into a digestion buffer cocktail (1 mL of 0.5 mg/mL Liberase TH research grade, no. 05401151001, Millipore Sigma), 20 U/mL DNase I (no. D4513, Sigma-Aldrich), 10 mmol/L HEPES (Invitrogen), and 0.1% sodium azide in HBSS with Ca^{2+} and Mg^{2+} (Invitrogen). The tissue was then shaken at 37°C for 5 min, and cells were then passed through a 40- μ m nylon mesh. The digestion process was repeated four times, cell suspension was collected after it was passed through nylon mesh each time, and finally

the total pooled cell suspension was centrifuged (10 min, 500 g, 4°C). Up to 10^8 cells were reconstituted with 180 μ L of MACS buffer (Miltenyi Biotec, 130-091-376). Cells in MACS buffer were incubated with 20 μ L of Anti-Ly-6G MicroBeads UltraPure (Cat. No. 130-120-337), incubated for 10 min at 4°C, and then washed once and centrifuged. The cells were resuspended in MACS buffer and passed through a MS column (Cat. No. 130-042-201) in a MACS separator (Miltenyi Biotec, 130-090-312). The magnetically labeled Ly6G⁺ cells were retained on the column. The unlabeled cells (Ly-6G negative flow through) were collected and washed once with MACS buffer (Ly6G⁻ cells) and centrifuged at 500 g for 10 min. Subsequently, the cell pellet (per 10^8 Ly6G⁻ cells) was again resuspended in 180 μ L of MACS buffer, incubated with 20 μ L of CD11b microBeads (Miltenyi Biotec, Cat. No. 130-049-601) at 4°C for 15 min, and then washed once and centrifuged. Resuspended cells went through a MACS column set in

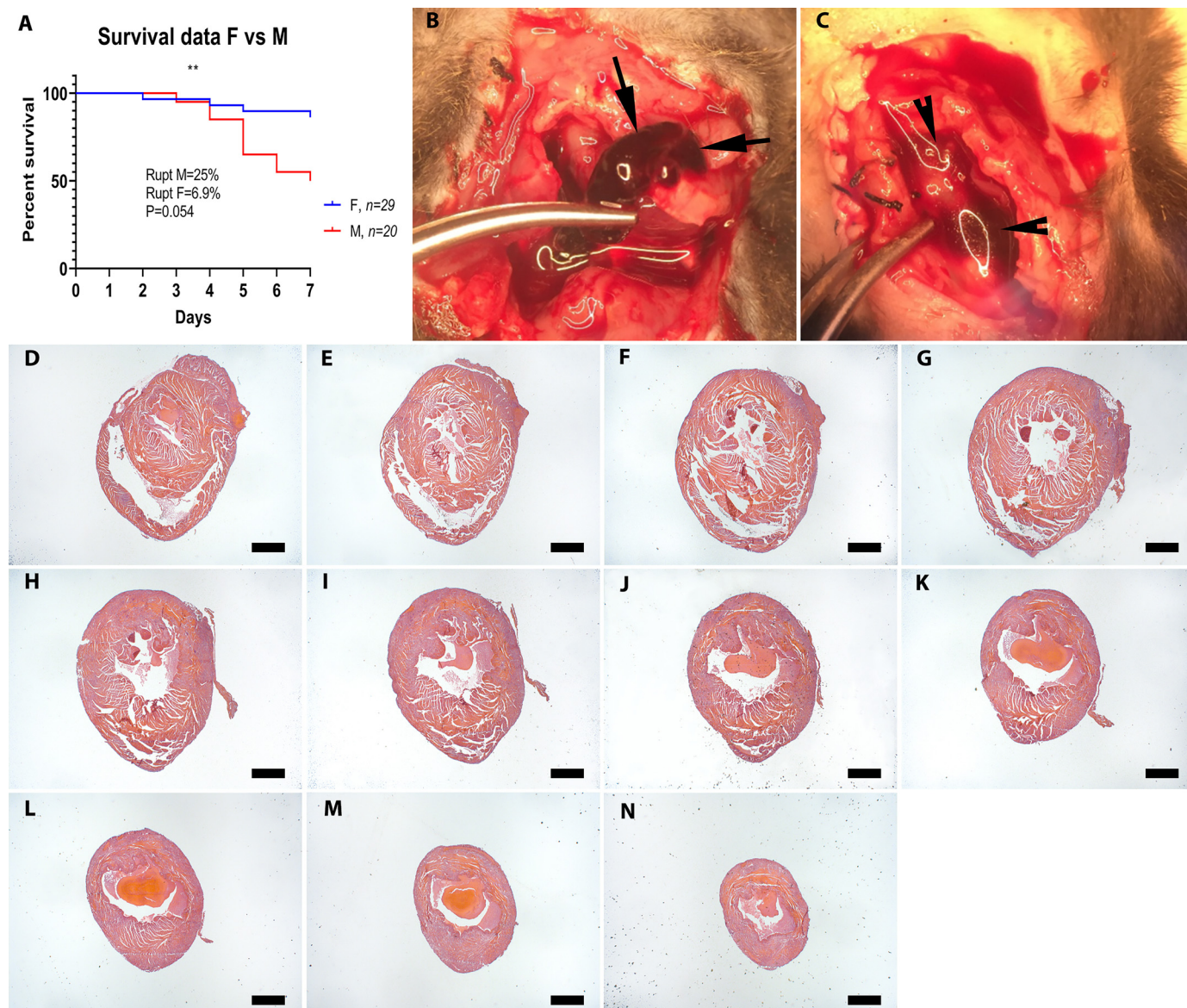


Fig. 2. Sex-specific mortality in infarcted mice and use of visual inspection vs. systematic histological analysis to identify the cause of death. A: when compared with female (F) C57BL/6J mice, male (M) animals had significantly higher post-myocardial infarction (MI) mortality (** $P < 0.009$), and a trend toward increased cardiac rupture rates ($P = 0.054$, $n = 29$ F, 20 M). To identify rupture-related deaths, visual inspection criteria were used. Criteria for rupture included a blood clot or blood in the chest (hemothorax; B and C, arrows) or presence of a cardiac rupture site. D–N: systematic histological analysis was performed by sectioning the entire heart from base to apex at 300- μ m partitions and staining the first section of each partition (D–N shows consecutive myocardial sections used to systematically study the cause the death. Scale bar, 1 mm.

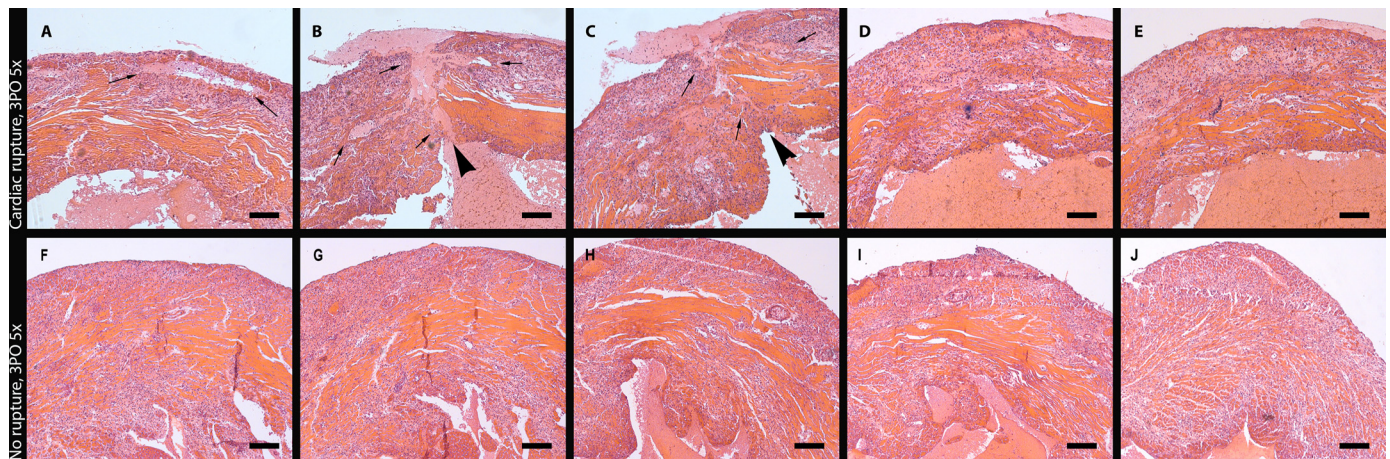


Fig. 3. Histological documentation of left ventricular free wall rupture in mice dying after myocardial infarction (MI). A–E: consecutive sections show the site of the intramural rupture track (arrowheads) in an animal dying of rupture 3 days after permanent coronary occlusion. Arrows show the borders of the ruptured area. F–J: systematic histological analysis of myocardial sections documents the absence of rupture in a representative mouse that died 3 days after coronary occlusion. Scale bar, 200 μ m.

a MACS separator. The magnetically labeled CD11b⁺ cells were retained on the column. Ly6G-CD11b⁺ cells (macrophages) were flushed out and harvested for RNA isolation.

PCR array. Gene expression in macrophages harvested from male and female mice was compared after 4 days of coronary occlusion. For PCR array, total RNA was extracted using the TRIzol reagent (Qiagen, 79306). A total of 400 ng of RNA was transcribed into cDNA using the RT² first-strand kit (Qiagen, 330404). Quantitative PCR was then performed using the RT² Profiler Mouse PCR Array Chemokines & Receptors (PAMM-022ZE-4) from Qiagen according to the manufacturer's protocol. The same thermal profile conditions were used for all primer sets: 95°C for 10 min, 40 cycles at 95°C for 15 s, followed at 60°C for 1 min. The data obtained were analyzed using the Δ Cq method. Gene expression levels were normalized to the levels of GAPDH.

Statistical analysis. For all analyses, normal distribution was tested using the Shapiro–Wilk normality test. For comparisons of two groups unpaired two-tailed Student's *t* test using (when appropriate) Welch's correction for unequal variances was performed. The Mann–Whitney test was used for comparisons between two groups that did not show Gaussian distribution. For comparisons of multiple groups, one-way ANOVA was performed followed by Tukey's multiple comparison test. The Kruskal–Wallis test, followed by Dunn's multiple comparison posttest was used when one or more groups did not show Gaussian distribution. Survival analysis was performed using the Kaplan–Meier method. Mortality was compared using the log rank test. Correlation analysis between manual and AI-based quantifications was done using the Pearson correlation coefficient (Pearson's *r*). Data are expressed as means \pm SE. Statistical significance was set at *P* < 0.05.

RESULTS

Male C57BL/6J mice exhibit higher mortality than female animals following nonreperfused MI. Forty-nine mice on a C57BL/6J background (20 males and 29 females) underwent nonreperfused MI protocols and were followed for 7 days. Mortality during the first week post-MI was 28.6%; deaths occurred between days 2 and 7 (mean: 4.9 ± 0.38 , *n* = 14). Male animals had significantly higher mortality than female mice (Fig. 2A, males: 50% vs, females: 13.79%, *P* = 0.0067). There was no significant difference in the time of death between male and female animals [male, 5 ± 0.37 days, *n* = 10; female, 4.5 ± 1.04 days, *n* = 4, *P* = not significant (NS)].

Visual inspection has low specificity for identification of cardiac rupture in mice dying following MI. The majority of published studies use visual inspection criteria to determine whether rupture is the cause of death in mice undergoing MI protocols. In our study, visual inspection during autopsy (Fig. 2, B and C) suggested that 10 of 14 deaths (71.4%) were due to cardiac rupture based on the identification of a rupture site or the presence of hemothorax. To validate the findings of visual inspection, we performed systematic histopathological analysis of all dead mouse hearts, examining myocardial sections from base (Fig. 2D) to apex (Fig. 2N) at 250- μ m intervals (Fig. 2, D–N). Histological evidence of rupture was found in only 50% of dead mice (Fig. 3, A–E), typically involving the left ventricular free wall at an apical level. In the other 50% of the dead mice, histological analysis documented the absence of rupture (Fig. 3, F–J). Next, we validated specific gross-pathological criteria for documentation of rupture, using systematic histological analysis as the “gold standard.” The presence of hemothorax, or the combined criterion of hemothorax and an identifiable rupture site had a high sensitivity (85.7%) but a relatively low specificity (42.8%) for documentation of rupture in infarcted mice (Table 1). On the other hand, identification of a rupture site or the combined presence of hemothorax and a rupture site were highly specific (85.7%) but had low sensitivity (28.6%). Both rupture-related and rupture-independent deaths were more common in male mice (25% of male mice and only 6.9% of female mice had post-MI cardiac rupture, *P* = 0.054). There was no significant difference in the time of death due to rupture (mean: 5 ± 0.53 days, *n* = 7, range: 3–7 days) versus no rupture (4.7 ± 0.56 days, *n* = 7, range: 2–7 days) for male (rupture: 4.8 ± 0.58 , *n* = 5 versus no rupture:

Table 1. Sensitivity and specificity of gross pathological criteria used for documentation of rupture

	RS	Hem	RS and Hem	RS or Hem
Sensitivity	28.6	85.7	28.6	85.7
Specificity	85.7	42.8	85.7	42.8

RS, rupture site; Hem, hemothorax.

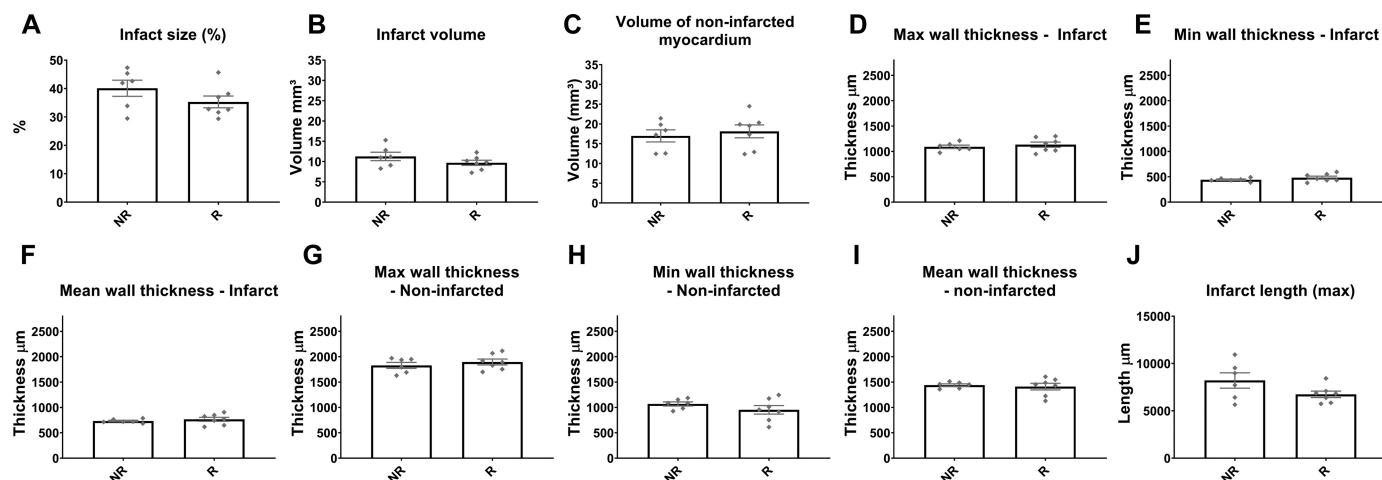


Fig. 4. Rupture is not associated with larger infarcts or thinner infarct walls. Comparison of morphometric end points between mice dying of rupture (R) and animals dying in the absence of rupture (no rupture, NR) showed no significant differences between groups. Infarct size (A), infarct volume (B), volume of noninfarcted myocardium (C), maximal, minimal, and mean thickness of the infarcted wall (D, E, F, respectively), maximal, minimal, and mean wall thickness of the noninfarcted myocardial segments (G, H, I, respectively), and infarct length (J) were comparable between groups ($P =$ not significant, $n = 6-7$ /group). Time points studied histologically were comparable between groups, as there was no significant difference in time of death (R group: 5.0 ± 0.53 days, $n = 7$; NR group: 5.16 ± 0.4 , $n = 6$).

5.2 ± 0.49 , $n = 5$) or female mice (rupture: 5.5 ± 1.5 , $n = 2$; versus no rupture: 3.5 ± 1.5 , $n = 2$).

Mice dying of rupture and animals with rupture-independent deaths have comparable infarct size and infarct wall thickness. To examine whether rupture was associated with larger infarcts, we compared the morphometric characteristics of the infarcted and noninfarcted myocardial segments between mice dying of rupture and animals that died from non-rupture-related causes. Systematic quantitative analysis of hearts sectioned serially from base to apex showed that mice with rupture and those dying from other infarct-related causes had comparable infarct size (Fig. 4A), infarct volume (Fig. 4B), and

volume of noninfarcted myocardium (Fig. 4C), maximal, minimal, and mean thickness of the infarcted and noninfarcted myocardium (Fig. 4, D–I) and infarct length (Fig. 4J). Thus, rupture of the infarcted heart was independent of the size of the infarct or the thickness of the infarcted and noninfarcted segments.

Mice dying of rupture have lower myofibroblast density and a trend toward reduced collagen content in the infarcted area. We next examined whether cardiac rupture might reflect impaired infiltration of the infarct with activated myofibroblasts. Myofibroblast density in the infarct zone was markedly lower in mice dying of cardiac rupture compared with animals dying

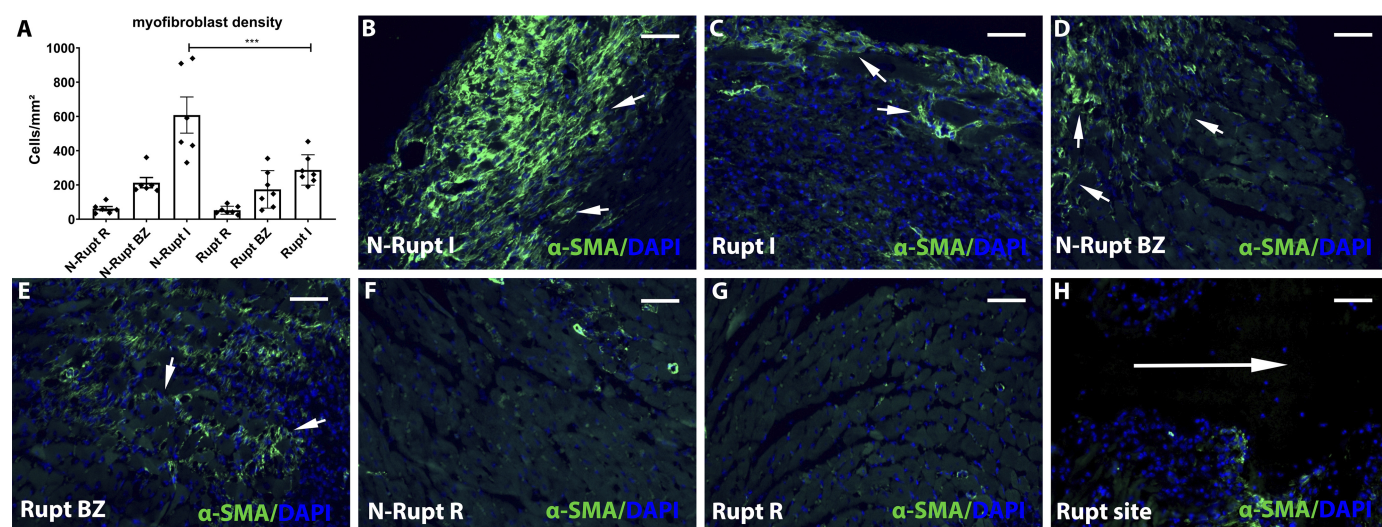


Fig. 5. Rupture is associated with attenuated myofibroblast infiltration in the healing infarct. A: artificial intelligence (AI)-based quantitative analysis showed that mice dying of cardiac rupture had markedly lower myofibroblast density in the infarcted myocardium (I) compared with mice dying the absence of rupture ($***P < 0.0001$, $n = 6-7$ /group). No significant differences were noted in the border zone (BZ) and in the remote remodeling myocardium (R). B–H: representative images show identification of α -smooth muscle actin (α -SMA) + myofibroblasts in infarcted hearts (short arrows). Infarcted segments in mice dying of rupture (C) have attenuated myofibroblast infiltration. H: please note the absence of myofibroblasts in the rupture site (long arrow). Time points studied histologically were comparable between groups, as there was no significant difference in the time of death (rupture group: 5.0 ± 0.53 days, $n = 7$; no rupture group: 5.16 ± 0.4 , $n = 6$). Scale bar, 50μ m.

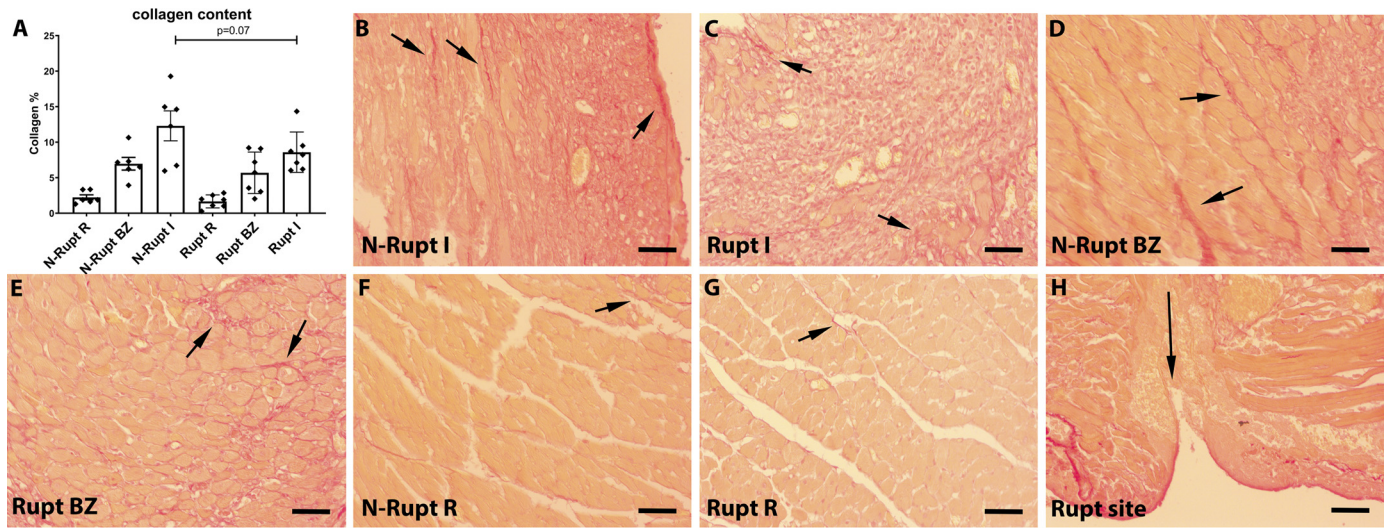


Fig. 6. Rupture is associated with a trend toward reduced collagen deposition in the healing infarct. *A*: quantitative analysis using a machine learning approach showed that collagen content in the infarct (I) was lower in mice dying of rupture (Rupt) compared with animals dying without rupture (N-rupt). However, the difference did not reach statistical significance ($P = 0.07$, $n = 6-7$ /group). No significant differences were noted in the border zone (BZ) and in the remote remodeling myocardium (R). *B-H*: representative images show labeling of collagen fibers using Picrosirius red staining (short arrows). *H*: collagen was absent in the rupture site (long arrow). Time points studied histologically were comparable between groups, as there was no significant difference in the time of death (rupture group: 5.0 ± 0.53 days, $n = 7$; no rupture group: 5.16 ± 0.4 , $n = 6$). Scale bar, 50 μm .

due to rupture-independent pathology ($P < 0.001$; Fig. 5, *A-C*). Very few myofibroblasts could be identified in the area around the rupture track (Fig. 5*H*). In contrast, no significant differences were noted in myofibroblast density in border and remote areas of the noninfarcted myocardium (Fig. 5, *A* and *D-G*).

Picrosirius red staining was used to label collagen fibers. Mice dying from cardiac rupture exhibited a trend toward reduced collagen content in the infarct zone ($P = 0.07$; Fig. 6, *A-C*). Collagen was virtually absent in the areas neighboring the rupture site (Fig. 6*H*). No significant differences in collagen

content were noted in the noninfarcted border and remote myocardial segments (Fig. 6, *A* and *D-G*).

Mice dying of rupture have higher macrophage density in the infarct zone. Mac2 immunohistochemistry was used to label macrophages. Mice dying of rupture had significantly higher macrophage density in the infarct zone ($P < 0.05$; Fig. 7, *A-C*). Abundant Mac2⁺ macrophages were found along the edges of the rupture track (Fig. 7*H*). In contrast, macrophage density in the noninfarcted border and remote myocardial segments was comparable between groups (Fig.

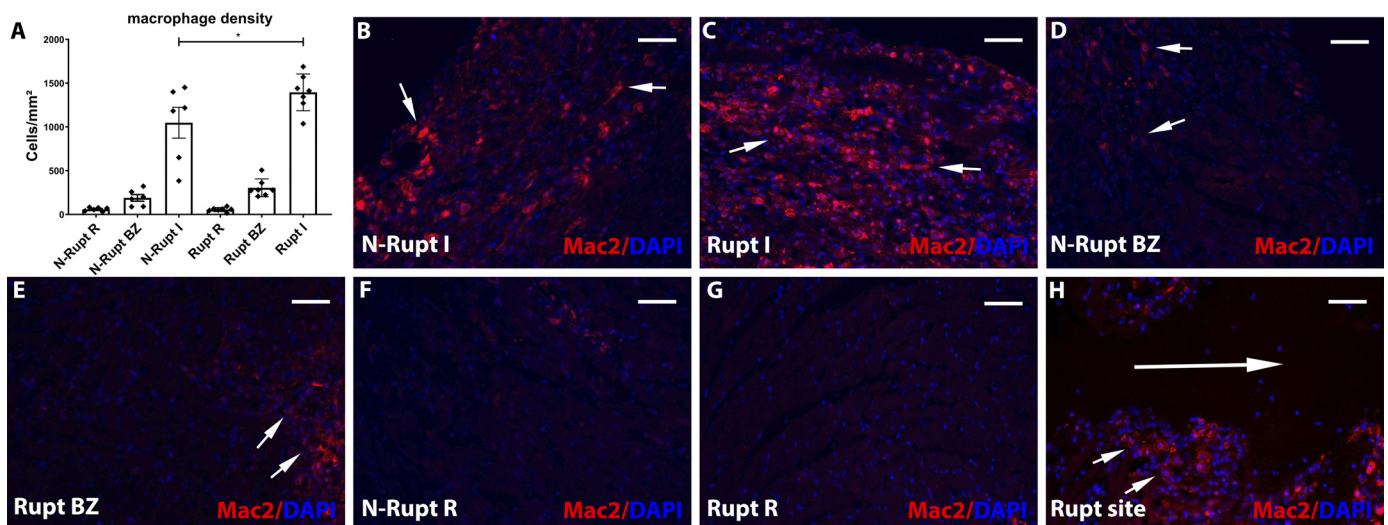


Fig. 7. Rupture is associated with increased macrophage infiltration in the infarcted segment. *A*: quantitative analysis using a machine learning approach showed that macrophage density in the infarct (I) was lower in mice dying of rupture (Rupt) compared with animals dying without rupture (N-rupt) ($*P < 0.05$, $n = 6-7$ /group). No significant differences in macrophage density were noted in the border zone (BZ) and in the remote remodeling myocardium (R). *B-H*: representative images show labeling of macrophages using Mac2 immunofluorescence (short arrows). Mice dying of rupture had significantly increased macrophage infiltration (C). *H*: a significant number of Mac2⁺ macrophages (short arrows) are noted in the edge of the rupture site (long arrow). Time points studied histologically were comparable between groups, as there was no significant difference in the time of death (rupture group: 5.0 ± 0.53 days, $n = 7$; no rupture group: 5.16 ± 0.4 , $n = 6$). Scale bar, 50 μm .

7, A and D–G). To examine potential associations between rupture-related death and macrophage polarization, we identified M₁-like and M₂-like macrophages by using the M₁ marker iNOS and the M₂ marker Arg1. No significant differences were noted in the density of M₁ or M₂ macrophages between animals with rupture and mice that died without rupture (Fig. 8).

Infarct myeloid cells harvested from male and female mice have comparable inflammatory gene expression profiles. To examine whether the increased incidence of rupture in male mice reflected overactive inflammatory responses in myeloid cells, we compared cytokine and chemokine gene expression in sorted myocardial CD11b⁺ myeloid cells harvested from male

and female mice after 4 days of permanent coronary occlusion (the time point corresponding to the peak incidence of cardiac rupture). Expressions of most inflammatory mediators involved in postinfarction remodeling [including C-C motif ligand (CCL)2, CCL3, CCL4, CCL5, CCL9, C-X3-C motif ligand (CX3CL)1, C-X-C motif ligand (CXCL)10, IL-1 β , IL-6, and TNF α] were comparable between cells harvested from male and female animals (Table 2). Expressions of CCL8 and CXCL2 were significantly higher in cells harvested from female mouse infarcts. There were no significant differences in β_2 -integrin, chemokine receptor or Toll-like receptor (TLR)2 and TLR4 levels between groups (Table 2). Thus, the increased incidence of cardiac rupture in male mice could not be attrib-

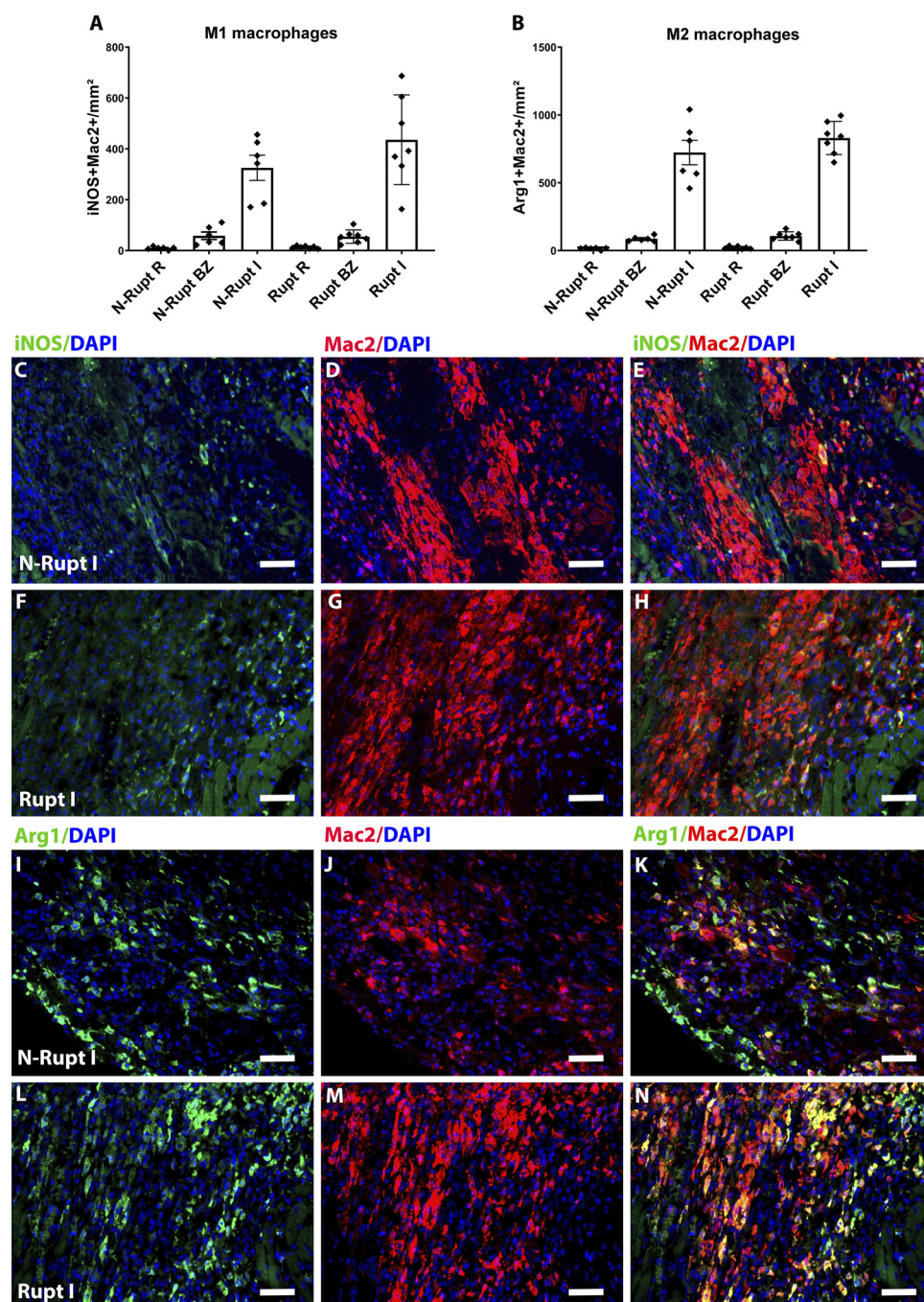


Fig. 8. Rupture is not associated with significant changes in the density of M₁ vs. M₂ macrophages. Quantitative analysis showed no significant differences in the density of inducible NO synthase (iNOS)⁺/Mac2⁺ M₁-like macrophages (A) and arginase-1 (Arg1)⁺/Mac2⁺ M₂-like macrophages (B) between groups ($n = 6-7$ /groups). C–H: dual immunofluorescence for macrophage marker Mac2 (red) and M₁ marker iNOS was used to identify M₁ macrophages. I–N: dual immunofluorescence for Mac2 (red), and M₂ marker Arg1 was used to identify M₂ macrophages. Time points studied histologically were comparable between groups, as there was no significant difference in the time of death (rupture group: 5.0 ± 0.53 days, $n = 7$; no rupture group: 5.16 ± 0.4 , $n = 6$). Scale bar, 50 μ m.

Table 2. *Inflammatory gene expression in infarct myeloid cells from male and female mice*

Gene Name	Gene: GAPDH		P Value
	M	F	
Complement component 5a receptor 1	0.01384	0.01186	0.7648
Chemokine (C-C motif) ligand 11	0.001534	0.005988	0.1437
Chemokine (C-C motif) ligand 12	0.004248	0.002895	0.7157
Chemokine (C-C motif) ligand 17	0.001263	0.002920	0.4909
Chemokine (C-C motif) ligand 19	0.004525	0.004905	0.9018
Chemokine (C-C motif) ligand 2	0.01989	0.01860	0.9172
Chemokine (C-C motif) ligand 22	0.002595	0.0006138	0.4856
Chemokine (C-C motif) ligand 24	0.001781	0.0004637	0.4692
Chemokine (C-C motif) ligand 25	0.0005090	ND	0.3559
Chemokine (C-C motif) ligand 26	0.001375	0.002190	0.4123
Chemokine (C-C motif) ligand 3	0.01030	0.009001	0.8329
Chemokine (C-C motif) ligand 4	0.008491	0.01264	0.4811
Chemokine (C-C motif) ligand 5	0.004289	0.002758	0.5280
Chemokine (C-C motif) ligand 6	0.1727	0.07732	0.3568
Chemokine (C-C motif) ligand 7	0.01639	0.02507	0.3653
Chemokine (C-C motif) ligand 8	0.005768	0.01586	0.0257
Chemokine (C-C motif) ligand 9	0.009111	0.003166	0.1254
Chemokine (C-C motif) receptor 1	0.006143	0.01291	0.2774
Chemokine (C-C motif) receptor 10	0.003331	ND	0.4226
Chemokine (C-C motif) receptor 1-like 1	0.003002	ND	0.4226
Chemokine (C-C motif) receptor 2	0.007806	0.01448	0.4072
Chemokine (C-C motif) receptor 3	0.006727	0.004839	0.5371
Chemokine (C-C motif) receptor 4	0.0005084	0.001546	0.2750
Chemokine (C-C motif) receptor 5	0.004950	0.01017	0.2352
Chemokine (C-C motif) receptor 6	0.0003573	0.0005493	0.7640
Chemokine (C-C motif) receptor 7	0.005574	0.007365	0.6991
Chemokine (C-C motif) receptor 8	ND	ND	
Chemokine (C-C motif) receptor 9	0.003901	ND	0.3912
Chemokine (C-C motif) receptor-like 1	0.0006560	0.0006533	0.9972
Chemokine (C-C motif) receptor-like 2	0.004157	0.001810	0.3649
Chemokine-like receptor 1	0.003178	0.002272	0.7852
Cklf-like Marvel Tm domain containing 2a	ND	0.0004849	0.3559
Cklf-like Marvel Tm domain containing 3	0.01266	0.01048	0.7589
Cklf-like Marvel Tm domain containing 4	0.003410	0.0006223	0.4047
Cklf-like Marvel Tm domain containing 5	ND	ND	
Cklf-like Marvel Tm domain containing 6	0.003730	0.01734	0.0642
Chemokine (C-X3-C motif) ligand 1	0.001861	0.001978	0.9398
Chemokine (C-X3-C) receptor 1	0.001722	0.002541	0.6002
Chemokine (C-X-C motif) ligand 1	0.002253	0.002495	0.8746
Chemokine (C-X-C motif) ligand 10	0.01534	0.008975	0.0814
Chemokine (C-X-C motif) ligand 11	ND	ND	
Chemokine (C-X-C motif) ligand 12	0.05222	0.1065	0.3271
Chemokine (C-X-C motif) ligand 13	0.002535	0.007473	0.1327
Chemokine (C-X-C motif) ligand 14	0.0001556	ND	0.3559
Chemokine (C-X-C motif) ligand 15	0.0009104	0.0005166	0.6322
Chemokine (C-X-C motif) ligand 16	0.008578	0.009264	0.8886
Chemokine (C-X-C motif) ligand 2	0.01357	0.02451	0.0080
Chemokine (C-X-C motif) ligand 3	0.003016	0.002059	0.4415
Chemokine (C-X-C motif) ligand 5	0.003116	0.001180	0.5320
Chemokine (C-X-C motif) ligand 9	0.0001775	ND	0.3559
Chemokine (C-X-C motif) receptor 1	ND	ND	
Chemokine (C-X-C motif) receptor 2	0.0004524	ND	0.4226
Chemokine (C-X-C motif) receptor 3	ND	ND	
Chemokine (C-X-C motif) receptor 4	0.02041	0.01743	0.7842
Chemokine (C-X-C motif) receptor 5	0.001828		0.1638
Chemokine (C-X-C motif) receptor 6	ND	0.001712	0.3559
Chemokine (C-X-C motif) receptor 7	0.001689	0.002191	0.7732

Continued

Gene Name	Gene: GAPDH		P Value
	M	F	
Duffy blood group, chemokine receptor	ND	0.0005270	0.3559
Formyl peptide receptor 1	0.001797	0.001522	0.9107
G protein-coupled receptor 17	0.002156	0.001442	0.6295
Hypoxia-inducible factor 1 α	0.01286	0.01349	0.9058
Interferon- γ	ND	ND	
Interleukin-16	0.0009023	0.0002709	0.3070
Interleukin-1 β	0.04332	0.03605	0.6744
Interleukin-4	0.003591	0.00005937	0.3314
Interleukin-6	0.01221	0.008579	0.5687
Integrin- α M	0.02596	0.02443	0.8738
Integrin- β 2	0.04285	0.04131	0.9220
Mitogen-activated protein kinase-1	0.02609	0.01908	0.4511
Mitogen-activated protein kinase-14	0.008821	0.009484	0.8759
Platelet factor 4	0.06353	0.04216	0.2131
Pro-platelet basic protein	0.006339	0.007147	0.8091
Slit homolog 2 (<i>Drosophila</i>)	0.0004225	ND	0.1389
Transforming growth factor- β 1	0.05729	0.05662	0.9558
Toll-like receptor 2	0.01014	0.008979	0.7833
Toll-like receptor 4	0.003651	0.0007350	0.1473
Tumor necrosis factor	0.001179	0.0009175	0.8138
Thymidine phosphorylase	ND	ND	
Chemokine (C motif) ligand 1	0.006992		0.4226
Chemokine (C motif) receptor 1	ND	ND	

M, male; F, female; ND, not determined.

uted to differences in leukocyte inflammatory gene expression levels.

DISCUSSION

The majority of published studies suggest that left ventricular free wall rupture is the predominant cause of death in mice undergoing nonreperused MI protocols (27, 65, 71, 97). However, there is substantial variation in the reported rupture rates, which is dependent not only on sex and the genetic background of the animals but also on the specific criteria used for documentation of rupture (Table 3). Although most studies use gross pathology to document rupture, the specific criteria vary. Typically, studies using hemothorax as a diagnostic criterion for rupture report very high rupture rates, whereas investigations requiring identification of a perforation site upon autopsy report much lower rupture rates (Table 4). Our study clarifies the basis for the conflicting findings. Systematic histological analysis of the infarcted heart from base to apex (Fig. 2) identified a rupture site in only 50% of mice dying following nonreperused MI (Figs. 2 and 3), consistent with other histopathological studies in C57BL/6 mice (Table 3). Our findings show that hemothorax is highly sensitive for identification of rupture but has relatively low specificity. In contrast, gross identification of a perforation site is very specific for rupture but has low sensitivity, missing a large number of rupture events (Table 1).

Moreover, our experiments provide a systematic characterization of the histopathological characteristics of cardiac rupture in mice. When compared with infarcted mice dying in the absence of rupture, ruptured hearts had comparable infarct size and infarct wall thickness but exhibited increased macrophage infiltration accompanied by reduced myofibroblast content. Male mice had a significantly higher incidence of rupture than female animals. However, the increased susceptibility of male mice to rupture could not be explained by increased inflam-

Table 3. Rupture-related mortality in wild-type mice undergoing nonreperfused myocardial infarction protocols

Strain	Sex	Age, wk	Mortality, %	Duration of Follow-up	Rupture rates, rupture × 100/total deaths	Rupture Assessment Criteria	Ref.
C57BL/6J	M+F	18	45	7	33	Hem or RS	(43)
C57BL/6	M	8–10	35.6	28	78.7	Autopsy (not otherwise specified)	(46)
C57BL/6J	M+F	10–12	35	28	100	Hem and RS	(14)
C57BL/6	M	12	46.6	56	92	Hem and RS	(87)
C57BL/6	M	8–12	22.7	7	80	Hem and RS	(93)
C57BL/6J	M+F	12	42	28	63 (M), 38.5 (F)	Hem and RS	(48)
C57BL/6	M	8–10	52	7	60.6	Hem	(45)
C57BI/6J	M+F	N/A	45	14	100	Autopsy (not otherwise specified)	(15)
C57BL/6	M	8–16	75	28	100	Autopsy (not otherwise specified)	(2)
N/A	M+F	N/A	12	7	100	Autopsy (not otherwise specified)	(26)
C57BI/6J	M+F	N/A	40	7	100	Autopsy (not otherwise specified)	(75)
C57BL/6	M	10	55	28	96	Hem and/or RS	(96)
C57BL/6J	M	8–12	40	28	100	Autopsy (not otherwise specified)	(77)
C57BL/6	M	8–12	41	56	80	RS	(7)
C57BL/6	M	8–12	20	14	83	Autopsy (not otherwise specified)	(12)
C57BL/6	M	12–20	65	14	26.1	Autopsy (not otherwise specified)	(84)
C57BL/6/129/svj	M	8–12	34.6	42	11.5	RS	(50)
C57BL/6	M	8–12	39.3	28	57.7	Histology	(64)
C57BL/6	M	10–12	35	28	85	Autopsy (not otherwise specified)	(53)
C57BL/6J	M+F	8–12	16	28	73	Hem or RS	(85)
C57BL/6	M	12	58	28	92	Autopsy (not otherwise specified)	(81)
C57BL/6	M	10–12	48	28	62.5	Hem and RS	(58)
C57BL/6	M+F	N/A	44	28	63.6	Histology	(46)
C57BL/6J	M	16	60	28	100	Autopsy (not otherwise specified)	(39)
C57BL/6 × FVB	F	12–14	15	7	100	Hem and/or RS	(83)
C57BL/6	M	10–16	51	28	70	Hem or RS	(97)
C57BL/6	M	10	50	7	100	Autopsy (not otherwise specified)	(92)
C57BL/6	M	9–12	50	28	87.4	Hem and RS	(82)
C57BL/6	M+F	7–8	60	120	100	Autopsy (not otherwise specified)	(70)
C57BL/6	M	8–10	22	14	100	Hem and RS	(71)
C57BI/6	M	8–10	53	7	55.8	Histology	(59)
C57BL/6	M	8	31	5	33.6	RS	(54)
C57BL/6	M	8–10	41	28	69.7	Hem and RS	(44)
C57BL/6	M	9–12	27.1	7	100	Hem	(63)
C57BL/6	M+F	N/A	40	28	85.5	Hem	(34)
C57BL/6	M	10–12	19.8	28	100	Autopsy (not otherwise specified)	(3)
C57BL/6	M+F	12–16	6	14	50	RS and Histology	(88)
C57BL/6J	M	11–12	28	10	75	Hem and Infusion	(67)
FVB	M+F	N/A	43.2	20	55	Hem	(86)
C57BL/6	M	N/A	66	7	40	Autopsy (not otherwise specified)	(61)
C57BL/6	M	8–28	25	30	33.6	Infusion	(32)
C57BL/6	M	10–12	40	28	80	Hem	(49)
FVB/njcl	F	8–12	35	28	88	Hem	(37)
C57BL/6J	M	10–18	15%	14	60	Histology	(78)
C57BL/6	M	N/A	40	10	100	Autopsy (not otherwise specified)	(69),
C57BL/6J	M	8	46	7	68	Autopsy (not otherwise specified)	(79)
C57BL/6J	M	12–13	54	28	38.5	Histology	(65)
C57BL/6	M	12–16	23.5	7	100	Autopsy (not otherwise specified)	(42)
C57BL/6	M	8–12	N/A	N/A	30	RS	(36)
BalbC	M	10–12	6	28	33.3	Hem	(89)
C57BL/6	M	10–12	19	28	81.8	Hem	(89)
FVB	M	10–12	37	28	45.8	Hem	(89)
129S6	M	10–12	42.8	28	93.3	Hem	(89)
Swiss	M	10–12	14.5	28	75	Hem	(89)
FVB/N	M+F	12–16	16.5 (M), 15.7 (F)	7	7.8 (M), 0 (F)	Hem and RS	(27)
C57BL/6	M+F	12–16	25.5 (M), 11.2 (F)	7	56 (M), 45.5 (F)	Hem and RS	(27)
129sv	M+F	12–16	45.6 (M), 11.3 (F)	7	93.4 (M), 72.8 (F)	Hem and RS	(27)

M, male; F, female; N/A, not available; Hem, hemothorax (clot or blood in chest); RS, rupture site in gross pathology.

matory activation of immune cells. Myeloid cells isolated from male and female mouse infarcts had comparable expressions of a wide range of inflammatory genes (Table 2).

Why are mice so susceptible to post-MI cardiac rupture? Even when the most rigorous and specific approaches for documentation are used, the incidence of rupture in young adult mice with coronary occlusion remains remarkably high

compared with the incidence of similar events in human MI patients. Several factors related to the characteristics of the MI model and the quality of cardiac repair in mice may explain the high susceptibility of mice to rupture. First, the extensive transmural MI induced by coronary occlusion in mice and the absence of significant collateral circulation increase the likelihood of cardiac rupture. In human MI patients, rupture is more

Table 4. Postinfarction rupture rates in male C57Bl6 mice based on assessment through various strategies

Strategy	Rupture Deaths (%) (mean)	Rupture Deaths (%) median	Rupture Deaths (%) (range)	Number of Studies (n)
Gross pathology (any criteria)	77.9	81.8	26.1–100	31
RS	47.9	33.6	30–80	3
Hem	80.6	80.9	60.6–100	4
RS + Hem	77.7	75.0	56–100	10
Gross pathology (criteria not specified)	83.8	96.0	26.1–100	14
Histology	53	56.8	38.5–60	4

RS, rupture site, Hem, hemothorax.

common in individuals with single-vessel disease that lack collateral circulation (62, 72), a situation more likely to result in transmural infarction. The mouse model of permanent coronary occlusion recapitulates this clinical scenario. Second, the absence of significant hypertrophy and fibrosis in young adult mice increases the likelihood of rupture. In contrast, in human patients MI typically affects older subjects who may exhibit baseline hypertrophic and fibrotic changes due to preexisting coronary disease or other comorbid conditions (such as hypertension, diabetes, obesity, and metabolic dysfunction). The typical patient with rupture has a first infarct without any preexisting fibrotic or hypertrophic remodeling (21). Third, myocardial scars in mice exhibit marked thinning during infarct healing compared with large animals (11, 17) and may be more susceptible to rupture. According to Laplace's law, tension in the ventricular wall is proportional to the radius and inversely proportional to the thickness of the wall. Although direct comparisons with human infarcts are impossible, the marked reduction in wall thickness in mouse infarcts, coupled with the impressive dilative remodeling in infarcted mouse hearts, may significantly increase wall stress, resulting in rupture. Finally, patients with MI are typically admitted to the coronary care unit, resting and receiving treatment. The continuous activity of infarcted mice may result in exercise-related systemic and intracardiac pressure increases that may precipitate rupture.

The cell biological response in ruptured hearts. Following MI, massive necrosis of cardiomyocytes triggers an intense myocardial inflammatory reaction, inducing recruitment of neutrophils (13) and proinflammatory monocytes (18). Subsequent activation of fibrogenic macrophages in the infarct results in secretion of growth factors, such as TGF β , that mediate formation of organized myofibroblast arrays in the infarct (52), triggering secretion and deposition of extracellular matrix (ECM) proteins. Dysregulation in the sequence of inflammatory and reparative cellular responses may play an important role in the pathogenesis of cardiac rupture.

In human patients, left ventricular free wall rupture can occur as early as a few hours or as late as several weeks after MI (94). Early rupture has been suggested to account for a significant percentage of pre-hospitalization deaths in MI patients (41). These rupture events occur before the infarct is infiltrated with significant numbers of leukocytes (6) and well before replacement with scar tissue. Thus, rupture events occurring during the first 24 h after MI cannot be attributed to overactive inflammatory cell infiltration or to perturbed activation of reparative cells. Massive cardiomyocyte death, accompanied by rapid activation of proteases in the interstitium of myocardial segments subjected to high wall stress, may account for early rupture in human patients. In C57BL6J mice,

we did not observe rupture-related deaths within the first 24 h of MI. Thus, the cellular mechanisms underlying early rupture cannot be studied using the mouse model.

All rupture events in mice with nonreperfused MI occurred between *days 3* and *7* following coronary occlusion at time points corresponding to the inflammatory and early reparative phase of cardiac repair (23). Comparison of the cellular composition of mice dying with and without rupture identified several distinct characteristics of ruptured hearts:

First, macrophage density is significantly increased in infarcted segments of mice dying of rupture, and significant numbers of macrophages are noted in the edge of the rupture track (Fig. 7). Increased influx of proinflammatory macrophages may result in local activation of proteases, thus degrading the cardiac ECM and precipitating rupture. To examine whether rupture is associated with perturbations in the ratio of proinflammatory vs. anti-inflammatory macrophages, we performed immunofluorescent staining for the M₁ marker iNOS and the M₂ marker Arg1. No significant differences in the density of M₁-like and M₂-like macrophages were noted in animals dying with or without rupture (Fig. 8). The findings do not support the notion that macrophage polarization is directly involved in cardiac rupture. However, it should be emphasized that systematic study of inflammatory mediator expression (rather than assessment of single M₁/M₂ markers) is required to gain insights into the phenotypic characteristics of macrophages in tissues. Unfortunately, harvesting macrophages from ruptured hearts to examine relations between inflammatory gene expression and rupture events is impractical.

Second, ruptured hearts exhibited reduced myofibroblast density in the infarct zone (Fig. 5). Recruitment and activation of fibroblasts play a crucial role in repair of the infarcted heart, generating a scar that protects the ventricle from catastrophic mechanical failure (52, 69). In mice with reduced activation of myofibroblasts, attenuated collagen synthesis may fall below the threshold needed to maintain the structural integrity of the infarct wall, thus leading to cardiac rupture. This notion was also supported by findings showing a trend toward reduced collagen content in ruptured hearts (Fig. 6).

Balance between proinflammatory and matrix-preserving cascades in the pathogenesis of cardiac rupture. A large body of evidence derived from in vivo experiments in genetically manipulated mice suggests that uncontrolled activation of proinflammatory signaling cascades (reviewed in Table 5), impaired fibroblast activation, and overactive matrix degradation (reviewed in Table 6) are the predominant mechanisms that mediate postinfarction cardiac rupture. It should be noted that in most studies documentation of rupture was based on visual inspection criteria; thus, the findings may more accu-

Table 5. *Inflammatory signals involved in the pathogenesis of cardiac rupture*

Gene/Protein	Mechanism	Ref.
Cyclic GMP-AMP synthase (cGAS)	cGAS was suggested to cause rupture following MI by acting as a pattern recognition receptor that stimulates proinflammatory programs and by inhibiting activation of reparative macrophages.	(8)
CD8	Mice deficient in functional CD8 ⁺ T cells had improved survival but increased incidence of cardiac rupture, suggesting that CD8 ⁺ T cells may be involved in effective scar formation.	(43)
IL-35	IL-35 protected from post-MI cardiac rupture, promoting reparative macrophage responses and improving repair.	(46)
Toll-like receptor 7 (TLR7)	TLR7 was implicated in cardiac rupture through effects on leukocyte cytokine expression.	(14)
Muscle atrophy F-box (MAFbx)	The E3 ubiquitin ligase MAFbx was implicated in cardiac rupture post-MI, presumably by inducing inflammatory cell infiltration.	(87)
Heat shock protein-B1 (HSPB1)	Cardiomyocyte-specific HSPB1 signaling was found to protect from post-MI cardiac rupture by inhibiting inflammatory activation.	(93)
12/15-Lipoxygenase (LOX)	12/15 LOX was implicated in the pathogenesis of cardiac rupture, presumably by enhancing synthesis of proinflammatory lipid mediators.	(48)
Apoptosis inhibitor of macrophage (AIM)	AIM was implicated in the pathogenesis of post-MI cardiac rupture, presumably through recruitment of proinflammatory macrophages.	(45)
CD36	Activation of a CD36-Mertk axis protects from cardiac rupture by promoting phagocytosis of dead cells by activated macrophages.	(15)
Granulocyte/macrophage colony-stimulating factor (GM-CSF)	Fibroblast-derived GM-CSF was implicated in post-MI cardiac rupture, presumably through recruitment of proteolytic/inflammatory neutrophils and monocytes.	(2)
Glucocorticoid receptor (GR)	Inactivation of GR altered the functional differentiation of monocyte-derived macrophages in the infarcted myocardium and was suggested to cause higher rupture-related mortality.	(26)
β -Adrenergic receptor (β_2 AR)	Myeloid β_2 ARKO (through bone marrow transplantation) mice displayed 100% mortality resulting from post-MI cardiac rupture. β_2 ARKO mice had reduced leukocyte infiltration in infarcted hearts.	(30)
Calpastatin	Male mice overexpressing calpastatin had increased rates of post-MI cardiac rupture. KO mice exhibited reduced infiltration of M ₂ macrophages and CD4 ⁺ T cells.	(91)
TGF β receptor 1 (T β RI)	Conditional cardiomyocyte specific TGF β receptor 1 knockout displayed marked decline in neutrophil recruitment and attenuated MMP9 activity with reduced post-MI cardiac rupture rates.	(75)
MIF	MIF-deficient mice had lower rates of post-MI cardiac rupture, associated with reduced myocardial leukocyte infiltration, and reduced activity of MMP-2 and -9, p38, and JNK MAPK.	(96)
IL-23	IL-23KO mice exhibited increased post-MI cardiac rupture rates, presumably through higher expression of proinflammatory cytokines and increased infiltration with immune cells.	(77)
Haptoglobin	Haptoglobin-deficient mice displayed increased post-MI cardiac rupture rates, presumably through increased leukocyte infiltration in the infarct, reduced PAI-1 activity and enhanced VEGF α expression.	(4)
5-Lipoxygenase	5-Lipoxygenase-null mice exhibited higher post-MI cardiac rupture rates, with more abundant proinflammatory macrophages and decreased collagen deposition and fibroblast migration.	(7)
D6	D6-null mice exhibited increased post-MI cardiac rupture rates, presumably through enhanced infiltration of neutrophils and Ly6Chi monocytes and increased MMP-9 and -2 activity in the infarct.	(12)
Fibulin-2	Fibulin-2 mice exhibited lower post-MI cardiac rupture rates with attenuated inflammatory cell infiltration and MMP-2 and -9 expression.	(84)
GDF-15	GDF-15 deficient mice had enhanced recruitment of PMN leukocytes associated with increased rates of post-MI cardiac rupture.	(50)
Syndecan-4 (Syn4)	Syn4 KO mice exhibited increased rates of post-MI cardiac rupture, associated with suppressed inflammation and impaired granulation tissue formation in the heart after MI.	(64)
Gp130	Cardiomyocyte-specific Gp130 KO was associated with increased post-MI cardiac rupture rates, presumably through enhanced STAT3 activation and increased expression of IL-6.	(38)
Timp4	Timp4 ^{-/-} mice had increased post-MI cardiac rupture rates, associated with increased neutrophil infiltration.	(53)
Class A macrophage scavenger receptor (SR-A)	SR-A ^{-/-} mice exhibited higher rates of post-MI cardiac rupture, presumably due to augmented gelatinolytic activity, increased MMP-9 and TNF α and reduced IL-10 mRNA in the infarcted myocardium.	(85)
TNF α	TNF α ^{-/-} mice exhibited markedly reduced post-MI cardiac rupture rates, presumably due to reduced inflammatory cell infiltration, cytokines, and MMP-9 and -2 expression in the infarct.	(81)
FrzA	FrzA overexpression protected from rupture, attenuating leukocyte infiltration and reducing MMP9 and MMP2 expression in the infarct.	(5)

MI, myocardial infarction; KO, knockout.

rately reflect effects on total mortality rather than rupture-specific deaths.

Direct activation of inflammatory cascades in leukocytes (14) and indirect stimulation of proinflammatory signals through release of cardiomyocyte- or fibroblast-derived mediators (93) (2) have been implicated in the pathogenesis of rupture. Moreover, loss of critical suppressive signals that inhibit or restrain inflammation has also been found to increase the incidence of cardiac rupture accentuating leukocyte infiltration (50). However, inflammation is not uniformly detrimental: some inflammatory pathways are critical for repair of the

infarcted heart and protect from rupture, presumably by activating matrix-secreting mesenchymal cells (29, 64).

On the other hand, activation of reparative fibroblasts and stimulation of matrix-preserving pathways play a critical role in protection of the infarcted heart from rupture. Several members of the matrix metalloproteinase (MMP) family may promote rupture by degrading the cardiac ECM (36, 65). Several matricellular proteins that promote myofibroblast activation [such as periostin (69, 79), osteoglycin (88), and SPARC (secreted protein, acidic, cysteine-rich) (78)] were found to protect from cardiac rupture. Moreover, fibroblast-

Table 6. Role of fibroblast activation and extracellular matrix remodeling in cardiac rupture

Gene/Protein	Mechanism	Ref.
Hsp47	Fibroblast-specific activation of Hsp47 was found to protect from cardiac rupture by promoting reparative myofibroblast activation.	(51)
TLR9	TLR9 signaling protects from rupture by activating myofibroblasts possibly through an interaction with HMGB1.	(58)
Smad3	Myofibroblast-specific Smad3, but not Smad2, signaling protects from late rupture post-MI by triggering an integrin-mediated response in myofibroblasts, thus contributing to formation of an organized scar.	(40, 52)
IL-35	IL-35 protects from post-MI cardiac rupture promoting reparative macrophage responses and improving repair.	(46)
miR-144	miR-144 was implicated in the pathogenesis of cardiac rupture, presumably through effects on ECM remodeling.	(35)
Mast cell protease 4	Chymase mast cell protease 4 was implicated in post-MI cardiac rupture, presumably through effects on matrix remodeling.	(39)
Heme oxygenase-1 (Hmox1)	Mice deficient in Hmox1 had lower rates of post-MI cardiac rupture, with greater collagen type I production compared with wild-type mice.	(83)
Dectin-2	Dectin-2 KO mice demonstrated lower post-MI cardiac rupture rates with increased expression of α -smooth muscle actin and collagen I/III and reduced MMP-2 and -9 expression.	(97)
miR-155	miR-155-deficient mice exhibited lower rates of post-MI cardiac rupture, associated with more abundant myofibroblasts and a increased collagen disposition in the infarct.	(92)
CD39	CD39-deficient mice demonstrated lower post-MI cardiac rupture rates associated with elevated fibrin and collagen deposition and increased reparative macrophage influx to the infarcted area.	(82)
NEIL3	Neil3 ^{-/-} mice showed increased post-MI myocardial rupture, presumably through ECM dysregulation and increased levels of MMP-2.	(70)
TLR9	TLR9 was suggested to reduce post-MI cardiac rupture rates presumably through proliferation and differentiation of cardiac fibroblasts.	(71)
Hand1	Hand1 ^{+/-} mice had decreased cardiac rupture rates associated with lower MMP-9 activity.	(59)
CD28	CD28KO mice had higher post-MI cardiac rupture rates, lower collagen deposition, and lower myofibroblast numbers.	(54)
Twinkle	Twinkle overexpression reduced post-MI cardiac rupture rates presumably through suppression of MMP-2 and -9 in the border zone of the infarct.	(44)
Follistatin-like 1	Conditional ablation of Fstl1 in S100a4-expressing fibroblast lineage cells was reported to reduce numbers of myofibroblasts and expression of ECM proteins in the infarct, and demonstrated increased post-MI cardiac rupture.	(63)
Girdin	Girdin S1416A knock-in mice (in which the Akt phosphorylation site is replaced with alanin) had reduced cardiac myofibroblast proliferation and collagen deposition that was implicated in higher rates of post-MI cardiac rupture.	(34)
Sirtuin 7	Sirt7 ^{-/-} mice showed high susceptibility to cardiac rupture, associated with reduced myofibroblast differentiation and perturbed TGF β responses.	(3)
Osteoglycin	Osteoglycin-null mice had significantly increased post-MI cardiac rupture rates. Tissue disruption and impaired collagen fibrillogenesis were implicated.	(88)
Phospholipase A ₂ receptor (PLA2R)	PLA2R-deficient mice exhibited higher rates of post-MI cardiac rupture, associated with decreased numbers of myofibroblasts and attenuated collagen deposition in the infarcted myocardium. PLA2R was implicated in migration and proliferation of myofibroblasts through interactions with integrin- β ₁ .	(67)
Melusin	Melusin overexpression reduced post-MI cardiac rupture rates, increasing matricellular protein expression in the infarcted area.	(86)
MMP-28	MMP-28 deletion increased post-MI cardiac rupture rates, presumably through impaired M ₂ macrophage activation and reduced deposition of ECM proteins.	(61)
Syndecan-4	Syndecan-4 KO mice exhibited increased rates of post-MI cardiac rupture, associated with suppressed inflammation and impaired granulation tissue formation in the heart post-MI.	(64)
TIMP3	TIMP3 ^{-/-} mice exhibited increased rates of post-MI cardiac rupture presumably through increased MMP activity, activated EGFR signaling, decreased myofibroblast numbers, and collagen deposition.	(32), (49)
Bcrp1/Abcg2	Bcrp1/Abcg2 KO mice exhibited higher post-MI cardiac rupture rates, with reduced capillary, myofibroblast, and macrophage densities in the peri-infarction area.	(37)
SPARC	SPARC-null mice exhibited increased rates of post-MI rupture, associated with disorganized granulation tissue formation and defective scar maturation.	(78)
Biglycan	Biglycan-deficient mice had higher post-MI rupture rates. Impaired collagen matrix organization was implicated.	(95)
Periostin	Periostin ^{-/-} mice had increased post-MI rupture rates, associated with lower numbers of myofibroblasts and impaired collagen fibril formation in the infarct.	(69, 79)
MMP-2	MMP-2-null mice exhibited reduced post-MI cardiac rupture, presumably through reduced gelatinolytic activity, and attenuated ECM degradation.	(65)
Factor XIII	FXIII ^{-/-} mice had markedly higher post-MI cardiac rupture rates, associated with lower collagen I and higher MMP-9 levels.	(68)
Angiotensin II receptor (AT2R)	AT2R-null mice had increased post-MI rupture rates, associated with reduced collagen deposition in the infarct.	(42)
uPA, TIMP1	uPA ^{-/-} mice exhibited low post-MI cardiac rupture rates. In addition, gene transfer of TIMP1 protected mice from rupture-related death.	(36)

MI, myocardial infarction; KO, knockout; MMP, matrix metalloproteinase.

specific TGF β /Smad3 signaling prevents late rupture following MI by stimulating integrin-dependent activation of infarct myofibroblasts (52). Considering that excessive ECM deposition in the infarcted heart may promote adverse remodeling and cause diastolic dysfunction, timely activation and suppression of fibroblast-driven matrix-preserving pathways are needed to protect from rupture while preventing exaggerated fibrosis (24). A recent study using single-cell transcriptomics suggested that mouse strains with lower susceptibility to cardiac rupture have early activation of matrix-producing myofibroblasts (22).

The male predilection for cardiac rupture: only in mice? Our findings confirm the increased susceptibility of male mice to cardiac rupture, reported in many published studies (9, 20, 27). Published studies have suggested sex-specific patterns of inflammatory mediator synthesis and release in male and female patients with myocardial infarction (31, 76). The reduced incidence of rupture in female mice has been attributed to reduced myocardial inflammation and lower levels of matrix-degrading proteases at time points corresponding to the peak of rupture (20). We used a PCR array to examine whether male mice have increased inflammatory gene expression in myeloid cells. Our findings did not show significant differences between male and female mice in levels of a wide range of inflammatory mediators, including the chemokines CCL2, CCL3, CCL4, CCL5, CCL9, CX3CL1, and CXCL10 and the cytokines IL-1 β , IL-6, and TNF α , β ₂-integrin and TLRs (Table 2). Our findings suggest that the increased susceptibility of male C57BL/6 mice to cardiac rupture is not due to differences in the gene expression profile of myeloid cells. Studies in mouse models of cardiac injury have suggested sex-specific differences in inflammatory gene expression patterns in neutrophils (16) and dendritic cells (74). Cardiomyocytes, fibroblasts (19), and vascular cells may also exhibit sex-specific differences in expression of inflammatory mediators or proteins involved in matrix remodeling that may explain the protective effects of female sex in postinfarction rupture. It should be emphasized that the male predilection for cardiac rupture seems to be specific to mice. In human patients, several studies have demonstrated that female sex is associated with an increased risk of rupture after MI (33, 55, 56). The species specificity may reflect, at least in part, the much younger age of mice undergoing experimental MI protocols compared with the human population. The vast majority of women suffering MI are elderly and postmenopausal. The protection noted in female mice may reflect hormonal actions of estrogens in young premenopausal animals (9).

Conclusions. Cardiac rupture remains a catastrophic complication and a significant cause of death for patients with MI. The mouse model of nonreperfused MI is associated with a high incidence of rupture. Although histopathology is the gold standard for documentation of cardiac rupture, systematic histological analysis of all mice dying following MI may be impractical, considering the costly and highly laborious process required for documentation. Thus, most published studies have used gross pathology for rupture assessment and have generated highly variable results. Our study demonstrates that, if appropriately performed, gross pathology can be a useful alternative to histology but has significant limitations depending on the specific autopsy criteria used for documentation of rupture. Hemothorax is highly sensitive but has relatively low

specificity, whereas gross identification of a perforation site is very specific but lacks sensitivity. Moreover, we characterize the cellular composition of the infarct in mice dying with or without rupture. We show that rupture is associated with increased macrophage infiltration and reduced myofibroblast recruitment in the infarcted segments. In the era of single-cell transcriptomics, identification of subsets of immune and reparative cells that may be associated with cardiac rupture may provide key insights into the cellular mechanisms underpinning this catastrophic complication.

GRANTS

This work was supported by National Heart, Lung, and Blood Institute Grants R01 HL-76246, R01 HL-85440, and R01 HL-149407 and United States Department of Defense Grants PR151029 and PR181464.

DISCLOSURES

No conflicts of interest, financial or otherwise, are declared by the authors.

AUTHOR CONTRIBUTIONS

A.H. and N.G.F. conceived and designed research; A.H. and A.V.S. performed experiments; A.H. and A.V.S. analyzed data; A.H. and N.G.F. interpreted results of experiments; A.H. prepared figures; A.H. and N.G.F. drafted manuscript; A.H., A.V.S., and N.G.F. edited and revised manuscript; A.H., A.V.S., and N.G.F. approved final version of manuscript.

REFERENCES

- Alex L, Russo I, Holoborodko V, Frangogiannis NG. Characterization of a mouse model of obesity-related fibrotic cardiomyopathy that recapitulates features of human heart failure with preserved ejection fraction. *Am J Physiol Heart Circ Physiol* 315: H934–H949, 2018. doi:10.1152/ajpheart.00238.2018.
- Anzai A, Choi JL, He S, Fenn AM, Nairz M, Rattik S, McAlpine CS, Mindur JE, Chan CT, Iwamoto Y, Tricot B, Wojtkiewicz GR, Weissleder R, Libby P, Nahrendorf M, Stone JR, Becher B, Swirski FK. The infarcted myocardium solicits GM-CSF for the detrimental oversupply of inflammatory leukocytes. *J Exp Med* 214: 3293–3310, 2017. doi:10.1084/jem.20170689.
- Araki S, Izumiya Y, Rokutanda T, Ianni A, Hanatani S, Kimura Y, Onoue Y, Senokuchi T, Yoshizawa T, Yasuda O, Koitabashi N, Kurabayashi M, Braun T, Bober E, Yamagata K, Ogawa H. Sirt7 contributes to myocardial tissue repair by maintaining transforming growth factor- β signaling pathway. *Circulation* 132: 1081–1093, 2015. doi:10.1161/CIRCULATIONAHA.114.014821.
- Arslan F, Smeets MB, Buttari B, Profumo E, Riganò R, Akeroyd L, Kara E, Timmers L, Sluijter JP, van Middelaar B, den Ouden K, Pasterkamp G, Lim SK, de Kleijn DP. Lack of haptoglobin results in unbalanced VEGF α /angiopoietin-1 expression, intramural hemorrhage and impaired wound healing after myocardial infarction. *J Mol Cell Cardiol* 56: 116–128, 2013. doi:10.1016/j.yjmcc.2012.12.012.
- Barandon L, Couffinhal T, Ezan J, Dufourcq P, Costet P, Alzieu P, Leroux L, Moreau C, Dare D, Dupl a C. Reduction of infarct size and prevention of cardiac rupture in transgenic mice overexpressing FrzA. *Circulation* 108: 2282–2289, 2003. doi:10.1161/01.CIR.0000093186.22847.4C.
- Becker AE, van Mantgem JP. Cardiac tamponade. A study of 50 hearts. *Eur J Cardiol* 3: 349–358, 1975.
- Bl mer N, Pachel C, Hofmann U, Nordbeck P, Bauer W, Mathes D, Frey A, Bayer B, Vogel B, Ertl G, Bauersachs J, Frantz S. 5-Lipoxygenase facilitates healing after myocardial infarction. *Basic Res Cardiol* 108: 367, 2013. doi:10.1007/s00395-013-0367-8.
- Cao DJ, Schiattarella GG, Villalobos E, Jiang N, May HI, Li T, Chen ZJ, Gillette TG, Hill JA. Cytosolic DNA sensing promotes macrophage transformation and governs myocardial ischemic injury. *Circulation* 137: 2613–2634, 2018. doi:10.1161/CIRCULATIONAHA.117.031046.
- Cavasin MA, Tao ZY, Yu AL, Yang XP. Testosterone enhances early cardiac remodeling after myocardial infarction, causing rupture and degrading cardiac function. *Am J Physiol Heart Circ Physiol* 290: H2043–H2050, 2006. doi:10.1152/ajpheart.01121.2005.

10. Chen B, Huang S, Su Y, Wu YJ, Hanna A, Brickshawana A, Graff J, Frangogiannis NG. Macrophage Smad3 Protects the infarcted heart, stimulating phagocytosis and regulating inflammation. *Circ Res* 125: 55–70, 2019. doi:10.1161/CIRCRESAHA.119.315069.
11. Christia P, Bujak M, Gonzalez-Quesada C, Chen W, Dobaczewski M, Reddy A, Frangogiannis NG. Systematic characterization of myocardial inflammation, repair, and remodeling in a mouse model of reperfused myocardial infarction. *J Histochem Cytochem* 61: 555–570, 2013. doi:10.1369/0022155413493912.
12. Cochain C, Auvynet C, Poupel L, Vilar J, Dumeau E, Richart A, Récalde A, Zouggari Y, Yin KY, Bruneval P, Renault G, Marchiol C, Bonnin P, Lévy B, Bonecchi R, Locati M, Combadière C, Silvestre JS. The chemokine decoy receptor D6 prevents excessive inflammation and adverse ventricular remodeling after myocardial infarction. *Arterioscler Thromb Vasc Biol* 32: 2206–2213, 2012. doi:10.1161/ATVBAHA.112.254409.
13. Daseke MJ 2nd, Valerio FM, Kalusche WJ, Ma Y, DeLeon-Pennell KY, Lindsey ML. Neutrophil proteome shifts over the myocardial infarction time continuum. *Basic Res Cardiol* 114: 37, 2019. doi:10.1007/s00395-019-0746-x.
14. de Kleijn DP, Chong SY, Wang X, Yatim SM, Fairhurst AM, Vernooij F, Zharkova O, Chan MY, Foo RS, Timmers L, Lam CS, Wang JW. Toll-like receptor 7 deficiency promotes survival and reduces adverse left ventricular remodeling after myocardial infarction. *Cardiovasc Res* 115: 1791–1803, 2019. doi:10.1093/cvr/cvz057.
15. Dehn S, Thorp EB. Myeloid receptor CD36 is required for early phagocytosis of myocardial infarcts and induction of Nr4a1-dependent mechanisms of cardiac repair. *FASEB J* 32: 254–264, 2018. doi:10.1096/fj.201700450r.
16. DeLeon-Pennell KY, Mouton AJ, Ero OK, Ma Y, Padmanabhan Iyer R, Flynn ER, Espinoza I, Musani SK, Vasani RS, Hall ME, Fox ER, Lindsey ML. LXR/RXR signaling and neutrophil phenotype following myocardial infarction classify sex differences in remodeling. *Basic Res Cardiol* 113: 40, 2018. doi:10.1007/s00395-018-0699-5.
17. Dewald O, Ren G, Duerr GD, Zoerlein M, Klemm C, Gersch C, Tincey S, Michael LH, Entman ML, Frangogiannis NG. Of mice and dogs: species-specific differences in the inflammatory response following myocardial infarction. *Am J Pathol* 164: 665–677, 2004. doi:10.1016/S0002-9440(10)63154-9.
18. Dewald O, Zymek P, Winkelmann K, Koerting A, Ren G, Aboukhamis T, Michael LH, Rollins BJ, Entman ML, Frangogiannis NG. CCL2/monocyte chemoattractant protein-1 regulates inflammatory responses critical to healing myocardial infarcts. *Circ Res* 96: 881–889, 2005. doi:10.1161/01.RES.0000163017.13772.3a.
19. Dworatzek E, Mahmoodzadeh S, Schriever C, Kusumoto K, Kramer L, Santos G, Fliegner D, Leung YK, Ho SM, Zimmermann WH, Lutz S, Regitz-Zagrosek V. Sex-specific regulation of collagen I and III expression by 17 β -estradiol in cardiac fibroblasts: role of estrogen receptors. *Cardiovasc Res* 115: 315–327, 2019. doi:10.1093/cvr/cvy185.
20. Fang L, Gao XM, Moore XL, Kiriazis H, Su Y, Ming Z, Lim YL, Dart AM, Du XJ. Differences in inflammation, MMP activation and collagen damage account for gender difference in murine cardiac rupture following myocardial infarction. *J Mol Cell Cardiol* 43: 535–544, 2007. doi:10.1016/j.yjmcc.2007.06.011.
21. Figueras J, Alcalde O, Barrabés JA, Serra V, Alguersuari J, Cortadellas J, Lidón RM. Changes in hospital mortality rates in 425 patients with acute ST-elevation myocardial infarction and cardiac rupture over a 30-year period. *Circulation* 118: 2783–2789, 2008. doi:10.1161/CIRCULATIONAHA.108.776690.
22. Forte E, Skelly DA, Chen M, Daigle S, Morelli KA, Hon O, Philip VM, Costa MW, Rosenthal NA, Furtado MB. Dynamic interstitial cell response during myocardial infarction predicts resilience to rupture in genetically diverse mice. *Cell Rep* 30: 3149–3163, 2020. doi:10.1016/j.celrep.2020.02.008.
23. Frangogiannis NG. The inflammatory response in myocardial injury, repair, and remodeling. *Nat Rev Cardiol* 11: 255–265, 2014. doi:10.1038/nrcardio.2014.28.
24. Frangogiannis NG. The extracellular matrix in myocardial injury, repair, and remodeling. *J Clin Invest* 127: 1600–1612, 2017. doi:10.1172/JCI87491.
25. Frunza O, Russo I, Saxena A, Shinde AV, Humeres C, Hanif W, Rai V, Su Y, Frangogiannis NG. Myocardial galectin-3 expression is associated with remodeling of the pressure-overloaded heart and may delay the hypertrophic response without affecting survival, dysfunction, and cardiac fibrosis. *Am J Pathol* 186: 1114–1127, 2016. doi:10.1016/j.ajpath.2015.12.017.
26. Galuppo P, Vettorazzi S, Hövelmann J, Scholz CJ, Tuckermann JP, Bauersachs J, Fraccarollo D. The glucocorticoid receptor in monocyte-derived macrophages is critical for cardiac infarct repair and remodeling. *FASEB J* 31: 5122–5132, 2017. doi:10.1096/fj.201700317R.
27. Gao XM, Xu Q, Kiriazis H, Dart AM, Du XJ. Mouse model of post-infarct ventricular rupture: time course, strain- and gender-dependency, tensile strength, and histopathology. *Cardiovasc Res* 65: 469–477, 2005. doi:10.1016/j.cardiores.2004.10.014.
28. Gao XM, White DA, Dart AM, Du XJ. Post-infarct cardiac rupture: recent insights on pathogenesis and therapeutic interventions. *Pharmacol Ther* 134: 156–179, 2012. doi:10.1016/j.pharmthera.2011.12.010.
29. Grisanti LA, Gumpert AM, Traynham CJ, Gorsky JE, Repas AA, Gao E, Carter RL, Yu D, Calvert JW, García AP, Ibáñez B, Rabinowitz JE, Koch WJ, Tilley DG. Leukocyte-expressed β 2-adrenergic receptors are essential for survival after acute myocardial injury. *Circulation* 134: 153–167, 2016. doi:10.1161/CIRCULATIONAHA.116.022304.
30. Grisanti LA, Traynham CJ, Repas AA, Gao E, Koch WJ, Tilley DG. β 2-Adrenergic receptor-dependent chemokine receptor 2 expression regulates leukocyte recruitment to the heart following acute injury. *Proc Natl Acad Sci USA* 113: 15126–15131, 2016. doi:10.1073/pnas.1611023114.
31. Halade GV, Kain V, Dillion C, Beasley M, Dudenbostel T, Oparil S, Limdi NA. Race-based and sex-based differences in bioactive lipid mediators after myocardial infarction. *ESC Heart Fail* 7: 1700–1710, 2020. doi:10.1002/ehf2.12730.
32. Hammoud L, Lu X, Lei M, Feng Q. Deficiency in TIMP-3 increases cardiac rupture and mortality post-myocardial infarction via EGFR signaling: beneficial effects of cetuximab. *Basic Res Cardiol* 106: 459–471, 2011. doi:10.1007/s00395-010-0147-7.
33. Hao Z, Ma J, Dai J, Shao Q, Shen L, He B, Jiang L. A real-world analysis of cardiac rupture on incidence, risk factors and in-hospital outcomes in 4190 ST-elevation myocardial infarction patients from 2004 to 2015. *Coron Artery Dis* 31: 424–429, 2020. doi:10.1097/MCA.0000000000000877.
34. Hayano S, Takefuji M, Maeda K, Noda T, Ichimiya H, Kobayashi K, Enomoto A, Asai N, Takahashi M, Murohara T. Akt-dependent Girdin phosphorylation regulates repair processes after acute myocardial infarction. *J Mol Cell Cardiol* 88: 55–63, 2015. doi:10.1016/j.yjmcc.2015.09.012.
35. He Q, Wang F, Honda T, James J, Li J, Redington A. Loss of miR-144 signaling interrupts extracellular matrix remodeling after myocardial infarction leading to worsened cardiac function. *Sci Rep* 8: 16886, 2018. doi:10.1038/s41598-018-35314-6.
36. Heymans S, Lutun A, Nuyens D, Theilmeier G, Creemers E, Moons L, Dyspersin GD, Cleutjens JP, Shipley M, Angellilo A, Levi M, Nübe O, Baker A, Keshet E, Lupu F, Herbert JM, Smits JF, Shapiro SD, Baes M, Borgers M, Collen D, Daemen MJ, Carmeliet P. Inhibition of plasminogen activators or matrix metalloproteinases prevents cardiac rupture but impairs therapeutic angiogenesis and causes cardiac failure. *Nat Med* 5: 1135–1142, 1999. doi:10.1038/13459.
37. Higashikuni Y, Sainz J, Nakamura K, Takaoka M, Enomoto S, Iwata H, Sahara M, Tanaka K, Koibuchi N, Ito S, Kusuhara H, Sugiyama Y, Hirata Y, Nagai R, Sata M. The ATP-binding cassette transporter BCRP1/ABCG2 plays a pivotal role in cardiac repair after myocardial infarction via modulation of microvascular endothelial cell survival and function. *Arterioscler Thromb Vasc Biol* 30: 2128–2135, 2010. doi:10.1161/ATVBAHA.110.211755.
38. Hilfiker-Kleiner D, Shukla P, Klein G, Schaefer A, Stapel B, Hoch M, Müller W, Scherr M, Theilmeier G, Ernst M, Hilfiker A, Drexler H. Continuous glycoprotein-130-mediated signal transducer and activator of transcription-3 activation promotes inflammation, left ventricular rupture, and adverse outcome in subacute myocardial infarction. *Circulation* 122: 145–155, 2010. doi:10.1161/CIRCULATIONAHA.109.933127.
39. Houde M, Schwertani A, Toul H, Desbiens L, Sarrhini O, Lecomte R, Lepage M, Gagnon H, Takai S, Pejler G, Jacques D, Gobeil F Jr, Day R, D'Orléans-Juste P. Mouse mast cell protease 4 deletion protects heart function and survival after permanent myocardial infarction. *Front Pharmacol* 9: 868, 2018. doi:10.3389/fphar.2018.00868.
40. Huang S, Chen B, Su Y, Alex L, Humeres C, Shinde AV, Conway SJ, Frangogiannis NG. Distinct roles of myofibroblast-specific Smad2 and Smad3 signaling in repair and remodeling of the infarcted heart. *J Mol Cell Cardiol* 132: 84–97, 2019. doi:10.1016/j.yjmcc.2019.05.006.

41. Hutchins KD, Skurnick J, Lavenhar M, Natarajan GA. Cardiac rupture in acute myocardial infarction: a reassessment. *Am J Forensic Med Pathol* 23: 78–82, 2002. doi:10.1097/0000433-200203000-00017.
42. Ichihara S, Senbonmatsu T, Price E Jr, Ichiki T, Gaffney FA, Inagami T. Targeted deletion of angiotensin II type 2 receptor caused cardiac rupture after acute myocardial infarction. *Circulation* 106: 2244–2249, 2002. doi:10.1161/01.CIR.0000033826.52681.37.
43. Ilatovskaya DV, Pitts C, Clayton J, Domondon M, Troncoso M, Pippin S, DeLeon-Pennell KY. CD8⁺ T-cells negatively regulate inflammation post-myocardial infarction. *Am J Physiol Heart Circ Physiol* 317: H581–H596, 2019. doi:10.1152/ajpheart.00112.2019.
44. Inoue T, Ikeda M, Ide T, Fujino T, Matsuo Y, Arai S, Saku K, Sunagawa K. Twinkle overexpression prevents cardiac rupture after myocardial infarction by alleviating impaired mitochondrial biogenesis. *Am J Physiol Heart Circ Physiol* 311: H509–H519, 2016. doi:10.1152/ajpheart.00044.2016.
45. Ishikawa S, Noma T, Fu HY, Matsuzaki T, Ishizawa M, Ishikawa K, Murakami K, Nishimoto N, Nishiyama A, Minamino T. Apoptosis inhibitor of macrophage depletion decreased M1 macrophage accumulation and the incidence of cardiac rupture after myocardial infarction in mice. *PLoS One* 12: e0187894, 2017. doi:10.1371/journal.pone.0187894.
46. Jia D, Jiang H, Weng X, Wu J, Bai P, Yang W, Wang Z, Hu K, Sun A, Ge J. Interleukin-35 promotes macrophage survival and improves wound healing after myocardial infarction in mice. *Circ Res* 124: 1323–1336, 2019. doi:10.1161/CIRCRESAHA.118.314569.
47. Julian DG. Why do patients die after myocardial infarction? *J Cardiovasc Pharmacol* 18, Suppl 2: S80–S82, 1991. doi:10.1097/00005344-199106182-00017.
48. Kain V, Ingle KA, Kabarowski J, Barnes S, Limdi NA, Prabhu SD, Halade GV. Genetic deletion of 12/15 lipoxygenase promotes effective resolution of inflammation following myocardial infarction. *J Mol Cell Cardiol* 118: 70–80, 2018. doi:10.1016/j.yjmcc.2018.03.004.
49. Kandam V, Basu R, Abraham T, Wang X, Awad A, Wang W, Lopaschuk GD, Maeda N, Oudit GY, Kassiri Z. Early activation of matrix metalloproteinases underlies the exacerbated systolic and diastolic dysfunction in mice lacking TIMP3 following myocardial infarction. *Am J Physiol Heart Circ Physiol* 299: H1012–H1023, 2010. doi:10.1152/ajpheart.00246.2010.
50. Kempf T, Zarbock A, Widera C, Butz S, Stadtmann A, Rossaint J, Bolomini-Vittori M, Korf-Klingebiel M, Napp LC, Hansen B, Kanwischer A, Bavendiek U, Beutel G, Hapke M, Sauer MG, Laudanna C, Hogg N, Vestweber D, Wollert KC. GDF-15 is an inhibitor of leukocyte integrin activation required for survival after myocardial infarction in mice. *Nat Med* 17: 581–588, 2011. doi:10.1038/nm.2354.
51. Khalil H, Kanisicak O, Vagnozzi RJ, Johansen AK, Maliken BD, Prasad V, Boyer JG, Brody MJ, Schips T, Kilian KK, Correll RN, Kawasaki K, Nagata K, Molkenin JD. Cell-specific ablation of Hsp47 defines the collagen-producing cells in the injured heart. *JCI Insight* 4: e128722, 2019. doi:10.1172/jci.insight.128722.
52. Kong P, Shinde AV, Su Y, Russo I, Chen B, Saxena A, Conway SJ, Graff JM, Frangogiannis NG. Opposing actions of fibroblast and cardiomyocyte Smad3 signaling in the infarcted myocardium. *Circulation* 137: 707–724, 2018. doi:10.1161/CIRCULATIONAHA.117.029622.
53. Koskivirta I, Kassiri Z, Rahnkonen O, Kiviranta R, Oudit GY, McKee TD, Kytö V, Saraste A, Jokinen E, Liu PP, Vuorio E, Khokha R. Mice with tissue inhibitor of metalloproteinases 4 (Timp4) deletion succumb to induced myocardial infarction but not to cardiac pressure overload. *J Biol Chem* 285: 24487–24493, 2010. doi:10.1074/jbc.M110.136820.
54. Kubota A, Hasegawa H, Tadokoro H, Hirose M, Kobara Y, Yamada-Inagawa T, Takemura G, Kobayashi Y, Takano H. Deletion of CD28 co-stimulatory signals exacerbates left ventricular remodeling and increases cardiac rupture after myocardial infarction. *Circ J* 80: 1971–1979, 2016. doi:10.1253/circj.CJ-16-0327.
55. Lanz J, Wyss D, Rüber L, Stortelky S, Hunziker L, Blöchliger S, Reineke D, Englberger L, Zanchin T, Valgimigli M, Heg D, Windecker S, Pilgrim T. Mechanical complications in patients with ST-segment elevation myocardial infarction: a single centre experience. *PLoS One* 14: e0209502, 2019. doi:10.1371/journal.pone.0209502.
56. Lewis AJ, Burchell HB, Titus JL. Clinical and pathologic features of postinfarction cardiac rupture. *Am J Cardiol* 23: 43–53, 1969. doi:10.1016/0002-9149(69)90240-9.
57. Lindsey ML, Bolli R, Cauty JM Jr, Du XJ, Frangogiannis NG, Frantz S, Gourdie RG, Holmes JW, Jones SP, Kloner RA, Lefer DJ, Liao R, Murphy E, Ping P, Przyklenk K, Recchia FA, Schwartz Longacre L, Ripplinger CM, Van Eyk JE, Heusch G. Guidelines for experimental models of myocardial ischemia and infarction. *Am J Physiol Heart Circ Physiol* 314: H812–H838, 2018. doi:10.1152/ajpheart.00335.2017.
58. Liu FY, Fan D, Yang Z, Tang N, Guo Z, Ma SQ, Ma ZG, Wu HM, Deng W, Tang QZ. TLR9 is essential for HMGB1-mediated post-myocardial infarction tissue repair through affecting apoptosis, cardiac healing, and angiogenesis. *Cell Death Dis* 10: 480, 2019. doi:10.1038/s41419-019-1718-7.
59. Lu S, Du P, Shan C, Wang Y, Ma C, Dong J. Haploinsufficiency of Hand1 improves mice survival after acute myocardial infarction through preventing cardiac rupture. *Biochem Biophys Res Commun* 478: 1726–1731, 2016. doi:10.1016/j.bbrc.2016.09.012.
60. Luo M, Guan X, Luczak ED, Lang D, Kutschke W, Gao Z, Yang J, Glynn P, Sossalla S, Swaminathan PD, Weiss RM, Yang B, Rokita AG, Maier LS, Efimov IR, Hund TJ, Anderson ME. Diabetes increases mortality after myocardial infarction by oxidizing CaMKII. *J Clin Invest* 123: 1262–1274, 2013. doi:10.1172/JCI65268.
61. Ma Y, Halade GV, Zhang J, Ramirez TA, Levin D, Voorhees A, Jin YF, Han HC, Manicone AM, Lindsey ML. Matrix metalloproteinase-28 deletion exacerbates cardiac dysfunction and rupture after myocardial infarction in mice by inhibiting M2 macrophage activation. *Circ Res* 112: 675–688, 2013. doi:10.1161/CIRCRESAHA.111.300502.
62. Mann JM, Roberts WC. Rupture of the left ventricular free wall during acute myocardial infarction: analysis of 138 necropsy patients and comparison with 50 necropsy patients with acute myocardial infarction without rupture. *Am J Cardiol* 62: 847–859, 1988. doi:10.1016/0002-9149(88)90881-8.
63. Maruyama S, Nakamura K, Papanicolaou KN, Sano S, Shimizu I, Asami Y, van den Hoff MJ, Ouchi N, Recchia FA, Walsh K. Follistatin-like 1 promotes cardiac fibroblast activation and protects the heart from rupture. *EMBO Mol Med* 8: 949–966, 2016. doi:10.15252/emmm.201506151.
64. Matsui Y, Ikese M, Danzaki K, Morimoto J, Sato M, Tanaka S, Kojima T, Tsutsui H, Uede T. Syndecan-4 prevents cardiac rupture and dysfunction after myocardial infarction. *Circ Res* 108: 1328–1339, 2011. doi:10.1161/CIRCRESAHA.110.235689.
65. Matsumura S, Iwanaga S, Mochizuki S, Okamoto H, Ogawa S, Okada Y. Targeted deletion or pharmacological inhibition of MMP-2 prevents cardiac rupture after myocardial infarction in mice. *J Clin Invest* 115: 599–609, 2005. doi:10.1172/JCI22304.
66. Michael LH, Entman ML, Hartley CJ, Youker KA, Zhu J, Hall SR, Hawkins HK, Berens K, Ballantyne CM. Myocardial ischemia and reperfusion: a murine model. *Am J Physiol* 269: H2147–H2154, 1995. doi:10.1152/ajpheart.1995.269.6.H2147.
67. Mishina H, Watanabe K, Tamaru S, Watanabe Y, Fujioka D, Takahashi S, Suzuki K, Nakamura T, Obata JE, Kawabata K, Yokota Y, Inoue O, Murakami M, Hanasaki K, Kugiyama K. Lack of phospholipase A2 receptor increases susceptibility to cardiac rupture after myocardial infarction. *Circ Res* 114: 493–504, 2014. doi:10.1161/CIRCRESAHA.114.302319.
68. Nahrendorf M, Hu K, Frantz S, Jaffer FA, Tung CH, Hiller KH, Voll S, Nordbeck P, Sosnovik D, Gattenlöhner S, Novikov M, Dickneite G, Reed GL, Jakob P, Rosenzweig A, Bauer WR, Weissleder R, Ertl G. Factor XIII deficiency causes cardiac rupture, impairs wound healing, and aggravates cardiac remodeling in mice with myocardial infarction. *Circulation* 113: 1196–1202, 2006. doi:10.1161/CIRCULATIONAHA.105.602094.
69. Oka T, Xu J, Kaiser RA, Melendez J, Hambleton M, Sargent MA, Lorts A, Brunskill EW, Dorn GW 2nd, Conway SJ, Aronow BJ, Robbins J, Molkenin JD. Genetic manipulation of periostin expression reveals a role in cardiac hypertrophy and ventricular remodeling. *Circ Res* 101: 313–321, 2007. doi:10.1161/CIRCRESAHA.107.149047.
70. Olsen MB, Hildrestrand GA, Scheffler K, Vinge LE, Alfsnes K, Palibrk V, Wang J, Neurauder CG, Luna L, Johansen J, Øgaard JDS, Ohm IK, Slupphaug G, Kuśnierczyk A, Fiane AE, Brorson SH, Zhang L, Gullestad L, Louch WE, Iversen PO, Østlie I, Klungland A, Christensen G, Sjaastad I, Sætrom P, Yndestad A, Aukrust P, Bjørås M, Finsen AV. NEIL3-dependent regulation of cardiac fibroblast proliferation prevents myocardial rupture. *Cell Reports* 18: 82–92, 2017. doi:10.1016/j.celrep.2016.12.009.
71. Omiya S, Omori Y, Taneike M, Protti A, Yamaguchi O, Akira S, Shah AM, Nishida K, Otsu K. Toll-like receptor 9 prevents cardiac rupture after myocardial infarction in mice independently of inflammation. *Am J*

- Physiol Heart Circ Physiol* 311: H1485–H1497, 2016. doi:10.1152/ajpheart.00481.2016.
72. Pohjola-Sintonen S, Muller JE, Stone PH, Willich SN, Antman EM, Davis VG, Parker CB, Braunwald E. Ventricular septal and free wall rupture complicating acute myocardial infarction: experience in the multicenter investigation of limitation of infarct size. *Am Heart J* 117: 809–818, 1989. doi:10.1016/0002-8703(89)90617-0.
 73. Puerto E, Viana-Tejedor A, Martínez-Sellés M, Domínguez-Pérez L, Moreno G, Martín-Asenjo R, Bueno H. Temporal trends in mechanical complications of acute myocardial infarction in the elderly. *J Am Coll Cardiol* 72: 959–966, 2018. doi:10.1016/j.jacc.2018.06.031.
 74. Pullen AB, Kain V, Serhan CN, Halade GV. Molecular and cellular differences in cardiac repair of male and female mice. *J Am Heart Assoc* 9: e015672, 2020. doi:10.1161/JAHA.119.015672.
 75. Rainer PP, Hao S, Vanhoutte D, Lee DL, Koitabashi N, Molkentin JD, Kass DA. Cardiomyocyte-specific transforming growth factor β suppression blocks neutrophil infiltration, augments multiple cytoprotective cascades, and reduces early mortality after myocardial infarction. *Circ Res* 114: 1246–1257, 2014. doi:10.1161/CIRCRESAHA.114.302653.
 76. Samnegård A, Hulthe J, Silveira A, Ericsson CG, Hamsten A, Eriksson P. Gender specific associations between matrix metalloproteinases and inflammatory markers in post myocardial infarction patients. *Atherosclerosis* 202: 550–556, 2009. doi:10.1016/j.atherosclerosis.2008.05.050.
 77. Savvatis K, Pappritz K, Becher PM, Lindner D, Zietsch C, Volk HD, Westermann D, Schultheiss HP, Tschöpe C. Interleukin-23 deficiency leads to impaired wound healing and adverse prognosis after myocardial infarction. *Circ Heart Fail* 7: 161–171, 2014. doi:10.1161/CIRCHEARTFAILURE.113.000604.
 78. Schellings MW, Vanhoutte D, Swinnen M, Cleutjens JP, Debets J, van Leeuwen RE, d'Hooge J, Van de Werf F, Carmeliet P, Pinto YM, Sage EH, Heymans S. Absence of SPARC results in increased cardiac rupture and dysfunction after acute myocardial infarction. *J Exp Med* 206: 113–123, 2009. doi:10.1084/jem.20081244.
 79. Shimazaki M, Nakamura K, Kii I, Kashima T, Amizuka N, Li M, Saito M, Fukuda K, Nishiyama T, Kitajima S, Saga Y, Fukayama M, Sata M, Kudo A. Periostin is essential for cardiac healing after acute myocardial infarction. *J Exp Med* 205: 295–303, 2008. doi:10.1084/jem.20071297.
 80. Shinde AV, Humeres C, Frangogiannis NG. The role of α -smooth muscle actin in fibroblast-mediated matrix contraction and remodeling. *Biochim Biophys Acta Mol Basis Dis* 1863: 298–309, 2017. doi:10.1016/j.bbadis.2016.11.006.
 81. Sun M, Dawood F, Wen WH, Chen M, Dixon I, Kirshenbaum LA, Liu PP. Excessive tumor necrosis factor activation after infarction contributes to susceptibility of myocardial rupture and left ventricular dysfunction. *Circulation* 110: 3221–3228, 2004. doi:10.1161/01.CIR.0000147233.10318.23.
 82. Sutton NR, Hayasaki T, Hyman MC, Anyanwu AC, Liao H, Petrovic-Djergovic D, Badri L, Baek AE, Walker N, Fukase K, Kanthi Y, Visovatti SH, Horste EL, Ray JJ, Goonewardena SN, Pinsky DJ. Ectonucleotidase CD39-driven control of postinfarction myocardial repair and rupture. *JCI Insight* 2: e89504, 2017. doi:10.1172/jci.insight.89504.
 83. Tomczyk M, Kraszewska I, Szade K, Bukowska-Strakova K, Meloni M, Jozkowicz A, Dulak J, Jazwa A. Splenic Ly6C^{hi} monocytes contribute to adverse late post-ischemic left ventricular remodeling in heme oxygenase-1 deficient mice. *Basic Res Cardiol* 112: 39, 2017. doi:10.1007/s00395-017-0629-y.
 84. Tsuda T, Wu J, Gao E, Joyce J, Markova D, Dong H, Liu Y, Zhang H, Zou Y, Gao F, Miller T, Koch W, Ma X, Chu ML. Loss of fibulin-2 protects against progressive ventricular dysfunction after myocardial infarction. *J Mol Cell Cardiol* 52: 273–282, 2012. doi:10.1016/j.yjmcc.2011.11.001.
 85. Tsujita K, Kaikita K, Hayasaki T, Honda T, Kobayashi H, Sakashita N, Suzuki H, Kodama T, Ogawa H, Takeya M. Targeted deletion of class A macrophage scavenger receptor increases the risk of cardiac rupture after experimental myocardial infarction. *Circulation* 115: 1904–1911, 2007. doi:10.1161/CIRCULATIONAHA.106.671198.
 86. Unsöld B, Kaul A, Sbroggiò M, Schubert C, Regitz-Zagrosek V, Brancaccio M, Damilano F, Hirsch E, Van Bilsen M, Munts C, Sipido K, Bito V, Detre E, Wagner NM, Schäfer K, Seidler T, Vogt J, Neef S, Bleckmann A, Maier LS, Balligand JL, Bouzin C, Ventura-Clapier R, Garnier A, Eschenhagen T, El-Armouche A, Knöll R, Tarone G, Hasenfuß G. Melusin protects from cardiac rupture and improves functional remodelling after myocardial infarction. *Cardiovasc Res* 101: 97–107, 2014. doi:10.1093/cvr/cvt235.
 87. Usui S, Chikata A, Takatori O, Takashima SI, Inoue O, Kato T, Murai H, Furusho H, Nomura A, Zablocki D, Kaneko S, Sadoshima J, Takamura M. Endogenous muscle atrophy F-box is involved in the development of cardiac rupture after myocardial infarction. *J Mol Cell Cardiol* 126: 1–12, 2019. doi:10.1016/j.yjmcc.2018.11.002.
 88. Van Aelst LN, Voss S, Carai P, Van Leeuwen R, Vanhoutte D, Sanders-van Wijk S, Eurlings L, Swinnen M, Verheyen FK, Verbeke E, Neff H, Troïd C, Cook SA, Brunner-La Rocca HP, Möllmann H, Papageorgiou AP, Heymans S. Osteoglycin prevents cardiac dilatation and dysfunction after myocardial infarction through infarct collagen strengthening. *Circ Res* 116: 425–436, 2015. doi:10.1161/CIRCRESAHA.116.304599.
 89. van den Borne SW, van de Schans VA, Strzelecka AE, Vervoort-Peters HT, Lijnen PM, Cleutjens JP, Smits JF, Daemen MJ, Janssen BJ, Blankesteyn WM. Mouse strain determines the outcome of wound healing after myocardial infarction. *Cardiovasc Res* 84: 273–282, 2009. doi:10.1093/cvr/cvp207.
 90. Virani SS, Alonso A, Benjamin EJ, Bittencourt MS, Callaway CW, Carson AP, Chamberlain AM, Chang AR, Cheng S, Delling FN, Djousse L, Elkind MSV, Ferguson JF, Fornage M, Khan SS, Kissela BM, Knutson KL, Kwan TW, Lackland DT, Lewis TT, Lichtman JH, Longenecker CT, Loop MS, Lutsey PL, Martin SS, Matsushita K, Moran AE, Mussolino ME, Perak AM, Rosamond WD, Roth GA, Sampson UKA, Satou GM, Schroeder EB, Shah SH, Shay CM, Spartano NL, Stokes A, Tirschwell DL, VanWagner LB, Tsao CW; American Heart Association Council on Epidemiology and Prevention Statistics Committee and Stroke Statistics Subcommittee. Heart disease and stroke statistics-2020 update: a report from the American heart association. *Circulation* 141: e139–e596, 2020. doi:10.1161/CIR.0000000000000757.
 91. Wan F, Letavernier E, Le Saux CJ, Houssaini A, Abid S, Czibik G, Sawaki D, Marcos E, Dubois-Rande JL, Baud L, Adnot S, Derumeaux G, Gellen B. Calpastatin overexpression impairs postinfarct scar healing in mice by compromising reparative immune cell recruitment and activation. *Am J Physiol Heart Circ Physiol* 309: H1883–H1893, 2015. doi:10.1152/ajpheart.00594.2015.
 92. Wang C, Zhang C, Liu L, A X, Chen B, Li Y, Du J. Macrophage-derived mir-155-containing exosomes suppress fibroblast proliferation and promote fibroblast inflammation during cardiac injury. *Mol Ther* 25: 192–204, 2017. doi:10.1016/j.ymthe.2016.09.001.
 93. Wang Y, Liu J, Kong Q, Cheng H, Tu F, Yu P, Liu Y, Zhang X, Li C, Li Y, Min X, Du S, Ding Z, Liu L. Cardiomyocyte-specific deficiency of HSPB1 worsens cardiac dysfunction by activating NF κ B-mediated leukocyte recruitment after myocardial infarction. *Cardiovasc Res* 115: 154–167, 2019. doi:10.1093/cvr/cvy163.
 94. Wehrens XH, Doevendans PA. Cardiac rupture complicating myocardial infarction. *Int J Cardiol* 95: 285–292, 2004. doi:10.1016/j.ijcard.2003.06.006.
 95. Westermann D, Mersmann J, Melchior A, Freudenberger T, Petrik C, Schaefer L, Lüllmann-Rauch R, Lettau O, Jacoby C, Schrader J, Brand-Herrmann SM, Young MF, Schultheiss HP, Levkau B, Baba HA, Unger T, Zacharowski K, Tschöpe C, Fischer JW. Biglycan is required for adaptive remodeling after myocardial infarction. *Circulation* 117: 1269–1276, 2008. doi:10.1161/CIRCULATIONAHA.107.714147.
 96. White DA, Su Y, Kanellakis P, Kiriazis H, Morand EF, Bucala R, Dart AM, Gao XM, Du XJ. Differential roles of cardiac and leukocyte derived macrophage migration inhibitory factor in inflammatory responses and cardiac remodelling post myocardial infarction. *J Mol Cell Cardiol* 69: 32–42, 2014. doi:10.1016/j.yjmcc.2014.01.015.
 97. Yan X, Zhang H, Fan Q, Hu J, Tao R, Chen Q, Iwakura Y, Shen W, Lu L, Zhang Q, Zhang R. Dectin-2 deficiency modulates Th1 differentiation and improves wound healing after myocardial infarction. *Circ Res* 120: 1116–1129, 2017. doi:10.1161/CIRCRESAHA.116.310260.

The significance of COVID-19-associated myocardial injury: how overinterpretation of scientific findings can fuel media sensationalism and spread misinformation

Nikolaos G. Frangogiannis  *

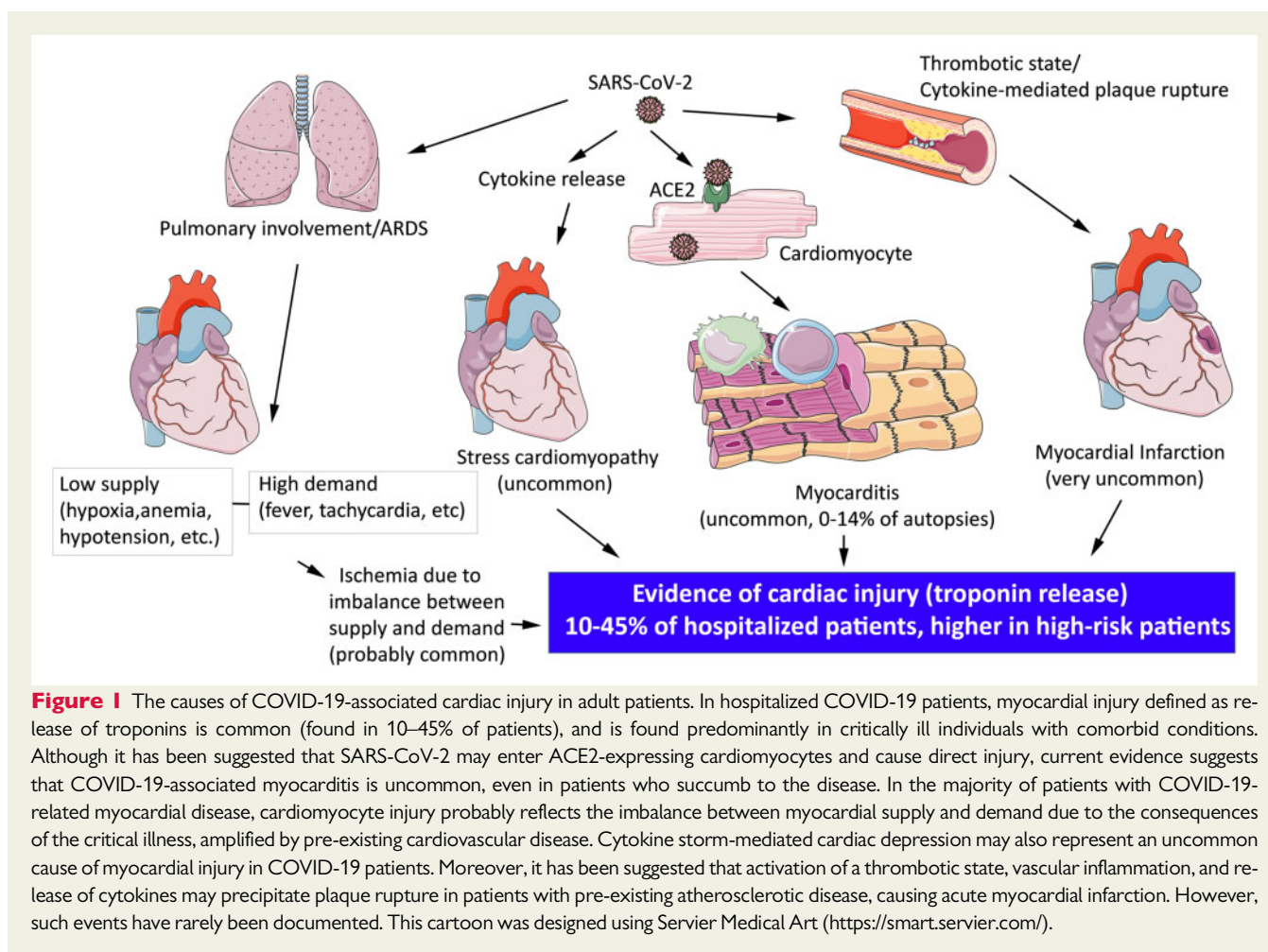
The Wilf Family Cardiovascular Research Institute, Department of Medicine (Cardiology), Albert Einstein College of Medicine, 1300 Morris Park Avenue, Forchheimer G46B, Bronx, NY 10461, USA

This editorial refers to ‘Pathological features of COVID-19-associated myocardial injury: a multicentre cardiovascular pathology study’, by C. Basso et al., doi:10.1093/eurheartj/ehaa664.

Evidence of myocardial injury is found in a significant fraction of hospitalized coronavirus disease 2019 (COVID-19) patients. Elevation of serum troponins, the most common COVID-19-associated myocardial abnormality, is found predominantly in patients with underlying cardiovascular disease, and is associated with increased mortality.^{1,2} Whether biochemical evidence of myocardial injury reflects primary severe acute respiratory syndrome coronavirus-2 (SARS-CoV-2)-mediated cardiac disease or secondary consequences of demand ischaemia remains unknown. Although it has been suggested that SARS-CoV-2 may gain entry into cardiomyocytes by binding to the abundant angiotensin-converting enzyme 2 (ACE2) expressed on the cell membrane, evidence supporting the role of myocarditis in COVID-19 myocardial pathology remains scant. Importantly, characterization of the pathological myocardial changes in COVID-19 patients is limited to case reports and small case series.^{3,4}

In the current issue of the *European Heart Journal*, Basso and co-workers⁵ provide the first systematic histopathological analysis of the myocardial alterations in patients dying from COVID-19. In an international multicentre study, the authors assessed cardiac pathology in 21 consecutive autopsies. The mechanism of death for the majority of the patients was adult respiratory distress syndrome (ARDS). All but one of the patients had underlying conditions known to cause

cardiac remodelling, including a prior history of ischaemic heart disease, hypertension, diabetes, and renal failure. The authors report that 86% of the patients exhibited widespread myocardial macrophage infiltration. A small fraction of patients (14%) had changes consistent with lymphocytic myocarditis, defined as the presence of multifocal inflammatory infiltrates associated with cardiomyocyte injury, not due to some other cause. Evidence of a recent myocardial infarction was found in one patient, whereas microvascular thrombi were noted in four patients. The study highlights the broad spectrum of cardiac injury patterns noted in critically ill COVID-19 patients, that may include acute coronary events, microvascular thrombosis, and myocardial inflammation. However, the study also has significant limitations. First, the findings cannot be generalized to all COVID-19 patients, but only represent subjects who died of the disease due to respiratory failure. Secondly, relationships between myocardial pathology and perturbations of systolic or diastolic function were not studied. Thirdly, the study cannot establish a causative relationship between SARS-CoV-2 and myocardial inflammation. Older patients with hypertension, diabetes, chronic renal failure, and chronic ischaemic heart disease often exhibit chronic low level myocardial inflammatory activation associated with interstitial macrophage infiltration.^{6,7} Due to the absence of a control group with comorbidities comparable with the COVID-19 patient population, the role of the viral infection in the pathogenesis of the myocardial changes cannot be determined. Interpretation is further complicated by the potential impact of demand ischaemia, due to fever and tachycardia typically associated with respiratory failure, on myocardial pathology. Moreover, in the absence of molecular evidence documenting the



presence of the virus, the lymphocytic infiltrate found in a small number of COVID-19 patients may not represent myocarditis. Thus, the myocardial pathological alterations observed in the current study may not reflect specific effects of the virus, but rather the consequences of critical illness in a population with a high prevalence of underlying conditions.

The findings of the current study are consistent with the notion that direct COVID-19-mediated cardiac pathology may be uncommon (Figure 1). In hospitalized COVID-19 patients, elevated serum troponin levels are commonly found and are more prominent in patients with underlying conditions.⁸ However, biochemical evidence of cardiac injury is not unique to COVID-19. Patients with severe community-acquired pneumonia, requiring intensive care, typically exhibit increased troponin levels.⁹ Increased myocardial demand due to fever and tachycardia, and reduced supply due to hypoxaemia and hypotension, can result in myocardial ischaemia in vulnerable patients, and may explain the evidence of myocardial injury commonly found in high-risk COVID-19 patients.¹⁰ Moreover, systemic inflammatory activation leading to cytokine storm may promote dysfunction, whereas prothrombotic effects may trigger plaque rupture, precipitating coronary events.¹¹ The evidence documenting SARS-CoV-2 myocarditis as a cause of cardiac dysfunction is limited to case reports. In a case series studying 14 patients who succumbed

to COVID-19 in Washington State, one patient with lymphocytic myocarditis and evidence of myocardial viral RNA was identified. In a study of 39 consecutive COVID-19 autopsy cases from Germany, 41% of patients had evidence of myocardial viral presence in the absence of significant inflammation.¹² The long-term significance of viral infection in COVID-19 patients remains unknown.

The authors should be complimented, not only for producing the first systematic investigation of myocardial pathological changes in COVID-19, but also for an objective and unbiased discussion that acknowledges the limitations of the study, without overinterpretations and hype. Adoption of careful and objective approaches for data interpretation and dissemination of scientific findings is critical to overcome the challenges of the pandemic. In most research fields, interest in specialized scientific articles typically remains limited within specific groups of researchers with related interests, and overinterpreted findings are filtered through the collective perspective of the scientific community. In contrast, the COVID-19 literature generates broad interest and can have an immediate impact on the public. Throughout the world, hundreds of journalists scan the COVID-19 literature; most of them have no scientific background. Considering that the attention generated by a news article, quantified by the number of readers, clicks, and comments, is a major measure of journalistic success, it is not surprising that many journalists tend to prioritize

sensationalism over accuracy. As a result, overinterpreted scientific studies can fuel sensationalist news stories, ultimately leading to misinformation of the public.

Recent dramatic headlines regarding the 'devastating' and 'lingering' consequences of COVID-19 on the myocardium illustrate this major problem. Cardiac magnetic resonance imaging in 100 patients who recovered from COVID-19 showed that the majority (78%) had subtle increases in non-specific indicators associated with inflammation (1.9% higher native T1 and an 8.3% increase in native T2) in comparison with a risk factor-matched control group that had no history of a respiratory infection.¹³ All patients had normal systolic function. Despite the absence of any robust evidence of inflammatory activity, these observations were interpreted by the authors as suggestive of an 'ongoing perimyocarditis' and indicative of a 'considerable burden of inflammatory disease in large and growing parts of the population'. These statements fuelled dramatic warnings in the lay and scientific press suggesting that SARS-CoV-2 has a 'devastating impact on the myocardium', 'ravages the heart in many ways', and 'can have lasting effects on heart health' (<https://www.sciencemag.org/news/2020/07/brain-fog-heart-damage-covid-19-s-lingering-problems-alarm-scientists>; [Supplementary material online, Table S1](#)). Such sensationalist statements are currently not supported by evidence. We simply have no information on any long-term effects of SARS-CoV-2 in the heart.

Speculative discussions and dissemination of doomsday scenarios can have a major negative impact in our fight against the pandemic, not only by increasing anxiety levels and by spreading fear, but also by undermining public confidence in science. It is up to the scientific community to ensure that the messages communicated in scientific manuscripts are supported by robust evidence. Our goal should not be to publish a 'newsworthy' paper in order to attract attention, but rather to present the facts and to support data-driven conclusions.

Supplementary material

[Supplementary material](#) is available at *European Heart Journal* online.

Funding

N.G.F.'s laboratory is supported by National Institutes of Health grants R01 HL76246, R01 HL85440, and R01 HL149407, and by U.S. Department of Defense grants PR151029 and PR181464.

Conflict of interest: none declared.

References

- Shi S, Qin M, Shen B, Cai Y, Liu T, Yang F, Gong W, Liu X, Liang J, Zhao Q, Huang H, Yang B, Huang C. Association of cardiac injury with mortality in hospitalized patients with COVID-19 in Wuhan, China. *JAMA Cardiol* 2020;**5**: 802–810.
- Shi S, Qin M, Cai Y, Liu T, Shen B, Yang F, Cao S, Liu X, Xiang Y, Zhao Q, Huang H, Yang B, Huang C. Characteristics and clinical significance of myocardial injury in patients with severe coronavirus disease 2019. *Eur Heart J* 2020;**41**: 2070–2079.
- Buja LM, Wolf DA, Zhao B, Akkanti B, McDonald M, Lelenwa L, Reilly N, Ottaviani G, Elghetany MT, Trujillo DO, Aisenberg GM, Madjid M, Kar B. The emerging spectrum of cardiopulmonary pathology of the coronavirus disease 2019 (COVID-19): report of 3 autopsies from Houston, Texas, and review of autopsy findings from other United States cities. *Cardiovasc Pathol* 2020;**48**: 107233.
- Bradley BT, Maioli H, Johnston R, Chaudhry I, Fink SL, Xu H, Najafian B, Deutsch G, Lacy JM, Williams T, Yarid N, Marshall DA. Histopathology and ultrastructural findings of fatal COVID-19 infections in Washington State: a case series. *Lancet* 2020;**396**:320–332.
- Basso C, Leone O, Rizzo S, De Gaspari M, Van der Wal AC, Aubry M-C, Bois MC, Lin PT, Maleszewski JJ, Stone JR. Pathological features of COVID-19-associated myocardial injury: a multicentre cardiovascular pathology study. *Eur Heart J* 2020;doi: 10.1093/eurheartj/ehaa664.
- Yoshizawa S, Uto K, Nishikawa T, Hagiwara N, Oda H. Histological features of endomyocardial biopsies in patients undergoing hemodialysis: comparison with dilated cardiomyopathy and hypertensive heart disease. *Cardiovasc Pathol* 2020; **49**:107256.
- Frangogiannis NG, Shimoni S, Chang SM, Ren G, Shan K, Aggeli C, Reardon MJ, Letsou GV, Espada R, Ramchandani M, Entman ML, Zoghbi WA. Evidence for an active inflammatory process in the hibernating human myocardium. *Am J Pathol* 2002;**160**:1425–1433.
- Deng Q, Hu B, Zhang Y, Wang H, Zhou X, Hu W, Cheng Y, Yan J, Ping H, Zhou Q. Suspected myocardial injury in patients with COVID-19: evidence from front-line clinical observation in Wuhan, China. *Int J Cardiol* 2020;**311**:116–121.
- Frencken JF, van Baal L, Kappen TH, Donker DVW, Horn J, van der Poll T, van Klei WA, Bonten MJM, Cremer OL, Members of the MARS Consortium. Myocardial injury in critically ill patients with community-acquired pneumonia. A cohort study. *Ann Am Thorac Soc* 2019;**16**:606–612.
- Libby P. The heart in COVID19: primary target or secondary bystander? *JACC Basic Transl Sci* 2020;**5**:537–542.
- Tomasoni D, Italia L, Adamo M, Inciardi RM, Lombardi CM, Solomon SD, Metra M. COVID-19 and heart failure: from infection to inflammation and angiotensin II stimulation. Searching for evidence from a new disease. *Eur J Heart Fail* 2020;**22**: 957–966.
- Lindner D, Fitzek A, Brauning H, Aleshcheva G, Edler C, Meissner K, Scherschel K, Kirchhof P, Escher F, Schultheiss HP, Blankenberg S, Puschel K, Westermann D. Association of cardiac infection with SARS-CoV-2 in confirmed COVID-19 autopsy cases. *JAMA Cardiol* 2020;doi:10.1001/jamacardio.2020.3551.
- Puntmann VO, Carerj ML, Wieters I, Fahim M, Arendt C, Hoffmann J, Shchendrygina A, Escher F, Vasa-Nicotera M, Zeiher AM, Vahreschild M, Nagel E. Outcomes of cardiovascular magnetic resonance imaging in patients recently recovered from coronavirus disease 2019 (COVID-19). *JAMA Cardiol* 2020;doi: 10.1001/jamacardio.2020.3557.

Inflammatory Cytokines and Chemokines as Therapeutic Targets in Heart Failure

**Anis Hanna & Nikolaos
G. Frangogiannis**

Cardiovascular Drugs and Therapy

ISSN 0920-3206

Cardiovasc Drugs Ther

DOI 10.1007/s10557-020-07071-0



Your article is protected by copyright and all rights are held exclusively by Springer Science+Business Media, LLC, part of Springer Nature. This e-offprint is for personal use only and shall not be self-archived in electronic repositories. If you wish to self-archive your article, please use the accepted manuscript version for posting on your own website. You may further deposit the accepted manuscript version in any repository, provided it is only made publicly available 12 months after official publication or later and provided acknowledgement is given to the original source of publication and a link is inserted to the published article on Springer's website. The link must be accompanied by the following text: "The final publication is available at link.springer.com".



Inflammatory Cytokines and Chemokines as Therapeutic Targets in Heart Failure

Anis Hanna¹ · Nikolaos G. Frangogiannis¹

Accepted: 1 September 2020

© Springer Science+Business Media, LLC, part of Springer Nature 2020

Abstract

Heart failure exhibits remarkable pathophysiologic heterogeneity. A large body of evidence suggests that regardless of the underlying etiology, heart failure is associated with induction of cytokines and chemokines that may contribute to the pathogenesis of adverse remodeling, and systolic and diastolic dysfunction. The pro-inflammatory cytokines tumor necrosis factor (TNF)- α , interleukin (IL)-1, and IL-6 have been extensively implicated in the pathogenesis of heart failure. Inflammatory cytokines modulate phenotype and function of all myocardial cells, suppressing contractile function in cardiomyocytes, inducing inflammatory activation in macrophages, stimulating microvascular inflammation and dysfunction, and promoting a matrix-degrading phenotype in fibroblasts. Moreover, cytokine-induced growth factor synthesis may exert chronic fibrogenic actions contributing to the pathogenesis of heart failure with preserved ejection fraction (HFpEF). In addition to their role in adverse cardiac remodeling, some inflammatory cytokines may also exert protective actions on cardiomyocytes under conditions of stress. Chemokines, such as CCL2, are also upregulated in failing hearts and may stimulate recruitment of pro-inflammatory leukocytes, promoting myocardial injury, fibrotic remodeling, and dysfunction. Although experimental evidence suggests that cytokine and chemokine targeting may hold therapeutic promise in heart failure, clinical translation remains challenging. This review manuscript summarizes our knowledge on the role of TNF- α , IL-1, IL-6, and CCL2 in the pathogenesis of heart failure, and discusses the promises and challenges of targeted anti-cytokine therapy. Dissection of protective and maladaptive cellular actions of cytokines in the failing heart, and identification of patient subsets with overactive or dysregulated myocardial inflammatory responses are required for design of successful therapeutic approaches.

Keywords Heart failure · Cytokine · Chemokine · Inflammation · Interleukin-1 · TNF- α

Introduction

Heart failure is a condition in which the heart either cannot pump enough blood to meet the needs of various tissues or can do so only at the cost of increased filling pressures [1, 2]. Based on the ejection fraction, the most commonly used indicator of systolic function, heart failure patients can be classified into two major groups. Heart failure patients with reduced ejection fraction (HFrEF) exhibit depressed systolic function. On the other hand, the term heart failure with preserved

ejection fraction (HFpEF) is used for patients who have the same heart failure symptoms, in the absence of significant reductions in ejection fraction. Elevated filling pressures in HFpEF patients are caused predominantly by perturbations in diastolic function. Epidemiologic studies have demonstrated that HFpEF accounts for almost half of all incident heart failure [3]. Both HFrEF and HFpEF have a poor prognosis. Although approaches targeting neurohumoral pathways have shown beneficial effects in patients with HFrEF, effective therapeutic strategies for HFpEF are lacking.

A major obstacle that hampers development of new therapeutics in heart failure is the pathophysiologic heterogeneity of the disease. The clinical syndrome of heart failure can be triggered by a wide range of pathophysiologic changes, including myocardial ischemia and infarction, pressure or volume overload, metabolic dysregulation, genetic perturbations in sarcomeric protein function, and responses to viral infections. Regardless of underlying etiology, heart failure is

✉ Nikolaos G. Frangogiannis
nikolaos.frangogiannis@einstein.yu.edu

¹ Department of Medicine (Cardiology), The Wilf Family Cardiovascular Research Institute, Albert Einstein College of Medicine, 1300 Morris Park Avenue Forchheimer G46B, Bronx, NY 10461, USA

associated with both local and systemic activation of inflammatory signaling cascades [4]. In patients with myocarditis or inflammatory cardiomyopathies, inflammation is the primary cause of heart failure [5]. Moreover, cytokine-mediated inflammation has been implicated in acute stress-induced cardiomyopathy [6], an enigmatic entity that may be associated with major emotional or physical stress [7], and may also be a rare cause of myocardial injury in patients with coronavirus disease 2019 (COVID-19) [8, 9]. In most other cases, activation of an inflammatory program reflects a reparative or protective response to other primary injurious processes. Regardless of the underlying etiology, excessive, unrestrained, or dysregulated inflammation may exacerbate myocardial injury, thus contributing to the progression of heart failure. The inflammatory response in the failing heart is characterized by induction and activation of a wide range of pleiotropic cytokines and chemokines that modulate phenotype and function of all myocardial cells. The complexity and pleiotropy of inflammatory mediators have hampered therapeutic implementation of therapeutic strategies targeting the inflammatory response.

This review manuscript discusses the potential role of the best-studied and most promising pro-inflammatory cytokines and chemokines as therapeutic targets in heart failure. We focus on the prototypic inflammatory cytokines tumor necrosis factor (TNF)- α , interleukin (IL)-1 and IL-6, and on the CC chemokine CCL2/monocyte chemoattractant protein (MCP)-1. We summarize the cell biological actions of these mediators in the failing heart and their potential contribution to dysfunction and heart failure progression. Finally, we discuss the promises and challenges of cytokine and chemokine targeting in heart failure patients.

Inflammatory Cytokines in the Pathogenesis of Chronic Heart Failure

A large body of evidence, derived through both experimental and clinical studies, supports an important role for inflammatory cytokines and chemokines in the pathogenesis of myocardial dysfunction and adverse cardiac remodeling. Marked elevations of circulating pro-inflammatory cytokines are consistently noted in heart failure patients, in both HFrEF and HFpEF subpopulations [10, 11]. Cytokine levels are further increased in patients exhibiting an acute decompensation [12] and seem to predict clinical outcome [13]. Patients with ischemic cardiomyopathy in the absence of myocardial infarction exhibit induction of chemokines in chronically ischemic myocardial segments, accompanied by recruitment of inflammatory leukocytes [14]. Moreover, several studies using experimental animal models of heart failure induced through a wide range of pathophysiologic perturbations showed that disruption of pro-inflammatory cytokine signaling may exert

beneficial actions [15–17]. However, this evidence should not be interpreted as suggestive of unidimensional deleterious effects of inflammatory cytokine signaling in failing hearts. Inflammatory cytokines are highly pleiotropic and multifunctional. Several members of the cytokine and chemokine families are upregulated in response to myocardial injury and may exert important protective actions on cardiomyocytes [18], while activating reparative programs [19]. Although there is little doubt that dysregulated, excessive, or prolonged inflammatory responses precipitate or worsen heart failure in human patients, the relative contribution of inflammatory signaling likely depends on the underlying etiology of the disease. In patients developing heart failure due to viral myocarditis, inflammatory injury may be the primary cause of dysfunction and adverse remodeling [5, 20]. In contrast, in other heart failure etiologies, the role of inflammatory cytokines is less convincingly documented. All types of myocardial injury result in secondary activation of an immune response. Several lines of evidence support the notion that regardless of the underlying etiology of heart failure, cytokine and chemokine induction promote dysfunction and progressive remodeling of the myocardium. First, inflammatory cytokines have negative inotropic effects [21]. Second, inflammatory cytokines may promote cardiomyocyte apoptosis [22]. Third, pro-inflammatory cytokines may activate a matrix-degrading program, inducing matrix metalloproteinases, and triggering extracellular matrix degradation [23], thus depriving cardiomyocytes from key matrix-driven signals that preserve homeostatic function. Fourth, chronic pro-inflammatory cytokine activation may stimulate a fibrogenic program, leading to induction of fibrogenic growth factors, expansion of activated fibroblasts, and subsequent deposition of extracellular matrix (ECM) proteins in the cardiac interstitium. Inflammation-mediated interstitial fibrosis may increase myocardial stiffness, contributing to the pathogenesis of HFpEF [24, 25]. To what extent these detrimental actions outweigh any protective effects of the inflammatory mediators is dependent on the pathophysiologic context and on the cytokine-specific patterns of inflammatory activation.

Pro-Inflammatory Cytokines in Heart Failure

TNF- α

The multifunctional cytokine TNF- α is the best-studied inflammatory mediator in heart failure. In the early 1990s, observations suggesting that HFrEF patients have markedly elevated circulating TNF- α levels [10] triggered a large body of experimental work to investigate the effects of TNF- α in the failing heart. Although clinical trials showed that anti-TNF approaches do not benefit human heart failure patients, the insights gained by studying the role of TNF- α in the

myocardium contributed significantly to our understanding of the complex role of inflammation in heart disease, and the clinical investigations highlighted the challenges of therapeutic translation.

Expression and Role of TNF- α in Heart Failure

Increased myocardial expression of TNF- α has been consistently documented in experimental models of heart failure [26, 27] and in human patients with cardiomyopathic conditions [28]. Several different cell types contribute to the increased expression of TNF- α in injured and failing hearts, including cardiomyocytes [27], macrophages [29], vascular cells [29], and mast cells [30]. The mechanisms of TNF- α induction may involve activation of mechanosensitive signaling cascades [27], neurohumoral signaling, or responses to damage-associated molecular patterns (DAMPs) released by injured cardiomyocytes. Several lines of evidence support the notion that TNF- α may play a causative role in heart failure. First, mice with cardiac-specific overexpression of TNF- α develop dilated cardiomyopathy [22, 31, 32] and infusion of TNF- α impairs LV systolic and diastolic function in dogs [33]. Second, *TNF* deletion attenuated dysfunction in a model of left ventricular pressure overload [15], and TNF- α antagonism reduced adverse remodeling and improved hemodynamics in models of volume overload and post-infarction heart failure [34, 35]. Third, in human heart failure patients, higher circulating levels of TNF- α were associated with increased mortality rates in both HFrEF and HFpEF subpopulations [36].

Cell Biological Mechanisms Responsible for the Effects of TNF- α in Heart Failure

TNF- α -mediated adverse remodeling and heart failure progression may involve effects on cardiomyocytes, macrophages, and the extracellular matrix (Fig. 1). In cardiomyocytes, TNF- α exerts negative inotropic actions by perturbing calcium homeostasis [37] and may trigger an apoptotic response by activating intrinsic cell death pathways [38]. In macrophages, TNF- α may stimulate synthesis of other pro-inflammatory cytokines with pro-apoptotic, negative inotropic, and matrix-degrading properties [39], and may upregulate expression of inducible nitric oxide synthase (iNOS) [40]. In fibroblasts, TNF- α may disrupt the balance between matrix metalloproteinases (MMPs) and their inhibitors, leading to ECM degradation [41, 42]. Finally, in the microvasculature, TNF- α increases permeability through modulation of endothelial cyclooxygenase-2, [43] and induces expression of endothelial adhesion molecules, such as intercellular adhesion molecule (ICAM)-1 and vascular cell adhesion molecule (VCAM)-1 [44], thus enhancing adhesive interactions between circulating leukocytes and the endothelial lining. Neutrophils or pro-inflammatory monocytes may be trapped in the cardiac microcirculation, thus contributing to tissue injury and cardiac dysfunction.

Several studies have suggested that in addition to its effects in progression and accentuation of adverse remodeling and dysfunction, TNF- α may also exert protective actions on injured or stressed cardiomyocytes. In a model of non-reperfused MI, global deletion of TNF receptors (*TNFRs*) was associated with increased infarct size, suggesting that TNF- α signaling may transduce cytoprotective signals [18]. In a genetic model of cardiomyopathy due to desmin loss, TNF- α was found to have cytoprotective actions by promoting formation of an alternative cytoskeletal network that prevents deterioration of cardiac function [45]. Whether this mechanism can be generalized in other models of heart failure remains unknown. In isolated rat hearts, low-dose TNF- α improved hemodynamics; the favorable actions were attributed to the inhibitory effect of TNF- α on cardiomyocyte calcium influx that may have reduced intracellular calcium overload [46]. In addition, TNF- α protected mitochondrial respiratory function following anoxia/reoxygenation injury presumably due to modulation of reactive oxygen species (ROS) and sphingolipids [47]. The conflicting findings suggesting both protective and injurious effects of TNF- α in vivo may reflect dose-dependent effects or differences in the balance between TNFR1 versus TNFR2 signaling in various cell types and experimental models. It has been suggested that the deleterious effects of TNF- α on cardiac remodeling may be mediated through TNFR1 signaling; in contrast, TNFR2 actions may be beneficial [39]. However, the cell-specific actions of TNFR signaling in vivo and their role in mediating cardiac remodeling have not been systematically investigated.

TNF- α Antagonism in Patients with Heart Failure

The in vivo evidence on the deleterious effects of TNF- α in the failing myocardium, and early clinical studies suggesting attenuated dysfunction in small groups of patients receiving TNF- α antagonists [48] fueled large clinical trials to investigate the effectiveness of TNF- α blockade in HFrEF patients. Unfortunately, the results were disappointing [49]. The Randomized Etanercept North American Strategy to Study Antagonism of Cytokines (RENAISSANCE) and Research into Etanercept Cytokine antagonism in VENTRICULAR dysfunction (RECOVER) trials tested the effects of TNF- α antagonism through administration of soluble TNFR (etanercept) in patients with heart failure and systolic dysfunction. Both trials were halted prematurely due to the lack of clinical benefit. In addition, the data from both trials were combined in the Randomized Etanercept Worldwide Evaluation (RENEWAL) trial; however, again etanercept had no effect on the primary endpoint of death or heart failure hospitalization in HFrEF patients [50]. The phase II Anti-TNF- α in Congestive Heart Failure (ATTACH) trial examined the effects of infliximab, a chimeric monoclonal anti-TNF- α antibody in HFrEF patients. TNF- α antagonism using

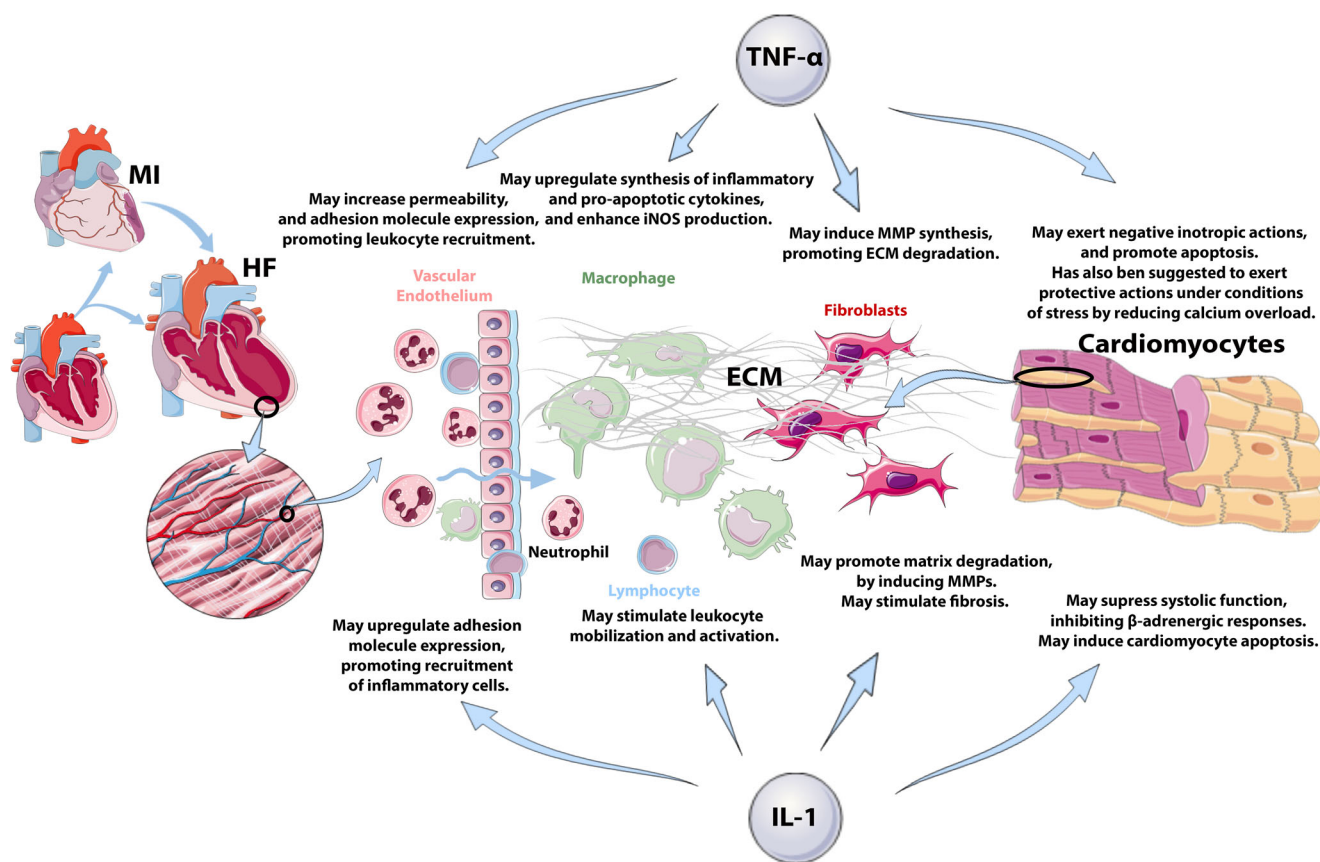


Fig. 1 Cellular actions of TNF- α and IL-1 in heart failure. The pleiotropic cytokines TNF- α and IL-1 have been implicated in both post-infarction heart failure (HF) and in non-ischemic HF by modulating phenotype and function of cardiomyocytes, immune cells, fibroblasts, and vascular cells. Both TNF- α and IL-1 have negative inotropic actions and induce apoptosis in cardiomyocytes. Moreover, both TNF- α and IL-1 induce MMP expression,

promoting degradation of the cardiac extracellular matrix (ECM), and stimulate inflammatory signaling in leukocytes and vascular endothelial cells. However, several studies have suggested that TNF- α may exert protective actions on cardiomyocytes under conditions of stress, by regulating calcium homeostasis and by preserving mitochondrial function. The cartoon was designed using Servier Medical Art (<https://smart.servier.com/>)

infliximab had adverse effects, increasing all-cause mortality and heart failure hospitalizations in comparison with conventional treatment [51]. The conflicting findings between the highly promising animal model investigations and early clinical studies, and the disappointing large clinical trials are frustrating, but may be explained considering the heterogeneity of heart failure and the pleiotropic effects of the cytokines. First, in human patients the (well-described) protective effects of TNF- α on cardiomyocytes may be more prominent than any deleterious actions. Second, human heart failure populations are pathophysiologically heterogeneous. Thus, TNF- α antagonism may afford benefit in a yet unidentified subset of patients with prominent cytokine-mediated injury. Third, dose-dependent effects of the cytokine may complicate design of effective therapy. Failing hearts may require an optimal level of TNF- α activity to preserve function and to prevent excessive remodeling. In addition, intrinsic biological actions of the anti-TNF agents may have contributed to the adverse effects of the treatment in some clinical trials. TNFR antagonists may also act as agonists (referred to as “stimulating antagonists”) and may stabilize the cytokine under certain conditions [52].

IL-1

The IL-1 family has 11 cytokine members and 10 receptors [53]; IL-1 α /IL-1 β , IL-18, and the IL-33/ST2 axis are the best-studied members of the family in the cardiovascular system. A large body of experimental evidence supports the notion that members of the IL-1 family may play an important role in progression of heart failure and in the pathogenesis of systolic dysfunction [54, 55]. However, the potential effectiveness of IL-1 targeting in patients with heart failure has not been established.

Expression and Role of IL-1 in Heart Failure

IL-1 is consistently upregulated in experimental models of heart failure due to a wide range of etiologies, including myocardial infarction [56], left ventricular pressure overload [57, 58], transgenic overexpression of calcineurin [59], and diabetic cardiomyopathy [60]. Moreover, myocardial IL-1 β induction has been reported in patients with cardiomyopathic conditions [61]. Heart failure is also associated with activation of

the inflammasome [62], a molecular platform of several components that is involved in caspase-1-mediated processing of pro-IL-1 β into its active form. Several cell types may contribute to IL-1 synthesis and activation in injured and failing hearts, including immune cells, fibroblasts, vascular cells, and cardiomyocytes [57, 62–64].

Extensive experimental evidence suggests an important role for IL-1 signaling in the pathogenesis of cardiac dysfunction and adverse remodeling associated with heart failure. Mice with genetic disruption of IL-1 signaling due to loss of *IL1RI*, the signaling receptor for IL-1, had attenuated adverse remodeling after myocardial infarction, exhibiting suppressed inflammatory responses [16]. Pharmacologic targeting of IL-1 cascades also showed protective effects in experimental models. Administration of recombinant IL-1Ra (anakinra) protected the heart from adverse remodeling in rodent models of post-infarction and non-ischemic heart failure [65, 66]. Treatment with anti-IL-1 β antibodies was also effective in heart failure models. In both diabetic and non-diabetic rats with post-infarction heart failure, administration of the anti-IL-1 β antibody gevokizumab attenuated dilative remodeling and improved ventricular function, reducing hypertrophy and fibrosis [67]. However, some studies have suggested that endogenous activation of sub-inflammatory levels of IL- β may also play an adaptive role following pressure overload mediating growth factor-induced compensatory hypertrophy [68].

What Are the Cellular Mechanisms of IL-1-Mediated Heart Failure?

As the prototypical pleiotropic pro-inflammatory cytokine, IL-1 acts on many different cell types (Fig. 1). Although the cellular basis for IL-1-driven cardiac remodeling and dysfunction has not been systematically studied, associative data and in vitro experiments suggest several potential mechanisms. First, much like TNF- α , IL-1 suppresses systolic cardiomyocyte function through effects that may involve disruption of calcium handling [69] or suppression of β -adrenergic responses [70]. Second, IL-1 exerts pro-apoptotic actions on cardiomyocytes [71]. Third, IL-1 induces leukocyte mobilization and activation, thus stimulating downstream inflammatory responses [72, 73]. Fourth, IL-1 may stimulate adhesion molecule expression in endothelial cells [74], promoting adhesive interactions with circulating leukocytes and increasing recruitment of inflammatory cells in the myocardium. Fifth, IL-1 promotes a matrix-degrading phenotype in fibroblasts, contributing to disruption of critical matrix–cardiomyocyte interactions required for cell survival [73]. Sixth, IL-1-driven matrix degradation may ultimately activate fibroblast-mediated matrix protein synthesis, resulting in accentuated fibrosis [75] through increased expression of fibrogenic

growth factors. Seventh, IL-1 may increase arterial stiffness [76] and microvascular inflammation, thus contributing to the pathogenesis of HFpEF. Finally, in heart failure associated with autoimmune myocarditis, the effects of IL-1 may involve dendritic cell activation and subsequent stimulation of autoreactive CD4⁺ T cells [77].

Targeting the IL-1 System in Human Heart Failure Patients

In the Canakinumab Anti-Inflammatory Thrombosis Outcomes Study (CANTOS) trial, treatment of patients with prior myocardial infarction and evidence of active inflammation (suggested by elevated high sensitivity C-reactive protein (hsCRP)) with the anti-IL1 β monoclonal antibody canakinumab had modest favorable effects, reducing the risk of the composite endpoint (non-fatal myocardial infarction, non-fatal stroke or death) by 15% in comparison with standard treatment [78]. The study supported the role of IL-1 β in the pathogenesis of atherothrombotic disease and also generated observations that may be important in understanding and treating heart failure. A pre-specified exploratory analysis of the CANTOS data showed that IL-1 β inhibition reduced the rate of heart failure hospitalizations or heart failure–related death in a dose-dependent manner [79]. Although the CANTOS trial was not designed to examine the effectiveness of IL-1 β targeting in heart failure, the findings are consistent with animal model experiments and suggest that canakinumab may have therapeutic benefit in subsets of heart failure patients. Animal model studies also support protective actions of gevokizumab, another anti-IL-1 β antibody, in patients with post-infarction heart failure [67]. In addition, other smaller studies further support this concept. In two small clinical studies in HFrEF patients, anakinra treatment improved indicators of systolic function [80]. In a small group of patients with HFpEF and elevated hsCRP, treatment with anakinra reduced NT-proBNP, but failed to improve indicators of cardiorespiratory fitness [81]. Moreover, in patients with rheumatoid arthritis, treatment with anakinra improved indicators of left ventricular and vascular function [76, 82]. Thus, IL-1 inhibition may hold promise as therapy for subpopulations of heart failure patients exhibiting prominent pro-inflammatory activation.

IL-6

IL-6 is the prototypical member of the gp130 cytokine family of cytokines that also includes several other cytokines that have been implicated in the pathogenesis of cardiovascular diseases, such as IL-11, leukemia inhibitory factor (LIF), cardiotrophin-1, and oncostatin-M. These cytokines transduce signals through the common signaling receptor subunit gp130 [83], activating Janus kinases and triggering STAT3 phosphorylation.

Expression and Role of IL-6 in Heart Failure

IL-6 is consistently upregulated in experimental models of cardiac injury and heart failure regardless of the underlying etiology, and is expressed by cardiomyocytes, infiltrating mononuclear cells, and fibroblasts [30, 84–86]. Moreover, in pressure-overloaded hearts, IL-6 induction is accompanied by upregulation of the IL-6 receptor (IL-6R α) [86]. Increased IL-6 expression may reflect the stimulatory effects of neurohumoral pathways, Toll-like receptor (TLR) agonists, or other pro-inflammatory cytokines (such as TNF- α and IL-1) on myocardial cells, or infiltrating leukocytes. During heart failure progression, negative regulatory mechanisms may be activated to restrain expression of IL-6 and other pro-inflammatory cytokines. Degradation of IL-6 mRNA by the RNase regnase-1 has been suggested as a mechanism restraining IL-6 expression and pro-inflammatory actions in the pressure-overloaded myocardium [87]. Although several clinical studies have demonstrated that failing hearts have increased myocardial IL-6 expression in comparison with non-failing myocardium [88], other investigations failed to show increased IL-6 synthesis in heart failure [89], but reported increased levels of downstream components of the IL-6 signaling cascade, such as gp130. The conflicting findings may reflect sampling at different stages of the disease, study of different subsets of heart failure patients, or activation of the IL-6/IL-6R axis [90] in rejected donor hearts, typically used as controls in many studies.

Experimental studies on the role of IL-6 in heart failure have produced conflicting findings, dependent on the model, the pathophysiologic context, and the type of interventions used to study the effects of IL-6 signaling. The bulk of the evidence suggests that the effects of IL-6 signaling in the failing heart are primarily pro-inflammatory and may accentuate dysfunction. Persistent gp130/STAT3 signaling enhanced inflammation in remodeling infarcted hearts [91]. Moreover, in the pressure-overloaded myocardium, genetic loss of *IL6* improved cardiac function and attenuated hypertrophy through actions attributed to abrogation of CaMKII-dependent effects on cardiomyocytes [92]. However, other investigations using similar genetic approaches found no significant effects of *IL6* deletion on the pressure-overloaded heart [93]. Pharmacologic blockade of IL-6 through administration of an anti-IL6R antibody attenuated dilation and improved function in a model of post-infarction heart failure [94].

The Pleiotropic Actions of IL-6 in the Failing Heart: The Impact of Cell-Specific Effects and Trans-Signaling

IL-6 is notorious for its pleiotropic actions on many different cell types involved in heart failure, including macrophages, lymphocytes, cardiomyocytes, fibroblasts, and vascular cells. Moreover, the concept of IL-6 trans-signaling contributes an

additional layer of complexity to IL-6-mediated actions. Classic IL-6 signaling involves binding of the cytokine to the IL-6R on the cell surface, and subsequent association of the IL-6/IL-6R complex with gp130, which dimerizes and initiates signaling. However, IL-6 can also signal in the absence of cell surface IL-6R. A Disintegrin and Metalloprotease (ADAM) proteases can cleave IL-6R from the cells, generating soluble IL-6R (sIL-6R), which may associate with IL-6, stimulating gp130 signaling on cells that do not express IL-6R on their surface [95]. This mechanism called “trans-signaling” significantly expands the cellular repertoire of IL-6 and complicates interpretation of its cellular actions (Fig. 2) [83]. Unfortunately, very little is known regarding the relative in vivo role of classic and trans IL-6 signaling in the failing heart.

In heart failure, IL-6 has important modulatory effects on several different cell types. In cardiomyocytes, IL-6 exerts negative inotropic effects [96] and promotes a hypertrophic response [97–99] through the gp130/STAT3 pathway, but may also exert protective actions, mediated through preservation of mitochondrial function [100]. In fibroblasts, IL-6 promotes proliferation and stimulates ECM synthesis [101–103]. The combined effects of IL-6 on cardiomyocytes and fibroblasts may play an important role in the pathogenesis of HFpEF. In experimental mouse studies, infusion of IL-6 caused concentric hypertrophy and fibrosis, and increased myocardial stiffness [97]. IL-6 also has potent modulatory effects on macrophages and lymphocytes. Both pro- and anti-inflammatory effects of IL-6 have been reported [104–107]; trans-signaling has been suggested to exert pro-inflammatory actions, whereas canonical IL-6 signaling may be anti-inflammatory [108]. The in vivo role of IL-6 in inflammation is likely dependent on the relative contribution of macrophage and lymphocyte subsets, and on the relative role of classic versus trans-signaling in each specific inflammatory condition. In the absence of cell-specific dissection in vivo, it is impossible to define the role of inflammatory signaling in mediating the in vivo effects of IL-6 in failing hearts.

Targeting IL-6 in Human Heart Failure

Extensive evidence suggests that IL-6 plays a crucial role in the post-inflammatory hepatic acute phase response and is implicated in autoimmunity. Based on this evidence, IL-6 has been considered an attractive therapeutic target in many conditions associated with inflammation. The IL-6 receptor neutralizing antibody tocilizumab has been approved as effective therapy for patients with moderate to severe rheumatoid arthritis and temporal arteritis, and for the treatment of the cytokine release syndrome associated with CAR-T cell therapies. Experimental evidence demonstrating involvement of IL-6 signaling in the pathogenesis of heart failure suggests that treatment with tocilizumab may also be effective in heart failure patients. However, clinical studies supporting this

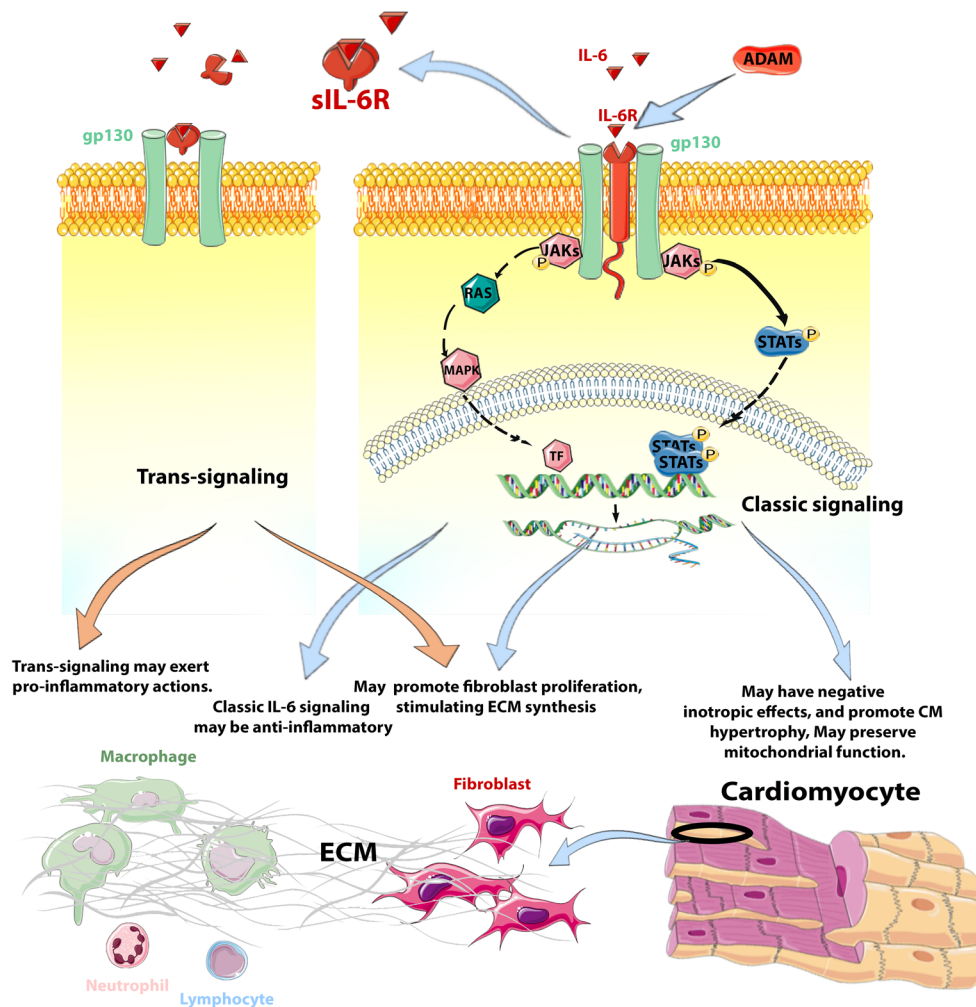


Fig. 2 IL-6 signaling and cellular actions in the failing heart. The wide range of cellular targets of IL-6 and the complexity of IL-6 signaling may explain its pleiotropic actions in heart failure. IL-6 has been reported to exert both pro- and anti-inflammatory actions, stimulates fibroblast proliferation and ECM synthesis, and promotes cardiomyocyte hypertrophy. The potential role of trans-signaling adds a layer of complexity to IL-6 actions. Classically, IL-6 signals through binding to the IL-6 receptor (IL-6R) which in turn associates with the dimerized gp130 receptor subunit gp130 to form a receptor complex that activates Janus kinases and

triggers STAT3 phosphorylation. Cells lacking the IL-6R may also be affected by IL-6 through trans-signaling. ADAM proteases can cleave IL-6R from cell surface, generating soluble IL-6R (sIL-6R), which may associate with IL-6, stimulating gp130/STAT3 signaling on cells lacking IL-6R. While classic IL-6 signaling may be anti-inflammatory, trans-signaling has been suggested to exert pro-inflammatory actions. The relative contributions of canonical and trans IL-6 signaling in heart failure have not been systematically studied. This cartoon was designed using Servier Medical Art (<https://smart.servier.com/>)

notion are lacking. In patients with rheumatoid arthritis in the absence of cardiovascular disease, tocilizumab reduced the circulating levels of N-terminal pro-B-type natriuretic peptide (NT-proBNP) [109]; this finding may reflect cardioprotective actions that may attenuate heart failure development. A phase II clinical trial tested the effectiveness of tocilizumab in reducing ischemic myocardial injury in acute coronary syndromes. In non-ST elevation myocardial infarction (non-STEMI) patients, a single dose of tocilizumab administered prior to coronary angiography was safe and attenuated troponin T release and systemic inflammation [110]. Although IL-6 blockade reduced serum CRP, levels of the chemokines CXCL10 and CCL4 were increased, highlighting the complexity of IL-6 actions on inflammatory cascades [111].

It should be noted that the use of anti-IL-6 therapeutics is complicated by the classic versus trans-signaling actions of the cytokine. Anti-IL-6R antibodies block all modes of IL-6 signaling, whereas soluble gp130 selectively inhibits IL-6 trans-signaling by binding to the IL-6-sIL-6R complex. The effects of various IL-6 targeting strategies on the failing heart have not been systematically investigated.

CCL2 and the Chemokines

Chemokines are small (8–12 kDa) chemotactic cytokines that regulate cell migration and positioning in development, homeostasis, and inflammation [112]. On a structural basis,

chemokines can be subclassified into four subfamilies: the XC, CC, CXC, and CX3C chemokines. From a functional perspective, chemokines can be “homeostatic” (constitutively expressed in certain tissues and involved in basal leukocyte trafficking and formation of lymphoid organs), “inflammatory” (members inducible following injury with effects in leukocyte recruitment and activation) [113–115], or may exhibit both homeostatic and inflammatory roles. The inflammatory CC chemokine CCL2/MCP-1 is the best-studied member of the family in heart failure and has been suggested as a therapeutic target in conditions associated with myocardial injury and adverse remodeling [116].

Expression and Role of CCL2 in Failing Hearts

CCL2 is markedly and consistently upregulated in experimental models of cardiac injury, remodeling and heart failure [19, 57, 117–119]. In infarcted and in failing hearts, CCL2 has been localized in endothelial cells [117], vascular smooth muscle cells [120], mononuclear cells [17], and cardiomyocytes [119]; its induction may involve activation of TLR signaling, neurohumoral cascades, or pro-inflammatory cytokine-mediated pathways [115]. Studies in human patients also demonstrated CCL2 upregulation in failing hearts. CCL2 was overexpressed in myocardial samples from patients with ischemic [14], dilated [121], or hypertrophic cardiomyopathy [122].

Extensive experimental evidence suggests that CCL2 contributes to adverse remodeling, dysfunction, and fibrosis in models of infarctive and non-infarctive heart failure (Table 1). In models of myocardial infarction, CCL2 deletion and anti-CCL2 gene therapy improved adverse remodeling [124], at the expense of delayed phagocytosis of dead cardiomyocytes with granulation tissue [19]. In a model of ischemic fibrotic cardiomyopathy induced through brief repetitive ischemia followed by reperfusion, CCL2 contributed to macrophage recruitment, fibrotic remodeling, and systolic dysfunction [17]. Moreover, in a model of left ventricular pressure overload, CCL2 neutralization attenuated diastolic dysfunction, reducing fibrosis [120]. Clinical studies have also generated associative data consistent with an important role of CCL2 in heart failure. In HF_{rEF} patients, high circulating CCL2 levels were associated with more severe symptoms and worse systolic dysfunction [130]. Moreover, in patients with advanced heart failure, high circulating levels of CCL2 were associated with increased mortality [131].

What Is the Cellular Basis for the Effects of CCL2 on Cardiac Remodeling and Dysfunction?

Immune cells are the most likely major cellular targets of CCL2 in failing hearts. As an inducible inflammatory CC chemokine, CCL2 is markedly upregulated following injury, binds to

proteoglycans on the endothelium or the ECM, and promotes recruitment of pro-inflammatory CCR2⁺ monocytes. In the infarcted and remodeling myocardium, CCR2⁺ monocytes may promote injury and exacerbate dysfunction by secreting pro-inflammatory cytokines and matrix-degrading proteases. CCL2-driven pro-inflammatory signaling may accentuate cardiomyocyte death; disruption of the CCL2/CCR2 axis in experimental models of myocardial infarction was reported to reduce infarct size in many [132–135] but not in all studies [19].

CCL2 may also exert potent fibrogenic actions on the remodeling myocardium [17]. CCL2-mediated fibrosis has been attributed primarily to recruitment and activation of monocytes and macrophages, resulting in increased synthesis of fibrogenic mediators, such as TGF- β and osteopontin [17, 19, 136]. Whether CCL2 may also exert direct fibrogenic actions through effects on resident cardiac fibroblasts or their progenitors remains controversial. Although CCL2 has been reported to stimulate pro-fibrotic signaling in skin, liver, and lung fibroblasts [137–139], in cardiac fibroblasts, CCL2 did not affect matrix gene synthesis or proliferative activity [17]. It has also been suggested that CCL2 may exert fibrogenic actions through recruitment of circulating fibroblast progenitors [126, 140]. However, the evidence supporting this notion is associative, based on colocalization of relatively non-specific hematopoietic cell and fibroblast markers in the same cells. Lineage tracing studies have consistently demonstrated that most activated fibroblasts in failing hearts are derived from resident fibroblast populations, and not from circulating hematopoietic cells [141–143]. Thus, the potential role of CCL2-mediated recruitment of fibroblast progenitors in cardiac fibrosis remains unclear [144].

It has also been suggested that CCL2 may exert direct actions on cardiomyocytes, increasing injury-associated death and promoting dysfunction. Some studies have suggested that CCL2 may promote cardiomyocyte apoptosis through induction of the ribonuclease monocyte chemoattractant protein-1-induced protein (MCPIP, originally proposed to function as a transcription factor), also known as regnase-1 [145, 146]. However, regnase-1/MCPIP can be induced by a wide range of inflammatory mediators, and is known to restrain inflammation by degrading cytokine RNAs in immune and non-immune cells [147]. Although the bulk of the experimental evidence suggests that CCL2 contributes to adverse remodeling (while playing a role in cardiac repair), some studies using CCL2-overexpressing mice have suggested cardioprotective actions of CCL2 in ischemia/reperfusion, mediated through effects that may involve attenuation of oxidative stress [148]. These findings may reflect the consequences of baseline alterations in the cardiac microenvironment in CCL2-overexpressing mice undergoing ischemia protocols, rather than direct protective actions of CCL2 on cardiomyocytes.

Table 1 Experimental studies investigating the role of the CCL2/CCR2 axis in heart failure

Heart failure model	Intervention	Effects on cardiac function and remodeling	Cellular target and molecular mechanism	Reference
Rat model of pressure overload through suprarenal aortic constriction	Anti-CCL2 neutralizing antibody	Anti-CCL2 antibody ameliorated diastolic dysfunction.	Decreased macrophage recruitment, fibroblast proliferation and TGF- β production associated with attenuated myocardial fibrosis	[120]
Mouse model of left ventricular pressure overload	CCR2 antagonist and antibody-mediated CCR2+ cell depletion	CCR2 antagonist and depletion of CCR2+ cells attenuated LV dilation and systolic dysfunction	Attenuated CCR2+ macrophage recruitment, cardiomyocyte hypertrophy, and cardiac fibrosis	[123]
Mouse model of non-reperfused myocardial infarction	Anti-CCL2 gene therapy	Anti-CCL2 therapy attenuated LV dilatation and systolic dysfunction, and increased post-MI survival	Attenuated interstitial fibrosis, macrophage infiltration, and TNF- α and TGF- β 1 levels	[124]
Mouse model of reperfused myocardial infarction	CCL2 KO and antibody neutralization	CCL2 KO mice had reduced post-infarction dilative remodeling	Attenuated myofibroblast proliferation, reduced macrophage recruitment and activation, associated with reduced fibrosis and delayed granulation tissue formation	[19]
Mouse model of ischemic cardiomyopathy induced through brief repetitive ischemia/reperfusion	CCL2 KO and antibody neutralization	CCL2 KO mice had improved systolic function, evidenced by increased fractional shortening	Reduced fibroblast proliferation and macrophage recruitment associated with attenuated interstitial fibrosis	[17]
Mouse model of ischemia/reperfusion	Depletion of CCR2+ macrophages (by injecting DT in CCR2-DTR mice)	Depletion of CCR2+ macrophages improved LV systolic function, and reduced LV dilation	Reduced infarct size and attenuated cardiomyocyte hypertrophy	[125]
Mouse model of angiotensin II-induced cardiac remodeling	CCL2 KO	CCL2 loss did not affect systolic function, but attenuated fibrosis	Attenuated fibrogenic effects of Ang-II, and the expression of TNF- α and TGF- β 1	[126]
Mouse model of aging	CCL2 KO	Aged CCL2 KO mice had attenuated diastolic dysfunction	Reduced leukocyte infiltration, associated with attenuated fibrosis	[127]
Mouse model of streptozotocin-induced diabetes	CCR2 KO CCR2 inhibitor	CCR2 KO and inhibitor improved cardiac function and reduced LV dilation in diabetic mice	Attenuated cardiomyocyte apoptosis and induced polarization of M2 macrophages. In addition, CCR2 KO reduced myocardial fibrosis presumably due to decreased macrophage-driven inflammation and oxidative stress	[128]
N/A	Transgenic Cardiomyocyte-specific CCL2 overexpression	Cardiomyocyte-specific CCL2 overexpression in mice induced cardiac hypertrophy and dilation	Induced myocardial inflammation and fibrotic changes attributed to inflammatory cell recruitment and activation	[129]

KO knockout

CCL2 as a Therapeutic Target in Heart Failure

Considering the extensive evidence suggesting a causative role for CCL2 in cardiac remodeling and dysfunction, antagonism of the CCL2:CCR2 axis holds promise as heart failure therapy. Other CC chemokines may also be involved in recruitment of pro-inflammatory leukocytes; thus, combined targeting of several CC chemokine receptors may increase the effectiveness of the approach. Despite decades of experimental work on the biology of the chemokines, implementation of chemokine-targeting therapeutics in inflammatory conditions remains at an early stage. In a phase II clinical trial, treatment with an anti-CCR2 antibody failed to improve symptoms in patients

with rheumatoid arthritis [149]. Another phase II trial using the dual CCR2/CCR5 inhibitor cenicriviroc in patients with non-alcoholic steatohepatitis showed promise, suggesting attenuation of inflammation-driven fibrosis [150]. The effectiveness of CC chemokine targeting in human patients with heart failure has not been tested. Despite the established role of the CCL2/CCR2 axis in cardiac remodeling, several concerns are raised regarding the potential effects of CC chemokine inhibition. First, macrophages do not exert solely pro-inflammatory actions, but also serve to downregulate inflammation and to stimulate angiogenesis. Experimental studies have suggested that CCL2 may play a role in arteriogenesis [151], a process that may be important for preservation of myocardial perfusion in

patients with heart failure. Targeting CCR2 may not selectively inhibit recruitment of pro-inflammatory macrophages, but may also perturb downstream inflammatory responses that recruit protective leukocyte subsets in the remodeling myocardium. Second, use of dual CC chemokine inhibitors to target inflammation in heart failure may also reduce recruitment of lymphocyte subpopulations involved in suppression of inflammation, such as regulatory T cells (Tregs) [152].

The Challenges of Clinical Translation

Therapeutic translation is always challenging, especially when dealing with a pathophysiologically heterogeneous condition, such as heart failure. Despite the promising experimental findings in animal models, targeting pro-inflammatory chemokines and cytokines has not yet produced therapeutic benefit in patients with heart failure. Several major challenges have hampered therapeutic translation. First, documentation of clinical benefits in human heart failure populations requires well-designed and very expensive clinical trials with long follow-up. Thus, the pace of testing candidate agents in clinical trials is predictably slow. Second, animal models are inherently suboptimal tools for prediction of therapeutic efficacy. The strength of animal model studies lies in the provision of cell biological insights using reductionist approaches and standardized protocols. No animal model can recapitulate the pathophysiologic heterogeneity of human heart failure. Thus, a major priority in clinical heart failure research is the pathophysiologic stratification of human patient populations and the identification of patient subsets with excessive or dysregulated inflammatory responses. Use of inflammatory biomarkers and imaging strategies may contribute to identification of patients that may benefit from targeted cytokine therapeutics [153]. Third, the need for chronic administration of cytokine or chemokine inhibitors to delay progression of heart failure is a major concern. Pro-inflammatory signaling plays an important role in the defense against infections, in reparative responses to injury, and in control of tumors. Moreover, some members of the cytokine family have been suggested to exert important protective actions on cardiomyocytes under conditions of stress. Considering the perils of chronic administration of anti-cytokine therapeutics, it may be preferable to focus on clinical settings associated with rapid inflammation-driven cardiac remodeling, such as post-infarction heart failure [154] or acute myocarditis. In these conditions, brief cytokine inhibition may have lasting effects on the remodeling process, protecting from the development of heart failure.

Conclusions

Over the last 30 years, experimental and clinical studies have greatly contributed to our understanding of the role of inflammation in the pathogenesis of heart failure. Despite early disappointments in clinical translation, targeting inflammatory mediators remains a promising and attractive direction in heart failure therapeutics. Successful implementation of cytokine targeting approaches in heart failure patients will require dissection of specific pro-inflammatory pathways with a critical role in dysfunction and progression of adverse remodeling, and identification of patient subpopulations with dysregulated or overactive inflammatory responses that may derive maximal benefit from targeted cytokine or chemokine inhibition.

Availability of Data and Material N/A

Code Availability N/A

Funding N.G.F.'s laboratory is supported by NIH grants R01 HL76246, R01 HL85440, and R01 HL149407 and by U.S. Department of Defense grants PR151029 and PR181464.

Compliance with Ethical Standards

Conflicts of Interest/Competing Interests None.

Ethics Approval N/A

Consent to Participate N/A

Consent for Publication N/A

References

1. Pfeffer MA, Shah AM, Borlaug BA. Heart failure with preserved ejection fraction in perspective. *Circ Res.* 2019;124:1598–617. <https://doi.org/10.1161/CIRCRESAHA.119.313572>.
2. Braunwald E. Heart disease. A textbook of cardiovascular medicine. 4th Ed. Philadelphia: WB Saunders; 1992.
3. Senni M, Tribouilloy CM, Rodeheffer RJ, Jacobsen SJ, Evans JM, Bailey KR, et al. Congestive heart failure in the community: a study of all incident cases in Olmsted County, Minnesota, in 1991. *Circulation.* 1998;98:2282–9. <https://doi.org/10.1161/01.cir.98.21.2282>.
4. Dick SA, Epelman S. Chronic heart failure and inflammation: what do we really know? *Circ Res.* 2016;119:159–76. <https://doi.org/10.1161/CIRCRESAHA.116.308030>.
5. Trachtenberg BH, Hare JM. Inflammatory cardiomyopathic syndromes. *Circ Res.* 2017;121:803–18. <https://doi.org/10.1161/CIRCRESAHA.117.310221>.
6. Wilson HM, Cheyne L, Brown PAJ, Kerr K, Hannah A, Srinivasan J, et al. Characterization of the myocardial inflammatory response in acute stress-induced (Takotsubo) cardiomyopathy. *JACC Basic Transl Sci.* 2018;3:766–78. <https://doi.org/10.1016/j.jacbts.2018.08.006>.

7. Scally C, Abbas H, Ahearn T, Srinivasan J, Mezincescu A, Rudd A, et al. Myocardial and systemic inflammation in acute stress-induced (Takotsubo) cardiomyopathy. *Circulation*. 2019;139:1581–92. <https://doi.org/10.1161/CIRCULATIONAHA.118.037975>.
8. Giustino G, Croft LB, Oates CP, Rahman K, Lerakis S, Reddy VY, et al. Takotsubo cardiomyopathy in COVID-19. *J Am Coll Cardiol*. 2020;76:628–9. <https://doi.org/10.1016/j.jacc.2020.05.068>.
9. Jabri A, Kalra A, Kumar A, Alameh A, Adroja S, Bashir H, et al. Incidence of stress cardiomyopathy during the coronavirus disease 2019 pandemic. *JAMA Netw Open*. 2020;3:e2014780. <https://doi.org/10.1001/jamanetworkopen.2020.14780>.
10. Levine B, Kalman J, Mayer L, Fillit HM, Packer M. Elevated circulating levels of tumor necrosis factor in severe chronic heart failure. *N Engl J Med*. 1990;323:236–41.
11. Sanders-van Wijk S, van Empel V, Davarzani N, Maeder MT, Handschin R, Pfisterer ME, et al. Circulating biomarkers of distinct pathophysiological pathways in heart failure with preserved vs. reduced left ventricular ejection fraction. *Eur J Heart Fail*. 2015;17:1006–14. <https://doi.org/10.1002/ejhf.414>.
12. Abemethy A, Raza S, Sun JL, Anstrom KJ, Tracy R, Steiner J, et al. Pro-inflammatory biomarkers in stable versus acutely decompensated heart failure with preserved ejection fraction. *J Am Heart Assoc*. 2018;7. <https://doi.org/10.1161/JAHA.117.007385>.
13. Chirinos JA, Orlenko A, Zhao L, Basso MD, Cvijic ME, Li Z, et al. Multiple plasma biomarkers for risk stratification in patients with heart failure and preserved ejection fraction. *J Am Coll Cardiol*. 2020;75:1281–95. <https://doi.org/10.1016/j.jacc.2019.12.069>.
14. Frangogiannis NG, Shimoni S, Chang SM, Ren G, Shan K, Aggeli C, et al. Evidence for an active inflammatory process in the hibernating human myocardium. *Am J Pathol*. 2002;160:1425–33.
15. Sun M, Chen M, Dawood F, Zurawska U, Li JY, Parker T, et al. Tumor necrosis factor- α mediates cardiac remodeling and ventricular dysfunction after pressure overload state. *Circulation*. 2007;115:1398–407.
16. Bujak M, Dobaczewski M, Chatila K, Mendoza LH, Li N, Reddy A, et al. Interleukin-1 receptor type I signaling critically regulates infarct healing and cardiac remodeling. *Am J Pathol*. 2008;173:57–67.
17. Frangogiannis NG, Dewald O, Xia Y, Ren G, Haudek S, Leucker T, et al. Critical role of monocyte chemoattractant protein-1/CC chemokine ligand 2 in the pathogenesis of ischemic cardiomyopathy. *Circulation*. 2007;115:584–92.
18. Kurrelmeyer KM, Michael LH, Baumgarten G, Taffet GE, Peschon JJ, Sivasubramanian N, et al. Endogenous tumor necrosis factor protects the adult cardiac myocyte against ischemic-induced apoptosis in a murine model of acute myocardial infarction. *Proc Natl Acad Sci U S A*. 2000;97:5456–61.
19. Dewald O, Zymek P, Winkelmann K, Koerting A, Ren G, Aboukhamis T, et al. CCL2/monocyte chemoattractant protein-1 regulates inflammatory responses critical to healing myocardial infarcts. *Circ Res*. 2005;96:881–9.
20. Zhao L, Fu Z. Roles of host immunity in viral myocarditis and dilated cardiomyopathy. *J Immunol Res*. 2018;2018:5301548. <https://doi.org/10.1155/2018/5301548>.
21. Finkel MS, Oddis CV, Jacob TD, Watkins S, Hattler B, Simmons R. Negative inotropic effects of cytokines on the heart mediated by nitric oxide. *Science*. 1992;257:387–9.
22. Kubota T, McTiernan CF, Frye CS, et al. Dilated cardiomyopathy in transgenic mice with cardiac-specific overexpression of tumor necrosis factor- α . *Circ Res*. 1997;81:627–35. <https://doi.org/10.1161/01.res.81.4.627>.
23. Siwik DA, Chang DL, Colucci WS. Interleukin-1 β and tumor necrosis factor- α decrease collagen synthesis and increase matrix metalloproteinase activity in cardiac fibroblasts in vitro. *Circ Res*. 2000;86:1259–65.
24. Packer M, Kitzman DW. Obesity-related heart failure with a preserved ejection fraction: the mechanistic rationale for combining inhibitors of aldosterone, neprilysin, and sodium-glucose cotransporter-2. *JACC Heart Fail*. 2018;6:633–9. <https://doi.org/10.1016/j.jchf.2018.01.009>.
25. Frangogiannis NG. The extracellular matrix in ischemic and nonischemic heart failure. *Circ Res*. 2019;125:117–46. <https://doi.org/10.1161/CIRCRESAHA.119.311148>.
26. Kapadia S, Lee J, Torre-Amione G, Birdsall HH, Ma TS, Mann DL. Tumor necrosis factor- α gene and protein expression in adult feline myocardium after endotoxin administration. *J Clin Invest*. 1995;96:1042–52. <https://doi.org/10.1172/JCI118090>.
27. Kapadia SR, Oral H, Lee J, Nakano M, Taffet GE, Mann DL. Hemodynamic regulation of tumor necrosis factor- α gene and protein expression in adult feline myocardium. *Circ Res*. 1997;81:187–95. <https://doi.org/10.1161/01.res.81.2.187>.
28. Torre-Amione G, Kapadia S, Lee J, Durand JB, Bies RD, Young JB, et al. Tumor necrosis factor- α and tumor necrosis factor receptors in the failing human heart. *Circulation*. 1996;93:704–11.
29. Shioi T, Matsumori A, Sasayama S. Persistent expression of cytokine in the chronic stage of viral myocarditis in mice. *Circulation*. 1996;94:2930–7.
30. Frangogiannis NG, Lindsey ML, Michael LH, Youker KA, Bressler RB, Mendoza LH, et al. Resident cardiac mast cells degranulate and release preformed TNF- α , initiating the cytokine cascade in experimental canine myocardial ischemia/reperfusion. *Circulation*. 1998;98:699–710.
31. Janczewski AM, Kadokami T, Lemster B, Frye CS, McTiernan CF, Feldman AM. Morphological and functional changes in cardiac myocytes isolated from mice overexpressing TNF- α . *Am J Physiol Heart Circ Physiol*. 2003;284:H960–9. <https://doi.org/10.1152/ajpheart.0718.2001>.
32. Bryant D, Becker L, Richardson J, Shelton J, Franco F, Peshock R, et al. Cardiac failure in transgenic mice with myocardial expression of tumor necrosis factor- α . *Circulation*. 1998;97:1375–81.
33. Pagani FD, Baker LS, Hsi C, Knox M, Fink MP, Visner MS. Left ventricular systolic and diastolic dysfunction after infusion of tumor necrosis factor- α in conscious dogs. *J Clin Invest*. 1992;90:389–98. <https://doi.org/10.1172/JCI115873>.
34. Jobe LJ, Melendez GC, Levick SP, et al. TNF- α inhibition attenuates adverse myocardial remodeling in a rat model of volume overload. *Am J Physiol Heart Circ Physiol*. 2009;297:H1462–8. <https://doi.org/10.1152/ajpheart.00442.2009>.
35. Berry MF, Woo YJ, Pirulli TJ, Bish LT, Moise MA, Burdick JW, et al. Administration of a tumor necrosis factor inhibitor at the time of myocardial infarction attenuates subsequent ventricular remodeling. *J Heart Lung Transplant*. 2004;23:1061–8. <https://doi.org/10.1016/j.healun.2004.06.021>.
36. Dunlay SM, Weston SA, Redfield MM, Killian JM, Roger VL. Tumor necrosis factor- α and mortality in heart failure: a community study. *Circulation*. 2008;118:625–31. <https://doi.org/10.1161/CIRCULATIONAHA.107.759191>.
37. Yokoyama T, Vaca L, Rossen RD, Durante W, Hazarika P, Mann DL. Cellular basis for the negative inotropic effects of tumor necrosis factor- α in the adult mammalian heart. *J Clin Invest*. 1993;92:2303–12.
38. Haudek SB, Taffet GE, Schneider MD, Mann DL. TNF provokes cardiomyocyte apoptosis and cardiac remodeling through activation of multiple cell death pathways. *J Clin Invest*. 2007;117:2692–701.

39. Hamid T, Gu Y, Ortines RV, Bhattacharya C, Wang G, Xuan YT, et al. Divergent tumor necrosis factor receptor-related remodeling responses in heart failure: role of nuclear factor-kappaB and inflammatory activation. *Circulation*. 2009;119:1386–97.
40. Sanders DB, Larson DF, Hunter K, Gorman M, Yang B. Comparison of tumor necrosis factor-alpha effect on the expression of iNOS in macrophage and cardiac myocytes. *Perfusion*. 2001;16:67–74. <https://doi.org/10.1177/026765910101600110>.
41. Sivasubramanian N, Coker ML, Kurrelmeyer KM, MacLellan WR, DeMayo FJ, Spinale FG, et al. Left ventricular remodeling in transgenic mice with cardiac restricted overexpression of tumor necrosis factor. *Circulation*. 2001;104:826–31. <https://doi.org/10.1161/hc3401.093154>.
42. Li YY, Feng YQ, Kadokami T, McTiernan CF, Draviam R, Watkins SC, et al. Myocardial extracellular matrix remodeling in transgenic mice overexpressing tumor necrosis factor alpha can be modulated by anti-tumor necrosis factor alpha therapy. *Proc Natl Acad Sci U S A*. 2000;97:12746–51. <https://doi.org/10.1073/pnas.97.23.12746>.
43. Mark KS, Trickler WJ, Miller DW. Tumor necrosis factor-alpha induces cyclooxygenase-2 expression and prostaglandin release in brain microvessel endothelial cells. *J Pharmacol Exp Ther*. 2001;297:1051–8.
44. Mattila P, Majuri ML, Mattila PS, Renkonen R. TNF alpha-induced expression of endothelial adhesion molecules, ICAM-1 and VCAM-1, is linked to protein kinase C activation. *Scand J Immunol*. 1992;36:159–65. <https://doi.org/10.1111/j.1365-3083.1992.tb03087.x>.
45. Papathanasiou S, Rickelt S, Soriano ME, Schips TG, Maier HJ, Davos CH, et al. Tumor necrosis factor-alpha confers cardioprotection through ectopic expression of keratins K8 and K18. *Nat Med*. 2015;21:1076–84. <https://doi.org/10.1038/nm.3925>.
46. Rathi SS, Xu YJ, Dhalla NS. Mechanism of cardioprotective action of TNF-alpha in the isolated rat heart. *Exp Clin Cardiol*. 2002;7:146–50.
47. Lacerda L, McCarthy J, Mungly SF, et al. TNFalpha protects cardiac mitochondria independently of its cell surface receptors. *Basic Res Cardiol*. 2010;105:751–62. <https://doi.org/10.1007/s00395-010-0113-4>.
48. Deswal A, Bozkurt B, Seta Y, Pariltili-Eiswirth S, Hayes FA, Blosch C, et al. Safety and efficacy of a soluble P75 tumor necrosis factor receptor (Enbrel, etanercept) in patients with advanced heart failure. *Circulation*. 1999;99:3224–6. <https://doi.org/10.1161/01.cir.99.25.3224>.
49. Adamo L, Rocha-Resende C, Prabhu SD, Mann DL. Reappraising the role of inflammation in heart failure. *Nat Rev Cardiol*. 2020;17:269–85. <https://doi.org/10.1038/s41569-019-0315-x>.
50. Mann DL, McMurray JJ, Packer M, et al. Targeted anticytokine therapy in patients with chronic heart failure: results of the randomized etanercept worldwide evaluation (RENEWAL). *Circulation*. 2004;109:1594–602.
51. Chung ES, Packer M, Lo KH, Fasanmade AA, Willerson JT, Anti-TNF Therapy Against Congestive Heart Failure Investigators. Randomized, double-blind, placebo-controlled, pilot trial of infliximab, a chimeric monoclonal antibody to tumor necrosis factor-alpha, in patients with moderate-to-severe heart failure: results of the anti-TNF therapy against congestive heart failure (ATTACH) trial. *Circulation*. 2003;107:3133–40. <https://doi.org/10.1161/01.CIR.0000077913.60364.D2>.
52. Klein B, Brailly H. Cytokine-binding proteins: stimulating antagonists. *Immunol Today*. 1995;16:216–20. [https://doi.org/10.1016/0167-5699\(95\)80161-8](https://doi.org/10.1016/0167-5699(95)80161-8).
53. Dinarello CA. Overview of the IL-1 family in innate inflammation and acquired immunity. *Immunol Rev*. 2018;281:8–27. <https://doi.org/10.1111/imr.12621>.
54. Bujak M, Frangogiannis NG. The role of IL-1 in the pathogenesis of heart disease. *Arch Immunol Ther Exp*. 2009;57:165–76.
55. Abbate A, Toldo S, Marchetti C, Kron J, van Tassel BW, Dinarello CA. Interleukin-1 and the Inflammasome as therapeutic targets in cardiovascular disease. *Circ Res*. 2020;126:1260–80. <https://doi.org/10.1161/CIRCRESAHA.120.315937>.
56. Dewald O, Ren G, Duerr GD, Zoerlein M, Klemm C, Gersch C, et al. Of mice and dogs: species-specific differences in the inflammatory response following myocardial infarction. *Am J Pathol*. 2004;164:665–77.
57. Shioi T, Matsumori A, Kihara Y, Inoko M, Ono K, Iwanaga Y, et al. Increased expression of interleukin-1 beta and monocyte chemoattractant and activating factor/monocyte chemoattractant protein-1 in the hypertrophied and failing heart with pressure overload. *Circ Res*. 1997;81:664–71.
58. Xia Y, Lee K, Li N, Corbett D, Mendoza L, Frangogiannis NG. Characterization of the inflammatory and fibrotic response in a mouse model of cardiac pressure overload. *Histochem Cell Biol*. 2009;131:471–81.
59. Bracey NA, Beck PL, Muruve DA, Hirota SA, Guo J, Jabagi H, et al. The Nlrp3 inflammasome promotes myocardial dysfunction in structural cardiomyopathy through interleukin-1beta. *Exp Physiol*. 2013;98:462–72. <https://doi.org/10.1113/expphysiol.2012.068338>.
60. Luo B, Li B, Wang W, Liu X, Xia Y, Zhang C, et al. NLRP3 gene silencing ameliorates diabetic cardiomyopathy in a type 2 diabetes rat model. *PLoS One*. 2014;9:e104771. <https://doi.org/10.1371/journal.pone.0104771>.
61. Francis SE, Holden H, Holt CM, Duff GW. Interleukin-1 in myocardium and coronary arteries of patients with dilated cardiomyopathy. *J Mol Cell Cardiol*. 1998;30:215–23.
62. Suetomi T, Willeford A, Brand CS, Cho Y, Ross RS, Miyamoto S, et al. Inflammation and NLRP3 inflammasome activation initiated in response to pressure overload by Ca(2+)/calmodulin-dependent protein kinase II delta signaling in cardiomyocytes are essential for adverse cardiac remodeling. *Circulation*. 2018;138:2530–44. <https://doi.org/10.1161/CIRCULATIONAHA.118.034621>.
63. Mezzaroma E, Toldo S, Farkas D, Seropian IM, van Tassel BW, Salloum FN, et al. The inflammasome promotes adverse cardiac remodeling following acute myocardial infarction in the mouse. *Proc Natl Acad Sci U S A*. 2011;108:19725–30.
64. Kawaguchi M, Takahashi M, Hata T, Kashima Y, Usui F, Morimoto H, et al. Inflammasome activation of cardiac fibroblasts is essential for myocardial ischemia/reperfusion injury. *Circulation*. 2011;123:594–604.
65. Abbate A, Salloum FN, Vecile E, Das A, Hoke NN, Straino S, et al. Anakinra, a recombinant human interleukin-1 receptor antagonist, inhibits apoptosis in experimental acute myocardial infarction. *Circulation*. 2008;117:2670–83.
66. Zhu J, Zhang J, Xiang D, Zhang Z, Zhang L, Wu M, et al. Recombinant human interleukin-1 receptor antagonist protects mice against acute doxorubicin-induced cardiotoxicity. *Eur J Pharmacol*. 2010;643:247–53. <https://doi.org/10.1016/j.ejphar.2010.06.024>.
67. Harouki N, Nicol L, Remy-Jouet I, Henry JP, Dumesnil A, Lejeune A, et al. The IL-1beta antibody gevokizumab limits cardiac remodeling and coronary dysfunction in rats with heart failure. *JACC Basic Transl Sci*. 2017;2:418–30. <https://doi.org/10.1016/j.jacbts.2017.06.005>.
68. Honsho S, Nishikawa S, Amano K, Zen K, Adachi Y, Kishita E, et al. Pressure-mediated hypertrophy and mechanical stretch induces IL-1 release and subsequent IGF-1 generation to maintain compensative hypertrophy by affecting Akt and JNK pathways. *Circ Res*. 2009;105:1149–58. <https://doi.org/10.1161/CIRCRESAHA.109.208199>.

69. Kumar A, Thota V, Dee L, Olson J, Uretz E, Parrillo JE. Tumor necrosis factor alpha and interleukin 1beta are responsible for in vitro myocardial cell depression induced by human septic shock serum. *J Exp Med*. 1996;183:949–58.
70. Gulick T, Chung MK, Pieper SJ, Lange LG, Schreiner GF. Interleukin 1 and tumor necrosis factor inhibit cardiac myocyte beta-adrenergic responsiveness. *Proc Natl Acad Sci U S A*. 1989;86:6753–7.
71. Ing DJ, Zang J, Dzau VJ, Webster KA, Bishopric NH. Modulation of cytokine-induced cardiac myocyte apoptosis by nitric oxide, Bak, and Bcl-x. *Circ Res*. 1999;84:21–33.
72. Sager HB, Heidt T, Hulsmans M, Dutta P, Courties G, Sebas M, et al. Targeting interleukin-1beta reduces leukocyte production after acute myocardial infarction. *Circulation*. 2015;132:1880–90. <https://doi.org/10.1161/CIRCULATIONAHA.115.016160>.
73. Saxena A, Chen W, Su Y, Rai V, Uche OU, Li N, et al. IL-1 induces proinflammatory leukocyte infiltration and regulates fibroblast phenotype in the infarcted myocardium. *J Immunol*. 2013;191:4838–48.
74. Leszczynski D, Josephs MD, Foegh ML. IL-1 beta-stimulated leucocyte-endothelial adhesion is regulated, in part, by the cyclic-GMP-dependent signal transduction pathway. *Scand J Immunol*. 1994;39:551–6. <https://doi.org/10.1111/j.1365-3083.1994.tb03412.x>.
75. Bageghni SA, Hemmings KE, Yuldasheva NY, Maqbool A, Gamboa-Esteves FO, Humphreys NE, et al. Fibroblast-specific deletion of interleukin-1 receptor-1 reduces adverse cardiac remodeling following myocardial infarction. *JCI Insight*. 2019;5. <https://doi.org/10.1172/jci.insight.125074>.
76. Ikonomidis I, Tzortzis S, Lekakis J, Paraskevaidis I, Andreadou I, Nikolaou M, et al. Lowering interleukin-1 activity with anakinra improves myocardial deformation in rheumatoid arthritis. *Heart*. 2009;95:1502–7. <https://doi.org/10.1136/hrt.2009.168971>.
77. Eriksson U, Kurrer MO, Sonderegger I, Iezzi G, Tafuri A, Hunziker L, et al. Activation of dendritic cells through the interleukin 1 receptor 1 is critical for the induction of autoimmune myocarditis. *J Exp Med*. 2003;197:323–31.
78. Ridker PM, Everett BM, Thuren T, MacFadyen JG, Chang WH, Ballantyne C, et al. Antiinflammatory therapy with canakinumab for atherosclerotic disease. *N Engl J Med*. 2017;377:1119–31. <https://doi.org/10.1056/NEJMoa1707914>.
79. Everett BM, Cornel JH, Lainscak M, Anker SD, Abbate A, Thuren T, et al. Anti-inflammatory therapy with canakinumab for the prevention of hospitalization for heart failure. *Circulation*. 2019;139:1289–99. <https://doi.org/10.1161/CIRCULATIONAHA.118.038010>.
80. Buckley LF, Carbone S, Trankle CR, Canada JM, Erdle CO, Regan JA, et al. Effect of Interleukin-1 blockade on left ventricular systolic performance and work: a post hoc pooled analysis of 2 clinical trials. *J Cardiovasc Pharmacol*. 2018;72:68–70. <https://doi.org/10.1097/FJC.0000000000000591>.
81. Van Tassel BW, Trankle CR, Canada JM, et al. IL-1 blockade in patients with heart failure with preserved ejection fraction. *Circ Heart Fail*. 2018;11:e005036. <https://doi.org/10.1161/CIRCHEARTFAILURE.118.005036>.
82. Ikonomidis I, Lekakis JP, Nikolaou M, Paraskevaidis I, Andreadou I, Kaplanoglou T, et al. Inhibition of interleukin-1 by anakinra improves vascular and left ventricular function in patients with rheumatoid arthritis. *Circulation*. 2008;117:2662–9.
83. Rose-John S. Interleukin-6 family cytokines. *Cold Spring Harb Perspect Biol*. 2018;10. <https://doi.org/10.1101/cshperspect.a028415>.
84. Yue P, Massie BM, Simpson PC, Long CS. Cytokine expression increases in nonmyocytes from rats with postinfarction heart failure. *Am J Phys*. 1998;275:H250–8.
85. Gwechenberger M, Mendoza LH, Youker KA, Frangogiannis NG, Smith CW, Michael LH, et al. Cardiac myocytes produce interleukin-6 in culture and in viable border zone of reperfused infarctions. *Circulation*. 1999;99:546–51.
86. Baumgarten G, Knuefermann P, Kalra D, Gao F, Taffet GE, Michael L, et al. Load-dependent and -independent regulation of proinflammatory cytokine and cytokine receptor gene expression in the adult mammalian heart. *Circulation*. 2002;105:2192–7.
87. Omiya S, Omori Y, Taneike M, Murakawa T, Ito J, Tanada Y, et al. Cytokine mRNA degradation in cardiomyocytes restrains sterile inflammation in pressure-overloaded hearts. *Circulation*. 2020;141:667–77. <https://doi.org/10.1161/CIRCULATIONAHA.119.044582>.
88. Kubota T, Miyagishima M, Alvarez RJ, et al. Expression of pro-inflammatory cytokines in the failing human heart: comparison of recent-onset and end-stage congestive heart failure. *J Heart Lung Transplant*. 2000;19:819–24. [https://doi.org/10.1016/s1053-2498\(00\)00173-x](https://doi.org/10.1016/s1053-2498(00)00173-x).
89. Eiken HG, Oie E, Damas JK, Yndestad A, Bjerkeli V, Aass H, et al. Myocardial gene expression of leukaemia inhibitory factor, interleukin-6 and glycoprotein 130 in end-stage human heart failure. *Eur J Clin Invest*. 2001;31:389–97. <https://doi.org/10.1046/j.1365-2362.2001.00795.x>.
90. Plenz G, Eschert H, Erren M, Wichter T, Böhm M, Flesch M, et al. The interleukin-6/interleukin-6-receptor system is activated in donor hearts. *J Am Coll Cardiol*. 2002;39:1508–12. [https://doi.org/10.1016/s0735-1097\(02\)01791-6](https://doi.org/10.1016/s0735-1097(02)01791-6).
91. Hilfiker-Kleiner D, Shukla P, Klein G, Schaefer A, Stapel B, Hoch M, et al. Continuous glycoprotein-130-mediated signal transducer and activator of transcription-3 activation promotes inflammation, left ventricular rupture, and adverse outcome in subacute myocardial infarction. *Circulation*. 2010;122:145–55.
92. Zhao L, Cheng G, Jin R, Afzal MR, Samanta A, Xuan YT, et al. Deletion of interleukin-6 attenuates pressure overload-induced left ventricular hypertrophy and dysfunction. *Circ Res*. 2016;118:1918–29. <https://doi.org/10.1161/CIRCRESAHA.116.308688>.
93. Lai NC, Gao MH, Tang E, Tang R, Guo T, Dalton ND, et al. Pressure overload-induced cardiac remodeling and dysfunction in the absence of interleukin 6 in mice. *Lab Invest*. 2012;92:1518–26. <https://doi.org/10.1038/labinvest.2012.97>.
94. Kobara M, Noda K, Kitamura M, Okamoto A, Shiraishi T, Toba H, et al. Antibody against interleukin-6 receptor attenuates left ventricular remodeling after myocardial infarction in mice. *Cardiovasc Res*. 2010;87:424–30.
95. Mackiewicz A, Schooltink H, Heinrich PC, Rose-John S. Complex of soluble human IL-6-receptor/IL-6 up-regulates expression of acute-phase proteins. *J Immunol*. 1992;149:2021–7.
96. Kinugawa K, Takahashi T, Kohmoto O, Yao A, Aoyagi T, Momomura S, et al. Nitric oxide-mediated effects of interleukin-6 on [Ca²⁺]_i and cell contraction in cultured chick ventricular myocytes. *Circ Res*. 1994;75:285–95. <https://doi.org/10.1161/01.res.75.2.285>.
97. Melendez GC, McLarty JL, Levick SP, et al. Interleukin 6 mediates myocardial fibrosis, concentric hypertrophy, and diastolic dysfunction in rats. *Hypertension*. 2010;56:225–31. <https://doi.org/10.1161/HYPERTENSIONAHA.109.148635>.
98. Sano M, Fukuda K, Kodama H, Pan J, Saito M, Matsuzaki J, et al. Interleukin-6 family of cytokines mediate angiotensin II-induced cardiac hypertrophy in rodent cardiomyocytes. *J Biol Chem*. 2000;275:29717–23. <https://doi.org/10.1074/jbc.M003128200>.
99. Kunisada K, Tone E, Fujio Y, Matsui H, Yamauchi-Takahara K, Kishimoto T. Activation of gp130 transduces hypertrophic signals via STAT3 in cardiac myocytes. *Circulation*. 1998;98:346–52. <https://doi.org/10.1161/01.cir.98.4.346>.
100. Smart N, Mojet MH, Latchman DS, et al. IL-6 induces PI 3-kinase and nitric oxide-dependent protection and preserves mitochondrial

- function in cardiomyocytes. *Cardiovasc Res.* 2006;69:164–77. <https://doi.org/10.1016/j.cardiores.2005.08.017>.
101. Chou CH, Hung CS, Liao CW, Wei LH, Chen CW, Shun CT, et al. IL-6 trans-signalling contributes to aldosterone-induced cardiac fibrosis. *Cardiovasc Res.* 2018;114:690–702. <https://doi.org/10.1093/cvr/cvy013>.
 102. Leicht M, Briest W, Zimmer HG. Regulation of norepinephrine-induced proliferation in cardiac fibroblasts by interleukin-6 and p42/p44 mitogen activated protein kinase. *Mol Cell Biochem.* 2003;243:65–72. <https://doi.org/10.1023/a:1021655023870>.
 103. Mir SA, Chatterjee A, Mitra A, Pathak K, Mahata SK, Sarkar S. Inhibition of signal transducer and activator of transcription 3 (STAT3) attenuates interleukin-6 (IL-6)-induced collagen synthesis and resultant hypertrophy in rat heart. *J Biol Chem.* 2012;287:2666–77. <https://doi.org/10.1074/jbc.M111.246173>.
 104. Mitani H, Katayama N, Araki H, Ohishi K, Kobayashi K, Suzuki H, et al. Activity of interleukin 6 in the differentiation of monocytes to macrophages and dendritic cells. *Br J Haematol.* 2000;109:288–95. <https://doi.org/10.1046/j.1365-2141.2000.02020.x>.
 105. Mauer J, Chaurasia B, Goldau J, Vogt MC, Ruud J, Nguyen KD, et al. Signaling by IL-6 promotes alternative activation of macrophages to limit endotoxemia and obesity-associated resistance to insulin. *Nat Immunol.* 2014;15:423–30. <https://doi.org/10.1038/ni.2865>.
 106. Sackett SD, Otto T, Mohs A, Sander LE, Strauch S, Streetz KL, et al. Myeloid cells require gp130 signaling for protective anti-inflammatory functions during sepsis. *FASEB J.* 2019;33:6035–44. <https://doi.org/10.1096/fj.201802118R>.
 107. Scheller J, Chalaris A, Schmidt-Arras D, Rose-John S. The pro- and anti-inflammatory properties of the cytokine interleukin-6. *Biochim Biophys Acta.* 2011;1813:878–88. <https://doi.org/10.1016/j.bbamcr.2011.01.034>.
 108. Kraakman MJ, Kammoun HL, Allen TL, Deswaerte V, Henstridge DC, Estevez E, et al. Blocking IL-6 trans-signaling prevents high-fat diet-induced adipose tissue macrophage recruitment but does not improve insulin resistance. *Cell Metab.* 2015;21:403–16. <https://doi.org/10.1016/j.cmet.2015.02.006>.
 109. Yokoe I, Kobayashi H, Kobayashi Y, Giles JT, Yoneyama K, Kitamura N, et al. Impact of tocilizumab on N-terminal pro-brain natriuretic peptide levels in patients with active rheumatoid arthritis without cardiac symptoms. *Scand J Rheumatol.* 2018;47:364–70. <https://doi.org/10.1080/03009742.2017.1418424>.
 110. Kleveland O, Kunszt G, Bratlie M, Ueland T, Broch K, Holte E, et al. Effect of a single dose of the interleukin-6 receptor antagonist tocilizumab on inflammation and troponin T release in patients with non-ST-elevation myocardial infarction: a double-blind, randomized, placebo-controlled phase 2 trial. *Eur Heart J.* 2016;37:2406–13. <https://doi.org/10.1093/eurheartj/ehw171>.
 111. Kleveland O, Ueland T, Kunszt G, Bratlie M, Yndestad A, Broch K, et al. Interleukin-6 receptor inhibition with tocilizumab induces a selective and substantial increase in plasma IP-10 and MIP-1beta in non-ST-elevation myocardial infarction. *Int J Cardiol.* 2018;271:1–7. <https://doi.org/10.1016/j.ijcard.2018.04.136>.
 112. Sokol CL, Luster AD. The chemokine system in innate immunity. *Cold Spring Harb Perspect Biol.* 2015;7. <https://doi.org/10.1101/cshperspect.a016303>.
 113. Clark-Lewis I, Kim KS, Rajarathnam K, Gong JH, Dewald B, Moser B, et al. Structure–activity relationships of chemokines. *J Leukoc Biol.* 1995;57:703–11.
 114. Zlotnik A, Morales J, Hedrick JA. Recent advances in chemokines and chemokine receptors. *Crit Rev Immunol.* 1999;19:1–47.
 115. Chen B, Frangogiannis NG. Chemokines in myocardial infarction. *J Cardiovasc Transl Res.* 2020. <https://doi.org/10.1007/s12265-020-10006-7>.
 116. Xia Y, Frangogiannis NG. MCP-1/CCL2 as a therapeutic target in myocardial infarction and ischemic cardiomyopathy. *Inflamm Allergy Drug Targets.* 2007;6:101–7.
 117. Kumar AG, Ballantyne CM, Michael LH, Kukielka GL, Youker KA, Lindsey ML, et al. Induction of monocyte chemoattractant protein-1 in the small veins of the ischemic and reperfused canine myocardium. *Circulation.* 1997;95:693–700.
 118. Dewald O, Frangogiannis NG, Zoerlein M, Duerr GD, Klemm C, Knuefermann P, et al. Development of murine ischemic cardiomyopathy is associated with a transient inflammatory reaction and depends on reactive oxygen species. *Proc Natl Acad Sci U S A.* 2003;100:2700–5.
 119. Behr TM, Wang X, Aiyar N, Coatney RW, Li X, Koster P, et al. Monocyte chemoattractant protein-1 is upregulated in rats with volume-overload congestive heart failure. *Circulation.* 2000;102:1315–22.
 120. Kuwahara F, Kai H, Tokuda K, Takeya M, Takeshita A, Egashira K, et al. Hypertensive myocardial fibrosis and diastolic dysfunction: another model of inflammation? *Hypertension.* 2004;43:739–45.
 121. Lehmann MH, Kuhnert H, Muller S, Sigusch HH. Monocyte chemoattractant protein 1 (MCP-1) gene expression in dilated cardiomyopathy. *Cytokine.* 1998;10:739–46.
 122. Iwasaki J, Nakamura K, Matsubara H, Nakamura Y, Nishii N, Banba K, et al. Relationship between circulating levels of monocyte chemoattractant protein-1 and systolic dysfunction in patients with hypertrophic cardiomyopathy. *Cardiovasc Pathol.* 2009;18:317–22. <https://doi.org/10.1016/j.carpath.2008.12.004>.
 123. Patel B, Bansal SS, Ismail MA, Hamid T, Rokosh G, Mack M, et al. CCR2(+) monocyte-derived infiltrating macrophages are required for adverse cardiac remodeling during pressure overload. *JACC Basic Transl Sci.* 2018;3:230–44. <https://doi.org/10.1016/j.jacbs.2017.12.006>.
 124. Hayashidani S, Tsutsui H, Shiomi T, Ikeuchi M, Matsusaka H, Suematsu N, et al. Anti-monocyte chemoattractant protein-1 gene therapy attenuates left ventricular remodeling and failure after experimental myocardial infarction. *Circulation.* 2003;108:2134–40.
 125. Bajpai G, Bredemeyer A, Li W, Zaitsev K, Koenig AL, Lokshina I, et al. Tissue resident CCR2– and CCR2+ cardiac macrophages differentially orchestrate monocyte recruitment and fate specification following myocardial injury. *Circ Res.* 2019;124:263–78. <https://doi.org/10.1161/CIRCRESAHA.118.314028>.
 126. Haudek SB, Cheng J, Du J, et al. Monocytic fibroblast precursors mediate fibrosis in angiotensin-II-induced cardiac hypertrophy. *J Mol Cell Cardiol.* 2010;49:499–507.
 127. Trial J, Heredia CP, Taffet GE, Entman ML, Cieslik KA. Dissecting the role of myeloid and mesenchymal fibroblasts in age-dependent cardiac fibrosis. *Basic Res Cardiol.* 2017;112:34. <https://doi.org/10.1007/s00395-017-0623-4>.
 128. Tan X, Hu L, Shu Z, Chen L, Li X, du M, et al. Role of CCR2 in the development of streptozotocin-treated diabetic cardiomyopathy. *Diabetes.* 2019;68:2063–73. <https://doi.org/10.2337/db18-1231>.
 129. Kolattukudy PE, Quach T, Bergese S, Breckenridge S, Hensley J, Altschuld R, et al. Myocarditis induced by targeted expression of the MCP-1 gene in murine cardiac muscle. *Am J Pathol.* 1998;152:101–11.
 130. Stumpf C, Lehner C, Raaz D, Yilmaz A, Anger T, Daniel WG, et al. Platelets contribute to enhanced MCP-1 levels in patients with chronic heart failure. *Heart.* 2008;94:65–9. <https://doi.org/10.1136/hrt.2007.115006>.
 131. Hohensinner PJ, Rychli K, Zorn G, Hülsmann M, Berger R, Mörtl D, et al. Macrophage-modulating cytokines predict adverse outcome in heart failure. *Thromb Haemost.* 2010;103:435–41. <https://doi.org/10.1160/TH09-06-0399>.

132. Grisanti LA, Traynham CJ, Repas AA, Gao E, Koch WJ, Tilley DG. beta2-adrenergic receptor-dependent chemokine receptor 2 expression regulates leukocyte recruitment to the heart following acute injury. *Proc Natl Acad Sci U S A*. 2016;113:15126–31. <https://doi.org/10.1073/pnas.1611023114>.
133. Wang J, Seo MJ, Deci MB, Weil BR, Canty JM, Nguyen J. Effect of CCR2 inhibitor-loaded lipid micelles on inflammatory cell migration and cardiac function after myocardial infarction. *Int J Nanomedicine*. 2018;13:6441–51. <https://doi.org/10.2147/IJN.S178650>.
134. Leuschner F, Dutta P, Gorbato R, Novobrantseva TI, Donahoe JS, Courties G, et al. Therapeutic siRNA silencing in inflammatory monocytes in mice. *Nat Biotechnol*. 2011;29:1005–10. <https://doi.org/10.1038/nbt.1989>.
135. Lu W, Xie Z, Tang Y, Bai L, Yao Y, Fu C, et al. Photoluminescent mesoporous silicon nanoparticles with siCCR2 improve the effects of mesenchymal stromal cell transplantation after acute myocardial infarction. *Theranostics*. 2015;5:1068–82. <https://doi.org/10.7150/thno.11517>.
136. Sakai N, Wada T, Furuichi K, Shimizu K, Kokubo S, Hara A, et al. MCP-1/CCR2-dependent loop for fibrogenesis in human peripheral CD14-positive monocytes. *J Leukoc Biol*. 2006;79:555–63.
137. Kruglov EA, Nathanson RA, Nguyen T, Dranoff JA. Secretion of MCP-1/CCL2 by bile duct epithelia induces myofibroblastic transdifferentiation of portal fibroblasts. *Am J Physiol Gastrointest Liver Physiol*. 2006;290:G765–71.
138. Yamamoto T, Eckes B, Mauch C, Hartmann K, Krieg T. Monocyte chemoattractant protein-1 enhances gene expression and synthesis of matrix metalloproteinase-1 in human fibroblasts by an autocrine IL-1 alpha loop. *J Immunol*. 2000;164:6174–9.
139. Gharaee-Kermani M, Denholm EM, Phan SH. Costimulation of fibroblast collagen and transforming growth factor beta1 gene expression by monocyte chemoattractant protein-1 via specific receptors. *J Biol Chem*. 1996;271:17779–84.
140. Haudek SB, Xia Y, Huebener P, Lee JM, Carlson S, Crawford JR, et al. Bone marrow-derived fibroblast precursors mediate ischemic cardiomyopathy in mice. *Proc Natl Acad Sci U S A*. 2006;103:18284–9.
141. Moore-Morris T, Cattaneo P, Guimaraes-Camboa N, et al. Infarct fibroblasts do not derive from bone marrow lineages. *Circ Res*. 2018;122:583–90. <https://doi.org/10.1161/CIRCRESAHA.117.311490>.
142. Moore-Morris T, Guimaraes-Camboa N, Banerjee I, et al. Resident fibroblast lineages mediate pressure overload-induced cardiac fibrosis. *J Clin Invest*. 2014;124:2921–34. <https://doi.org/10.1172/JCI74783>.
143. Kanisicak O, Khalil H, Ivey MJ, Karch J, Maliken BD, Correll RN, et al. Genetic lineage tracing defines myofibroblast origin and function in the injured heart. *Nat Commun*. 2016;7:12260. <https://doi.org/10.1038/ncomms12260>.
144. Alex L, Frangogiannis NG. The cellular origin of activated fibroblasts in the infarcted and remodeling myocardium. *Circ Res*. 2018;122:540–2. <https://doi.org/10.1161/CIRCRESAHA.118.312654>.
145. Zhou L, Azfer A, Niu J, Graham S, Choudhury M, Adamski FM, et al. Monocyte chemoattractant protein-1 induces a novel transcription factor that causes cardiac myocyte apoptosis and ventricular dysfunction. *Circ Res*. 2006;98:1177–85.
146. Zhang W, Zhu T, Chen L, Luo W, Chao J. MCP-1 mediates ischemia-reperfusion-induced cardiomyocyte apoptosis via MCP1P1 and CaSR. *Am J Physiol Heart Circ Physiol*. 2020;318:H59–71. <https://doi.org/10.1152/ajpheart.00308.2019>.
147. Mao R, Yang R, Chen X, Harhaj EW, Wang X, Fan Y. Regnase-1, a rapid response ribonuclease regulating inflammation and stress responses. *Cell Mol Immunol*. 2017;14:412–22. <https://doi.org/10.1038/cmi.2016.70>.
148. Morimoto H, Hirose M, Takahashi M, Kawaguchi M, Ise H, Kolattukudy PE, et al. MCP-1 induces cardioprotection against ischaemia/reperfusion injury: role of reactive oxygen species. *Cardiovasc Res*. 2008;78:554–62. <https://doi.org/10.1093/cvr/cvn035>.
149. Vergunst CE, Gerlag DM, Lopatinskaya L, Klareskog L, Smith MD, van den Bosch F, et al. Modulation of CCR2 in rheumatoid arthritis: a double-blind, randomized, placebo-controlled clinical trial. *Arthritis Rheum*. 2008;58:1931–9. <https://doi.org/10.1002/art.23591>.
150. Ratziu V, Sanyal A, Harrison SA, Wong VWS, Francque S, Goodman Z, et al. Cenicriviroc treatment for adults with nonalcoholic steatohepatitis and fibrosis: final analysis of the phase 2b CENTAUR study. *Hepatology*. 2020. <https://doi.org/10.1002/hep.31108>.
151. Scholz D, Ito W, Fleming I, Deindl E, Sauer A, Wiesnet M, et al. Ultrastructure and molecular histology of rabbit hind-limb collateral artery growth (arteriogenesis). *Virchows Arch*. 2000;436:257–70. <https://doi.org/10.1007/s004280050039>.
152. Dobaczewski M, Xia Y, Bujak M, Gonzalez-Quesada C, Frangogiannis NG. CCR5 signaling suppresses inflammation and reduces adverse remodeling of the infarcted heart, mediating recruitment of regulatory T cells. *Am J Pathol*. 2010;176:2177–87.
153. Frangogiannis NG. The inflammatory response in myocardial injury, repair, and remodeling. *Nat Rev Cardiol*. 2014;11:255–65.
154. Christia P, Frangogiannis NG. Targeting inflammatory pathways in myocardial infarction. *Eur J Clin Invest*. 2013;43:986–95.

Publisher's Note Springer Nature remains neutral with regard to jurisdictional claims in published maps and institutional affiliations.

**JACC FOCUS SEMINAR: EXTRACELLULAR MATRIX IN
CARDIOVASCULAR HEALTH AND DISEASE**

JACC FOCUS SEMINAR

Extracellular Matrix in Ischemic Heart Disease, Part 4/4



JACC Focus Seminar

Nikolaos G. Frangogiannis, MD,^a Jason C. Kovacic, MD, PhD^{b,c}

ABSTRACT

Myocardial ischemia and infarction, both in the acute and chronic phases, are associated with cardiomyocyte loss and dramatic changes in the cardiac extracellular matrix (ECM). It has long been appreciated that these changes in the cardiac ECM result in altered mechanical properties of ischemic or infarcted myocardial segments. However, a growing body of evidence now clearly demonstrates that these alterations of the ECM not only affect the structural properties of the ischemic and post-infarct heart, but they also play a crucial and sometimes direct role in mediating a range of biological pathways, including the orchestration of inflammatory and reparative processes, as well as the pathogenesis of adverse remodeling. This final part of a 4-part JACC Focus Seminar reviews the evidence on the role of the ECM in relation to the ischemic and infarcted heart, as well as its contribution to cardiac dysfunction and adverse clinical outcomes. (J Am Coll Cardiol 2020;75:2219-35) © 2020 by the American College of Cardiology Foundation.

So far in this JACC Focus Seminar we have covered basic extracellular matrix (ECM) biology in Part 1, the role of ECM in vascular disease in Part 2, and the involvement of ECM in myocardial interstitial fibrosis (MIF) in nonischemic heart disease in Part 3. Here, in Part 4, we address the role of ECM in ischemic heart disease.

In the majority of patients, ischemic heart disease is caused by atherosclerosis of the epicardial coronary arteries, which leads to an imbalance between oxygen supply and demand. Typically, a coronary luminal narrowing of >75% does not cause a reduction in resting blood flow, but precludes an increase in oxygen supply when myocardial demand is increased (upon exercise, during tachyarrhythmia, and so on), resulting in ischemia. When atherosclerotic disease is

complicated by superimposed thrombosis, acute coronary occlusion results in myocardial infarction (MI). Complete and prolonged interruption of blood flow to the area subserved by the vessel leads to cessation of oxidative phosphorylation, depletion of high energy phosphates, and increased accumulation of metabolites in the ischemic myocardium. After 15 to 20 min of occlusion, disruption of aerobic metabolism in cardiomyocytes results in irreversible changes that eventually lead to cardiomyocyte death. As we review in this paper, both chronic ischemia and acute MI are associated with profound changes in the ECM network. Furthermore, mounting evidence suggests that in ischemic and infarcted hearts, ECM alterations not only accompany the pathological changes in cardiomyocytes, but also play a crucial role in mediating



Listen to this manuscript's audio summary by Editor-in-Chief Dr. Valentin Fuster on JACC.org.

From the ^aWilf Family Cardiovascular Research Institute, Department of Medicine (Cardiology), Albert Einstein College of Medicine, Bronx, New York; ^bThe Zena and Michael A. Wiener Cardiovascular Institute, Icahn School of Medicine at Mount Sinai, New York, New York; and the ^cVictor Chang Cardiac Research Institute and St. Vincent's Clinical School, University of New South Wales, Darlinghurst, New South Wales, Australia. Dr. Frangogiannis' laboratory is supported by National Institutes of Health grants R01HL76246 and R01HL85440 and by grants PR151029, PR151134, and PR181464 from the Department of Defense Congressionally Directed Medical Research Programs. Dr. Kovacic has received research support from the National Institutes of Health (R01HL130423, R01HL135093). Thomas Wight, MD, served as Guest Associate Editor for this paper.

Manuscript received November 3, 2019; revised manuscript received February 27, 2020, accepted March 3, 2020.

ABBREVIATIONS AND ACRONYMS

ECM = extracellular matrix

MI = myocardial infarction

MIF = myocardial interstitial fibrosis

MMP = matrix metalloprotease

PGP = proline-glycine-proline

TGF = transforming growth factor

VEGF = vascular endothelial growth factor

injurious pathways, orchestrating inflammatory and reparative processes, and contributing to the pathogenesis of adverse remodeling.

THE ECM IN THE INFARCTED HEART

In adult mammals with MI, massive loss of cardiomyocytes overwhelms the extremely limited endogenous regenerative capacity of the heart (1). Thus, the infarcted myocardium heals through replacement of dead myocardium with a matrix-based scar. The myocardial reparative response can be divided into 3 distinct, but overlapping phases: inflammatory, proliferative, and maturation. As the infarcted myocardial segments heal, noninfarcted areas remodel in response to hemodynamic loading and to the effects of immune cells and fibroblasts accumulating in the infarct border zone. The dynamic changes in ECM composition not only affect the structure and mechanics of the heart, but also play a critical role in regulation of the cellular responses in the infarcted and remodeling myocardium. During the inflammatory phase, fragments of ECM generated through early activation of proteases may serve as damage-associated molecular patterns that activate immune cells, triggering an inflammatory reaction. Moreover, extravasated plasma proteins enrich the ECM, generating a plastic network of provisional matrix that serves as a conduit for immune and reparative cells. Phagocytosis of dead cells and matrix debris by professional phagocytes inhibits inflammation, leading to the proliferative phase of infarct healing, characterized by activation of myofibroblasts and neovessel formation. Enrichment of the cardiac ECM through deposition of matricellular proteins plays a critical role in spatial regulation of growth factor signaling cascades, restricting the fibrotic response to areas of injury. In addition, activated fibroblasts secrete large amounts of structural ECM proteins, forming a scar. As the infarct matures, cross-linking of the ECM provides structural stability, while increasing ventricular stiffness. In viable myocardial segments, pressure and volume loads cooperate to induce chronic progressive deposition of collagen in the interstitium, thus contributing to the pathogenesis of post-infarction heart failure.

cardial reparative response can be divided into 3 distinct, but overlapping phases: inflammatory, proliferative, and maturation. As the infarcted myocardial segments heal, noninfarcted areas remodel in response to hemodynamic loading and to the effects of immune cells and fibroblasts accumulating in the infarct border zone. The dynamic changes in ECM composition not only affect the structure and mechanics of the heart, but also play a critical role in regulation of the cellular responses in the infarcted and remodeling myocardium. During the inflammatory phase, fragments of ECM generated through early activation of proteases may serve as damage-associated molecular patterns that activate immune cells, triggering an inflammatory reaction. Moreover, extravasated plasma proteins enrich the ECM, generating a plastic network of provisional matrix that serves as a conduit for immune and reparative cells. Phagocytosis of dead cells and matrix debris by professional phagocytes inhibits inflammation, leading to the proliferative phase of infarct healing, characterized by activation of myofibroblasts and neovessel formation. Enrichment of the cardiac ECM through deposition of matricellular proteins plays a critical role in spatial regulation of growth factor signaling cascades, restricting the fibrotic response to areas of injury. In addition, activated fibroblasts secrete large amounts of structural ECM proteins, forming a scar. As the infarct matures, cross-linking of the ECM provides structural stability, while increasing ventricular stiffness. In viable myocardial segments, pressure and volume loads cooperate to induce chronic progressive deposition of collagen in the interstitium, thus contributing to the pathogenesis of post-infarction heart failure.

THE ROLE OF ECM IN THE INFLAMMATORY PHASE OF INFARCT HEALING. Activation of matrix-degrading proteases and generation of matrix fragments are the earliest ECM perturbations in infarcted hearts. In some studies, ischemic changes in the interstitial matrix have been reported to precede

HIGHLIGHTS

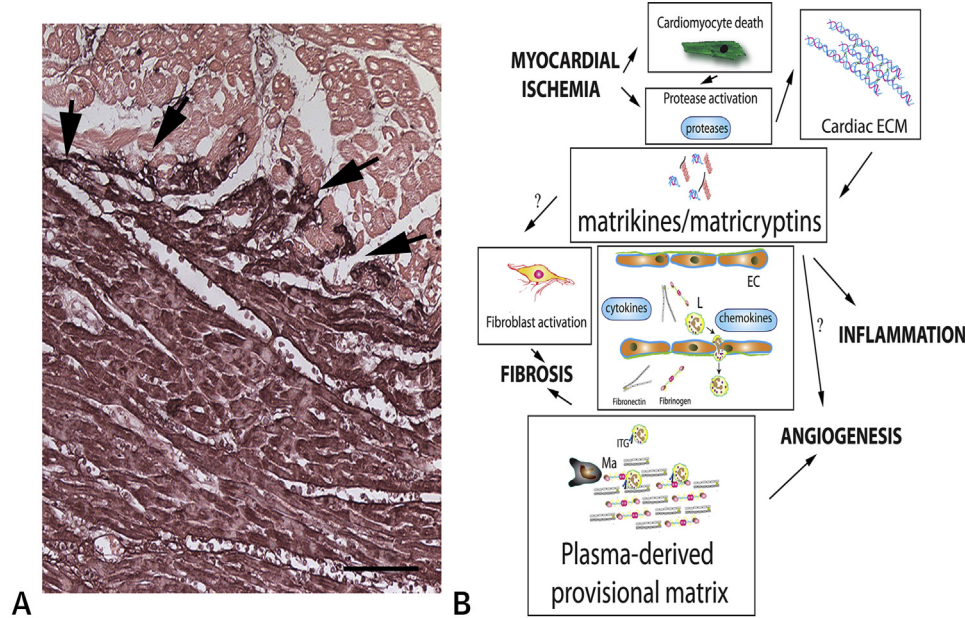
- Myocardial ischemia and infarction are associated with dynamic changes in the composition of the ECM network.
- In addition to their structural role, ECM proteins modulate cellular phenotype and function.
- Specialized matrix proteins transduce signals that regulate inflammation, fibrosis, and angiogenesis.
- Targeting the ECM may attenuate remodeling and enhance repair and regeneration following infarction.

irreversible cardiomyocyte injury. In a porcine model, matrix metalloproteinase (MMP) activation was first detected in the cardiac interstitium after 10 min of coronary occlusion (2). Early MMP activation is followed by fragmentation of fibrillar collagens and other structural ECM proteins. In a pig MI model, release of type I collagen fragments in the serum was documented after 30 min of coronary occlusion (3). In ultrastructural studies, the earliest alterations in collagen morphology, described as “irregular arrangement” of collagen fibers, were noted after 40 min of coronary occlusion and were followed by a reduction in the density of collagen fibrils 2 h after the acute event (4). Early increases in MMP activity in the ischemic myocardium reflect activation of latent stores, presumably through reactive oxygen species-mediated pathways (5). At a later stage, ischemic cardiomyocytes, fibroblasts, vascular cells, and immune cells synthesize and release large amounts of proteases in the infarcted myocardium (6). Members of the collagenase family (such as MMP1), gelatinases (including MMP2 and MMP9), and cathepsins are up-regulated in the infarcted heart (7,8) and also contribute to ECM fragmentation.

ECM FRAGMENTS AS REGULATORS OF THE INFLAMMATORY AND REPARATIVE RESPONSE.

Protease-mediated ECM fragmentation generates bioactive peptides that can modulate inflammatory, fibrogenic, or angiogenic responses (9,10) (Figure 1). The terms *matrikines* and *matricryptins* have been used to describe these biologically active matrix fragments. Although universally accepted definitions are lacking, the term *matrikine* is typically used to describe any fragment of an ECM molecule with biological properties distinct from those of the full-length molecule. On the other hand, the term *matricryptin* refers to a subtype of matrikines that

FIGURE 1 Generation of Matrix Fragments and Formation of a Plasma-Derived Provisional Matrix During the Inflammatory Phase of Cardiac Repair



(A) Immunohistochemistry for fibrinogen/fibrin (**black**) shows deposition of plasma-derived proteins (including fibrin and fibronectin) that enrich the cardiac extracellular matrix (ECM) during the early stages of infarct healing (**arrows**). Counterstained with eosin. Scale bar = 120 μ m. Data from our own work in a canine model of reperfused myocardial infarction (13). **(B)** Schematic cartoon illustrating the dramatic changes in the interstitial ECM network during the inflammatory phase of infarct healing. Rapid activation and induction of proteases, such as matrix metalloproteases (MMPs) and cathepsins, in the infarcted myocardium generates ECM fragments (matrikines and matricryptins) that modulate the phenotype of fibroblasts, macrophages (Ma) and endothelial cells (EC). MMPs have a wide range of substrates and process cytokines and chemokines, regulating their proinflammatory actions. Recruitment and migration of leukocytes (L), fibroblasts, and vascular cells in the infarcted heart requires interactions between cell surface integrins (ITG) and provisional matrix proteins (such as fibrin and fibronectin). Thus, the provisional matrix plays an important role in regulation of inflammatory, fibrogenic, and angiogenic responses.

require proteolytic processing to expose a functional domain and exert their biological actions (11). Although the rapid and prolonged activation of proteases may release a wide range of matrix fragments in the cardiac interstitium, their profile, time course of release, and potential involvement in regulation of myocardial inflammation and repair remain poorly understood. In the infarcted myocardium, all constituents of the cardiac ECM (including fibrillar collagens, elastin, basement membrane proteins, fibronectin, hyaluronan, and newly-secreted matricellular macromolecules) (12-15) may be targeted by proteases to generate fragments (Table 1). Peptides derived from fibrillar collagens and elastin have been implicated in activation of immune cells in models of inflammation and tissue injury (10,16). Extensive evidence in models of pulmonary inflammation suggests that the tripeptide proline-glycine-proline (PGP) and its acetylated form ac-PGP are generated from collagen

through a multistep proteolytic cascade that involves MMP8, MMP9, and prolyl endopeptidase (17), and may act as a potent neutrophil chemoattractant signaling through activation of the chemokine receptor CXCR2 (18). Although PGP generation has been demonstrated in pressure-overloaded hearts (19), evidence implicating this proinflammatory matrikine in post-MI inflammation is lacking. Low molecular weight hyaluronan fragments may also exert potent proinflammatory actions in injured tissues by activating toll-like receptor signaling pathways (20). Interestingly, it has been suggested that impaired clearance of these fragments may prolong and accentuate proinflammatory signaling in leukocytes and vascular cells (21,22), thus accentuating adverse remodeling after MI. Proteolytic processing of laminins by MMP2 and MMP14 has also been demonstrated to yield neutrophil chemoattractant peptides (23), while fibronectin fragments have been identified in the infarcted heart and are suggested to reduce

TABLE 1 Generation of ECM Protein Fragments in the Infarcted Heart

ECM Protein	Animal Models	Human Patients	Proposed Role
Fibrillar collagens (collagen I, collagen III)	In the pig MI model, release of type I collagen fragments in the serum has been documented after 30 min of coronary occlusion (3). Experiments in the isolated perfused heart showed that global ischemia generates collagen I and III fragments (153). Cathepsin K-specific collagen I fragments were found in infarcted mouse hearts (8). The collagen I $\alpha 1$ C-1158/59 fragment was identified in infarcted mouse hearts, generated through effects of MMP2 and MMP9 (24).	In patients with MI, an early increase in collagen degradation markers is noted (154). Plasma levels of carboxy-terminal telopeptide of type I collagen (CITP) reflect collagen I degradation, are higher in MI patients with systolic dysfunction (155), and correlate with the extent of acute injury (156). Plasma CITP levels 24 or 72 h after acute MI are associated with late mortality (157) and adverse remodeling (158). A reduction in the ratio of biomarkers reflecting synthesis vs. degradation of collagen was also associated with worse post-MI remodeling (159).	Although collagen fragments have been suggested to exert proinflammatory actions, their role in initiation and progression of the post-MI inflammatory response has not been documented. Late generation of the collagen I $\alpha 1$ C-1158/59 matricryptin may promote repair by activating fibroblasts and vascular cells (4).
Elastin	N/A	Elastin fragments were identified in the serum of patients with MI (160).	Overexpression of elastin fragments (typically absent from myocardial infarcts) attenuated adverse remodeling in a rat MI model (161).
Collagen IV	Canstatin, a 24kDa polypeptide cleaved from the $\alpha 2$ chain of type IV collagen is found in infarcted rat hearts (30).	N/A	Canstatin may promote activation of infarct myofibroblasts (30). Tumstatin, a cleaved fragment of collagen type IV $\alpha 3$ chain, may generate a matricryptin that modulates fibroblast activation, angiogenesis, and cardiomyocyte survival (28,162).
Collagen XVIII	Endostatin, a 20 kDa fragment of collagen XVIII, is up-regulated in a rat MI model (163).	Serum endostatin levels were increased in patients with MI (164).	Endostatin inhibition in a rat MI model was reported to worsen outcomes (163). Endostatin may stimulate fibroblast proliferation (25), while exerting potent angiostatic actions (26).
Fibronectin	Fibronectin fragments were identified in the post-ischemic cardiac lymph (reflecting the cardiac extracellular environment) in a canine model of reperfused MI.	N/A	Fibronectin fragments reduced monocyte very late antigen-5 expression, attenuating the migratory capacity of monocytes in response to chemokines (15).

CITP = carboxy-terminal telopeptide of collagen type I; MI = myocardial infarction.

monocyte migratory capacity in response to chemokines (15).

It should be emphasized that the effects of matrixins and matricryptins are not limited to the inflammatory phase of infarct healing. Prolonged activation of proteases in the infarcted myocardium generates ECM fragments for several days after MI. In addition to their effects on immune cells, matrix fragments may also modulate the fibroblast and vascular cell phenotype (24). Endostatin, a 20kDa fragment of collagen XVIII, may stimulate fibroblast proliferation (25) while exerting potent angiostatic actions (26). MMP9-mediated cleavage of collagen IV generates tumstatin, a fragment with angiostatic properties (27) that can be further degraded to produce fragments that promote a proliferative and migratory phenotype in cardiac fibroblasts (28). Canstatin, another collagen IV-derived fragment, may also activate fibroblasts, stimulating their proliferation and enhancing fibroblast-derived MMP synthesis (29,30).

BROAD EFFECTS OF MMPs IN REGULATION OF THE INFLAMMATORY RESPONSE. In addition to their role in ECM remodeling, MMPs regulate inflammatory and reparative cascades through proteolytic processing of

cytokines, chemokines, and growth factors. Several members of the MMP family can process the cell membrane-anchored precursor of tumor necrosis factor- α to generate the active cytokine (31). MMP3 and the gelatinases MMP2 and MMP9 can also process interleukin-1 β , generating the biologically active form of the cytokine in a caspase 1-independent manner (32). Furthermore, MMPs are implicated in the complex multistep cascade that leads to generation of mature transforming growth factor (TGF)- β from secreted latent complexes (33). MMPs also process several members of the chemokine family, including CXCL12/stromal cell-derived factor (SDF)-1 and CCL2/monocyte chemoattractant protein (MCP)-1, exerting diverse and often conflicting actions that may either potentiate or inactivate the effects of the chemokine (34-38). Furthermore, MMPs may disperse chemokine gradients by degrading glycosaminoglycan binding sites that are critical for chemokine immobilization on the endothelial cell surface and subsequent interaction with activated leukocytes (39). Considering the critical involvement of chemokines and cytokines in leukocyte recruitment, repair, and remodeling of the infarcted myocardium (40-42), MMP-dependent processing of

inflammatory mediators may be a central regulatory mechanism in the post-infarct heart.

Discoveries suggesting subcellular localizations of some MMP family members in the cytosol, mitochondria, or the nucleus have added complexity to our understanding of the role of MMPs in cardiac repair. It has been suggested that intracellular MMPs may have a wide range of substrates, including cytoskeletal proteins, signal transducers, enzymes, and transcriptional regulators (43). MMP-mediated degradation of contractile proteins, such as myosin and actinin, has been implicated in the pathogenesis of ischemic myocardial dysfunction (44,45). In vitro studies demonstrated that MMPs may also function in a nonproteolytic manner, regulating signal transduction or transcription (46). The in vivo significance of these functions remains to be fully defined.

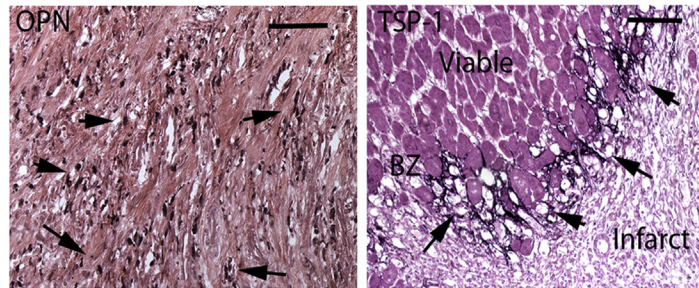
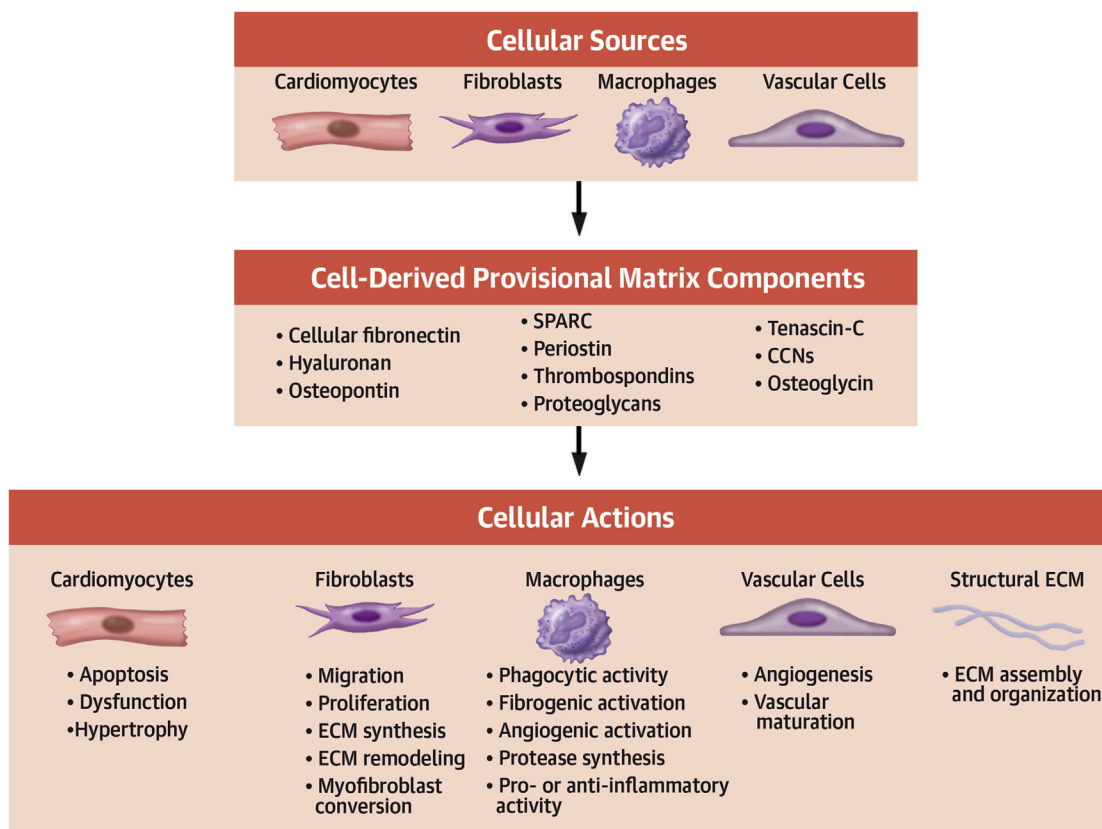
THE DEPOSITION OF A PLASMA-DERIVED PROVISIONAL MATRIX REGULATES THE POST-INFARCTION INFLAMMATORY RESPONSE. Proteolytic degradation of the native myocardial ECM is accompanied by the formation of a highly plastic provisional matrix network that supports migration and differentiation of immune, vascular, and reparative cells, contributing to scar formation (13,47). In models of vascular injury and of cutaneous repair, progressive changes in the composition of the provisional matrix have been described (48). Early provisional matrix is comprised predominantly of extravasated proteins (such as fibrinogen-derived fibrin and plasma fibronectin) (49). As immune cells and fibroblasts migrate into the injured tissue, the provisional matrix is enriched with a cell-derived component, comprised of cellular fibronectin and proteoglycans (50). Studies describing the cellular events in infarcted mammalian hearts suggest a similar transition ECM composition (13,51). Rapid induction and release of cytokines and growth factors, such as tumor necrosis factor- α and vascular endothelial growth factor (VEGF), may be responsible for increased vascular permeability (52,53), leading to extravasation of fibrinogen and fibronectin in the infarct zone (13,54). The role of the components of the provisional matrix in regulation of the inflammatory response following MI remains poorly supported by experimental in vivo evidence. In a mouse model of reperfused MI, fibrin-mediated proinflammatory actions were suggested to extend ischemic injury (55). Both fibrinogen and fibronectin contain integrin binding sites that may play a crucial role in adhesion and migration of leukocytes in the infarcted heart (56,57), and which may transduce signals that modulate cytokine and chemokine expression by macrophages (58-60). In addition to

the direct effects of its components on inflammatory cells, the provisional matrix may also serve as a reservoir for cytokines and growth factors that mediate the transition to the proliferative phase of cardiac repair.

THE ROLE OF ECM IN THE PROLIFERATIVE PHASE OF INFARCT HEALING.

The clearance of dead cells and matrix debris from the infarcted myocardium triggers a series of anti-inflammatory cascades that suppress leukocyte recruitment and generate a reparative environment. Infarct macrophages undergo phenotypic transitions, expressing and releasing mediators (like TGF- β and interleukin-10) that suppress inflammation, while promoting myofibroblast activation (61-63). Resident cardiac fibroblasts undergo myofibroblast conversion (64), expressing contractile proteins such as α -smooth muscle actin, and secreting collagens and other structural ECM proteins that are necessary for protection of the infarcted myocardium from catastrophic rupture (65). Although other cell types such as macrophages may produce collagen following myocardial injury (66), their relative contribution as a source of structural ECM proteins is limited, and activated myofibroblasts represent the main collagen-synthesizing cells in the healing infarct. Myofibroblast activation requires the cooperation of several different cell types, including macrophages, lymphocytes, vascular cells, and border zone cardiomyocytes, which secrete growth factors and matricellular proteins, converting the ECM into a signaling hub that localizes fibroblast-activating mediators into the infarct zone.

Transition to the proliferative phase of cardiac repair is marked by dramatic changes in the composition of the provisional matrix. The fibrin-based plasma-derived provisional network is lysed by fibrinolytic enzymes (67). In vivo studies suggest that the timely clearance of the fibrin-based provisional matrix by the plasminogen/plasmin system plays a crucial role in regulation of the reparative response. Plasminogen null mice exhibit marked defects in infarct healing, associated with impaired recruitment of reparative cells and perturbed replacement of dead cardiomyocytes with granulation tissue (68,69). As the fibrin network is lysed, activated macrophages and interstitial cells generate a cell-derived ECM that contains cellular fibronectin, hyaluronan, and proteoglycans (51,70). The cell-derived provisional matrix is further enriched with a range of matricellular macromolecules (13,71) and transduces key activating signals in fibroblasts, immune cells, vascular cells, and

CENTRAL ILLUSTRATION Matricellular Proteins Regulate Inflammatory, Reparative, Angiogenic and Fibrogenic Cellular Responses During the Proliferative Phase of Infarct Healing**A. Matricellular Protein Expression After Myocardial Infarction****B. Cellular Sources and Actions of Specialized Matrix Proteins in the Infarcted Heart**Frangogiannis, N.G. et al. *J Am Coll Cardiol.* 2020;75(17):2219-35.

(A) Immunohistochemical staining using a peroxidase-based strategy (black) shows expression of the matricellular proteins osteopontin (OPN) (left) and thrombospondin (TSP)-1 (right) in the infarcted myocardium. Counterstained with eosin. Scale bar = 100 μ m. Data are from our own work in a canine model of reperfused myocardial infarction (13,152). Each matricellular protein shows a unique pattern of localization, likely reflecting distinct cellular sources and mechanisms of regulation. OPN is predominantly expressed by macrophages (left, arrows), whereas TSP-1 is deposited in the infarct border zone (right, arrows). (B) Schematic cartoon illustrating the complex matrix environment in the proliferative phase of infarct healing. Cell-derived fibronectin, hyaluronan, and a wide range of matricellular proteins (OPN, TSP-1, TNC/tenascin-C, periostin, SPARC, osteoglycin, and members of the CCN family) and proteoglycans enrich the infarct ECM and regulate assembly of the collagen-based structural matrix, while modulating a variety of cellular responses in cardiomyocytes, fibroblasts, macrophages, and vascular cells. CCN = CYR61 (cysteine-rich angiogenic inducer 61)/CTGF(connective tissue growth factor)/NOV(nephroblastoma overexpressed).

TABLE 2 Expression and Role of Matricellular Proteins in Myocardial Infarction

Matricellular Protein	Expression Following MI	Function	Possible Mechanisms of Action
Thrombospondin (TSP)-1	Transient up-regulation and deposition in the infarct border zone during the proliferative phase of healing in mouse, rat, and canine models of MI (71,165). In human patients with end-stage heart failure, TSP-1 expression may be reduced, suggesting that injury-associated TSP-1 induction is transient (166).	Protects the infarcted heart from adverse remodeling, limiting expansion of inflammation and extension of fibrosis (71).	May activate TGF- β (167,168). May inhibit MMPs (169,170). May exert angiostatic actions (171). May modulate nitric oxide signaling and inflammation (172). May regulate ECM assembly and cross-linking (173). The relative contribution of these actions in TSP-1-mediated modulation of the reparative and remodeling responses following MI has not been studied.
TSP-4	Markedly up-regulated in experimental models of MI (174).	Although TSP-4 has been suggested to exert protective actions in pressure-overloaded hearts (175,176), its role in MI has not been systematically studied.	Unknown.
Tenascin C	Transient up-regulation in infarcted area, border zone, and remote remodeling myocardium has been documented in animal models of MI (177,178) and in human patients with ischemic heart disease.	May contribute to myocardial regeneration in fish and amphibians (147,179). Promotes fibrosis and accelerates adverse t-MI remodeling in adult mammals (85,180).	May exert proinflammatory actions, in part through activation of Toll-like receptor signaling (181). May promote fibrogenic actions and may drive persistence of fibrotic lesions (182). May promote recruitment of myofibroblasts (85). May modulate angiogenesis (183). May regulate macrophage recruitment (184) and polarization (87).
SPARC	Abundant, but transient up-regulation in infarcted myocardium, predominantly localized in macrophages and myofibroblasts (185,186).	Protects from cardiac rupture. May promote systolic dysfunction during the early post-ischemic phase (185,186).	May play a role in procollagen processing and collagen fibril assembly (185,187). May accentuate growth factor signaling, promoting fibroblast activation (185). May exert inotropic actions on cardiomyocytes (188). May restrain angiogenesis (189), and inhibit angiogenic actions of VEGF in endothelial cells (190).
Osteopontin	Markedly and transiently up-regulated following MI, primarily localized in galectin-3 ^{hi} /CD206+ macrophages (42,191,192).	Protects from adverse remodeling (35).	May promote proliferation and integrin-dependent activation of cardiac fibroblasts (193). May transduce survival signals (194), and activate a matrix-synthetic program in fibroblasts (195). May promote cardiomyocyte hypertrophy (196), and regulate metabolic pathways involved in diastolic dysfunction (197). May promote angiogenic responses (198). May activate macrophages to express galectin-3, promoting a fibrogenic phenotype (198).
Periostin	Marked, but transient up-regulation in activated myofibroblasts in the infarct, border zone, and remodeling area (199,200).	Protects from cardiac rupture, while promoting late fibrosis in remodeling segments (199,200). Has been suggested to promote a regenerative response in neonatal mouse myocardial injury (201) and may even activate a regenerative program in adult mice (151).	May promote migration and activate a matrix-synthetic program in cardiac fibroblasts (199,200). May regulate collagen fibrillogenesis (202). Has been suggested to promote cell cycle entry in cardiomyocyte progenitors and in cardiomyocytes (151). However, genetic manipulations of periostin in mouse models failed to confirm the significance of these actions (203).
CCN2	Marked, but transient up-regulation in infarcted hearts (204-206).	Cardiomyocyte-specific CCN2 overexpression studies suggested that CCN2 reduces infarct size following ischemia/reperfusion and attenuates adverse remodeling in nonreperfused infarction (204,205). In contrast, antagonism of endogenous CCN2 using a neutralizing antibody had no effects on infarct size (207). CCN2 inhibition experiments in a model of nonreperfused MI suggested that CCN2 may accentuate adverse remodeling, promoting hypertrophy and fibrosis (207).	May activate prosurvival pathways in cardiomyocytes. May attenuate inflammation and promote fibrogenic activation (207). Studies using genetic approaches in models of cardiac remodeling did not support the proposed critical role of CCN2 as a downstream effector of TGF- β (208). CCN2 and CCN5 have been suggested to exert opposing actions in remodeling and fibrosis of the pressure-overloaded heart (206); however, interactions between CCN family members in MI have not been investigated.

CCN = CYR61 (cysteine-rich angiogenic inducer 61)/CTGF(connective tissue growth factor)/NOV(nephroblastoma overexpressed); ECM = extracellular matrix; MI = myocardial infarction; MMP, matrix metalloprotease; SPARC = secreted protein, acidic and rich in cysteine; TGF = tissue growth factor; TSP = thrombospondin; VEGF = vascular endothelial growth factor.

surviving border zone cardiomyocytes (Central Illustration).

The conversion of fibroblasts to activated myofibroblasts also occurs, which requires a close association with TGF- β -secreting macrophages (72) and local

activation of latent TGF- β in the infarcted area. The deposition of specialized components of the matrix network plays a critical role in spatially-restricted TGF- β activation in the healing infarct. In vitro and in vivo evidence suggest that the ED-A splice variant

of fibronectin mediates TGF- β 1-induced myofibroblast conversion (73,74). However, the interactions between ED-A fibronectin and the TGF- β signaling cascade remain poorly understood. It has been suggested that ED-A fibronectin may act by immobilizing the large latent TGF- β complex within the ECM (75), thus localizing this growth factor in the area of fibroblast accumulation. Proteases, cell surface integrins, and matricellular proteins may then cooperate to liberate the active TGF- β dimer from latent stores, triggering downstream fibrogenic signaling pathways (76). In addition to its role in stimulating TGF- β -driven fibroblast-activating responses, fibronectin may also play an important role in angiogenesis. The heparin II domain of fibronectin binds to VEGF (77) and may promote angiogenic activation of endothelial cells, thus stimulating neovessel formation in the infarct.

The modulation of interactions between growth factors and proteoglycans has profound effects on reparative, fibrogenic, and angiogenic cascades. Induction of sulfatases in the infarcted heart can remove 6-*O*-sulfate groups from heparan sulfate in the extracellular compartment, thus perturbing interactions between VEGF-A and heparan sulfate, and increasing responsiveness to the angiogenic effects of VEGF (78). Inhibition of heparin sulfate sulfation may also affect bioactivity of several other cytokines, chemokines, and growth factors, including CXCL12 and TGF- β s.

THE EFFECTS OF MATRICELLULAR PROTEINS. The term “matricellular protein” was coined to highlight the effects of structurally unrelated, injury-associated ECM components that regulate cellular functions by modulating signaling cascades (79,80). Prototypical matricellular proteins have a limited structural role, but are overexpressed in injured and remodeling tissues, and bind to structural matrix proteins and cell surface receptors (like integrins or syndecans), transducing cytokine and growth factor signals, or modulating the activity of proteases and other bioactive mediators (71). The family includes secreted protein, acidic and rich in cysteine (SPARC); thrombospondins (TSP)-1, -2, and -4; tenascin-C and -X; periostin; osteopontin; and the members of the CCN (Cystein rich protein 61/ Connective tissue growth factor)/Nephroblastoma overexpressed gene) family (81). The term is also used to describe other secreted proteins that may exhibit some matricellular functions within the broad range of their effects (including the galectins, fibulins, and small leucine rich proteoglycans such as osteoglycin). Considering the growing evidence suggesting that even prototypical matricellular proteins may act

as intracellular mediators or exert cytokine-like functions, the term may be more useful to describe specific functions that govern the interactions between the ECM and cellular elements, rather than to define a group of proteins. In the infarcted heart, neurohumoral signals, cytokines, and growth factors induce the expression and secretion of a wide range of matricellular proteins in fibroblasts, macrophages, cardiomyocytes, and vascular cells (**Central Illustration**) (13,82,83). Our current understanding of the role of matricellular proteins in the infarcted heart is derived from studies using genetically targeted mice (71,84). Although each member appears to exert unique actions in vivo (**Table 2**), several unifying patterns have emerged on the functional properties of matricellular macromolecules. First, matricellular proteins act on many cell types, modulating fibroblast, macrophage, and vascular cell phenotypes, and regulating survival, hypertrophy, and dysfunction of border zone cardiomyocytes (85-87). However, the relative significance of these cell-specific actions of matricellular proteins is unclear. Second, matricellular proteins may also contribute to the cellular plasticity of interstitial cells observed in healing infarcts (88-91), both through direct actions and via modulation of growth factor-mediated pathways. Third, several members of the family exhibit a highly selective localization in the infarct border zone (92), possibly reflecting macrophage-derived secretion in this leukocyte-rich environment, or the unique interactions between surviving cardiomyocytes, macrophages, and fibroblasts in this area. The localized induction of matricellular proteins in the infarct border zone highlights their role in spatial regulation of cellular responses. Large amounts of growth factors and cytokines are secreted in the infarct border zone and could diffuse into neighboring viable areas, promoting fibrogenic or inflammatory responses. The selective induction and deposition of matricellular proteins may serve to localize inflammation and fibroblast activation within the area of injury, restraining the fibrotic response and protecting from adverse remodeling. Fourth, members of the matricellular family are transiently up-regulated in the healing infarct. Although the mechanisms responsible for removal of matricellular proteins from the healing area remain poorly understood, the signals involved in their clearance may protect the infarcted heart from expansion of the fibrotic response following injury.

DEPOSITION OF FIBRILLAR COLLAGENS IN THE INFARCTED HEART. De novo fibrillar collagen synthesis (i.e., collagens I and III) confers mechanical strength to the healing scar, thus protecting the

infarcted myocardium from rupture and attenuating dilative remodeling. In addition to their structural role, fibrillar collagens may also transduce signals to interstitial immune and vascular cells. Infarct myofibroblasts are capable of secreting large amounts of collagens in response to neurohumoral stimuli or growth factors (such as TGF- β), and are the major collagen-synthesizing cells in the healing infarct (93). Although the functional heterogeneity of fibroblasts is increasingly appreciated (94,95), whether exaggerated matrix synthesis marks a distinct subset of myofibroblasts remains unknown.

In experimental models of MI, type III procollagen exhibits early induction, followed by the marked up-regulation of procollagen I synthesis (93,96). Whether the time course of collagen isoform synthesis reflects isoform-specific effects of various fibrogenic stimuli is unknown. The relative expression of collagen I and III has been suggested to regulate cardiac compliance. Collagen I forms thick and stiff fibers; in contrast, the fine reticular collagen III fibers are more compliant and may improve elasticity of the infarcted ventricle.

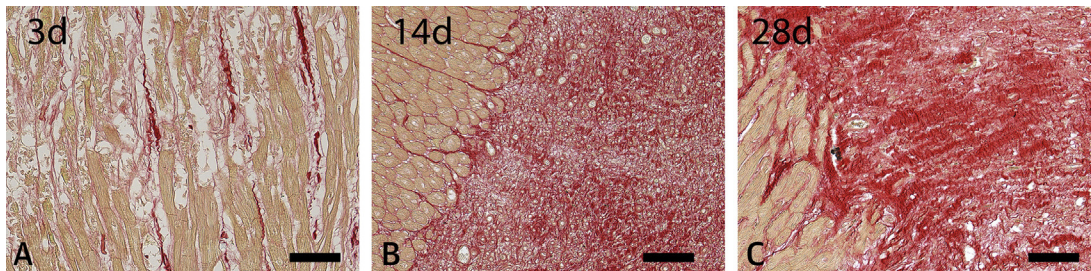
The synthesis of procollagens by infarct myofibroblasts is followed by secretion of soluble procollagen protein in the infarct zone (Figure 2). Subsequent processing of procollagen chains and assembly of fibrils is of critical significance for formation of an organized scar. Cleavage of the C-terminal propeptide attached to procollagen involves the C proteinase bone morphogenetic protein 1 (97), which is induced in the infarcted heart (98,99). Secreted frizzled-related protein 2 (Sfrp2) is also up-regulated in infarct fibroblasts and likely enhances the bone morphogenetic protein 1-procollagen interaction, promoting collagen processing (99). In addition, collagen processing may require further interactions with matricellular proteins, such as SPARC (100).

THE ROLE OF NONFIBRILLAR COLLAGENS. Myocardial infarction is also associated with the induction of nonfibrillar collagens: a subfamily of collagens that do not form large fibrillar bundles, but that can associate with type I or III collagen fibrils to regulate anchoring, networking, and organization of the ECM (101). Some nonfibrillar collagens may exert signaling functions through binding to cell surface receptors. Other members of the family may be proteolytically cleaved, generating bioactive fragments that regulate the fibroblast or vascular cell phenotype. Collagen VI, the best studied nonfibrillar collagen in MI, has been suggested to exert protective effects, reducing the size of the infarct and attenuating adverse remodeling (102). Specific actions of collagen VI on cardiomyocyte survival and activation of reparative

myofibroblasts have been proposed to explain the protective effects (103,104).

THE ECM IN SCAR MATURATION. Maturation of the healing infarct is associated with cross-linking of the collagenous ECM and reduction of the cellular content of the scar. The molecular signals suppressing fibrogenic activation in the mature scar remain enigmatic. As the scar matures, there is a progressive reduction of the density of activated myofibroblasts in the infarct zone (105). Some descriptive studies have documented apoptosis of infarct fibroblasts, suggesting that cell-specific activation of an apoptotic program may be involved (106,107). Depletion of growth factors and clearance of matricellular proteins required for fibroblast survival may be sufficient to trigger fibroblast death or quiescence in the mature infarct (108,109). Whether active secretion of specific proapoptotic or deactivating signals that target infarct fibroblasts also plays a role in negative regulation of the fibrogenic response remains unknown. Recent lineage tracing approaches have suggested that fibroblasts persist in the mature infarct, but that they transition to a distinct phenotype that produces tendon genes and that may be specialized to support the scar (110). However, the mechanisms responsible for cell-specific activation of a proapoptotic program in the late phase of infarct healing have not been investigated, and the acquisition of a quiescent phenotype may precede apoptosis of infarct myofibroblasts. Vascular cells may also respond to the mature ECM environment by undergoing changes that profoundly affect the morphology and function of the infarct microvasculature. As the scar matures, infarct microvessels acquire a coat of mural cells through activation of platelet-derived growth factor receptor (PDGFR)- β signaling (105,111), while uncoated vessels regress. The composition of the ECM modulates interactions between pericytes and endothelial cells (112,113); however, the role of such actions in the maturation of infarct microvessels has not been investigated.

CHRONIC ECM EXPANSION IN THE NONINFARCTED REMODELING MYOCARDIUM MAY PLAY A ROLE IN HEART FAILURE PROGRESSION. In the presence of a large MI, massive loss of contractile tissue results in increased ventricular filling pressures, and typically also with progressive fibrotic changes in viable myocardial segments (114). The deposition of interstitial collagen in the noninfarct zone is attributed to the pathophysiological effects of pressure and volume loads, and may be dependent on neurohumoral pathway activation (115). Moreover, in viable

FIGURE 2 The Time Course of Collagen Deposition in the Healing Infarct

Staining of canine infarct border zones with picosirius red to identify collagen fibers at 3, 14, and 28 days after reperfused myocardial MI (1 h of coronary occlusion followed by reperfusion). Collagen is identified by the red staining, with cardiomyocytes in light brown. Note the early disruption of the collagen network, accompanied by limited de novo synthesis at 3 days (**A**). After 14 days, extensive collagen deposition is noted in the healing infarct (**B**). The mature scar (28 days [**C**]) exhibits a dense matrix network, typically associated with collagen cross-linking. Data from our own work in a canine model of reperfused MI (13). Scalebar = 100 μ m.

segments, increased wall stress may locally activate mechanosensitive cascades in macrophages and fibroblasts, triggering MIF (see Part 3 of this review series) and expansion of the cardiac interstitial matrix network (116,117).

THE ECM IN CHRONIC ISCHEMIC CARDIOMYOPATHY

Alterations in the ECM network have been extensively documented in patients with ischemic cardiomyopathy, even in the absence of frank MI. Patients with chronic ischemic cardiomyopathy typically exhibit MIF (118), and have increased myocardial collagen levels (119) associated with accentuated MMP expression (120,121) and increased deposition of matricellular proteins such as tenascin-C (122). Considering the high prevalence of comorbidities (including hypertension, diabetes, and metabolic dysfunction) that may profoundly affect ECM deposition and remodeling, the relative impact of chronic ischemia in the matrix remodeling patterns noted in ischemic cardiomyopathy patients is unclear.

Pathophysiologically oriented studies examining the effects of brief intermittent ischemic insults, or low-flow ischemia on the myocardial ECM are limited. Some animal evidence suggests that ischemia may cause significant alterations in the ECM network, even in the absence of infarction. In a pig model, reduction of coronary flow to 50% of baseline for 90 min was sufficient to activate MMP9, but had no effects on the structure of cardiac ECM (123). Whether longer intervals of chronic ischemia stimulate MMP-mediated matrix degradation remains unknown. In a mouse model, daily brief repetitive myocardial ischemia and reperfusion for 7 days was associated with interstitial collagen deposition and increased

expression of the matricellular protein tenascin-C in the absence of a completed infarction (124). The activation of oxidative stress pathways by brief repetitive ischemic insults was implicated in the observed fibrotic changes. This suggests that repetitive ischemic events of low duration or intensity may be sufficient to trigger remodeling of the cardiac ECM in the absence of cardiomyocyte necrosis (125). A small clinical study supports this notion, demonstrating that in patients undergoing aortocoronary bypass surgery, MMP2 and MMP9 are activated in the myocardium following reperfusion after cardioplegia (126).

THERAPEUTIC OPPORTUNITIES: TARGETING THE ECM IN ISCHEMIC HEART DISEASE

MATRIX-BASED STRATEGIES TO PRESERVE THE STRUCTURE, GEOMETRY AND FUNCTION OF THE REMODELING HEART AFTER MI. Because of its importance in preserving cardiac structural integrity and function (127), and its role in the regulation of cellular responses in cardiac injury, repair, and remodeling (71), the cardiac ECM may provide unique opportunities for therapeutic interventions. Following acute MI, cardiac rupture is an uncommon but dramatic complication, typically associated with accentuated matrix degradation (128), perturbed deposition of new structural matrix (129), or disorganized architecture of the scar (65). The application of patches containing ECM proteins may be sufficient to restore the structural integrity of the ventricle in acute left ventricular free wall rupture (130).

The effects of biomaterial scaffolds have been extensively studied in experimental MI models. Implantation of cellular or acellular ECM bioscaffolds

and administration of injectable materials have been reported to exert beneficial actions on the infarcted heart (131-135), not only by improving the mechanical properties of the healing scar, but also by modulating inflammatory and reparative signals, by stimulating prosurvival pathways and promoting angiogenesis (136). Composite cell-matrix scaffolds can also be effective cell delivery platforms to enhance the reparative actions of cell therapy (137). Recently, transendocardial injection of VentriGel (Ventrix, San Diego, California), a cardiac ECM hydrogel derived from decellularized porcine myocardium, was tested in 15 patients with chronic remodeling and moderate left ventricular dysfunction following MI (138). Although the study supported the safety and feasibility of the approach, it was not designed to evaluate efficacy, and large randomized clinical trials testing the efficacy of ECM hydrogels have not been performed. More importantly, despite extensive experimental work, there is currently no consensus regarding the optimal composition and method of administration of biomaterials following MI. Systematic study of the effects of various strategies in large animal models of MI is needed prior to attempts for therapeutic translation.

In chronic ischemic heart disease, there is little doubt that ECM deposition needs to be tightly regulated: excessive accumulation of cross-linked collagens may increase stiffness, promoting diastolic dysfunction, whereas overactive protease-driven matrix degradation pathways may promote dilative remodeling, causing systolic dysfunction. Established therapeutic approaches, such as angiotensin-converting enzyme inhibition, angiotensin type 1 receptor blockade, β -adrenergic receptor antagonism, and mechanical unloading, all act to modulate the deposition and metabolism of ECM proteins (139) and may exert their protective actions (at least in part) by targeting the ECM network. However, the implementation of direct approaches to target matrix remodeling has been hampered by the broad effects of proteases in the infarcted myocardium, while attempts to inhibit MMPs in patients with MI have produced mixed results. Thus, early nonselective MMP inhibition with doxycycline attenuated dilative remodeling in patients surviving MI complicated by left ventricular systolic dysfunction (140). In contrast, administration of a selective oral MMP inhibitor in patients with MI and reduced ejection fraction showed no significant protection from adverse remodeling (141). The wide range of actions of MMPs that may affect not only ECM remodeling, but also the molecular signals involved in inflammation and repair,

complicates interpretation of these findings. As also suggested in the context of MIF in the nonischemic heart (see Part 3 of this series), it is likely that successful approaches targeting the ECM may require the development and validation of biomarkers or imaging methods to identify patient subpopulations with specific patterns of ECM alterations (142). Thus, individuals with overactive matrix synthetic responses following infarction may require different approaches compared to patients with predominantly protease-driven matrix degradation.

TARGETING THE MATRICELLULAR PROTEINS. The critical role of the ECM in repair and remodeling of the infarcted heart suggests that therapeutic approaches modulating the biochemical composition and mechanical properties of the matrix may hold promise for patients with MI. Strategies based on matricellular proteins seem particularly attractive, as they could allow localized modulation of growth factor and cytokine signaling in the infarct area. However, despite evidence suggesting the critical actions of matricellular proteins in the infarcted heart, therapeutic translation is hampered by the complexity of their biological actions. The effects of the matricellular proteins are exerted through many cell types and may be context-dependent, depending on the local cytokine environment and the ECM composition. Moreover, matricellular proteins have multiple functional domains with different actions. Thus, successful therapeutic implementation of therapies based on matricellular proteins will likely require the identification of the functional domains responsible for their protective or detrimental actions *in vivo* (71,143). Considering the known limitations of *in vivo* models, this is a daunting task.

MATRIX INTERVENTIONS FOR CARDIAC REGENERATION. ECM modulation may also hold the key to a visionary research goal: cardiac regeneration. This notion is based on several findings. First, in cardiomyocyte progenitors and neonatal cardiomyocytes, a compliant, elastin-containing ECM promotes cell cycle entry (144,145). Second, in zebrafish, fibronectin deposition has been suggested to play a critical role in myocardial regeneration (146), and in amphibians, a matrix network containing fibronectin, hyaluronan, and the matricellular protein tenascin-C has been suggested to activate a regenerative program (147). Third, in experimental cell therapy studies in mammalian models of cardiac injury, the application of matrix-based patches containing progenitor cells showed enhanced effectiveness (148,149). Whether

such effects may be due to direct actions of specific matrix proteins on cardiac progenitors, or reflect matrix-dependent activation of other cell types (like immune or vascular cells) remains unknown. Fourth, mammalian models of infarction have suggested regenerative actions of certain matricellular macromolecules that may promote the proliferation of differentiated cardiomyocytes. For example, agrin, a large extracellular heparan sulfate proteoglycan, promotes cardiomyocyte cell cycle re-entry in both neonatal and adult mice (150). In addition, the matricellular protein periostin triggers cell cycle re-entry in differentiated adult cardiomyocytes through integrin-dependent mechanisms, which results in improved cardiac function when administered as an epicardial gelfoam patch following infarction (151). Nevertheless, these promising early findings should be viewed with caution. Considering that the specialized ECM proteins suggested to be critical in regeneration of fish, amphibian, and neonatal mouse hearts are also induced following adult mammalian cardiac injury in the absence of regeneration, it is unlikely that simple ECM-modulatory strategies will be sufficient to remuscularize adult mammalian hearts. Myocardial regeneration may require not only a “regenerative” matrix profile, but also enhanced phenotypic plasticity of

progenitor cell populations, and a favorable local cytokine and growth factor microenvironment.

SUMMARY AND CONCLUSIONS

Both acute MI and chronic myocardial ischemia are associated with profound changes in the ECM network. Furthermore, these ECM changes not only alter the cardiac interstitial milieu and its functional properties, but a growing body of evidence suggests that the ECM itself plays a key role in modulating both beneficial and adverse pathways, including inflammation and post-MI remodeling, but also cardiac repair. In this context, and also the broader context of the entire cardiovascular system as reviewed in this series, the therapeutic targeting of the ECM and its many players is a compelling clinical avenue of research that is certain to see intense future interest.

ADDRESS FOR CORRESPONDENCE: Dr. Nikolaos G. Frangogiannis, Albert Einstein College of Medicine, 1300 Morris Park Avenue, Forchheimer G46B, Bronx, New York 10461. E-mail: nikolaos.frangogiannis@einstein.yu.edu. OR Dr. Jason Kovacic, Mount Sinai Medical Center, One Gustave L. Levy Place, Box 1030, New York, New York 10029-6574. E-mail: jason.kovacic@mountsinai.org. Twitter: [@ICahnMountSinai](https://twitter.com/ICahnMountSinai).

REFERENCES

- Santini MP, Forte E, Harvey RP, Kovacic JC. Developmental origin and lineage plasticity of endogenous cardiac stem cells. *Development* 2016;143:1242-58.
- Etoh T, Joffs C, Deschamps AM, et al. Myocardial and interstitial matrix metalloproteinase activity after acute myocardial infarction in pigs. *Am J Physiol Heart Circ Physiol* 2001;281:H987-94.
- Villarreal F, Omens J, Dillmann W, Risteli J, Nguyen J, Covell J. Early degradation and serum appearance of type I collagen fragments after myocardial infarction. *J Mol Cell Cardiol* 2004;36:597-601.
- Sato S, Ashraf M, Millard RW, Fujiwara H, Schwartz A. Connective tissue changes in early ischemia of porcine myocardium: an ultrastructural study. *J Mol Cell Cardiol* 1983;15:261-75.
- Wang W, Sawicki G, Schulz R. Peroxynitrite-induced myocardial injury is mediated through matrix metalloproteinase-2. *Cardiovasc Res* 2002;53:165-74.
- Alfonso-Jaume MA, Bergman MR, Mahimkar R, et al. Cardiac ischemia-reperfusion injury induces matrix metalloproteinase-2 expression through the AP-1 components FosB and JunB. *Am J Physiol Heart Circ Physiol* 2006;291:H1838-46.
- Danielsen CC, Wiggers H, Andersen HR. Increased amounts of collagenase and gelatinase in porcine myocardium following ischemia and reperfusion. *J Mol Cell Cardiol* 1998;30:1431-42.
- Fang W, He A, Xiang MX, et al. Cathepsin K-deficiency impairs mouse cardiac function after myocardial infarction. *J Mol Cell Cardiol* 2019;127:44-56.
- Gaggar A, Weathington N. Bioactive extracellular matrix fragments in lung health and disease. *J Clin Invest* 2016;126:3176-84.
- Wells JM, Gaggar A, Blalock JE. MMP-generated matrikines. *Matrix Biol* 2015;44-46:122-9.
- Ricard-Blum S, Salza R. Matricryptins and matrikines: biologically active fragments of the extracellular matrix. *Exp Dermatol* 2014;23:457-63.
- Lauten A, Gerhard-Garcia A, Suhr F, Fischer JH, Figulla HR, Bloch W. Impact of ischemia-reperfusion on extracellular matrix processing and structure of the basement membrane of the heart. *PLoS One* 2014;9:e92833.
- Dobaczewski M, Bujak M, Zymek P, Ren G, Entman ML, Frangogiannis NG. Extracellular matrix remodeling in canine and mouse myocardial infarcts. *Cell Tissue Res* 2006;324:475-88.
- Huebener P, Abou-Khamis T, Zymek P, et al. CD44 is critically involved in infarct healing by regulating the inflammatory and fibrotic response. *J Immunol* 2008;180:2625-33.
- Trial J, Baughn RE, Wygant JN, et al. Fibronectin fragments modulate monocyte VLA-5 expression and monocyte migration. *J Clin Invest* 1999;104:419-30.
- Senior RM, Griffin GL, Mecham RP. Chemotactic activity of elastin-derived peptides. *J Clin Invest* 1980;66:859-62.
- Gaggar A, Jackson PL, Noerager BD, et al. A novel proteolytic cascade generates an extracellular matrix-derived chemoattractant in chronic neutrophilic inflammation. *J Immunol* 2008;180:5662-9.
- Weathington NM, van Houwelingen AH, Noerager BD, et al. A novel peptide CXCR ligand derived from extracellular matrix degradation during airway inflammation. *Nat Med* 2006;12:317-23.
- Russo I, Cavalera M, Huang S, et al. Protective effects of activated myofibroblasts in the pressure-overloaded myocardium are mediated through Smad-dependent activation of a matrix-preserving program. *Circ Res* 2019;124:1214-27.
- Jiang D, Liang J, Fan J, et al. Regulation of lung injury and repair by Toll-like receptors and hyaluronan. *Nat Med* 2005;11:1173-9.
- Taylor KR, Trowbridge JM, Rudisill JA, Termeer CC, Simon JC, Gallo RL. Hyaluronan fragments stimulate endothelial recognition of

- injury through TLR4. *J Biol Chem* 2004;279:17079-84.
22. Teder P, Vandivier RW, Jiang D, et al. Resolution of lung inflammation by CD44. *Science* 2002;296:155-8.
23. Mydel P, Shipley JM, Adair-Kirk TL, et al. Neutrophil elastase cleaves laminin-332 (laminin-5) generating peptides that are chemotactic for neutrophils. *J Biol Chem* 2008;283:9513-22.
24. Lindsey ML, Iyer RP, Zamilpa R, et al. A Novel Collagen Matricryptin Reduces Left Ventricular Dilation Post-Myocardial Infarction by Promoting Scar Formation and Angiogenesis. *J Am Coll Cardiol* 2015;66:1364-74.
25. Okada M, Oba Y, Yamawaki H. Endostatin stimulates proliferation and migration of adult rat cardiac fibroblasts through PI3K/Akt pathway. *Eur J Pharmacol* 2015;750:20-6.
26. O'Reilly MS, Boehm T, Shing Y, et al. Endostatin: an endogenous inhibitor of angiogenesis and tumor growth. *Cell* 1997;88:277-85.
27. Hamano Y, Zeisberg M, Sugimoto H, et al. Physiological levels of tumstatin, a fragment of collagen IV alpha3 chain, are generated by MMP-9 proteolysis and suppress angiogenesis via alphaV beta3 integrin. *Cancer Cell* 2003;3:589-601.
28. Yasuda J, Fukui K, Okada M, Yamawaki H. T3 peptide, a fragment of tumstatin, stimulates proliferation and migration of cardiac fibroblasts through activation of Akt signaling pathway. *Naunyn Schmiedeberg Arch Pharmacol* 2017;390:1135-44.
29. Okada M, Murata N, Yamawaki H. Canstatin stimulates migration of rat cardiac fibroblasts via secretion of matrix metalloproteinase-2. *Am J Physiol Cell Physiol* 2017;312:C199-208.
30. Sugiyama A, Okada M, Yamawaki H. Pathophysiological roles of canstatin on myofibroblasts after myocardial infarction in rats. *Eur J Pharmacol* 2017;807:32-43.
31. Gearing AJ, Beckett P, Christodoulou M, et al. Matrix metalloproteinases and processing of pro-TNF-alpha. *J Leukoc Biol* 1995;57:774-7.
32. Schonbeck U, Mach F, Libby P. Generation of biologically active IL-1 beta by matrix metalloproteinases: a novel caspase-1-independent pathway of IL-1 beta processing. *J Immunol* 1998;161:3340-6.
33. Dayer C, Stamenkovic I. Recruitment of matrix metalloproteinase-9 (MMP-9) to the fibroblast cell surface by lysyl hydroxylase 3 (LH3) triggers transforming growth factor-beta (TGF-beta) activation and fibroblast differentiation. *J Biol Chem* 2015;290:13763-78.
34. Van Lint P, Libert C. Chemokine and cytokine processing by matrix metalloproteinases and its effect on leukocyte migration and inflammation. *J Leukoc Biol* 2007;82:1375-81.
35. Feng G, Hao D, Chai J. Processing of CXCL12 impedes the recruitment of endothelial progenitor cells in diabetic wound healing. *FEBS J* 2014;281:5054-62.
36. Peng H, Wu Y, Duan Z, Ciborowski P, Zheng JC. Proteolytic processing of SDF-1alpha by matrix metalloproteinase-2 impairs CXCR4 signaling and reduces neural progenitor cell migration. *Protein Cell* 2012;3:875-82.
37. Denney H, Clench MR, Woodroffe MN. Cleavage of chemokines CCL2 and CXCL10 by matrix metalloproteinases-2 and -9: implications for chemotaxis. *Biochem Biophys Res Commun* 2009;382:341-7.
38. Song J, Wu C, Zhang X, Sorokin LM. In vivo processing of CXCL5 (LIX) by matrix metalloproteinase (MMP)-2 and MMP-9 promotes early neutrophil recruitment in IL-1beta-induced peritonitis. *J Immunol* 2013;190:401-10.
39. Cox JH, Dean RA, Roberts CR, Overall CM. Matrix metalloproteinase processing of CXCL11/I-TAC results in loss of chemoattractant activity and altered glycosaminoglycan binding. *J Biol Chem* 2008;283:19389-99.
40. Bujak M, Dobaczewski M, Chatila K, et al. Interleukin-1 receptor type I signaling critically regulates infarct healing and cardiac remodeling. *Am J Pathol* 2008;173:57-67.
41. Bujak M, Dobaczewski M, Gonzalez-Quesada C, et al. Induction of the CXC chemokine interferon-gamma-inducible protein 10 regulates the reparative response following myocardial infarction. *Circ Res* 2009;105:973-83.
42. Dewald O, Zymek P, Winkelmann K, et al. CCL2/monocyte chemoattractant protein-1 regulates inflammatory responses critical to healing myocardial infarcts. *Circ Res* 2005;96:881-9.
43. Cauwe B, Opendakker G. Intracellular substrate cleavage: a novel dimension in the biochemistry, biology and pathology of matrix metalloproteinases. *Crit Rev Biochem Mol Biol* 2010;45:351-423.
44. Ali MA, Cho WJ, Hudson B, Kassiri Z, Granzier H, Schulz R. Titin is a target of matrix metalloproteinase-2: implications in myocardial ischemia/reperfusion injury. *Circulation* 2010;122:2039-47.
45. Schulz R. Intracellular targets of matrix metalloproteinase-2 in cardiac disease: rationale and therapeutic approaches. *Annu Rev Pharmacol Toxicol* 2007;47:211-42.
46. Jobin PG, Butler GS, Overall CM. New intracellular activities of matrix metalloproteinases shine in the moonlight. *Biochim Biophys Acta Mol Cell Res* 2017;1864:2043-55.
47. Frangogiannis NG. The extracellular matrix in myocardial injury, repair, and remodeling. *J Clin Invest* 2017;127:1600-12.
48. Barker TH, Engler AJ. The provisional matrix: setting the stage for tissue repair outcomes. *Matrix Biol* 2017;60-61:1-4.
49. Clark RA, Lanigan JM, DellaPelle P, Manseau E, Dvorak HF, Colvin RB. Fibronectin and fibrin provide a provisional matrix for epidermal cell migration during wound reepithelialization. *J Invest Dermatol* 1982;79:264-9.
50. Magnusson MK, Mosher DF. Fibronectin: structure, assembly, and cardiovascular implications. *Arterioscler Thromb Vasc Biol* 1998;18:1363-70.
51. Ulrich MM, Janssen AM, Daemen MJ, et al. Increased expression of fibronectin isoforms after myocardial infarction in rats. *J Mol Cell Cardiol* 1997;29:2533-43.
52. Andersson L, Scharin Tang M, Lundqvist A, et al. Rip2 modifies VEGF-induced signalling and vascular permeability in myocardial ischaemia. *Cardiovasc Res* 2015;107:478-86.
53. Frangogiannis NG, Lindsey ML, Michael LH, et al. Resident cardiac mast cells degranulate and release preformed TNF-alpha, initiating the cytokine cascade in experimental canine myocardial ischemia/reperfusion. *Circulation* 1998;98:699-710.
54. Brown LF, Yeo KT, Berse B, et al. Expression of vascular permeability factor (vascular endothelial growth factor) by epidermal keratinocytes during wound healing. *J Exp Med* 1992;176:1375-9.
55. Petzelbauer P, Zacharowski PA, Miyazaki Y, et al. The fibrin-derived peptide Bbeta15-42 protects the myocardium against ischemia-reperfusion injury. *Nat Med* 2005;11:298-304.
56. Flick MJ, Du X, Witte DP, et al. Leukocyte engagement of fibrin(ogen) via the integrin receptor alphaMbeta2/Mac-1 is critical for host inflammatory response in vivo. *J Clin Invest* 2004;113:1596-606.
57. Silva LM, Lum AG, Tran C, et al. Plasmin-mediated fibrinolysis enables macrophage migration in a murine model of inflammation. *Blood* 2019;134:291-303.
58. Corbett SA, Schwarzbauer JE. Fibronectin-fibrin cross-linking: a regulator of cell behavior. *Trends Cardiovasc Med* 1998;8:357-62.
59. Smiley ST, King JA, Hancock WW. Fibrinogen stimulates macrophage chemokine secretion through toll-like receptor 4. *J Immunol* 2001;167:2887-94.
60. White ES, Livant DL, Markwart S, Arenberg DA. Monocyte-fibronectin interactions, via alpha(5)beta(1) integrin, induce expression of CXC chemokine-dependent angiogenic activity. *J Immunol* 2001;167:5362-6.
61. Shiraishi M, Shintani Y, Shintani Y, et al. Alternatively activated macrophages determine repair of the infarcted adult murine heart. *J Clin Invest* 2016;126:2151-66.
62. Honold L, Nahrendorf M. Resident and monocyte-derived macrophages in cardiovascular disease. *Circ Res* 2018;122:113-27.
63. Chen B, Huang S, Su Y, et al. Macrophage Smad3 protects the infarcted heart, stimulating phagocytosis and regulating inflammation. *Circ Res* 2019;125:55-70.
64. Kanisicak O, Khalil H, Ivey MJ, et al. Genetic lineage tracing defines myofibroblast origin and function in the injured heart. *Nat Commun* 2016;7:12260.
65. Kong P, Shinde AV, Su Y, et al. Opposing actions of fibroblast and cardiomyocyte Smad3 signaling in the infarcted myocardium. *Circulation* 2018;137:707-24.
66. Simoes FC, Cahill TJ, Kenyon A, et al. Macrophages directly contribute collagen to scar formation during zebrafish heart regeneration and mouse heart repair. *Nat Commun* 2020;11:600.

- 67.** Schafer BM, Maier K, Eickhoff U, Todd RF, Kramer MD. Plasminogen activation in healing human wounds. *Am J Pathol* 1994;144:1269-80.
- 68.** Creemers E, Cleutjens J, Smits J, et al. Disruption of the plasminogen gene in mice abolishes wound healing after myocardial infarction. *Am J Pathol* 2000;156:1865-73.
- 69.** Gong Y, Zhao Y, Li Y, Fan Y, Hoover-Plow J. Plasminogen regulates cardiac repair after myocardial infarction through its noncanonical function in stem cell homing to the infarcted heart. *J Am Coll Cardiol* 2014;63:2862-72.
- 70.** Brown LF, Dubin D, Lavigne L, Logan B, Dvorak HF, Van de Water L. Macrophages and fibroblasts express embryonic fibronectins during cutaneous wound healing. *Am J Pathol* 1993;142:793-801.
- 71.** Frangogiannis NG. Matricellular proteins in cardiac adaptation and disease. *Physiol Rev* 2012;92:635-88.
- 72.** Lodyga M, Cambridge E, Karvonen HM, et al. Cadherin-11-mediated adhesion of macrophages to myofibroblasts establishes a profibrotic niche of active TGF- β . *Sci Signal* 2019;12:eaao3469.
- 73.** Arslan F, Smeets MB, Riem Vis PW, et al. Lack of fibronectin-EDA promotes survival and prevents adverse remodeling and heart function deterioration after myocardial infarction. *Circ Res* 2011;108:582-92.
- 74.** Serini G, Bochaton-Piallat ML, Ropraz P, et al. The fibronectin domain ED-A is crucial for myofibroblastic phenotype induction by transforming growth factor- β 1. *J Cell Biol* 1998;142:873-81.
- 75.** Klingberg F, Chau G, Walraven M, et al. The fibronectin ED-A domain enhances recruitment of latent TGF- β -binding protein-1 to the fibroblast matrix. *J Cell Sci* 2018;131:jcs201293.
- 76.** Frangogiannis NG. The role of transforming growth factor (TGF)- β in the infarcted myocardium. *J Thorac Dis* 2017;9:552-63.
- 77.** Wijelath ES, Rahman S, Namekata M, et al. Heparin-II domain of fibronectin is a vascular endothelial growth factor-binding domain: enhancement of VEGF biological activity by a singular growth factor/matrix protein synergism. *Circ Res* 2006;99:853-60.
- 78.** Korf-Klingebiel M, Reboll MR, Grote K, et al. Heparan Sulfate-Editing Extracellular Sulfatases Enhance VEGF Bioavailability for Ischemic Heart Repair. *Circ Res* 2019;125:787-801.
- 79.** Bornstein P. Matricellular proteins: an overview. *J Cell Commun Signal* 2009;3:163-5.
- 80.** Murphy-Ullrich JE. The de-adhesive activity of matricellular proteins: is intermediate cell adhesion an adaptive state? *J Clin Invest* 2001;107:785-90.
- 81.** Bornstein P, Sage EH. Matricellular proteins: extracellular modulators of cell function. *Curr Opin Cell Biol* 2002;14:608-16.
- 82.** Mackie EJ, Scott-Burden T, Hahn AW, et al. Expression of tenascin by vascular smooth muscle cells. Alterations in hypertensive rats and stimulation by angiotensin II. *Am J Pathol* 1992;141:377-88.
- 83.** Hashimoto S, Suzuki T, Dong HY, Yamazaki N, Matsushima K. Serial analysis of gene expression in human monocytes and macrophages. *Blood* 1999;94:837-44.
- 84.** Schellings MW, Pinto YM, Heymans S. Matricellular proteins in the heart: possible role during stress and remodeling. *Cardiovasc Res* 2004;64:24-31.
- 85.** Tamaoki M, Imanaka-Yoshida K, Yokoyama K, et al. Tenascin-C regulates recruitment of myofibroblasts during tissue repair after myocardial injury. *Am J Pathol* 2005;167:71-80.
- 86.** Imanaka-Yoshida K, Hiroe M, Nishikawa T, et al. Tenascin-C modulates adhesion of cardiomyocytes to extracellular matrix during tissue remodeling after myocardial infarction. *Lab Invest* 2001;81:1015-24.
- 87.** Shimojo N, Hashizume R, Kanayama K, et al. Tenascin-C may accelerate cardiac fibrosis by activating macrophages via the integrin α V- β 3/nuclear factor- κ B/interleukin-6 axis. *Hypertension* 2015;66:757-66.
- 88.** Aisagbonhi O, Rai M, Ryzhov S, Atria N, Feoktistov I, Hatzopoulos AK. Experimental myocardial infarction triggers canonical Wnt signaling and endothelial-to-mesenchymal transition. *Dis Model Mech* 2011;4:469-83.
- 89.** Ubil E, Duan J, Pillai IC, et al. Mesenchymal-endothelial transition contributes to cardiac neovascularization. *Nature* 2014;514:585-90.
- 90.** Zeisberg EM, Tarnavski O, Zeisberg M, et al. Endothelial-to-mesenchymal transition contributes to cardiac fibrosis. *Nat Med* 2007;13:952-61.
- 91.** Saxena A, Chen W, Su Y, et al. IL-1 induces proinflammatory leukocyte infiltration and regulates fibroblast phenotype in the infarcted myocardium. *J Immunol* 2013;191:4838-48.
- 92.** Frangogiannis NG, Ren G, Dewald O, et al. Critical role of endogenous thrombospondin-1 in preventing expansion of healing myocardial infarcts. *Circulation* 2005;111:2935-42.
- 93.** Cleutjens JP, Verluyten MJ, Smiths JF, Daemen MJ. Collagen remodeling after myocardial infarction in the rat heart. *Am J Pathol* 1995;147:325-38.
- 94.** Frangogiannis NG. The functional pluralism of fibroblasts in the infarcted myocardium. *Circ Res* 2016;119:1049-51.
- 95.** Tallquist MD. Cardiac fibroblast diversity. *Annu Rev Physiol* 2020;82:63-78.
- 96.** Inoue K, Kusachi S, Niiya K, Kajikawa Y, Tsuji T. Sequential changes in the distribution of type I and III collagens in the infarct zone: immunohistochemical study of experimental myocardial infarction in the rat. *Coron Artery Dis* 1995;6:153-8.
- 97.** Baicu CF, Zhang Y, Van Laer AO, Renaud L, Zile MR, Bradshaw AD. Effects of the absence of procollagen C-endopeptidase enhancer-2 on myocardial collagen accumulation in chronic pressure overload. *Am J Physiol Heart Circ Physiol* 2012;303:H234-40.
- 98.** He W, Zhang L, Ni A, et al. Exogenously administered secreted frizzled related protein 2 (Sfrp2) reduces fibrosis and improves cardiac function in a rat model of myocardial infarction. *Proc Natl Acad Sci U S A* 2010;107:21110-5.
- 99.** Kobayashi K, Luo M, Zhang Y, et al. Secreted Frizzled-related protein 2 is a procollagen C proteinase enhancer with a role in fibrosis associated with myocardial infarction. *Nat Cell Biol* 2009;11:46-55.
- 100.** Bradshaw AD, Baicu CF, Rentz TJ, et al. Pressure overload-induced alterations in fibrillar collagen content and myocardial diastolic function: role of secreted protein acidic and rich in cysteine (SPARC) in post-synthetic procollagen processing. *Circulation* 2009;119:269-80.
- 101.** Shamhart PE, Meszaros JG. Non-fibrillar collagens: key mediators of post-infarction cardiac remodeling? *J Mol Cell Cardiol* 2010;48:530-7.
- 102.** Luther DJ, Thodeti CK, Shamhart PE, et al. Absence of type VI collagen paradoxically improves cardiac function, structure, and remodeling after myocardial infarction. *Circ Res* 2012;110:851-6.
- 103.** Naugle JE, Olson ER, Zhang X, et al. Type VI collagen induces cardiac myofibroblast differentiation: implications for postinfarction remodeling. *Am J Physiol Heart Circ Physiol* 2006;290:H323-30.
- 104.** Skrbic B, Engebretsen KV, Strand ME, et al. Lack of collagen VIII reduces fibrosis and promotes early mortality and cardiac dilatation in pressure overload in mice. *Cardiovasc Res* 2015;106:32-42.
- 105.** Ren G, Michael LH, Entman ML, Frangogiannis NG. Morphological characteristics of the microvasculature in healing myocardial infarcts. *J Histochem Cytochem* 2002;50:71-9.
- 106.** Takemura G, Ohno M, Hayakawa Y, et al. Role of apoptosis in the disappearance of infiltrated and proliferated interstitial cells after myocardial infarction. *Circ Res* 1998;82:1130-8.
- 107.** Zhao W, Lu L, Chen SS, Sun Y. Temporal and spatial characteristics of apoptosis in the infarcted rat heart. *Biochem Biophys Res Commun* 2004;325:605-11.
- 108.** Hinz B. Formation and function of the myofibroblast during tissue repair. *J Invest Dermatol* 2007;127:526-37.
- 109.** Tomasek JJ, Gabbiani G, Hinz B, Chaponnier C, Brown RA. Myofibroblasts and mechano-regulation of connective tissue remodeling. *Nat Rev Mol Cell Biol* 2002;3:349-63.
- 110.** Fu X, Khalil H, Kanisicak O, et al. Specialized fibroblast differentiated states underlie scar formation in the infarcted mouse heart. *J Clin Invest* 2018;128:2127-43.
- 111.** Zymek P, Bujak M, Chatila K, et al. The role of platelet-derived growth factor signaling in healing myocardial infarcts. *J Am Coll Cardiol* 2006;48:2315-23.
- 112.** Davis GE, Norden PR, Bowers SL. Molecular control of capillary morphogenesis and maturation by recognition and remodeling of the extracellular matrix: functional roles of endothelial cells and pericytes in health and disease. *Connect Tissue Res* 2015;56:392-402.
- 113.** Rivera LB, Brekken RA. SPARC promotes pericyte recruitment via inhibition of endoglin-

- dependent TGF- β 1 activity. *J Cell Biol* 2011;193:1305-19.
- 114.** Volders PG, Willems IE, Cleutjens JP, Arends JW, Havenith MG, Daemen MJ. Interstitial collagen is increased in the non-infarcted human myocardium after myocardial infarction. *J Mol Cell Cardiol* 1993;25:1317-23.
- 115.** van Krimpen C, Smits JF, Cleutjens JP, et al. DNA synthesis in the non-infarcted cardiac interstitium after left coronary artery ligation in the rat: effects of captopril. *J Mol Cell Cardiol* 1991;23:1245-53.
- 116.** Chen B, Frangogiannis NG. Macrophages in the Remodeling Failing Heart. *Circ Res* 2016;119:776-8.
- 117.** Sager HB, Hulsmans M, Lavine KJ, et al. Proliferation and recruitment contribute to myocardial macrophage expansion in chronic heart failure. *Circ Res* 2016;119:853-64.
- 118.** Beltrami CA, Finato N, Rocco M, et al. Structural basis of end-stage failure in ischemic cardiomyopathy in humans. *Circulation* 1994;89:151-63.
- 119.** Mukherjee D, Sen S. Alteration of collagen phenotypes in ischemic cardiomyopathy. *J Clin Invest* 1991;88:1141-6.
- 120.** Reinhardt D, Sigusch HH, Hense J, Tyagi SC, Korfer R, Figulla HR. Cardiac remodelling in end stage heart failure: upregulation of matrix metalloproteinase (MMP) irrespective of the underlying disease, and evidence for a direct inhibitory effect of ACE inhibitors on MMP. *Heart* 2002;88:525-30.
- 121.** Spinale FG, Coker ML, Heung LJ, et al. A matrix metalloproteinase induction/activation system exists in the human left ventricular myocardium and is upregulated in heart failure. *Circulation* 2000;102:1944-9.
- 122.** Frangogiannis NG, Shimoni S, Chang SM, et al. Active interstitial remodeling: an important process in the hibernating human myocardium. *J Am Coll Cardiol* 2002;39:1468-74.
- 123.** Lu L, Gunja-Smith Z, Woessner JF, et al. Matrix metalloproteinases and collagen ultrastructure in moderate myocardial ischemia and reperfusion in vivo. *Am J Physiol Heart Circ Physiol* 2000;279:H601-9.
- 124.** Dewald O, Frangogiannis NG, Zoerlein M, et al. Development of murine ischemic cardiomyopathy is associated with a transient inflammatory reaction and depends on reactive oxygen species. *Proc Natl Acad Sci U S A* 2003;100:2700-5.
- 125.** Frangogiannis NG. The Extracellular matrix in ischemic and nonischemic heart failure. *Circ Res* 2019;125:117-46.
- 126.** Lalu MM, Pasini E, Schulze CJ, et al. Ischaemia-reperfusion injury activates matrix metalloproteinases in the human heart. *Eur Heart J* 2005;26:27-35.
- 127.** Clarke SA, Richardson WJ, Holmes JW. Modifying the mechanics of healing infarcts: is better the enemy of good? *J Mol Cell Cardiol* 2016;93:115-24.
- 128.** Honda S, Asaumi Y, Yamane T, et al. Trends in the clinical and pathological characteristics of cardiac rupture in patients with acute myocardial infarction over 35 years. *J Am Heart Assoc* 2014;3:e000984.
- 129.** Hayashidani S, Tsutsui H, Ikeuchi M, et al. Targeted deletion of MMP-2 attenuates early LV rupture and late remodeling after experimental myocardial infarction. *Am J Physiol Heart Circ Physiol* 2003;285:H1229-35.
- 130.** Holubec T, Caliskan E, Bettex D, Maisano F. Repair of post-infarction left ventricular free wall rupture using an extracellular matrix patch. *Eur J Cardiothorac Surg* 2015;48:800-3.
- 131.** Pattar SS, Fatehi Hassanabad A, Fedak PWM. Acellular extracellular matrix bioscaffolds for cardiac repair and regeneration. *Front Cell Dev Biol* 2019;7:63.
- 132.** Mewhort HEM, Svystonyuk DA, Turnbull JD, et al. Bioactive Extracellular Matrix Scaffold Promotes Adaptive Cardiac Remodeling and Repair. *J Am Coll Cardiol Basic Transl Sci* 2017;2:450-64.
- 133.** Singelyn JM, Christman KL. Injectable materials for the treatment of myocardial infarction and heart failure: the promise of decellularized matrices. *J Cardiovasc Transl Res* 2010;3:478-86.
- 134.** Seif-Naraghi SB, Singelyn JM, Salvatore MA, et al. Safety and efficacy of an injectable extracellular matrix hydrogel for treating myocardial infarction. *Sci Transl Med* 2013;5:173ra25.
- 135.** McLaughlin S, McNeill B, Podrebarac J, et al. Injectable human recombinant collagen matrices limit adverse remodeling and improve cardiac function after myocardial infarction. *Nat Commun* 2019;10:4866.
- 136.** Wassenaar JW, Gaetani R, Garcia JJ, et al. Evidence for mechanisms underlying the functional benefits of a myocardial matrix hydrogel for post-MI treatment. *J Am Coll Cardiol* 2016;67:1074-86.
- 137.** Godier-Furnemont AF, Martens TP, Koeckert MS, et al. Composite scaffold provides a cell delivery platform for cardiovascular repair. *Proc Natl Acad Sci U S A* 2011;108:7974-9.
- 138.** Traverse JH, Henry TD, Dib N, et al. First-in-man study of a cardiac extracellular matrix hydrogel in early and late myocardial infarction patients. *J Am Coll Cardiol Basic Transl Sci* 2019;4:659-69.
- 139.** Silvestre JS, Heymes C, Oubenaissa A, et al. Activation of cardiac aldosterone production in rat myocardial infarction: effect of angiotensin II receptor blockade and role in cardiac fibrosis. *Circulation* 1999;99:2694-701.
- 140.** Cerisano G, Buonamici P, Valenti R, et al. Early short-term doxycycline therapy in patients with acute myocardial infarction and left ventricular dysfunction to prevent the ominous progression to adverse remodeling: the TIPTOP trial. *Eur Heart J* 2014;35:184-91.
- 141.** Hudson MP, Armstrong PW, Ruzyllo W, et al. Effects of selective matrix metalloproteinase inhibitor (PG-116800) to prevent ventricular remodeling after myocardial infarction: results of the PREMIER (Prevention of Myocardial Infarction Early Remodeling) trial. *J Am Coll Cardiol* 2006;48:15-20.
- 142.** Frangogiannis NG. The inflammatory response in myocardial injury, repair, and remodeling. *Nat Rev Cardiol* 2014;11:255-65.
- 143.** Sawyer AJ, Kyriakides TR. Matricellular proteins in drug delivery: therapeutic targets, active agents, and therapeutic localization. *Adv Drug Deliv Rev* 2016;97:56-68.
- 144.** Yahalom-Ronen Y, Rajchman D, Sarig R, Geiger B, Tzahor E. Reduced matrix rigidity promotes neonatal cardiomyocyte dedifferentiation, proliferation and clonal expansion. *Elife* 2015;4:e07455.
- 145.** Qiu Y, Bayomy AF, Gomez MV, et al. A role for matrix stiffness in the regulation of cardiac side population cell function. *Am J Physiol Heart Circ Physiol* 2015;308:H990-7.
- 146.** Wang J, Karra R, Dickson AL, Poss KD. Fibronectin is deposited by injury-activated epicardial cells and is necessary for zebrafish heart regeneration. *Dev Biol* 2013;382:427-35.
- 147.** Mercer SE, Odelberg SJ, Simon HG. A dynamic spatiotemporal extracellular matrix facilitates epicardial-mediated vertebrate heart regeneration. *Dev Biol* 2013;382:457-69.
- 148.** Gaetani R, Feyen DA, Verhage V, et al. Epicardial application of cardiac progenitor cells in a 3D-printed gelatin/hyaluronic acid patch preserves cardiac function after myocardial infarction. *Biomaterials* 2015;61:339-48.
- 149.** Serpooshan V, Zhao M, Metzler SA, et al. Use of bio-mimetic three-dimensional technology in therapeutics for heart disease. *Bioengineered* 2014;5:193-7.
- 150.** Bassat E, Mutlak YE, Genzelinakh A, et al. The extracellular matrix protein agrin promotes heart regeneration in mice. *Nature* 2017;547:179-84.
- 151.** Kuhn B, del Monte F, Hajjar RJ, et al. Periostin induces proliferation of differentiated cardiomyocytes and promotes cardiac repair. *Nat Med* 2007;13:962-9.
- 152.** Huebener P, Frangogiannis NG. Matricellular proteins in myocardial infarction. *Current Cardiology Reviews* 2006;2:163-71.
- 153.** Takahashi S, Geenen D, Nieves E, Iwazumi T. Collagenase degrades collagen in vivo in the ischemic heart. *Biochim Biophys Acta* 1999;1428:251-9.
- 154.** Manhenke C, Ueland T, Jugdutt BI, et al. The relationship between markers of extracellular cardiac matrix turnover: infarct healing and left ventricular remodelling following primary PCI in patients with first-time STEMI. *Eur Heart J* 2014;35:395-402.
- 155.** McGavigan AD, Maxwell PR, Dunn FG. Serological evidence of altered collagen homeostasis reflects early ventricular remodeling following acute myocardial infarction. *Int J Cardiol* 2006;111:267-74.
- 156.** Murakami T, Kusachi S, Murakami M, et al. Time-dependent changes of serum carboxy-terminal peptide of type I procollagen and carboxy-terminal telopeptide of type I collagen

- concentrations in patients with acute myocardial infarction after successful reperfusion: correlation with left ventricular volume indices. *Clin Chem* 1998;44:2453-61.
- 157.** Barthelemy O, Beygui F, Vicaut E, et al. Relation of high concentrations of plasma carboxy-terminal telopeptide of collagen type I with outcome in acute myocardial infarction. *Am J Cardiol* 2009;104:904-9.
- 158.** Cerisano G, Pucci PD, Sulla A, et al. Relation between plasma brain natriuretic peptide, serum indexes of collagen type I turnover, and left ventricular remodeling after reperfused acute myocardial infarction. *Am J Cardiol* 2007;99:651-6.
- 159.** Eschaliel R, Fertin M, Fay R, et al. Extracellular matrix turnover biomarkers predict long-term left ventricular remodeling after myocardial infarction: insights from the REVE-2 study. *Circ Heart Fail* 2013;6:1199-205.
- 160.** Skjot-Arkil H, Clausen RE, Rasmussen LM, et al. Acute myocardial infarction and pulmonary diseases result in two different degradation profiles of elastin as quantified by two novel ELISAs. *PLoS One* 2013;8:e00936.
- 161.** Mizuno T, Mickle DA, Kiani CG, Li RK. Overexpression of elastin fragments in infarcted myocardium attenuates scar expansion and heart dysfunction. *Am J Physiol Heart Circ Physiol* 2005;288:H2819-27.
- 162.** Yasuda J, Okada M, Yamawaki H. Protective effect of T3 peptide, an active fragment of tumstatin, against ischemia/reperfusion injury in rat heart. *J Pharmacol Sci* 2019;139:193-200.
- 163.** Isobe K, Kuba K, Maejima Y, Suzuki J, Kubota S, Isobe M. Inhibition of endostatin/collagen XVIII deteriorates left ventricular remodeling and heart failure in rat myocardial infarction model. *Circ J* 2010;74:109-19.
- 164.** Seko Y, Fukuda S, Nagai R. Serum levels of endostatin, vascular endothelial growth factor (VEGF) and hepatocyte growth factor (HGF) in patients with acute myocardial infarction undergoing early reperfusion therapy. *Clin Sci (Lond)* 2004;106:439-42.
- 165.** Sezaki S, Hirohata S, Iwabu A, et al. Thrombospondin-1 is induced in rat myocardial infarction and its induction is accelerated by ischemia/reperfusion. *Exp Biol Med (Maywood)* 2005;230:621-30.
- 166.** Battle M, Perez-Villa F, Lazaro A, et al. Decreased expression of thrombospondin-1 in failing hearts may favor ventricular remodeling. *Transplant Proc* 2009;41:2231-3.
- 167.** Belmadani S, Bernal J, Wei CC, et al. A thrombospondin-1 antagonist of transforming growth factor-beta activation blocks cardiomyopathy in rats with diabetes and elevated angiotensin II. *Am J Pathol* 2007;171:777-89.
- 168.** Schultz-Cherry S, Murphy-Ullrich JE. Thrombospondin causes activation of latent transforming growth factor-beta secreted by endothelial cells by a novel mechanism. *J Cell Biol* 1993;122:923-32.
- 169.** Bein K, Simons M. Thrombospondin type 1 repeats interact with matrix metalloproteinase 2. Regulation of metalloproteinase activity. *J Biol Chem* 2000;275:32167-73.
- 170.** Xia Y, Dobaczewski M, Gonzalez-Quesada C, et al. Endogenous thrombospondin 1 protects the pressure-overloaded myocardium by modulating fibroblast phenotype and matrix metabolism. *Hypertension* 2011;58:902-11.
- 171.** Iruela-Arispe ML, Lombardo M, Krutzsch HC, Lawler J, Roberts DD. Inhibition of angiogenesis by thrombospondin-1 is mediated by 2 independent regions within the type 1 repeats. *Circulation* 1999;100:1423-31.
- 172.** Isenberg JS, Qin Y, Maxhimer JB, et al. Thrombospondin-1 and CD47 regulate blood pressure and cardiac responses to vasoactive stress. *Matrix Biol* 2009;28:110-9.
- 173.** Rosini S, Pugh N, Bonna AM, Hulmes DJS, Farndale RW, Adams JC. Thrombospondin-1 promotes matrix homeostasis by interacting with collagen and lysyl oxidase precursors and collagen cross-linking sites. *Sci Signal* 2018;11:eaar2566.
- 174.** Mustonen E, Leskinen H, Aro J, et al. Metoprolol treatment lowers thrombospondin-4 expression in rats with myocardial infarction and left ventricular hypertrophy. *Basic Clin Pharmacol Toxicol* 2010;107:709-17.
- 175.** Cingolani OH, Kirk JA, Seo K, et al. Thrombospondin-4 is required for stretch-mediated contractility augmentation in cardiac muscle. *Circ Res* 2011;109:1410-4.
- 176.** Frolova EG, Sopko N, Blech L, et al. Thrombospondin-4 regulates fibrosis and remodeling of the myocardium in response to pressure overload. *FASEB J* 2012;26:2363-73.
- 177.** Willems IE, Arends JW, Daemen MJ. Tenascin and fibronectin expression in healing human myocardial scars. *J Pathol* 1996;179:321-5.
- 178.** Bujak M, Ren G, Kweon HJ, et al. Essential role of smad3 in infarct healing and in the pathogenesis of cardiac remodeling. *Circulation* 2007;116:2127-38.
- 179.** Chablais F, Jazwinska A. The regenerative capacity of the zebrafish heart is dependent on TGFbeta signaling. *Development* 2012;139:1921-30.
- 180.** Kimura T, Tajiri K, Sato A, et al. Tenascin-C accelerates adverse ventricular remodeling after myocardial infarction by modulating macrophage polarization. *Cardiovasc Res* 2019;115:614-24.
- 181.** Midwood K, Sacre S, Piccinini AM, et al. Tenascin-C is an endogenous activator of Toll-like receptor 4 that is essential for maintaining inflammation in arthritic joint disease. *Nat Med* 2009;15:774-80.
- 182.** Bhattacharyya S, Wang W, Morales-Nebreda L, et al. Tenascin-C drives persistence of organ fibrosis. *Nat Commun* 2016;7:11703.
- 183.** Ballard VL, Sharma A, Duignan I, et al. Vascular tenascin-C regulates cardiac endothelial phenotype and neovascularization. *FASEB J* 2006;20:717-9.
- 184.** Abbadi D, Laroumanie F, Bizou M, et al. Local production of tenascin-C acts as a trigger for monocyte/macrophage recruitment that provokes cardiac dysfunction. *Cardiovasc Res* 2018;114:123-37.
- 185.** Schellings MW, Vanhoutte D, Swinnen M, et al. Absence of SPARC results in increased cardiac rupture and dysfunction after acute myocardial infarction. *J Exp Med* 2009;206:113-23.
- 186.** McCurdy SM, Dai Q, Zhang J, et al. SPARC mediates early extracellular matrix remodeling following myocardial infarction. *Am J Physiol Heart Circ Physiol* 2011;301:H497-505.
- 187.** Harris BS, Zhang Y, Card L, Rivera LB, Brekken RA, Bradshaw AD. SPARC regulates collagen interaction with cardiac fibroblast cell surfaces. *Am J Physiol Heart Circ Physiol* 2011;301:H841-7.
- 188.** Deckx S, Johnson DM, Rienks M, et al. Extracellular SPARC increases cardiomyocyte contraction during health and disease. *PLoS One* 2019;14:e0209534.
- 189.** Bradshaw AD, Reed MJ, Carbon JG, Pinney E, Brekken RA, Sage EH. Increased fibrovascular invasion of subcutaneous polyvinyl alcohol sponges in SPARC-null mice. *Wound Repair Regen* 2001;9:522-30.
- 190.** Kupprion C, Motamed K, Sage EH. SPARC (BM-40, osteonectin) inhibits the mitogenic effect of vascular endothelial growth factor on microvascular endothelial cells. *J Biol Chem* 1998;273:29635-40.
- 191.** Murry CE, Giachelli CM, Schwartz SM, Vracco R. Macrophages express osteopontin during repair of myocardial necrosis. *Am J Pathol* 1994;145:1450-62.
- 192.** Shirakawa K, Endo J, Kataoka M, et al. IL (Interleukin)-10-STAT3-galectin-3 axis is essential for osteopontin-producing reparative macrophage polarization after myocardial infarction. *Circulation* 2018;138:2021-35.
- 193.** Ashizawa N, Graf K, Do YS, et al. Osteopontin is produced by rat cardiac fibroblasts and mediates A(II)-induced DNA synthesis and collagen gel contraction. *J Clin Invest* 1996;98:2218-27.
- 194.** Lorenzen JM, Schauerte C, Hubner A, et al. Osteopontin is indispensable for AP1-mediated angiotensin II-related miR-21 transcription during cardiac fibrosis. *Eur Heart J* 2015;36:2184-96.
- 195.** Sawaki D, Czibik G, Pini M, et al. Visceral adipose tissue drives cardiac aging through modulation of fibroblast senescence by osteopontin production. *Circulation* 2018;138:809-22.
- 196.** Trueblood NA, Xie Z, Communal C, et al. Exaggerated left ventricular dilation and reduced collagen deposition after myocardial infarction in mice lacking osteopontin. *Circ Res* 2001;88:1080-7.
- 197.** Yousefi K, Irion CI, Takeuchi LM, et al. Osteopontin promotes left ventricular diastolic dysfunction through a mitochondrial pathway. *J Am Coll Cardiol* 2019;73:2705-18.
- 198.** Zhao X, Johnson JN, Singh K, Singh M. Impairment of myocardial angiogenic response in the absence of osteopontin. *Microcirculation* 2007;14:233-40.

- 199.** Oka T, Xu J, Kaiser RA, et al. Genetic manipulation of periostin expression reveals a role in cardiac hypertrophy and ventricular remodeling. *Circ Res* 2007;101:313-21.
- 200.** Shimazaki M, Nakamura K, Kii I, et al. Periostin is essential for cardiac healing after acute myocardial infarction. *J Exp Med* 2008;205:295-303.
- 201.** Chen Z, Xie J, Hao H, et al. Ablation of periostin inhibits post-infarction myocardial regeneration in neonatal mice mediated by the phosphatidylinositol 3 kinase/glycogen synthase kinase 3beta/cyclin D1 signalling pathway. *Cardiovasc Res* 2017;113:620-32.
- 202.** Norris RA, Damon B, Mironov V, et al. Periostin regulates collagen fibrillogenesis and the biomechanical properties of connective tissues. *J Cell Biochem* 2007;101:695-711.
- 203.** Lorts A, Schwanekamp JA, Elrod JW, Sargent MA, Molkentin JD. Genetic manipulation of periostin expression in the heart does not affect myocyte content, cell cycle activity, or cardiac repair. *Circ Res* 2009;104:e1-7.
- 204.** Ahmed MS, Gravning J, Martinov VN, et al. Mechanisms of novel cardioprotective functions of CCN2/CTGF in myocardial ischemia/reperfusion injury. *Am J Physiol Heart Circ Physiol* 2011;300:H1291-302.
- 205.** Gravning J, Orn S, Kaasboll OJ, et al. Myocardial connective tissue growth factor (CCN2/CTGF) attenuates left ventricular remodeling after myocardial infarction. *PLoS One* 2012;7:e52120.
- 206.** Jeong D, Lee MA, Li Y, et al. Matricellular protein CCN5 reverses established cardiac fibrosis. *J Am Coll Cardiol* 2016;67:1556-68.
- 207.** Vainio LE, Szabo Z, Lin R, et al. Connective tissue growth factor inhibition enhances cardiac repair and limits fibrosis after myocardial infarction. *J Am Coll Cardiol Basic Transl Sci* 2019;4:83-94.
- 208.** Accornero F, van Berlo JH, Correll RN, et al. Genetic analysis of connective tissue growth factor as an effector of transforming growth factor beta signaling and cardiac remodeling. *Mol Cell Biol* 2015;35:2154-64.
-
- KEY WORDS** biomarker, collagen, fibroblast, heart failure, ischemic heart disease

Chemokines in Myocardial Infarction

Bijun Chen & Nikolaos G. Frangogiannis

**Journal of Cardiovascular
Translational Research**

ISSN 1937-5387

J. of Cardiovasc. Trans. Res.
DOI 10.1007/s12265-020-10006-7



Your article is protected by copyright and all rights are held exclusively by Springer Science+Business Media, LLC, part of Springer Nature. This e-offprint is for personal use only and shall not be self-archived in electronic repositories. If you wish to self-archive your article, please use the accepted manuscript version for posting on your own website. You may further deposit the accepted manuscript version in any repository, provided it is only made publicly available 12 months after official publication or later and provided acknowledgement is given to the original source of publication and a link is inserted to the published article on Springer's website. The link must be accompanied by the following text: "The final publication is available at link.springer.com".



Chemokines in Myocardial Infarction

Bijun Chen¹ · Nikolaos G. Frangogiannis¹

Received: 13 January 2020 / Accepted: 15 April 2020
© Springer Science+Business Media, LLC, part of Springer Nature 2020

Abstract

In the infarcted myocardium, cardiomyocyte necrosis triggers an intense inflammatory reaction that not only is critical for cardiac repair, but also contributes to adverse remodeling and to the pathogenesis of heart failure. Both CC and CXC chemokines are markedly induced in the infarcted heart, bind to endothelial glycosaminoglycans, and regulate leukocyte trafficking and function. ELR+ CXC chemokines (such as CXCL8) control neutrophil infiltration, whereas CC chemokines (such as CCL2) mediate recruitment of mononuclear cells. Moreover, some members of the chemokine family (such as CXCL10 and CXCL12) may mediate leukocyte-independent actions, directly modulating fibroblast and vascular cell function. This review manuscript discusses our understanding of the role of the chemokines in regulation of injury, repair, and remodeling following myocardial infarction. Although several chemokines may be promising therapeutic targets in patients with myocardial infarction, clinical implementation of chemokine-based therapeutics is hampered by the broad effects of the chemokines in both injury and repair.

Keywords Chemokine · Leukocyte · Myocardial infarction · Cardiac remodeling · CCL2 · CXCL12

Introduction

Myocardial infarction (MI) is a leading cause of morbidity and mortality worldwide [1]. Sudden occlusion of a coronary artery results in complete loss of perfusion in the myocardial segments subserved by the vessel. Severe and sustained ischemia triggers a wavefront of cardiomyocyte death [2], leading to loss of large amounts of cardiac muscle. Because the adult mammalian heart has negligible regenerative capacity, repair of the infarcted heart is dependent on inflammation-driven formation of a scar.

Over the last 40 years, new pharmacologic therapies [3, 4] and the successful implementation of early reperfusion [5] have significantly reduced mortality in patients presenting with acute MI. However, improved survival resulted in an expanding pool of MI patients who survive the acute event, but remain at a high risk for development of chronic heart failure. The pathobiology of post-infarction heart failure is

linked with “cardiac remodeling,” a complex process that involves both infarcted and non-infarcted myocardial segments and results in progressive functional deterioration and an increased incidence of arrhythmias, typically associated with chamber dilation. The severity of post-infarction remodeling is dependent not only on the size of the infarct, but also on the qualitative characteristics of the reparative response [6]. Thus, following infarction, the cellular responses involved in repair may also contribute to adverse remodeling of the heart.

Inflammation is a key driver of repair and remodeling of the infarcted heart. Chemokines, a family of chemotactic cytokines with critical roles in leukocyte trafficking, are crucial mediators of inflammation in injury and repair. Over the last 20 years, a growing body of evidence has suggested that sequential mobilization of immune cell subpopulations in the infarcted heart is orchestrated by the chemokines and may play an important role in cardiac repair and remodeling [7, 8]. This review manuscript discusses our current understanding of the role of the chemokines in the infarcted heart.

Associate Editor Saskia de Jager oversaw the review of this article

✉ Nikolaos G. Frangogiannis
nikolaos.frangogiannis@einstein.yu.edu

¹ The Wilf Family Cardiovascular Research Institute, Department of Medicine (Cardiology), Albert Einstein College of Medicine, 1300 Morris Park Avenue Forchheimer G46B, Bronx, NY, USA

The chemokine Family

Chemokines are small (8–12 kDa) chemotactic cytokines that regulate cell migration and positioning in development,

homeostasis, and inflammatory injury [9]. In mammals, the chemokine family consists of more than 50 ligands that can be classified into 4 groups based on the positioning of their initial cysteine residues: XC, CC, CXC, and CX3C chemokine ligands. Thus, the CC chemokine ligands (CCLs) have two cysteine residues adjacent to each other, whereas the CXC-chemokine subfamily (CXCLs) has two cysteine residues separated by an amino acid [10]. The CX3C chemokine group has three amino acids between two cysteine residues and the XC chemokine group has only one N-terminal cysteine residue. Of the four chemokine groups, CCLs (28 members) are the largest subfamily, followed by the CXC-chemokines (17 members), whereas the CX3C and XC chemokine classes only have 1 and 2 members, respectively. Two subgroups of CXCLs have been identified based on the presence of the glutamic acid-leucine-arginine (ELR) motif in the aminoterminal region: the ELR+ and ELR- CXC chemokines [10]. This structural classification has important functional implications. Most CC chemokines are strong mononuclear cell chemoattractants, whereas ELR+ CXC chemokines have been implicated in neutrophil recruitment [11].

From a functional perspective, many members of the chemokine family can be categorized into inflammatory or homeostatic subgroups. The homeostatic chemokines are constitutively expressed in certain tissues and may be implicated in basal leukocyte trafficking and in formation of lymphoid organs. Inflammatory chemokines, on the other hand, are markedly upregulated in injured tissues and are key mediators in inflammatory reactions, controlling leukocyte recruitment and activation [12, 13]. This classification is crude and may represent an oversimplification, as several members of the chemokine family are expressed in normal tissues and play a role in homeostasis, but may also be induced following injury regulating inflammatory cell infiltration. However, the differences between inflammatory and homeostatic chemokines have an evolutionary origin. In mammals, inflammatory chemokines evolved rapidly, presumably in response to strong selective pressures when each species faced a new pathogen [14, 15]. For this reason, the profile and functional properties of inflammatory chemokines exhibit species-specific differences. In contrast, homeostatic chemokines are relatively ancient in evolutionary terms, and their functions are well conserved between species.

In sites of injury, inducible inflammatory chemokines are bound to glycosaminoglycans on the endothelial surface and on the extracellular matrix, and are presented to circulating or trafficking leukocytes, thus interacting with the corresponding chemokine receptors on the leukocyte surface [16, 17]. Chemokine receptors are G protein-coupled and signal via pertussis toxin-sensitive Gi-type G proteins. Most receptors recognize more than one chemokine, and certain chemokines may bind to several receptors. Despite their promiscuity, chemokine receptors only bind chemokines within the same group: CCR chemokine receptors bind to CCL chemokines,

whereas CXCR receptors bind CXCL chemokines. Some studies have suggested that certain non-chemokine ligands, such as extracellular matrix degradation peptides [18], and the cytokine macrophage migration inhibitory factor (MIF) [19] can also signal through chemokine receptor binding [20–22].

The Phases of Cardiac Repair

Following myocardial infarction, severe and prolonged loss of perfusion in the myocardium subserved by the occluded vessel results in massive necrosis of cardiomyocytes. Because the adult mammalian heart has negligible regenerative capacity, repair of the infarcted myocardium is dependent on formation of a collagen-based scar. The reparative response following infarction can be divided into three distinct, but overlapping, phases: the inflammatory phase, the proliferative phase, and the maturation phase [6]. During the inflammatory phase, danger signals released from necrotic cardiomyocytes trigger both systemic and myocardial inflammatory reactions, associated with induction of cytokines and chemokines, and subsequent mobilization of abundant neutrophils, monocytes, and lymphocytes that infiltrate the infarcted myocardium. Professional phagocytes clear the infarct from dead cells and matrix debris and undergo conversion to an anti-inflammatory phenotype that sets the stage for recruitment and activation of mesenchymal reparative cells, leading to the transition to the proliferative phase of healing [23–25]. During the proliferative phase of cardiac repair, activated myofibroblasts infiltrate the infarct predominantly derived from resident fibroblast populations [26], and deposit large amounts of extracellular matrix proteins in the infarcted area. Recruitment and organization of the myocardial scar, containing aligned myofibroblasts, is critical for protection of the infarcted myocardium from catastrophic rupture and provides mechanical support attenuating chamber dilation [27]. At this stage, activation of angiogenic pathways promotes formation of neovessels, ensuring sufficient perfusion of the highly cellular and metabolically active infarct. The maturation phase follows, associated with cross-linking of the extracellular matrix and quiescence of fibroblasts that no longer exhibit myofibroblast characteristics [28], but serve a supportive role for the mature scar [29]. Tight temporal regulation, sequential activation, and spatial containment of the cellular events associated with cardiac repair are critical to protect the infarcted heart from adverse remodeling and from the development of heart failure. Although early inflammatory activation may be required for leukocyte-mediated clearance of the infarct from dead cells and debris and for stimulation of a reparative program, excessive, prolonged, or expanding inflammation may cause sustained tissue damage, promoting adverse remodeling and accentuating fibrosis, and causing dysfunction. Given

their critical role in regulating inflammation and repair, it is not surprising that several members of the chemokine family have been implicated in repair and remodeling of the infarcted heart, and in the pathogenesis of post-infarction heart failure. Most inducible chemokines are markedly upregulated during the inflammatory phase of cardiac repair and mediate recruitment and activation of leukocyte subpopulations. However, some members of the family exert important actions during the proliferative phase, modulating angiogenic and fibrogenic responses (Fig. 1).

Regulation of Chemokine Synthesis in the Infarcted Myocardium

Both CC and CXC chemokines are markedly upregulated during the inflammatory phase of infarct healing. Many different cell types, including activated monocytes, macrophages [30], and lymphocytes [31], cytokine-stimulated vascular

endothelial cells [32, 33] and fibroblasts [34–36], and ischemic, hypoxic, or stressed cardiomyocytes [37–39] have been suggested to serve as a cellular source of chemokines in the infarcted heart. In the infarcted myocardium, necrotic and stressed/injured cells, and the damaged extracellular matrix, release bioactive mediators that act as danger signals, termed danger-associated molecular patterns (DAMPs). DAMPs bind to cognate pattern recognition receptors (PRRs) of the innate immune system on surviving parenchymal cells and infiltrating leukocytes to activate chemokine transcription.

Which DAMPs Stimulate Chemokine Synthesis Following Myocardial Infarction?

Although necrotic cardiomyocytes and damaged extracellular matrix can release a broad range of DAMPs, whether specific bioactive alarmins are responsible for chemokine upregulation in the infarct remains unknown. High mobility group box-1 (HMGB1) released by dying cells has been identified as a key

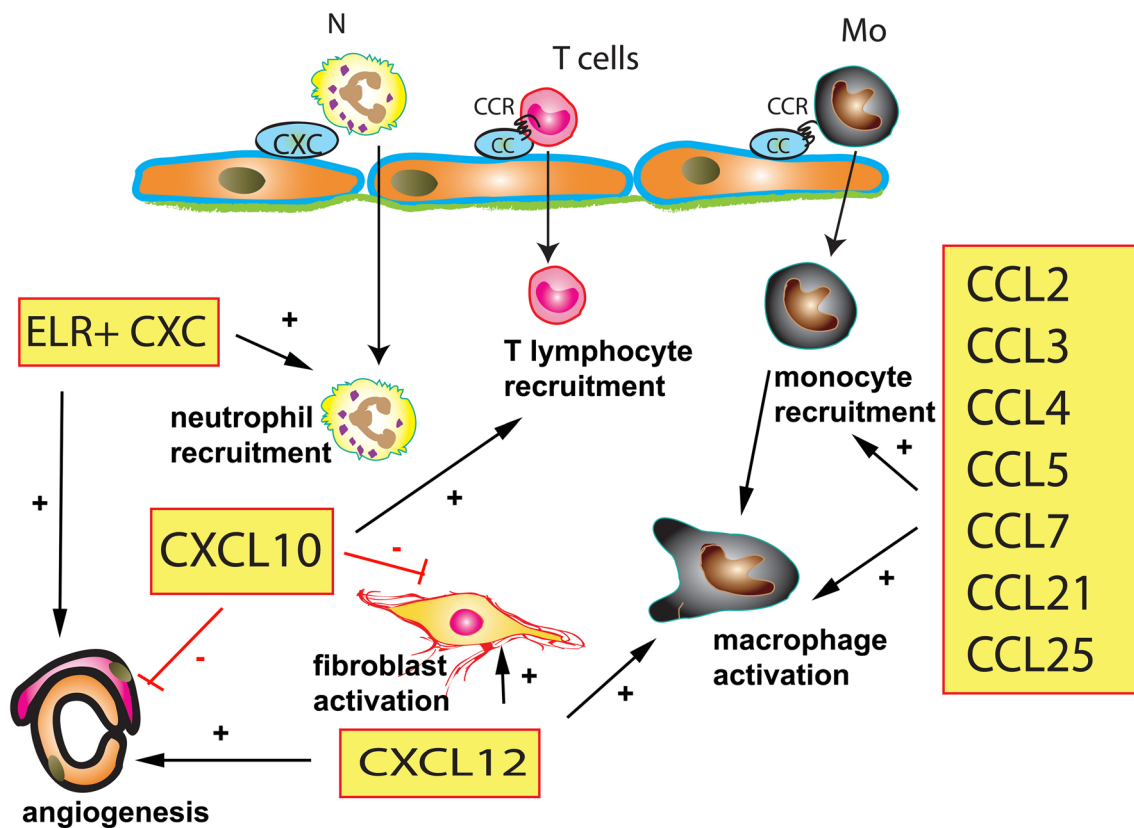


Fig. 1 The role of the chemokines in the infarcted myocardium. Induction of chemokines in the infarcted myocardium plays a critical role in leukocyte trafficking, but may also modulate phenotype and function of non-immune cells. Inflammatory CC and CXC chemokines bind to glycosaminoglycans on the endothelial surface and interact with leukocytes expressing the corresponding chemokine receptors. ELR+ CXC chemokines mediate neutrophil (N) infiltration, but may also act on the microvasculature (MV), exerting angiogenic actions. CXCL10

may act as an anti-fibrotic and angiostatic mediator. CXCL12 has been reported to exert a wide range of actions on leukocytes, cardiomyocytes, endothelial cells, and fibroblasts and may promote recruitment and differentiation of progenitor cells, stimulating angiogenesis. CC chemokines (including CCL2, CCL3, CCL4, CCL5, CCL7, CCL21, and CCL25) are involved in recruitment of mononuclear cell subpopulations and may modulate macrophage phenotype. Mo, monocyte

alarmin following myocardial infarction [40, 41], and can stimulate chemokine synthesis by endothelial cells [42] and fibroblasts [43] through activation of RAGE (receptor for advanced glycation end products). Necrotic cardiomyocytes also release large amounts of interleukin (IL)-1 α [44], a key early damage signal that may stimulate chemokine synthesis in macrophages, vascular cells, and fibroblasts through MyD88-dependent signaling. RNA released by necrotic or injured cells also serves as an important pro-inflammatory stimulus in the infarcted heart [45], and may activate chemokine transcription. Heat shock proteins released by injured cardiomyocytes may also stimulate chemokine upregulation, contributing to activation of the post-infarction inflammatory response [46, 47] (Fig. 2).

Activation of Toll-like Receptor (TLR)-Mediated Pathways

DAMP-mediated chemokine induction in the infarcted heart involves activation of TLRs, the major PRRs on myocardial cells [48]. Following MI, TLRs expressed on leukocytes or

parenchymal cells recognize DAMPs released by necrotic cells, triggering downstream NF- κ B and MAPK pathways that stimulate chemokine induction. Experimental studies have suggested important roles for TLR2, TLR3, TLR4, and TLR7 in activation of the post-infarction inflammatory response. TLR4 signaling increased leukocyte infiltration in the infarcted myocardium [49–51], accentuating chemokine synthesis and release [52]. TLR4 activation in leukocytes has been consistently reported in patients with myocardial infarction and was associated with enhanced inflammatory activity [53, 54]. Leukocyte TLR2 has also been implicated in post-infarction inflammation [55], and may act, at least in part, through stimulation of chemokine synthesis [56]. TLR3 may also be involved in mediating chemokine-induced inflammation following myocardial infarction [45, 57]. Leukocyte TLR7 was also found to enhance post-infarction inflammation, promoting cardiac rupture following infarction [58], through actions that may involve increased chemokine expression [59]. It should be emphasized that the *in vivo* actions of TLRs in the infarcted heart extend beyond induction of chemokine synthesis and may also involve modulation of

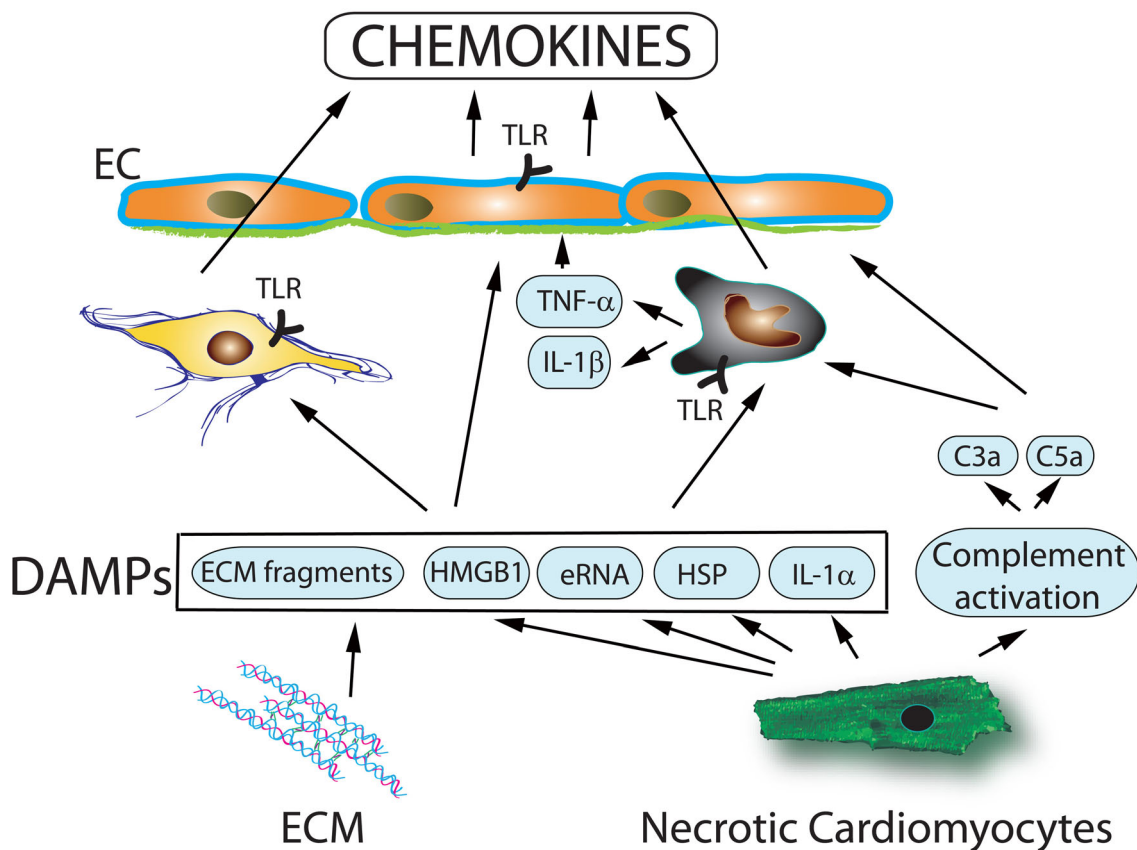


Fig. 2 Mechanisms of chemokine induction in the infarcted heart. Following myocardial infarction, dying cardiomyocytes release damage-associated molecular patterns (DAMPs) including high mobility group box-1 (HMGB1), heat shock proteins (HSP), extracellular RNA (eRNA), and interleukin (IL)-1 α . DAMPs induce chemokine expression by endothelial cells (EC), macrophages, and fibroblasts through

activation of innate immune pathways. Moreover, activation of the complement cascade, extracellular matrix (ECM) fragments generated through protease actions, and newly synthesized cytokines (such as TNF- α and IL-1 β) also stimulate chemokine synthesis in the infarcted heart, promoting leukocyte infiltration. TLR, Toll-like receptor

cardiomyocyte survival [60] and effects on fibroblast phenotype and activity [61, 62].

DAMP-mediated TLR signaling triggers chemokine synthesis in the myocardium by activating the nuclear factor (NF)- κ B system in resident myocardial cells and in hematopoietic cells. NF- κ B activation in myocardial cells following infarction may involve an MyD88/IRAK-1 pathway [63] that ultimately leads to nuclear translocation of NF- κ B and subsequent transcription of a large portfolio of genes including inflammatory cytokines, CXC and CC chemokines, and adhesion molecules. NF- κ B activation is well documented following myocardial infarction in both experimental animals and human patients [64–66], and has been demonstrated to mediate upregulation of both CXC [65] and CC chemokines [67–70].

The role of the Complement Cascade in Stimulating Chemokine Synthesis in the Infarcted Heart

The complement system is an important component of the innate immune response following myocardium infarction. Necrotic myocardial cells release subcellular membrane constituents rich in mitochondria, which are capable of triggering the early acting components (C1, C4, C2, and C3) of the complement cascade [71]. Ischemic myocardial injury rapidly activates C3 cleavage leukotactic products in the infarcted myocardium [72]. In vitro studies have suggested that the pro-inflammatory actions of complement components (such as C5a) may be mediated at least in part through chemokine upregulation [73]. The role of the complement cascade in activating the chemokine response following myocardial infarction is supported by some limited in vivo evidence. C6-deficient rabbits exhibited reduced neutrophil infiltration following infarction, associated with attenuated myocardial CXCL8/interleukin (IL)-8 expression [74].

Cytokine-Induced Chemokine Upregulation in the Infarcted Myocardium

A large body of evidence suggests that induction of chemokines in the infarcted myocardium may be amplified by effects of pro-inflammatory cytokines, such as tumor necrosis factor (TNF)- α and interleukin (IL)-1 β . TNF- α -deficient mice exhibit lower expression of chemokines and adhesion molecules after reperfused infarction [75]. Mice lacking the type I IL-1R (the only signaling receptor for IL-1) exhibit decreased chemokine expression associated with attenuated neutrophil and macrophage infiltration in the infarcted myocardium [76, 77]. In addition to the chemokine-inducing effects of pro-inflammatory cytokines, mast cell-derived pro-inflammatory mediators, such as histamine and tryptase, are also released in the infarcted myocardium [78] and can induce endothelial chemokine synthesis and secretion [79, 80].

The role of the Chemokines in myocardial Injury, Repair, and Remodeling

In the infarcted heart, the chemokine system orchestrates leukocyte migration [7, 8] by forming chemotactic gradients, which are localized to the area of injury. Gradient formation is dependent on binding of chemokines to glycosaminoglycans located on the endothelial surface and on the extracellular matrix. Endothelial chemokines interact with rolling leukocytes that express the corresponding chemokine receptors. Chemokine signaling promotes leukocyte integrin activation, triggering adhesive interactions between leukocytes and endothelial cells that ultimately lead to extravasation of the inflammatory cells in the infarct border zone [81, 82]. In extravasated leukocytes, chemokine:chemokine receptor interactions induce directed cell migration to the site of injury through activation of phosphoinositide-specific phospholipase C (PLC) and phosphoinositide 3-kinase (PI3K) pathways [83–85]. In addition to their effects on immune cells, some members of the chemokine family have been suggested to modulate behavior of other cell types involved in cardiac repair and remodeling, including vascular cells, fibroblasts, and cardiomyocytes [33, 86–88].

CXC Chemokines

ELR+ CXC Chemokines

ELR+ CXC chemokines not only are critically involved in chemotactic recruitment of neutrophils, but also exhibit angiogenic properties [89]. Several members of the ELR+ CXC subfamily are upregulated in the infarcted myocardium and have been suggested to play a role in neutrophil infiltration, regulation of cardiomyocyte injury, and angiogenesis. The prototypic ELR+ CXC chemokine CXCL8/IL-8 is markedly upregulated in infarcted myocardial segments in experimental animal models of myocardial infarction, and its expression is accentuated by reperfusion [90, 91]. Although as a potent neutrophil chemoattractant IL-8 would be expected to play an important role in recruitment of neutrophils in infarcted segments [92], robust experimental data documenting specific cellular actions of IL-8 in vivo are lacking. The absence of an IL-8 homolog in rodents precludes study of its role in myocardial infarction using mouse models. In a canine model, recombinant IL-8 markedly increased adhesion of neutrophils to isolated cardiomyocytes [90]. In contrast, an in vivo study in a rabbit model of reperfused myocardial infarction showed that administration of a neutralizing anti-IL-8 antibody prior to reperfusion reduced infarct size without affecting neutrophil infiltration [93]. Another study in mice suggested that effects on both leukocytes and cardiomyocytes may mediate the actions of ELR+ CXC chemokines in the infarcted heart. Loss of CXCR2, the main receptor for the ELR+ CXCLs, markedly

reduced inflammatory leukocyte recruitment in murine infarcts *in vivo* [87]; however, experiments in a Langendorff system suggested that, in the absence of circulating leukocytes, CXCR2 may protect ischemic cardiomyocytes [87]. In addition to their potential role in acute injury following myocardial infarction, IL-8 and other CXCR2 ligands may also modulate repair by exerting angiogenic actions. In a mouse model of myocardial infarction, CXCR2 blockade attenuated infarct angiogenesis [94]. Moreover, in a rabbit model, lentiviral IL-8 overexpression significantly enhanced neovessel formation in the infarcted heart [95].

A potential role of IL-8 in accentuating myocardial injury following infarction is also supported by clinical investigations. In patients with acute STEMI undergoing percutaneous coronary intervention (PCI), higher plasma IL-8 levels were associated with larger infarcts and adverse outcome [96].

ELR-Negative CXC Chemokines

In contrast to ELR-containing CXC chemokines, CXC chemokines lacking the ELR motif fail to attract granulocytes, but have been implicated in lymphocyte chemotaxis [97–99], and may exert pronounced effects on vascular cells and fibroblasts, exhibiting angiostatic and anti-fibrotic properties [100–102]. The ELR-negative CXC chemokine CXCL10/interferon- γ -inducible protein (IP)-10 is markedly upregulated in both canine and mouse myocardial infarcts [33, 103], and is predominantly localized in microvascular endothelial cells [33]. Experiments using global knockout mice suggested that endogenous CXCL10 protects the infarcted heart from excessive fibrotic remodeling, limiting infiltration of the infarct with activated myofibroblasts [86]. The anti-fibrotic effects of CXCL10 are mediated, at least in part, through inhibition of growth factor-induced fibroblast migration [86]. CXCL10-mediated inhibition of fibrosis was not mediated through CXCR3, the main functional receptor of the chemokine [104], but involved interactions with proteoglycans [105].

Stromal cell-derived factor (SDF)-1/CXCL12 is a non-ELR containing CXC chemokine with a critical role in cardiovascular development [106] and angiogenesis [107, 108]. CXCL12 induction is noted in healing infarcts [109–115] and has been suggested to exert a wide range of actions on vascular cells, cardiomyocytes, and immune cells. Extensive evidence suggested that CXCL12 accentuates infarct angiogenesis through recruitment of endothelial progenitor cells, or via direct stimulation of angiogenesis pathways [116–127]. Effects of CXCL12 on cardiomyocytes are controversial. Several studies have suggested protective actions of CXCL12 on cardiomyocyte survival, mediated through activation of anti-apoptotic pathways [122, 125, 128]. In contrast, other studies have suggested that high concentrations of CXCL12 may trigger apoptosis through a TNF- α -mediated

pathway [88]. CXCL12-induced activation of inflammatory cells may also accentuate injury following infarction [129].

Experiments using pharmacologic inhibition of CXCL12 have also produced contradictory results (Table 1). Continuous inhibition of CXCR4, the main receptor for CXCL12, resulted in scar expansion and exacerbated cardiac systolic and diastolic dysfunction after myocardial infarction [130]. In contrast, other studies suggested beneficial effects of CXCR4 inhibition in rat and mouse models of myocardial infarction [131, 132]. The conflicting observations likely reflect the context and dose-dependent, multifunctional, and pleiotropic actions of CXCL12/CXCR4 signaling, and the complexity of the cardiac reparative process. Therapeutic manipulation of the CXCL12/CXCR4 axis following infarction requires careful consideration of the timing and spatial localization of the intervention, the specific cellular targets affected, and the local concentration of the chemokine. An additional layer of complexity may be contributed by effects of CXCL12 mediated through the CXCR7 receptor. CXCL12/CXCR7 signaling has been suggested to protect the infarcted heart from adverse remodeling, presumably through effects on the microvasculature [133].

Because of its prominent role in progenitor cell homing and differentiation [110], CXCL12 may hold promise in the ongoing quest for cardiac regenerative strategies. Although in adult infarcted hearts, CXCL12 overexpression does not induce cardiomyocyte proliferation [117], a recent study suggested that the unique ability of the neonatal mammalian heart to regenerate may involve CXCL12 actions. In neonatal myocardial injury, cardiac regeneration required CXCL12/CXCR4-dependent arterial reassembly, mediated through migration of arterial endothelial cells that formed collateral neovessels [134].

The Proinflammatory Actions of the CC Chemokines

Members of the CC chemokine subfamily are potent mononuclear cell chemoattractants and have been implicated in chemotactic recruitment of proinflammatory monocytes in the infarcted region [135]. CCL2/Monocyte chemoattractant protein (MCP)-1, the best-studied CC chemokine in myocardial pathology, is rapidly upregulated in the infarcted myocardium and is predominantly expressed by endothelial cells and infiltrating leukocytes [30, 32, 103, 136, 137]. Over the last 15 years, experimental studies in animal models have revealed a critical role for CCL2 in recruitment, activation, and differentiation of monocytes and macrophages in the infarcted heart (Fig. 3). These actions were found to have major implications in cardiac injury, repair, and remodeling.

The adult heart contains a significant population of resident macrophages [138]. Based on their expression of the CCL2 receptor CCR2, resident myocardial macrophages can be divided into CCR2⁻ and CCR2⁺ subsets derived from embryonic and adult hematopoietic lineages, respectively

Table 1 Studies examining the role of the CXCL12/CXCR4 axis in myocardial infarction (MI)

MI model	Species	Experimental tool	Major findings	Ref.
Non-reperfused MI	Mouse	Conditional cardiomyocyte-specific CXCR4 $-/-$ mouse models	Cardiomyocyte-specific CXCR4 loss did not affect infarct size, collagen content, and cardiac function following MI	[177]
Reperfused MI	Rats	Adenoviral CXCR4 overexpression	CXCR4 overexpression accentuated infarct size and worsened cardiac dysfunction following MI. These effects were associated with increased influx of inflammatory cells and enhanced cardiomyocyte apoptosis	[129]
Non-reperfused MI	Mouse	Cxcr4 $+/-$ mice	CXCR4 $+/-$ mice had smaller infarcts, associated with decreased neutrophil content, but also exhibited impaired angiogenesis following MI	[178]
Non-reperfused MI	Rat and mouse	Cardiomyocyte-specific CXCL12-overexpressing transgenic (Tg) rats and CXCL12 conditional knockout (cKO) mice	Cardiomyocyte-specific CXCL12 KO mice had preserved cardiac function, reduced remodeling, and attenuated fibrosis following MI CXCL12 overexpressing rats had impaired cardiac function post-MI, accompanied by enhanced fibrosis	[37]
Non-reperfused MI	Rats	Transplantation of CXCL12-expressing cardiac fibroblasts into the peri-infarct zone	Transplantation of CXCL12-expressing fibroblasts improved left ventricular function and increased left ventricular mass post-MI	[110]
Non-reperfused MI	Mouse	Injection of CXCL12 into the center of the infarct	CXCL12 treatment reduced scar size and improved cardiac function by promoting angiogenesis	[118]
Non-reperfused MI	Rat	Tail vein infusion of syngeneic CXCL12-overexpressing mesenchymal stem cells	Cell therapy with CXCL12-overexpressing MSCs increased cardiac myocyte survival, vascular density, and cardiac myosin-positive area within the infarct zone. There was no evidence of cardiac regeneration	[117]
Non-reperfused MI	Rat	Transplantation of CXCL12-expressing syngeneic skeletal myoblasts	Cell therapy with CXCL12-expressing myoblasts promoted stem and progenitor cell migration, activated cell survival signaling, and enhanced angiogenesis in the infarcted heart	[121]
Reperfused MI	Mouse	CXCL12 treatment prior to coronary ischemia Administration of the CXCR4 antagonist AMD3100	Pretreatment with CXCL12 decreased infarct size by inhibiting apoptosis in cardiomyocytes. CXCL12-induced attenuation of infarct size was blocked by CXCR4 inhibition	[128]
Non-reperfused MI	Rat	Administration of the CXCR4 antagonist AMD3100	CXCR4 blockade reduced infarct size, improved systolic function, and partially suppressed the increased expression of atrial natriuretic peptide mRNA in the non-infarcted left ventricle	[131]
Non-reperfused MI	Mouse	Intracardiac CXCL12 administration	CXCL12 treatment attenuated dysfunction and decreased cardiac dilation after MI, promoting survival of cardiomyocytes, increasing infarct angiogenesis. These effects were attributed to enhanced Akt activation and accentuated VEGF expression	[116]
Non-reperfused MI	Mouse	Chronic administration of the CXCR4 antagonist AMD3100	CXCR4 blockade increased scar size and exacerbated cardiac systolic and diastolic dysfunction	[130]
Non-reperfused MI	Mouse	Acute or chronic administration of the CXCR4 antagonist AMD3100	Single-dose AMD3100 injection administered after the onset of myocardial infarction increased circulating endothelial progenitor cell (EPC) counts and myocardial vascularity, reduced fibrosis, and improved cardiac function and survival in mice. In contrast, continuous infusion of AMD3100 over a 2-week period worsened outcome following MI by blocking EPC incorporation	[132]
Non-reperfused MI	Rats	Sustained release of a CXCL12 analog from injectable hydrogels	Sustained release of CXCL12 analog enhanced endothelial progenitor cell chemotaxis, improved vascularity, ventricular geometry, ejection fraction, cardiac output, and contractility post-MI	[119]
Non-reperfused MI	Sheep	Injection of a CXCL12 analog in the infarct border zone	Treatment with the CXCL12 analog enhanced endothelial progenitor cell chemotaxis, increased capillary and arteriolar density, reduced infarct size, and attenuated dysfunction post-MI	[120]
Non-reperfused MI	Rat	Intracardiac administration of recombinant CXCL12, or infusion of anti-CXCL12 antibody	CXCL12 administration reduced cell apoptosis, increased vessel density, and improved cardiac function. Treatment with the anti-CXCL12 antibody had the opposite effects	[127]
Non-reperfused MI	Mouse	Intramyocardial injection of CXCL12	CXCL12 injection improved ventricular function, and increased border zone vessel density post-MI	[126]
Non-reperfused MI	Mouse	CXCL12-Annexin V fusion protein to localize CXCL12 in the area of necrosis	CXCL12-Annexin V treatment attenuated cell apoptosis, enhanced angiogenesis, reduced infarcted size, and improved cardiac function post-MI	[125]

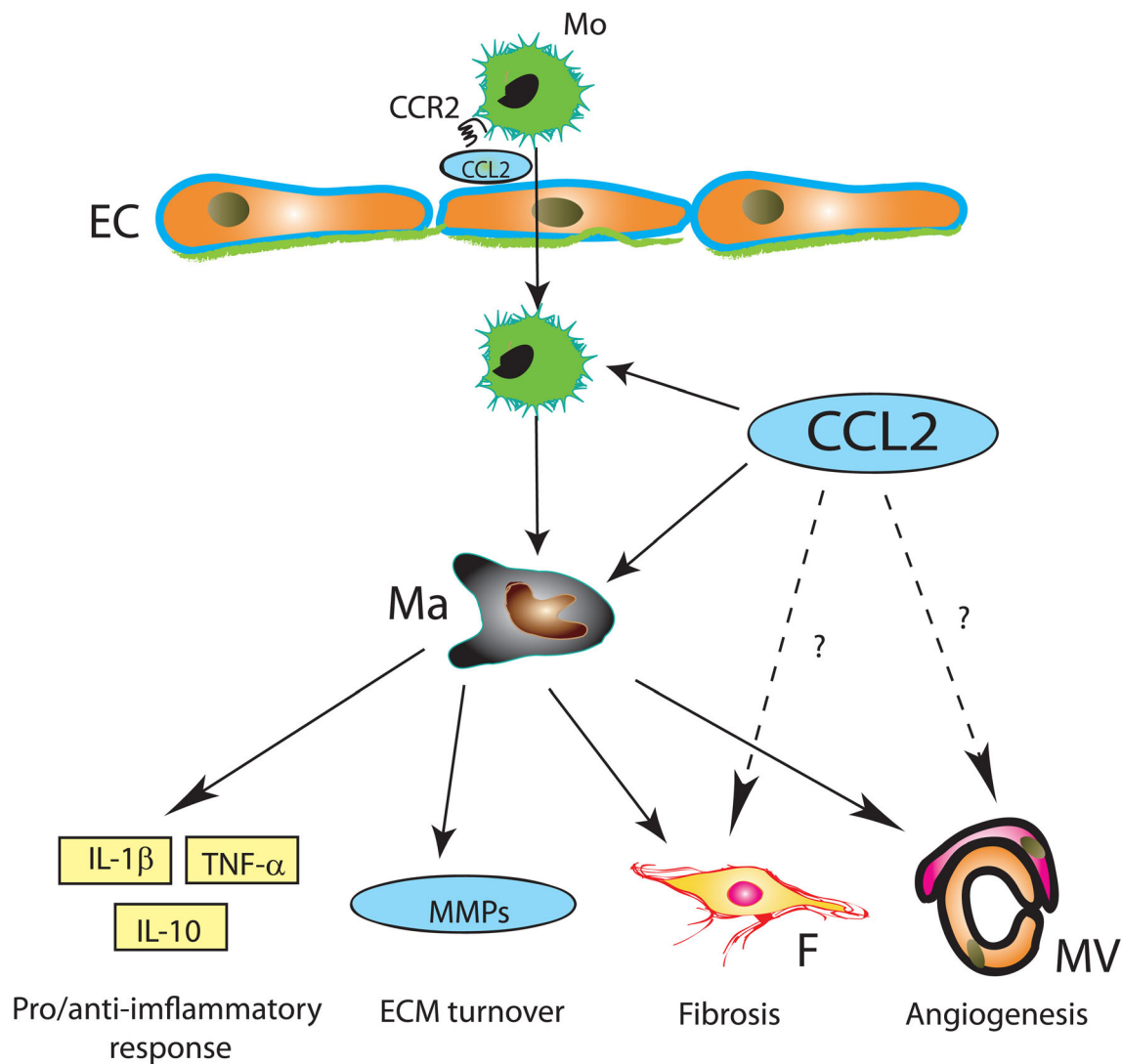


Fig. 3 Role of CCL2 in the infarcted myocardium. CCL2 plays a crucial role in recruitment of proinflammatory CCR2+ monocytes (Mo), but may also modulate macrophage (Ma) phenotype, promoting expression of cytokines and matrix metalloproteinases (MMPs). In vivo, CCL2 has been implicated in myofibroblast activation and in angiogenesis;

however, whether these actions are due to direct effects of the chemokine on fibroblasts (F) and vascular cells (MV, microvessels), or simply reflect alterations in the profile of infiltrating macrophages, remains unknown. EC, endothelial cell

[139–142]. Cardiomyocyte death triggers alarmin-mediated activation of resident CCR2+ macrophages, stimulating MyD88-dependent chemokine synthesis [143] and subsequent recruitment of inflammatory leukocytes. Fate mapping and flow cytometric studies revealed that the marked expansion of the macrophage population in the infarcted myocardium is predominantly driven by recruitment of circulating monocytes [144]. During the proliferative phase of cardiac repair, proliferation of mature macrophages serves to maintain the infarct macrophage population [144, 145]. In the remodeling of non-infarcted myocardium, chronic expansion of macrophage populations is noted, derived both from increased local macrophage proliferation and through recruitment of monocytes [146].

The critical role of CCL2 in recruitment of monocytes and expansion of macrophages following myocardial infarction is supported both by antibody inhibition and by genetic loss-of-function experiments (Table 2) [135, 147–150]. Disruption of the CCL2/CCR2 axis in experimental models of myocardial infarction was reported to reduce infarct size in many [149–152], but not in all, studies [135]. Moreover, CCL2/CCR2 inhibition was associated with attenuated adverse remodeling following myocardial infarction [135, 153]. Importantly, in addition to its protective actions against dilative post-infarction remodeling, complete global loss of CCL2 also delayed replacement of dead cardiomyocytes with granulation tissue, suggesting impaired phagocytic removal of dead cells, and/or perturbation of the reparative response

Table 2 Selected studies examining the role of CC chemokines in experimental myocardial infarction (MI)

Chemokine/ chemokine receptor pair	MI model	Species	Chemokine-related model	Major findings	Ref.
CCL2/CCR2	Non-reperfusion MI	Mouse	CCR2 ^{-/-} mice	CCR2 loss impaired infiltration of macrophages in infarcted tissue, reduced infarct size and collagen deposition, and ameliorated post-MI remodeling	[153]
	Reperfusion MI	Mouse	CCL2 ^{-/-} mice, anti-CCL2 antibody	CCL2 ^{-/-} mice exhibited decreased and delayed macrophage infiltration in the healing infarct and delayed replacement of injured cardiomyocytes with granulation tissue; decreased mRNA expression of the cytokines TNF- α , IL-1 β , TGF- β 2, TGF- β 3, and IL-10; diminished myofibroblast accumulation, attenuated left ventricular remodeling, but similar infarct size when compared with wild-type animals. Infarct angiogenesis was comparable between CCL2 ^{-/-} and wild-type animals. CCL2 antibody inhibition resulted in defects comparable with the pathological findings noted in infarcted CCL2 ^{-/-} animals without an effect on macrophage recruitment, suggesting that CCL2 may modulate macrophage phenotype or may alter the profile of recruited cells	[135]
	Reperfusion MI	Mouse	CCR2 ^{-/-} mice	CCR2 loss reduced macrophage infiltration and decreased infarct size	[179]
	Non-reperfusion MI	Mouse	CCR2 antagonist and CCR2 ^{-/-} mice	CCR2 disruption decreased monocyte/macrophage and neutrophil recruitment	[149]
	Reperfusion MI	Rat	Intravenous injection of anti-CCL2 antibody	CCL2 blockade reduced infarct size and decreased intercellular adhesion molecule (ICAM)-1 mRNA expression and infiltration of macrophages	[136]
	Non-reperfusion MI	Mouse	Anti-CCL2 gene therapy	Anti-CCL2 therapy reduced post-MI mortality and attenuated dilative remodeling and contractile dysfunction, reducing interstitial fibrosis, recruitment of macrophages, and myocardial cytokine gene expression	[180]
	Reperfusion MI	Mouse	Cardiac-specific CCL2 overexpression	Transgenic overexpression of CCL2 attenuated post-MI dysfunction	[181]
	Reperfusion MI	Mouse	Administration of a non-agonist (competitive) CCL2 mutant	CCL2 inhibition reduced infarct size, decreased monocyte infiltration, and attenuated fibrosis post-MI	[147]
	Reperfusion MI	Mouse	CCR2-siRNA knockdown in Ly-6C ^{high} monocytes	CCR2 inhibition reduced infarct size and attenuated infiltration of the infarct with monocytes and macrophages	[151]
	Reperfusion MI	Mouse	Anti-CCL2	Reduced the infarct size and lessened myocardial inflammation	[148]
	Non-reperfusion MI	Mouse	CCR2 siRNA	Decreased early infiltration of pro-inflammatory monocytes and apoptotic cardiomyocytes in the infarcted heart; promoted angiogenesis and reduced infarcted size	[152]
	Non-reperfusion MI	Mouse	CCR2 antagonist	CCR2 inhibition reduced infarct size, decreasing recruitment of Ly6C ^{high} inflammatory cells	[150]
	CCL7/CCRs	Non-reperfusion MI	Rat	Transplantation of CCL7 (MCP-3)-expressing cardiac fibroblasts into the infarct border zone	Transplanted CCL7-expressing cells enhanced homing of injected mesenchymal stem cells in the infarcted myocardium, reduced cardiac dilation, and improved cardiac function
Non-reperfusion MI		Mouse	B cell-selective CCL7 defi- ciency	Loss of CCL7 in B cells reduced monocyte mobilization, limited myocardial injury, and improved heart function post-MI	[31]
CCL5/CCRs	Non-reperfusion MI	Mouse	Rat anti-mouse CCL5/ RANTES mAb	Anti-CCL5 reduced infarct size, reduced infiltration with neutrophils and macrophages, and attenuated systolic dysfunction	[160]
CCLs/CCRs	Non-reperfusion MI	Mouse	Treatment with the CC chemokine binding protein evasin-4	The CC chemokine inhibitor reduced macrophage and neutrophil recruitment and superoxide production in the infarcted heart, reduced infarct size, and improved cardiac function and survival	[164]
CCL21/CCR7	Non-reperfusion MI	Mouse	Anti-CCL21 monoclonal antibody	Anti-CCL21 diminished neutrophil and macrophage recruitment in the infarct; and ameliorated cardiac dilation and dysfunction post-MI	[162]
CCLs/CCR1	Non-reperfusion MI	Mouse	CCR1 ^{-/-} mice	CCR1 loss reduced early recruitment of neutrophils, but also accelerated monocyte/lymphocyte infiltration and improved infarct healing	[165]
CCLs/CCR5	Reperfusion MI	Mouse	CCR5 ^{-/-} mice	CCR5 loss markedly increased proinflammatory cytokine and chemokine levels in the infarct associated, perturbing	[167]

Table 2 (continued)

Chemokine/ chemokine receptor pair	MI model	Species	Chemokine-related model	Major findings	Ref.
	Non-reperfusion MI	Mouse	CCR5 $-/-$ mice	recruitment of CD4 ⁺ /foxp3 ⁺ regulatory T cells and anti-inflammatory monocytes; impaired repression of post-MI inflammation was associated with worse cardiac dilation	[168]
	Reperfusion MI	Rat	Anti-CCR5 antibody and CCR5 agonist	CCR5 inhibition diminished inflammatory response and infarct size, while CCR5 agonist accentuated cardiac injury	[182]
CCL2/CCR9	Non-reperfusion MI	Mouse	CCR9 $-/-$ mice	CCR9 loss attenuated inflammation, apoptosis, and structural and electrical remodeling through suppression of NF- κ B and MAPK signaling. CCR9 loss also improved survival rate and attenuated dysfunction, decreasing infarct size	[161]

[135]. CCL2 actions in cardiac repair and remodeling may involve several cellular mechanisms. First, CCL2 may be crucial for recruitment of specific subsets of proinflammatory and phagocytic monocytes to the infarct area [135, 154]. Second, CCL2 may modulate macrophage phenotype. In vitro studies have suggested diverse and often contradictory effects of CCL2 on monocyte and macrophage cytokine expression profiles. CCL2 induced IL-1 [155] and IL-6 synthesis [156] in monocytes, but was also found to suppress M1-associated cytokine synthesis by macrophages, while promoting IL-10 expression [157]. Third, at least some of the effects of CCL2 may involve actions on fibroblasts, cardiomyocytes, or vascular endothelial cells. Although in vitro studies have demonstrated effects of CCL2 on interstitial and vascular cells, the in vivo significance of these actions remains poorly documented. In vivo, CCL2 loss markedly reduced myofibroblast density in the infarct [135]; however, this effect may reflect attenuated activation and recruitment of fibrogenic macrophages, rather than loss of direct effects of CCL2 on cardiac fibroblasts. In vitro, CCL2 stimulation did not affect expression of fibrosis-associated genes by isolated mouse cardiac fibroblasts [158].

Evidence supporting the role of other CC chemokines in repair and remodeling of the infarcted heart is more limited. In experimental models, CCL3, CCL4, CCL5, CCL7, CCL21, and CCL25 were found to be significantly upregulated in infarcted myocardium [31, 103, 159–162]. Moreover, small clinical studies have demonstrated increased circulating levels of CC chemokines in patients with myocardial infarction [163]. CCL5 neutralization significantly reduced infarct size and attenuated systolic dysfunction in a mouse model of non-reperfusion infarction [160, 164]; considering the negligible amounts of salvageable myocardium in permanent coronary occlusion models (due to the complete and permanent absence of perfusion), the mechanism of protection remains enigmatic. Deletion of CCR1, a receptor binding to CCL3, CCL5, CCL7, and CCL23, loss of CCR9, the receptor for CCL25, and

CCL21 inhibition were also reported to reduce the size of the infarct, decrease inflammation, and attenuate dysfunction following myocardial infarction [161, 162, 165].

Do CC Chemokines Mediate Suppression of Inflammation by Recruiting Anti-inflammatory Leukocytes?

CCR5 acts as a receptor for several CC chemokines, including CCL3, CCL4, and CCL5 [166]. Surprisingly, in a mouse model of myocardial infarction, CCR5 loss was associated with accentuated adverse remodeling and increased inflammatory activity [167, 168]. Adverse outcome in the absence of CCR5 was attributed to impaired recruitment of anti-inflammatory monocytes and regulatory T cells (Tregs) [167]. These findings suggest that certain chemokine-chemokine receptor interactions may attenuate inflammation by promoting recruitment of leukocyte subsets with anti-inflammatory properties.

The Role of CX3CL1/Fractalkine

Fractalkine/CX3CL1, the only member of the CX3C chemokine subfamily, is expressed by NK cells, monocytes, and T cells and has unique functions, both as a leukocyte chemoattractant and as an adhesion molecule. Increased myocardial CX3CL1 expression has been reported in infarcted and remodeling hearts [169, 170]. Moreover, in human patients with myocardial infarction, circulating CX3CL1 levels rapidly increase after reperfusion [171], and may independently predict major adverse cardiac events [172]. CX3CL1 neutralization delayed the progression of left ventricular enlargement following myocardial infarction [169, 173]. CX3CL1-mediated post-infarction remodeling has been attributed to accentuation of fibroblast proliferation [173], to enhanced MMP expression, to injurious effects on cardiomyocytes, to accentuated endothelial adhesion molecule expression [169], and to increased leukocyte recruitment [174].

Chemokines as Therapeutic Targets Following Myocardial Infarction

Considering their marked induction in the infarcted myocardium and their proposed role in mediating inflammatory injury, proinflammatory chemokines, such as CCL2, are attractive therapeutic targets for patients with myocardial infarction. It should be emphasized that some chemokine-driven inflammation and macrophage activation is needed for clearance of the infarct from dead cells and for activation of a reparative program [135]. However, the chemokine response needs to be tightly controlled. Prolonged, overactive, and spatially unrestrained chemokine signaling following infarction may result in accentuated inflammation, promoting adverse remodeling. Therapeutic implementation of chemokine targeting approaches will require identification of patient subpopulations with overactive chemokine responses following infarction. These patients may require chemokine inhibition to protect the myocardium from adverse remodeling [175].

Chemokine-based therapeutics may also hold promise in optimization of cardiac repair. CXCL12 administration may promote recruitment of reparative cells, increasing infarct angiogenesis, attenuating dysfunction, and improving left ventricular mechanics [116, 119, 120, 128]. Experimental studies suggest that pro-survival effects of CXCL12 on ischemic cardiomyocytes may also contribute significant therapeutic benefit [116]. Despite these promising findings, clinical translation is challenging. CXCL12 is also known to exert proinflammatory actions [131, 132] that may have injurious consequences, accentuating or prolonging inflammatory cascades. Identification of the optimal temporal window for spatially restricted administration of CXCL12 may be important in order to design effective therapy. Clinical evidence on the effects of CXCL12 therapy in human patients with myocardial infarction is lacking. However, in a phase II clinical trial in patients with ischemic heart failure, CXCL12 gene therapy was safe but did not meet the primary endpoint for functional improvement [176].

Conclusions

Over the last 25 years, we have identified members of the chemokine family as key mediators in cardiac injury, repair, and remodeling. Experimental studies have suggested that certain chemokines may represent attractive therapeutic targets for patients with myocardial infarction. Unfortunately, the biological complexity of the chemokine system, the challenges in identification of reparative and detrimental cellular function of each chemokine, and the remarkable pathophysiologic heterogeneity of post-infarction cardiac remodeling in human patients pose major challenges for clinical translation. Development of successful therapeutic approaches targeting

the chemokines will require not only understanding of the cell specific actions of chemokines in the infarcted heart and the underlying mechanisms, but also development of strategies for pathophysiologic stratification of myocardial infarction patients, in order to identify subjects with overactive myocardial inflammation that may be likely to benefit from targeted interventions inhibiting proinflammatory chemokines.

Funding Information Dr Frangogiannis' laboratory is supported by NIH R01 grants HL76246, HL85440, and HL149407, and by Department of Defense grants PR151029 and PR181464. Dr Chen is supported by an American Heart Association post-doctoral award.

Compliance with Ethical Standards

Conflict of Interest The authors declare that they have no conflict of interest.

Ethical Approval This article does not contain any studies with human participants or animals performed by any of the authors.

References

1. Roth, G. A., Huffman, M. D., Moran, A. E., Feigin, V., Mensah, G. A., Naghavi, M., et al. (2015). Global and regional patterns in cardiovascular mortality from 1990 to 2013. *Circulation*, *132*(17), 1667–1678. <https://doi.org/10.1161/CIRCULATIONAHA.114.008720>.
2. Reimer, K. A., Lowe, J. E., Rasmussen, M. M., & Jennings, R. B. (1977). The wavefront phenomenon of ischemic cell death. 1. Myocardial infarct size vs duration of coronary occlusion in dogs. *Circulation*, *56*(5), 786–794.
3. Hjalmarson, A., Elmfeldt, D., Herlitz, J., Holmberg, S., Malek, I., Nyberg, G., et al. (1981). Effect on mortality of metoprolol in acute myocardial infarction. A double-blind randomised trial. *Lancet*, *2*(8251), 823–827. [https://doi.org/10.1016/s0140-6736\(81\)91101-6](https://doi.org/10.1016/s0140-6736(81)91101-6).
4. Pfeffer, M. A., Braunwald, E., Moye, L. A., Basta, L., Brown Jr., E. J., Cuddy, T. E., et al. (1992). Effect of captopril on mortality and morbidity in patients with left ventricular dysfunction after myocardial infarction. Results of the survival and ventricular enlargement trial. *The SAVE Investigators. N Engl J Med*, *327*(10), 669–677.
5. Effectiveness of intravenous thrombolytic treatment in acute myocardial infarction. Gruppo Italiano per lo Studio della Streptochinasi nell'Infarto Miocardico (GISSI) (1986). *Lancet*, *1*(8478), 397–402.
6. Frangogiannis, N. G. (2014). The inflammatory response in myocardial injury, repair, and remodelling. *Nature Reviews. Cardiology*, *11*(5), 255–265. <https://doi.org/10.1038/ncardio.2014.28>.
7. Cavallera, M., & Frangogiannis, N. G. (2014). Targeting the chemokines in cardiac repair. *Current Pharmaceutical Design*, *20*(12), 1971–1979. <https://doi.org/10.2174/13816128113199990449>.
8. Frangogiannis, N. G. (2007). Chemokines in ischemia and reperfusion. *Thrombosis and Haemostasis*, *97*(5), 738–747.
9. Sokol, C. L., & Luster, A. D. (2015). The chemokine system in innate immunity. *Cold Spring Harbor Perspectives in Biology*, *7*(5). <https://doi.org/10.1101/cshperspect.a016303>.

10. Kufareva, I., Salanga, C. L., & Handel, T. M. (2015). Chemokine and chemokine receptor structure and interactions: implications for therapeutic strategies. *Immunology and Cell Biology*, *93*(4), 372–383. <https://doi.org/10.1038/icb.2015.15>.
11. Ahuja, S. K., & Murphy, P. M. (1996). The CXC chemokines growth-regulated oncogene (GRO) alpha, GRObeta, GROgamma, neutrophil-activating peptide-2, and epithelial cell-derived neutrophil-activating peptide-78 are potent agonists for the type B, but not the type A, human interleukin-8 receptor. *The Journal of Biological Chemistry*, *271*(34), 20545–20550. <https://doi.org/10.1074/jbc.271.34.20545>.
12. Clark-Lewis, I., Kim, K. S., Rajarathnam, K., Gong, J. H., Dewald, B., Moser, B., et al. (1995). Structure-activity relationships of chemokines. *Journal of Leukocyte Biology*, *57*(5), 703–711. <https://doi.org/10.1002/jlb.57.5.703>.
13. Zlotnik, A., Morales, J., & Hedrick, J. A. (1999). Recent advances in chemokines and chemokine receptors. *Critical Reviews in Immunology*, *19*(1), 1–47.
14. Zlotnik, A., & Yoshie, O. (2012). The chemokine superfamily revisited. *Immunity*, *36*(5), 705–716. <https://doi.org/10.1016/j.immuni.2012.05.008>.
15. Islam, S. A., Chang, D. S., Colvin, R. A., Byrne, M. H., McCully, M. L., Moser, B., et al. (2011). Mouse CCL8, a CCR8 agonist, promotes atopic dermatitis by recruiting IL-5+ T(H)2 cells. *Nature Immunology*, *12*(2), 167–177. <https://doi.org/10.1038/ni.1984>.
16. Jung, S., & Littman, D. R. (1999). Chemokine receptors in lymphoid organ homeostasis. *Current Opinion in Immunology*, *11*(3), 319–325.
17. Murphy, P. M. (1996). Chemokine receptors: structure, function and role in microbial pathogenesis. *Cytokine & Growth Factor Reviews*, *7*(1), 47–64.
18. Weathington, N. M., van Houwelingen, A. H., Noerager, B. D., Jackson, P. L., Kraneveld, A. D., Galin, F. S., et al. (2006). A novel peptide CXCR ligand derived from extracellular matrix degradation during airway inflammation. *Nature Medicine*, *12*(3), 317–323.
19. Bernhagen, J., Krohn, R., Lue, H., Gregory, J. L., Zernecke, A., Koenen, R. R., et al. (2007). MIF is a noncognate ligand of CXC chemokine receptors in inflammatory and atherogenic cell recruitment. *Nature Medicine*, *13*(5), 587–596. <https://doi.org/10.1038/nm1567>.
20. Lacy, M., Kontos, C., Brandhofer, M., Hille, K., Groning, S., Sinitski, D., et al. (2018). Identification of an Arg-Leu-Arg tripeptide that contributes to the binding interface between the cytokine MIF and the chemokine receptor CXCR4. *Scientific Reports*, *8*(1), 5171. <https://doi.org/10.1038/s41598-018-23554-5>.
21. Alampour-Rajabi, S., El Bounkari, O., Rot, A., Muller-Newen, G., Bachelier, F., Gawaz, M., et al. (2015). MIF interacts with CXCR7 to promote receptor internalization, ERK1/2 and ZAP-70 signaling, and lymphocyte chemotaxis. *The FASEB Journal*, *29*(11), 4497–4511. <https://doi.org/10.1096/fj.15-273904>.
22. Soppert, J., Kraemer, S., Beckers, C., Averdunk, L., Mollmann, J., Denecke, B., et al. (2018). Soluble CD74 reroutes MIF/CXCR4/AKT-mediated survival of cardiac myofibroblasts to necroptosis. *Journal of the American Heart Association*, *7*(17), e009384. <https://doi.org/10.1161/JAHA.118.009384>.
23. Frangogiannis, N. G. (2012). Regulation of the inflammatory response in cardiac repair. *Circulation Research*, *110*(1), 159–173. <https://doi.org/10.1161/CIRCRESAHA.111.243162>.
24. Chen, B., Huang, S., Su, Y., Wu, Y. J., Hanna, A., Brickshawana, A., et al. (2019). Macrophage Smad3 protects the infarcted heart, stimulating phagocytosis and regulating inflammation. *Circulation Research*, *125*(1), 55–70. <https://doi.org/10.1161/CIRCRESAHA.119.315069>.
25. Shinde, A. V., & Frangogiannis, N. G. (2014). Fibroblasts in myocardial infarction: a role in inflammation and repair. *Journal of Molecular and Cellular Cardiology*, *70C*, 74–82.
26. Kanisicak, O., Khalil, H., Ivey, M. J., Karch, J., Maliken, B. D., Correll, R. N., et al. (2016). Genetic lineage tracing defines myofibroblast origin and function in the injured heart. *Nature Communications*, *7*, 12260. <https://doi.org/10.1038/ncomms12260>.
27. Kong, P., Shinde, A. V., Su, Y., Russo, I., Chen, B., Saxena, A., et al. (2018). Opposing actions of fibroblast and cardiomyocyte Smad3 signaling in the infarcted myocardium. *Circulation*, *137*(7), 707–724. <https://doi.org/10.1161/CIRCULATIONAHA.117.029622>.
28. Frangogiannis, N. G., Michael, L. H., & Entman, M. L. (2000). Myofibroblasts in reperfused myocardial infarcts express the embryonic form of smooth muscle myosin heavy chain (SMemb). *Cardiovascular Research*, *48*(1), 89–100.
29. Fu, X., Khalil, H., Kanisicak, O., Boyer, J. G., Vagnozzi, R. J., Maliken, B. D., et al. (2018). Specialized fibroblast differentiated states underlie scar formation in the infarcted mouse heart. *The Journal of Clinical Investigation*, *128*(5), 2127–2143. <https://doi.org/10.1172/JCI98215>.
30. Kakio, T., Matsumori, A., Ono, K., Ito, H., Matsushima, K., & Sasayama, S. (2000). Roles and relationship of macrophages and monocyte chemoattractant and activating factor/monocyte chemoattractant protein-1 in the ischemic and reperfused rat heart. *Laboratory Investigation*, *80*(7), 1127–1136.
31. Zouggar, Y., Ait-Oufella, H., Bonnin, P., Simon, T., Sage, A. P., Guerin, C., et al. (2013). B lymphocytes trigger monocyte mobilization and impair heart function after acute myocardial infarction. *Nature Medicine*, *19*(10), 1273–1280.
32. Kumar, A. G., Ballantyne, C. M., Michael, L. H., Kukielka, G. L., Youker, K. A., Lindsey, M. L., et al. (1997). Induction of monocyte chemoattractant protein-1 in the small veins of the ischemic and reperfused canine myocardium. *Circulation*, *95*(3), 693–700.
33. Frangogiannis, N. G., Mendoza, L. H., Lewallen, M., Michael, L. H., Smith, C. W., & Entman, M. L. (2001). Induction and suppression of interferon-inducible protein 10 in reperfused myocardial infarcts may regulate angiogenesis. *The FASEB Journal*, *15*(8), 1428–1430.
34. Mylonas, K. J., Turner, N. A., Bageghni, S. A., Kenyon, C. J., White, C. I., McGregor, K., et al. (2017). 11beta-HSD1 suppresses cardiac fibroblast CXCL2, CXCL5 and neutrophil recruitment to the heart post MI. *The Journal of Endocrinology*, *233*(3), 315–327. <https://doi.org/10.1530/JOE-16-0501>.
35. Turner, N. A., Das, A., O'Regan, D. J., Ball, S. G., & Porter, K. E. (2011). Human cardiac fibroblasts express ICAM-1, E-selectin and CXC chemokines in response to proinflammatory cytokine stimulation. *The International Journal of Biochemistry & Cell Biology*, *43*(10), 1450–1458. <https://doi.org/10.1016/j.biocel.2011.06.008>.
36. Zymek, P., Nah, D. Y., Bujak, M., Ren, G., Koerting, A., Leucker, T., et al. (2007). Interleukin-10 is not a critical regulator of infarct healing and left ventricular remodeling. *Cardiovascular Research*, *74*(2), 313–322. <https://doi.org/10.1016/j.cardiores.2006.11.028>.
37. Muhlstedt, S., Ghadge, S. K., Duchene, J., Qadri, F., Jarve, A., Vilianovich, L., et al. (2016). Cardiomyocyte-derived CXCL12 is not involved in cardiogenesis but plays a crucial role in myocardial infarction. *Journal of Molecular Medicine (Berlin, Germany)*, *94*(9), 1005–1014. <https://doi.org/10.1007/s00109-016-1432-1>.
38. Segret, A., Rucker-Martin, C., Pavoin, C., Flavigny, J., Deroubaix, E., Chatel, M. A., et al. (2007). Structural localization and expression of CXCL12 and CXCR4 in rat heart and isolated cardiac myocytes. *The Journal of Histochemistry and Cytochemistry*, *55*(2), 141–150. <https://doi.org/10.1369/jhc.6A7050.2006>.

39. Ban, K., Ikeda, U., Takahashi, M., Kanbe, T., Kasahara, T., & Shimada, K. (1994). Expression of intercellular adhesion molecule-1 on rat cardiac myocytes by monocyte chemoattractant protein-1. *Cardiovascular Research*, 28(8), 1258–1262.
40. Herzog, C., Lorenz, A., Gillmann, H. J., Chowdhury, A., Larmann, J., Harendza, T., et al. (2014). Thrombomodulin's lectin-like domain reduces myocardial damage by interfering with HMGB1-mediated TLR2 signalling. *Cardiovascular Research*, 101(3), 400–410. <https://doi.org/10.1093/cvr/cvt275>.
41. Andrassy, M., Volz, H. C., Igwe, J. C., Funke, B., Eichberger, S. N., Kaya, Z., et al. (2008). High-mobility group box-1 in ischemia-reperfusion injury of the heart. *Circulation*, 117(25), 3216–3226.
42. Fiuza, C., Bustin, M., Talwar, S., Tropea, M., Gerstenberger, E., Shelhamer, J. H., et al. (2003). Inflammation-promoting activity of HMGB1 on human microvascular endothelial cells. *Blood*, 101(7), 2652–2660. <https://doi.org/10.1182/blood-2002-05-1300>.
43. Rossini, A., Zacheo, A., Mocini, D., Totta, P., Facchiano, A., Castoldi, R., et al. (2008). HMGB1-stimulated human primary cardiac fibroblasts exert a paracrine action on human and murine cardiac stem cells. *Journal of Molecular and Cellular Cardiology*, 44(4), 683–693. <https://doi.org/10.1016/j.yjmcc.2008.01.009>.
44. Lugin, J., Parapanov, R., Rosenblatt-Velin, N., Rignault-Clerc, S., Feihl, F., Waeber, B., et al. (2015). Cutting edge: IL-1 α is a crucial danger signal triggering acute myocardial inflammation during myocardial infarction. *Journal of Immunology*, 194(2), 499–503. <https://doi.org/10.4049/jimmunol.1401948>.
45. Chen, C., Feng, Y., Zou, L., Wang, L., Chen, H. H., Cai, J. Y., et al. (2014). Role of extracellular RNA and TLR3-Trif signaling in myocardial ischemia-reperfusion injury. *Journal of the American Heart Association*, 3(1), e000683. <https://doi.org/10.1161/JAHA.113.000683>.
46. Ghigo, A., Franco, I., Morello, F., & Hirsch, E. (2014). Myocyte signalling in leucocyte recruitment to the heart. *Cardiovascular Research*, 102(2), 270–280. <https://doi.org/10.1093/cvr/cvu030>.
47. Dybdahl, B., Slordahl, S. A., Waage, A., Kierulf, P., Espevik, T., & Sundan, A. (2005). Myocardial ischaemia and the inflammatory response: release of heat shock protein 70 after myocardial infarction. *Heart*, 91(3), 299–304.
48. Newton, K., & Dixit, V. M. (2012). Signaling in innate immunity and inflammation. *Cold Spring Harbor Perspectives in Biology*, 4(3). <https://doi.org/10.1101/cshperspect.a006049>.
49. Oyama, J., Blais Jr., C., Liu, X., Pu, M., Kobzik, L., Kelly, R. A., et al. (2004). Reduced myocardial ischemia-reperfusion injury in toll-like receptor 4-deficient mice. *Circulation*, 109(6), 784–789. <https://doi.org/10.1161/01.CIR.0000112575.66565.84>.
50. Kaczorowski, D. J., Nakao, A., Mollen, K. P., Vallabhaneni, R., Sugimoto, R., Kohmoto, J., et al. (2007). Toll-like receptor 4 mediates the early inflammatory response after cold ischemia/reperfusion. *Transplantation*, 84(10), 1279–1287. <https://doi.org/10.1097/01.tp.0000287597.87571.17>.
51. Feng, Y., Zhao, H., Xu, X., Buys, E. S., Raheer, M. J., Bopassa, J. C., et al. (2008). Innate immune adaptor MyD88 mediates neutrophil recruitment and myocardial injury after ischemia-reperfusion in mice. *American Journal of Physiology. Heart and Circulatory Physiology*, 295(3), H1311–H1318. <https://doi.org/10.1152/ajpheart.00119.2008>.
52. Ao, L., Zou, N., Cleveland Jr., J. C., Fullerton, D. A., & Meng, X. (2009). Myocardial TLR4 is a determinant of neutrophil infiltration after global myocardial ischemia: mediating KC and MCP-1 expression induced by extracellular HSC70. *American Journal of Physiology. Heart and Circulatory Physiology*, 297(1), H21–H28. <https://doi.org/10.1152/ajpheart.00292.2009>.
53. Methe, H., Kim, J. O., Kofler, S., Weis, M., Nabauer, M., & Koglin, J. (2005). Expansion of circulating Toll-like receptor 4-positive monocytes in patients with acute coronary syndrome. *Circulation*, 111(20), 2654–2661. <https://doi.org/10.1161/CIRCULATIONAHA.104.498865>.
54. Satoh, M., Shimoda, Y., Maesawa, C., Akatsu, T., Ishikawa, Y., Minami, Y., et al. (2006). Activated toll-like receptor 4 in monocytes is associated with heart failure after acute myocardial infarction. *International Journal of Cardiology*, 109(2), 226–234. <https://doi.org/10.1016/j.ijcard.2005.06.023>.
55. Arslan, F., Smeets, M. B., O'Neill, L. A., Keogh, B., McGuirk, P., Timmers, L., et al. (2010). Myocardial ischemia/reperfusion injury is mediated by leukocytic toll-like receptor-2 and reduced by systemic administration of a novel anti-toll-like receptor-2 antibody. *Circulation*, 121(1), 80–90.
56. Wang, J. W., Fontes, M. S. C., Wang, X., Chong, S. Y., Kessler, E. L., Zhang, Y. N., et al. (2017). Leukocytic Toll-like receptor 2 deficiency preserves cardiac function and reduces fibrosis in sustained pressure overload. *Scientific Reports*, 7(1), 9193. <https://doi.org/10.1038/s41598-017-09451-3>.
57. Lu, C., Ren, D., Wang, X., Ha, T., Liu, L., Lee, E. J., et al. (2014). Toll-like receptor 3 plays a role in myocardial infarction and ischemia/reperfusion injury. *Biochimica et Biophysica Acta*, 1842(1), 22–31.
58. de Kleijn, D. P. V., Chong, S. Y., Wang, X., Yatim, S., Fairhurst, A. M., Vernooij, F., et al. (2019). Toll-like receptor 7 deficiency promotes survival and reduces adverse left ventricular remodeling after myocardial infarction. *Cardiovascular Research*, 115(12), 1791–1803. <https://doi.org/10.1093/cvr/cvz057>.
59. Feng, Y., Chen, H., Cai, J., Zou, L., Yan, D., Xu, G., et al. (2015). Cardiac RNA induces inflammatory responses in cardiomyocytes and immune cells via Toll-like receptor 7 signaling. *J Biol Chem*, 290(44), 26688–26698. doi:10.1074/jbc.M115.661835.
60. Frantz, S., Kelly, R. A., & Bourcier, T. (2001). Role of TLR-2 in the activation of nuclear factor kappaB by oxidative stress in cardiac myocytes. *The Journal of Biological Chemistry*, 276(7), 5197–5203. <https://doi.org/10.1074/jbc.M009160200>.
61. Yang, R., Song, Z., Wu, S., Wei, Z., Xu, Y., & Shen, X. (2018). Toll-like receptor 4 contributes to a myofibroblast phenotype in cardiac fibroblasts and is associated with autophagy after myocardial infarction in a mouse model. *Atherosclerosis*, 279, 23–31. <https://doi.org/10.1016/j.atherosclerosis.2018.10.018>.
62. Zhang, W., Lavine, K. J., Epelman, S., Evans, S. A., Weinheimer, C. J., Barger, P. M., et al. (2015). Necrotic myocardial cells release damage-associated molecular patterns that provoke fibroblast activation in vitro and trigger myocardial inflammation and fibrosis in vivo. *Journal of the American Heart Association*, 4(6), e001993. <https://doi.org/10.1161/JAHA.115.001993>.
63. Li, Y., Si, R., Feng, Y., Chen, H. H., Zou, L., Wang, E., et al. (2011). Myocardial ischemia activates an injurious innate immune signaling via cardiac heat shock protein 60 and Toll-like receptor 4. *The Journal of Biological Chemistry*, 286(36), 31308–31319.
64. Ritchie, M. E. (1998). Nuclear factor-kappaB is selectively and markedly activated in humans with unstable angina pectoris. *Circulation*, 98(17), 1707–1713. <https://doi.org/10.1161/01.cir.98.17.1707>.
65. Chandrasekar, B., Smith, J. B., & Freeman, G. L. (2001). Ischemia-reperfusion of rat myocardium activates nuclear factor-kappaB and induces neutrophil infiltration via lipopolysaccharide-induced CXC chemokine. *Circulation*, 103(18), 2296–2302. <https://doi.org/10.1161/01.cir.103.18.2296>.
66. Chandrasekar, B., & Freeman, G. L. (1997). Induction of nuclear factor kappaB and activation protein 1 in postischemic myocardium. *FEBS Letters*, 401(1), 30–34. [https://doi.org/10.1016/s0014-5793\(96\)01426-3](https://doi.org/10.1016/s0014-5793(96)01426-3).
67. Onai, Y., Suzuki, J., Kakuta, T., Maejima, Y., Haraguchi, G., Fukasawa, H., et al. (2004). Inhibition of IkappaB phosphorylation in cardiomyocytes attenuates myocardial ischemia/

- reperfusion injury. *Cardiovascular Research*, 63(1), 51–59. <https://doi.org/10.1016/j.cardiores.2004.03.002>.
68. Li, H. L., Zhuo, M. L., Wang, D., Wang, A. B., Cai, H., Sun, L. H., et al. (2007). Targeted cardiac overexpression of A20 improves left ventricular performance and reduces compensatory hypertrophy after myocardial infarction. *Circulation*, 115(14), 1885–1894. <https://doi.org/10.1161/CIRCULATIONAHA.106.656835>.
 69. Timmers, L., van Keulen, J. K., Hoefler, I. E., Meijs, M. F., van Middelaar, B., den Ouden, K., et al. (2009). Targeted deletion of nuclear factor kappaB p50 enhances cardiac remodeling and dysfunction following myocardial infarction. *Circulation Research*, 104(5), 699–706. <https://doi.org/10.1161/CIRCRESAHA.108.189746>.
 70. Frantz, S., Tillmanns, J., Kuhlencordt, P. J., Schmidt, I., Adamek, A., Dienesch, C., et al. (2007). Tissue-specific effects of the nuclear factor kappaB subunit p50 on myocardial ischemia-reperfusion injury. *The American Journal of Pathology*, 171(2), 507–512. <https://doi.org/10.2353/ajpath.2007.061042>.
 71. Pinckard, R. N., Olson, M. S., Giclas, P. C., Terry, R., Boyer, J. T., & O'Rourke, R. A. (1975). Consumption of classical complement components by heart subcellular membranes in vitro and in patients after acute myocardial infarction. *The Journal of Clinical Investigation*, 56(3), 740–750. <https://doi.org/10.1172/JCI108145>.
 72. Hill, J. H., & Ward, P. A. (1971). The phlogistic role of C3 leukotactic fragments in myocardial infarcts of rats. *The Journal of Experimental Medicine*, 133(4), 885–900. <https://doi.org/10.1084/jem.133.4.885>.
 73. Czermak, B. J., Sarma, V., Bless, N. M., Schmal, H., Friedl, H. P., & Ward, P. A. (1999). In vitro and in vivo dependency of chemokine generation on C5a and TNF-alpha. *Journal of Immunology*, 162(4), 2321–2325.
 74. Kilgore, K. S., Park, J. L., Tanhehco, E. J., Booth, E. A., Marks, R. M., & Lucchesi, B. R. (1998). Attenuation of interleukin-8 expression in C6-deficient rabbits after myocardial ischemia/reperfusion. *Journal of Molecular and Cellular Cardiology*, 30(1), 75–85. <https://doi.org/10.1006/jmcc.1997.0573>.
 75. Maekawa, N., Wada, H., Kanda, T., Niwa, T., Yamada, Y., Saito, K., et al. (2002). Improved myocardial ischemia/reperfusion injury in mice lacking tumor necrosis factor-alpha. *Journal of the American College of Cardiology*, 39(7), 1229–1235. [https://doi.org/10.1016/s0735-1097\(02\)01738-2](https://doi.org/10.1016/s0735-1097(02)01738-2).
 76. Bujak, M., Dobaczewski, M., Chatila, K., Mendoza, L. H., Li, N., Reddy, A., et al. (2008). Interleukin-1 receptor type I signaling critically regulates infarct healing and cardiac remodeling. *The American Journal of Pathology*, 173(1), 57–67. <https://doi.org/10.2353/ajpath.2008.070974>.
 77. Saxena, A., Chen, W., Su, Y., Rai, V., Uche, O. U., Li, N., et al. (2013). IL-1 induces proinflammatory leukocyte infiltration and regulates fibroblast phenotype in the infarcted myocardium. *Journal of Immunology*, 191(9), 4838–4848. <https://doi.org/10.4049/jimmunol.1300725>.
 78. Frangogiannis, N. G., Lindsey, M. L., Michael, L. H., Youker, K. A., Bressler, R. B., Mendoza, L. H., et al. (1998). Resident cardiac mast cells degranulate and release preformed TNF-alpha, initiating the cytokine cascade in experimental canine myocardial ischemia/reperfusion. *Circulation*, 98(7), 699–710. <https://doi.org/10.1161/01.cir.98.7.699>.
 79. Somasundaram, P., Ren, G., Nagar, H., Kraemer, D., Mendoza, L., Michael, L. H., et al. (2005). Mast cell tryptase may modulate endothelial cell phenotype in healing myocardial infarcts. *The Journal of Pathology*, 205(1), 102–111. <https://doi.org/10.1002/path.1690>.
 80. Oynebraten, I., Bakke, O., Brandtzaeg, P., Johansen, F. E., & Haraldsen, G. (2004). Rapid chemokine secretion from endothelial cells originates from 2 distinct compartments. *Blood*, 104(2), 314–320. <https://doi.org/10.1182/blood-2003-08-2891>.
 81. Detmers, P. A., Lo, S. K., Olsen-Egbert, E., Walz, A., Baggiolini, M., & Cohn, Z. A. (1990). Neutrophil-activating protein 1/interleukin 8 stimulates the binding activity of the leukocyte adhesion receptor CD11b/CD18 on human neutrophils. *The Journal of Experimental Medicine*, 171(4), 1155–1162. <https://doi.org/10.1084/jem.171.4.1155>.
 82. Herter, J., & Zarbock, A. (2013). Integrin regulation during leukocyte recruitment. *Journal of Immunology*, 190(9), 4451–4457. <https://doi.org/10.4049/jimmunol.1203179>.
 83. Knall, C., Worthen, G. S., & Johnson, G. L. (1997). Interleukin 8-stimulated phosphatidylinositol-3-kinase activity regulates the migration of human neutrophils independent of extracellular signal-regulated kinase and p38 mitogen-activated protein kinases. *Proceedings of the National Academy of Sciences of the United States of America*, 94(7), 3052–3057. <https://doi.org/10.1073/pnas.94.7.3052>.
 84. Legler, D. F., & Thelen, M. (2018). New insights in chemokine signaling. *F1000Res*, 7, 95, doi:<https://doi.org/10.12688/f1000research.13130.1>.
 85. Sotsios, Y., & Ward, S. G. (2000). Phosphoinositide 3-kinase: a key biochemical signal for cell migration in response to chemokines. *Immunological Reviews*, 177, 217–235.
 86. Bujak, M., Dobaczewski, M., Gonzalez-Quesada, C., Xia, Y., Leucker, T., Zymek, P., et al. (2009). Induction of the CXC chemokine interferon-gamma-inducible protein 10 regulates the reparative response following myocardial infarction. *Circulation Research*, 105(10), 973–983. <https://doi.org/10.1161/CIRCRESAHA.109.199471>.
 87. Tarzami, S. T., Miao, W., Mani, K., Lopez, L., Factor, S. M., Berman, J. W., et al. (2003). Opposing effects mediated by the chemokine receptor CXCR2 on myocardial ischemia-reperfusion injury: recruitment of potentially damaging neutrophils and direct myocardial protection. *Circulation*, 108(19), 2387–2392. <https://doi.org/10.1161/01.CIR.0000093192.72099.9A>.
 88. Jarrah, A. A., Schwarskopf, M., Wang, E. R., LaRocca, T., Dhume, A., Zhang, S., et al. (2018). SDF-1 induces TNF-mediated apoptosis in cardiac myocytes. *Apoptosis*, 23(1), 79–91. <https://doi.org/10.1007/s10495-017-1438-3>.
 89. Strieter, R. M., Polverini, P. J., Kunkel, S. L., Arenberg, D. A., Burdick, M. D., Kasper, J., et al. (1995). The functional role of the ELR motif in CXC chemokine-mediated angiogenesis. *The Journal of Biological Chemistry*, 270(45), 27348–27357.
 90. Kukielka, G. L., Smith, C. W., LaRosa, G. J., Manning, A. M., Mendoza, L. H., Daly, T. J., et al. (1995). Interleukin-8 gene induction in the myocardium after ischemia and reperfusion in vivo. *The Journal of Clinical Investigation*, 95(1), 89–103. <https://doi.org/10.1172/JCI117680>.
 91. Ivey, C. L., Williams, F. M., Collins, P. D., Jose, P. J., & Williams, T. J. (1995). Neutrophil chemoattractants generated in two phases during reperfusion of ischemic myocardium in the rabbit. Evidence for a role for C5a and interleukin-8. *The Journal of Clinical Investigation*, 95(6), 2720–2728. <https://doi.org/10.1172/JCI117974>.
 92. Zeilhofer, H. U., & Schorr, W. (2000). Role of interleukin-8 in neutrophil signaling. *Current Opinion in Hematology*, 7(3), 178–182.
 93. Boyle Jr, E. M., Kovacich, J. C., Hebert, C. A., Canty Jr, T. G., Chi, E., Morgan, E. N., et al. (1998). Inhibition of interleukin-8 blocks myocardial ischemia-reperfusion injury. *The Journal of Thoracic and Cardiovascular Surgery*, 116(1), 114–121. [https://doi.org/10.1016/S0022-5223\(98\)70249-1](https://doi.org/10.1016/S0022-5223(98)70249-1).
 94. Oral, H., Kanzler, I., Tuhscheerer, N., Curaj, A., Simsekylmaz, S., Sonmez, T. T., et al. (2013). CXC chemokine KC fails to induce neutrophil infiltration and neoangiogenesis in a mouse

- model of myocardial infarction. *Journal of Molecular and Cellular Cardiology*, 60, 1–7. <https://doi.org/10.1016/j.yjmcc.2013.04.006>.
95. Xie, Q., Sun, Z., Chen, M., Zhong, Q., Yang, T., & Yi, J. (2015). IL-8 up-regulates proliferative angiogenesis in ischemic myocardium in rabbits through phosphorylation of Akt/GSK-3 β (ser9) dependent pathways. *International Journal of Clinical and Experimental Medicine*, 8(8), 12498–12508.
 96. Shetelig, C., Limalanathan, S., Hoffmann, P., Seljeflot, I., Gran, J. M., Eritsland, J., et al. (2018). Association of IL-8 with infarct size and clinical outcomes in patients With STEMI. *Journal of the American College of Cardiology*, 72(2), 187–198. <https://doi.org/10.1016/j.jacc.2018.04.053>.
 97. Moser, B., & Loetscher, P. (2001). Lymphocyte traffic control by chemokines. *Nature Immunology*, 2(2), 123–128. <https://doi.org/10.1038/84219>.
 98. Fiorina, P., Ansari, M. J., Jurewicz, M., Barry, M., Ricchiuti, V., Smith, R. N., et al. (2006). Role of CXC chemokine receptor 3 pathway in renal ischemic injury. *J Am Soc Nephrol*, 17(3), 716–723. <https://doi.org/10.1681/ASN.2005090954>.
 99. Khan, I. A., MacLean, J. A., Lee, F. S., Casciotti, L., DeHaan, E., Schwartzman, J. D., et al. (2000). IP-10 is critical for effector T cell trafficking and host survival in *Toxoplasma gondii* infection. *Immunity*, 12(5), 483–494. [https://doi.org/10.1016/S1074-7613\(00\)80200-9](https://doi.org/10.1016/S1074-7613(00)80200-9).
 100. Shiraha, H., Glading, A., Gupta, K., & Wells, A. (1999). IP-10 inhibits epidermal growth factor-induced motility by decreasing epidermal growth factor receptor-mediated calpain activity. *The Journal of Cell Biology*, 146(1), 243–254. <https://doi.org/10.1083/jcb.146.1.243>.
 101. Strieter, R. M., Polverini, P. J., Arenberg, D. A., Walz, A., Opendakker, G., Van Damme, J., et al. (1995). Role of C-X-C chemokines as regulators of angiogenesis in lung cancer. *Journal of Leukocyte Biology*, 57(5), 752–762. <https://doi.org/10.1002/jlb.57.5.752>.
 102. Strieter, R. M., Polverini, P. J., Kunkel, S. L., Arenberg, D. A., Burdick, M. D., Kasper, J., et al. (1995). The functional role of the ELR motif in CXC chemokine-mediated angiogenesis. *The Journal of Biological Chemistry*, 270(45), 27348–27357. <https://doi.org/10.1074/jbc.270.45.27348>.
 103. Dewald, O., Ren, G., Duerr, G. D., Zoerlein, M., Klemm, C., Gersch, C., et al. (2004). Of mice and dogs: species-specific differences in the inflammatory response following myocardial infarction. *The American Journal of Pathology*, 164(2), 665–677. [https://doi.org/10.1016/S0002-9440\(10\)63154-9](https://doi.org/10.1016/S0002-9440(10)63154-9).
 104. Loetscher, M., Gerber, B., Loetscher, P., Jones, S. A., Piali, L., Clark-Lewis, I., et al. (1996). Chemokine receptor specific for IP10 and mig: structure, function, and expression in activated T-lymphocytes. *The Journal of Experimental Medicine*, 184(3), 963–969. <https://doi.org/10.1084/jem.184.3.963>.
 105. Saxena, A., Bujak, M., Frunza, O., Dobaczewski, M., Gonzalez-Quesada, C., Lu, B., et al. (2014). CXCR3-independent actions of the CXC chemokine CXCL10 in the infarcted myocardium and in isolated cardiac fibroblasts are mediated through proteoglycans. *Cardiovascular Research*, 103(2), 217–227. <https://doi.org/10.1093/cvr/cvu138>.
 106. Nagasawa, T., Hirota, S., Tachibana, K., Takakura, N., Nishikawa, S., Kitamura, Y., et al. (1996). Defects of B cell lymphopoiesis and bone-marrow myelopoiesis in mice lacking the CXC chemokine PBSF/SDF-1. *Nature*, 382(6592), 635–638. <https://doi.org/10.1038/382635a0>.
 107. Salvucci, O., Yao, L., Villalba, S., Sajewicz, A., Pittaluga, S., & Tosato, G. (2002). Regulation of endothelial cell branching morphogenesis by endogenous chemokine stromal-derived factor-1. *Blood*, 99(8), 2703–2711. <https://doi.org/10.1182/blood.v99.8.2703>.
 108. Salcedo, R., Wasserman, K., Young, H. A., Grimm, M. C., Howard, O. M., Anver, M. R., et al. (1999). Vascular endothelial growth factor and basic fibroblast growth factor induce expression of CXCR4 on human endothelial cells: In vivo neovascularization induced by stromal-derived factor-1 α . *The American Journal of Pathology*, 154(4), 1125–1135. [https://doi.org/10.1016/S0002-9440\(10\)65365-5](https://doi.org/10.1016/S0002-9440(10)65365-5).
 109. Pillarisetti, K., & Gupta, S. K. (2001). Cloning and relative expression analysis of rat stromal cell derived factor-1 (SDF-1): SDF-1 α mRNA is selectively induced in rat model of myocardial infarction. *Inflammation*, 25(5), 293–300. <https://doi.org/10.1023/a:1012808525370>.
 110. Askari, A. T., Unzek, S., Popovic, Z. B., Goldman, C. K., Forudi, F., Kiedrowski, M., et al. (2003). Effect of stromal-cell-derived factor 1 on stem-cell homing and tissue regeneration in ischaemic cardiomyopathy. *Lancet*, 362(9385), 697–703. [https://doi.org/10.1016/S0140-6736\(03\)14232-8](https://doi.org/10.1016/S0140-6736(03)14232-8).
 111. Frangogiannis, N. G. (2011). The stromal cell-derived factor-1/CXCR4 axis in cardiac injury and repair. *Journal of the American College of Cardiology*, 58(23), 2424–2426. <https://doi.org/10.1016/j.jacc.2011.08.031>.
 112. Uematsu, M., Yoshizaki, T., Shimizu, T., Obata, J. E., Nakamura, T., Fujioka, D., et al. (2015). Sustained myocardial production of stromal cell-derived factor-1 α was associated with left ventricular adverse remodeling in patients with myocardial infarction. *American Journal of Physiology. Heart and Circulatory Physiology*, 309(10), H1764–H1771. <https://doi.org/10.1152/ajpheart.00493.2015>.
 113. Ceradini, D. J., Kulkarni, A. R., Callaghan, M. J., Tepper, O. M., Bastidas, N., Kleinman, M. E., et al. (2004). Progenitor cell trafficking is regulated by hypoxic gradients through HIF-1 induction of SDF-1. *Nature Medicine*, 10(8), 858–864. <https://doi.org/10.1038/nm1075>.
 114. Abbott, J. D., Huang, Y., Liu, D., Hickey, R., Krause, D. S., & Giordano, F. J. (2004). Stromal cell-derived factor-1 α plays a critical role in stem cell recruitment to the heart after myocardial infarction but is not sufficient to induce homing in the absence of injury. *Circulation*, 110(21), 3300–3305. <https://doi.org/10.1161/01.CIR.0000147780.30124.CF>.
 115. Ma, J., Ge, J., Zhang, S., Sun, A., Shen, J., Chen, L., et al. (2005). Time course of myocardial stromal cell-derived factor 1 expression and beneficial effects of intravenously administered bone marrow stem cells in rats with experimental myocardial infarction. *Basic Research in Cardiology*, 100(3), 217–223. <https://doi.org/10.1007/s00395-005-0521-z>.
 116. Saxena, A., Fish, J. E., White, M. D., Yu, S., Smyth, J. W., Shaw, R. M., et al. (2008). Stromal cell-derived factor-1 α is cardioprotective after myocardial infarction. *Circulation*, 117(17), 2224–2231. <https://doi.org/10.1161/CIRCULATIONAHA.107.694992>.
 117. Zhang, M., Mal, N., Kiedrowski, M., Chacko, M., Askari, A. T., Popovic, Z. B., et al. (2007). SDF-1 expression by mesenchymal stem cells results in trophic support of cardiac myocytes after myocardial infarction. *The FASEB Journal*, 21(12), 3197–3207. <https://doi.org/10.1096/fj.06-6558com>.
 118. Sasaki, T., Fukazawa, R., Ogawa, S., Kanno, S., Nitta, T., Ochi, M., et al. (2007). Stromal cell-derived factor-1 α improves infarcted heart function through angiogenesis in mice. *Pediatrics International*, 49(6), 966–971. <https://doi.org/10.1111/j.1442-200X.2007.02491.x>.
 119. MacArthur Jr., J. W., Purcell, B. P., Shudo, Y., Cohen, J. E., Fairman, A., Trubelja, A., et al. (2013). Sustained release of engineered stromal cell-derived factor 1- α from injectable hydrogels effectively recruits endothelial progenitor cells and preserves ventricular function after myocardial infarction.

- Circulation*, 128(11 Suppl 1), S79–S86. <https://doi.org/10.1161/CIRCULATIONAHA.112.000343>.
120. MacArthur Jr., J. W., Cohen, J. E., McCarvey, J. R., Shudo, Y., Patel, J. B., Trubelja, A., et al. (2014). Preclinical evaluation of the engineered stem cell chemokine stromal cell-derived factor 1alpha analog in a translational ovine myocardial infarction model. *Circulation Research*, 114(4), 650–659. <https://doi.org/10.1161/CIRCRESAHA.114.302884>.
 121. Elmadbouh, I., Haider, H., Jiang, S., Idris, N. M., Lu, G., & Ashraf, M. (2007). Ex vivo delivered stromal cell-derived factor-1alpha promotes stem cell homing and induces angiomyogenesis in the infarcted myocardium. *Journal of Molecular and Cellular Cardiology*, 42(4), 792–803. <https://doi.org/10.1016/j.yjmcc.2007.02.001>.
 122. Mayorga, M. E., Kiedrowski, M., McCallinhardt, P., Forudi, F., Ockunzzi, J., Weber, K., et al. (2018). Role of SDF-1:CXCR4 in impaired post-myocardial infarction cardiac repair in diabetes. *Stem Cells Translational Medicine*, 7(1), 115–124. <https://doi.org/10.1002/sctm.17-0172>.
 123. Cheng, M., Huang, K., Zhou, J., Yan, D., Tang, Y. L., Zhao, T. C., et al. (2015). A critical role of Src family kinase in SDF-1/CXCR4-mediated bone-marrow progenitor cell recruitment to the ischemic heart. *Journal of Molecular and Cellular Cardiology*, 81, 49–53. <https://doi.org/10.1016/j.yjmcc.2015.01.024>.
 124. Wang, M., Hu, R., Yang, Y., Xiang, L., & Mu, Y. (2019). In vivo ultrasound molecular imaging of SDF-1 expression in a swine model of acute myocardial infarction. *Frontiers in Pharmacology*, 10, 899. <https://doi.org/10.3389/fphar.2019.00899>.
 125. Huang, F. Y., Xia, T. L., Li, J. L., Li, C. M., Zhao, Z. G., Lei, W. H., et al. (2019). The bifunctional SDF-1-AnxA5 fusion protein protects cardiac function after myocardial infarction. *Journal of Cellular and Molecular Medicine*, 23(11), 7673–7684. <https://doi.org/10.1111/jcmm.14640>.
 126. Goldstone, A. B., Burnett, C. E., Cohen, J. E., Paulsen, M. J., Eskandari, A., Edwards, B. E., et al. (2018). SDF 1-alpha attenuates myocardial injury without altering the direct contribution of circulating cells. *Journal of Cardiovascular Translational Research*, 11(4), 274–284. <https://doi.org/10.1007/s12265-017-9772-y>.
 127. Liu, Y., Gao, S., Wang, Z., Yang, Y., Huo, H., & Tian, X. (2016). Effect of stromal cell-derived factor-1 on myocardial apoptosis and cardiac function recovery in rats with acute myocardial infarction. *Experimental and Therapeutic Medicine*, 12(5), 3282–3286. <https://doi.org/10.3892/etm.2016.3770>.
 128. Hu, X., Dai, S., Wu, W. J., Tan, W., Zhu, X., Mu, J., et al. (2007). Stromal cell derived factor-1 alpha confers protection against myocardial ischemia/reperfusion injury: role of the cardiac stromal cell derived factor-1 alpha CXCR4 axis. *Circulation*, 116(6), 654–663. <https://doi.org/10.1161/CIRCULATIONAHA.106.672451>.
 129. Chen, J., Chemaly, E., Liang, L., Kho, C., Lee, A., Park, J., et al. (2010). Effects of CXCR4 gene transfer on cardiac function after ischemia-reperfusion injury. *The American Journal of Pathology*, 176(4), 1705–1715. <https://doi.org/10.2353/ajpath.2010.090451>.
 130. Dai, S., Yuan, F., Mu, J., Li, C., Chen, N., Guo, S., et al. (2010). Chronic AMD3100 antagonism of SDF-1alpha-CXCR4 exacerbates cardiac dysfunction and remodeling after myocardial infarction. *Journal of Molecular and Cellular Cardiology*, 49(4), 587–597. <https://doi.org/10.1016/j.yjmcc.2010.07.010>.
 131. Proulx, C., El-Helou, V., Gosselin, H., Clement, R., Gillis, M. A., Villeneuve, L., et al. (2007). Antagonism of stromal cell-derived factor-1alpha reduces infarct size and improves ventricular function after myocardial infarction. *Pflügers Archiv*, 455(2), 241–250. <https://doi.org/10.1007/s00424-007-0284-5>.
 132. Jujo, K., Hamada, H., Iwakura, A., Thorne, T., Sekiguchi, H., Clarke, T., et al. (2010). CXCR4 blockade augments bone marrow progenitor cell recruitment to the neovasculature and reduces mortality after myocardial infarction. *Proceedings of the National Academy of Sciences of the United States of America*, 107(24), 11008–11013. <https://doi.org/10.1073/pnas.0914248107>.
 133. Hao, H., Hu, S., Chen, H., Bu, D., Zhu, L., Xu, C., et al. (2017). Loss of endothelial CXCR7 impairs vascular homeostasis and cardiac remodeling after myocardial infarction: implications for cardiovascular drug discovery. *Circulation*, 135(13), 1253–1264. <https://doi.org/10.1161/CIRCULATIONAHA.116.023027>.
 134. Das, S., Goldstone, A. B., Wang, H., Farry, J., D'Amato, G., Paulsen, M. J., et al. (2019). A unique collateral artery development program promotes neonatal heart regeneration. *Cell*, 176(5), 1128–1142 e1118. doi:<https://doi.org/10.1016/j.cell.2018.12.023>.
 135. Dewald, O., Zymek, P., Winkelmann, K., Koerting, A., Ren, G., Abou-Khamis, T., et al. (2005). CCL2/Monocyte chemoattractant protein-1 regulates inflammatory responses critical to healing myocardial infarcts. *Circulation Research*, 96(8), 881–889. <https://doi.org/10.1161/01.RES.0000163017.13772.3a>.
 136. Ono, K., Matsumori, A., Furukawa, Y., Igata, H., Shioi, T., Matsushima, K., et al. (1999). Prevention of myocardial reperfusion injury in rats by an antibody against monocyte chemotactic and activating factor/monocyte chemoattractant protein-1. *Laboratory Investigation*, 79(2), 195–203.
 137. Tarzami, S. T., Cheng, R., Miao, W., Kitsis, R. N., & Berman, J. W. (2002). Chemokine expression in myocardial ischemia: MIP-2 dependent MCP-1 expression protects cardiomyocytes from cell death. *Journal of Molecular and Cellular Cardiology*, 34(2), 209–221. <https://doi.org/10.1006/jmcc.2001.1503>.
 138. Pinto, A. R., Ilinykh, A., Ivey, M. J., Kuwabara, J. T., D'Antoni, M. L., Debuque, R., et al. (2016). Revisiting cardiac cellular composition. *Circulation Research*, 118(3), 400–409. <https://doi.org/10.1161/CIRCRESAHA.115.307778>.
 139. Epelman, S., Lavine, K. J., Beaudin, A. E., Sojka, D. K., Carrero, J. A., Calderon, B., et al. (2014). Embryonic and adult-derived resident cardiac macrophages are maintained through distinct mechanisms at steady state and during inflammation. *Immunity*, 40(1), 91–104. <https://doi.org/10.1016/j.immuni.2013.11.019>.
 140. Epelman, S., Lavine, K. J., & Randolph, G. J. (2014). Origin and functions of tissue macrophages. *Immunity*, 41(1), 21–35. <https://doi.org/10.1016/j.immuni.2014.06.013>.
 141. Lavine, K. J., Epelman, S., Uchida, K., Weber, K. J., Nichols, C. G., Schilling, J. D., et al. (2014). Distinct macrophage lineages contribute to disparate patterns of cardiac recovery and remodeling in the neonatal and adult heart. *Proceedings of the National Academy of Sciences of the United States of America*, 111(45), 16029–16034. <https://doi.org/10.1073/pnas.1406508111>.
 142. Leid, J., Carrelha, J., Boukarabila, H., Epelman, S., Jacobsen, S. E., & Lavine, K. J. (2016). Primitive embryonic macrophages are required for coronary development and maturation. *Circulation Research*, 118(10), 1498–1511. <https://doi.org/10.1161/CIRCRESAHA.115.308270>.
 143. Bajpai, G., Bredemeyer, A., Li, W., Zaitsev, K., Koenig, A. L., Lokshina, I., et al. (2019). Tissue resident CCR2- and CCR2+ cardiac macrophages differentially orchestrate monocyte recruitment and fate specification following myocardial injury. *Circulation Research*, 124(2), 263–278. <https://doi.org/10.1161/CIRCRESAHA.118.314028>.
 144. Heidt, T., Courties, G., Dutta, P., Sager, H. B., Sebas, M., Iwamoto, Y., et al. (2014). Differential contribution of monocytes to heart macrophages in steady-state and after myocardial infarction. *Circulation Research*, 115(2), 284–295. <https://doi.org/10.1161/CIRCRESAHA.115.303567>.
 145. Frangogiannis, N. G., Mendoza, L. H., Ren, G., Akrivakis, S., Jackson, P. L., Michael, L. H., et al. (2003). MCSF expression is

- induced in healing myocardial infarcts and may regulate monocyte and endothelial cell phenotype. *American Journal of Physiology. Heart and Circulatory Physiology*, 285(2), H483–H492.
146. Sager, H. B., Hulsmans, M., Lavine, K. J., Moreira, M. B., Heidt, T., Courties, G., et al. (2016). Proliferation and recruitment contribute to myocardial macrophage expansion in chronic heart failure. *Circulation Research*, 119(7), 853–864. <https://doi.org/10.1161/CIRCRESAHA.116.309001>.
 147. Liehn, E. A., Piccinini, A. M., Koenen, R. R., Soehnlein, O., Adage, T., Fatu, R., et al. (2010). A new monocyte chemotactic protein-1/chemokine CC motif ligand-2 competitor limiting neointima formation and myocardial ischemia/reperfusion injury in mice. *Journal of the American College of Cardiology*, 56(22), 1847–1857. <https://doi.org/10.1016/j.jacc.2010.04.066>.
 148. Al-Amran, F. G., Manson, M. Z., Hanley, T. K., & Hainz, D. L. (2014). Blockade of the monocyte chemoattractant protein-1 receptor pathway ameliorates myocardial injury in animal models of ischemia and reperfusion. *Pharmacology*, 93(5-6), 296–302. <https://doi.org/10.1159/000363657>.
 149. Grisanti, L. A., Traynham, C. J., Repas, A. A., Gao, E., Koch, W. J., & Tilley, D. G. (2016). beta2-Adrenergic receptor-dependent chemokine receptor 2 expression regulates leukocyte recruitment to the heart following acute injury. *Proceedings of the National Academy of Sciences of the United States of America*, 113(52), 15126–15131. <https://doi.org/10.1073/pnas.1611023114>.
 150. Wang, J., Seo, M. J., Deci, M. B., Weil, B. R., Canty, J. M., & Nguyen, J. (2018). Effect of CCR2 inhibitor-loaded lipid micelles on inflammatory cell migration and cardiac function after myocardial infarction. *International Journal of Nanomedicine*, 13, 6441–6451. <https://doi.org/10.2147/IJN.S178650>.
 151. Leuschner, F., Dutta, P., Gorbato, R., Novobrantseva, T. I., Donahoe, J. S., Courties, G., et al. (2011). Therapeutic siRNA silencing in inflammatory monocytes in mice. *Nature Biotechnology*, 29(11), 1005–1010. <https://doi.org/10.1038/nbt.1989>.
 152. Lu, W., Xie, Z., Tang, Y., Bai, L., Yao, Y., Fu, C., et al. (2015). Photoluminescent mesoporous silicon nanoparticles with siCCR2 improve the effects of mesenchymal stromal cell transplantation after acute myocardial infarction. *Theranostics*, 5(10), 1068–1082. <https://doi.org/10.7150/thno.11517>.
 153. Kaikita, K., Hayasaki, T., Okuma, T., Kuziel, W. A., Ogawa, H., & Takeya, M. (2004). Targeted deletion of CC chemokine receptor 2 attenuates left ventricular remodeling after experimental myocardial infarction. *The American Journal of Pathology*, 165(2), 439–447. [https://doi.org/10.1016/S0002-9440\(10\)63309-3](https://doi.org/10.1016/S0002-9440(10)63309-3).
 154. Nahrendorf, M., Swirski, F. K., Aikawa, E., Stangenberg, L., Wurdinger, T., Figueiredo, J. L., et al. (2007). The healing myocardium sequentially mobilizes two monocyte subsets with divergent and complementary functions. *The Journal of Experimental Medicine*, 204(12), 3037–3047. <https://doi.org/10.1084/jem.20070885>.
 155. Gavrilin, M. A., Deucher, M. F., Boeckman, F., & Kolattukudy, P. E. (2000). Monocyte chemotactic protein 1 upregulates IL-1beta expression in human monocytes. *Biochemical and Biophysical Research Communications*, 277(1), 37–42. <https://doi.org/10.1006/bbrc.2000.3619>.
 156. Jiang, Y., Beller, D. I., Frenzl, G., & Graves, D. T. (1992). Monocyte chemoattractant protein-1 regulates adhesion molecule expression and cytokine production in human monocytes. *Journal of Immunology*, 148(8), 2423–2428.
 157. Sierra-Filardi, E., Nieto, C., Dominguez-Soto, A., Barroso, R., Sanchez-Mateos, P., Puig-Kroger, A., et al. (2014). CCL2 shapes macrophage polarization by GM-CSF and M-CSF: identification of CCL2/CCR2-dependent gene expression profile. *Journal of Immunology*, 192(8), 3858–3867. <https://doi.org/10.4049/jimmunol.1302821>.
 158. Frangogiannis, N. G., Dewald, O., Xia, Y., Ren, G., Haudek, S., Leucker, T., et al. (2007). Critical role of monocyte chemoattractant protein-1/CC chemokine ligand 2 in the pathogenesis of ischemic cardiomyopathy. *Circulation*, 115(5), 584–592.
 159. Schenk, S., Mal, N., Finan, A., Zhang, M., Kiedrowski, M., Popovic, Z., et al. (2007). Monocyte chemotactic protein-3 is a myocardial mesenchymal stem cell homing factor. *Stem Cells*, 25(1), 245–251. <https://doi.org/10.1634/stemcells.2006-0293>.
 160. Montecucco, F., Braunersreuther, V., Lenglet, S., Delattre, B. M., Pelli, G., Buatois, V., et al. (2012). CC chemokine CCL5 plays a central role impacting infarct size and post-infarction heart failure in mice. *European Heart Journal*, 33(15), 1964–1974. <https://doi.org/10.1093/eurheartj/ehr127>.
 161. Huang, Y., Wang, D., Wang, X., Zhang, Y., Liu, T., Chen, Y., et al. (2016). Abrogation of CC chemokine receptor 9 ameliorates ventricular remodeling in mice after myocardial infarction. *Scientific Reports*, 6, 32660. <https://doi.org/10.1038/srep32660>.
 162. Jiang, Y., Bai, J., Tang, L., Zhang, P., & Pu, J. (2015). Anti-CCL21 antibody attenuates infarct size and improves cardiac remodeling after myocardial infarction. *Cellular Physiology and Biochemistry*, 37(3), 979–990. <https://doi.org/10.1159/000430224>.
 163. Parisis, J. T., Adamopoulos, S., Venetsanou, K. F., Mentzikof, D. G., Karas, S. M., & Kremastinos, D. T. (2002). Serum profiles of C-C chemokines in acute myocardial infarction: possible implication in postinfarction left ventricular remodeling. *Journal of Interferon & Cytokine Research*, 22(2), 223–229. <https://doi.org/10.1089/107999002753536194>.
 164. Braunersreuther, V., Montecucco, F., Pelli, G., Galan, K., Proudfoot, A. E., Belin, A., et al. (2013). Treatment with the CC chemokine-binding protein Evasin-4 improves post-infarction myocardial injury and survival in mice. *Thrombosis and Haemostasis*, 110(4), 807–825. <https://doi.org/10.1160/TH13-04-0297>.
 165. Liehn, E. A., Merx, M. W., Postea, O., Becher, S., Djalali-Talab, Y., Shagdarsuren, E., et al. (2008). Ccr1 deficiency reduces inflammatory remodelling and preserves left ventricular function after myocardial infarction. *Journal of Cellular and Molecular Medicine*, 12(2), 496–506. <https://doi.org/10.1111/j.1582-4934.2007.00194.x>.
 166. Combadiere, C., Ahuja, S. K., Tiffany, H. L., & Murphy, P. M. (1996). Cloning and functional expression of CC CKR5, a human monocyte CC chemokine receptor selective for MIP-1(alpha), MIP-1(beta), and RANTES. *Journal of Leukocyte Biology*, 60(1), 147–152. <https://doi.org/10.1002/jlb.60.1.147>.
 167. Dobaczewski, M., Xia, Y., Bujak, M., Gonzalez-Quesada, C., & Frangogiannis, N. G. (2010). CCR5 signaling suppresses inflammation and reduces adverse remodeling of the infarcted heart, mediating recruitment of regulatory T cells. *The American Journal of Pathology*, 176(5), 2177–2187. <https://doi.org/10.2353/ajpath.2010.090759>.
 168. Zamilpa, R., Kanakia, R., Cigarroa, J. t., Dai, Q., Escobar, G. P., Martinez, H., et al. (2011). CC chemokine receptor 5 deletion impairs macrophage activation and induces adverse remodeling following myocardial infarction. *American Journal of Physiology. Heart and Circulatory Physiology*, 300(4), H1418–H1426. <https://doi.org/10.1152/ajpheart.01002.2010>.
 169. Xuan, W., Liao, Y., Chen, B., Huang, Q., Xu, D., Liu, Y., et al. (2011). Detrimental effect of fractalkine on myocardial ischaemia and heart failure. *Cardiovascular Research*, 92(3), 385–393. <https://doi.org/10.1093/cvr/cvr221>.
 170. Husberg, C., Nygard, S., Finsen, A. V., Damas, J. K., Frigessi, A., Oie, E., et al. (2008). Cytokine expression profiling of the myocardium reveals a role for CX3CL1 (fractalkine) in heart failure. *Journal of Molecular and Cellular Cardiology*, 45(2), 261–269.

171. Boag, S. E., Das, R., Shmeleva, E. V., Bagnall, A., Egred, M., Howard, N., et al. (2015). T lymphocytes and fractalkine contribute to myocardial ischemia/reperfusion injury in patients. *The Journal of Clinical Investigation*, 125(8), 3063–3076. <https://doi.org/10.1172/JCI80055>.
172. Xu, B., Qian, Y., Zhao, Y., Fang, Z., Tang, K., Zhou, N., et al. (2019). Prognostic value of fractalkine/CX3CL1 concentration in patients with acute myocardial infarction treated with primary percutaneous coronary intervention. *Cytokine*, 113, 365–370. <https://doi.org/10.1016/j.cyto.2018.10.006>.
173. Gu, X., Xu, J., Yang, X. P., Peterson, E., & Harding, P. (2015). Fractalkine neutralization improves cardiac function after myocardial infarction. *Experimental Physiology*, 100(7), 805–817. <https://doi.org/10.1113/EP085104>.
174. Draganova, L., Redgrave, R., Tual-Chalot, S., Marsh, S., Arthur, H., & Spyridopoulos, I. (2019). BS31 The role of fractalkine and CX3CR1-expressing lymphocytes during myocardial ischaemia/reperfusion injury. *Heart*, 105(Suppl 6), A160–A160. <https://doi.org/10.1136/heartjnl-2019-BCS.194>.
175. Huang, S., & Frangogiannis, N. G. (2018). Anti-inflammatory therapies in myocardial infarction: failures, hopes and challenges. *British Journal of Pharmacology*, 175(9), 1377–1400. <https://doi.org/10.1111/bph.14155>.
176. Chung, E. S., Miller, L., Patel, A. N., Anderson, R. D., Mendelsohn, F. O., Traverse, J., et al. (2015). Changes in ventricular remodelling and clinical status during the year following a single administration of stromal cell-derived factor-1 non-viral gene therapy in chronic ischaemic heart failure patients: the STOP-HF randomized phase II trial. *European Heart Journal*, 36(33), 2228–2238. <https://doi.org/10.1093/eurheartj/ehv254>.
177. Agarwal, U., Ghalayini, W., Dong, F., Weber, K., Zou, Y. R., Rabbany, S. Y., et al. (2010). Role of cardiac myocyte CXCR4 expression in development and left ventricular remodeling after acute myocardial infarction. *Circulation Research*, 107(5), 667–676. <https://doi.org/10.1161/CIRCRESAHA.110.223289>.
178. Liehn, E. A., Tuchscheerer, N., Kanzler, I., Drechsler, M., Fraemohs, L., Schuh, A., et al. (2011). Double-edged role of the CXCL12/CXCR4 axis in experimental myocardial infarction. *Journal of the American College of Cardiology*, 58(23), 2415–2423. <https://doi.org/10.1016/j.jacc.2011.08.033>.
179. Hayasaki, T., Kaikita, K., Okuma, T., Yamamoto, E., Kuziel, W. A., Ogawa, H., et al. (2006). CC chemokine receptor-2 deficiency attenuates oxidative stress and infarct size caused by myocardial ischemia-reperfusion in mice. *Circulation Journal*, 70(3), 342–351. <https://doi.org/10.1253/circj.70.342>.
180. Hayashidani, S., Tsutsui, H., Shiomi, T., Ikeuchi, M., Matsusaka, H., Suematsu, N., et al. (2003). Anti-monocyte chemoattractant protein-1 gene therapy attenuates left ventricular remodeling and failure after experimental myocardial infarction. *Circulation*, 108(17), 2134–2140. <https://doi.org/10.1161/01.CIR.0000092890.29552.22>.
181. Morimoto, H., Hirose, M., Takahashi, M., Kawaguchi, M., Ise, H., Kolattukudy, P. E., et al. (2008). MCP-1 induces cardioprotection against ischaemia/reperfusion injury: role of reactive oxygen species. *Cardiovascular Research*, 78(3), 554–562. <https://doi.org/10.1093/cvr/cvn035>.
182. Shen, B., Li, J., Gao, L., Zhang, J., & Yang, B. (2013). Role of CC-chemokine receptor 5 on myocardial ischemia-reperfusion injury in rats. *Molecular and Cellular Biochemistry*, 378(1-2), 137–144. <https://doi.org/10.1007/s11010-013-1604-z>.

Publisher's Note Springer Nature remains neutral with regard to jurisdictional claims in published maps and institutional affiliations.



The role of Smad2 and Smad3 in regulating homeostatic functions of fibroblasts in vitro and in adult mice

Shuaibo Huang, Bijun Chen, Claudio Humeres, Linda Alex, Anis Hanna, Nikolaos G. Frangogiannis*

The Wilf Family Cardiovascular Research Institute, Department of Medicine (Cardiology), Albert Einstein College of Medicine, Bronx, NY, United States of America

ARTICLE INFO

Keywords

Fibroblast
Myocardium
Extracellular matrix
TGF- β
Smad
Collagen

ABSTRACT

The heart contains an abundant fibroblast population that may play a role in homeostasis, by maintaining the extracellular matrix (ECM) network, by regulating electrical impulse conduction, and by supporting survival and function of cardiomyocytes and vascular cells. Despite an explosion in our understanding of the role of fibroblasts in cardiac injury, the homeostatic functions of resident fibroblasts in adult hearts remain understudied. TGF- β -mediated signaling through the receptor-activated Smads, Smad2 and Smad3 critically regulates fibroblast function. We hypothesized that baseline expression of Smad2/3 in fibroblasts may play an important role in cardiac homeostasis. Smad2 and Smad3 were constitutively expressed in normal mouse hearts and in cardiac fibroblasts. In cultured cardiac fibroblasts, Smad2 and Smad3 played distinct roles in regulation of baseline ECM gene synthesis. Smad3 knockdown attenuated collagen I, collagen IV and fibronectin mRNA synthesis and reduced expression of the matricellular protein thrombospondin-1. Smad2 knockdown on the other hand attenuated expression of collagen V mRNA and reduced synthesis of fibronectin, periostin and versican. In vivo, inducible fibroblast-specific Smad2 knockout mice and fibroblast-specific Smad3 knockout mice had normal heart rate, preserved cardiac geometry, ventricular systolic and diastolic function, and normal myocardial structure. Fibroblast-specific Smad3, but not Smad2 loss modestly but significantly reduced collagen content. Our findings suggest that fibroblast-specific Smad3, but not Smad2, may play a role in regulation of baseline collagen synthesis in adult hearts. However, at least short term, these changes do not have any impact on homeostatic cardiac function.

1. Introduction

The adult mammalian heart contains a large population of fibroblasts [1–3] located in the cardiac interstitium. Resident cardiac fibroblasts can be activated in response to a wide range of injurious stimuli and play an important role in cardiac repair [4] [5], while contributing to adverse remodeling of the injured ventricle [6–10]. A growing body of evidence challenges the notion that fibroblasts are unidimensional cells that simply serve to produce extracellular matrix (ECM) proteins. Fibroblasts exhibit remarkable transcriptomic heterogeneity [11], and can sense microenvironmental cues, undergoing phenotypic and functional changes [12,13]. In response to stimulation with neurohumoral signals, cytokines, growth factors, and components of the ECM, fibroblasts can acquire inflammatory, matrix-synthetic, matrix-degrading, or angiogenic phenotypes [4,14,15] [5,16], serving as key orchestrators of reparative, fibrogenic and angiogenic cellular responses.

The members of the Transforming Growth Factor (TGF)- β superfamily are crucial activators of fibroblasts in injured and remodeling hearts [17,18]. In vitro, stimulation of cardiac fibroblasts with TGF- β s trig-

gers myofibroblast conversion, and promotes a matrix-preserving phenotype, inducing synthesis of structural collagens and upregulating expression of tissue inhibitors of metalloproteinases (TIMPs) [19,20]. Following binding to their receptors, TGF- β s act through signaling cascades involving intracellular effectors, the receptor-activated Smads (R-Smads) [4,21,22], or by transducing Smad-independent pathways [23–25]. Although both Smad2 and Smad3 are activated in fibroblasts infiltrating infarcted and remodeling hearts, cell-specific loss-of-function studies suggested that Smad3 signaling plays a more important role in fibroblast activation in models of myocardial infarction and left ventricular pressure overload [4,21,26,27]. In contrast, myofibroblast-specific Smad2 loss had only transient effects on the reparative and fibrotic response to myocardial infarction [26].

Considering the evidence suggesting involvement of fibroblasts in cardiac repair and remodeling [9,28], the focus on the role of fibroblasts in myocardial injury models is well-justified. However, cardiac fibroblasts may also be implicated in myocardial homeostasis, preserving structural integrity, facilitating impulse conduction, and supporting cardiomyocyte and microvascular function. The cardiac intersti-

* Corresponding author at: Albert Einstein College of Medicine, 1300 Morris Park Avenue Forchheimer G46B, Bronx, NY 10461, United States of America.

E-mail address: nikolaos.frangogiannis@einstein.yu.edu (N.G. Frangogiannis)

tial ECM, produced and maintained predominantly by fibroblast-like cells, provides essential structural support to the myocardium, preserving the mechanical properties of the ventricle. Moreover, the interstitial ECM proteins may transduce key signals to cardiomyocytes, promoting survival and supporting contractile function. Thus, baseline activity of cardiac fibroblasts may be important in cardiac homeostasis.

We hypothesized that fibroblast-specific Smad2 and/or Smad3 signaling may be important in regulation of baseline fibroblast function in adult mouse hearts. In order to test this hypothesis, we generated mice with inducible Smad2 and Smad3 disruption in quiescent collagen-expressing fibroblasts, and we performed *in vitro* experiments investigating the effects of Smad2/Smad3 loss on baseline ECM gene expression in cultured cardiac fibroblasts.

2. Materials and methods

2.1. Smad2 and Smad3 knockdown experiments in cultured cardiac fibroblasts

In order to examine the effects of Smad2 and Smad3 knockdown on cardiac fibroblast gene expression, fibroblasts were isolated and cultured from normal mouse (C57/BL6J) hearts as previously described [20,29]. Freshly dissected whole mouse hearts were minced and incubated in Liberase TM (Roche, 540119001) supplemented with RNase I (Invitrogen™, AM2294) at recommended concentration for 30 min at 37 °C. Tissues were disrupted by pipetting up and down with a 1000 µL tip. Cell suspensions were seeded in culture dishes (Corning, Cat#: 353003, Falcon® 100 mm × 15 mm) with DMEM/F12 (Gibco™, 11320082) plus 10% FBS (Gibco™, 10100147), without antibiotic-antimycotic added. After 48 h incubation at 37 °C in 5% carbon dioxide, the medium and nonadherent cells were aspirated and fresh medium was added instead. Cells were ready to passage after another 48 h incubation, when they grew to 80%–90% confluence. Mouse cardiac fibroblasts at passage 1 were seeded at 80% confluence (100 mm dishes) in DMEM/F12 + 10% FBS and were either transfected with 50 nM ON-TARGET plus mouse Smad2 siRNA, Smad3 siRNA, Smad2 siRNA + Smad3 siRNA, or transfected with a non-silencing control siRNA (Dharmacon) using Lipofectamine® 3000 Reagent (ThermoFisher Scientific). The ON-TARGET modification is shown to dramatically decrease the off-target effects of the siRNA [30]. Fibroblasts cultured in plates were transfected with Smad2, Smad3, Smad2 + Smad3, or control scrambled siRNA for 72 h in DMEM/F12 with 10% FBS. Afterwards, cells were rinsed twice with DPBS, and then 1 mL Trizol solution was added in each dish for cell lysis and RNA extraction. Extracted RNA was used for PCR array analysis ($n = 4/\text{group}$).

2.2. Generation of conditional fibroblast-specific Smad2 and Smad3 KO mice

All animal studies were approved by the Institutional Animal Care and Use Committee at Albert Einstein College of Medicine. All animals were housed in the Albert Einstein College of Medicine animal institute (Ullman Building), a disease-free rodent facility. Animal care was in strict accordance with AAALAC and NIH guidelines. In order to study the role of fibroblast-specific Smad2 and Smad3 in homeostasis, Col1 α 2-CreERT mice (purchased from The Jackson Laboratory, Stock No: 029235) were bred with Smad2 fl/fl mice (purchased from The Jackson Laboratory, Stock No: 022074) or Smad3 fl/fl mice (from our colony) [4] to generate Col1 α 2-Cre;Smad2 fl/fl animals, Col1 α 2-Cre;Smad3 fl/fl animals and corresponding Smad2 fl/fl, Smad3 fl/fl controls. The Col1 α 2-CreERT line has been previously demonstrated to selectively target cardiac fibroblasts [31–33]. Tamoxifen (Sigma, T5648) was dissolved in 5% ethanol and 95% corn oil to make a 20 mg/mL stock solution. Tamoxifen was administered intraperi-

toneally every 24 h for 5 consecutive days (75 mg/kg/day) to generate mice with inducible Smad2 loss (FS2KO, Col1 α 2-Cre; Smad2 fl/fl animals treated with tamoxifen), animals with inducible Smad3 loss (FS3KO, Col1 α 2-Cre; Smad3 fl/fl animals treated with tamoxifen), and corresponding tamoxifen-treated Smad2 fl/fl and Smad3 fl/fl controls. Mice were 4 weeks old during initiation of tamoxifen treatment and were followed up for 8 weeks. Both male (M) and female (F) mice were studied. A total of 27 Smad2 fl/fl (M, $n = 13$, F, $n = 14$), 25 FS2KO (M, $n = 12$, F, $n = 13$), 20 Smad3 fl/fl (M, $n = 11$, F, $n = 9$), and 21 FS3KO mice (M, $n = 11$, F, $n = 10$) were studied.

2.3. Isolation and culture of cardiac fibroblasts from FS2KO, FS3KO and control mice, protein extraction and western blotting

In order to confirm loss of Smad2 and Smad3 in cardiac fibroblasts, cells were isolated from Smad2 fl/fl, FS2KO, Smad3 fl/fl, and FS3KO mice at 4 weeks after tamoxifen injection and cultured in DMEM/F12 (Gibco™, 11320082) with 10% FBS (Gibco™, 10100147) as described above. Briefly, medium was changed every 48 h and experiments were performed on fibroblasts at passage 1, when cells grew to 80%–90% confluence (100 mm dish). Protein was extracted from cardiac fibroblasts as previously described [34]. Western blotting was performed using antibodies to Smad2 (Cell Signaling Technology, 5339), Smad3 (Cell Signaling Technology, 9523), and GAPDH (Santa Cruz, 25778). The gels were imaged by ChemiDoc™ MP System (Bio Rad) and analyzed by Image Lab 3.0 software (Bio Rad).

2.4. Echocardiography

Echocardiographic studies were performed in FS2KO, FS3KO and corresponding Smad2 fl/fl and Smad3 fl/fl control animals at baseline, and 4 weeks and 8 weeks after tamoxifen administration, using the Vevo 2100 system (VisualSonics, Toronto ON), as previously described [35]. Parasternal long-axis (PSLAX) M-mode was used for measurement of systolic and diastolic ventricular and wall diameters. PSLAX IVS tool was used to measure the end-diastolic thickness of the left ventricular anterior wall (LVAWd), and the end-diastolic thickness of the left ventricular posterior wall (LVPWd), The left ventricular end-diastolic volume (LVEDV) and the left ventricular end-systolic volume (LVESV) were measured as indicators of dilative remodeling. The left ventricular ejection fraction (LVEF = $[(\text{LVEDV} - \text{LVESV}) / \text{LVEDV}] \times 100\%$) was measured for assessment of systolic ventricular function. Dimensions of the ascending aorta were measured using PSLAX-B mode images. Electrocardiography was used to calculate heart rate from > 10 cardiac cycles. For assessment of diastolic function, we performed Doppler echocardiography and tissue Doppler imaging (TDI), as previously described [36]. Transmittal LV inflow velocities were measured by pulsed-wave Doppler. Peak early E wave (E) and late A wave (A) filling velocities were measured. TDI was obtained by placing a 1.0-mm sample volume at the medial annulus of the mitral valve. Analysis was performed for the early (e') and late (a') diastolic velocity. The mitral inflow E velocity-to-tissue Doppler e' wave velocity ratio (E/ e') was calculated to assess diastolic function. All Doppler spectra were recorded for 3–5 cardiac cycles at a sweep speed of 100 mm/s. The echocardiographic offline analysis was performed by a sonographer blinded to the study groups.

2.5. Assessment of Smad2 and Smad3 expression and phosphorylation in normal mouse tissues and in cultured cardiac fibroblasts

In order to assess baseline expression and phosphorylation levels of Smad2 and Smad3, organs (heart, lung, spleen, liver, kidney, skin, pancreas and thymus) were harvested from 8 week-old WT C57Bl6J mice. Protein was extracted as previously described [34]. Halt™ Phos-

phatase Inhibitor Cocktail (Thermo Scientific™, 78420) was used to preserve the phosphorylation state of proteins during and after tissue lysis or protein extraction. Fibroblasts isolated from WT C57/BL6J and Smad3 KO mouse hearts [19] were cultured in 100 mm dishes with DMEM/F12 plus 10% FBS. When cells at passage 1 grew to 80%–90% confluence, medium was changed to DMEM/F12 without serum overnight. TGF- β 1 (10 ng/mL, 30 min) was added as positive control for phosphorylation of Smad2 and Smad3. Western blotting was performed using antibodies to p-Smad2 (Cell Signaling Technology, 3108), Smad2 (Cell Signaling Technology, 5339), pSmad3 (Cell Signaling Technology, 9520), Smad3 (Cell Signaling Technology, 9523), and GAPDH (Santa Cruz, 25778).

2.6. Histology and machine learning-based quantitative analysis of myocardial collagen content

For histopathological analysis murine tissues were fixed in zinc-formalin (Z-fix; Anatech, Battle Creek, MI), and embedded in paraffin. In order to assess collagen content, sections were stained with picosirius red to label the collagen fibers. Picosirius red-stained slides were scanned using the bright field settings of Zen 2.6 Pro software and the Zeiss Imager M2 microscope (Carl Zeiss Microscopy, New York NY). Using default algorithms of the Intellesis Trainable Segmentation module of Zen 2.6 Pro software (Carl Zeiss Microscopy, New York NY), a model was trained on multiple fields of different regions of the baseline myocardium to segment SR stained collagen fibers. Red fibrillar staining representing interstitial and perivascular collagen was considered the object of interest, while the rest of myocardium was considered as background. Automatic analysis of 10 fields from 3 different sections from each mouse heart was performed using the trained model. Collagen content was expressed as the percentage of the picosirius red-stained area to the total myocardial area.

2.7. RNA extraction, qPCR and qPCR array analysis

TRIzol (Invitrogen™) based method was used to extract total RNA from cultured fibroblasts at passage 1 according to the manufacturer's instructions. RNA concentration was measured by a spectrophotometer at 260 nm and 280 nm. For each reverse transcription reaction, 1 μ g of total RNA was converted to cDNA using iScript™ cDNA synthesis kit (Bio-Rad, 1708890). Quantitative PCR (qPCR) was performed using SsoFast EvaGreen Supermix reagent (Bio-Rad) on the CFX384™ Real-Time PCR Detection System (Bio-Rad) and the thermal cycler apparatus from Bio-Rad follow the manufacturer's recommendations: enzyme was activated at 95 °C for 30 s, followed by 40 cycles of 5 s at 95 °C, 5 s at 60 °C. In order to confirm loss of Smad3 and Smad2 in vivo, qPCR was performed with the following primer pairs: GAPDH forward 5'-AGGTCGGTGTGAACGGATTG-3', GAPDH reverse 5'-TGTAGACCATGTAGTTGAGGTCA-3', Smad2 forward 5'-ATCTTGCCATTCACCTCCGCC-3', Smad2 reverse 5'-TCTGAGTGGTGATGGCTTCTC -3', Smad3 forward 5'-CACGCAGAACGTGAACACC-3', and Smad3 reverse 5'-GGCAGTAGATAACGTGAGGGA-3'. The housekeeping gene GAPDH was used as internal control. The qPCR procedure was repeated three times in independent runs; gene expression levels were calculated using the Δ CT method.

In order to assess gene expression of extracellular matrix-related genes in cultured fibroblasts following Smad2 or Smad3 knockdown, we used the RT² Profiler™ PCR Array Mouse Extracellular Matrix & Adhesion Molecules (QIAGEN, PAMM-013ZE) according to manufacturer's protocol. RNA extraction was performed using Trizol. A total of 400 ng RNA was reverse-transcribed into cDNA using the RT² first strand kit. The same thermal profile conditions were used for all primers sets: 95 °C for 10 min, 40 cycles at 95 °C for 15 s followed at 60 °C for 1 min. The data obtained were exported to SABiosciences

PCR array web-based template where it was analyzed using the Δ CT method.

2.8. Statistical analysis

For comparisons of two groups unpaired, 2-tailed Student's *t*-test using (when appropriate) Welch's correction for unequal variances was performed. The Shapiro-Wilk test was used to assess normality of the distributions. The Mann-Whitney test was used for comparisons between 2 groups that did not show Gaussian distribution. For comparisons of multiple groups, 1-way ANOVA was performed followed by Tukey's multiple comparison test. For comparisons of several groups with control Dunnett's test was used. The Kruskal-Wallis test, followed by Dunn's multiple comparison post-test was used when one or more groups did not show Gaussian distribution.

3. Results

3.1. Constitutive expression of Smad2 and Smad3 in normal mouse tissues and in cultured cardiac fibroblasts

We used western blotting to study the expression of Smad2 and Smad3 in normal mouse tissues and in cultured cardiac fibroblasts. All tissues studied showed significant constitutive expression of Smad2 (Fig. 1A). The thymus, pancreas, skin, spleen and lung had the highest levels of Smad2 expression (Fig. 1A, C). Constitutive expression of p-Smad2 was low in all organs studied. The skin, lung and heart exhibited identifiable bands of p-Smad2 (Fig. 1A). Smad3 was also ubiquitously expressed in mouse tissues (Fig. 1B, D). The liver, kidney and heart had the highest levels of Smad3 expression (Fig. 1B, D). Constitutive p-Smad3 expression was low in all organs studied. Cultured cardiac fibroblasts had high levels of baseline Smad2 and Smad3 expression, but low levels of Smad2 and Smad3 phosphorylation (Fig. 1A–B). As expected, TGF- β 1 stimulation triggered Smad2 and Smad3 phosphorylation in cardiac fibroblasts. Specificity of the antibodies was confirmed using Smad3 KO cells (Fig. 1A–B).

3.2. Smad3 mediates collagen I transcription, whereas Smad2 stimulates collagen V synthesis in cultured cardiac fibroblasts

qPCR demonstrated that Smad2 siRNA KD (for 72 h) in cultured serum-stimulated cardiac fibroblasts specifically reduced Smad2 levels without affecting Smad3 expression (Fig. 2A). A PCR array was used to examine the effects of Smad2 and Smad3 KD on matrix gene synthesis (Table 1). Smad3 KD markedly attenuated Smad3 synthesis without affecting Smad2 levels (Fig. 2B). Combined Smad2 and Smad3 knock-down markedly reduced levels of both Smad2 and Smad3 (Fig. 2A–B). Smad3, but not Smad2 KD significantly attenuated collagen I α 1 expression (Fig. 2C) mRNA expression. Neither Smad2 nor Smad3 KD significantly affected transcription of collagen II α 1 and collagen III α 1 (Fig. 2D–E). Combined Smad2 and Smad3 KD attenuated synthesis of collagen I α 1 and collagen II α 1, but did not affect collagen III α 1 levels (Fig. 2C–E). Smad2, but not Smad3 KD significantly reduced collagen V α 1 expression (Fig. 2F), whereas collagen VI levels were not affected by Smad2, Smad3 or combined Smad2 and Smad3 KD (Fig. 2G).

3.3. Smad3, but not Smad2 mediates collagen IV α 1 mRNA synthesis in cardiac fibroblasts

Next, we examined the effects of Smad2 and Smad3 on expression of basement membrane genes by cardiac fibroblasts. Smad3 KD, but not Smad2 KD attenuated collagen IV α 1 synthesis; however, effects on collagen IV α 2 and collagen IV α 3 gene expression did not reach statistical significance (Fig. 3A–C).

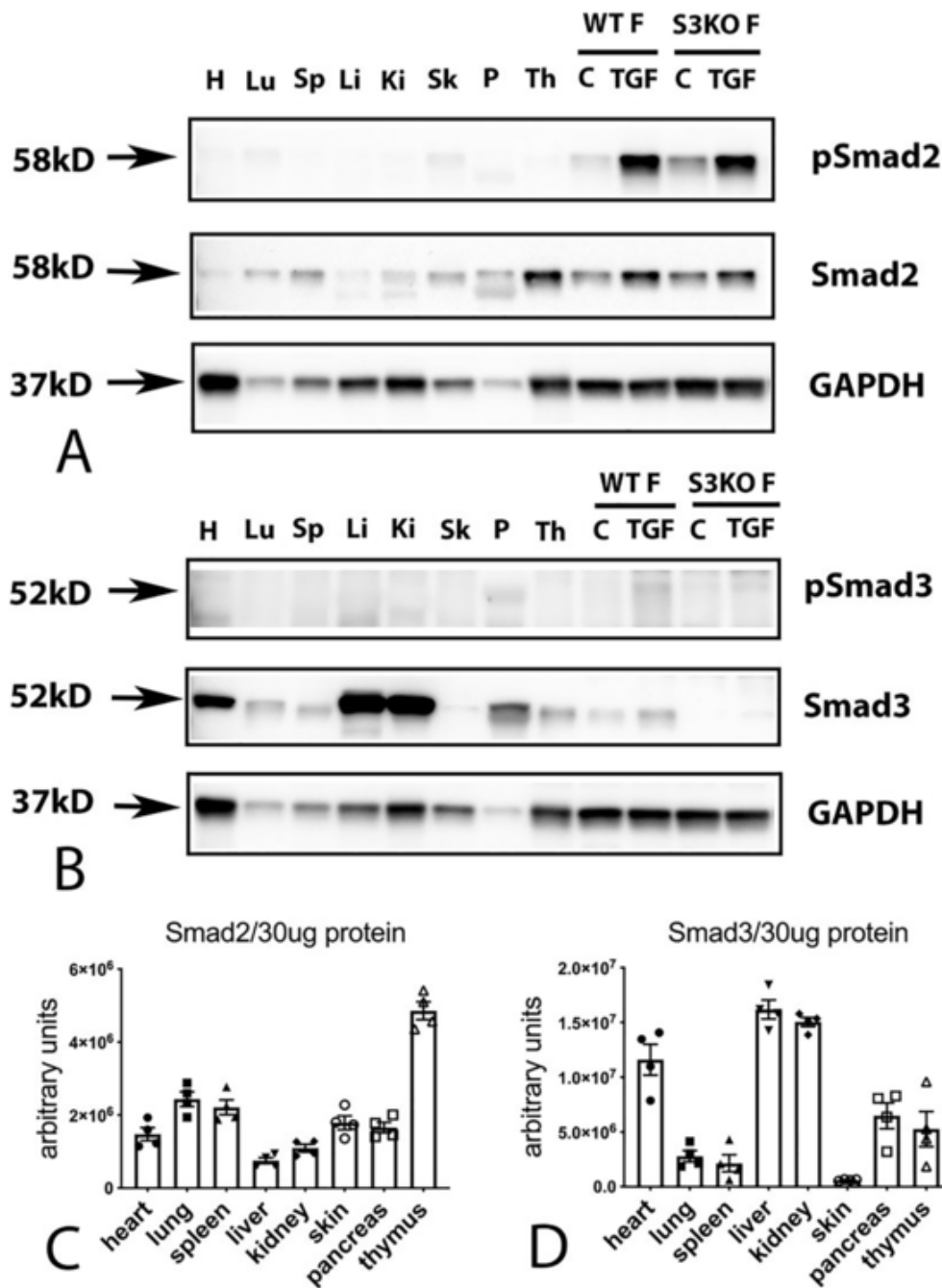


Fig. 1. Constitutive expression of Smad2 and Smad3 in mouse tissues and in cultured cardiac fibroblasts. All mouse tissues had significant constitutive expression of Smad2 (A). The thymus (Th), pancreas (P), skin (Sk), spleen (Sp) and lung (Lu) had the highest levels of Smad2 expression (A, C). Constitutive expression of p-Smad2 was low in all organs studied (A). The skin (Sk), lung (Lu) and heart (H) had identifiable bands of p-Smad2 (A). Smad3 was also ubiquitously expressed in mouse tissues (B, D). The liver (Li), kidney (Ki) and heart (H) had the highest levels of Smad3 expression (B, D). Constitutive p-Smad3 expression was low in all organs studied. Relative expression of Smad2 (C) and Smad3 (D) was normalized to the total amount of protein, due to marked differences in baseline expression of the housekeeping protein GAPDH between tissues. Cultured cardiac fibroblasts (WT F) had high levels of baseline Smad2 and Smad3 expression, but low levels of Smad2 and Smad3 phosphorylation (A–B). TGF- β 1 stimulation (TGF) triggered Smad2 and Smad3 phosphorylation in cardiac fibroblasts. Specificity of the antibodies was confirmed using Smad3 KO cells (S3KO F) (A–B). $n = 4$.

3.4. Smad2 restrains laminin α 2 chain mRNA synthesis

Smad3 KD had no significant effects on laminin α 1, α 2 and β 2 expression (Fig. 3D–F). In contrast, Smad2 KD significantly increased laminin α 2 transcription (Fig. 3E) without affecting laminin α 1 and β 2 levels (Fig. 3D, F).

3.5. Role of Smad2 and Smad3 in expression of specialized matrix proteins by cultured cardiac fibroblasts

Next, we examined the role of Smad2 and Smad3 in expression of fibronectin and matricellular genes by cardiac fibroblasts. Smad2, Smad3 and combined Smad2/Smad3 KD attenuated expression of fibronectin in cardiac fibroblasts (Fig. 4A), suggesting that both Smad2 and Smad3 are involved in mediating fibronectin transcription in car-

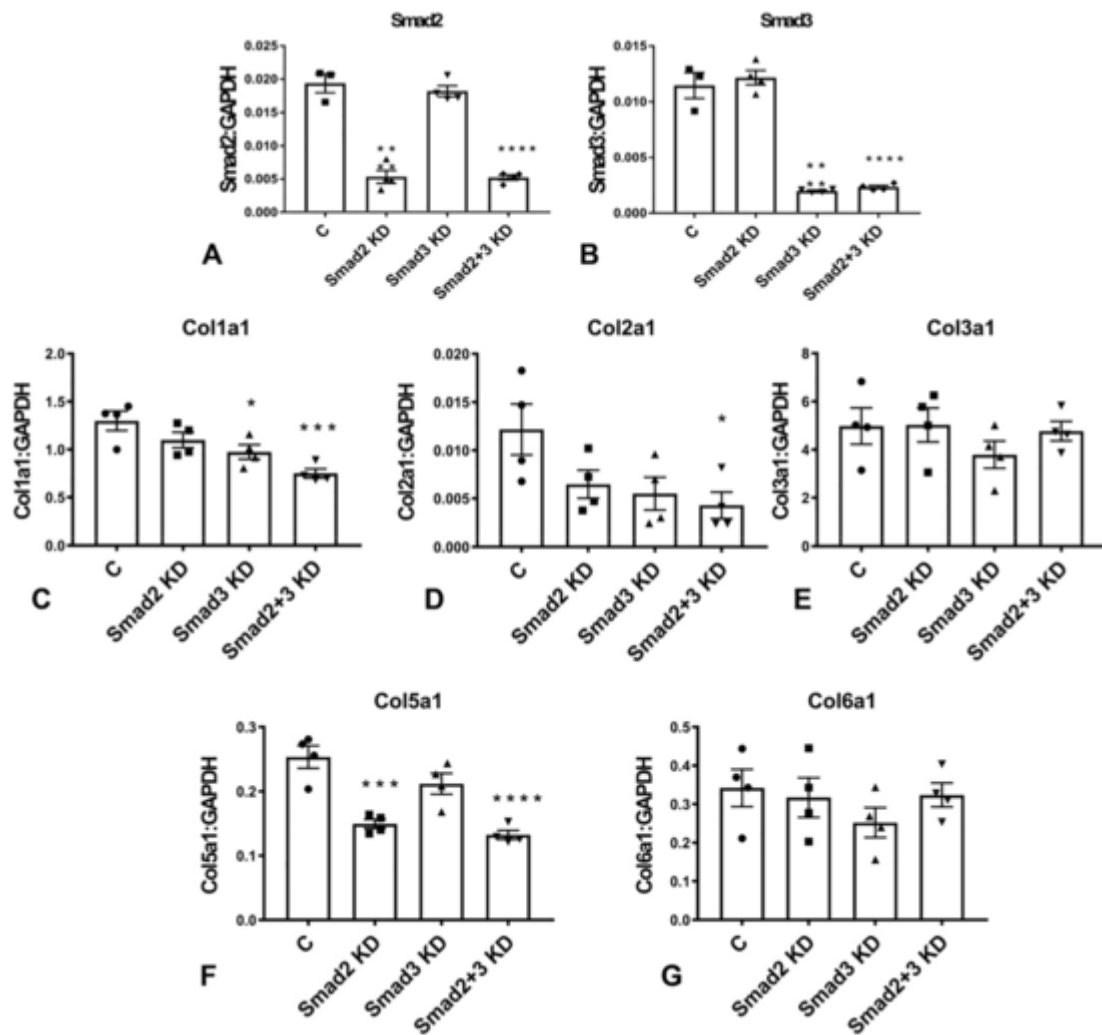


Fig. 2. Effects of Smad2 and Smad3 on baseline collagen gene transcription in cardiac fibroblasts. The effectiveness and specificity of Smad2 and Smad3 KD was demonstrated using qPCR (A–B). Full PCR array data on the effects of Smad2 and Smad3 KD on ECM and adhesion molecules gene synthesis are provided in Table 1. Smad3, but not Smad2 KD significantly attenuated collagen I a1 mRNA expression (C). Neither Smad2 nor Smad3 KD affected transcription of collagen II a1 and collagen III a1 levels (D–E). Smad2, but not Smad3 KD significantly reduced collagen V a1 expression (F), whereas collagen VI levels were not affected by Smad2, Smad3 or combined Smad2 and Smad3 KD (G). (* $p < 0.05$, ** $p < 0.01$, *** $p < 0.001$, **** $p < 0.0001$ vs control (C), $n = 4$ /group, ANOVA followed by Dunnett's multiple comparisons test).

diac fibroblasts. In contrast, Smad2 and Smad3 had distinct effects on synthesis of matricellular genes. Tenascin-C expression was significantly reduced in Smad2 and Smad2/Smad3 KD cells, but not in Smad3 KD fibroblasts (Fig. 4B). Effects of Smad2 and Smad3 KD on SPARC expression were not statistically significant (Fig. 4C). Smad3 KD significantly increased osteopontin/Spp1 mRNA expression (Fig. 4D). Smad2KD and combined Smad2/Smad3 KD, but not Smad3 KD attenuated expression of periostin (Fig. 4E). Versican expression was attenuated in Smad2, but not in Smad3 KD cells (Fig. 4F). Thrombospondin (TSP)-1/Thbs1 was the highest expressed TSP in cultured cardiac fibroblasts. Smad3 KD and combined Smad2/Smad3 KD, but not Smad2 KD significantly reduced TSP-1 synthesis (Fig. 4G). In contrast, effects of Smad2 and Smad3 KD on TSP-2/Thbs2 expression did not reach statistical significance (Fig. 4H). Low levels of TSP-3/Thbs3 expression were noted in cardiac fibroblasts; Smad2 KD, but not Smad3 KD increased TSP-3 expression levels (Fig. 4I).

3.6. Effects of Smad2 and Smad3 on fibroblast expression of proteases

Cardiac fibroblasts expressed high levels of several proteases, including members of the ADAMTS (a disintegrin and metallopro-

teinase with thrombospondin motifs) and matrix metalloproteinase (MMP) families. Smad3 loss significantly reduced baseline mRNA expression of ADAMTS1 and ADAMTS5. In contrast, Smad2 KD did not affect ADAMTS1 levels, but significantly increased ADAMTS5 expression (Fig. 5A–B). Smad2 and Smad3 had distinct effects in regulation of MMP and TIMP mRNA synthesis. Smad2 KD increased MMP1a, MMP2 and MMP14 mRNA expression, suggesting that Smad2-mediated actions restrain MMP synthesis (Fig. 5C–E). In contrast, Smad3 KD had no effects on MMP1a, but reduced MMP2 expression and increased MMP14 synthesis (Fig. 5C–E). Smad3, but not Smad2 disruption significantly reduced TIMP-3 expression (Fig. 5F).

3.7. Effects of Smad2 and Smad3 on fibroblast adhesion molecule expression

Expression of adhesion molecules by fibroblasts modulates their matrix-synthetic and matrix remodeling properties [37]. Both Smad2 and Smad3 mediated ICAM-1 synthesis by cardiac fibroblasts. Smad2 KD, Smad3 KD and cells with combined Smad2 and Smad3 KD had significantly attenuated expression of ICAM-1 (Fig. 6A). Fibroblasts also exhibited significant expression of NCAM-1 (Fig. 6B) and VCAM-1 (

Table 1
Effects of Smad2, Smad3 and combined Smad2/Smad3 loss on extracellular matrix gene synthesis by cardiac fibroblasts.

Gene name	Gene symbol	Smad2 KD		Smad3 KD		Smad2 + Smad3 KD	
		Fold	p-Value	Fold	p-Value	Fold	p-Value
A disintegrin-like and metalloproteinase (reprolysin type) with thrombospondin type 1 motif, 1	<i>Adams1</i>	1.20	0.1026	0.57	0.0004 [†]	1.07	0.9612
A disintegrin-like and metalloproteinase (reprolysin type) with thrombospondin type 1 motif, 2	<i>Adams2</i>	1.00	> 0.9999	0.79	0.4414	0.95	0.9259
A disintegrin-like and metalloproteinase (reprolysin type) with thrombospondin type 1 motif, 5	<i>Adams5</i>	1.79	0.0011 [†]	0.46	0.0172 [†]	1.21	0.5691
A disintegrin-like and metalloproteinase (reprolysin type) with thrombospondin type 1 motif, 8	<i>Adams8</i>	0.71	0.3369	1.99	0.0009 [†]	0.91	0.9268
CD44 antigen	<i>Cd44</i>	0.85	0.0811	0.57	0.0006 [†]	0.64	0.002 [†]
Cadherin 1	<i>Cdh1</i>	ND	-	ND	-	ND	-
Cadherin 2	<i>Cdh2</i>	0.78	0.0617	0.77	0.0421 [†]	0.83	0.1401
Cadherin 3	<i>Cdh3</i>	0.44	0.0342 [†]	1.40	0.2144	0.62	0.0955
Cadherin 4	<i>Cdh4</i>	ND	-	ND	-	ND	-
Contactin 1	<i>Cntn1</i>	0.82	0.9399	0.63	0.8804	1.31	0.9942
Collagen type I, alpha1	<i>Col1a1</i>	0.86	0.2259	0.75	0.034 [†]	0.58	0.001 [†]
Collagen type II, alpha1	<i>Col2a1</i>	0.53	0.1216	0.42	0.0645	0.34	0.028 [†]
Collagen type III, alpha1	<i>Col3a1</i>	1.02	> 0.9999	0.76	0.4218	0.99	0.99
Collagen type IV, alpha1	<i>Col4a1</i>	0.89	0.2537	0.57	0.0001 [†]	0.79	0.0168 [†]
Collagen type IV, alpha2	<i>Col4a2</i>	0.97	0.8428	0.86	0.2308	0.85	0.0984
Collagen type IV, alpha3	<i>Col4a3</i>	1.23	0.9918	0.66	0.5862	0.81	0.7044
Collagen type V, alpha1	<i>Col5a1</i>	0.59	0.0003 [†]	0.83	0.1002	0.53	< 0.0001 [†]
Collagen type VI, alpha1	<i>Col6a1</i>	0.93	0.9558	0.73	0.3592	0.98	0.9818
Connective tissue growth factor	<i>Ctgf</i>	0.96	0.9705	0.73	0.1052	0.58	0.0115 [†]
Catenin (Cadherin associated protein), alpha1	<i>Ctnna1</i>	0.96	0.8678	0.90	0.3221	1.00	0.9981
Catenin (Cadherin associated protein), alpha2	<i>Ctnna2</i>	1.19	0.9997	0.58	0.3288	1.03	0.8801
Catenin (Cadherin associated protein), beta1	<i>Ctnnb1</i>	1.00	> 0.9999	0.95	0.8839	1.20	0.0875
Extracellular matrix protein 1	<i>Ecm1</i>	0.92	0.6037	1.20	0.0914	1.26	0.0351 [†]
Elastin microfibril interfacer 1	<i>Emilin1</i>	1.13	0.8245	0.75	0.2225	0.86	0.4733
Ectonucleoside triphosphate diphosphohydrolase 1	<i>Entpd1</i>	0.88	0.7972	0.66	0.1511	0.90	0.9441
Fibulin 1	<i>Fbn1</i>	0.63	0.2275	0.93	0.9068	0.90	0.8722
Fibronectin 1	<i>Fn1</i>	0.71	0.0011 [†]	0.76	0.0061 [†]	0.63	0.0002 [†]
Hyaluronan and proteoglycan link protein 1	<i>Hapln1</i>	4.11	0.0337 [†]	3.29	0.4624	1.20	> 0.9999
Hemolytic complement	<i>Hc</i>	1.32	0.7713	1.30	0.79	0.81	0.8101
Intercellular adhesion molecule 1	<i>Icam1</i>	0.66	0.0003 [†]	0.81	0.0217 [†]	0.71	0.0011 [†]
Integrin alpha2	<i>Itga2</i>	0.72	0.1937	0.63	0.0375 [†]	0.77	0.2425
Integrin alpha3	<i>Itga3</i>	1.23	0.5389	1.27	0.419	1.07	0.9919
Integrin alpha4	<i>Itga4</i>	0.85	0.0618	0.54	< 0.0001 [†]	0.59	< 0.0001 [†]
Integrin alpha5	<i>Itga5</i>	0.84	0.1638	1.07	0.689	0.90	0.5138
Integrin alpha1, epithelial-associated	<i>Itgae</i>	ND	-	ND	-	ND	-
Integrin alpha L	<i>Itgal</i>	2.13	0.0003 [†]	0.39	0.0185 [†]	0.95	0.977
Integrin alpha M	<i>Itgam</i>	1.27	0.4943	1.33	0.3749	1.18	0.7086
Integrin alpha V	<i>Itgav</i>	0.86	0.1827	1.03	0.964	0.95	0.8274
Integrin alpha X	<i>Igtax</i>	1.42	0.278	1.30	0.5194	1.30	0.4876
Integrin beta1	<i>Itgb1</i>	0.69	< 0.0001 [†]	0.96	0.7791	0.78	0.0017 [†]
Integrin beta2	<i>Itgb2</i>	1.45	0.1434	1.06	0.983	1.12	0.8774
Integrin beta3	<i>Itgb3</i>	0.75	0.2061	0.92	0.7783	0.85	0.3933
Integrin beta4	<i>Itgb4</i>	0.88	0.3398	0.93	0.553	0.92	0.4494
Laminin, alpha1	<i>Lama1</i>	0.69	0.9534	0.94	> 0.9999	0.59	0.6767
Laminin, alpha2	<i>Lama2</i>	1.91	0.003 [†]	1.11	0.9619	1.36	0.2962
Laminin, alpha3	<i>Lama3</i>	0.86	0.7634	0.37	0.2565	0.78	0.6245
Laminin, beta2	<i>Lamb2</i>	1.36	0.2233	1.13	0.8831	1.46	0.1447
Laminin, beta3	<i>Lamb3</i>	0.94	> 0.9999	0.55	0.4203	0.65	0.5299
Laminin, gamma1	<i>Lamc1</i>	1.14	0.1251	1.06	0.6642	0.96	0.8442
Matrix metalloproteinase 10	<i>Mmp10</i>	0.77	0.3023	1.21	0.9662	0.57	0.0399 [†]
Matrix metalloproteinase 11	<i>Mmp11</i>	1.34	0.1113	1.42	0.0496 [†]	1.46	0.0414 [†]
Matrix metalloproteinase 12	<i>Mmp12</i>	1.37	0.8689	1.90	0.2164	1.60	0.4346
Matrix metalloproteinase 13	<i>Mmp13</i>	1.56	0.0317 [†]	0.54	0.0739	0.99	> 0.9999
Matrix metalloproteinase 14	<i>Mmp14</i>	1.27	0.0205 [†]	1.31	0.0108 [†]	1.44	0.001 [†]
Matrix metalloproteinase 15	<i>Mmp15</i>	0.51	0.0092 [†]	1.03	0.9927	0.72	0.1573

Table 1 (Continued)

Gene name	Gene symbol	Smad2 KD		Smad3 KD		Smad2 + Smad3 KD	
		Fold	p-Value	Fold	p-Value	Fold	p-Value
Matrix metalloproteinase 1, alpha	<i>Mmp1a</i>	2.23	<0.0001 [†]	0.88	0.7969	1.94	0.0004 [†]
Matrix metalloproteinase 2	<i>Mmp2</i>	1.42	0.0098 [†]	0.65	0.0085 [†]	0.96	0.7422
Matrix metalloproteinase 3	<i>Mmp3</i>	1.52	0.5465	1.08	0.9911	2.01	0.1364
Matrix metalloproteinase 7	<i>Mmp7</i>	ND	–	ND	–	ND	–
Matrix metalloproteinase 8	<i>Mmp8</i>	1.90	0.1009	1.26	0.9574	1.13	0.9999
Matrix metalloproteinase 9	<i>Mmp9</i>	1.91	0.1663	1.52	0.3911	1.24	0.9028
Neural cell adhesion molecule 1	<i>Ncam1</i>	0.56	0.0071 [†]	0.85	0.4708	0.33	0.0003 [†]
Neural cell adhesion molecule 2	<i>Ncam2</i>	ND	–	ND	–	ND	–
Platelet/endothelial cell adhesion molecule 1	<i>Pecam1</i>	1.01	0.9991	1.11	0.6413	1.20	0.1953
Periostin, osteoblast specific factor	<i>Postn</i>	0.62	0.0017 [†]	0.86	0.2503	0.38	<0.0001 [†]
Selectin, endothelial cell	<i>Sele</i>	0.83	0.6299	1.22	0.5334	1.71	0.0076 [†]
Selectin, lymphocyte	<i>Sell</i>	ND	–	ND	–	ND	–
Selectin, platelet	<i>Selp</i>	0.99	0.9978	0.69	0.0193 [†]	1.02	>0.9999
Sarcoglycan, epsilon	<i>Sgce</i>	1.57	0.0127 [†]	0.98	0.9993	1.27	0.357
Secreted acidic cysteine rich glycoprotein	<i>Sparc</i>	1.19	0.1279	0.92	0.6975	1.05	0.9429
Sparc/osteonectin, cwcv and kazal-like domains proteoglycan 1	<i>Spock1</i>	ND	–	ND	–	ND	–
Secreted phosphoprotein 1	<i>Spp1</i>	1.59	0.6204	2.31	0.028 [†]	1.39	0.7043
synaptotagmin 1	<i>Syt1</i>	1.72	0.8436	1.12	0.9061	0.92	0.9725
Transforming growth factor, beta induced	<i>Tgfb1</i>	0.68	0.0226 [†]	1.27	0.0538 [†]	0.72	0.0414 [†]
Thrombospondin 1	<i>Thbs1</i>	0.90	0.4343	0.76	0.0224 [†]	0.70	0.0045 [†]
Thrombospondin 2	<i>Thbs2</i>	0.52	0.0658	0.89	0.8188	0.56	0.0745
Thrombospondin 3	<i>Thbs3</i>	1.66	0.0525 [†]	1.30	0.8955	0.97	>0.9999
Tissue inhibitor of metalloproteinase 1	<i>Timp1</i>	1.10	0.8511	0.81	0.5181	0.99	>0.9999
Tissue inhibitor of metalloproteinase 2	<i>Timp2</i>	1.12	0.7962	1.51	0.0167 [†]	1.59	0.0067 [†]
Tissue inhibitor of metalloproteinase 3	<i>Timp3</i>	0.77	0.3058	0.43	0.0078 [†]	0.30	0.0016 [†]
Tenascin C	<i>Tnc</i>	0.64	0.0067 [†]	0.80	0.1059	0.72	0.0196 [†]
Vascular cell adhesion molecule 1	<i>Vcam1</i>	1.87	0.0008 [†]	1.00	0.9944	1.62	0.0221 [†]
Versican	<i>Vcan</i>	0.61	0.0092 [†]	1.06	0.9172	0.84	0.3146
Vitronectin	<i>Vtn</i>	ND	–	ND	–	ND	–

ND-not detected.

[†] P value <0.05.

Fig. 6C). Smad2 KD, but not Smad3 KD reduced NCAM-1 mRNA expression. In contrast, Smad2 KD increased VCAM-1 mRNA levels, suggesting that Smad2 signaling may restrain VCAM-1 synthesis. CD44 has been critically implicated in fibroblast activation [38], serving as a ligand for hyaluronan [39] and osteopontin [40], and accentuating TGF- β signaling. Smad3 KD, but not Smad2 KD significantly attenuated CD44 expression in cardiac fibroblasts (Fig. 6D).

3.8. Effects of Smad2 and Smad3 on *Ecm1* and *emilin1* expression

The extracellular matrix protein ECM1 is upregulated in aging hearts and has been suggested to act as a fibroblast activator [41]. Cardiac fibroblasts synthesized significant amounts of ECM1 mRNA. Neither Smad2 nor Smad3 KD had significant effects on ECM1 expression; however, combined KD of Smad2 and Smad3 increased ECM1 mRNA levels (Fig. 6E). Emilin-1 is a member of the emilin family of extracellular matrix proteins, involved in elastogenesis and in regulation of fibroblast proliferation. Cardiac fibroblasts expressed significant amounts of EMILIN-1; however, Smad2 and Smad3 KD did not affect EMILIN-1 expression (Fig. 6F).

3.9. Generation of mice with fibroblast-specific Smad2 and Smad3 loss

Our in vitro studies suggested an important role of Smad2 and Smad3 in regulating matrix gene transcription in cardiac fibroblasts cultured in serum. In order to test the in vivo role of Smad2 and Smad3 in regulating structure and function of the adult heart, we generated mice with inducible fibroblast-specific loss of Smad2 and

Smad3 (FS2KO and FS3KO mice respectively) using the Col1 α 2-CreERT driver. In order to document cell-specific loss of Smad2 and Smad3, cardiac fibroblasts were harvested from the hearts of FS2KO, Smad2 fl/fl, FS3KO and Smad3 fl/fl mice, 4 weeks after tamoxifen injection. Subsequently, hearts were digested with Liberase and cell suspensions were seeded in dishes with DMEM/F12 plus 10% FBS. Medium was changed every 48 h until fibroblasts grew to 80%–90% confluence. Documentation of Smad2 and Smad3 loss were performed on cells at passage 1. FS2KO cardiac fibroblasts had a significant 50% reduction in Smad2 mRNA and protein expression, when compared with cardiac fibroblasts harvested from Smad2 fl/fl hearts (Fig. 7A–C). In contrast, fibroblasts from FS3KO and Smad3 fl/fl mice had comparable Smad2 expression levels (Fig. 7A, D–E). FS3KO mice had a statistically significant 60% reduction in Smad3 mRNA and protein levels (Fig. 7F, I–J). Smad3 expression was comparable between FS2KO and Smad2 fl/fl cardiac fibroblasts (Fig. 7F, G–H).

3.10. FS2KO mice have normal baseline cardiac geometry, and preserved systolic and diastolic function

In order to examine whether fibroblast-specific Smad2 disruption affects baseline cardiac geometry and function, we performed echocardiographic analysis in FS2KO and Smad2 fl/fl mice at baseline and 4–8 weeks after tamoxifen injection. Male and female FS2KO mice had comparable left ventricular ejection fraction, LVEDV and LVESV with corresponding Smad2 fl/fl controls (Fig. 8A–F). End-diastolic left ventricular anterior wall thickness was comparable between groups in both male and female mice (Fig. 8G–H). Female FS2KO mice had a mod-

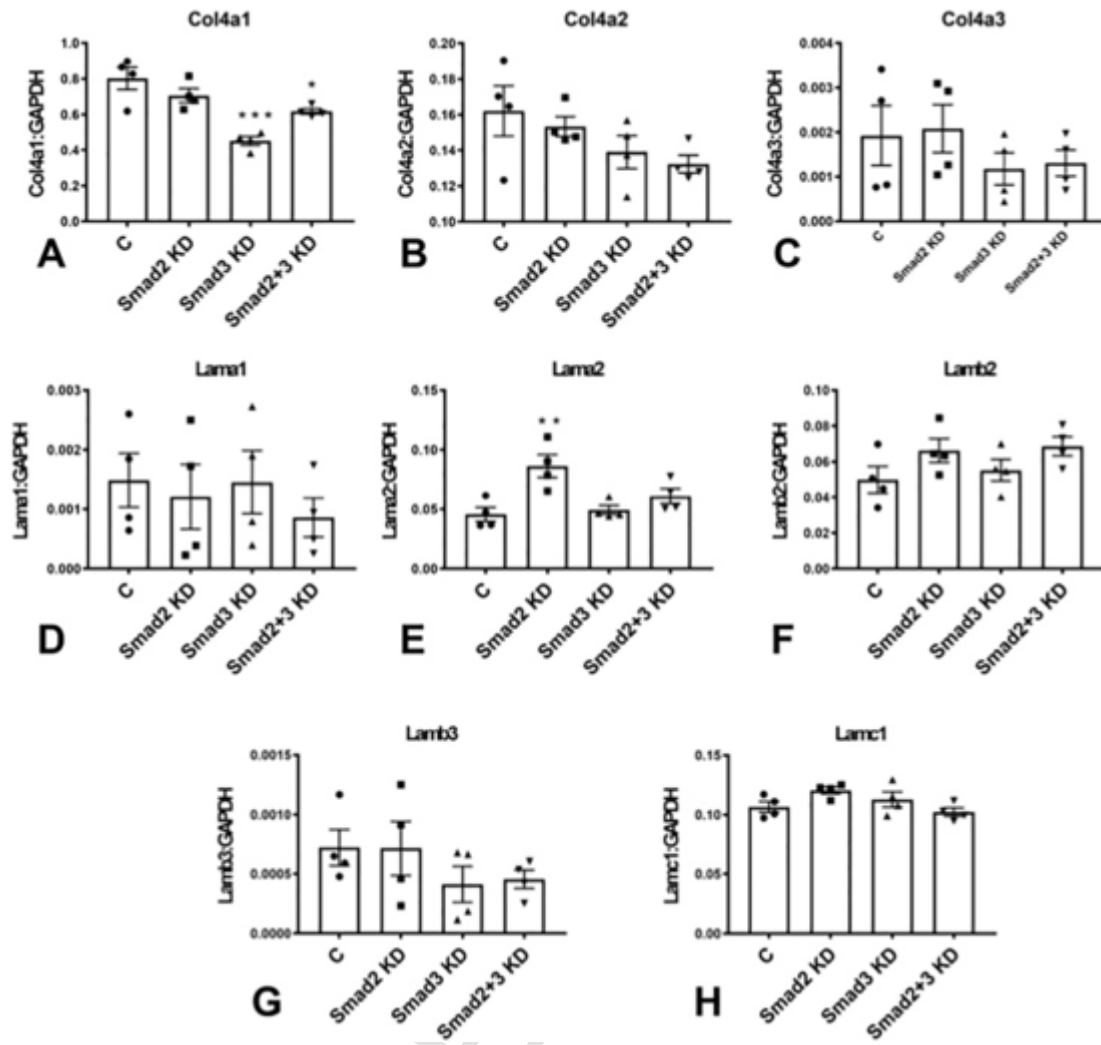


Fig. 3. Effects of Smad2 and Smad3 KD on fibroblast expression of basement membrane genes. Smad3 KD, but not Smad2 KD attenuated collagen IV a1 synthesis (A); however, effects on collagen IV a2 and collagen IV a3 gene expression did not reach statistical significance (B–C). Smad3 KD had no significant effects on laminin α 1, α 2 and β 2 mRNA expression (D–F). In contrast, Smad2 KD significantly increased laminin α 2 transcription (E) without affecting laminin α 1 and β 2 levels (D, F). (* $p < 0.05$, ** $p < 0.01$, *** $p < 0.001$ vs control (C), $n = 4$ /group, ANOVA followed by Dunnett's multiple comparisons test).

est but statistically significant reduction in left ventricular posterior wall thickness (* $p < 0.05$), when compared with age- and sex-matched Smad2 fl/fl controls (Fig. 8J). Dimensions of the ascending aorta were comparable between groups (Fig. 8K–L). No significant differences in heart rate were noted (Fig. 8M–N). Tissue Doppler imaging showed that FS2KO mice and corresponding Smad2 fl/fl controls had comparable E/E' ratio, suggesting that Smad2 loss in cardiac fibroblasts does not significantly affect baseline diastolic function (Fig. 8O–P).

3.11. FS3KO mice have normal left ventricular geometry and preserved systolic and diastolic function

In order to examine the effects of fibroblast-specific Smad3 disruption on cardiac geometry and function, we compared echocardiographic endpoints between FS3KO and Smad3 fl/fl mice at baseline and 4–8 weeks after tamoxifen injection. Male and female FS3KO mice had comparable left ventricular ejection fraction, LVEDV, LVESV, and end-diastolic left ventricular anterior and posterior wall thickness with corresponding Smad3 fl/fl controls (Fig. 9A–J). Dimensions of the ascending aorta (Fig. 9K–L) and heart rate (Fig. 9M–N) were also comparable between groups. Tissue Doppler imaging showed that FS3KO mice and corresponding Smad3 fl/fl controls had comparable E/E' ratio, sug-

gesting that Smad3 loss in cardiac fibroblasts does not significantly affect baseline diastolic function (Fig. 9O–P).

3.12. Fibroblast-specific Smad3, but not Smad2, loss reduces collagen content in uninjured myocardium

In order to examine the effects of fibroblast-specific Smad2 and Smad3 on the extracellular matrix network, we stained myocardial sections with Sirius red to label collagen fibers. 8 weeks after tamoxifen injection, FS2KO and FS3KO mice appeared to have normal patterns of endomyocardial, perimysial and perivascular collagen (Fig. 10A–H). In order to perform unbiased quantitative analysis of collagen content with validated a machine learning approach using Zen intellesis software (Fig. 10I–K). Quantitation of collagen content showed that FS2KO and Smad2 fl/fl controls had comparable myocardial collagen content (Fig. 10L). In contrast, FS3KO mice had a modest, but significant reduction in myocardial collagen content when compared with Smad3 fl/fl animals (Fig. 10M), suggesting that Smad3 may play a role in regulation of tissue collagen content under homeostatic conditions. In order to examine whether these changes are associated with alterations in fibroblast expression of matrix genes, we compared matrix gene expression between fibroblasts harvested from FS3KO and FS2KO mice and corre-

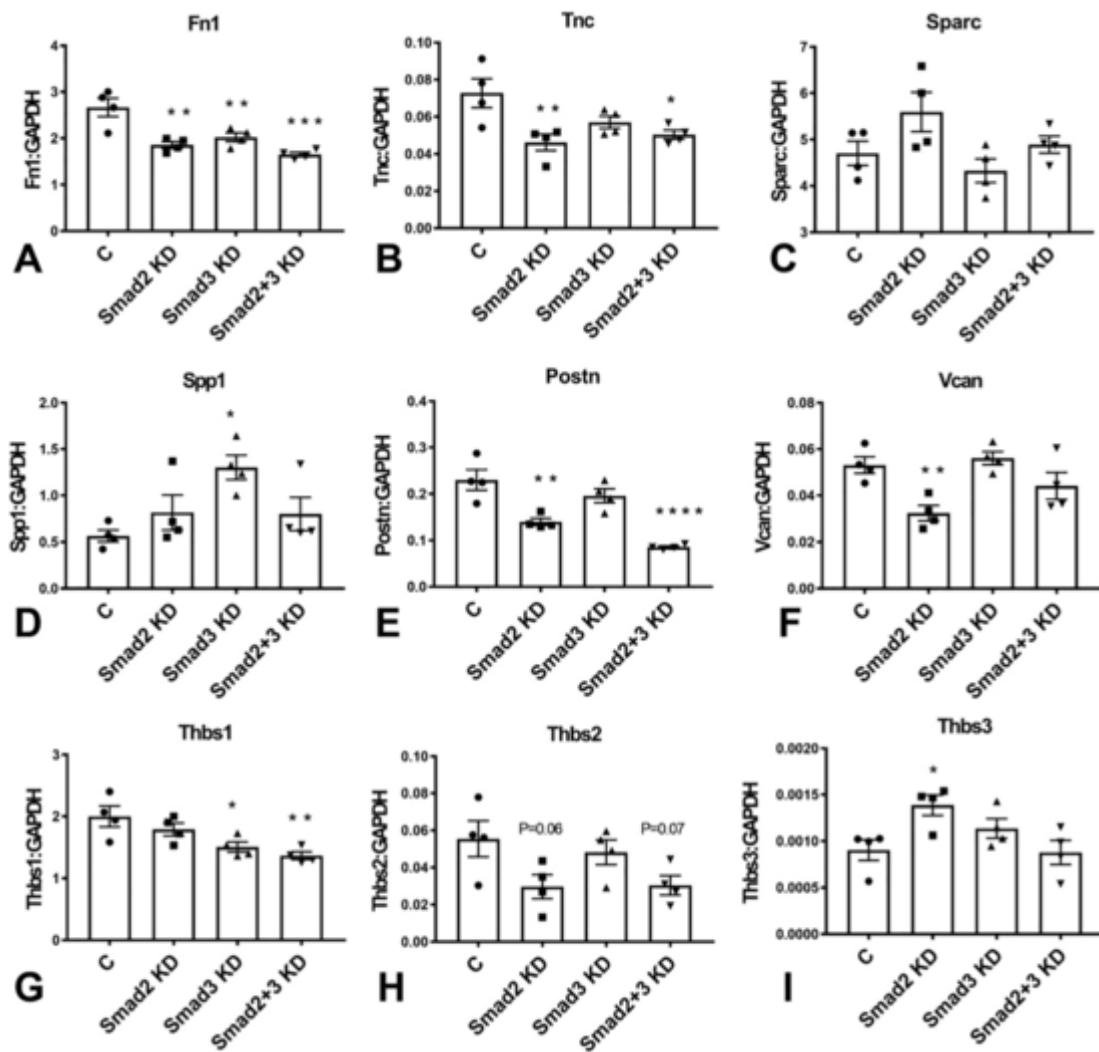


Fig. 4. Effects of Smad2 and Smad3 on fibroblast expression of fibronectin and matricellular genes. Smad2, Smad3 and combined Smad2/Smad3 KD attenuated expression of fibronectin mRNA (*Fn1*) in cardiac fibroblasts (A). Tenascin-C (*Tnc*) expression was significantly reduced in Smad2 and Smad2/Smad3 KD cells, but not in Smad3 KD fibroblasts (B). Effects of Smad2 and Smad3 KD on *SPARC* expression were not statistically significant (C). Smad3 KD significantly increased osteopontin/*Spp1* mRNA expression (D). Smad2KD and combined Smad2/Smad3 KD, but not Smad3 KD attenuated expression of periostin (*Postn*, E). Versican (*Vcan*) expression was attenuated in Smad2, but not in Smad3 KD cells (F). Smad3 KD and combined Smad2/Smad3 KD, but not Smad2 KD significantly reduced TSP-1 synthesis (G). In contrast, effects of Smad2 and Smad3 KD on TSP-2/*Thbs2* expression did not reach statistical significance (H). Smad2 KD, but not Smad3 KD increased TSP-3/*Thbs3* expression levels (I). (* $p < 0.05$, ** $p < 0.01$, *** $p < 0.001$, **** $p < 0.0001$ vs. control (C), $n = 4$ /group, ANOVA followed by Dunnett's multiple comparisons test).

sponding controls (Fig. 11, Tables 2 and 3). Cardiac fibroblasts from FS3KO mice had significantly reduced baseline expression of Col2a1 (Fig. 11C), Col4a1 (Fig. 11G), Col4a2 (Fig. 11I), thrombospondin-1 (Fig. 11M) and TIMP3 (Fig. 11O), and trends towards decreased expression levels of Col1a1, Col3a1 and Col5a1 that did not reach statistical significance (Fig. 11A, E, K). These findings supported the notion that fibroblast Smad3 plays a role in regulation of baseline matrix synthesis in normal adult hearts. In contrast, fibroblasts from FS2KO only exhibited a modest but significant reduction in TSP-1 expression levels (Fig. 11N), without any significant changes in expression levels of any other matrix genes (Fig. 11). Thus, the findings of the fibroblast-specific analysis of gene expression were consistent with the histological quantification of collagen, suggesting that Smad3, but not Smad2, may play a role in regulation of baseline matrix gene expression in adult mice.

4. Discussion

Our study reports for the first time that Smad2 and Smad3 play important and distinct roles in regulation of baseline ECM gene synthesis in cultured cardiac fibroblasts. Moreover, in adult mouse hearts fibro-

last-specific Smad3, but not Smad2 is involved in regulation of collagen content. Although mice with fibroblast-specific Smad3 disruption had reduced myocardial collagen content and exhibited attenuated expression of several ECM genes in cardiac fibroblasts, these perturbations had no short-term consequences on left ventricular function.

4.1. Smad2 and Smad3 signaling activate distinct aspects of the ECM transcriptome

Both Smad2 and Smad3 have been suggested to transduce critical TGF- β -induced activating signals in fibroblasts. We have previously demonstrated that in cultured cardiac fibroblasts, Smad3 signaling stimulates TGF- β -driven fibroblast to myofibroblast conversion [19], and mediates, at least in part, the matrix-synthetic and matrix-preserving fibroblast response triggered by TGF- β [19,21]. Pro-fibrotic effects of Smad3 have also been reported in renal [42], lung [43] and dermal fibroblasts [44]. In contrast, the effects of Smad2 on fibroblast phenotype have been less consistent. Some studies have reported a role for Smad2 in mediating TGF- β -driven ECM gene synthesis by renal fibroblasts [45]. Other investigations suggested that Smad2 is not involved

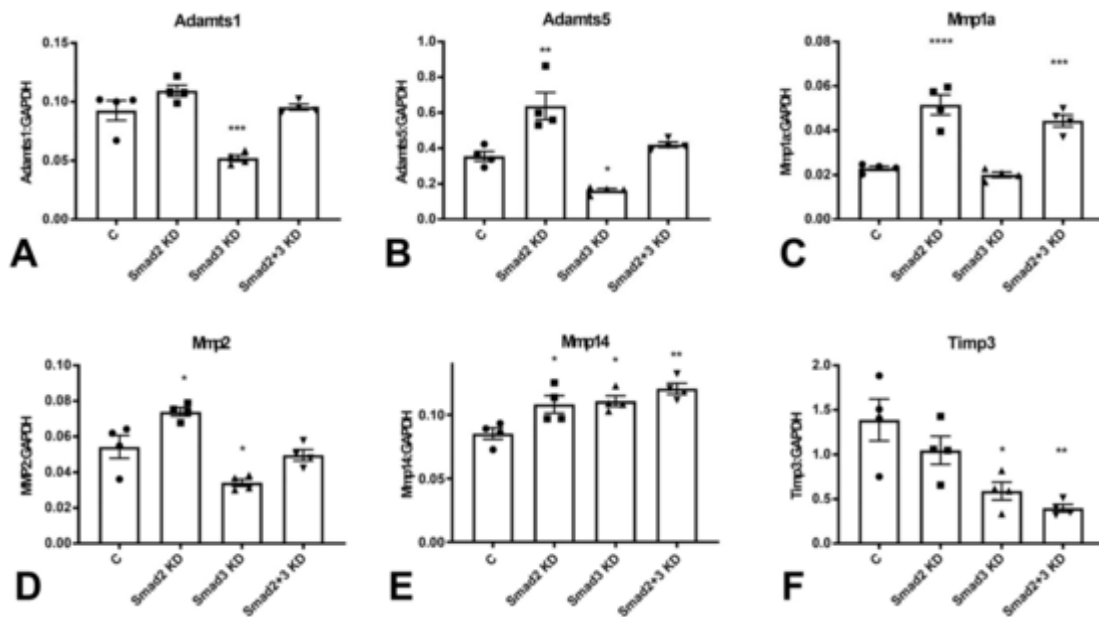


Fig. 5. Effects of Smad2 and Smad3 on fibroblast expression of ADAMTS and MMP family members. Smad3 KD significantly reduced *Adamts1* (A) and *Adamts5* (B) mRNA expression levels. In contrast, Smad2 KD had no effects on *Adamts1* expression and accentuated *Adamts5* synthesis (A–B). Smad2 KD increased expression of *MMP1a* (C), and *MMP2* (D). In contrast, Smad3 KD had no effects on *MMP1a* expression, and reduced *MMP2* levels (C–D). Smad2 and Smad3 KD significantly increased *MMP14* expression (E). *TIMP3* levels were markedly reduced following Smad3 KD (F). (* $p < 0.05$, ** $p < 0.01$, *** $p < 0.001$, **** $p < 0.0001$, vs. control (C), $n = 4$ /group, ANOVA followed by Dunnett's multiple comparisons test).

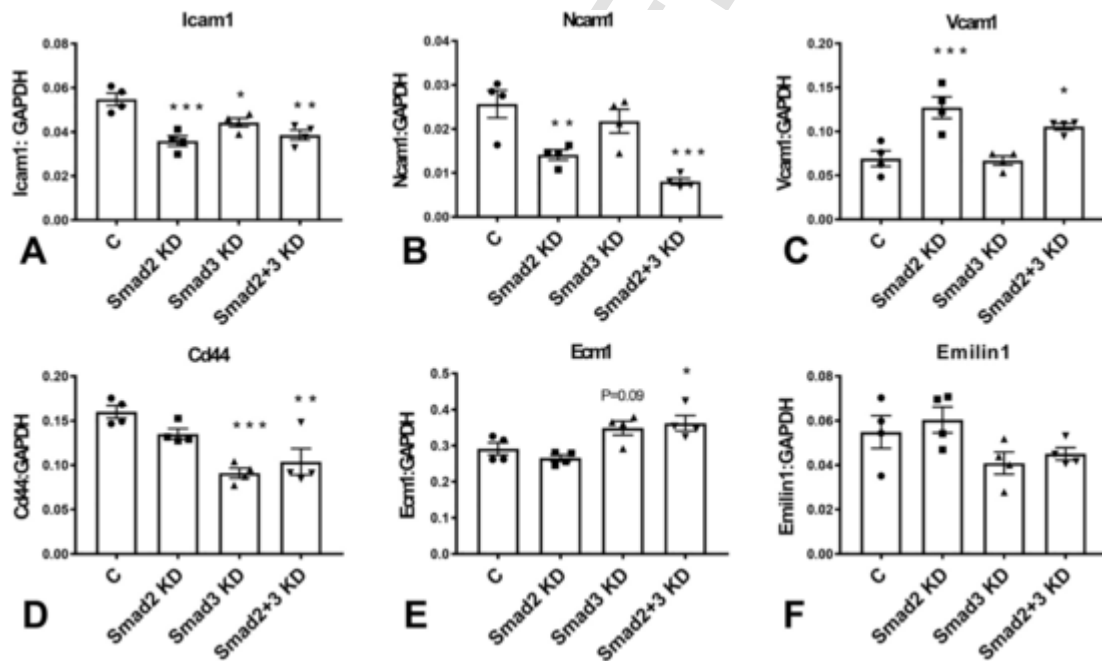


Fig. 6. Effects of Smad2 and Smad3 loss on fibroblast expression of adhesion molecules. Both Smad2 and Smad3 mediated ICAM-1 synthesis by cardiac fibroblasts. Smad2 KD, Smad3 KD and cells with combined Smad2 and Smad3 KD had significantly attenuated expression of ICAM-1 (A). Fibroblasts also exhibited significant expression of NCAM-1 (B) and VCAM-1 (C). Smad2 KD, but not Smad3 KD reduced NCAM-1 mRNA expression. In contrast, Smad2 KD increased VCAM-1 mRNA levels, suggesting that Smad2 signaling may restrain VCAM-1 synthesis. Smad3 KD, but not Smad2 KD significantly attenuated CD44 expression in cardiac fibroblasts (D). Cardiac fibroblasts synthesized significant amounts of ECM-1 mRNA. Neither Smad2 nor Smad3 KD had significant effects on ECM1 expression; however, combined KD of Smad2 and Smad3 increased ECM1 mRNA levels (E). Cardiac fibroblasts expressed significant amounts of EMILIN-1; however, Smad2 and Smad3 KD did not affect EMILIN-1 expression (F). (* $p < 0.05$, ** $p < 0.01$, *** $p < 0.001$, **** $p < 0.0001$ vs control (C), $n = 4$ /group, ANOVA followed by Dunnett's multiple comparisons test).

in regulation of ECM gene synthesis by activated myofibroblasts [46], and have suggested that Smad2 actions may oppose the fibrogenic effects of Smad3 [47]. Differences in the strategies used to disrupt Smad2 and Smad3, study of distinct fibrosis-associated genes that may be differentially regulated by Smad2 and Smad3, and the heterogeneity of fibroblasts harvested from various tissues may account for the conflicting findings. Our study suggests that in isolated cardiac fibroblasts cul-

tured in the presence of serum, both Smad2 and Smad3 are implicated in baseline ECM gene expression. Smad2 mediated *Col5a1*, *Lama2*, *TnC*, *Postn* and *Vcan* synthesis, whereas Smad3 stimulated *Col1a1*, *Col4a1* and *Thbs1* expression (Figs. 2–4). Fibronectin (*Fn1*) gene synthesis was mediated through both Smad2 and Smad3 (Fig. 4A). Our findings do not support the notion that Smad2 may oppose actions of Smad3 on ECM gene synthesis. The distinct targets of Smad2 and Smad3 may ex-

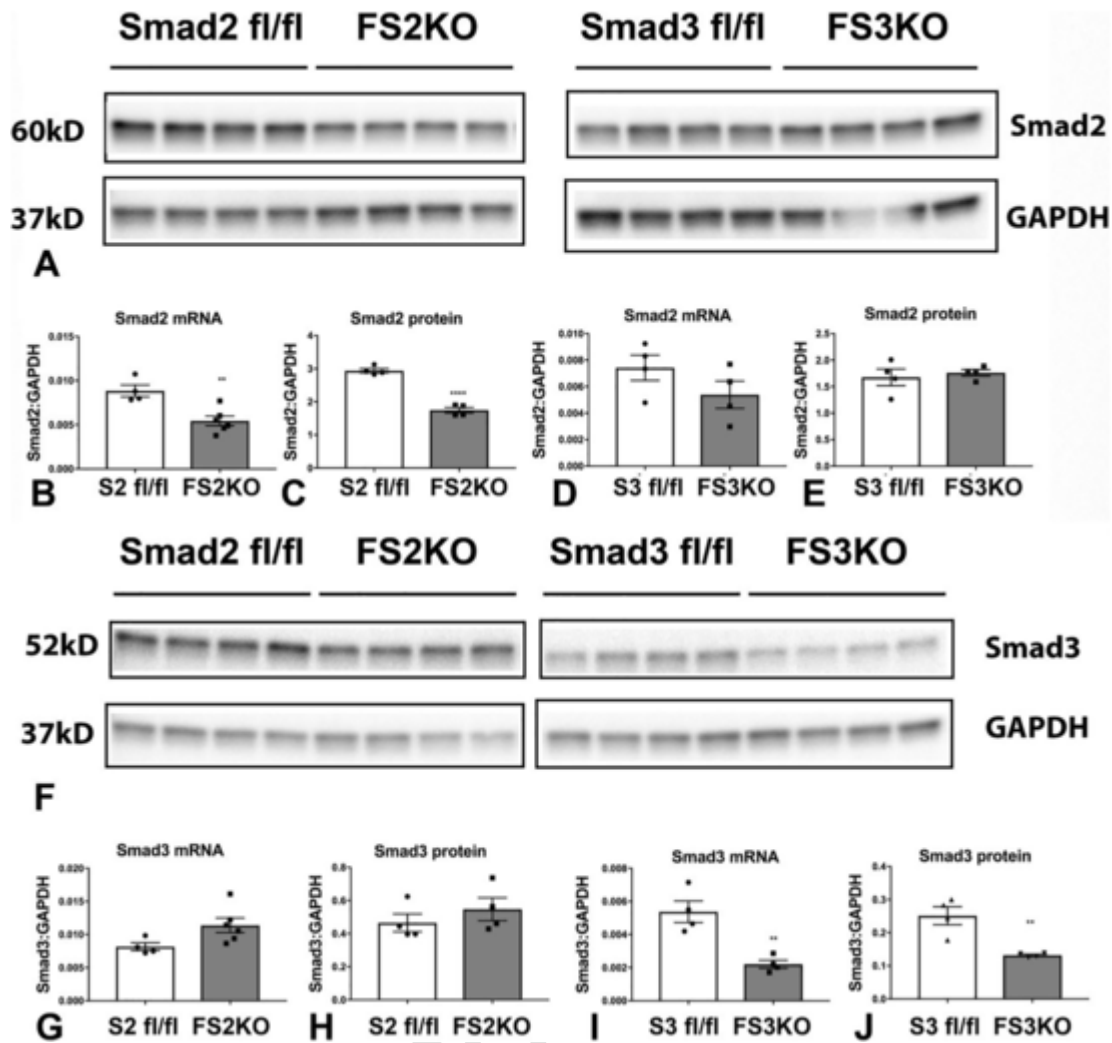


Fig. 7. Documentation of fibroblast-specific Smad2 and Smad3 loss in FS2KO and FS3KO animals. FS2KO cardiac fibroblasts had a significant 50% reduction in Smad2 mRNA and protein expression, when compared with cardiac fibroblasts harvested from Smad2 fl/fl hearts (A–C). In contrast, FS3KO fibroblasts and Smad3 fl/fl fibroblasts had comparable Smad2 expression levels (A, D–E). FS3KO mice had a statistically significant 60% reduction in Smad3 mRNA and protein levels (F, I–J). Smad3 expression was comparable between FS2KO and Smad2 fl/fl cardiac fibroblasts (F, G–H) (**p < 0.01, ****p < 0.0001, n = 4/group, unpaired t-test).

plain conflicting conclusions between various in vitro studies that may have assessed effects on the fibrogenic profile of fibroblasts on the basis of expression of selected ECM genes.

4.2. The role of fibroblasts in cardiac homeostasis

In developing hearts, fibroblasts have been suggested to play a role in formation of myocardial tissue [48,49]. However, whether fibroblasts in adult hearts play an important role in regulation of cardiac structure and function remains unknown. The adult mammalian heart contains a large population of fibroblasts [1], predominantly derived from epicardial sources [7,8]. In the adult myocardium, cardiac fibroblasts may regulate homeostatic function through several different pathways. First, continuous secretion of ECM proteins by fibroblasts may be important in preservation of the matrix network, providing mechanical support to the myocardium. Second, fibroblasts express gap junction proteins (such as Cx43 and Cx45) [50], and may be involved in regulation of cardiac electrical activity. Third, through their close spatial association with cardiomyocytes and vascular cells, fibroblasts may support cardiomyocyte survival and contractile function, and may control the density and function of the microvasculature. The signals involved in baseline regulation of fibroblast function are poorly understood. Fi-

broblast-specific loss-of-function approaches suggest that both activating and inhibitory signals may be involved in regulation of fibroblast populations in adult hearts. Platelet-derived growth factor receptor (PDGFR)- α signaling is critically involved in maintenance of the fibroblast population in adult mouse hearts [51]. On the other hand, constitutive activity of the Hippo pathway kinases large tumor suppressor kinase (LATS)1 and LATS2 promotes fibroblast quiescence in the myocardium [52], suggesting that maintaining the resting fibroblast state is an active process.

4.3. Fibroblast-specific Smad3 regulates collagen content in the adult mouse heart

In vivo, inducible fibroblast-specific disruption of Smad3 significantly reduced myocardial collagen content (Fig. 10). In contrast, fibroblast-specific Smad2 loss had no significant effects on myocardial collagen levels. Moreover cardiac fibroblasts harvested from FS3KO mice exhibited lower levels of expression of several ECM genes (Fig. 11). The effects of Smad3 loss on ECM gene synthesis were less impressive in cells harvested from FS3KO animals (Fig. 11), when compared to the effects of Smad3 siRNA KD (Figs. 2–7). This may be due to the higher efficiency of siRNA KD, or may reflect compensatory mecha-

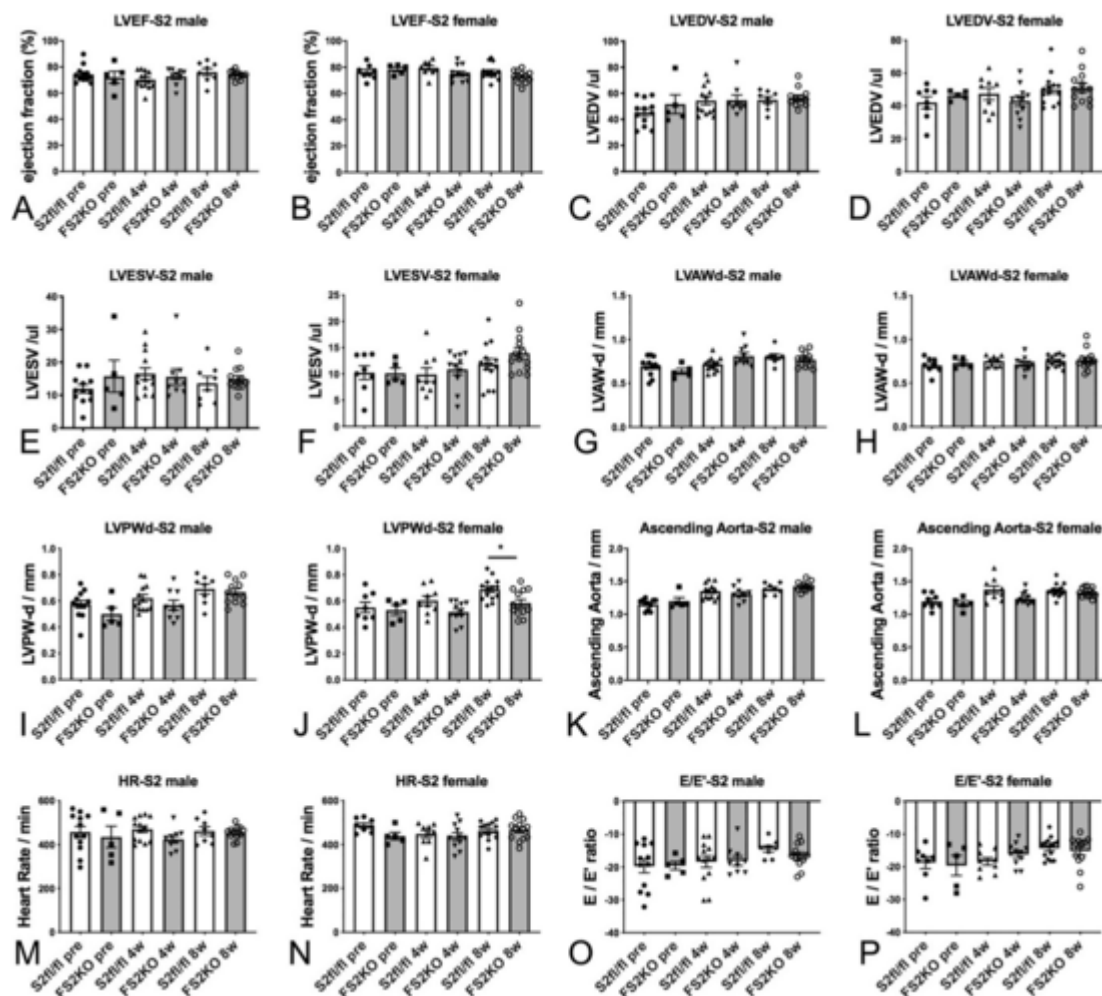


Fig. 8. Fibroblast-specific Smad2 loss does not affect baseline cardiac geometry, systolic and diastolic function. Echocardiographic analysis was performed in FS2KO and Smad2 fl/fl mice at baseline and 4–8 weeks after tamoxifen injection. Male and female FS2KO mice had comparable LVEF, LVEDV and LVESV with corresponding Smad2 fl/fl controls (A–F). End-diastolic left ventricular anterior wall thickness was comparable between groups in both male and female mice (G–H). Female FS2KO mice had a modest but statistically significant reduction in left ventricular posterior wall thickness ($*p < 0.05$), when compared with Smad2 fl/fl controls (J). Dimensions of the ascending aorta were comparable between groups (K–L). No significant differences in heart rate were noted (M–N). Tissue Doppler imaging showed that FS2KO mice and corresponding Smad2 fl/fl controls had comparable E/E' ratio, suggesting that Smad2 loss in cardiac fibroblasts does not significantly affect baseline diastolic function (O–P). Sample size: Smad2 fl/fl (males, $n = 13$; females, $n = 14$), FS2KO (males, $n = 12$; females, $n = 13$). ANOVA followed by Sidak's multiple comparisons tests.

nisms that may preserve ECM synthesis in vivo. Taken together, our findings suggest that Smad3, but not Smad2 plays a role in maintaining ECM synthesis in adult hearts.

4.4. Attenuated collagen deposition in FS3KO mice has no short-term impact on cardiac systolic and diastolic function

Despite the reduction in myocardial collagen content in FS3KO hearts, fibroblast-specific Smad3 loss had no effects on cardiac systolic and diastolic function (Fig. 9). Our observations and the recently reported absence of systolic dysfunction in fibroblast-specific PDGFR- α KO mice (despite a prolonged reduction in fibroblast density) [51] are consistent with a limited role for baseline fibroblast actions in function of the adult heart. Moreover, global loss of the transcription factor scleraxis, an important regulator of fibroblast function had no effects on echocardiographically-assessed left ventricular function [53,54], despite a marked reduction in fibroblast density and activity [53]. Thus, low level baseline activity of cardiac fibroblasts may be sufficient to preserve the structural integrity and function of the adult mammalian heart. Although this is a plausible interpretation of the data, several limitations of our study preclude definitive conclusions regarding the absence of a homeostatic role of fibroblast-specific R-Smads. First, us-

ing the Col1a2-CreERT driver, we achieved only 50–60% loss of Smad2 and Smad3 in cardiac fibroblasts. Residual Smad2/3 expression may be sufficient to support fibroblast function and preserve myocardial homeostasis. Second, functional and histological analyses were performed 8 weeks after tamoxifen administration for cell-specific Smad2 and Smad3 deletion. The relatively long half-life of many ECM proteins in normal adult hearts [55] may limit the consequences of reduced ECM gene transcription on cardiac function. Longer intervals of fibroblast-specific R-Smad deletion may be associated with significant changes in ECM structure and cardiac function. Third, we did not examine the effects of combined fibroblast-specific Smad2 and Smad3 loss in vivo. Disruption of both pathways may cause more pronounced perturbations in the ECM network that could be associated with dysfunction. Fourth, in young animals, a relatively modest attenuation of collagen content may not significantly affect myocardial mechanisms. However, the effects of fibroblast-specific Smad3 loss may become functionally significant in aging hearts, attenuating senescence-associated collagen deposition that may contribute to diastolic dysfunction [56]. Unfortunately, due to the practical challenges of cell-specific loss-of-function studies in senescent mice, the hypothesis that disruption of fibroblast activation may limit aging-associated diastolic dysfunction has not been tested.

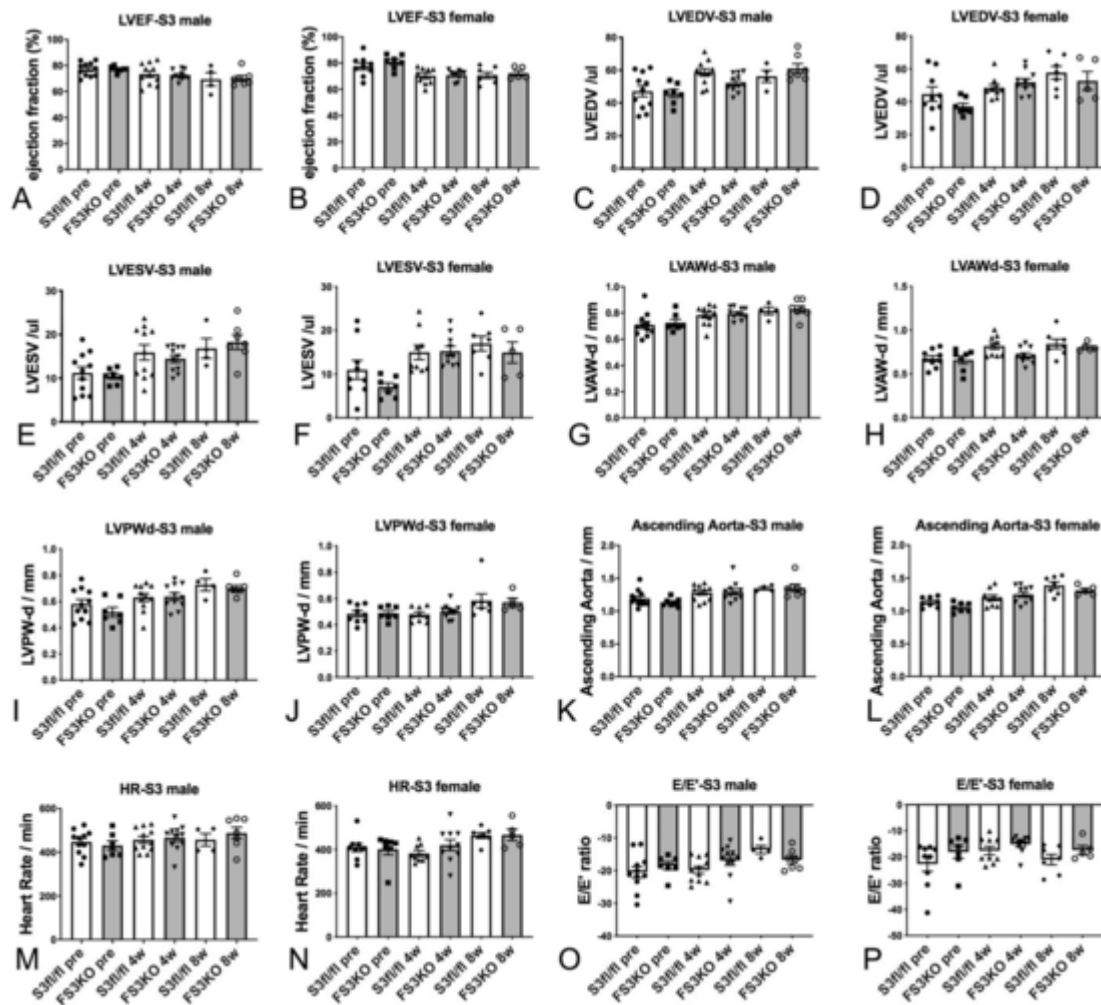


Fig. 9. Fibroblast-specific Smad3 loss does not affect baseline cardiac geometry, systolic and diastolic function. Echocardiographic endpoints were compared between FS3KO and Smad3 fl/fl mice at baseline and 4–8 weeks after tamoxifen injection. Male and female FS3KO mice had comparable LVEF, LVEDV, LVESV, and end-diastolic left ventricular anterior and posterior wall thickness with corresponding Smad3 fl/fl controls (A–J). Dimensions of the ascending aorta (K–L) and heart rate (M–N) were also comparable between groups. Tissue Doppler imaging showed that FS3KO mice and corresponding Smad3 fl/fl controls had comparable E/E' ratio, suggesting that fibroblast-specific Smad3 loss does not significantly affect baseline diastolic function (O–P). Sample size: Smad3 fl/fl (male, $n = 11$; female, $n = 9$), FS3KO mice (male, $n = 11$; female, $n = 10$). ANOVA followed by Sidak's multiple comparisons test.

4.5. What is the basis for the contrasting *in vivo* and *in vitro* observations?

The impressive effects of Smad2 and Smad3 KD on baseline gene expression of cultured cardiac fibroblasts seem to contrast the unimpressive *in vivo* consequences of fibroblast-specific Smad2 and Smad3 loss. The contrasting findings of *in vitro* and *in vivo* experiments reported in our study reflect, at least in part, the inherent problems in studying resting fibroblasts using *in vitro* models. Fibroblasts are highly dynamic cells; their phenotype is dependent on the culture environment. When cultured in plates, a significant proportion of cardiac fibroblasts undergoes myofibroblast conversion, thus exhibiting characteristics of injury-associated cells [57]. The use of serum during the culture process may have further accentuated fibroblast activation in our experiments assessing ECM gene synthesis. Thus, the significant effects of Smad2 and Smad3 on baseline gene expression in cultured cardiac fibroblasts may reflect activation responses, rather than a role for R-Smads in fibroblast homeostasis.

4.6. Conclusions

In recent years, the cardiovascular community has focused on the role of fibroblasts in pathologic conditions, such as myocardial infarc-

tion and heart failure. This is very well-justified, considering the important role of fibroblasts in reparative, fibrotic and remodeling responses. However, the potential role of fibroblasts in cardiac homeostasis has been neglected. Our findings suggest that fibroblast-specific Smad3 signaling may play a role in regulating collagen content in normal adult hearts. Although attenuated collagen deposition in FS3KO hearts had no impact on left ventricular function in young adult mice, chronic modulation of baseline fibroblast activity may have significant effects on age-associated fibrosis and diastolic dysfunction.

Sources of funding

This work was supported by NIH R01 grants HL76246 and HL85440, and by Department of Defense grants PR151029, PR151134, and PR181464. Dr. Shuaibo Huang was supported by China Scholarship Council grant 201603170222. Dr. Bijun Chen and Dr. Claudio Humeres are supported by American Heart Association post-doctoral grants.

CRediT authorship contribution statement

Shuaibo Huang:Methodology, Investigation, Formal analysis, Writing - original draft, Writing - review & editing.**Bijun Chen:**Investigation, Formal analysis, Writing - review & editing.**Claudio Humeres:**Investigation, Writing - review & editing.**Linda Alex:**Investigation, Writ-

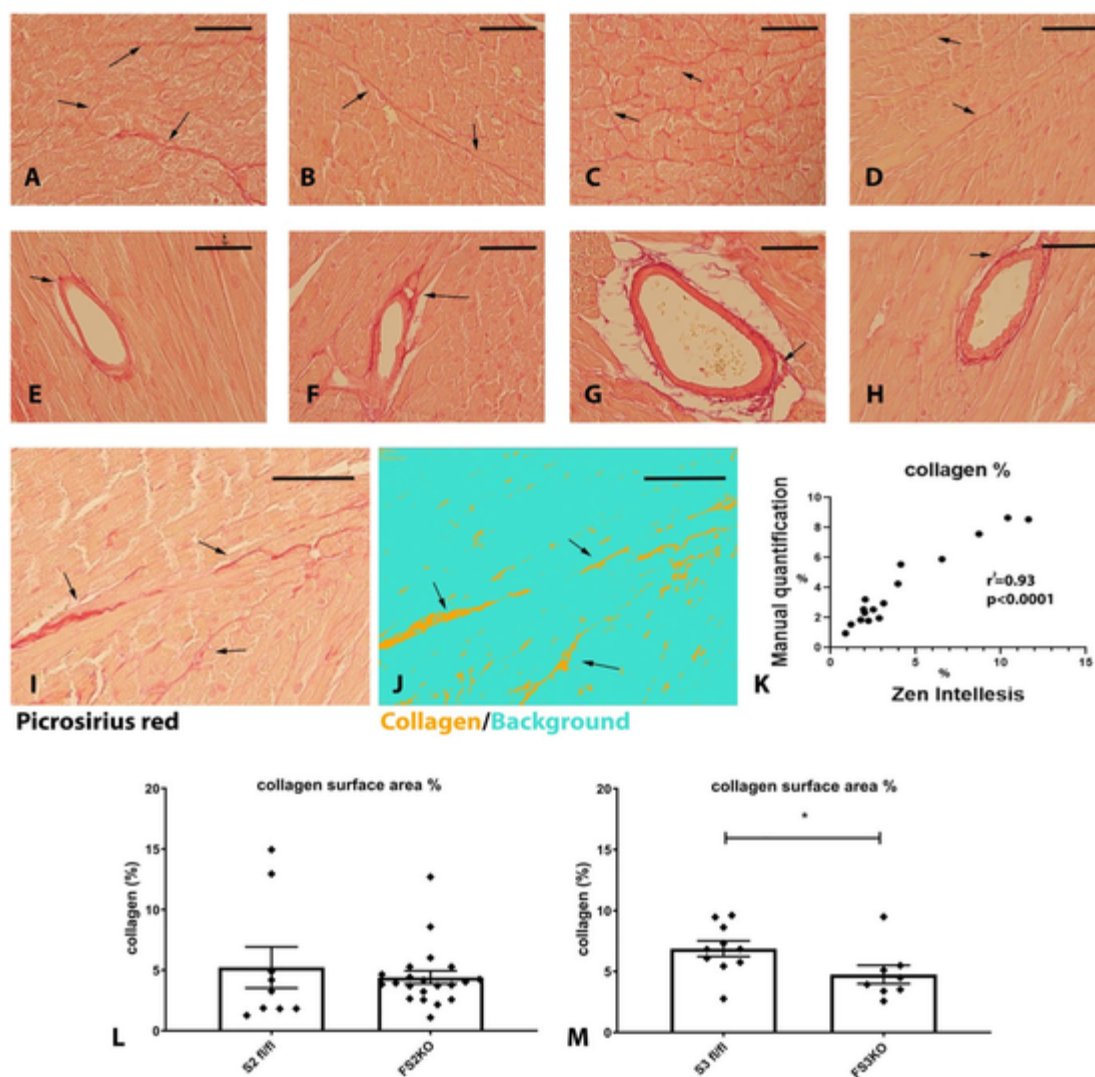


Fig. 10. Inducible fibroblast-specific Smad3 loss reduces myocardial collagen content. Myocardial sections from Smad2 fl/fl (A, E), FS2KO (B, F), Smad3 fl/fl (C, G) and FS3KO (D, H) mice were stained with Picosirius red to label interstitial (A–D) and perivascular (E–H) collagen fibers (arrows). Mice were studied 8 weeks after tamoxifen injection, FS2KO and FS3KO mice appeared to have preserved myocardial structure. Quantitative analysis of collagen content was performed using a machine learning-based system for objective unbiased analysis. I–K: The artificial intelligence-guided model was tested using 16 different field from 4 mice and showed excellent correlation ($r^2 = 0.93$, $p < 0.0001$, $n = 16$) with manual measurements. L: FS2KO mice and Smad2 fl/fl controls had comparable myocardial collagen content ($p = \text{NS}$, $n = 9\text{--}21/\text{group}$, Mann-Whitney test). M: When compared with Smad3 fl/fl animals, FS3KO mice had a modest, but significant reduction in myocardial collagen content ($p < 0.05$, $n = 8\text{--}10/\text{group}$, Mann-Whitney test). Scalebar = 50 μm .

ing - review & editing. **Anis Hanna:** Investigation, Formal analysis, Writing - review & editing. **Nikolaos G. Frangogiannis:** Methodology, Formal analysis, Writing - original draft, Writing - review & editing.

Declaration of competing interest

The authors declare that they have no known competing financial interests or personal relationships that could have appeared to influence the work reported in this paper.

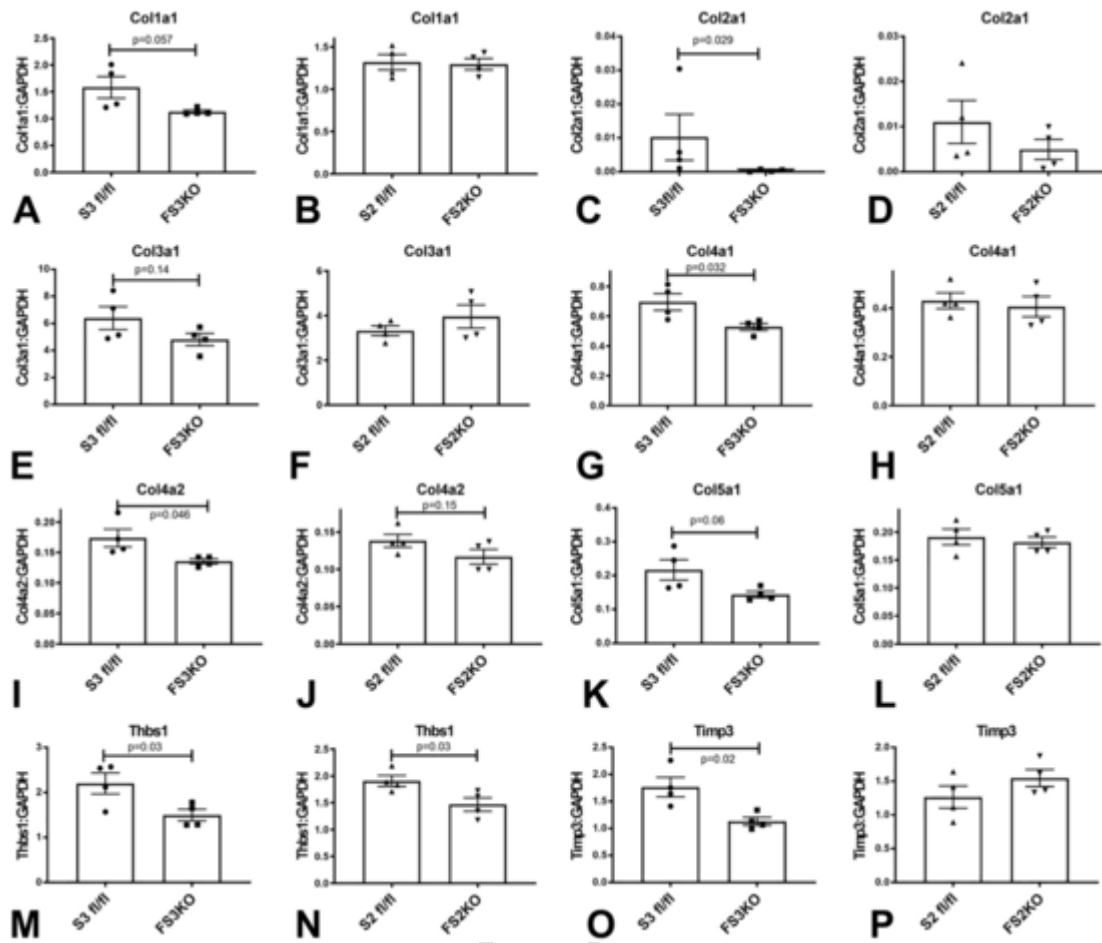


Fig. 11. Fibroblasts harvested from FS3KO hearts exhibit attenuated synthesis of ECM genes. When compared with Smad3 fl/fl cardiac fibroblasts, FS3KO fibroblasts had significantly lower mRNA expression of Col2a1(C), Col4a1 (G), Col4a2 (I), Thrombospondin-1/Thbs1 (M) and TIMP3 (O), and exhibited trends towards reduced expression of Col1a1 (A), Col3a1 (E) and Col5a1 (K). In contrast, when compared with corresponding Smad2 fl/fl controls, fibroblasts harvested from FS2KO hearts had comparable expression of Col1a1 (B), Col2a1 (D), Col3a1 (F), Col4a1 (H), Col4a2 (J), Col5a1 (L) and TIMP3 (P). Thbs1 levels were significantly reduced in the absence of Smad2 (N). n = 4/group. Unpaired t-test.

Table 2
Baseline extracellular matrix gene expression levels in cardiac fibroblasts from fibroblast-specific Smad2 KO (FS2KO) mice.

Gene name	Gene symbol	Smad2 fl/fl (mean ± SEM)	FS2KO (mean ± SEM)	p-Value
A disintegrin-like and metallopeptidase (reprolysin type) with thrombospondin type 1motif, 1	<i>Adams1</i>	0.05011 ± 0.004495	0.05468 ± 0.002875	0.4241
A disintegrin-like and metallopeptidase (reprolysin type) with thrombospondin type 1motif, 2	<i>Adams2</i>	0.1242 ± 0.008133	0.1495 ± 0.01546	0.1978
A disintegrin-like and metallopeptidase (reprolysin type) with thrombospondin type 1motif, 5	<i>Adams5</i>	0.07718 ± 0.01298	0.1003 ± 0.01372	0.2665
A disintegrin-like and metallopeptidase (reprolysin type) with thrombospondin type 1motif, 8	<i>Adams8</i>	4.250e-005 ± 4.787e-006	6.750e-005 ± 1.702e-005	0.2070
CD44 antigen	<i>Cd44</i>	0.1194 ± 0.003434	0.1327 ± 0.007079	0.1422
Cadherin 1	<i>Cdh1</i>	ND	ND	–
Cadherin 2	<i>Cdh2</i>	0.01873 ± 0.003922	0.02185 ± 0.002256	0.5166
Cadherin 3	<i>Cdh3</i>	0.0001700 ± 3.162e-005	0.0001100 ± 2.799e-005	0.2052
Cadherin 4	<i>Cdh4</i>	ND	ND	–
Contactin 1	<i>Cntn1</i>	ND	ND	–
Collagen type I, alpha1	<i>Col1a1</i>	1.322 ± 0.09085	1.298 ± 0.06676	0.8358
Collagen type II, alpha1	<i>Col2a1</i>	0.01105 ± 0.004770	0.004953 ± 0.002213	0.2907
Collagen type III, alpha1	<i>Col3a1</i>	3.325 ± 0.2212	3.958 ± 0.5178	0.3038
Collagen type IV, alpha1	<i>Col4a1</i>	0.4297 ± 0.03268	0.4059 ± 0.04170	0.6693
Collagen type IV, alpha2	<i>Col4a2</i>	0.1384 ± 0.008707	0.1169 ± 0.009966	0.1554
Collagen type IV, alpha3	<i>Col4a3</i>	0.0001200 ± 2.614e-005	0.0001700 ± 4.163e-005	0.3484
Collagen type V, alpha1	<i>Col5a1</i>	0.1914 ± 0.01411	0.1818 ± 0.009520	0.5945
Collagen type VI, alpha1	<i>Col6a1</i>	0.3600 ± 0.04680	0.3853 ± 0.03039	0.6657
Connective tissue growth factor	<i>Ctgf</i>	2.578 ± 0.2733	2.827 ± 0.1393	0.4485
Catenin (Cadherin associated protein), alpha1	<i>Ctnna1</i>	0.08657 ± 0.008150	0.1025 ± 0.007268	0.1950
Catenin (Cadherin associated protein), alpha2	<i>Ctnna2</i>	0.05011 ± 0.004495	0.05468 ± 0.002875	0.4241
Catenin (Cadherin associated protein), beta1	<i>Ctmb1</i>	0.1322 ± 0.005469	0.1472 ± 0.006247	0.1213
Extracellular matrix protein 1	<i>Ecm1</i>	0.05011 ± 0.004495	0.05468 ± 0.002875	0.4241
Elastin microfibril interfacer 1	<i>Emilin1</i>	0.08706 ± 0.006891	0.09406 ± 0.004824	0.4369
Ectonucleoside triphosphate diphosphohydrolase 1	<i>Entpd1</i>	0.05011 ± 0.004495	0.05468 ± 0.002875	0.4241
Fibulin 1	<i>Fbln1</i>	0.008356 ± 0.001318	0.007695 ± 0.001472	0.7491
Fibronectin 1	<i>Fn1</i>	0.05011 ± 0.004495	0.05468 ± 0.002875	0.4241
Hyaluronan and proteoglycan link protein 1	<i>Haph1</i>	ND	ND	–
Hemolytic complement	<i>Hc</i>	ND	ND	–
Intercellular adhesion molecule 1	<i>Icam1</i>	0.04526 ± 0.003715	0.08703 ± 0.008140	0.0034 †
Integrin alpha2	<i>Itga2</i>	0.05011 ± 0.004495	0.05468 ± 0.002875	0.4241
Integrin alpha3	<i>Itga3</i>	0.006343 ± 0.0004632	0.006505 ± 0.0006678	0.8489
Integrin alpha4	<i>Itga4</i>	0.004250 ± 0.0006292	0.008163 ± 0.001345	0.0388 †
Integrin alpha5	<i>Itga5</i>	0.07631 ± 0.01056	0.06432 ± 0.003967	0.3287
Integrin alpha1, epithelial-associated	<i>Itgae</i>	ND	ND	–
Integrin alpha L	<i>Itgal</i>	0.0002500 ± 8.165e-006	0.0002975 ± 3.705e-005	0.2922
Integrin alpha M	<i>Itgam</i>	2.250e-005 ± 9.465e-006	4.250e-005 ± 1.887e-005	0.3801
Integrin alpha V	<i>Itgav</i>	0.07016 ± 0.01001	0.07201 ± 0.007132	0.8854
Integrin alpha X	<i>Igtax</i>	0.05011 ± 0.004495	0.05468 ± 0.002875	0.4241
Integrin beta1	<i>Itgb1</i>	0.3718 ± 0.03817	0.4283 ± 0.02015	0.2390
Integrin beta2	<i>Itgb2</i>	0.05011 ± 0.004495	0.05468 ± 0.002875	0.4241
Integrin beta3	<i>Itgb3</i>	0.007356 ± 0.0006389	0.007835 ± 0.0005224	0.6857
Integrin beta4	<i>Itgb4</i>	0.05011 ± 0.004495	0.05468 ± 0.002875	0.4241
Laminin, alpha1	<i>Lama1</i>	0.0007726 ± 7.470e-005	0.0006245 ± 9.608e-005	0.6857
Laminin, alpha2	<i>Lama2</i>	0.008000 ± 0.001080	0.008758 ± 0.001548	0.7020
Laminin, alpha3	<i>Lama3</i>	ND	ND	–
Laminin, beta2	<i>Lamb2</i>	0.1242 ± 0.008133	0.1495 ± 0.01546	0.1978
Laminin, beta3	<i>Lamb3</i>	0.0001549 ± 2.649e-005	0.0002531 ± 9.019e-005	0.3365
Laminin, gama1	<i>Lamc1</i>	0.05011 ± 0.004495	0.05468 ± 0.002875	0.4241
Matrix metallopeptidase 10	<i>Mmp10</i>	0.0009981 ± 0.0002581	0.0009728 ± 5.866e-005	0.9291
Matrix metallopeptidase 11	<i>Mmp11</i>	0.05011 ± 0.004495	0.05468 ± 0.002875	0.4241
Matrix metallopeptidase 12	<i>Mmp12</i>	0.0001067 ± 2.493e-005	0.0001167 ± 4.918e-005	0.8617
Matrix metallopeptidase 13	<i>Mmp13</i>	0.05011 ± 0.004495	0.05468 ± 0.002875	0.4241
Matrix metallopeptidase 14	<i>Mmp14</i>	0.07840 ± 0.007007	0.07942 ± 0.004432	0.9059
Matrix metallopeptidase 15	<i>Mmp15</i>	0.0007500 ± 0.0002500	0.001201 ± 0.0001180	0.2857
Matrix metallopeptidase I, alpha	<i>Mmp1a</i>	0.0005438 ± 0.0001033	0.0004808 ± 7.519e-005	0.6394

Table 2 (Continued)

Gene name	Gene symbol	Smad2 fl/fl (mean \pm SEM)	FS2KO (mean \pm SEM)	p-Value
Matrix metalloproteinase 2	<i>Mmp2</i>	0.04275 \pm 0.006897	0.04616 \pm 0.003666	0.6781
Matrix metalloproteinase 3	<i>Mmp3</i>	0.1488 \pm 0.03419	0.1464 \pm 0.03906	0.9641
Matrix metalloproteinase 7	<i>Mmp7</i>	ND	ND	–
Matrix metalloproteinase 8	<i>Mmp8</i>	0.001260 \pm 0.0001659	0.001073 \pm 0.0002067	0.5064
Matrix metalloproteinase 9	<i>Mmp9</i>	ND	ND	–
Neural cell adhesion molecule 1	<i>Ncam1</i>	0.01511 \pm 0.001621	0.01639 \pm 0.002848	0.7091
Neural cell adhesion molecule 2	<i>Ncam2</i>	ND	ND	–
Platelet/endothelial cell adhesion molecule 1	<i>Pecam1</i>	0.05011 \pm 0.004495	0.05468 \pm 0.002875	0.4241
Periostin, osteoblast specific factor	<i>Postn</i>	0.01174 \pm 0.002937	0.008773 \pm 0.001060	0.3781
Selectin, endothelial cell	<i>Sele</i>	0.05011 \pm 0.004495	0.05468 \pm 0.002875	0.4241
Selectin, lymphocyte	<i>Sell</i>	ND	ND	–
Selectin, platelet	<i>Selp</i>	0.02509 \pm 0.007001	0.04889 \pm 0.01727	0.3429
Sarcoglycan, epsilon	<i>Sgce</i>	0.03075 \pm 0.003301	0.03869 \pm 0.003668	0.1588
Secreted acidic cysteine rich glycoprotein	<i>Sparc</i>	3.999 \pm 0.08188	4.519 \pm 0.4423	0.3261
Sparc/osteonectin, cwcv and kazal-like domains proteoglycan 1	<i>Spock1</i>	ND	ND	–
Secreted phosphoprotein 1	<i>Spp1</i>	0.1475 \pm 0.004519	0.1012 \pm 0.03215	0.2461
synaptotagmin 1	<i>Syt1</i>	ND	ND	–
Transforming growth factor, beta induced	<i>Tgfb1</i>	0.002250 \pm 0.0002500	0.002053 \pm 0.0004777	0.8000
Thrombospondin 1	<i>Thbs1</i>	1.907 \pm 0.1020	1.467 \pm 0.1256	0.0349 [†]
Thrombospondin 2	<i>Thbs2</i>	0.05250 \pm 0.008005	0.03626 \pm 0.002433	0.2000
Thrombospondin 3	<i>Thbs3</i>	0.002192 \pm 0.0001814	0.001634 \pm 0.0002342	0.1087
Tissue inhibitor of metalloproteinase 1	<i>Timp1</i>	0.05011 \pm 0.004495	0.05468 \pm 0.002875	0.4241
Tissue inhibitor of metalloproteinase 2	<i>Timp2</i>	1.399 \pm 0.05310	1.565 \pm 0.1505	0.3375
Tissue inhibitor of metalloproteinase 3	<i>Timp3</i>	1.265 \pm 0.1647	1.547 \pm 0.1258	0.2228
Tenascin C	<i>Tnc</i>	0.1975 \pm 0.02316	0.1565 \pm 0.006735	0.1399
Vascular cell adhesion molecule 1	<i>Vcam1</i>	0.1053 \pm 0.01070	0.1123 \pm 0.008587	0.6282
Versican	<i>Vcan</i>	0.01832 \pm 0.005616	0.01193 \pm 0.0009556	0.3399
Vitronectin	<i>Vtn</i>	ND	ND	–

ND-not detected.

† P value < 0.05.

Table 3
Baseline extracellular matrix gene expression levels in cardiac fibroblasts from fibroblast-specific Smad3 KO (FS3KO) mice.

Gene name	Gene symbol	Smad3 fl/fl (mean ± SEM)	FS3KO (mean ± SEM)	p-Value
A disintegrin-like and metallopeptidase (reprolysin type) with thrombospondin type 1 motif, 1	<i>Adams1</i>	0.08552 ± 0.008394	0.08235 ± 0.004471	0.7504
A disintegrin-like and metallopeptidase (reprolysin type) with thrombospondin type 1 motif, 2	<i>Adams2</i>	0.2270 ± 0.04090	0.1796 ± 0.01951	0.3359
A disintegrin-like and metallopeptidase (reprolysin type) with thrombospondin type 1 motif, 5	<i>Adams5</i>	0.1784 ± 0.02840	0.1528 ± 0.01668	0.4669
A disintegrin-like and metallopeptidase (reprolysin type) with thrombospondin type 1 motif, 8	<i>Adams8</i>	5.750e-005 ± 1.109e-005	5.750e-005 ± 1.315e-005	> 0.9999
CD44 antigen	<i>Cd44</i>	0.1203 ± 0.008070	0.1126 ± 0.007737	0.5179
Cadherin 1	<i>Cdh1</i>	ND	ND	-
Cadherin 2	<i>Cdh2</i>	0.03067 ± 0.004226	0.02008 ± 0.001042	0.0510
Cadherin 3	<i>Cdh3</i>	0.0001100 ± 2.273e-005	8.250e-005 ± 3.065e-005	0.4982
Cadherin 4	<i>Cdh4</i>	ND	ND	-
Contactin 1	<i>Cntr1</i>	ND	ND	-
Collagen type I, alpha1	<i>Col1a1</i>	1.584 ± 0.2012	1.129 ± 0.03113	0.0571
Collagen type II, alpha1	<i>Col2a1</i>	0.01022 ± 0.006811	0.0003875 ± 0.0001616	0.0286 †
Collagen type III, alpha1	<i>Col3a1</i>	6.392 ± 0.8426	4.811 ± 0.4546	0.1496
Collagen type IV, alpha1	<i>Col4a1</i>	0.6953 ± 0.05561	0.5286 ± 0.02332	0.0327 †
Collagen type IV, alpha2	<i>Col4a2</i>	0.1737 ± 0.01462	0.1355 ± 0.004078	0.0457 †
Collagen type IV, alpha3	<i>Col4a3</i>	0.0001325 ± 1.493e-005	7.000e-005 ± 8.165e-006	0.0104 †
Collagen type V, alpha1	<i>Col5a1</i>	0.2166 ± 0.03011	0.1440 ± 0.009342	0.0609
Collagen type VI, alpha1	<i>Col6a1</i>	0.4923 ± 0.03000	0.4311 ± 0.03351	0.2223
Connective tissue growth factor	<i>Ctgf</i>	2.001 ± 0.05805	1.694 ± 0.2973	0.3795
Catenin (Cadherin associated protein), alpha1	<i>Ctnna1</i>	0.1082 ± 0.008349	0.07824 ± 0.004927	0.0215 †
Catenin (Cadherin associated protein), alpha2	<i>Ctnna2</i>	0.08552 ± 0.008394	0.08235 ± 0.004471	0.7504
Catenin (Cadherin associated protein), beta1	<i>Ctnnb1</i>	0.1350 ± 0.006237	0.1192 ± 0.005547	0.1065
Extracellular matrix protein 1	<i>Ecm1</i>	0.08552 ± 0.008394	0.08235 ± 0.004471	0.7504
Elastin microfibril interfacer 1	<i>Emilin1</i>	0.1401 ± 0.01728	0.1160 ± 0.005231	0.2288
Ectonucleoside triphosphate diphosphohydrolase 1	<i>Entpd1</i>	0.08552 ± 0.008394	0.08235 ± 0.004471	0.7504
Fibulin 1	<i>Fbln1</i>	0.006493 ± 0.001556	0.004165 ± 0.0005900	0.2114
Fibronectin 1	<i>Fn1</i>	0.08552 ± 0.008394	0.08235 ± 0.004471	0.7504
Hyaluronan and proteoglycan link protein 1	<i>Hapln1</i>	ND	ND	-
Hemolytic complement	<i>Hc</i>	ND	ND	-
Intercellular adhesion molecule 1	<i>Icam1</i>	0.05568 ± 0.004796	0.05175 ± 0.002562	0.4975
Integrin alpha2	<i>Itga2</i>	0.08552 ± 0.008394	0.08235 ± 0.004471	0.7504
Integrin alpha3	<i>Itga3</i>	0.003108 ± 0.0003279	0.002097 ± 0.0005673	0.1739
Integrin alpha4	<i>Itga4</i>	0.008000 ± 0.001954	0.006000 ± 0.0009129	0.3895
Integrin alpha5	<i>Itga5</i>	0.04811 ± 0.007806	0.03566 ± 0.001261	0.2090
Integrin alpha1, epithelial-associated	<i>Itgae</i>	ND	ND	-
Integrin alpha L	<i>Itgal</i>	0.0005550 ± 0.0001202	0.002135 ± 0.0004533	0.0151 †
Integrin alpha M	<i>Itgam</i>	0.007605 ± 0.0006380	0.02065 ± 0.006379	0.1330
Integrin alpha V	<i>Itgav</i>	0.07837 ± 0.008046	0.06176 ± 0.002823	0.0994
Integrin alpha X	<i>Igtax</i>	0.08552 ± 0.008394	0.08235 ± 0.004471	0.7504
Integrin beta1	<i>Itgb1</i>	0.4998 ± 0.04867	0.3983 ± 0.03534	0.1425
Integrin beta2	<i>Itgb2</i>	0.08552 ± 0.008394	0.08235 ± 0.004471	0.7504
Integrin beta3	<i>Itgb3</i>	0.006515 ± 0.0007208	0.005433 ± 0.0005200	0.2691
Integrin beta4	<i>Itgb4</i>	0.08552 ± 0.008394	0.08235 ± 0.004471	0.7504
Laminin, alpha1	<i>Lama1</i>	0.0006850 ± 0.0004440	0.0003373 ± 0.0001388	0.8857
Laminin, alpha2	<i>Lama2</i>	0.01510 ± 0.002387	0.01050 ± 0.001041	0.1276
Laminin, alpha3	<i>Lama3</i>	ND	ND	-
Laminin, beta2	<i>Lamb2</i>	0.2270 ± 0.04090	0.1796 ± 0.01951	0.3359
Laminin, beta3	<i>Lamb3</i>	0.0003100 ± 5.642e-005	0.0003403 ± 4.560e-005	0.6912
Laminin, gama1	<i>Lamc1</i>	0.08552 ± 0.008394	0.08235 ± 0.004471	0.7504
Matrix metallopeptidase 10	<i>Mmp10</i>	0.0009200 ± 0.0002996	0.0007273 ± 7.612e-005	0.5724
Matrix metallopeptidase 11	<i>Mmp11</i>	0.08552 ± 0.008394	0.08235 ± 0.004471	0.7504
Matrix metallopeptidase 12	<i>Mmp12</i>	0.02601 ± 0.0005370	0.02907 ± 0.007396	0.7067
Matrix metallopeptidase 13	<i>Mmp13</i>	0.08552 ± 0.008394	0.08235 ± 0.004471	0.7504
Matrix metallopeptidase 14	<i>Mmp14</i>	0.08783 ± 0.006574	0.08574 ± 0.006208	0.8857
Matrix metallopeptidase 15	<i>Mmp15</i>	0.0005925 ± 7.157e-005	0.0005000 ± 0.0002887	> 0.9999
Matrix metallopeptidase 1, alpha	<i>Mmp1a</i>	0.007983 ± 0.002195	0.006278 ± 0.001565	0.5505
Matrix metallopeptidase 2	<i>Mmp2</i>	0.04454 ± 0.006701	0.04175 ± 0.001250	0.7081

Table 3 (Continued)

Gene name	Gene symbol	Smad3 fl/fl (mean ± SEM)	FS3KO (mean ± SEM)	p-Value
Matrix metalloproteinase 3	<i>Mmp3</i>	0.3447 ± 0.08269	0.3010 ± 0.07823	0.7144
Matrix metalloproteinase 7	<i>Mmp7</i>	ND	ND	–
Matrix metalloproteinase 8	<i>Mmp8</i>	0.004628 ± 0.001785	0.002308 ± 0.0005025	0.2574
Matrix metalloproteinase 9	<i>Mmp9</i>	ND	ND	–
Neural cell adhesion molecule 1	<i>Ncam1</i>	0.01641 ± 0.003805	0.008610 ± 0.0006935	0.1313
Neural cell adhesion molecule 2	<i>Ncam2</i>	ND	ND	–
Platelet/endothelial cell adhesion molecule 1	<i>Pecam1</i>	0.08552 ± 0.008394	0.08235 ± 0.004471	0.7504
Periostin, osteoblast specific factor	<i>Postn</i>	0.01017 ± 0.001744	0.005487 ± 0.001245	0.0714
Selectin, endothelial cell	<i>Sele</i>	0.08552 ± 0.008394	0.08235 ± 0.004471	0.7504
Selectin, lymphocyte	<i>Sell</i>	ND	ND	–
Selectin, platelet	<i>Selp</i>	0.01438 ± 0.001676	0.008881 ± 0.0005781	0.0211 †
Sarcoglycan, epsilon	<i>Sgce</i>	0.03166 ± 0.002014	0.03925 ± 0.002428	0.0571
Secreted acidic cysteine rich glycoprotein	<i>Sparc</i>	4.222 ± 0.3581	3.930 ± 0.2464	0.5262
Sparc/osteonectin, cwcv and kazal-like domains proteoglycan 1	<i>Spock1</i>	ND	ND	–
Secreted phosphoprotein 1	<i>Spp1</i>	0.2215 ± 0.04578	0.08450 ± 0.03218	0.0499 †
synaptotagmin 1	<i>Syt1</i>	ND	ND	–
Transforming growth factor, beta induced	<i>Tgfb1</i>	0.002168 ± 0.0003201	0.004750 ± 0.001031	0.0538
Thrombospondin 1	<i>Thbs1</i>	2.199 ± 0.2340	1.497 ± 0.1276	0.0389 †
Thrombospondin 2	<i>Thbs2</i>	0.05461 ± 0.01732	0.03425 ± 0.005618	0.6857
Thrombospondin 3	<i>Thbs3</i>	0.0009700 ± 0.0001891	0.0006808 ± 0.0001137	0.2378
Tissue inhibitor of metalloproteinase 1	<i>Timp1</i>	0.08552 ± 0.008394	0.08235 ± 0.004471	0.7504
Tissue inhibitor of metalloproteinase 2	<i>Timp2</i>	1.001 ± 0.04551	1.126 ± 0.1519	0.4593
Tissue inhibitor of metalloproteinase 3	<i>Timp3</i>	1.766 ± 0.1795	1.133 ± 0.07485	0.0173 †
Tenascin C	<i>Tnc</i>	0.1372 ± 0.01384	0.1166 ± 0.006884	0.2324
Vascular cell adhesion molecule 1	<i>Vcam1</i>	0.05594 ± 0.009035	0.04700 ± 0.002160	0.4002
Versican	<i>Vcan</i>	0.008155 ± 0.001039	0.005431 ± 0.0008986	0.0946
Vitronectin	<i>Vtn</i>	ND	ND	–

ND-not detected.

† P value < 0.05.

References

- [1] A R Pinto, A Ilyikh, M J Ivey, J T Kuwabara, M L D'Antoni, R Debuque, A Chandran, L Wang, K Arora, N A Rosenthal, et al., Revisiting cardiac cellular composition, *Circ. Res.* 118 (3) (2016) 400–409.
- [2] C A Souders, S L Bowers, T A Baudino, Cardiac fibroblast: the renaissance cell, *Circ. Res.* 105 (12) (2009) 1164–1176.
- [3] M D Tallquist, J D Molkenin, Redefining the identity of cardiac fibroblasts, *Nat. Rev. Cardiol.* 14 (8) (2017) 484–491.
- [4] P Kong, A V Shinde, Y Su, I Russo, B Chen, A Saxena, S J Conway, J M Graff, N G Frangogiannis, Opposing actions of fibroblast and cardiomyocyte Smad3 signaling in the infarcted myocardium, *Circulation.* 137 (7) (2018) 707–724.
- [5] S Maruyama, K Nakamura, K N Papanicolaou, S Sano, I Shimizu, Y Asaumi, M J van den Hoff, N Ouchi, F A Recchia, K Walsh, Follistatin-like 1 promotes cardiac fibroblast activation and protects the heart from rupture, *EMBO Mol. Med.* 8 (8) (2016) 949–966.
- [6] S A Bageghni, K E Hemmings, N Y Yuldasheva, A Maqbool, F O Gamboa-Esteves, N E Humphreys, M S Jackson, C P Denton, S Francis, K E Porter, et al., Fibroblast-specific deletion of interleukin-1 receptor-1 reduces adverse cardiac remodeling following myocardial infarction, *JCI Insight* 5 (2019).
- [7] S R Ali, S Ranjbarvaziri, M Talkhabi, P Zhao, A Subat, A Hojjat, P Kamran, A M Muller, K S Volz, Z Tang, et al., Developmental heterogeneity of cardiac fibroblasts does not predict pathological proliferation and activation, *Circ. Res.* 115 (7) (2014) 625–635.
- [8] T Moore-Morris, N Guimaraes-Cambao, I Banerjee, A C Zambon, T Kisseleva, A Velayoudon, W B Stallcup, Y Gu, N D Dalton, M Cedenilla, et al., Resident fibroblast lineages mediate pressure overload-induced cardiac fibrosis, *J. Clin. Invest.* 124 (7) (2014) 2921–2934.
- [9] O Kanisicak, H Khalil, M J Ivey, J Karch, B D Maliken, R N Correll, M J Brody, S C JL, B J Aronow, M D Tallquist, et al., Genetic lineage tracing defines myofibroblast origin and function in the injured heart, *Nat. Commun.* 7 (12260) (2016).
- [10] A Ruiz-Villalba, A M Simon, C Pogontke, M I Castillo, G Abizanda, B Pelacho, R Sanchez-Dominguez, J C Segovia, F Prosper, J M Perez-Pomares, Interacting resident epicardium-derived fibroblasts and recruited bone marrow cells form myocardial infarction scar, *J. Am. Coll. Cardiol.* 65 (19) (2015) 2057–2066.
- [11] R Vidal, Wagner JUG, C Braeuning, C Fischer, R Patrick, L Tombor, M Muhly-Reinholz, D John, M Kliem, T Conrad, et al., Transcriptional heterogeneity of fibroblasts is a hallmark of the aging heart, *JCI Insight* 4 (22) (2019).
- [12] C Humeres, N G Frangogiannis, Fibroblasts in the infarcted, remodeling, and failing heart, *JACC Basic Transl. Sci.* 4 (3) (2019) 449–467.
- [13] P L Roche, K L Filomeno, R A Bagchi, M P Czubyrt, Intracellular signaling of cardiac fibroblasts, *Compr. Physiol.* 5 (2) (2015) 721–760.
- [14] A J Mouton, Y Ma, O J Rivera Gonzalez, M J Daseke 2nd, E R Flynn, T C Freeman, M R Garrett, K Y DeLeon-Pennell, M L Lindsey, Fibroblast polarization over the myocardial infarction time continuum shifts roles from inflammation to angiogenesis, *Basic Res. Cardiol.* 114 (2) (2019) 6.
- [15] A Anzai, J L Choi, S He, A M Fenn, M Nairz, S Rattik, C S McAlpine, J E Mindur, C T Chan, Y Iwamoto, et al., The infarcted myocardium solicits GM-CSF for the detrimental oversupply of inflammatory leukocytes, *J. Exp. Med.* 214 (11) (2017) 3293–3310.
- [16] J G Travers, F A Kamal, J Robbins, K E Yutzey, B C Blaxall, Cardiac fibrosis: the fibroblast awakens, *Circ. Res.* 118 (6) (2016) 1021–1040.
- [17] A Hanna, N G Frangogiannis, The role of the TGF-beta superfamily in myocardial infarction, *Front Cardiovasc. Med.* 6 (140) (2019).
- [18] N G Frangogiannis, Transforming Growth Factor (TGF)-beta in tissue fibrosis, *J. Exp. Med.* 217 (3) (2020) e20190103, doi:10.1084/jem.
- [19] M Dobaczewski, M Bujak, N Li, C Gonzalez-Quesada, L H Mendoza, X F Wang, N G Frangogiannis, Smad3 signaling critically regulates fibroblast phenotype and function in healing myocardial infarction, *Circ. Res.* 107 (3) (2010) 418–428.
- [20] M Bujak, G Ren, H J Kweon, M Dobaczewski, A Reddy, G Taffet, X F Wang, N G Frangogiannis, Essential role of Smad3 in infarct healing and in the pathogenesis of cardiac remodeling, *Circulation.* 116 (2007) 2127–2138.
- [21] I Russo, M Cavallera, S Huang, Y Su, A Hanna, B Chen, A V Shinde, S J Conway, J Graff, N G Frangogiannis, Protective effects of activated myofibroblasts in the pressure-overloaded myocardium are mediated through Smad-dependent activation of a matrix-preserving program, *Circ. Res.* 124 (8) (2019) 1214–1227.
- [22] A Biernacka, M Dobaczewski, N G Frangogiannis, TGF-beta signaling in fibrosis, *Growth Factors* 29 (5) (2011) 196–202.
- [23] J D Molkenin, D Bugg, N Ghearing, L E Dorn, P Kim, M A Sargent, J Gunaje, K Otsu, J Davis, Fibroblast-specific genetic manipulation of p38 mitogen-activated protein kinase in vivo reveals its central regulatory role in fibrosis, *Circulation.* 136 (6) (2017) 549–561.
- [24] S A Bageghni, K E Hemmings, N Zava, C P Denton, K E Porter, J F X Ainscough, M J Drinkhill, N A Turner, Cardiac fibroblast-specific p38alpha MAP kinase promotes cardiac hypertrophy via a putative paracrine interleukin-6 signaling mechanism, *FASEB J.* (2018) fj201701455RR.
- [25] M R Zeglinski, P Roche, M Hnatowich, D S Jassal, J T Wigle, M P Czubyrt, I M Dixon, TGFbeta1 regulates Scleraxis expression in primary cardiac myofibroblasts by a Smad-independent mechanism, *Am. J. Physiol. Heart Circ. Physiol.* 310 (2) (2016) H239–H249.
- [26] S Huang, B Chen, Y Su, L Alex, C Humeres, A V Shinde, S J Conway, N G Frangogiannis, Distinct roles of myofibroblast-specific Smad2 and Smad3 signaling in repair and remodeling of the infarcted heart, *J. Mol. Cell. Cardiol.* 132 (2019) 84–97.

- [27] H Khalil, O Kanisicak, V Prasad, R N Correll, X Fu, T Schips, R J Vagnozzi, R Liu, T Huynh, S J Lee, et al., Fibroblast-specific TGF-beta-Smad2/3 signaling underlies cardiac fibrosis, *J. Clin. Invest.* 127 (10) (2017) 3770–3783.
- [28] H Kaur, M Takefuji, C Y Ngai, J Carvalho, J Bayer, A Wietelmann, A Poetsch, S Hoelper, S J Conway, H Mollmann, et al., Targeted ablation of periostin-expressing activated fibroblasts prevents adverse cardiac remodeling in mice, *Circ. Res.* 118 (12) (2016) 1906–1917.
- [29] M Bujak, M Dobaczewski, C Gonzalez-Quesada, Y Xia, T Leucker, P Zymek, V Veeranna, A M Tager, A D Luster, N G Frangogiannis, Induction of the CXC chemokine interferon-gamma-inducible protein 10 regulates the reparative response following myocardial infarction, *Circ. Res.* 105 (10) (2009) 973–983.
- [30] A L Jackson, J Burchard, D Leake, A Reynolds, J Schelzer, J Guo, J M Johnson, L Lim, J Karpilow, K Nichols, et al., Position-specific chemical modification of siRNAs reduces “off-target” transcript silencing, *RNA*. 12 (7) (2006) 1197–1205.
- [31] H Lal, F Ahmad, J Zhou, J E Yu, R J Vagnozzi, Y Guo, D Yu, E J Tsai, J Woodgett, E Gao, et al., Cardiac fibroblast glycogen synthase kinase-3beta regulates ventricular remodeling and dysfunction in ischemic heart, *Circulation*. 130 (5) (2014) 419–430.
- [32] E Ubil, J Duan, I C Pillai, M Rosa-Garrido, Y Wu, F Bargiacchi, Y Lu, S Stanbouly, J Huang, M Rojas, et al., Mesenchymal-endothelial transition contributes to cardiac neovascularization, *Nature*. 514 (7524) (2014) 585–590.
- [33] J M Swonger, J S Liu, M J Ivey, M D Tallquist, Genetic tools for identifying and manipulating fibroblasts in the mouse, *Differentiation*. 92 (3) (2016) 66–83.
- [34] A Biernacka, M Cavallera, J Wang, I Russo, A Shinde, P Kong, C Gonzalez-Quesada, V Rai, M Dobaczewski, D W Lee, et al., Smad3 signaling promotes fibrosis while preserving cardiac and aortic geometry in obese diabetic mice, *Circ. Heart Fail.* 8 (4) (2015) 788–798.
- [35] M Dobaczewski, Y Xia, M Bujak, C Gonzalez-Quesada, N G Frangogiannis, CCR5 signaling suppresses inflammation and reduces adverse remodeling of the infarcted heart, mediating recruitment of regulatory T cells, *Am. J. Pathol.* 176 (5) (2010) 2177–2187.
- [36] L Alex, I Russo, V Holoborodko, N G Frangogiannis, Characterization of a mouse model of obesity-related fibrotic cardiomyopathy that recapitulates features of human heart failure with preserved ejection fraction, *Am. J. Physiol. Heart Circ. Physiol.* 315 (4) (2018) (H934-H49).
- [37] Y Matsushita, M Hasegawa, T Matsushita, M Fujimoto, M Horikawa, T Fujita, A Kawasuji, F Ogawa, D A Steeber, T F Tedder, et al., Intercellular adhesion molecule-1 deficiency attenuates the development of skin fibrosis in tight-skin mice, *J. Immunol.* 179 (1) (2007) 698–707.
- [38] P Huebener, T Abou-Khamis, P Zymek, M Bujak, X Ying, K Chatila, S Haudek, G Thakker, N G Frangogiannis, CD44 is critically involved in infarct healing by regulating the inflammatory and fibrotic response, *J. Immunol.* 180 (4) (2008) 2625–2633.
- [39] A C Midgley, M Rogers, M B Hallett, A Clayton, T Bowen, A O Phillips, R Steadman, Transforming growth factor-beta1 (TGF-beta1)-stimulated fibroblast to myofibroblast differentiation is mediated by hyaluronan (HA)-facilitated epidermal growth factor receptor (EGFR) and CD44 co-localization in lipid rafts, *J. Biol. Chem.* 288 (21) (2013) 14824–14838.
- [40] A Anwar, M Li, M G Frid, B Kumar, E V Gerasimovskaya, S R Riddle, B A McKeon, R Thukaram, B O Meyrick, M A Fini, et al., Osteopontin is an endogenous modulator of the constitutively activated phenotype of pulmonary adventitial fibroblasts in hypoxic pulmonary hypertension, *Am. J. Phys. Lung Cell. Mol. Phys.* 303 (1) (2012) L1–L11.
- [41] S A Hardy, N S Mabotuwana, L A Murtha, B Coulter, S Sanchez-Bezanilla, M S Al-Omary, T Senanayake, S Loering, M Starkey, R J Lee, et al., Novel role of extracellular matrix protein 1 (ECM1) in cardiac aging and myocardial infarction, *PLoS One* 14 (2) (2019) e0212230.
- [42] X L Qu, X L Li, Y W Zheng, Y Ren, V G Puelles, G Caruana, D J Nikolic-Paterson, J H Li, Regulation of renal fibrosis by Smad3 Thr388 phosphorylation, *Am. J. Pathol.* 184 (4) (2014) 944–952.
- [43] A M Ramirez, S Takagawa, M Sekosan, H A Jaffe, J Varga, J Roman, Smad3 deficiency ameliorates experimental obliterative bronchiolitis in a heterotopic tracheal transplantation model, *Am. J. Pathol.* 165 (4) (2004) 1223–1232.
- [44] F Verrecchia, M L Chu, A Mauviel, Identification of novel TGF-beta/Smad gene targets in dermal fibroblasts using a combined cDNA microarray/promoter transactivation approach, *J. Biol. Chem.* 276 (20) (2001) 17058–17062.
- [45] M H J Heeg, M J Koziolk, R Vasko, L Schaefer, K Sharma, G A Muller, F Strutz, The antifibrotic effects of relaxin in human renal fibroblasts are mediated in part by inhibition of the Smad2 pathway, *Kidney Int.* 68 (1) (2005) 96–109.
- [46] W J Duan, X Yu, X R Huang, J W Yu, H Y Lan, Opposing roles for Smad2 and Smad3 in peritoneal fibrosis in vivo and in vitro, *Am. J. Pathol.* 184 (8) (2014) 2275–2284.
- [47] X M Meng, X R Huang, A C K Chung, W Qin, X L Shao, P Igarashi, W J Ju, E P Bottinger, H Y Lan, Smad2 protects against TGF-beta/Smad3-mediated renal fibrosis, *J. Am. Soc. Nephrol.* 21 (9) (2010) 1477–1487.
- [48] M B Furtado, M W Costa, N A Rosenthal, The cardiac fibroblast: origin, identity and role in homeostasis and disease, *Differentiation*. 92 (3) (2016) 93–101.
- [49] M B Furtado, M W Costa, E A Pranoto, E Salimova, A R Pinto, N T Lam, A Park, P Snider, A Chandran, R P Harvey, et al., Cardiogenic genes expressed in cardiac fibroblasts contribute to heart development and repair, *Circ. Res.* 114 (9) (2014) 1422–1434.
- [50] P Camelliti, T K Borg, P Kohl, Structural and functional characterisation of cardiac fibroblasts, *Cardiovasc. Res.* 65 (1) (2005) 40–51.
- [51] M J Ivey, J T Kuwabara, K L Riggsbee, M D Tallquist, Platelet-derived growth factor receptor-alpha is essential for cardiac fibroblast survival, *Am. J. Physiol. Heart Circ. Physiol.* 317 (2) (2019) (H330-H44).
- [52] Y Xiao, M C Hill, L Li, V Deshmukh, T J Martin, J Wang, J F Martin, Hippo pathway deletion in adult resting cardiac fibroblasts initiates a cell state transition with spontaneous and self-sustaining fibrosis, *Genes Dev.* 33 (21–22) (2019) 1491–1505.
- [53] R A Bagchi, P Roche, N Aroutiounova, L Espira, B Abrenica, R Schweitzer, M P Czubyrt, The transcription factor scleraxis is a critical regulator of cardiac fibroblast phenotype, *BMC Biol.* 14 (21) (2016).
- [54] A K Levay, J D Peacock, Y Lu, M Koch, R B Hinton Jr., K E Kadler, J Lincoln, Scleraxis is required for cell lineage differentiation and extracellular matrix remodeling during murine heart valve formation in vivo, *Circ. Res.* 103 (9) (2008) 948–956.
- [55] B I Jugdutt, Ventricular remodeling after infarction and the extracellular collagen matrix: when is enough enough?, *Circulation*. 108 (11) (2003) 1395–1403.
- [56] A Biernacka, N G Frangogiannis, Aging and cardiac fibrosis, *Aging Dis.* 2 (2) (2011) 158–173.
- [57] A V Shinde, C Humeres, N G Frangogiannis, The role of alpha-smooth muscle actin in fibroblast-mediated matrix contraction and remodeling, *Biochim. Biophys. Acta* 1863 (1) (2017) 298–309.



Contents lists available at ScienceDirect

Hellenic Journal of Cardiology

journal homepage: <http://www.journals.elsevier.com/hellenic-journal-of-cardiology/>



Editorial

Monocyte subsets as predictors of adverse events in patients with atherosclerosis

Human monocytes are divided into 3 major populations, classical, nonclassical, and intermediate, based on their surface expression of the pattern recognition receptor CD14 and the Fc gamma III receptor CD16.^{1,2} This classification has been suggested to have important implications in the pathophysiology of human disease, as the 3 subsets of human monocytes exhibit distinct transcriptional and functional profiles. Classical monocytes (CD14⁺⁺/CD16⁻) constitute the majority of circulating monocytes, and can be recruited to injured and inflamed tissues, where they secrete large amounts of proinflammatory cytokines. Nonclassical monocytes (CD14⁺/CD16⁺) represent the first line of defense in pathogen-related responses and have been traditionally associated with an anti-inflammatory phenotype. Intermediate monocytes (CD14⁺⁺/CD16⁺) exhibit a unique chemokine receptor profile and have been implicated in the pathogenesis of several distinct inflammatory conditions.

A large body of evidence implicates monocytes in the progression of atherosclerosis, and in the pathogenesis of plaque rupture that may lead to thrombosis-related organ infarction.³ Driven by the need to identify high-risk patients, several investigations have tested the hypothesis that a quantitative analysis of circulating monocyte subsets may be useful in cardiovascular risk assessment in both normal subjects and in patients with known atherosclerotic disease. Unfortunately, these studies have produced conflicting results, reflecting our limited understanding of the functional and transcriptomic heterogeneity of human monocytes.

In this issue of the journal, Hopfner and coworkers⁴ prospectively examined the relation between the number of circulating monocyte subsets and the incidence of acute cardiovascular events in a patient population with angiographically documented coronary artery disease. The authors found that a higher absolute number of classical monocytes was associated with increased incidence of the predefined combined endpoint (nonfatal myocardial infarction, cardiovascular death, and nonhemorrhagic cerebrovascular event). In contrast, intermediate, nonclassical, and total monocyte counts showed no significant association with cardiovascular events. The data are consistent with the notion that the proinflammatory phenotype of classical monocytes may contribute to adverse events in patients with atherosclerotic disease. However, the key question remains: can the quantitative assessment of circulating monocyte subsets be used to identify patients at high risk for cardiovascular events?

1. The relation between circulating monocyte subsets and cardiovascular risk

Published evidence paints a rather confusing picture regarding the value of classical monocytes in identifying high-risk patients with atherosclerotic disease. Consistent with the findings of this study, an investigation in 700 randomly selected subjects from the cardiovascular arm of the Malmo Diet and Cancer Study showed that the percentage and number of classical monocytes could predict cardiovascular events.⁵ However, links between increased circulating classical monocyte counts and vulnerable plaque pathology have not been demonstrated. In patients undergoing carotid endarterectomy, circulating classical monocytes did not associate with vulnerable plaque characteristics.⁶ In another study, circulating classical monocytes were reduced in patients with signs of plaque neovascularization, an event that may lead to plaque destabilization.⁷ The predictive value of other monocyte subsets also remains controversial. In contrast to the lack of an association between intermediate CD14⁺⁺/CD16⁺ monocytes and adverse events suggested by this study, other investigations demonstrated significant relations between intermediate cells and plaque stability. In two independent studies, circulating CD14⁺⁺/CD16⁺ monocyte counts were associated with the evidence of plaque vulnerability, as assessed by virtual histology intravascular ultrasound⁸, or through optical coherence tomography.⁹ The conflicting findings of the various studies may be due, at least in part to the study of patient populations with different baseline characteristics, and to the use of very different endpoints to assess clinical outcome or plaque vulnerability. Importantly, contrasting observations and confusing messages likely also reflect the limitations of traditional human monocyte phenotyping using the "classical/nonclassical/intermediate" subtype model. In the era of advanced cellular phenotyping and of single-cell transcriptomics, this model may have outlived its usefulness.

2. The need for more sophisticated approaches to subtype human monocytes

The reliance on CD14/CD16 flow cytometric analysis may provide a crude perspective on the profile of circulating cells, but is of relatively limited value in the assessment of functional phenotypes and in the identification of subtypes with distinct cytokine expression profiles. Several new and emerging strategies may be used to improve the functional phenotyping of monocytes in patients with atherosclerotic disease. First, standard flow cytometry using CD14 and CD16 is suboptimal for the study of intermediate

Peer review under responsibility of Hellenic Society of Cardiology.

<https://doi.org/10.1016/j.hjc.2019.11.009>

1109-9666/© 2020 Hellenic Society of Cardiology. Publishing services by Elsevier B.V. This is an open access article under the CC BY-NC-ND license (<http://creativecommons.org/licenses/by-nc-nd/4.0/>).

Please cite this article as: Frangiannis NG, Monocyte subsets as predictors of adverse events in patients with atherosclerosis, Hellenic Journal of Cardiology, <https://doi.org/10.1016/j.hjc.2019.11.009>

and nonclassical monocytes, which are frequently contaminated.¹⁰ New gating schemes, taking into account the shared coexpression of surface markers, may be helpful in improving the purity of monocyte subset populations. Second, even when optimally used, cell surface markers do not provide direct information on the cytokine expression profile of monocyte subsets. Studies identifying distinct monocyte subsets on the basis of cytokine expression, cytokine, and chemokine receptor levels, or investigations directly assessing the downstream activation of specific proinflammatory pathways may provide an improved definition of functional monocyte subtypes. Third, new single-cell transcriptomic approaches offer a unique new opportunity for the identification of novel monocyte subsets with distinct functional properties. Fourth, new studies should examine to what extent circulating monocyte subsets reflect plaque pathology. Considering the localized inflammatory activation that may be responsible for the rupture of an unstable plaque, the baseline profile of circulating monocytes may not provide information on the changes associated with the acute event. However, the systematic characterization of circulating monocytes may be helpful in the identification of vulnerable patients who may exhibit chronic activation of proinflammatory leukocyte subpopulations.

3. Assessment of monocyte profile may identify vulnerable patients who may benefit from anti-inflammatory interventions

The visionary therapeutic goal for patients with atherosclerosis is to replace nonspecific therapies with approaches targeting specific pathophysiological perturbations.¹¹ There is an urgent need for the pathophysiological stratification of patients with atherosclerosis, to identify subjects who may benefit from strategies targeting specific pathogenetic pathways. The characterization of circulating monocyte subsets in patients with atherosclerosis may identify vulnerable individuals with baseline inflammatory activation, who may benefit from aggressive anti-inflammatory therapy.

Sources of funding

Dr. Frangogiannis' laboratory is supported by NIH R01 grants HL76246 and HL85440, and by the United States Department of Defense grants PR151029 and PR181464.

References

1. Kapellos TS, Bonaguro L, Gemund I, et al. Human Monocyte Subsets and Phenotypes in Major Chronic Inflammatory Diseases. *Front Immunol.* 2019;10:2035.
2. Narasimhan PB, Marcovecchio P, Hamers AAJ, Hedrick CC. Nonclassical Monocytes in Health and Disease. *Annu Rev Immunol.* 2019;37:439–456.
3. Tabas I, Lichtman AH. Monocyte-Macrophages and T Cells in Atherosclerosis. *Immunity.* 2017;47:621–634.
4. Hopfner F, Jacob M, Ulrich C, et al. Subgroups of monocytes predict cardiovascular events in patients with coronary heart disease. The PHAMOS trial (Prospective Halle Monocytes Study). *Hellenic J Cardiol.* 2019 May 2;S1109–9666(18):30426–30433. <https://doi.org/10.1016/j.hjc.2019.04.012> (epub ahead of print).
5. Berg KE, Ljungcrantz I, Andersson L, et al. Elevated CD14⁺⁺CD16⁻ monocytes predict cardiovascular events. *Circ Cardiovasc Genet.* 2012;5:122–131.
6. Meeuwssen JAL, de Vries JJ, van Duijvenvoorde A, et al. Circulating CD14(+)CD16(-) classical monocytes do not associate with a vulnerable plaque phenotype, and do not predict secondary events in severe atherosclerotic patients. *J Mol Cell Cardiol.* 2019;127:260–269.
7. Ammirati E, Moroni F, Magnoni M, et al. Circulating CD14⁺ and CD14^(high)CD16⁻ classical monocytes are reduced in patients with signs of plaque neovascularization in the carotid artery. *Atherosclerosis.* 2016;255:171–178.
8. Yoshida N, Yamamoto H, Shinke T, et al. Impact of CD14⁽⁺⁺⁾CD16⁽⁺⁾ monocytes on plaque vulnerability in diabetic and non-diabetic patients with asymptomatic coronary artery disease: a cross-sectional study. *Cardiovasc Diabetol.* 2017;16:96.
9. Yamamoto H, Yoshida N, Shinke T, et al. Impact of CD14⁽⁺⁺⁾CD16⁽⁺⁾ monocytes on coronary plaque vulnerability assessed by optical coherence tomography in coronary artery disease patients. *Atherosclerosis.* 2018;269:245–251.
10. Thomas GD, Hamers AAJ, Nakao C, et al. Human Blood Monocyte Subsets: A New Gating Strategy Defined Using Cell Surface Markers Identified by Mass Cytometry. *Arterioscler Thromb Vasc Biol.* 2017;37:1548–1558.
11. Crea F, Libby P. Acute Coronary Syndromes: The Way Forward From Mechanisms to Precision Treatment. *Circulation.* 2017;136:1155–1166.

Nikolaos G. Frangogiannis*

The Wilf Family Cardiovascular Research Institute, Department of Medicine (Cardiology), Albert Einstein College of Medicine, Bronx NY, USA

* Corresponding author. Albert Einstein College of Medicine, 1300 Morris Park Avenue Forchheimer G46B, Bronx NY 10461. Tel: 1 718 430 3546, Fax: 1 718 430 8989.

E-mail address: nikolaos.frangogiannis@einstein.yu.edu.

25 November 2019
Available online xxx

The Vascular Wall: a Plastic Hub of Activity in Cardiovascular Homeostasis and Disease

Cassandra P. Awgulewitsch^{1,2} · Linh T. Trinh^{1,2} · Antonis K. Hatzopoulos^{1,2}

© Springer Science+Business Media New York 2017

Abstract

Purpose of Review This review aims to summarize recent findings regarding the plasticity and fate switching among somatic and progenitor cells residing in the vascular wall of blood vessels in health and disease.

Recent Findings Cell lineage tracing methods have identified multiple origins of stem cells, macrophages, and matrix-producing cells that become mobilized after acute or chronic injury of cardiovascular tissues. These studies also revealed that in the disease environment, resident somatic cells become plastic, thereby changing their stereotypical identities to adopt proinflammatory and profibrotic phenotypes.

Summary Currently, the functional significance of this heterogeneity among reparative cells is unknown. Furthermore, mechanisms that control cellular plasticity and fate decisions in the disease environment are poorly understood. Cardiovascular diseases are responsible for the majority of deaths worldwide. From a therapeutic perspective, these novel discoveries may identify new targets to improve the repair and regeneration of the cardiovascular system.

Keywords Endothelial-to-mesenchymal transition · Cellular plasticity · Vascular wall · Perivascular cells · Stem cells · Cardiovascular homeostasis

This article is part of the Topical Collection on *Regenerative Medicine*

✉ Antonis K. Hatzopoulos
antonis.hatzopoulos@vanderbilt.edu

¹ Division of Cardiovascular Medicine, Department of Medicine, Vanderbilt University Medical Center, 2213 Garland Avenue, Nashville, TN 37232-6300, USA

² Department of Cell and Developmental Biology, Vanderbilt University, Nashville, TN, USA

Introduction

In the last decade, a number of discoveries have revolutionized our view about how the cardiovascular system maintains its structure during homeostasis, repairs itself after acute injury, or responds to chronic pathological conditions such as atherosclerosis, hypertension, or heart failure. Specifically, the application of cell lineage tracing techniques—which were originally designed to identify the contribution of various cell types in organ development—has uncovered multiple origins of seemingly similar cell types, including stem cells, macrophages, and extracellular matrix (ECM)-producing cells that become mobilized to repair cardiovascular tissues [1–5]. They have documented that resident mature cells change their stereotypical identities to adopt proinflammatory and profibrotic phenotypes in the disease environment and also assume stem cell characteristics, thereby contributing to tissue maintenance under normal conditions [3, 6]. These findings have painted a new complex landscape of cardiovascular biology in adults. In this landscape, the vascular wall has emerged as the central hub of activity with endothelial cells (ECs) in the vascular wall intima, smooth muscle cells (SMCs) in the media, and perivascular progenitor cells in the adventitia showing a wide gamut of plasticity and differentiation potential. These recently recognized processes present new challenges to understand organ maintenance, but they also offer new opportunities to moderate disease progression, improve cardiovascular tissue repair, and promote regeneration.

Lineage Tracing or Cell Fate Mapping

Lineage tracing, also called cell fate mapping, is based on genetically tagging the genome of cells in permanent fashion with a gene expressing a fluorescent or other color marker. In this way, tagged cells and their progeny, no matter which cell types they

become, or how they respond to environmental conditions, can be followed throughout the organism [7, 8]. Genetic tagging depends on two components that are typically generated as two independent transgenic mouse lines. The first line is designed to express a recombinase enzyme, usually Cre in mice, under the regulatory elements of an endogenous gene promoter [9]. This is accomplished by embedding the Cre recombinase coding sequences within a gene locus or by creating a transgenic construct with Cre expression under the regulatory control of specific transcriptional elements. Depending on the gene locus and promoter/enhancer elements chosen in the design, Cre recombinase is expressed in select cell types, for example endothelial cells or cardiomyocytes [10, 11].

The second mouse line takes advantage of the ubiquitous ROSA locus that was originally described by the group of Philippe Soriano [12]. The ROSA locus is engineered to express a fluorescent or color marker such as green fluorescence protein or β -galactosidase in all cell types, but expression is blocked by a STOP signal [13]. The STOP signal is flanked by LoxP sites that can be recombined by Cre recombinase to remove the STOP signal, thus allowing expression of the marker gene in the cell where recombination took place. Expression is maintained in all of this cell's progeny, because the transcriptional elements of the ROSA locus are active in most cell types.

This technique allows precise tagging of cells based on their characteristic gene expression profiles and has provided an improved tool to trace cell lineages compared to previously used methods that were based on localized infection of cells with genetically modified viruses expressing traceable gene markers, or simple injection of carbon particles and other dyes to locally mark and follow cells during development.

Many variations on this basic theme have been developed over the years, including inducible recombinases like CreER^T that are activated by tamoxifen, thus allowing cell labeling at a defined time point [14, 15]. Inducible tagging is especially useful to lineage trace cells in adult mice, avoiding cell labeling during embryonic development, or for pulse chase experiments at distinct time points during disease progression. Another powerful tool is the Confetti mouse, which carries a multicolor reporter with four distinct fluorescent protein genes (red, yellow, nuclear green, and membrane-bound cyan) in the ROSA locus [16]. The fluorescent protein coding sequences are organized in tandem among alternating LoxP sites in a way that recombination of the ROSA-Confetti allele leads to stochastic expression of any of the four distinct fluorescent proteins. The construct is designed such that random recombination activates only one of the fluorescent protein genes, randomly labeling each targeted cell and its descendants with the same single color. As a result, this fate mapping strategy can distinguish cells that are clonally related, i.e., generated from a single originating cell versus independently derived. This powerful technique can also minimize the possibility that

cells were falsely labeled by ectopic Cre expression or Cre transfer between cells due to fusion. Alternative multi-color lineage tracing methods using the Rainbow mice have also been developed for clonal analyses [17, 18].

However, it should be noted that these techniques have several limitations that might lead to false conclusions. Most of these artifacts can be attributed to the promoter used to drive recombinase expression. Ectopic promoter expression or leaky or weak promoters can label the wrong cell types, or just a random subpopulation of relevant cells, thus leading to over- or underestimation of the contribution of different cell types to a biological process. Moreover, embryonic labeling, fusion, or genetic material transfer from cell to cell might lead to artificial labeling and incorrect inferences about genuine cellular progeny. Safeguarding against such potential artifacts by using multiple, independent, cell-specific and strong promoters, inducible Cre recombinases, Cre antibodies, pulse-labeling and chasing experiments, multicolor labeling for clonal analyses, and comparing lineage tracing results to mice expressing gene markers under the same promoter without Cre recombination is required to address these concerns and validate experimental conclusions [19].

Despite these limitations, application of lineage tracing tools in adult disease models has broadened our perspective about how cells behave under pathophysiological conditions and revealed an amazing plasticity, especially for cells located within and around the vascular wall of blood vessels.

Intima Layer—Endothelial Cell Plasticity

The quintessential plastic cell type in the vascular wall is the endothelial cells that line up the inner layer of all blood vessels in the body. The plasticity of endothelial cells has been first recognized in the embryo where it was discovered that hematopoietic stem cells emerge from endothelial cells in the ventral wall of the dorsal aorta and subsequently colonize a succession of hematopoiesis sites in the liver, the spleen, and finally the bone marrow [20–25]. The properties of the hemogenic endothelium have been recapitulated in vitro using human iPS cell-derived endothelial cells [26].

A second site where endothelial cells give rise to a different cell type is in the developing valves and septa in the heart [6, 27, 28]. During cardiac development, endothelial cells lining the endocardial cushions undergo endothelial-to-mesenchymal transition (EndMT), giving rise to valvular interstitial cells that proceed to migrate, colonize the cardiac jelly within valve tissue, and become the major extracellular matrix (ECM)-producing cell type in the developing and mature valves.

Endothelial-to-Mesenchymal Transition

EndMT is a specialized form of epithelial-to-mesenchymal transition or EMT [6, 29]. During this process, epithelial cells

lose expression of E-cadherin, or VE-cadherin in the case of endothelial cells, and replace them with N-cadherin. Either E-cadherin or VE-cadherin proteins are present in cellular junctions and required for cell-cell adhesion; thus, their suppression loosens cells within the epithelial or endothelial layers, allowing them to become mobile and migrate [30, 31]. EndMT is also accompanied by loss of typical endothelial-specific markers, such as CD31 and vWF [30]. The downregulation of endothelial properties is followed by upregulation of genes characteristic of mesenchymal cells such as SMA, Vimentin, Periostin, FSP-1, and PDGFR α/β as well as reorganization of the cytoskeleton that transforms endothelial cells to fibroblast-like cells [30]. The initial EndMT step of downregulation of cadherin expression is accomplished by a number of transcriptional repressors such as Snail, Twist and Slug [32–34]. These repressors are direct targets of EndMT-promoting pathways such as TGF β /BMP, Wnt, and Notch signaling [33–37, 38•, 39].

EndMT has now been recognized as taking place in various diseases, especially during fibrosis after acute injury or because of chronic pathological conditions [6, 29, 40]. Numerous studies using lineage tracing of endothelial cells have revealed that a significant portion of ECM-producing cells in various pathological conditions is of endothelial origin (estimates vary but usually range between 20 and 30%). Specifically, this has been shown in various models of lung fibrosis and pulmonary hypertension [41–44]; kidney fibrosis after acute or chronic injury [45–47]; the heart after acute ischemic injury such as myocardial infarction and chronic fibrosis caused by constant pressure overload [38•, 48•, 49, 50]; intestinal fibrosis [51]; stiffening of the arterial wall in hypertension [52•]; plaque formation in atherosclerosis [53•, 54•]; vascular graft stenosis [55•, 56]; vascular calcification [57]; diabetic retinopathy [58]; valve thickening [59]; and the generation of fibroblast-like cells that support tumor growth [60]. However, the field is not without controversy, since other studies have refuted the extent of EndMT contribution in fibrosis and pointed to proliferation and activation of resident fibroblasts as the main source of myofibroblasts after acute or chronic injury [61•, 62•].

Furthermore, EndMT has been identified as the cause of inherited or sporadically occurring cerebral cavernous malformations that lead to brain hemorrhages [63]. Cerebral cavernous malformations are vascular lesions that manifest when tight endothelial cell connections, which are required to maintain the integrity of the blood-brain barrier, break down due to acquisition of mesenchymal properties by endothelial cells.

Endothelial-to-Mesenchymal Transition Yields Mesenchymal Stem Cells

A fascinating aspect of EndMT is that besides yielding ECM-producing cells, it can also yield mesenchymal cells with stem

cell characteristics (MSCs) [34, 64]. At the moment, the relationship between the generation of profibrotic and regenerative cells is not clear. It is possible that EndMT is a naturally occurring phenomenon that is required for tissue homeostasis. It is also likely that this same process under various stress conditions turns functional tissue to scar formation as a necessary step to prevent tissue rupture, for example in the heart after myocardial infarction, or becomes maladaptive during chronic pathological conditions or aging [1].

Consistent with this scenario, we have recently discovered using lineage tracing that endothelial cells give rise to smooth muscle cells in the medial layer of coronary arteries, stem cell antigen-1 (Sca-1, alternatively known as lymphocyte antigen 6 complex, locus A, or Ly-6A) progenitor cells in the adventitial layer, and ventricular cardiomyocytes during cardiac homeostasis [19•]. Endothelial cell-derived cardiomyocytes were organized in clonal clusters, presumably of single-cell origin. Pulse-chase experiments showed that generation of individual clusters is rapid and efficient. These new endothelial cell-derived cardiomyocytes comprise approximately 0.3% of the total cardiomyocyte population, but they are confined to specific regions of the heart in the right and left ventricular walls and the junctions between the two ventricles [19•]. Endothelial derived-Sca1⁺ progenitor cells in the adventitia of coronary arteries constitute about 30–40% of the total Sca1⁺ population. Interestingly, the perivascular Sca1⁺ cells are the only endothelial progeny with high proliferation rates. The endothelial cell-fate maps are remarkably similar to those obtained by lineage tracing of Sca1⁺ cells, suggesting that endothelial cells or endothelial-like cells are upstream of Sca1⁺ progenitors [19•, 65•]. In support of these findings in the adult heart, a recent study showed that endothelial cells are a source of smooth muscle cells and pericytes in the heart during development [66].

Besides cardiomyocytes, endothelial cell progeny in other tissues include osteogenic cells, adipocytes, and skeletal muscle [29, 67–69]. This plasticity of endothelial cells in various tissues may be linked to their potential to transdifferentiate to multipotent MSCs.

Endothelial-to-Mesenchymal Transition Activation

What triggers EndMT in disease? Vascular inflammation has been implicated as a key inducer of EndMT in pathological conditions, and EndMT may be an adaptive response to endothelial injury [30, 51, 53•, 55•, 70, 71]. Shear stress is also known to induce EndMT [72]. Vascular inflammation stimulates signaling pathways such as TGF β /SMAD and Wnt/ β -catenin, which are key inducers of EndMT [38•, 48•, 73–77]. At the molecular level, evidence shows that FGF suppresses TGF β signaling and EndMT [78]. FGF binding to FGFR1 leads to phosphorylation and activation of ERK signaling that in turns induces expression of miR *let-7b* [55•]. *Let-7b* blocks

TGF β signaling by suppressing expression of TGF β and its receptor TGF β R1. Inflammatory cytokines induced after acute or in chronic injury inhibit FGFR signaling, reducing *let-7b* levels, further potentiating TGF β signaling in endothelial cells and, thus, inducing EndMT.

Inflammation and shear stress have been shown to activate expression of the transcription factor Kruppel-like factor 4 (KLF4), which is known to promote TGF β /BMP signaling in endothelial cells [79]. KLF4 activation has been recently identified as the major inducer of EndMT in cerebral cavernous malformations, suggesting that KLF4 might be a key trigger of pathological EndMT [80, 81]. Additional regulators of EndMT include Notch signaling, several miRs, endothelin 1, Tie1 tyrosine kinase receptors, and sonic hedgehog signaling, providing a wide range of potential targets to regulate EndMT in pathological conditions [29, 37, 82–87].

Media and Adventitia—Smooth Muscle and Perivascular Cells

Although most of our knowledge about cell plasticity in disease has so far come from studies on endothelial cells and EndMT, several reports have shown that smooth muscle cells (SMCs) in the media of blood vessels and adventitia perivascular cells have also the potential to transform to other cell types and acquire proinflammatory and profibrotic phenotypes.

Studies have hinted to the plasticity of SMCs in atherosclerotic lesions and their transformation to macrophage-like cells in both mouse models and atherosclerotic lesions in human patients [88, 89]. Recent studies using SMC-specific promoters such as *Myh11* and *SM22* to mark and lineage trace SMCs within atherosclerotic lesions found that SMCs lose their characteristics and give rise to cells that exhibit phenotypes of other cell lineages, including macrophages and mesenchymal stem cells (MSCs) [90, 91, 92]. Interestingly, using Confetti mice, it was shown that SMCs that lose SMC characteristics and undergo transition to macrophage phenotypes also begin to proliferate and clonally expand within atherosclerotic plaques, thus exacerbating plaque growth [93].

Although the mechanisms of SMC plasticity are not well understood, it appears that pathways implicated in EndMT are also in play in the transformation of SMCs. For example, FGF and TGF β appear to regulate SMC plasticity [94]. In addition, SMC-specific conditional knockout of KLF4 resulted in reduced numbers of SMC-derived MSC- and macrophage-like cells [91]. These findings indicate that KLF4-dependent transitions in SMC phenotype are critical in atherosclerosis. Of note, inactivation of KLF4 *in vivo* in mice led to a significant reduction in atherosclerotic lesion size and increased plaque stability, supporting the important role of the SMC-to-macrophage transition in atherosclerosis [91].

The adventitia not only has been long recognized as a niche for cardiovascular and mesenchymal progenitor cells that contribute to organ homeostasis but also respond to disease stimuli (recently reviewed in [95]). Lineage tracing of Tcf21⁺ cells in the adventitia of coronary arteries revealed that vascular wall cells expressing this basic helix-loop-helix transcription factor migrate into vascular lesions of ApoE^{-/-} and Ldlr^{-/-} mice before disease initiation. While Tcf21 lineage traced cells are distributed throughout the early lesions, in mature lesions, they contribute to the formation of a subcapsular layer of cells and become associated with the fibrous cap acquiring characteristics of SMCs [96].

Sca1⁺ progenitor cells reside in the vascular adventitia [97–99]. These pluripotent cells emerge during embryogenesis and persist into adulthood. In healthy arteries of adult mice, Sca1⁺ progenitors maintain ECs and SMCs and generate vascular-like branching structures when cultured on Matrigel [100]. However, in atherosclerosis and vascular injury, Sca1⁺ cells can transition into a mesenchymal phenotype and contribute to fibrosis [97, 101–103].

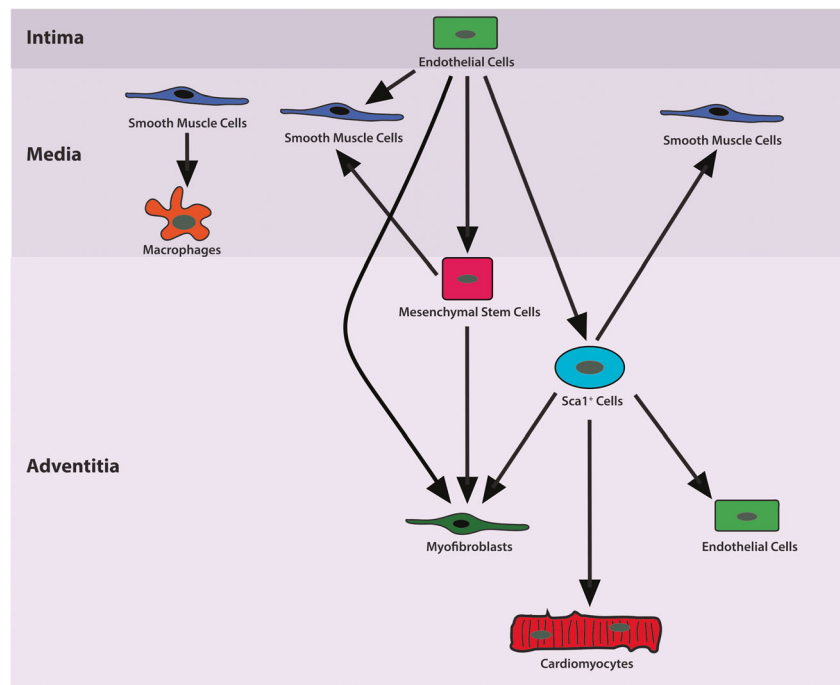
Hypertension causes arterial wall stiffening because of excessive production and deposition of collagen in the adventitia of large arteries, exacerbating blood pressure elevation and causing end-organ damage. A new study showed that most of the collagen-producing cells in the adventitia are Sca1⁺ cells [52]. Lineage tracing and flow cytometry analyses revealed that a portion of profibrotic cells is derived from transformation of resident Sca1⁺ progenitor cells to matrix-producing cells, a second portion is derived from EndMT, and a third portion is derived from circulating bone marrow fibrocytes.

A recent publication has shown that Gli1⁺ MSCs, residing in the perivascular area in many organs, including the kidney, lung, liver, and heart, expand after injury and transform to myofibroblasts after injury, substantially contributing to organ fibrosis [104]. Interestingly, genetic ablation of these Gli1⁺ MSCs attenuated fibrosis and improved organ function. Collectively, these lineage tracing studies suggest that progenitor cells in the adventitia of large vessels, which are necessary for vascular wall and tissue maintenance during homeostasis, become profibrotic under pathological conditions.

Conclusions

Recent discoveries have uncovered a complex picture of cellular activity around blood vessels that is important for organ homeostasis that also plays a critical role in various pathological processes. This activity depends partly on cell plasticity and the adoption of proinflammatory and profibrotic phenotypes by resident somatic cells in the intima, media, and adventitia layers, and partly on switching the differentiation potential of progenitor cells that normally regenerate organ structures during homeostasis to reparative cells that contribute to

Fig. 1 Cellular plasticity in the vascular wall. Schematic diagram of plasticity among various somatic and progenitor cell populations residing within and around blood vessels as revealed by cell lineage tracing approaches. Cellular plasticity may contribute to organ homeostasis under normal conditions, but generate proinflammatory and profibrotic cells in diseases such as atherosclerosis, myocardial infarction, heart failure, and hypertension



atherosclerotic plaque growth, interstitial fibrosis, and scar formation (Fig. 1).

The best understood process so far is EndMT that transforms endothelial cells to ECM-producing cells after acute injury or under chronic pathological conditions such as heart failure, hypertension, and atherosclerosis. It is conceivable that EndMT-derived ECM-producing cells have distinct functions than activated resident myofibroblasts, regarding their spatiotemporal contribution in the fibrotic process, the type of ECM proteins they synthesize, or their pro- and anti-inflammatory properties. On the other hand, it is also possible that the endothelial origin of ECM-producing cells is not important and that the disease environment is the primary determinant of cellular function. In this case, the multiple sources might be a means to generate the necessary cell numbers in a short period of time. It is also likely that both the origin and environment contribute to cellular heterogeneity. For example, the environment may dictate profibrotic properties during the initial stages of scar formation, but the origin may define long-term survival and specific roles in scar maintenance and neovascularization. In either case, targeting EndMT could regulate specific subpopulations of ECM-producing cells or just reduce the burden of collagen-producing cells.

Although the functional significance of cellular plasticity and fate switching in tissue repair and regeneration is poorly understood, there is evidence that these processes take place in human diseases as well. Histological analyses have identified hallmarks of EndMT in lung fibrosis, blood vessel graft stenosis, and vascular malformations [56, 105], recently reviewed in [40]. There is also evidence of SMC contribution to macrophages during atherosclerotic plaque formation in

human patients [89]. Determining the mechanisms regulating the transition of vascular and perivascular cells to proinflammatory and profibrotic cell types, and understanding the precise role of these cells in pathological conditions, should lead to new therapeutic strategies to improve clinical outcomes in patients with cardiovascular disease.

Acknowledgements This work was supported by grants from NIH (HL100398) and the Department of Defense (PR151029P1).

Compliance with Ethical Standards

Conflict of Interest Antonis K. Hatzopoulos declares that he has no conflict of interest.

Human and Animal Rights and Informed Consent This article does not contain any studies with human or animal subjects performed by any of the authors.

References

Papers of particular interest, published recently, have been highlighted as:

- Of importance
- Of major importance

1. Boudoulas KD, Hatzopoulos AK. Cardiac repair and regeneration: the Rubik's cube of cell therapy for heart disease. *Dis Model Mech.* 2009;2:344–58.
2. Swirski FK, Robbins CS, Nahrendorf M. Development and function of arterial and cardiac macrophages. *Trends Immunol.* 2016;37:2–40.

3. Santini MP, Forte E, Harvey RP, Kovacic JC. Developmental origin and lineage plasticity of endogenous cardiac stem cells. *Development*. 2016;143:1242–58.
4. Nieto MA, Huang RY, Jackson RA, Thiery JP. EMT: 2016. *Cell*. 2016;166:21–45.
5. Rios FJ, Harvey A, Lopes RA, Montezano AC, Touyz RM. Progenitor cells, bone marrow-derived fibrocytes and endothelial-to-mesenchymal transition: new players in vascular fibrosis. *Hypertension*. 2016;67:272–4.
6. Kovacic JC, Mercader N, Torres M, Boehm M, Fuster V. Epithelial-to-mesenchymal and endothelial-to-mesenchymal transition: from cardiovascular development to disease. *Circulation*. 2012;125:1795–808.
7. Kretzschmar K, Watt FM. Lineage tracing. *Cell*. 2012;148:33–45.
8. Rulands S, Simons BD. Tracing cellular dynamics in tissue development, maintenance and disease. *Curr Opin Cell Biol*. 2016;43:38–45.
9. Sauer B, Henderson N. Site-specific DNA recombination in mammalian cells by the Cre recombinase of bacteriophage P1. *Proc Natl Acad Sci U S A*. 1988;85:5166–70.
10. Gustafsson E, Brakebusch C, Hietanen K, Fassler R. 2001. Tie-1-directed expression of Cre recombinase in endothelial cells of embryoid bodies and transgenic mice. *J Cell Sci*. 2001;114:671–6.
11. Sohal DS, Nghiem M, Crackower MA, Witt SA, Kimball TR, Tymitz KM, Penninger JM, Molkentin JD. Temporally regulated and tissue-specific gene manipulations in the adult and embryonic heart using a tamoxifen-inducible Cre protein. *Circ Res*. 2001;89:20–5.
12. Soriano P. Generalized lacZ expression with the ROSA26 Cre reporter strain. *Nat Genet*. 1991;21:70–1.
13. Srinivas S, Watanabe T, Lin CS, William CM, Tanabe Y, Jessell TM, Costantini F. Cre reporter strains produced by targeted insertion of EYFP and ECFP into the ROSA26 locus. *BMC Dev Biol*. 2001;1:4.
14. Feil R, Brocard J, Mascrez B, LeMeur M, Metzger D, Chambon P. Ligand-activated site-specific recombination in mice. *Proc Natl Acad Sci U S A*. 1996;93:10887–90.
15. Verrou C, Zhang Y, Zürm C, Schamel WW, Reth M. Comparison of the tamoxifen regulated chimeric Cre recombinases MerCreMer and CreMer. *Biol Chem*. 1999;380:1435–8.
16. Snippert HJ, van der Flier LG, Sato T, van Es JH, van den Born M, Kroon-Veenboer C, Barker N, Klein AM, van Rheenen J, Simons BD, Clevers H. Intestinal crypt homeostasis results from neutral competition between symmetrically dividing Lgr5 stem cells. *Cell*. 2010;143:134–44.
17. Rinkevich Y, Lindau P, Ueno H, Longaker MT, Weissman IL. Germ-layer and lineage-restricted stem/progenitors regenerate the mouse digit tip. *Nature*. 2011;476:409–13.
18. Tabansky I, Lenarcic A, Draft RW, Loulier K, Keskin DB, Rosains J, Rivera-Feliciano J, Lichtman JW, Livet J, Stern JN, Sanes JR, Eggan K. Developmental bias in cleavage-stage mouse blastomeres. *Curr Biol*. 2013;23:21–31.
19. Fioret BA, Heimfeld JD, Paik DT, Hatzopoulos AK. Endothelial cells contribute to generation of adult ventricular myocytes during cardiac homeostasis. *Cell Rep*. 2014;2014(8):229–41. **Using lineage tracing, the authors identified endothelial cells as a source of cardiomyocytes, smooth muscle cells, and Sc α 1⁺ cells in the adventitia of coronary arteries.**
20. de Bruijn MF, Ma X, Robin C, Ottersbach K, Sanchez MJ, Dzierzak E. Hematopoietic stem cells localize to the endothelial cell layer in the midgestation mouse aorta. *Immunity*. 2002;16:673–83.
21. Zovein AC, Hofmann JJ, Lynch M, French WJ, Turlo KA, Yang Y, Becker MS, Zanetta L, Dejana E, Gasson JC, Tallquist MD, Iruela-Arispe ML. Fate tracing reveals the endothelial origin of hematopoietic stem cells. *Cell Stem Cell*. 2008;3:625–36.
22. Bertrand JY, Chi NC, Santoso B, Teng S, Stainier DY, Traver D. Hematopoietic stem cells derive directly from aortic endothelium during development. *Nature*. 2010;464:108–11.
23. Boisset JC, van Cappellen W, Andrieu-Soler C, Galjart N, Dzierzak E, Robin C. In vivo imaging of hematopoietic cells emerging from the mouse aortic endothelium. *Nature*. 2010;464:116–20.
24. Kissa K, Herbomel P. Blood stem cells emerge from aortic endothelium by a novel type of cell transition. *Nature*. 2010;464:112–5.
25. Ivanovs A, Rybtsov S, Welch L, Anderson RA, Turner ML, Medvinsky A. Highly potent human hematopoietic stem cells first emerge in the intraembryonic aorta-gonad-mesonephros region. *J Exp Med*. 2011;208:2417–27.
26. Choi KD, Vodyanik MA, Togarrati PP, Suknuntha K, Kumar A, Samarjeet F, Probasco MD, Tian S, Stewart R, Thomson JA, Slukvin II. Identification of the mesogenic endothelial progenitor and its direct precursor in human pluripotent stem cell differentiation cultures. *Cell Rep*. 2012;2:553–67.
27. Markwald RR, Fitzharris TP, Manasek FJ. Structural development of endocardial cushions. *Am J Anat*. 1977;148:85–119.
28. Kisanuki YY, Hammer RE, Miyazaki J, Williams SC, Richardson JA, Yanagisawa M. Tie2-Cre transgenic mice: a new model for endothelial cell-lineage analysis in vivo. *Dev Biol*. 2001;230:230–42.
29. Medici D. Endothelial-mesenchymal transition in regenerative medicine. *Stem Cells Int*. 2016;2016:6962801. doi:10.1155/2016/6962801.
30. Pérez L, Muñoz-Durango N, Riedel CA, Echeverría C, Kalergis AM, Cabello-Verrugio C, Simon F. Endothelial-to-mesenchymal transition: cytokine-mediated pathways that determine endothelial fibrosis under inflammatory conditions. *Cytokine Growth Factor Rev*. 2016; doi:10.1016/j.cytogfr.2016.09.002.
31. Lamouille S, Xu J, Derynck R. Molecular mechanisms of epithelial–mesenchymal transition. *Nat Rev Mol Cell Biol*. 2014;15:178–96.
32. Cano A, Perez-Moreno MA, Rodrigo I, Locascio A, Blanco MJ, del Barrio MG, Portillo F, Nieto MA. The transcription factor snail controls epithelial-mesenchymal transitions by repressing E-cadherin expression. *Nat Cell Biol*. 2000;2:76–83.
33. Diez M, Musri MM, Ferrer E, Barbera JA, Peinado VI. Endothelial progenitor cells undergo an endothelial-to-mesenchymal transition-like process mediated by TGF β RI. *Cardiovasc Res*. 2010;88:502–11.
34. Medici D, Shore EM, Lounev VY, Kaplan FS, Kalluri R, Olsen BR. Conversion of vascular endothelial cells into multipotent stem-like cells. *Nat Med*. 2010;16:1400–6.
35. Kokudo T, Suzuki Y, Yoshimatsu Y, Yamazaki T, Watabe T, Miyazono K. Snail is required for TGF β -induced endothelial-mesenchymal transition of embryonic stem cell-derived endothelial cells. *J Cell Sci*. 2008;121:3317–24.
36. Niessen K, Fu Y, Chang L, Hoodless PA, McFadden D, Karsan A. Slug is a direct Notch target required for initiation of cardiac cushion cellularization. *J Cell Biol*. 2008;182:315–25.
37. Luna-Zurita L, Prados B, Grego-Bessa J, Luxan G, del Monte G, Benguria A, Adams RH, Perez-Pomares JM, de la Pompa JL. Integration of a Notch-dependent mesenchymal gene program and Bmp2-driven cell invasiveness regulates murine cardiac valve formation. *J Clin Invest*. 2010;120:3493–507.
38. Aisagbonhi O, Rai M, Ryzhov S, Atria N, Feoktistov I, Hatzopoulos AK. Experimental myocardial infarction triggers canonical Wnt signaling and endothelial-to-mesenchymal transition. *Dis Model Mech*. 2011;4:469–83. **This paper was the first to show canonical Wnt signaling induction and the significant contribution of EndMT in cardiac fibrosis after acute ischemic injury.**

39. Cheng SL, Shao JS, Behrmann A, Krchma K, Towler DA. Dkk1 and MSX2-Wnt7b signaling reciprocally regulate the endothelial-mesenchymal transition in aortic endothelial cells. *Arterioscler Thromb Vasc Biol.* 2013;33:1679–89.
40. Piera-Velazquez S, Li Z, Jimenez SA. Role of endothelial-mesenchymal transition (EndoMT) in the pathogenesis of fibrotic disorders. *Am J Pathol.* 2011;179:1074–80.
41. Hashimoto N, Phan SH, Imaizumi K, Matsuo M, Nakashima H, Kawabe T, Shimokata K, Hasegawa Y. Endothelial-mesenchymal transition in bleomycin-induced pulmonary fibrosis. *Am J Respir Cell Mol Biol.* 2010;43:161–72.
42. Ranchoux B, Antigny F, Rucker-Martin C, Hautefort A, Pêchoux C, Bogaard HJ, Dorfmueller P, Remy S, Lecerf F, Planté S, Chat S, Fadel E, Houssaini A, Anegón I, Adnot S, Simonneau G, Humbert M, Cohen-Kaminsky S, Perros F. Endothelial-to-mesenchymal transition in pulmonary hypertension. *Circulation.* 2015;131:1006–18.
43. Good RB, Gilbane AJ, Trinder SL, Denton CP, Coghlan G, Abraham DJ, Holmes AM. Endothelial to mesenchymal transition contributes to endothelial dysfunction in pulmonary arterial hypertension. *Am J Pathol.* 2015;185:1850–8.
44. Hopper RK, Moonen JR, Diebold I, Cao A, Rhodes CJ, Tojais NF, Hennigs JK, Gu M, Wang L, Rabinovitch M. In pulmonary arterial hypertension, reduced BMPR2 promotes endothelial-to-mesenchymal transition via HMGA1 and its target Slug. *Circulation.* 2016;133:1783–94.
45. Zeisberg EM, Potenta SE, Sugimoto H, Zeisberg M, Kalluri R. Fibroblasts in kidney fibrosis emerge via endothelial-to-mesenchymal transition. *J Am Soc Nephrol.* 2008;19:2282–7.
46. Li J, Qu X, Yao J, Caruana G, Ricardo SD, Yamamoto Y, Yamamoto H, Bertram JF. Blockade of endothelial-mesenchymal transition by a Smad3 inhibitor delays the early development of streptozotocin-induced diabetic nephropathy. *Diabetes.* 2010;59:2612–24.
47. Xavier S, Vasko R, Matsumoto K, Zullo JA, Chen R, Maizel J, Chander PN, Goligorsky MS. Curtailing endothelial TGF- β signaling is sufficient to reduce endothelial-mesenchymal transition and fibrosis in CKD. *J Am Soc Nephrol.* 2015;26:817–29.
48. Zeisberg EM, Tarnavski O, Zeisberg M, Dorfman AL, McMullen JR, Gustafsson E, Chandraker A, Yuan X, Pu WT, Roberts AB, Neilson EG, Sayegh MH, Izumo S, Kalluri R. Endothelial-to-mesenchymal transition contributes to cardiac fibrosis. *Nat Med.* 2007;2007(13):952–61. **This landmark paper first discovered the impact of EndMT in cardiac fibrosis and its inhibition by BMP7.**
49. Widyantoro B, Emoto N, Nakayama K, Anggrahini DW, Adiarto S, Iwasa N, Yagi K, Miyagawa K, Rikitake Y, Suzuki T, Kisanuki YY, Yanagisawa M, Hirata K. Endothelial cell-derived endothelin-1 promotes cardiac fibrosis in diabetic hearts through stimulation of endothelial-to-mesenchymal transition. *Circulation.* 2010;121:2407–18.
50. Ghosh AK, Bradham WS, Gleaves LA, De Taeye B, Murphy SB, Covington JW, Vaughan DE. Genetic deficiency of plasminogen activator inhibitor-1 promotes cardiac fibrosis in aged mice: involvement of constitutive transforming growth factor-beta signaling and endothelial-to-mesenchymal transition. *Circulation.* 2010;122:1200–9.
51. Rieder F, Kessler SP, West GA, Bhilocha S, de la Motte C, Sadler TM, Gopalan B, Stylianou E, Fiocchi C. Inflammation-induced endothelial-to-mesenchymal transition: a novel mechanism of intestinal fibrosis. *Am J Pathol.* 2011;179:2660–73.
52. Wu J, Montaniel KR, Saleh MA, Xiao L, Chen W, Owens GK, Humphrey JD, Majesky MW, Paik DT, Hatzopoulos AK, Madhur MS, Harrison DG. Origin of matrix-producing cells that contribute to aortic fibrosis in hypertension. *Hypertension.* 2016;67:461–8. **This paper first identified EndMT, adventitial Sca1⁺ progenitor cells, resident fibroblasts, and bone marrow-recruited fibrocytes as diverse sources of collagen-producing cells in the aortic wall of hypertensive mice.**
53. Chen PY, Qin L, Baeyens N, Li G, Afolabi T, Budatha M, Tellides G, Schwartz MA, Simons M. Endothelial-to-mesenchymal transition drives atherosclerosis progression. *J Clin Invest.* 2015;125:4514–28. **Here, the authors described the contribution of EndMT in atherosclerotic lesions and the role of FGF and TGF β signaling in EndMT induction.**
54. Evrard SM, Lecce L, Michelis KC, Nomura-Kitabayashi A, Pandey G, Purushothaman KR, d'Escamard V, Li JR, Hadri L, Fujitani K, Moreno PR, Benard L, Rimmele P, Cohain A, Mecham B, Randolph GJ, Nabel EG, Hajjar R, Fuster V, Boehm M, Kovacic JC. Endothelial to mesenchymal transition is common in atherosclerotic lesions and is associated with plaque instability. *Nat Commun.* 2016;7:11853. doi:10.1038/ncomms11853. **Here, the authors tracked EndMT in mouse and human atherosclerotic lesions and showed its association with plaque instability.**
55. Chen PY, Qin L, Barnes C, Charisse K, Yi T, Zhang X, Ali R, Medina PP, Yu J, Slack FJ, Anderson DG, Kotlianski V, Wang F, Tellides G, Simons M. FGF regulates TGF- β signaling and endothelial-to-mesenchymal transition via control of *let-7* miRNA expression. *Cell Rep.* 2012;2:1684–96. **The authors identified let-7 miRNA as a key upstream regulator of EndMT.**
56. Cooley BC, Nevado J, Mellad J, Yang D, St Hilaire C, Negro A, Fang F, Chen G, San H, Walts AD, Schwartzbeck RL, Taylor B, Lanzer JD, Wragg A, Elagha A, Beltran LE, Berry C, Feil R, Virmani R, Ladich E, Kovacic JC, Boehm M. TGF- β signaling mediates endothelial-to-mesenchymal transition (EndMT) during vein graft remodeling. *Sci Transl Med.* 2014;6:227ra34. doi:10.1126/scitranslmed.3006927.
57. Yao J, Guihard PJ, Blazquez-Medela AM, Guo Y, Moon JH, Jumabay M, Boström KI, Yao Y. Serine protease activation essential for endothelial-mesenchymal transition in vascular calcification. *Circ Res.* 2015;117:758–69.
58. Cao Y, Feng B, Chen S, Chu Y, Chakrabarti S. Mechanisms of endothelial to mesenchymal transition in the retina in diabetes. *Invest Ophthalmol Vis Sci.* 2014;55:7321–31.
59. Shapero K, Wylie-Sears J, Levine RA, Mayer Jr JE, Bischoff J. Reciprocal interactions between mitral valve endothelial and interstitial cells reduce endothelial-to-mesenchymal transition and myofibroblastic activation. *J Mol Cell Cardiol.* 2015;80:175–85.
60. Zeisberg EM, Potenta S, Xie L, Zeisberg M, Kalluri R. Discovery of endothelial to mesenchymal transition as a source for carcinoma-associated fibroblasts. *Cancer Res.* 2007;67:10123–8.
61. Moore-Morris T, Guimarães-Cambo N, Banerjee I, Zambon AC, Kisseleva T, Velayoudon A, Stallcup WB, Gu Y, Dalton ND, Cedenilla M, Gomez-Amaro R, Zhou B, Brenner DA, Peterson KL, Chen J, Evans SM. Resident fibroblast lineages mediate pressure overload-induced cardiac fibrosis. *J Clin Invest.* 2014;124:2921–34. **Applying a pressure overload model, this manuscript shows that most myofibroblasts are generated by proliferation and activation of resident fibroblasts with minor EndMT contribution.**
62. Kanisicak O, Khalil H, Ivey MJ, Karch JMBD, Correll RN, Brody MJ, Lin SC J, Aronow BJ, Tallquist MD, Molkenin JD. Genetic lineage tracing defines myofibroblast origin and function in the injured heart. *Nat Commun.* 2016;7:12260. doi:10.1038/ncomms12260. **The authors use lineage tracing to identify resident Tcf21 cells as the main source of myofibroblasts after myocardial infarction.**
63. Maddaluno L, Rudini N, Cuttano R, Bravi L, Giampietro C, Corada M, Ferrarini L, Orsenigo F, Papa E, Boulday G, Tournier-Lasserre E, Chapon F, Richichi C, Retta SF,

- Lampugnani MG, Dejana E. EndMT contributes to the onset and progression of cerebral cavernous malformations. *Nature*. 2013;498:492–6.
64. Medici D, Kalluri R. Endothelial-mesenchymal transition and its contribution to the emergence of stem cell phenotype. *Semin Cancer Biol*. 2012;22:379–84.
 65. Uchida S, De Gaspari P, Kostin S, Jenniches K, Kilic A, Izumiya Y, Shiojima I, Grosse Kreymborg K, Renz H, Walsh K, Braun T. Sca1-derived cells are a source of myocardial renewal in the murine adult heart. *Stem Cell Reports*. 2013;1:397–410. **The authors found that Sca1 cells differentiate into cardiomyocytes during homeostasis.**
 66. Chen Q, Zhang H, Liu Y, Adams S, Eilken H, Stehling M, Corada M, Dejana E, Zhou B, Adams RH. Endothelial cells are progenitors of cardiac pericytes and vascular smooth muscle cells. *Nat Commun*. 2016;7:12422. doi:10.1038/ncomms12422.
 67. Shoshani O, Zipori D. Transition of endothelium to cartilage and bone. *Cell Stem Cell*. 2011;8:10–1.
 68. Tran KV, Gealekman O, Frontini A, Zingaretti MC, Morroni M, Giordano A, Smorlesi A, Perugini J, De Matteis R, Sbarbati A, Corvera S, Cinti S. The vascular endothelium of the adipose tissue gives rise to both white and brown fat cells. *Cell Metab*. 2012;15:222–9.
 69. Tang R, Gao M, Wu M, Liu H, Zhang X, Liu B. High glucose mediates endothelial-to-chondrocyte transition in human aortic endothelial cells. *Cardiovasc Diabetol*. 2012;11:11.
 70. Murdoch CE, Chaubey S, Zeng L, Yu B, Ivetic A, Walker SJ, Vanhoutte D, Heymans S, Grieve DJ, Cave AC, Brewer AC, Zhang M, Shah AM. Endothelial NADPH oxidase-2 promotes interstitial cardiac fibrosis and diastolic dysfunction through pro-inflammatory effects and endothelial-mesenchymal transition. *J Am Coll Cardiol*. 2014;63:2734–41.
 71. Ambrozova G, Fidlerova T, Verescakova H, Koudelka A, Rudolph TK, Woodcock SR, Freeman BA, Kubala L, Pekarova M. Nitro-oleic acid inhibits vascular endothelial inflammatory responses and the endothelial-mesenchymal transition. *Biochim Biophys Acta*. 1860;2016:2428–37.
 72. Moonen JR, Lee ES, Schmidt M, Maleszewska M, Koerts JA, Brouwer LA, van Kooten TG, van Luyn MJ, Zeebregts CJ, Krenning G, Harmsen MC. Endothelial-to-mesenchymal transition contributes to fibro-proliferative vascular disease and is modulated by fluid shear stress. *Cardiovasc Res*. 2015;108:377–86.
 73. Medici D, Potenta S, Kalluri R. Transforming growth factor-2 promotes snail-mediated endothelial-mesenchymal transition through convergence of smad-dependent and smad-independent signaling. *Biochem J*. 2011;437:515–20.
 74. Mahler GJ, Farrar EJ, Butcher JT. Inflammatory cytokines promote mesenchymal transformation in embryonic and adult valve endothelial cells. *Arterioscler Thromb Vasc Biol*. 2013;33:121–30.
 75. Maleszewska M, Moonen JR, Huijkman N, van de Sluis B, Krenning BG, Harmsen MC. IL-1 and TGF 2 synergistically induce endothelial to mesenchymal transition in an NFkB-dependent manner. *Immunobiology*. 2013;218:443–54.
 76. Liebner S, Cattelino A, Gallini R, Rudini N, Iurlaro M, Piccolo S, Dejana E. Beta-catenin is required for endothelial-mesenchymal transformation during heart cushion development in the mouse. *J Cell Biol*. 2004;166:359–67.
 77. van Meeteren LA, ten Dijke P. Regulation of endothelial cell plasticity by TGF- β . *Cell Tissue Res*. 2012;347:177–86.
 78. Chen PY, Qin L, Tellides G, Simons M. Fibroblast growth factor receptor 1 is a key inhibitor of TGF β signaling in the endothelium. *Sci Signal*. 2014;23(7):ra90. doi:10.1126/scisignal.2005504.
 79. Yoshida T, Hayashi M. Role of Krüppel-like factor 4 and its binding proteins in vascular disease. *J Atheroscler Thromb*. 2014;21:402–13.
 80. Cuttano R, Rudini N, Bravi L, Corada M, Giampietro C, Papa E, Morini MF, Maddaluno L, Baeyens N, Adams RH, Jain MK, Owens GK, Schwartz M, Lampugnani MG, Dejana E. KLF4 is a key determinant in the development and progression of cerebral cavernous malformations. *EMBO Mol Med*. 2015;8:6–24.
 81. Zhou Z, Tang AT, Wong WY, Bamezai S, Goddard LM, Shenkar R, Zhou S, Yang J, Wright AC, Foley M, Arthur JS, Whitehead KJ, Awad IA, Li DY, Zheng X, Kahn ML. Cerebral cavernous malformations arise from endothelial gain of MEKK3-KLF2/4 signalling. *Nature*. 2016;532:122–6.
 82. Zhao Y, Qiao X, Wang L, Tan TK, Zhao H, Zhang Y, Zhang J, Rao P, Cao Q, Wang Y, Wang Y, Wang YM, Lee VW, Alexander SI, Harris DC, Zheng G. Matrix metalloproteinase 9 induces endothelial-mesenchymal transition via Notch activation in human kidney glomerular endothelial cells. *BMC Cell Biol*. 2016;17:21. doi:10.1186/s12860-016-0101-0.
 83. Correia AC, Moonen JR, Brinker MG, Krenning G. FGF2 inhibits endothelial-mesenchymal transition through microRNA-20a-mediated repression of canonical TGF- β signaling. *J Cell Sci*. 2016;129:569–79.
 84. Feng B, Cao Y, Chen S, Chu X, Chu Y, Chakrabarti S. miR-200b mediates endothelial-to-mesenchymal transition in diabetic cardiomyopathy. *Diabetes*. 2016;65:768–79.
 85. Sun Y, Cai J, Yu S, Chen S, Li F, Fan C. miR-630 inhibits endothelial-mesenchymal transition by targeting Slug in traumatic heterotopic ossification. *Sci Rep*. 2016;6:22729. doi:10.1038/srep22729.
 86. Piera-Velazquez S, Mendoza FA, Jimenez SA. Role of endothelial-mesenchymal transition (EndoMT) in the pathogenesis of human fibrotic diseases. *J Clin Med*. 2016;5. doi:10.3390/jcm5040045.
 87. Garcia J, Sandi MJ, Cordelier P, Binétruy B, Pouyssegur J, Iovanna JL, Tournaire R. Tie1 deficiency induces endothelial-mesenchymal transition. *EMBO Rep*. 2012;13:431–9.
 88. Rong JX, Shapiro M, Trogan E, Fisher EA. Transdifferentiation of mouse aortic smooth muscle cells to a macrophage-like state after cholesterol loading. *Proc Natl Acad Sci U S A*. 2003;100:13531–6.
 89. Allahverdian S, Chehroudi AC, McManus BM, Abraham T, Francis GA. Contribution of intimal smooth muscle cells to cholesterol accumulation and macrophage-like cells in human atherosclerosis. *Circulation*. 2014;129:1551–9.
 90. Feil S, Fehrenbacher B, Lukowski R, Essmann F, Schulze-Osthoff K, Schaller M, Feil R. Transdifferentiation of vascular smooth muscle cells to macrophage-like cells during atherogenesis. *Circ Res*. 2014;115:662–7.
 91. Shankman LS, Gomez D, Cherepanova OA, Salmon M, Alencar GF, Haskins RM, Swiatlowska P, Newman AA, Greene ES, Straub AC, Isakson B, Randolph GJ, Owens GK. KLF4-dependent phenotypic modulation of smooth muscle cells has a key role in atherosclerotic plaque pathogenesis. *Nat Med*. 2015;21:628–37. **This study identified Krüppel-like factor 4 as a key contributing factor to atherosclerotic lesion formation by promoting the transition of smooth muscle cells to macrophages and mesenchymal stem cells.**
 92. Albarrán-Juárez J, Kaur H, Grimm M, Offermanns S, Wetschreck N. Lineage tracing of cells involved in atherosclerosis. *Atherosclerosis*. 2016;251:445–53.
 93. Chappell J, Harman JL, Narasimhan VM, Yu H, Foote K, Simons BD, Bennett MR, Jorgensen HF. Extensive proliferation of a subset of differentiated, yet plastic, medial vascular smooth muscle cells contribute to neointimal formation in mouse injury and atherosclerosis models. *Circ Res*. 2016;119:1313–23.
 94. Chen PY, Qin L, Li G, Tellides G, Simons M. Fibroblast growth factor (FGF) signaling regulates transforming growth factor beta

- (TGF β)-dependent smooth muscle cell phenotype modulation. *Sci Rep*. 2016;6:33407. doi:10.1038/srep33407.
95. Psaltis PJ, Simari RD. Vascular wall progenitor cells in health and disease. *Circ Res*. 2015;116:1392–412.
 96. Nurnberg ST, Cheng K, Raiesdana A, Kundu R, Miller CL, Kim JB, Arora K, Carcamo-Oribe I, Xiong Y, Tellakula N, Nanda V, Murthy N, Boisvert WA, Hedin U, Perisic L, Aldi S, Maegdefessel L, Pjanic M, Owens GK, Tallquist MD, Quertermous T. Coronary artery disease associated transcription factor TCF21 regulates smooth muscle precursor cells that contribute to the fibrous cap. *PLoS Genet*. 2015;11:e1005155. doi:10.1371/journal.pgen.1005155.
 97. Hu Y, Zhang Z, Torsney E, Afzal AR, Davison F, Metzler B, Xu Q. Abundant progenitor cells in the adventitia contribute to atherosclerosis of vein grafts in ApoE-deficient mice. *J Clin Invest*. 2004;113:1258–65.
 98. Passman JN, Dong XR, Wu SP, Maguire CT, Hogan KA, Bautch VL, Majesky MW. A sonic hedgehog signaling domain in the arterial adventitia supports resident Sc α 1⁺ smooth muscle progenitor cells. *Proc Natl Acad Sci U S A*. 2008;105:9349–54.
 99. Majesky MW, Dong XR, Høglund V, Mahoney Jr WM, Daum G. The adventitia: a dynamic interface containing resident progenitor cells. *Arterioscler Thromb Vasc Biol*. 2011;31:1530–9.
 100. Sainz J, Al Haj Zen A, Caligiuri G, Demerens C, Urbain D, Lemitre M, Lafont A. Isolation of “side population” progenitor cells from healthy arteries of adult mice. *Arterioscler Thromb Vasc Biol*. 2006;26:281–6.
 101. Ryzhov S, Sung BH, Zhang Q, Weaver A, Gumina RJ, Biaggioni I, Feoktistov I. Role of adenosine A2B receptor signaling in contribution of cardiac mesenchymal stem-like cells to myocardial scar formation. *Purinergic Signal*. 2014;10:477–86.
 102. Ieronimakis N, Hays AL, Janebodin K, Mahoney Jr WM, Duffield JS, Majesky MW, Reyes M. Coronary adventitial cells are linked to perivascular cardiac fibrosis via TGF β 1 signaling in the mdx mouse model of Duchenne muscular dystrophy. *J Mol Cell Cardiol*. 2013;63:122–34.
 103. Ieronimakis N, Hays A, Prasad A, Janebodin K, Duffield JS, Reyes M. PDGFR α signalling promotes fibrogenic responses in collagen-producing cells in Duchenne muscular dystrophy. *J Pathol*. 2016;241:410–24.
 104. Kramann R, Schneider RK, DiRocco DP, Machado F, Fleig S, Bondzie PA, Henderson JM, Ebert BL, Humphreys BD. Perivascular Gli1⁺ progenitors are key contributors to injury-induced organ fibrosis. *Cell Stem Cell*. 2015;16:51–66. **The authors identified a new resident perivascular cell population contributing to fibrosis across a variety of organs.**
 105. Mendoza FA, Piera-Velazquez S, Farber JL, Feghali-Bostwick C, Jiménez SA. Endothelial cells expressing endothelial and mesenchymal cell gene products in lung tissue from patients with systemic sclerosis-associated interstitial lung disease. *Arthritis Rheumatol*. 2016;68:210–7.

Coordinated Proliferation and Differentiation of Human-Induced Pluripotent Stem Cell-Derived Cardiac Progenitor Cells Depend on Bone Morphogenetic Protein Signaling Regulation by GREMLIN 2

Jeffery B. Bylund,^{1,2} Linh T. Trinh,¹ Cassandra P. Awgulewitsch,¹ David T. Paik,^{1,3,*}
Christopher Jetter,¹ Rajneesh Jha,⁴ Jianhua Zhang,⁵ Kristof Nolan,⁶ Chunhui Xu,⁴
Thomas B. Thompson,⁶ Timothy J. Kamp,⁵ and Antonis K. Hatzopoulos^{1,3}

Heart development depends on coordinated proliferation and differentiation of cardiac progenitor cells (CPCs), but how the two processes are synchronized is not well understood. Here, we show that the secreted Bone Morphogenetic Protein (BMP) antagonist GREMLIN 2 (GREM2) is induced in CPCs shortly after cardiac mesoderm specification during differentiation of human pluripotent stem cells. GREM2 expression follows cardiac lineage differentiation independently of the differentiation method used, or the origin of the pluripotent stem cells, suggesting that GREM2 is linked to cardiogenesis. Addition of GREM2 protein strongly increases cardiomyocyte output compared to established procardiogenic differentiation methods. Our data show that inhibition of canonical BMP signaling by GREM2 is necessary to promote proliferation of CPCs. However, canonical BMP signaling inhibition alone is not sufficient to induce cardiac differentiation, which depends on subsequent JNK pathway activation specifically by GREM2. These findings may have broader implications in the design of approaches to orchestrate growth and differentiation of pluripotent stem cell-derived lineages that depend on precise regulation of BMP signaling.

Keywords: cardiomyocyte differentiation, human pluripotent stem cells, BMP signaling, GREMLIN 2

Introduction

HUMAN EMBRYONIC STEM (ES) AND induced pluripotent stem (iPS) cells differentiate to a variety of distinct tissue-specific cell types, providing a unique resource to study human embryonic development and disease mechanisms [1–4]. A major challenge in this endeavor is to enrich the differentiation of pluripotent stem cell to specific cell types with desired characteristics [5–8]. Specifically for cardiomyocytes (CMs), several experimental protocols have emerged that stimulate differentiation of ES and iPS cells toward the cardiac lineage by exploiting pathways that regulate embryonic cardiovascular development, optimizing extracellular matrix substrates, using timely application of chemical compounds, or combinations of the above [9–13]; however, robust differentiation

has been based on empirical trial and error approaches without a clear understanding of how the balance between growth and differentiation of progenitor cells is regulated during expansion of the cardiac lineage.

We have previously shown in zebrafish that the secreted Bone Morphogenetic Protein (BMP) antagonist Gremlin 2 (Grem2), also called Protein Related to Dan and Cerberus (PRDC), is expressed in pharyngeal mesoderm during the initial formation of the cardiac tube and is necessary for cardiac laterality and proper differentiation of CMs [14,15]. More recently, we found that Grem2 promotes cardiac lineage expansion during differentiation of mouse ES cells [16,17]. However, whether GREM2 plays a role in the expansion or differentiation of human cardiac progenitor cells (CPCs), or both, is not known.

¹Division of Cardiovascular Medicine, Department of Medicine, Vanderbilt University Medical Center, Nashville, Tennessee.

²Department of Pharmacology, Vanderbilt University School of Medicine, Nashville, Tennessee.

³Department of Cell and Developmental Biology, Vanderbilt University School of Medicine, Nashville, Tennessee.

⁴Department of Pediatrics, Emory University School of Medicine, Atlanta, Georgia.

⁵Stem Cell and Regenerative Medicine Center, University of Wisconsin School of Medicine and Public Health, Madison, Wisconsin.

⁶Department of Molecular Genetics, Biochemistry and Microbiology, University of Cincinnati, Cincinnati, Ohio.

*Current affiliation: Stanford Cardiovascular Institute, Stanford University, Stanford, California.

Using human pluripotent stem cells, we show that GREM2 expression is induced in NKX2.5⁺ CPCs during the initial steps of their differentiation and promotes the formation of contracting CMs. The GREM2 effect depends on dual positive effects on CPC proliferation and differentiation that depend on sequential inhibition of the canonical, p-SMAD-mediated BMP signaling and activation of the noncanonical JNK pathway, respectively. This novel regulation of BMP signaling provides a unique mechanism to optimize the growth and differentiation of human CMs.

Materials and Methods

Human pluripotent stem cell culture

Human iPS (hiPS) cell lines iMR90 and DF 19-9-11 from WiCell were cultured under feeder-free conditions in mTeSR1 or Essential 8 (E8) media (Stem Cell Technologies) as previously described [18]. Briefly, cells were thawed and seeded onto six-well plates coated with 8.7 $\mu\text{g}/\text{cm}^2$ growth factor-reduced Matrigel (Corning) in mTeSR1 or E8 media supplemented with 10 μM Y-27632 dihydrochloride (Tocris Bioscience) to promote cell survival and attachment. Media were exchanged daily until cells reached ~60%–70% confluence. Cells were passaged using Versene EDTA cell dissociation reagent (Thermo Fisher Scientific/Gibco) and seeded onto Matrigel-coated plates in mTeSR1 or E8 media supplemented with 10 μM Y-27632 dihydrochloride at a split ratio of 1:15–1:20. Cells were kept in a copper-lined humidified incubator (Thermo Fisher Scientific) at 37°C with a 5% CO₂ atmosphere.

Human ES (hES) cells WA07 were cultured in conditioned media as previously described [19]. Briefly, cells were cultured in mouse embryonic fibroblast (MEF)-conditioned medium supplemented with basic fibroblast growth factor (bFGF) (8 ng/mL). Cells were cultured for 4–6 days or until colonies occupied 75%–80% of well surface area. Cells were then passaged by rinsing with Dulbecco's phosphate-buffered saline and incubating with collagenase (200 U/mL) for 5–10 min at 37°C to dissociate them into small clumps. Clumps were then plated onto six-well cell culture plates precoated with 1 mL/well of 50 $\mu\text{g}/\text{mL}$ Matrigel (Corning). Cells were kept in a copper-lined humidified incubator (Thermo Fisher Scientific) at 37°C with a 5% CO₂ atmosphere.

iPS cell differentiation

hiPS cells were differentiated using the “Matrix Sandwich” method, the GiWi method, or the BMP/Activin A method, as already described [11,20,21]. In all differentiation methods, cells were allowed to become 80%–90% confluent and then dissociated by incubating in Versene EDTA cell dissociation reagent (Thermo Fisher Scientific/Gibco) for 10 min at room temperature. After incubation, cells were triturated to dissociate into a single-cell suspension. Single-cell preparations were centrifuged for 5 min at 200 *g* and cell pellets were resuspended in cell culture media for plating.

For the “Matrix Sandwich” method, cells were resuspended in E8 or mTeSR1 media (Stem Cell Technologies) supplemented with 10 μM ROCKi (Y-27632 dihydrochloride; Tocris) and plated onto Matrigel-coated (8.7 $\mu\text{g}/\text{cm}^2$) 12-well culture plates at a density of 500,000 cells per well. Fresh E8

or mTeSR1 media were given daily until cells became 90% confluent. When 90% confluent, cells were overlaid with 8.7 $\mu\text{g}/\text{cm}^2$ growth factor-reduced Matrigel (Corning) in E8 or mTeSR1 media. After 24 h, the matrix coating solution was removed and fresh E8 or mTeSR1 media were added until cells were 100% confluent. Cells were then treated with 1 mL/well of day 0 media (RPMI 1640 media supplemented with B27 minus insulin, coated with 8.7 $\mu\text{g}/\text{cm}^2$ Matrigel, and 100 ng/mL Activin A; R&D Systems). Exactly 24 h later, day 0 media were aspirated and cells were treated with 1.5 mL/well of day 1 media (RPMI 1640 media supplemented with B27 minus insulin) (Life Technologies), 5 ng/mL of hBMP4 (R&D Systems), and 10 ng/mL human bFGF (Life Technologies).

Four days after addition of day 1 media, cells were treated with 1 mL/well basal differentiation media (RPMI 1640 media supplemented with B27 plus insulin). Cells treated with GREM2 received 1 mL/well of RPMI 1640 media with B27 minus insulin supplemented with 150 ng/mL GREM2 exactly 48 h after adding day 1 media (day 3). At day 5, GREM2-treated wells received basal differentiation medium with 150 ng/mL of GREM2. Media in all wells were replaced daily. Cells were treated in a similar manner with 50 ng/mL NOGGIN or 1.5 $\mu\text{g}/\text{mL}$ DAN, based on their specific activities (R&D Systems). GREM2 wild-type protein and mutated versions of GREM2 were synthesized, purified, and measured for activity as previously described [22–24].

The BMP/Activin A method followed the same protocol as described for the “Matrix Sandwich” method, but without the Matrigel overlay steps.

For the GiWi method, cells were resuspended in E8 media (Stem Cell Technologies) supplemented with 10 μM ROCKi (Y-27632 dihydrochloride; Tocris) and plated onto Matrigel-coated (8.7 $\mu\text{g}/\text{cm}^2$) 12-well culture plates at a density of 500,000 cells per well. Once cells were 100% confluent (typically 3–4 days after seeding), differentiation was started by adding 2 mL/well of day 0 media (RPMI 1640 with B27 minus insulin and 12 μM CHIR 99021). Exactly 24 h after adding day 0 media, cells were treated with 2 mL/well early differentiation media (RPMI 1640 with B27 minus insulin). After 48 h, 1 mL/well of conditioned media was removed from differentiating cells and combined with 1 mL early differentiation media and supplemented with 2 μM IWR-1 endo (Tocris). After 48 h, cells were treated with 2 mL/well of late differentiation media (RPMI 1640 with B27 plus insulin). Late differentiation media were then replaced daily.

The hES cells were differentiated as previously described [25]. Briefly, WA07 hES cells were rinsed with 2 mL DPBS and incubated with 2 mL Versene (EDTA; Life Technologies) for 10 min at 37°C. Versene was aspirated and replaced with 1 mL/well of MEF-conditioned media supplemented with 8 ng/mL of bFGF. hES cells were triturated to produce a single-cell suspension and seeded onto 24-well Matrigel-coated (8.7 $\mu\text{g}/\text{cm}^2$) plates at a density of 400,000 cells per well. Cells were given fresh media daily until 100% confluent. Once 100% confluent, cells were given 1 mL/well day 0 medium (RPMI 1640 with 2% B27 minus insulin and 100 ng/mL Activin A). Cells were incubated at 37°C for 24 h and then treated with 1 mL/well of day 1 medium (RPMI 1640 with 2% B27 minus insulin and 10 ng/mL BMP4). After 4 days, the medium was replaced with late differentiation medium (RPMI 1640 with 2% B27). 1 mL/well of fresh late differentiation media was added to each well every other day.

Reverse transcriptase quantitative polymerase chain reaction

Cells were collected from each well using Tryp-LE Select (Thermo Fisher Scientific) and centrifuged at 200 g for 5 min to pellet. Cell pellets were lysed using RLT buffer, and RNA was isolated using the RNeasy Mini Kit following the manufacturer's instructions (Qiagen). cDNA was generated by reverse transcription of 1–3 µg of RNA as we have previously reported [16]. cDNA samples were amplified using GoTaq qPCR Master Mix (Promega) in a Bio-Rad CFX thermocycler. Relative gene expression levels were calculated using the delta-delta Ct method [26,27]. Relative primer efficiencies were determined using the Real-time PCR Miner algorithm and confirmed experimentally using the slope of the standard curve from plotting log(DNA copy number) versus Ct value [28]. Amplification primer sequences are reported in Supplementary Table S1 (Supplementary Data are available online at www.liebertpub.com/scd).

Cell quantification

Cells were dissociated into single-cell suspensions using Tryp-LE Express (Life Technologies), stained with trypan blue (diluted 1:2 in PBS or cell culture media) to exclude dead cells and quantified using a Bio-Rad TC-10 automated cell counter. For DAPI-stained cells, cell numbers were quantified by dividing three fields of view from three independent wells per condition into quadrants and manually counting the number of nuclei visible in each quadrant.

Immunofluorescence

Cells were seeded onto Matrigel-coated (8.7 µg/cm²) 12-well plastic culture plates (Thermo Fisher Scientific) at a density of 500,000 cells per well and differentiated as described above for the "Matrix Sandwich" method. Cells were fixed at the desired time points (differentiation days 4, 5, 6, and 10) by rinsing with 500 µL DPBS and incubating in 4% paraformaldehyde in PBS at 4°C for 5 min. The PFA solution was then aspirated and cells were rinsed with 1×PBS five times. Fixed cells were permeabilized by incubating with 400 µL permeabilization buffer (0.2% Triton X-100 in 1×PBS) in each well at room temperature for 1 h. Nonspecific binding was then blocked using 400 µL/well of blocking solution (5% nonfat dry milk in permeabilization buffer) for 2 h at room temperature with gentle rocking. For all subsequent steps, a minimum of 350 µL of solution was added to each well. Cells were then washed 3×5 min with 400 µL/well of 1×PBS at room temperature. After washing, cells were incubated with primary antibodies in incubation buffer (0.1% Triton X-100, 1% BSA in 1×PBS) overnight at 4°C with gentle rocking. Next, cells were washed 3×3 min each, with PBST (0.2% Tween-20 in 1×PBS) followed by 3×3 min each with 1×PBS. Cells were then incubated with secondary antibodies diluted in incubation buffer for 1 h at room temperature in the dark. Finally, cells were then washed 2 times, 3 min each, with 1×PBS and stored in 400 µL 1×PBS for imaging.

Imaging was done using a Leica DM IRB Inverted Microscope or a Zeiss Laser Scanning Microscope (LSM 880). Image analysis and volume rendering were done using NIS Elements, Zen, ImageJ/FIJI, and Imaris software suites. Primary antibodies recognizing phospho-HISTONE H3 (Santa

Cruz Biotechnology; Cat. No. sc-8656-R, 1:500), NKX2.5 (Santa Cruz Biotechnology; sc-8697, 1:50), GREM2 (ProteinTech; 13892-1-AP, 1:100), and α -ACTININ (Sigma; A7811, 1:500) were applied. We have also tested anti-GREM2 rabbit polyclonal antibodies from GeneTex (GTKX108414), Abcam (ab102563), and R&D Systems (AF2069) at a 1:100 dilution. The fluorescent dye 4',6-diamidino-2-phenylindole (DAPI; Invitrogen) was added during the final 15 min of secondary incubation at a 1:10,000 dilution to stain nuclei.

Flow cytometry

Differentiated hiPS cells were washed once with DPBS minus Mg²⁺ and Ca²⁺, incubated with 1 mL/well Accutase at room temperature for 15 min, and triturated to break up into single cells. Accutase was diluted by adding two volumes of late differentiation medium per well and contents were transferred to 15-mL conical tubes through mesh strainer caps to remove large cell clumps. Before centrifugation and after visual confirmation of complete cell detachment and single-cell dissociation with Accutase, the total cell number per well was quantified using the Bio-Rad TC-10 automated cell counter as described above. Cell suspensions were then centrifuged at 200 g for 5 min to pellet cells. Cell pellets were rinsed 1× time with DPBS minus Mg²⁺ and Ca²⁺ and repelleted. Washed pellets were resuspended in 500 µL Fix/Perm buffer (fixation/permeabilization solution; BD Biosciences), transferred to 5-mL round-bottomed flow cytometry tubes (BD Biosciences), and incubated for 40 min on ice. Cells were then pelleted at 300 g for 5 min and supernatant was aspirated. Cells were washed 2× times with Perm/Wash buffer (BD Bioscience) and pelleted by centrifugation at 300 g for 5 min. Cells were blocked by adding 100 µL blocking buffer (BD Bioscience) to each tube and incubating on ice with gentle rocking for 30 min.

Primary antibodies recognizing NKX2.5 (Abcam; ab91196) and MYH6 (Abcam; ab50967) at a 1:100 dilution were added directly to the cell suspensions in each tube and incubated for 2 h on ice with gentle rocking. To wash out primary antibodies, 3 mL of Perm/Wash buffer was added to each tube and then centrifuged at 300 g for 5 min. Supernatant was aspirated and cells were washed with 2 mL/tube fresh Perm/Wash solution and centrifuged at 300 g for 5 min. For secondary antibody incubation, cell pellets were suspended in 100 µL blocking buffer with secondary antibodies at 1:400 dilutions. Cells were incubated with rocking for 30 min on ice and then washed twice with Perm/Wash buffer. Cells were then suspended in Flow Assay Buffer (BD Biosciences) and the percentage of NKX2.5⁺ and MYH6⁺ cells was determined using FACS Aria flow cytometer and analyzed using FACS Diva (BD Bioscience) or FlowJo (FlowJo, LLC) software in the Vanderbilt University Shared Flow Cytometry Resource Laboratory. The total number of CMs per well was calculated by multiplying the total cell number per well (as described above) by the percentage of NKX2.5⁺ or MYH6⁺ cells as determined by flow cytometry.

Western blotting

Protein samples from differentiated hiPS cells (DF 19-9-11; WiCell) were isolated using the RIPA buffer, including the protease inhibitor cocktail and phosphatase inhibitor cocktail 2 and 3 (Sigma) diluted at 1:100. Cell lysates were shaken at 4°C for 30 min and centrifuged at 12,000 rpm at

4°C for 15 min. Protein concentration in supernatants was measured using the Pierce BCA protein assay (Thermo Fisher Scientific). Fifteen micrograms of protein (adjusted to 7.5 μ L with distilled water) was then mixed with 7.5 μ L of 2 \times Laemmli sample buffer (Bio-Rad) containing β -mercaptoethanol (Sigma). Proteins were denatured at 95°C for 5 min and then placed on ice for another 5 min. Electrophoresis was run using sodium dodecyl sulfate polyacrylamide gels with 1 \times MOPS SDS running buffer (Life Technologies). Size fractionated proteins were transferred to nitrocellulose membranes (Bio-Rad) using the semidry system.

Membranes were blocked with 5% dry milk or 5% BSA (Sigma) in Tris-buffered saline (Corning) containing 1% Tween-20 (Sigma) (1 \times TBST) for 1 h at room temperature or 4°C, respectively. Next, membranes were incubated overnight with antibodies recognizing phosphorylated SMAD1/5/9 or total SMAD1 and phosphorylated or total JNK 1&2 (Cell Signaling) diluted at 1:1,000, NKX2.5 (Santa Cruz Biotechnology, sc-8697) diluted at 1:500, and β -ACTIN (Sigma Aldrich, A1978) diluted at 1:5,000 in 5% BSA in 1 \times TBST. Next day, membranes were washed 3 times, 5 min each with TBST and incubated for 2 h at room temperature with peroxidase-conjugated secondary antibodies (Jackson ImmunoResearch) diluted 1:5,000 in 5% dry milk-TBST. Three 5-min washes were performed to wash away unbound secondary antibodies. Signals were detected using SuperSignal West Pico Chemiluminescent Substrate (Thermo Fisher Scientific) and images were taken with ChemiDoc Touch System (Bio-Rad). Protein band intensities were quantified using ImageJ.

Luciferase assays

CGR8 mouse ES cells were transfected with the BRE₂-Luc reporter construct with *luciferase* expression under the control of two canonical BMP signaling responsive elements of the *Id2* gene [16,29]. Cells were treated for 8 h with 40 ng/mL BMP4, 50 ng/mL GREM2, and/or 300 ng/mL BMP decoy protein L51P [30]. Firefly luciferase activity was normalized to Renilla luciferase activity to account for transfection efficiency.

Results

GREM2 is expressed in differentiating human pluripotent stem cells during CPC expansion and differentiation

We have previously shown that *grem2* expression in zebrafish embryos first appears within the pharyngeal arch mesoderm, adjacent to the cardiac field, during the early stages of heart tube formation [14,15]. In mouse embryos, we found that *Grem2* expression appears around embryonic day 8 and overlaps with the nascent cardiac field area [16]. To determine whether GREM2 is associated with early human cardiac development, we cultured and differentiated the hiPS cell line DF 19-9-11, using the “Matrix Sandwich” method that was designed for efficient CM differentiation [20]. We then isolated RNA samples at consecutive days of differentiation and analyzed the temporal program of cardiogenic development by reverse transcriptase quantitative polymerase chain reaction (RT-qPCR). As shown in Fig. 1, expression of the *T BRY* gene that marks mesoderm for-

mation is transiently induced at days 2–3 after initiation of differentiation, followed by sequential expression of markers specific to early cardiogenic mesoderm (*MESP-1*), CPCs (*NKX2.5*, *ISL1*, and *KDR* or *VEGFR2*), and CMs (*TNNT2*, *MYH6*). Expression of endothelial and hematopoietic genes (*CD31*, *VE-CADHERIN*, *HBBY*) was at low levels (data not shown), likely because the “Matrix Sandwich” method is optimized specifically for cardiac differentiation.

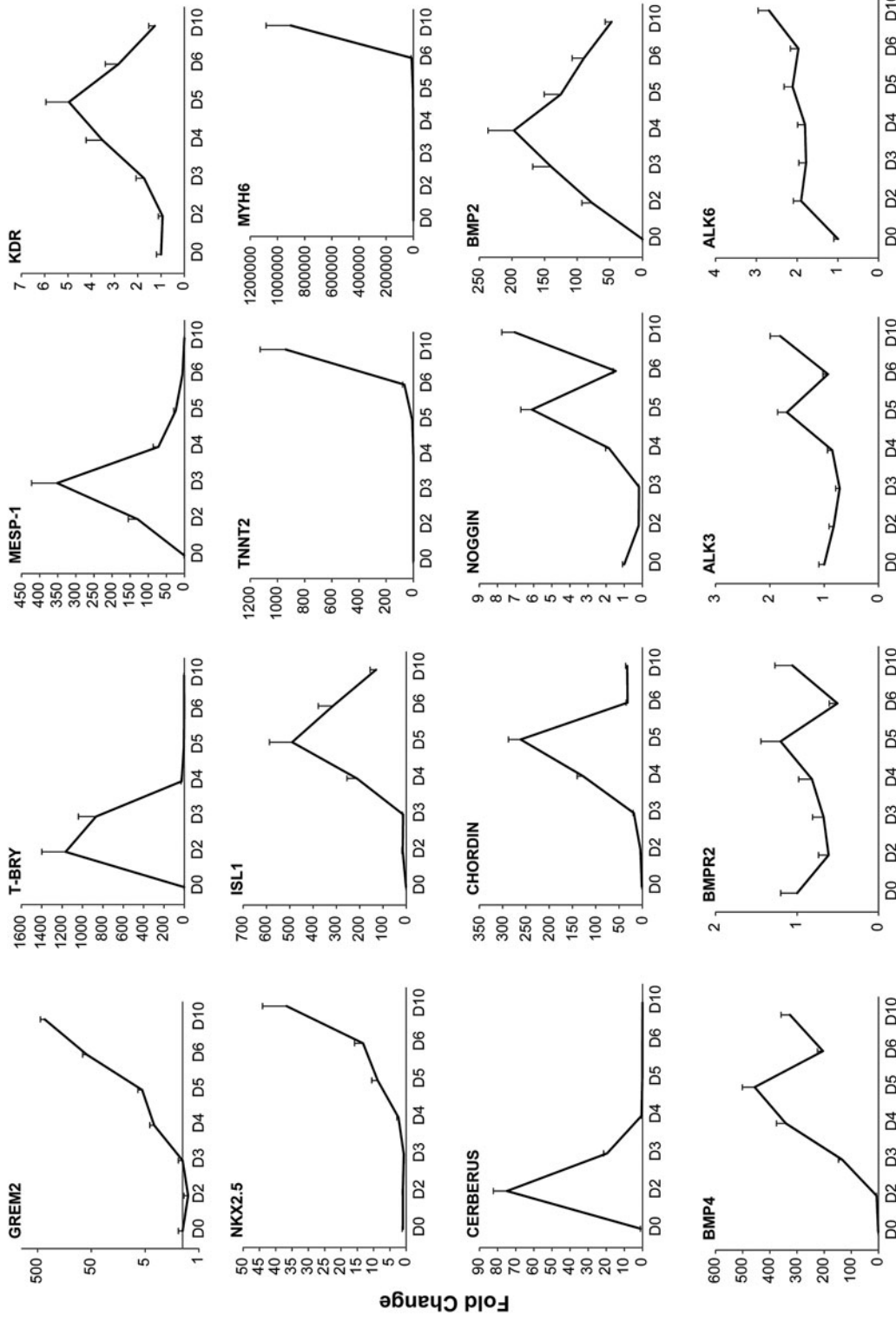
To place *GREM2* expression in the context of other BMP signaling components during hiPS cell differentiation, we analyzed expression of select BMP ligands, BMP receptors, and BMP antagonists. Our results show that *CERBERUS LIKE 1* and *CHORDIN* are transiently induced during mesoderm formation, in accordance with their expression patterns in other species [16,31–33], whereas *NOGGIN* is expressed at later time points of differentiation. *GREM2* expression appears after mesoderm formation, coincidentally with early cardiac markers such as *NKX2.5*, and continues to rise during cardiac differentiation (Fig. 1). The expression of *BMP2* and *BMP4* is in line with their respective roles in cardiac differentiation in mice, with *BMP2* being expressed first during cardiogenic specification and followed by *BMP4* [34,35]. In contrast to the dynamic expression of BMP ligands and BMP antagonists during cardiac differentiation, BMP receptors (*BMPR2*, *ALK3*, *ALK6*) appear to be constantly expressed throughout the differentiation process.

A similar expression pattern for *GREM2* was also observed in (1) the WA07 hES cells and (2) the independently reprogrammed hiPS cell line iMR90 C4 (Supplementary Fig. S1). Furthermore, because the “Matrix Sandwich” method of cardiac cell differentiation depends on timely activation and withdrawal of BMP signaling, which may influence expression of BMP ligands and antagonists, we used the distinct GiWi differentiation protocol that relies on sequential activation and inhibition of canonical Wnt signaling [11]. Our results show a similar induction profile of *GREM2* during cardiac differentiation following the GiWi protocol, indicating that the *GREM2* expression pattern is independent of the differentiation method used (Supplementary Fig. S1).

Taken together, our data demonstrate that *GREM2* expression starts after mesoderm formation, during the initial phase of CPC specification, and is retained throughout CPC expansion and differentiation to CMs. *GREM2* is unique among BMP antagonists to follow the cardiac differentiation pattern, although *NOGGIN* is also expressed within specific time windows of cardiac differentiation. The *GREM2* expression pattern is consistent with our previous studies in zebrafish and mouse development, as well as mouse ES cell differentiation [14–16], indicating that *GREM2* expression and possibly function have been conserved during evolution from lower vertebrates to humans. Furthermore, the *GREM2* expression pattern is consistent among different hES and iPS cell lines and independent of the applied differentiation protocol, suggesting that *GREM2* is inherently linked to the early stages of the cardiac differentiation process.

GREM2 is expressed in human CPCs and differentiated CMs

To determine the cellular source of *GREM2*, we performed immunofluorescence staining on fixed cells during



Day of Differentiation

FIG. 1. *GREM2* expression during hiPS cell cardiac differentiation follows the expression pattern of cardiac-specific genes. RT-qPCR gene expression analysis in DF 19-9-11 hiPS cells during cardiac differentiation [day 0 (D0) to day 10 (D10)] using the “Matrix Sandwich” method indicates cardiogenic mesoderm specification (*MESP-1*) and the appearance of cardiovascular progenitor cell gene markers (*KDR*, *NKX2.5*, *ISL1*). *GREM2* expression appears concurrently with cardiovascular progenitor cells and increases during differentiation to cardiomyocytes marked by *TNNT2* and *MYH6* genes. The expression pattern of BMP ligands *BMP2* and *BMP4*, BMP antagonists *CERBERUS-LIKE 1* and *NOGGIN*, as well as BMP receptors type 2 (*BMPR2*) and type 1 (*ALK3* and *ALK6*) is indicated. $n = 3$ replicates per condition. *ALK3* or 6, activin A receptor type II-like kinase 3 or 6, also *BMPRIA* or *BMPRIIB*; *BMP2* or 4, bone morphogenetic protein 2 or 4; *BMPR2*, bone morphogenetic protein receptor 2; *GREM2*, gremlin 2; *ISL-1*, insulin gene enhancer protein 1; hiPS, human-induced pluripotent stem; *KDR*, kinase insert domain receptor; *MESP-1*, mesoderm posterior bHLH transcription factor 1; *MYH6*, myosin heavy chain 6; *NKX2.5*, NK2 homeobox 5; *T-BRY*, T-brachyury; *TNNT2*, cardiac troponin T 2.

early (day 5 and 7) and late (day 10) differentiation stages using primary antibodies against GREM2, and antibodies recognizing typical cardiac-specific proteins, such as the transcription factor NKX2.5 and the sarcomeric component α -ACTININ.

To identify antibodies specific for detection of human GREM2 protein in cultured cells, we screened four distinct, commercially available, anti-GREM2 primary antibodies. To this end, we used HEK293 cells transiently transfected with a plasmid expressing the human *GREM2* cDNA under

the regulation of the CMV promoter, or empty vector as control. Transfected cells were fixed, stained, and imaged using a fluorescence microscope (Supplementary Fig. S2). Three antibodies gave a specific signal and the one with the best signal to noise ratio was subsequently selected for immunolabeling of differentiating iPS cells.

We found that GREM2 is expressed in NKX2.5⁺ cells at differentiation day 5 and 7 (Fig. 2A and Supplementary Fig. S3A, B). GREM2 protein expression persists in α -actinin⁺ CMs at day 10 of differentiation (Fig. 2B and

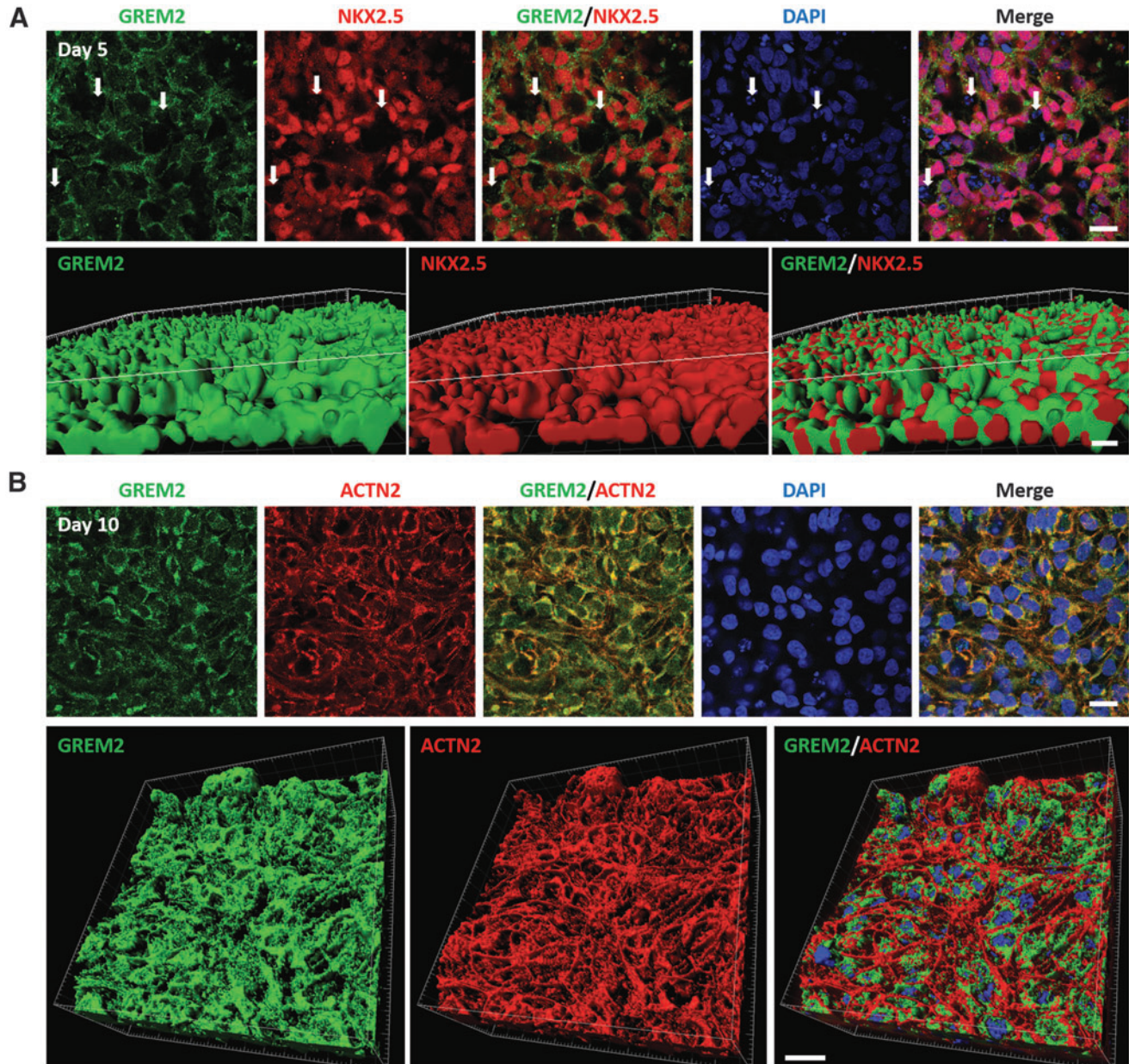


FIG. 2. GREM2 is expressed in CPCs and cardiomyocytes. Immunofluorescence analysis of differentiating hiPS cells. (A) CPCs at differentiation day 5, marked with NKX2.5 (red), express GREM2 (green). White arrows mark NKX2.5⁺ cells that also lack GREM2 expression (upper panels). Scale bar, 30 μ m. Three-dimensional reconstruction using z-stack confocal microscopy images illustrates GREM2 expression in NKX2.5⁺ cells (lower panels). Scale bar, 30 μ m. (B) Differentiated cardiomyocytes at differentiation day 10, marked with α -ACTININ (red), express GREM2 (green; upper panels). Scale bar, 30 μ m. Three-dimensional reconstruction of confocal microscopy images (lower panels) shows GREM2 expression in differentiated cardiomyocytes with sarcomeric structures. Scale bar, 20 μ m. DAPI staining (blue) marks cell nuclei. ACTN2, α -ACTININ; CPC, cardiac progenitor cell.

Supplementary Fig. S3C). GREM2 was not detected in NKX2.5⁺ cells, suggesting that GREM2 expression is confined to the cardiac lineage during iPS cell differentiation and acts in an autocrine manner.

BMP signaling antagonism is required for CM differentiation

The GREM2 expression data described above suggest that BMP signaling antagonism is necessary for CM differentiation. To test this possibility, we treated differentiating iPS cells with an L51P mutant of BMP2 that was shown to bind the BMP antagonist NOGGIN, but unable to bind BMPRI and activate BMP signaling, thus acting as a BMP ligand decoy [30]. To test the ability of the BMP decoy to block GREM2, we first transfected CGR8 mouse ES cells with a plasmid containing the firefly *luciferase* gene under the control of the BMP signaling response elements from the *Id2* gene promoter (BRE₂-Luc) [16,29]. Optimal concentrations for effective BMP signaling inhibition by GREM2 were first determined by titrating increasing concentrations of GREM2 in cells exposed to a constant BMP4 amount (Supplementary Fig. S4). The cells were then treated with BMP4, GREM2, and/or the BMP decoy. The results show that BMP4 induces canonical BMP (BRE₂-Luc) signaling, whereas the BMP decoy alone does not signal nor does it interfere with BMP4 signaling activation (Fig. 3A). GREM2 inhibits BMP4 activity, where GREM2 alone does not induce BRE₂-Luc activity, as expected. Moreover, co-incubation of BMP4, GREM2, and the BMP decoy restored canonical BMP signaling, indicating that the BMP decoy effectively blocks the inhibitory effect of GREM2 (Fig. 3A).

Treatment of differentiating human pluripotent stem cells with the BMP decoy protein starting at day 4 of differentiation, when CPCs first appear and GREM2 expression is induced, caused a significant reduction in cardiac gene

expression levels and reduced the percentage of contracting cells in culture (Fig. 3B). These data suggest that BMP signaling inhibition is required for cardiogenic differentiation of human pluripotent stem cells.

GREM2 enhances the cardiogenic potential of differentiating iPS cells

The results described above suggest inhibition of BMP signaling is necessary for CM differentiation of hiPS cells. To test whether GREM2 can further enhance human CM differentiation, we added GREM2 protein to differentiating iPS cells from day 3 onward, when cardiogenic mesoderm appears and endogenous *GREM2* expression begins to rise. The “Matrix Sandwich” protocol (SP) served as a positive control, whereas a modified, truncated “Matrix Sandwich” differentiation protocol (MP) without any factor addition after mesoderm induction at day 3 served as the baseline or negative control (Fig. 4A).

Visual comparison of cultures revealed that GREM2 protein addition accelerated the appearance of contracting cells, indicating the presence of CMs at day 7, which is 1 day earlier than the “Matrix Sandwich” method and 3 days earlier than the negative control. In addition, GREM2 also increased the overall areas of contracting cells, suggesting further expansion of the cardiac lineage (Fig. 4B, C).

In agreement with the visual observations, analysis of RNA samples prepared at days 10 and 14 of differentiation showed that addition of GREM2 leads to a further increase in cardiac-specific gene expression levels compared to the “Matrix Sandwich” method (Fig. 4D). To quantify the long-term effects of GREM2 on CM yields, we performed flow cytometry analysis at differentiation day 30 using antibodies recognizing the cardiac-specific myosin heavy chain MYH6. We also used antibodies recognizing NKX2.5, the expression of which is maintained in mature CMs, thus providing an

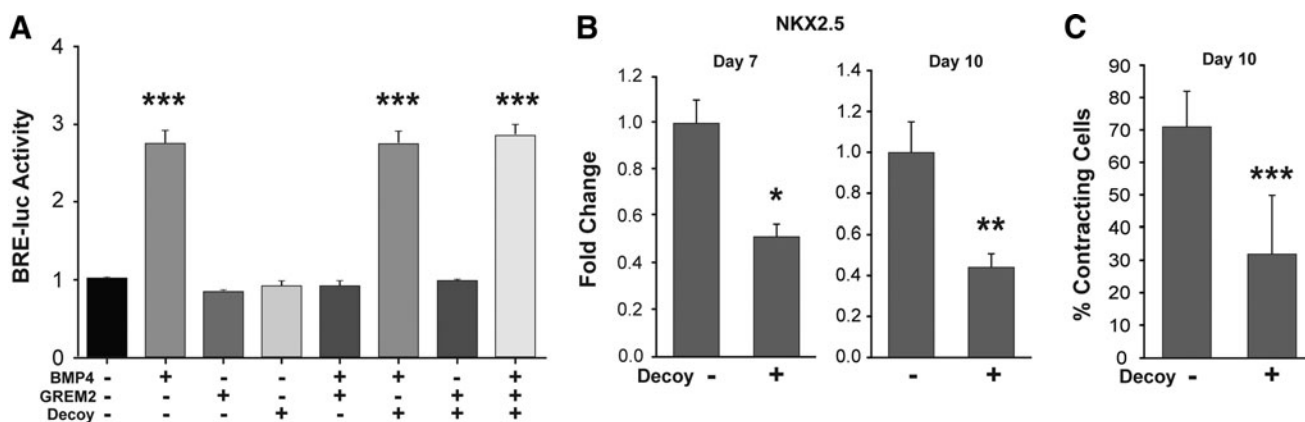


FIG. 3. BMP ligand antagonism is required for cardiac differentiation of hiPS cells. **(A)** BMP decoys block the inhibitory effects of GREM2. Mouse ES cells were transfected with the BRE₂-Luc reporter construct with *luciferase* expression under the control of two canonical BMP signaling responsive elements of the *Id2* gene. Cells were treated for 8 h with BMP4, GREM2, and the L51P BMP2 decoy in various combinations as indicated. In the presence of the BMP decoy, GREM2 inhibition of BMP signaling is aborted. One-way ANOVA with Dunnett’s test was performed to compare the experimental groups to the no treatment control group. *** $P < 0.001$. **(B)** RT-qPCR gene expression analysis of RNA samples isolated from DF 19-9-11 iPS cells at day 7 and 10 of differentiation with or without BMP decoy treatment shows a reduction in cardiac gene expression in samples treated with the BMP decoy. $n = 3$ replicates per condition. Student’s *t*-test. * $P < 0.05$; ** $P < 0.01$. **(C)** iPS cells treated with the BMP decoy BMP have a significant reduction in the percentage of contracting cells at differentiation day 10. $n = 3$ replicates per condition. Student’s *t*-test. *** $P < 0.001$. ES, embryonic stem; RT-qPCR, reverse transcriptase quantitative polymerase chain reaction.

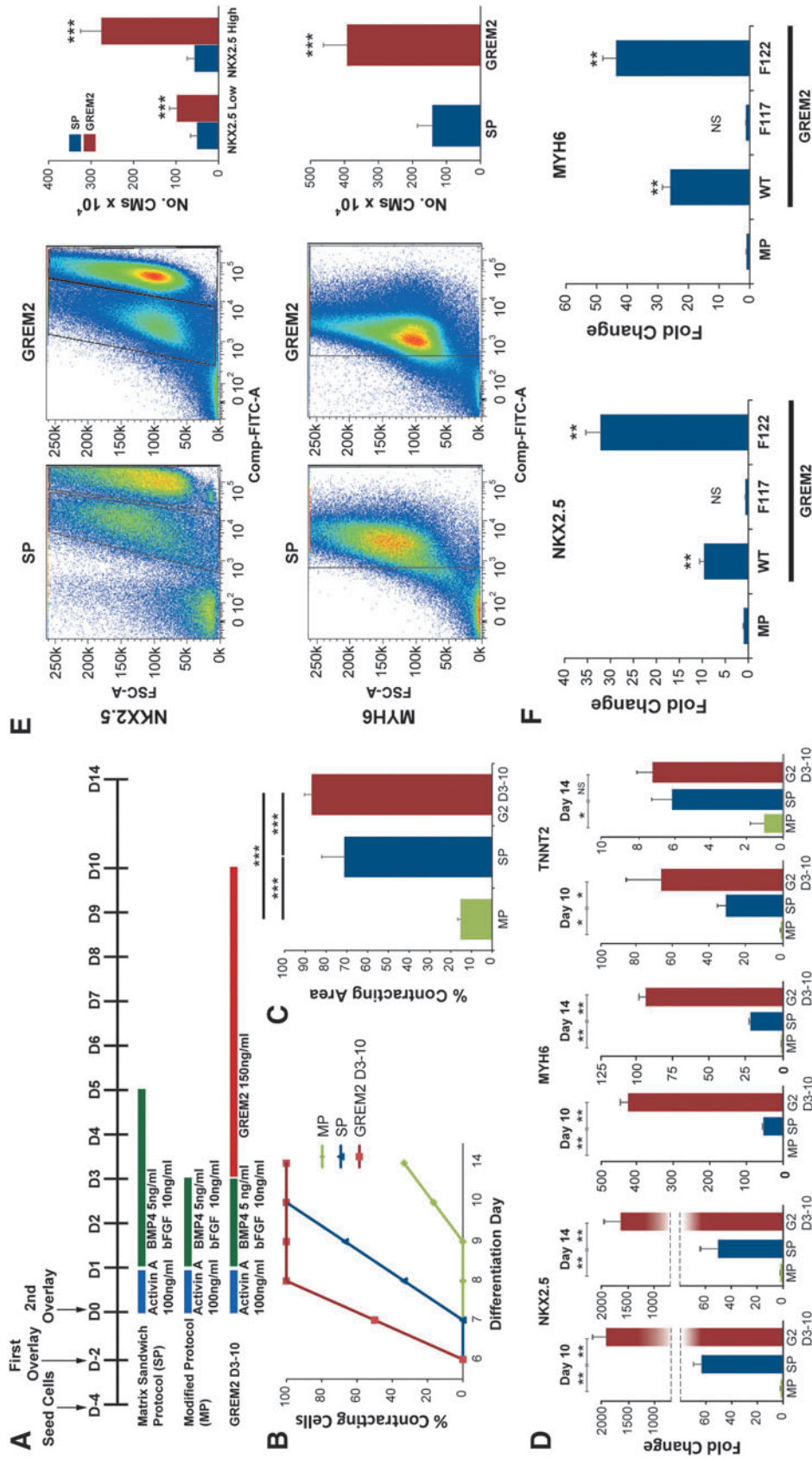


FIG. 4. GREM2 enhances the cardiogenic potential of differentiating iPS cells. (A) Schematic diagram showing treatment schedule and conditions of the three differentiation protocols using DF 19-9-11 iPS cells. Day minus 4 (D-4) to day 14 (D14) represents differentiation day minus 4 through day 14, respectively. Addition of growth factors and treatment duration are indicated below. (B) Differentiating iPS cells treated with GREM2 (GREM2 D3-10) start contracting earlier than the "Matrix Sandwich" protocol (SP) or the modified protocol (MP). (C) Percentage of contracting areas in each well was measured on differentiation day 14 (D14) for each condition. GREM2-treated wells had the highest percentage of contracting areas among the conditions tested, suggesting that GREM2 treatment is able to increase cardiac potential in differentiating iPS cells. $n = 9$ replicates per condition. Student's t -test was used to compare conditions as indicated. $***P < 0.001$. (D) RT-qPCR analysis of cardiac genes shows that GREM2 treatment increases expression of the early cardiac gene *NKX2.5* and the late cardiac genes *MYH6* and *TNNI2*. $n = 3$ replicates per condition. Student's t -test was used to compare conditions as indicated. $*P < 0.05$; $**P < 0.01$. (E) Flow cytometry of iPS cell-derived cardiomyocytes at differentiation day 30 using antibodies recognizing NKX2.5 and MYH6. GREM2 treatment increases the total number of cardiomyocytes compared to the "Matrix Sandwich" (SP) protocol. Cardiomyocytes were observed as both high and low NKX2.5⁺ populations. Cardiomyocytes with high NKX2.5 expression are particularly enriched by GREM2. Quantification of the flow cytometry data is shown to the right. $n = 8$ replicates. Student's t -test. $***P < 0.001$. (F) RT-qPCR analysis of cardiac genes in differentiated iPS cells at differentiation day 10. Cells were treated with 100 ng/mL of wild-type GREM2 (WT), a non-BMP binding GREM2 mutant (F117A), and a strongly binding mutant (F122A) during differentiation days 5–10. Both the WT and the F122A mutant induce cardiac genes. The F117A mutant was similar to nontreated controls (MP). $n = 3$ replicates per condition. Student's t -test, $**P < 0.01$. NS, not significant.

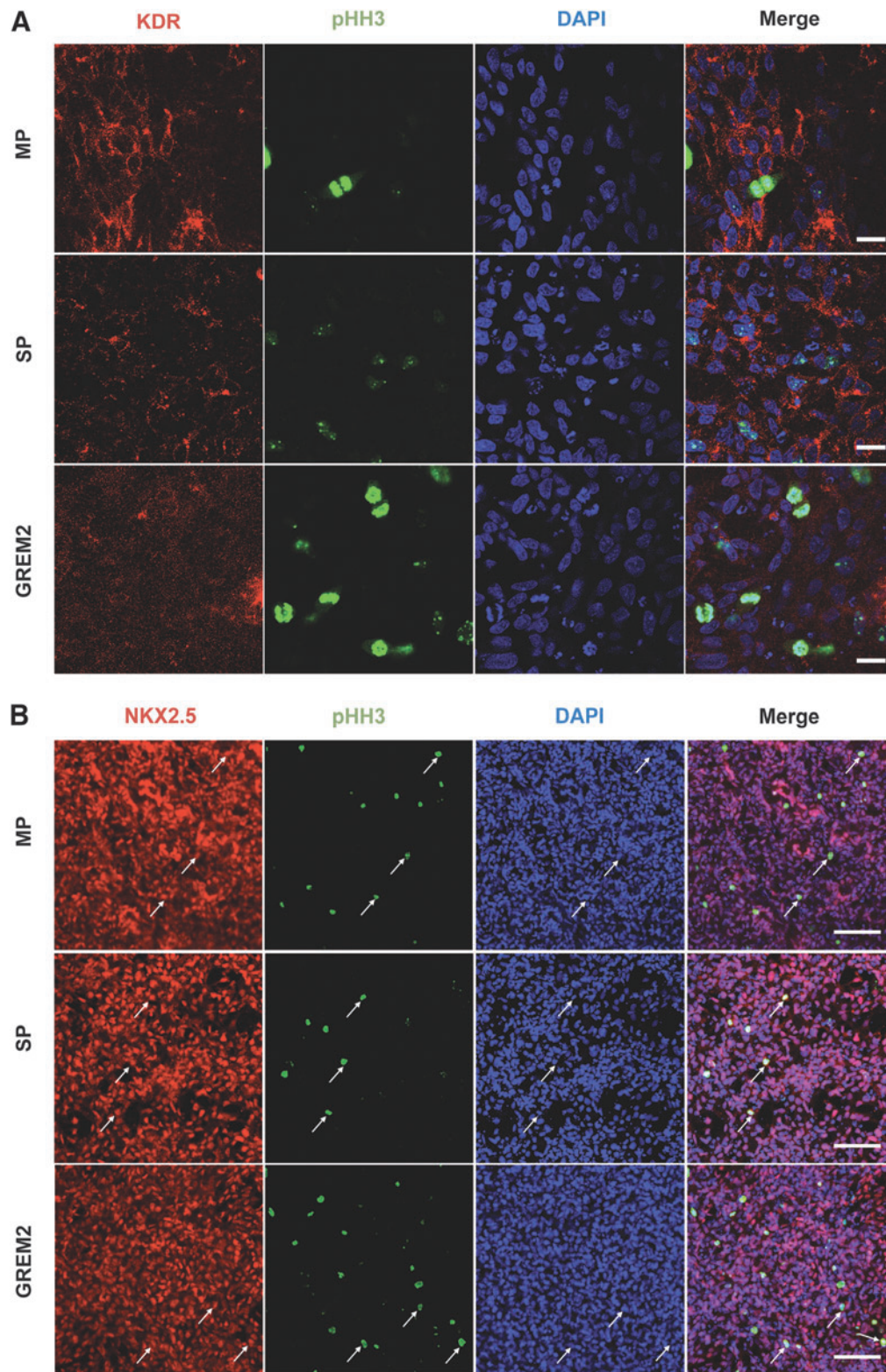


FIG. 5. GREM2 promotes proliferation of CPCs. Immunofluorescence staining of CPCs during iPS cell differentiation. Cells were treated with GREM2 and compared to “Matrix Sandwich” (SP) and baseline negative controls (MP) as described in Fig. 4A. **(A)** Representative images of cell cultures stained at differentiation day 4 with the cardiovascular progenitor marker KDR (*red*) and the active proliferation marker pHH3 (*green*) show that GREM2 treatment increases the total number of proliferative cells. Scale bars, 30 μ m. **(B)** Staining at day 5 with the CPC marker NKX2.5 (*red*) shows colocalization with pHH3 (*green*), indicating increased proliferation of CPCs in GREM2-treated cultures of differentiating iPS cells. Representative double-positive cells are marked by *arrows*. Scale bars, 100 μ m. DAPI staining (*blue*) marks cell nuclei. pHH3, phospho-HISTONE H3.

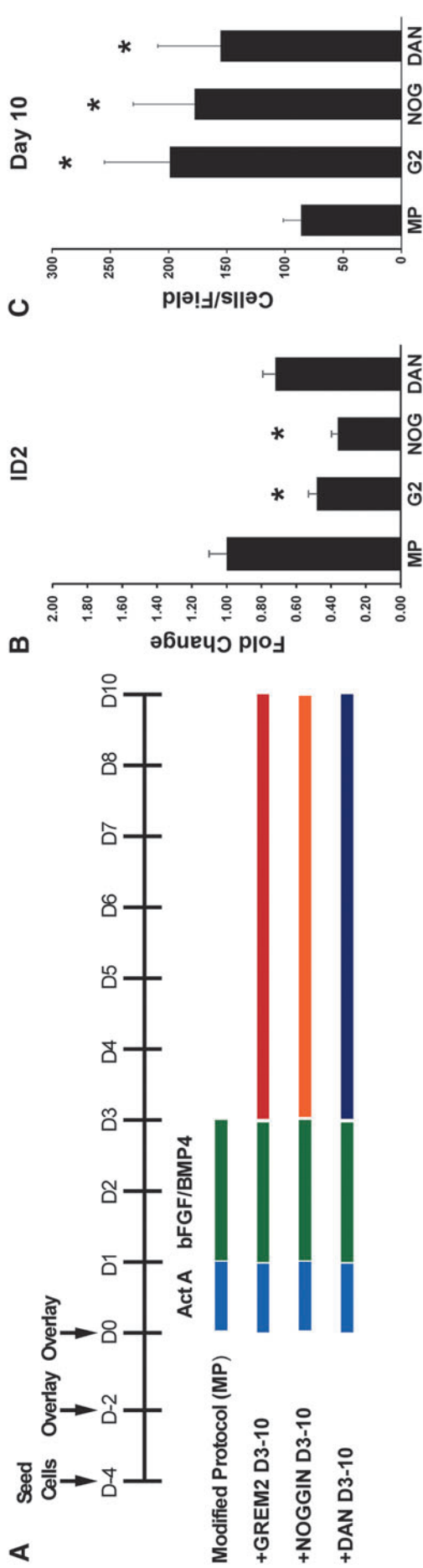


FIG. 6. BMP inhibition promotes proliferation of CPCs but is not sufficient to induce cardiac-specific genes. **(A)** Schematic diagram showing treatment schedule and conditions of iPS cell differentiation using DF 19-9-11 hiPS cells. Day minus 4 (D-4) to day 10 (D10) represents differentiation day minus 4 through day 10, respectively. Addition of various BMP antagonists is indicated on the left. **(B)** RT-qPCR analysis of the canonical BMP signaling target gene *ID2* at differentiation day 5. All 3 BMP antagonists, GREM2 (G2), NOGGIN (NOG), and DAN suppress *ID2* expression. $n = 3$ replicates per condition. $*P < 0.05$. One-way ANOVA with Tukey's HSD test. **(C)** Total cell numbers were quantified using the live nuclear stain Nuc Blue at day 10 of differentiation. All three BMP antagonists increase the total numbers of cells per well. $n = 6$ replicates per condition. $*P < 0.05$. One-way ANOVA with Tukey's HSD test. **(D)** Immunostaining of CPCs at day 6 of iPS cell differentiation with the proliferation marker pHH3 (*green*) and the CPC marker NKX2.5 (*red*). DAPI staining (*blue*) marks cell nuclei. Cells were treated with the BMP inhibitors GREM2, NOGGIN, and DAN as indicated in *panel A*. All three BMP inhibitors induce proliferation of CPCs. Scale bar, 100 μm . **(E)** RT-qPCR analysis of cardiac genes *MYH6*, *NKX2.5*, *TNNI2*, and *MYL7* at day 10 of differentiation shows an increase in cardiomyocyte gene induction at later time points in GREM2-treated iPS cells, while a similar increase in gene induction was not observed for the other BMP antagonists. $n = 3$ replicates per condition. $***P < 0.001$. One-way ANOVA with Tukey's HSD test.

(Continued →)

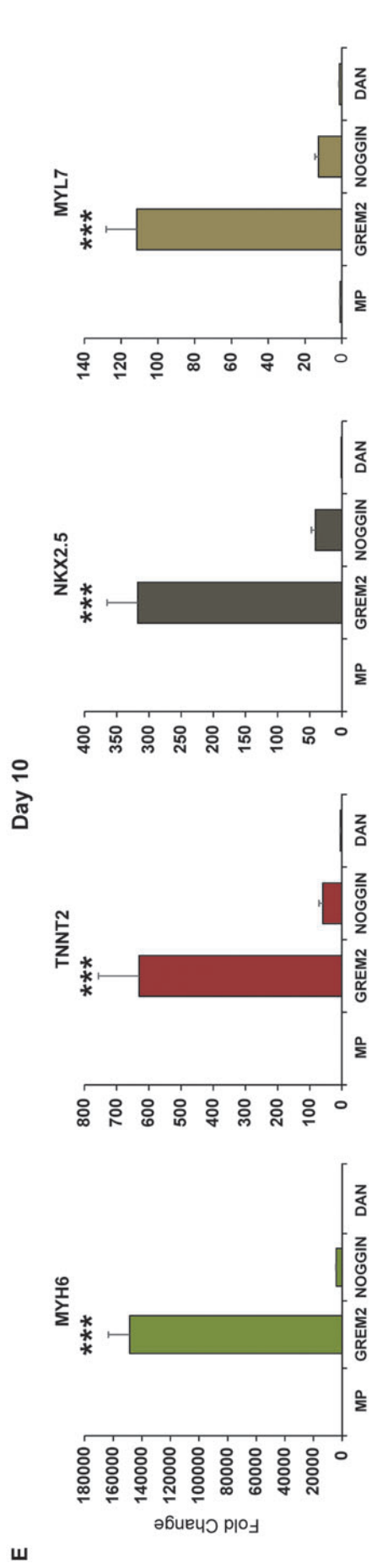
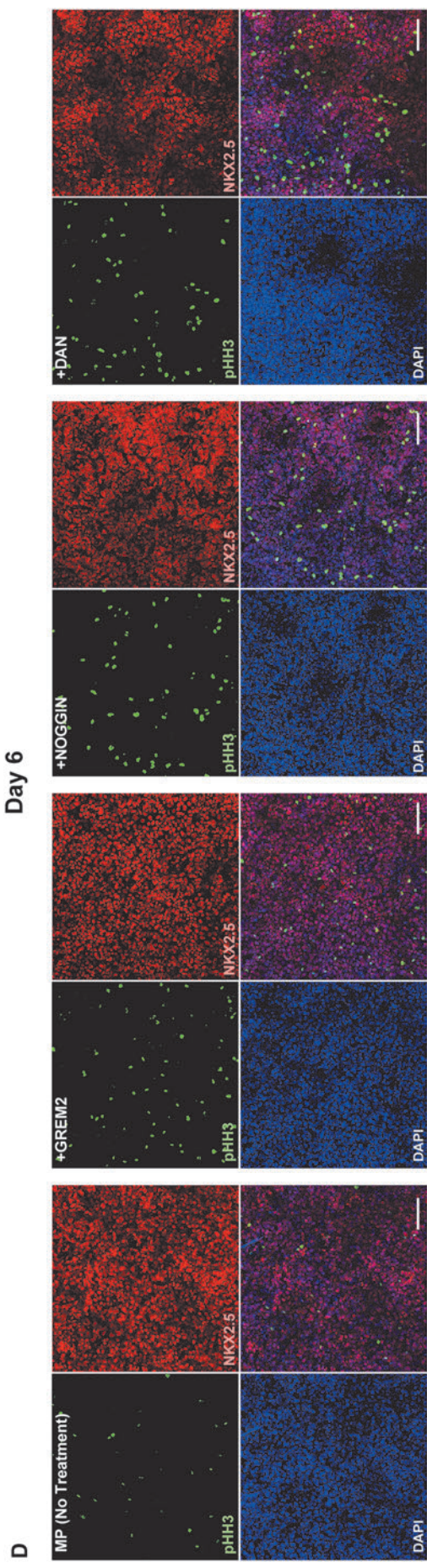


FIG. 6. (Continued).

independent marker to quantify cardiac cells. The data showed that GREM2 treatment gives rise to increased numbers of CMs compared to the “Matrix Sandwich” method (Fig. 4E). Specifically, GREM2 treatment increased the percentage of MYH6⁺ cells from ~83% in the optimal Sandwich protocol (SP) to ~93% and approximately doubled the total number of cells, thus increasing the total number of CMs/well, as shown in Fig. 4E. Similarly, the percentage of NKX2.5⁺ cells increased from ~70% to ~88%.

Using engineered GREM2 mutants that retain or lose BMP binding activity showed that BMP binding is required for cardiogenic differentiation (Fig. 4F). The positive effect of GREM2 was also evident using an independent hiPS cell line, iMR90 C-4, indicating that the procardiogenic properties of GREM2 are not limited to a single pluripotent stem cell line (Supplementary Fig. S5). Taken together, these data demonstrate that GREM2 protein addition during cardiac differentiation accelerates and enhances the cardiogenic potential of differentiating hiPS cells.

GREM2 promotes proliferation of CPCs

Using western blotting analysis of NKX2.5 protein, we found that GREM2 does not affect the initial induction of early cardiac genes, but leads to expansion of cardiac lineage markers at subsequent differentiation stages (Supplementary Fig. S6). Instead, the GREM2 expression during the initial appearance of CPCs and its stimulatory effect on cardiac differentiation raised the possibility that GREM2 promotes proliferation of CPCs. To directly test this possibility, we stained GREM2-treated differentiating iPS cells with antibodies recognizing the phosphorylated form of HISTONE H3 (pHH3) that is specifically phosphorylated during the mitosis and meiosis phases of cell division, thereby marking proliferating cells. The “Matrix Sandwich” (SP) and baseline (MP) protocols as outlined above in Fig. 4A served as positive and negative controls, respectively.

Our results demonstrate that addition of GREM2 protein at day 3 leads to a five- to sixfold increase in pHH3⁺ cells at day 4 (Fig. 5A and Supplementary Fig. S7). At this stage, pHH3 colocalizes with cell colonies expressing the early cardiovascular progenitor-specific membrane receptor KDR (or VEGFR2) [10]. Notably, KDR expression diminishes in SP cultures compared to MP and even more in GREM2-treated cells, likely due to acceleration of cardiac differentiation and loss of vascular markers, which is consistent with the timing of appearance of contracting cells under the different protocols at later stages (Fig. 4B). At day 5, pHH3 is specifically found in the nuclei of NKX2.5⁺ CPCs (Fig. 5B). The immunofluorescence analysis results show that GREM2 promotes proliferation of CPCs. Interestingly, the “Matrix Sandwich” protocol, which requires BMP4 addition at differentiation days 3–5, initially generates less proliferating CPCs than the other conditions (Fig. 5A, B, and Supplementary Fig. S7). However, the “Matrix Sandwich” protocol eventually promotes CM differentiation after BMP4 removal at day 5, but not to the same extent as addition of GREM2.

BMP inhibition promotes proliferation of CPCs

The results described in the previous sections show that GREM2 promotes proliferation of CPCs. To test whether

GREM2-mediated inhibition of BMP is sufficient to also stimulate cardiac differentiation, we compared the effects of GREM2 to two additional, distinct BMP antagonists, namely NOGGIN and DAN (Fig. 6A). All three BMP antagonists led to suppression of the canonical BMP signaling target gene *ID2*, respectively, showing they function as expected (Fig. 6B). Treatment with any of the three BMP antagonists led to a significant increase in overall cell numbers (Fig. 6C). Costaining of differentiating iPS cells at day 6 with antibodies recognizing NKX2.5 and pHH3 showed that GREM2-treated cells had higher proliferation rates than baseline. NOGGIN and DAN also increased CPC proliferation, compared to baseline (Fig. 6D). Of note, there were comparable numbers of NKX2.5⁺ cells at day 6 in control and BMP antagonist-treated differentiating iPS cells, further suggesting that GREM2 and BMP signaling antagonists do not affect the specification of CPCs.

To test whether BMP signaling inhibition is sufficient to promote CM differentiation, we isolated RNA samples at day 10 of differentiation from cells treated as shown in Fig. 6A. qPCR analysis showed that GREM2 led to induction of cardiac-specific gene markers characteristic of contracting CMs such as MYH6 and TNNT2, but NOGGIN and DAN had minimal or no effect (Fig. 6E). Therefore, although all three BMP antagonists enhanced proliferation of NKX2.5⁺ cells, induction of CM differentiation was a characteristic specific to GREM2.

GREM2 enhancement of cardiac differentiation requires JNK activation

We have previously shown that GREM2 inhibited canonical BMP, that is, SMAD1/5/8-mediated signaling shortly after treatment of differentiating mouse ES cells, followed by JNK signaling activation at later stages. Moreover, we found that this dual effect on canonical BMP signaling inhibition and the subsequent noncanonical JNK signaling activation is a unique property of GREM2 among BMP antagonists [16]. To test whether JNK activation drives cardiogenic differentiation of hiPS cells by GREM2, we prepared protein samples at differentiation days 4, 5, 6, 7, and 8 of GREM2- and NOGGIN-treated cells. The “Matrix Sandwich” and baseline protocols served as positive and negative controls, respectively (as described in Fig. 4A). Western blotting analysis using antibodies recognizing activated phospho-SMAD1/5/8 showed that both GREM2 and NOGGIN effectively blocked SMAD phosphorylation 24h after treatment (Fig. 7A). Phospho-SMAD1/5/8 levels became undetectable in all samples at subsequent time points (not shown). We did not detect JNK phosphorylation at days 4–7 (not shown). In contrast, western blotting showed that phospho-JNK1/2 protein was specifically activated by GREM2 at day 8, but not NOGGIN (Fig. 7A). Of note, we did not detect JNK activation by the Matrix Sandwich method at this stage, suggesting that either alternative procardiogenic mechanisms are induced by this method or that GREM2 accelerates JNK signaling activation.

To test whether JNK activation by GREM2 drives human CM differentiation, we exposed GREM2-treated differentiating iPS cells to the JNK signaling-specific chemical inhibitor TCS JNK 60 (JNKi 60) [36,37] or vehicle control. Visual observations and RNA analysis by qPCR showed that

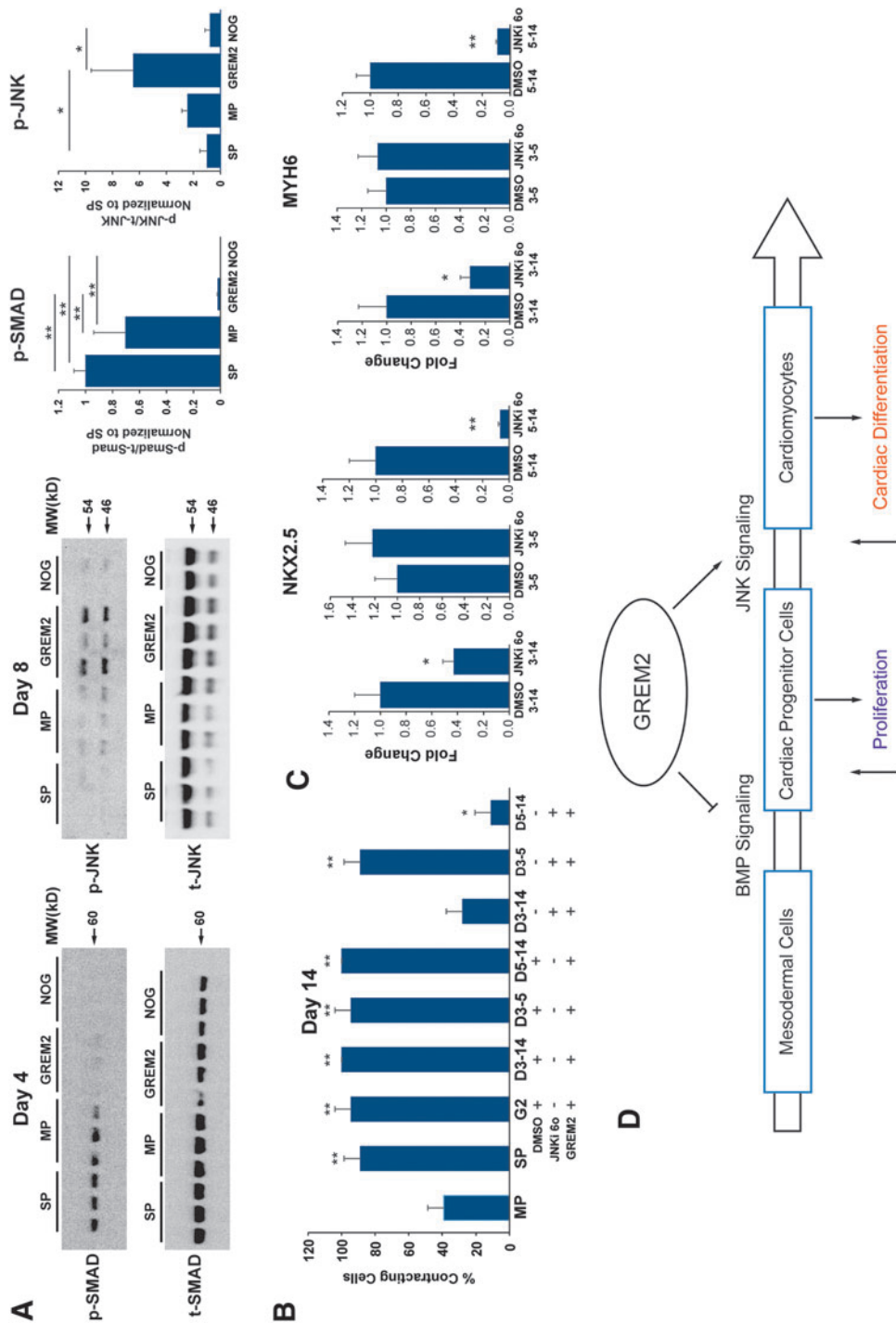


FIG. 7. JNK signaling is required for GREM2-induced cardiac differentiation. (A) DF 19-9-11 iPS cells were differentiated according to the Matrix Sandwich method (SP), baseline control method (MP), or treated with GREM2 or NOGGIN (NOG) from day 3 (as described in Figs. 4A and 6A). Protein lysates for western blotting analysis were collected at indicated differentiation time points and analyzed using antibodies recognizing the phosphorylated forms of SMAD1/5/8 (expected MW 60 kDa) and JNK1/2 isoforms (46 and 54 kDa, respectively) and total SMAD1 and JNK1/2 proteins. Both NOGGIN and GREM2 effectively inhibit SMAD phosphorylation at day 4. In contrast, only GREM2 treatment leads to strong upregulation of JNK phosphorylation at day 6. Graphs on the right represent quantification of phosphorylated SMAD and JNK forms relative to the corresponding total protein levels. One-way ANOVA with Tukey's HSD test. $*P < 0.05$, $**P < 0.01$. (B) Differentiating DF 19-9-11 iPS cells were treated with GREM2 alone and either with GREM2 and the selective small-molecule JNK inhibitor TCS JNK 60 (JNKi 60) or vehicle as control (DMSO). Addition of JNKi 60 to GREM2-treated wells during the entire cardiac differentiation phase (days 3–14) or just the late cardiac differentiation phase (days 5–14) reduced the total percentage of contracting cells in each well. $n = 3$ replicates per condition. One-way ANOVA with Tukey's HSD test. $*P < 0.05$, $**P < 0.01$. (C) RT-qPCR analysis of cardiac genes *NKX2.5* and *MYH6* at day 14 of differentiation shows a reduction of GREM2 expression in cells cotreated with GREM2 and JNKi 60. $n = 3$ replicates per condition. Unpaired *t*-test. $*P < 0.05$, $**P < 0.01$. (D) Schematic diagram of the proposed role of GREM2 in regulating cell signaling during human cardiac differentiation. As cells progress from cardiac progenitors toward more committed cardiac cells, GREM2 blocks BMP signaling to induce proliferation of CPCs and activates JNK signaling to promote differentiation. MW, molecular weight.

JNK signaling inhibition abolished the stimulatory effect of GREM2 on the cardiac lineage expansion (Fig. 7B, C). Of note, JNK inhibition was effective when applied during differentiation of CPCs after day 5. In summary, our data show that GREM2 coordinates cardiogenic output in a 2-step mechanism, initially inhibiting canonical BMP signaling to promote CPC proliferation followed by induction of differentiation through JNK signaling activation (Fig. 7D).

Discussion

Our data demonstrate that expression of the secreted BMP antagonist GREM2 is induced in pluripotent stem cell-derived human CPCs shortly after the specification of cardiac mesoderm. GREM2 expression is maintained in CPCs throughout their differentiation and persists in differentiated CMs. BMP signaling antagonism is required for cardiac lineage development, since BMP ligand decoys that bind antagonists, but do not activate BMP receptors, abort CM differentiation. Our results further show that GREM2 increases cardiac gene expression and CM differentiation, a process that depends on JNK signaling activation. Interestingly, although BMP antagonists such as NOGGIN and DAN equally stimulate CPC proliferation, only GREM2 efficiently promotes differentiation to CMs.

BMP ligands play crucial roles at various stages of cardiac development [38], starting from the initial cardiogenic specification of mesoderm [39], to subsequent cardiac tube assembly, asymmetric looping and jogging [40], ventricular identity [41], outflow track and cushion formation [35], and CM differentiation [42]. Although canonical BMP signaling induces *NKX2.5* gene in the cardiac crescent to generate CPCs, BMP signaling needs to be suppressed to allow proliferation and expansion of CPCs. Interestingly, during mouse secondary heart field development, *Nkx2.5* suppresses BMP signaling by blocking pSmad1, forming a negative regulatory loop that promotes proliferation of CPCs [43]. Our results show that this mechanism likely applies to human CPCs as BMP signaling inhibition by NOGGIN, GREM2, or DAN proteins promotes proliferation of CPCs.

On the contrary, elegant gain- and loss-of-function studies in mouse embryos have shown that persistent BMP signaling inhibition prevents differentiation of CPCs [43]. Our data confirm that NOGGIN and DAN prevent expression of genes specific to differentiated CMs, including sarcomere proteins such as MYH6 and TROPONIN T2. In contrast, GREM2, after the initial stimulation of CPC proliferation, leads to superinduction of cardiac differentiation. We have previously shown that GREM2 has the unique property among BMP antagonists, after its prescribed canonical BMP signaling inhibition, to subsequently induce JNK signaling activation that is required for cardiac differentiation [16]. Our results indicate that this GREM2 property is responsible for promotion of human cardiac cell differentiation as well, since JNK signaling inhibition aborts the procardiogenic effect of GREM2. These findings are consistent with previous reports that have implicated JNK signaling in cardiogenic differentiation of pluripotent stem cells [44,45].

Recent crystallographic evidence revealed that GREM2 folds into a unique tertiary shape that has not been described before. Specifically, GREM2 dimerizes in a head-to-tail

manner, unlike the head-to-head pairing of NOGGIN [24,46,47]. This head-to-tail arrangement gives rise to large, constrained, and arching hydrophobic surfaces on the three-dimensional structure, which precludes Grem2 from wrapping around BMP dimers as NOGGIN does [24,46,47]. We currently test whether this unique structural arrangement is also critical for the function of GREM2 in regulating both proliferation and differentiation of CPCs. Future biochemical analyses may further identify critical structural motifs that could be exploited to design molecules that mimic the biological effects of GREM2, such as the ability to selectively alter its BMP inhibitory and JNK activating properties. Recognizing these mechanisms may offer additional novel insights in the cardiac differentiation process. Moreover, due to the wide interest in regulating BMP signaling in a number of human diseases, BMP signaling inhibitors are being developed for clinical use [48,49]. Thus, our findings may facilitate future repurposing of these new pharmacological resources for coordinated growth and differentiation of stem cell populations.

We recently established that during embryonic development in zebrafish, *grem2* first appears in the pharyngeal mesoderm next to the forming heart tube [14,15]. Loss- and gain-of-function approaches demonstrated that Grem2 is necessary for proper cardiac tube jogging and looping, cardiac laterality, and CM differentiation by suppression of Smad1/5/8 phosphorylation [15]. Although left/right asymmetry and complex morphogenetic processes cannot be replicated in cell culture, our data show that the critical role of GREM2 in CM differentiation has been conserved across species and applies to human pluripotent stem cells. Moreover, we found that Grem2 is critical for atrium formation in zebrafish and promotes differentiation of pluripotent mouse ES cells to atrial-like CMs [16]. We did not detect preferential induction of atrial- versus ventricular-specific genes in the examined early stages of GREM2-treated hiPS cells (data not shown). Because human CMs take longer to mature in culture than mouse cells [50], it is likely that longer treatment periods might be required to test whether GREM2 can regulate chamber identity in iPS cell-derived CMs.

In the adult mouse heart, we recently discovered that Grem2 is highly induced in peri-infarct CMs at the end of the inflammatory phase after myocardial infarction. Using genetic gain- and loss-of-Grem2-function mouse models and chemical compounds that inhibit BMPs, we found that Grem2 modulates the magnitude of the inflammatory response and keeps inflammation in check through suppression of canonical BMP signaling [51]. Grem2 levels after myocardial infarction correlate with functional recovery, suggesting a new strategy to control inflammation of cardiac tissue after acute ischemic injury and improve cardiac function. It is intriguing that the BMP developmental pathway that initiates cardiac specification is also among the earliest induced after ischemic injury in the adult heart, but assumes a very different role. It is also intriguing that Grem2 induction takes place in peri-infarct CMs indicating that reactivation of CM-specific expression of Grem2 takes place under pathological conditions. However, unlike in developing CMs, Grem2 does not induce cell proliferation in the adult heart. Understanding how this property is lost in adult CMs might open the way to unlock cardiac regenerative mechanisms.

Acknowledgments

We thank the Vanderbilt FACS Core and the Cell Imaging Shared Resource for expert assistance. We are grateful to Gokhan Unlu and Dr. Ela Knapik for their assistance and advice with immunofluorescence imaging. This work was supported by NIH grants HL100398 to A.K.H. and GM114640 to T.B.T. and A.K.H.; and T32 Program in Cardiovascular Mechanisms: Training in Investigation (HL007411) fellowships to J.B.B. and D.T.P.

Author Disclosure Statement

No competing financial interests exist.

References

- Bellin M, MC Marchetto, FH Gage and CL Mummery. (2012). Induced pluripotent stem cells: the new patient? *Nat Rev Mol Cell Biol* 13:713–726.
- Sternecker JL, P Reinhardt and HR Schöler. (2014). Investigating human disease using stem cell models. *Nat Rev Genet* 15:625–639.
- Sayed N, C Liu and JC Wu. (2016). Translation of human-induced pluripotent stem cells: from clinical trial in a dish to precision medicine. *J Am Coll Cardiol* 67:2161–2176.
- Golos TG, M Giakoumopoulos and MA Garthwaite. (2010). Embryonic stem cells as models of trophoblast differentiation: progress, opportunities, and limitations. *Reproduction* 140:3–9.
- Garbern JC and RT Lee. (2013). Cardiac stem cell therapy and the promise of heart regeneration. *Cell Stem Cell* 12:689–698.
- Zhang J, GF Wilson, AG Soerens, CH Koonce, J Yu, SP Palecek, JA Thomson and TJ Kamp. (2009). Functional cardiomyocytes derived from human induced pluripotent stem cells. *Circ Res* 104:e30–e41.
- Saha K and R Jaenisch. (2009). Technical challenges in using human induced pluripotent stem cells to model disease. *Cell Stem Cell* 5:584–595.
- Tapia N and HR Schöler. (2016). Molecular obstacles to clinical translation of iPSCs. *Cell Stem Cell* 19:298–309.
- Xu C, S Police, N Rao and MK Carpenter. (2002). Characterization and enrichment of cardiomyocytes derived from human embryonic stem cells. *Circ Res* 91:501–508.
- Yang L, MH Soonpaa, ED Adler, TK Roepke, SJ Kattman, M Kennedy, E Henckaerts, K Bonham, GW Abbott, et al. (2008). Human cardiovascular progenitor cells develop from a KDR⁺ embryonic-stem-cell-derived population. *Nature* 453:524–528.
- Lian X, J Zhang, SM Azarin, K Zhu, LB Hazeltine, X Bao, C Hsiao, TJ Kamp and SP Palecek. (2013). Directed cardiomyocyte differentiation from human pluripotent stem cells by modulating Wnt/ β -catenin signaling under fully defined conditions. *Nat Protoc* 8:162–175.
- Burridge PW, E Matsa, P Shukla, ZC Lin, JM Churko, AD Ebert, F Lan, S Diecke, B Huber, et al. (2014). Chemically defined generation of human cardiomyocytes. *Nat Methods* 11:855–860.
- Feaster TK, AG Cadar, L Wang, CH Williams, YW Chun, JE Hempel, N Bloodworth, WD Merryman, CC Lim, et al. (2015). Matrigel mattress: a method for the generation of single contracting human-induced pluripotent stem cell-derived cardiomyocytes. *Circ Res* 117:995–1000.
- Müller II, EW Knapik and AK Hatzopoulos. (2006). Expression of the protein related to Dan and Cerberus gene—prdc—During eye, pharyngeal arch, somite, and swim bladder development in zebrafish. *Dev Dyn* 235:2881–2888.
- Müller II, DB Melville, V Tanwar, WM Rybski, A Mukherjee, MB Shoemaker, W-D Wang, JA Schoenhard, DM Roden, et al. (2013). Functional modeling in zebrafish demonstrates that the atrial-fibrillation-associated gene GREM2 regulates cardiac laterality, cardiomyocyte differentiation and atrial rhythm. *Dis Model Mech* 6:332–341.
- Tanwar V, JB Bylund, J Hu, J Yan, JM Walthall, A Mukherjee, WH Heaton, W-D Wang, F Potet, et al. (2014). Gremlin 2 promotes differentiation of embryonic stem cells to atrial fate by activation of the JNK signaling pathway. *Stem Cells* 32:1774–1788.
- Bylund JB and AK Hatzopoulos. (2016). Differentiation of atrial cardiomyocytes from pluripotent stem cells using the BMP antagonist Grem2. *J Vis Exp* DOI: 10.3791/53919.
- Beers J, DR Gulbranson, N George, LI Siniscalchi, J Jones, JA Thomson and G Chen. (2012). Passaging and colony expansion of human pluripotent stem cells by enzyme-free dissociation in chemically defined culture conditions. *Nat Protoc* 7:2029–2040.
- Xu C, MS Inokuma, J Denham, K Golds, P Kundu, JD Gold and MK Carpenter. (2001). Feeder-free growth of undifferentiated human embryonic stem cells. *Nat Biotechnol* 19:971–974.
- Zhang J, M Klos, GF Wilson, AM Herman, X Lian, KK Raval, MR Barron, L Hou, AG Soerens, et al. (2012). Extracellular matrix promotes highly efficient cardiac differentiation of human pluripotent stem cells: the matrix sandwich method. *Circ Res* 111:1125–1136.
- Laflamme MA, KY Chen, AV Naumova, V Muskheli, JA Fugate, SK Dupras, H Reinecke, C Xu, M Hassanipour, et al. (2007). Cardiomyocytes derived from human embryonic stem cells in pro-survival factors enhance function of infarcted rat hearts. *Nat Biotechnol* 25:1015–1024.
- Kattamuri C, DM Luedeke, K Nolan, SA Rankin, KD Greis, AM Zorn and TB Thompson. (2012). Members of the DAN family are BMP antagonists that form highly stable noncovalent dimers. *J Mol Biol* 424:313–327.
- Kattamuri C, DM Luedeke and TB Thompson. (2012). Expression and purification of recombinant protein related to DAN and cerberus (PRDC). *Protein Expr Purif* 82:389–395.
- Nolan K, C Kattamuri, DM Luedeke, X Deng, A Jagpal, F Zhang, RJ Linhardt, AP Kenny, AM Zorn and TB Thompson. (2013). Structure of protein related to Dan and Cerberus: insights into the mechanism of bone morphogenetic protein antagonism. *Structure* 21:1417–1429.
- Xu C, S Police, M Hassanipour, Y Li, Y Chen, C Priest, C O'Sullivan, MA Laflamme, W-Z Zhu, et al. (2011). Efficient generation and cryopreservation of cardiomyocytes derived from human embryonic stem cells. *Regen Med* 6:53–66.
- Livak KJ and TD Schmittgen. (2001). Analysis of relative gene expression data using real-time quantitative PCR and the 2(-Delta Delta C(T)) Method. *Methods* 25:402–408.
- Beck H, M Semisch, C Culmsee, N Plesnila and AK Hatzopoulos. (2008). Egr-1 regulates expression of the glial scar component phosphacan in astrocytes after experimental stroke. *Am J Pathol* 173:77–92.
- Zhao S and RD Fernald. (2005). Comprehensive algorithm for quantitative real-time polymerase chain reaction. *J Comput Biol* 12:1047–1064.

29. Monteiro RM, SMC de Sousa Lopes, O Korchynski, P ten Dijke and CL Mummery. (2004). Spatio-temporal activation of Smad1 and Smad5 in vivo: monitoring transcriptional activity of Smad proteins. *J Cell Sci* 117:4653–4663.
30. Albers CE, W Hofstetter, H-J Sebald, W Sebald, KA Siebenrock and FM Klenke. (2012). L51P—A BMP2 variant with osteoinductive activity via inhibition of Noggin. *Bone* 51:401–406.
31. Sasai Y, B Lu, H Steinbeisser, D Geissert, LK Gont and EM De Robertis. (1994). Xenopus chordin: a novel dorsalizing factor activated by organizer-specific homeobox genes. *Cell* 79:779–790.
32. Hsu DR, AN Economides, X Wang, PM Eimon and RM Harland. (1998). The Xenopus dorsalizing factor Gremlin identifies a novel family of secreted proteins that antagonize BMP activities. *Mol Cell* 1:673–683.
33. Biben C, E Stanley, L Fabri, S Kotecha, M Rhinn, C Drinkwater, M Lah, CC Wang, A Nash, et al. (1998). Murine cerberus homologue mCer-1: a candidate anterior patterning molecule. *Dev Biol* 194:135–151.
34. McCulley DJ, J-O Kang, JF Martin and BL Black. (2008). BMP4 is required in the anterior heart field and its derivatives for endocardial cushion remodeling, outflow tract septation, and semilunar valve development. *Dev Dyn* 237:3200–3209.
35. Ma L, M-F Lu, RJ Schwartz and JF Martin. (2005). Bmp2 is essential for cardiac cushion epithelial-mesenchymal transition and myocardial patterning. *Development* 132:5601–5611.
36. Szczepankiewicz BG, C Kosogof, LTJ Nelson, G Liu, B Liu, H Zhao, MD Serby, Z Xin, M Liu, et al. (2006). Aminopyridine-based c-Jun n-terminal kinase inhibitors with cellular activity and minimal cross-kinase activity. *J Med Chem* 49:3563–3580.
37. Kauskot A, F Adam, A Mazharian, N Ajzenberg, E Berrou, A Bonnefoy, J-P Rosa, MF Hoylaerts and M Bryckaert. (2007). Involvement of the mitogen-activated protein kinase c-Jun NH2-terminal kinase 1 in thrombus formation. *J Biol Chem* 282:31990–31999.
38. van Wijk B, AFM Moorman and MJB van den Hoff. (2007). Role of bone morphogenetic proteins in cardiac differentiation. *Cardiovasc Res* 74:244–255.
39. Kruithof BPT, B van Wijk, S Somi, M Kruithof-de Julio, JM Pérez Pomares, F Weesie, A Wessels, AFM Moorman and MJB van den Hoff. (2006). BMP and FGF regulate the differentiation of multipotential pericardial mesoderm into the myocardial or epicardial lineage. *Dev Biol* 295:507–522.
40. Breckenridge RA, TJ Mohun and E Amaya. (2001). A role for BMP signalling in heart looping morphogenesis in Xenopus. *Dev Biol* 232:191–203.
41. Marques SR and D Yelon. (2009). Differential requirement for BMP signaling in atrial and ventricular lineages establishes cardiac chamber proportionality. *Dev Biol* 328:472–482.
42. de Pater E, M Ciampricotti, F Priller, J Veerkamp, I Strate, K Smith, AK Lagendijk, TF Schilling, W Herzog, et al. (2012). Bmp signaling exerts opposite effects on cardiac differentiation. *Circ Res* 110:578–587.
43. Prall OWJ, MK Menon, MJ Solloway, Y Watanabe, S Zaffran, F Bajolle, C Biben, JJ McBride, BR Robertson, et al. (2007). An Nkx2-5/Bmp2/Smad1 negative feedback loop controls heart progenitor specification and proliferation. *Cell* 128:947–959.
44. Kempf H, M Lecina, S Ting, R Zweigerdt and S Oh. (2011). Distinct regulation of mitogen-activated protein kinase activities is coupled with enhanced cardiac differentiation of human embryonic stem cells. *Stem Cell Res* 7:198–209.
45. Ou D, Q Wang, Y Huang, D Zeng, T Wei, L Ding, X Li, Q Zheng and Y Jin. (2016). Co-culture with neonatal cardiomyocytes enhances the proliferation of iPSC-derived cardiomyocytes via FAK/JNK signaling. *BMC Dev Biol* 16:11.
46. Nolan K, C Kattamuri, SA Rankin, RJ Read, AM Zorn and TB Thompson. (2016). Structure of Gremlin-2 in complex with GDF5 gives insight into DAN-family-mediated BMP antagonism. *Cell Rep* 16:2077–2086.
47. Groppe J, J Greenwald, E Wiater, J Rodriguez-Leon, AN Economides, W Kwiatkowski, M Affolter, WW Vale, JC Izpisua Belmonte and S Choe. (2002). Structural basis of BMP signalling inhibition by the cystine knot protein Noggin. *Nature* 420:636–642.
48. Sanvitale CE, G Kerr, A Chaikuad, M-C Ramel, AH Moheidas, S Reichert, Y Wang, JT Triffitt, GD Cuny, et al. (2013). A new class of small molecule inhibitor of BMP signaling. *PLoS One* 8:e62721.
49. Cao Y, C Wang, X Zhang, G Xing, K Lu, Y Gu, F He and L Zhang. (2014). Selective small molecule compounds increase BMP-2 responsiveness by inhibiting Smurf1-mediated Smad1/5 degradation. *Sci Rep* 4:4965.
50. Mummery C, D Ward, C van den Brink, S Bird, P Doevendans, T Opthof, AB de la Riviere, L Tertoolen, M van der Heyden and M Pera. (2002). Cardiomyocyte differentiation of mouse and human embryonic stem cells. *J Anat* 200:233–242.
51. Sanders LN, JA Schoenhard, MA Saleh, A Mukherjee, S Ryzhov, WG McMaster, K Nolan, RJ Gumina, TB Thompson, et al. (2016). The BMP antagonist Gremlin 2 limits inflammation after myocardial infarction. *Circ Res* 119:434–449.

Address correspondence to:
 Antonis K. Hatzopoulos, PhD
 Division of Cardiovascular Medicine
 Department of Medicine
 Vanderbilt University Medical Center
 Nashville, TN 37232 6300

E-mail: antonis.hatzopoulos@vanderbilt.edu

Received for publication July 27, 2016

Accepted after revision January 25, 2017

Prepublished on Liebert Instant Online XXXX XX, XXXX

Cadherin-11 blockade reduces inflammation-driven fibrotic remodeling and improves outcomes after myocardial infarction

Alison K. Schroer, ... , Hind Lal, W. David Merryman

JCI Insight. 2019;4(18):e131545. <https://doi.org/10.1172/jci.insight.131545>.

Research Article

Cardiology

Over one million Americans experience myocardial infarction (MI) annually, and the resulting scar and subsequent cardiac fibrosis gives rise to heart failure. A specialized cell-cell adhesion protein, cadherin-11 (CDH11), contributes to inflammation and fibrosis in rheumatoid arthritis, pulmonary fibrosis, and aortic valve calcification but has not been studied in myocardium after MI. MI was induced by ligation of the left anterior descending artery in mice with either heterozygous or homozygous knockout of CDH11, wild-type mice receiving bone marrow transplants from *Cdh11*-deficient animals, and wild-type mice treated with a functional blocking antibody against CDH11 (SYN0012). Flow cytometry revealed significant CDH11 expression in noncardiomyocyte cells after MI. Animals given SYN0012 had improved cardiac function, as measured by echocardiogram, reduced tissue remodeling, and altered transcription of inflammatory and proangiogenic genes. Targeting CDH11 reduced bone marrow–derived myeloid cells and increased proangiogenic cells in the heart 3 days after MI. Cardiac fibroblast and macrophage interactions increased IL-6 secretion in vitro. Our findings suggest that CDH11-expressing cells contribute to inflammation-driven fibrotic remodeling after MI and that targeting CDH11 with a blocking antibody improves outcomes by altering recruitment of bone marrow–derived cells, limiting the macrophage-induced expression of IL-6 by fibroblasts and promoting vascularization.

Find the latest version:

<http://jci.me/131545/pdf>



Cadherin-11 blockade reduces inflammation-driven fibrotic remodeling and improves outcomes after myocardial infarction

Alison K. Schroer,¹ Matthew R. Bersi,¹ Cynthia R. Clark,¹ Qinkun Zhang,² Lehanna H. Sanders,² Antonis K. Hatzopoulos,² Thomas L. Force,² Susan M. Majka,³ Hind Lal,² and W. David Merryman¹

¹Department of Biomedical Engineering, ²Department of Cardiovascular Medicine, and ³Department of Allergy, Pulmonary, and Critical Care Medicine, Vanderbilt University, Nashville, Tennessee, USA.

Over one million Americans experience myocardial infarction (MI) annually, and the resulting scar and subsequent cardiac fibrosis gives rise to heart failure. A specialized cell-cell adhesion protein, cadherin-11 (CDH11), contributes to inflammation and fibrosis in rheumatoid arthritis, pulmonary fibrosis, and aortic valve calcification but has not been studied in myocardium after MI. MI was induced by ligation of the left anterior descending artery in mice with either heterozygous or homozygous knockout of CDH11, wild-type mice receiving bone marrow transplants from *Cdh11*-deficient animals, and wild-type mice treated with a functional blocking antibody against CDH11 (SYN0012). Flow cytometry revealed significant CDH11 expression in noncardiomyocyte cells after MI. Animals given SYN0012 had improved cardiac function, as measured by echocardiogram, reduced tissue remodeling, and altered transcription of inflammatory and proangiogenic genes. Targeting CDH11 reduced bone marrow-derived myeloid cells and increased proangiogenic cells in the heart 3 days after MI. Cardiac fibroblast and macrophage interactions increased IL-6 secretion *in vitro*. Our findings suggest that CDH11-expressing cells contribute to inflammation-driven fibrotic remodeling after MI and that targeting CDH11 with a blocking antibody improves outcomes by altering recruitment of bone marrow-derived cells, limiting the macrophage-induced expression of IL-6 by fibroblasts and promoting vascularization.

Introduction

Every year over one million Americans experience a myocardial infarction (MI), which significantly reduces cardiac function and potentiates the progression to heart failure by increasing the risk of recurrent infarctions (1). The process of infarct healing requires complex interactions between resident and recruited cells, which must coordinate the clearance and replacement of damaged tissue with a stable and robust collagen scar to prevent cardiac rupture.

Immune cells — including neutrophils, monocytes, and macrophages, among others — are recruited from the blood within the first few hours after MI and critically participate in the healing and remodeling process. Resident cardiac macrophages also participate in stabilizing the heart after cardiac injury (2). Following the successful clearance of necrotic tissue and cell debris by immune cells, resident mesenchymal cells — including cardiac fibroblasts (CFs) — proliferate and differentiate into an activated, hypersecretory, hypercontractile, tissue remodeling phenotype known as myofibroblasts. This highly cellularized stage of cardiac remodeling, termed the granulation phase, is characterized by the resolution of inflammatory signaling and the transition to fibrotic remodeling and scar formation by activated myofibroblasts. In the following weeks, myofibroblasts deposit and remodel collagen into a compact scar, which can sustain the biomechanical integrity of the myocardial wall (3). However, excess inflammation and reparative activity can ultimately lead to expansion of the infarct area and further diminished cardiac function (4, 5).

Development of treatment strategies for MI is made particularly challenging by the precise and necessary timing of both chemical signals and cellular activity throughout these phases of remodeling. Many treatments targeting specific growth factor cascades have failed to maintain the delicate balance between

Conflict of interest: The authors have declared that no conflict of interest exists.

Copyright: © 2019, American Society for Clinical Investigation.

Submitted: July 3, 2019

Accepted: August 21, 2019

Published: September 19, 2019.

Reference information: *JCI Insight*. 2019;4(18):e131545.
<https://doi.org/10.1172/jci.insight.131545>.

necessary and excessive inflammation and fibrosis and often have adverse side effects on the surviving cardiomyocytes (CMs), causing additional loss of contractile potential (6–8).

Cadherin-11 (CDH11) is a cell-cell adhesion protein expressed by inflammatory cells and activated fibroblast-like cells in multiple inflammatory and fibrotic disease models — including rheumatoid arthritis, pulmonary fibrosis, and aortic valve calcification (9–11) — but its function in infarct healing has not yet been studied. CDH11 (or OB-cadherin) was originally described in osteoblasts and has been shown to affect cell migration and exfiltration in cancer studies (12, 13), but the role of CDH11 in bone marrow–derived cell (BMDC) recruitment and CF contractility in the heart has not been studied. CDH11 expression has been observed in CFs but is minimally expressed by CMs in culture and has not been well studied in the myocardium in vivo (14). CDH11 engagement promotes the expression of the proinflammatory cytokine IL-6 as well as profibrotic signaling factors and myofibroblast markers, such as TGF- β 1, in diseased joints, lungs, and heart valves (9–11, 15, 16). Thus, we hypothesized that genetic and pharmacologic targeting of CDH11 after MI would reduce inflammation-driven fibrotic scar expansion and improve cardiac outcomes.

Results

To establish the therapeutic potential of targeting CDH11 in the heart after MI, we first wanted to identify the cardiac cell populations on which CDH11 is expressed. Flow cytometric analysis of non-CM cardiac cell populations — including cardiac endothelial cells (CECs: CD45⁻CD31⁺), cardiac mesenchymal cells (CMCs: CD45⁻CD31⁻), and BMDCs (CD45⁺) (Supplemental Figures 1 and 2; supplemental material available online with this article; <https://doi.org/10.1172/jci.insight.131545DS1>) — revealed that BMDCs constitute the majority of non-CMs in the heart 3 days after infarct (86.2% of live cells). By 7 days after infarct the largest cardiac cell population was CMCs (52.3% of live cells); activated myofibroblasts likely made up a majority of this population (Figure 1, A and B, and Supplemental Figure 3A). Gene expression analysis by qPCR confirmed higher *Cdh11* transcription in non-CMs relative to CMs and revealed a significant increase in non-CM *Cdh11* transcription that was nearly 10-fold higher than that in sham-operated hearts (sham) by 7 days after MI (Supplemental Figure 4, A and B).

Flow cytometry further revealed that each non-CM population in the heart had some level of CDH11 expression (Figure 1, A–C) and that the overall percentage of CDH11⁺ cells in infarcted hearts was increased relative to sham by 7 days after infarct (18.2% of live cells vs. 6.9% of live cells in sham; Supplemental Figure 4C). Percentages of both CDH11⁺ BMDCs and CDH11⁺ CMCs increased between days 3 and 7 after MI but remained unchanged over time in sham hearts. Despite constituting less than 3% of all live cells in the heart, the percentage of CDH11⁺ CECs was decreased relative to sham at both 3 and 7 days after MI and changed over time in both surgical conditions (Figure 1, A–C). While CDH11⁺ CECs comprised a markedly lower percentage of all CDH11⁺ cells identified in infarcted hearts relative to sham at both 3 and 7 days, CDH11⁺ CMCs made up the majority of all CDH11⁺ cells after 7 days in both surgical conditions. The percentage of BMDCs expressing CDH11 constituted a significant fraction of all CDH11⁺ cells in the heart 3 days after MI (63.6% of CDH11⁺ cells vs. 30.5% of CDH11⁺ cells in sham) and was reduced back to sham levels by 7 days after MI (Figure 1, A–C), consistent with the time course of inflammation resolution.

We next analyzed our flow cytometry data to determine which BMDC subsets had CDH11 expression (Figure 1, D–F). After infarct, we observed a significant increase in myeloid lineage cells (CD45⁺CD11b⁺) — including neutrophils (CD45⁺CD11b⁺Gr-1/CD86^{hi}), M1-like macrophages (CD45⁺CD11b⁺Gr-1/CD86^{int}CD206⁻), and M2-like macrophages (CD45⁺CD11b⁺Gr-1/CD86^{int}CD206⁺) (17) — as well as a reduction in bone marrow–derived proangiogenic cells (CD45⁺CD11b⁻CD31⁺) and nonmyeloid lineage BMDCs (CD45⁺CD11b⁻), which are predominately lymphocytes (Supplemental Figure 3A). Though most BMDC subsets had detectable amounts of CDH11 expression, less than 1% of all Gr-1/CD86^{lo} BMDCs — eosinophils and monocytes — were CDH11⁺. The largest population of CDH11⁺ BMDCs was M2-like macrophages (Figure 1D), and the percentage of BMDCs that were CDH11⁺ M2-like macrophages was increased relative to sham by 7 days after MI (14.1% of CD45⁺ cells vs. 9.5% of CD45⁺ cells in sham). Similar to CECs, there were fewer CDH11⁺ bone marrow–derived proangiogenic cells in the heart at both 3 and 7 days after infarct compared with sham (Figure 1F). Though CDH11⁺ neutrophils comprised a relatively small percentage of all BMDCs, they represented a significant percentage of all CDH11⁺ BMDCs and were elevated at day 3 after MI relative to sham (27.0% of CDH11⁺CD45⁺ cells vs. 10.1% CDH11⁺CD45⁺ cells in sham). CDH11⁺ M1-like macrophages were also elevated at day 3 after infarct, albeit not significantly. Nonetheless, the percentages of both CDH11⁺ neutrophils and CDH11⁺ M1-like macrophages

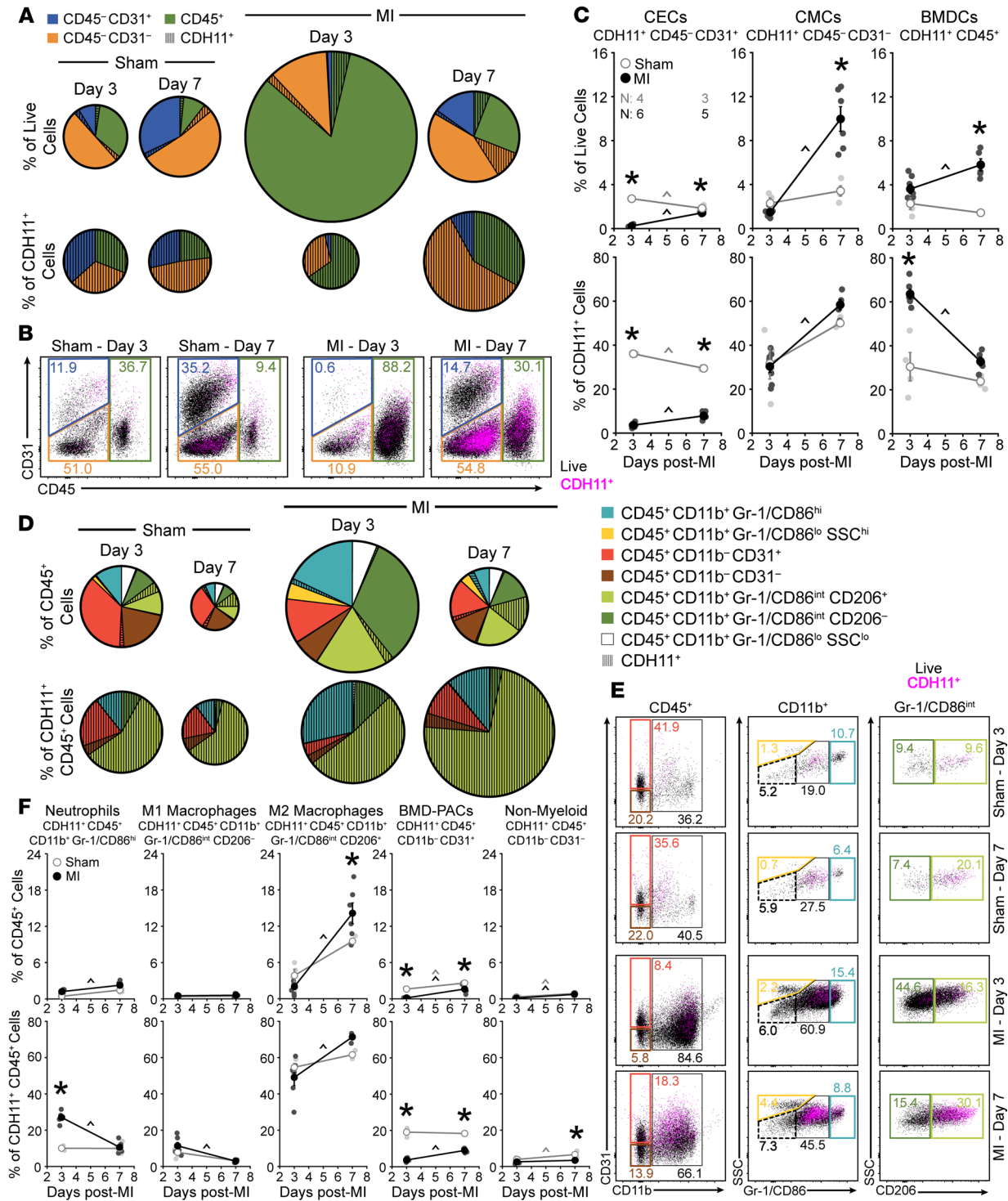


Figure 1. Specific cell populations in the heart express CDH11 after MI. Non-CM populations, including cardiac endothelial cells (CECs), cardiac mesenchymal cells (CMCs), and bone marrow–derived cells (BMDCs), express a baseline amount of CDH11 (hatched wedges) that is increased after MI. Pie chart radii (A) are scaled by either the number of live single cells (top) or the number of CDH11⁺ cells (bottom) relative to sham hearts at day 3. Representative dot plots (B) show changes in CDH11 expression (magenta) within each population (colored gates). CDH11⁺ cells (C) within each population are shown as either a percentage of live cells (top) or of all CDH11⁺ cells (bottom). CDH11 expression in BMDC (CD45⁺) subpopulations (D) revealed predominant expression in neutrophils and M1- and M2-like macrophages (light blue, dark green, and light green, respectively). Representative dot plots (E) show changes in CDH11 expression (magenta) within each subpopulation (colored gates). CDH11⁺ cells (F) within each subpopulation are shown as either a percentage of all BMDCs (top) or all CDH11⁺ BMDCs (bottom). Percentages of each population, relative to all live cell events, are denoted within colored gates. Data are presented as mean ± SEM, with *n* = 3–6 per group; dots in C and F denote individual animals. Pie charts represent average values. Significance was determined by 2-way ANOVA with a Holms–Sidak’s multiple comparison test. **P* < 0.05 between sham and MI at the same time, ^*P* < 0.05 over time; color of significance marker denotes group.

were decreased to sham levels by 7 days after infarct. In contrast, the percentage of all CDH11⁺ BMDCs that were either CDH11⁺ M2-like macrophages or CDH11⁺ bone marrow-derived proangiogenic cells increased between 3 and 7 days after infarct, whereas CDH11⁺ nonmyeloid cells remained unchanged after MI and were reduced at day 7 relative to sham (Figure 1F). A similar flow cytometric analysis profiling cells isolated from the peripheral blood after MI confirmed that the vast majority of cells (>90% of live cells) were CD45⁺ (Supplemental Figure 3B), and it revealed that only a small fraction of cells (<2% of live cells) expressed CDH11 (Supplemental Figure 4D). Of the CDH11⁺ cells in the blood, little difference was observed between sham and MI (Supplemental Figure 5).

Next, we sought to evaluate the effect of CDH11 signaling on cardiac remodeling *in vivo* and found that there was no difference in ejection fraction (EF) or left ventricular (LV) mass among *Cdh11*^{+/+}, *Cdh11*^{+/-}, and *Cdh11*^{-/-} mice following MI (Figure 2, A and B). However, LV volume was increased in *Cdh11*^{+/+} and *Cdh11*^{+/-} mice, but not in *Cdh11*^{-/-} mice, between 7 and 21 days after infarct. By day 21, LV diastolic volume was increased in *Cdh11*^{+/+} mice relative to that in *Cdh11*^{+/-} and *Cdh11*^{-/-} mice (Figure 2, C and D), and mixed-effects analysis identified a significant difference in LV diastolic volume among genotypes (Figure 2C). In addition, genetic deletion of CDH11 appeared to provide a survival benefit in the first week after MI, with an observed incidence of 29% survival for *Cdh11*^{+/+} mice, 63% survival for *Cdh11*^{+/-} mice, and 57% survival for *Cdh11*^{-/-} mice. To further investigate the role of CDH11 in BMDCs, we induced MI in wild-type mice receiving bone marrow from *Cdh11*^{+/+}, *Cdh11*^{+/-}, and *Cdh11*^{-/-} donors (Figure 2E and Supplemental Figure 6). Though most of the mice (8 of 10) that received *Cdh11*^{-/-} bone marrow died before complete bone marrow reconstitution at 6 weeks after transplantation, *Cdh11*^{+/-} bone marrow recipients showed improved EF between 7 and 21 days and reduced LV mass 7 days after MI, relative to *Cdh11*^{+/+} bone marrow recipients (Figure 2, F and G). Mixed-effects analysis identified a significant difference among genotypes and significant interaction between genotype and time for LV mass (Figure 2G). LV volume was not different between mice receiving either *Cdh11*^{+/+} or *Cdh11*^{+/-} bone marrow (Figure 2, H and I).

Having demonstrated a role for CDH11 in remodeling after MI, we hypothesized that blocking CDH11 adhesion and activity may therapeutically reduce MI-induced adverse ventricular remodeling and heart failure. Thus, we treated mice with *i.p.* injections of either a CDH11-blocking antibody (SYN0012) or IgG2a isotype control beginning 24 hours after induction of MI. EF (Figure 3A) and LV mass (Figure 3B) were preserved in SYN0012-treated animals relative to IgG2a for up to 56 days following MI. Further, the increased LV dilation observed in the IgG2a-treated mice was curtailed in the animals receiving SYN0012, resulting in preserved ventricular volume at both diastole (Figure 3C) and systole (Figure 3D) for up to 56 days after MI. Mixed-effects analysis identified an overall significant difference between treatment groups and significant interactions between treatment and day for EF and LV volume. Though survival after MI was improved with CDH11 blockade (82% survival for SYN0012 vs. 65% survival for IgG2a), it was not found to be statistically significant ($P = 0.20$; Supplemental Figure 7).

Given the changes in LV structure and function observed by echocardiography, we next wanted to quantify tissue mechanical properties and the extent of cardiac remodeling after infarct. In particular, median stiffness of infarcted areas from both SYN0012- and IgG2a-treated hearts, as measured by atomic force microscopy (AFM) (Supplemental Figure 8), was decreased below the measured range of sham myocardial stiffness by 7 days after MI (Figure 4A). However, by 21 days, infarct stiffness from both treatment groups was increased relative to sham, with the median and range of stiffness values from IgG2a-treated infarcts exceeding that of time-matched SYN0012-treated infarcts. By 56 days after MI, the median stiffness of SYN0012-treated infarcts had returned to the sham stiffness range, while the stiffness of IgG2a-treated infarcts remained elevated (Figure 4A). Automated histological quantification (Supplemental Figure 9) determined that infarcts from SYN0012-treated animals were thicker and spanned less of the LV circumference than IgG2a at both 21 and 56 days after MI (Figure 4, B–D, and Supplemental Figure 10, D and E). There were no measured differences in cardiac hypertrophy or remote interstitial fibrosis between treatments (Supplemental Figure 10, A–C), and despite differences in infarct remodeling, we observed no difference in CF contractility following SYN0012 treatment *in vitro*. Whereas *Cdh11*-knockout reduced collagen gel contraction by CFs (Supplemental Figure 11A), SYN0012 treatment did not affect CF contraction (Supplemental Figure 11B), suggesting a potentially critical role for CDH11 activation in modulating the myofibroblast phenotype and promoting interactions with specific immune cell populations in order to determine the extent of cardiac remodeling after infarct.

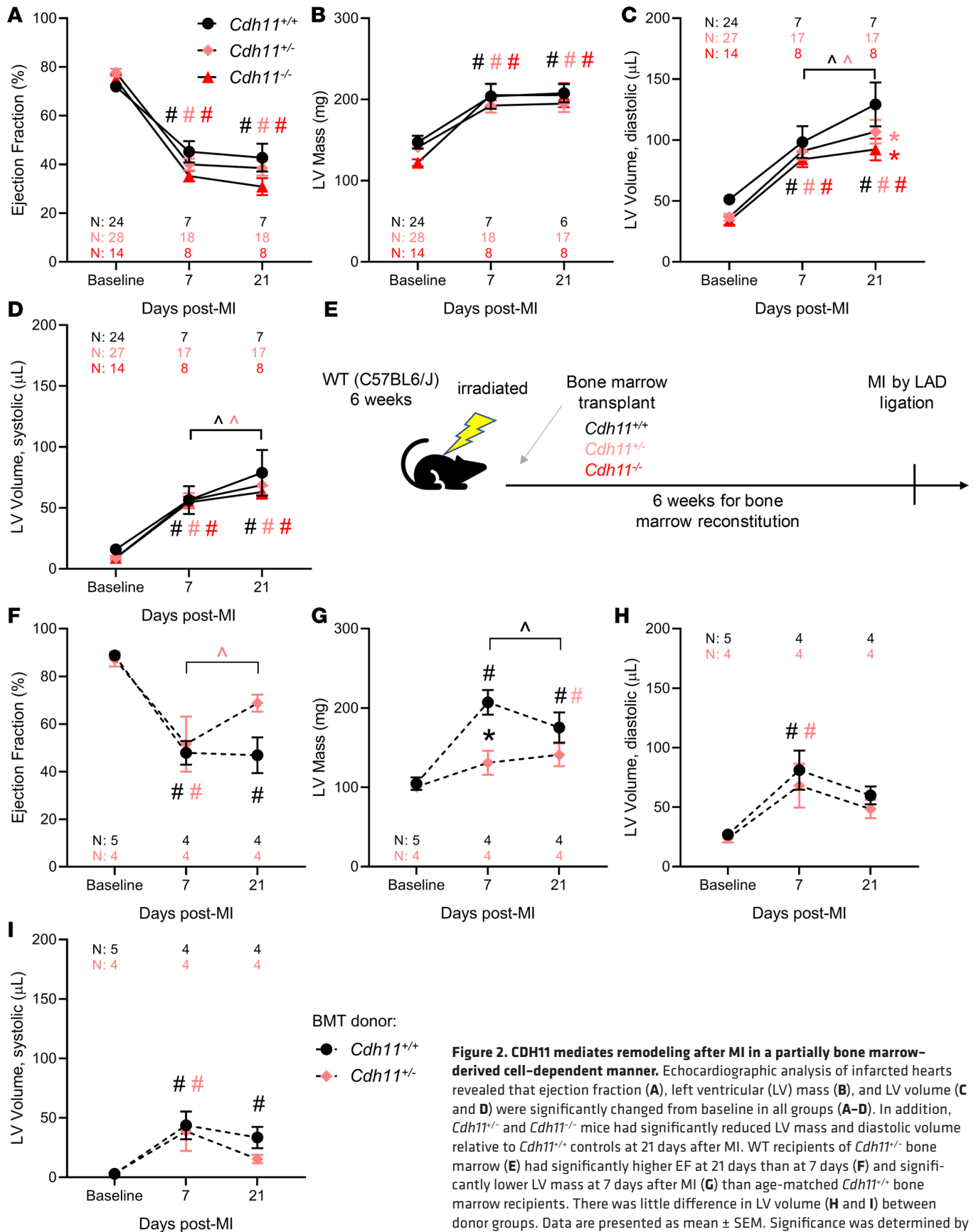


Figure 2. CDH11 mediates remodeling after MI in a partially bone marrow-derived cell-dependent manner. Echocardiographic analysis of infarcted hearts revealed that ejection fraction (A), left ventricular (LV) mass (B), and LV volume (C and D) were significantly changed from baseline in all groups (A–D). In addition, *Cdh11*^{-/-} and *Cdh11*^{+/-} mice had significantly reduced LV mass and diastolic volume relative to *Cdh11*^{+/+} controls at 21 days after MI. WT recipients of *Cdh11*^{-/-} bone marrow (E) had significantly higher EF at 21 days than at 7 days (F) and significantly lower LV mass at 7 days after MI (G) than age-matched *Cdh11*^{+/+} bone marrow recipients. There was little difference in LV volume (H and I) between donor groups. Data are presented as mean ± SEM. Significance was determined by mixed-effect analysis, with a Holms-Sidak’s multiple comparison test. **P* < 0.05 relative to *Cdh11*^{+/+}, #*P* < 0.05 relative to baseline, ^*P* < 0.05 between time points; color of significance marker denotes group.

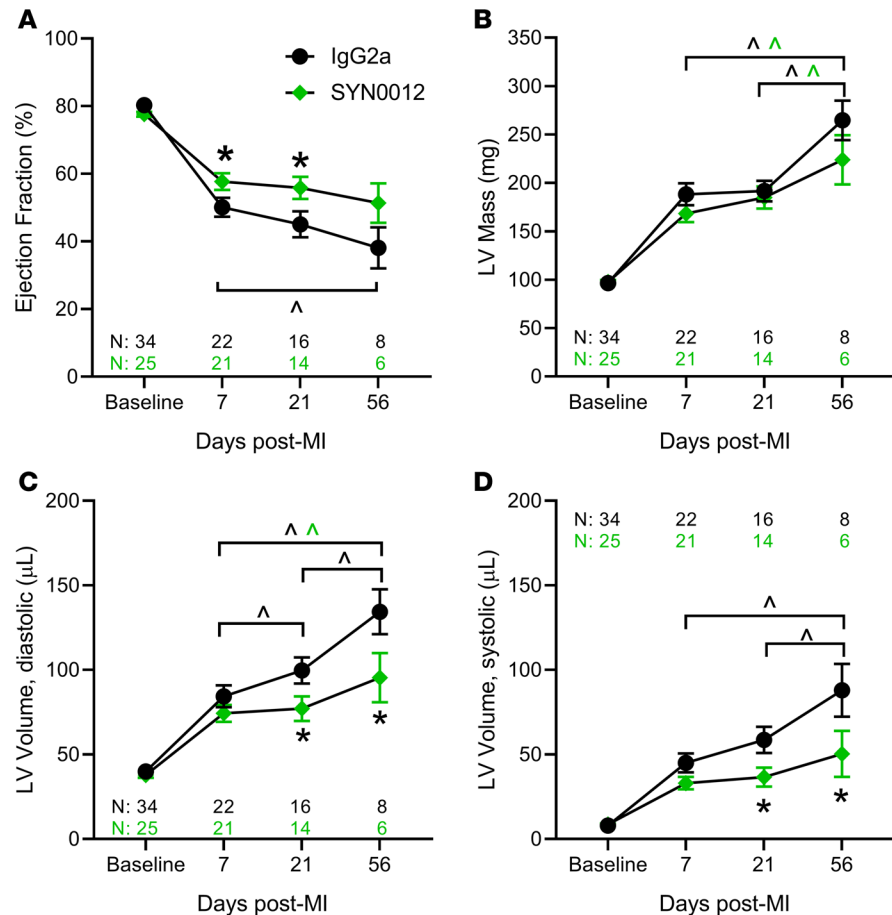


Figure 3. CDH11 blockade improves functional outcomes after MI. Echocardiographic analysis of infarcted hearts revealed that ejection fraction (A), left ventricular (LV) mass (B), and LV volume (C and D) was significantly changed from baseline in all groups. SYN0012-treated hearts had significantly higher ejection fraction at 7 and 21 days after infarct, and reduced LV volume at 21 and 56 days after infarct, compared with IgG2a-treated controls; LV mass was not different between treatments at any time point. Data are presented as mean \pm SEM. Significance was determined by mixed-effect analysis with a Holms-Sidak's multiple comparison test. * $P < 0.05$ between treatments, $\wedge P < 0.05$ between time points; color of significance marker denotes treatment group.

To determine which cells contribute to the preserved cardiac remodeling in response to pharmacologic CDH11 blockade, we again used flow cytometry to quantify the percentages of non-CMs in the heart and peripheral blood after infarct (Figure 5). SYN0012 treatment did not alter the percentages of the primary non-CM cardiac cell populations — CECs, CMCs, and BMDCs — relative to IgG2a treatment, despite trends toward decreased CMCs and increased BMDCs after infarct in SYN0012-treated hearts (Figure 5, A–C). Further examination of BMDC subsets revealed that SYN0012 treatment decreased the percentage of specific myeloid lineage cells — particularly, neutrophils and M1-like macrophages — in the heart at 3 days after MI (Figure 5, D–F). Though the ratio of M1/M2-like macrophages in the heart was not altered with SYN0012 treatment (Supplemental Figure 12, A–C), the early reduction in neutrophils and M1-like macrophages suggests that CDH11 blockade alters the expression of cell populations in the heart to result in a more proresolving inflammatory environment after infarct. SYN0012 also resulted in an increase in bone marrow–derived proangiogenic cells and nonmyeloid BMDCs in the heart 3 days after infarct; differences relative to IgG2a in all populations were gone by day 7, consistent with the time course of inflammation resolution. The distribution of circulating cells in the peripheral blood was largely unaffected by SYN0012 treatment, aside from a higher M1/M2-like macrophage ratio in the peripheral blood at day 3 after infarct, relative to IgG2a (Supplemental Figure 12F). The observed increase was a result of decreased circulating levels of M2-like macrophages and suggests that SYN0012 treatment may alter macrophage recruitment to the heart after infarct (Supplemental Figure 13, D–F).

We next examined transcriptional levels of multiple inflammatory and fibrotic genes over the 21-day time course of remodeling after MI (Figure 6 and Supplemental Figure 14). SYN0012 treatment decreased

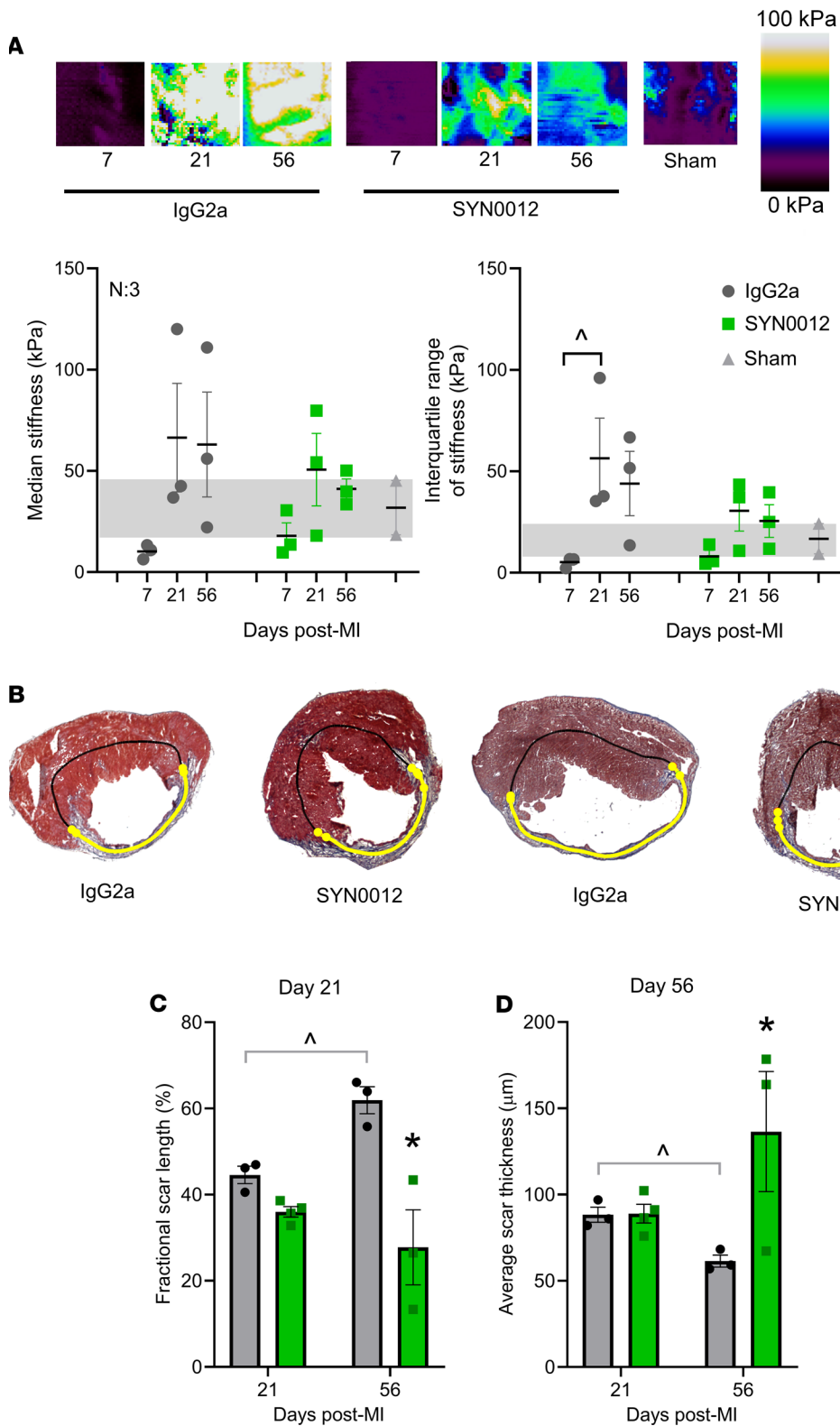


Figure 4. CDH11 blockade limits fibrotic remodeling after MI. Atomic force microscopy was used to quantify local tissue stiffness, as shown by representative stiffness color maps (A). Calculation of median stiffness values from each scan revealed a decrease at 7 days after MI, with all of the IgG2a hearts falling outside the range of the sham myocardium. Median stiffness values increased by 21 days and remained elevated out to 56 days in IgG2a-treated hearts, whereas SYN0012-treated hearts increased to a lesser extent at 21 days and were restored to sham levels by 56 days after MI; the interquartile range of stiffness values was larger in IgG2a-treated infarcts than SYN0012-treated infarcts, which were similar to the range of sham myocardium. Representative Masson's trichrome-stained sections denote scar location (yellow line), as identified by a custom image processing algorithm (B). Images were used to quantify the fractional scar length as a percentage of cardiac circumference (C) and the average thickness along the infarct length (D). Data are presented as mean \pm SEM; each dot represents the average of either 5 independent measurements (A) or 3 independent images (C and D) from individual animals, with $n = 3-4$. Significance was determined by 2-way ANOVA with Holm-Sidak's multiple comparison test. * $P < 0.05$ between treatments, $\wedge P < 0.05$ between time points

transcription of the proinflammatory cytokine *Il6* at 3 days after MI, relative to IgG2a treatment (Figure 6A). Representative immunostaining further confirmed that there was a reduction in IL-6 expression in the infarct region of SYN0012-treated hearts (~80% of staining intensity of sham; Figure 6B). Transcription of *Cdh11* was increased at both 7 and 21 days after MI, relative to sham but was not significantly affected by SYN0012 treatment (Figure 6C). Interestingly, SYN0012 treatment reduced transcription of proangiogenic signaling

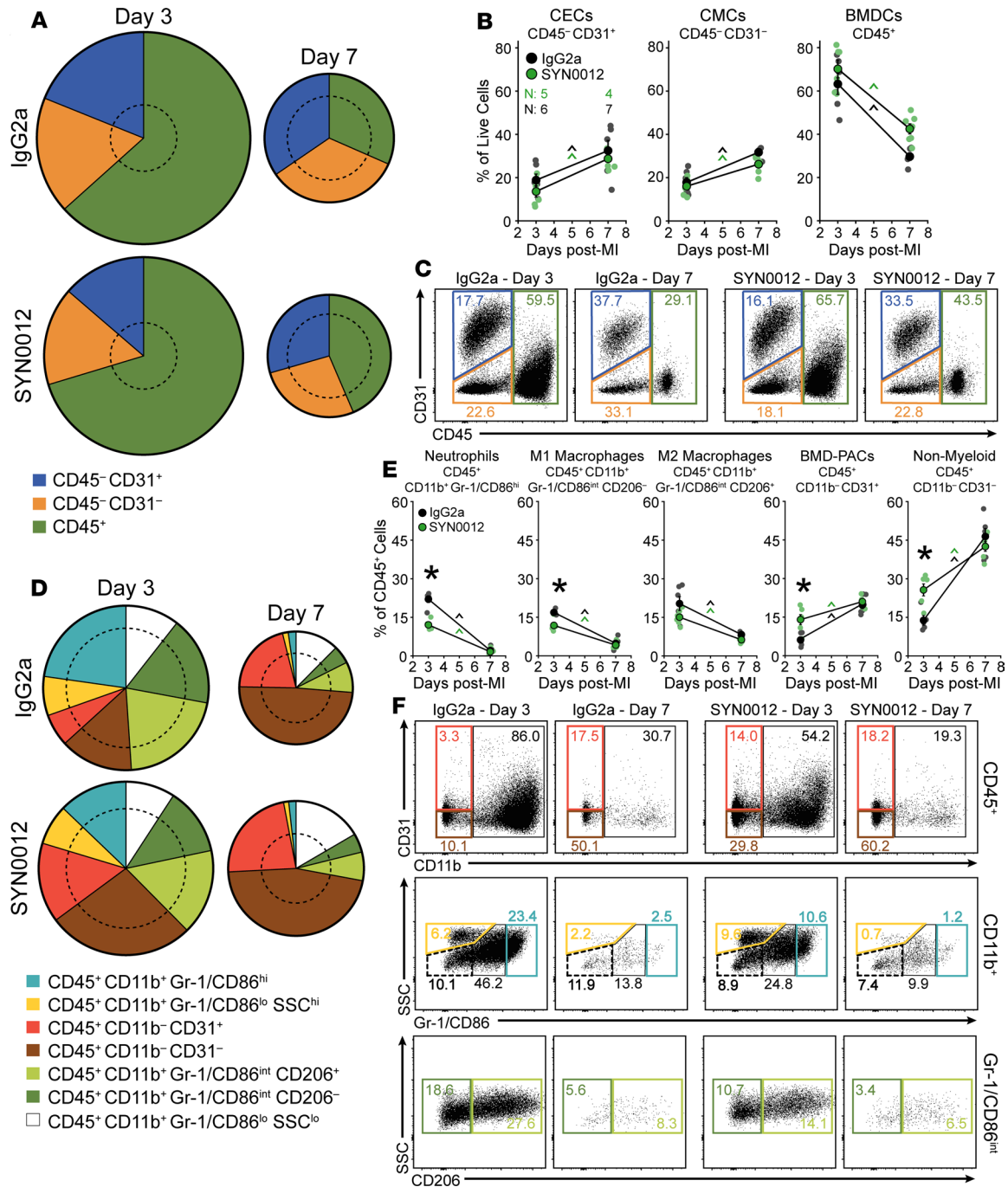


Figure 5. CDH11 blockade modulates expression of specific cell populations after MI. CDH11 blockade by SYN0012 treatment does not significantly alter the percentages of non-CM populations (cardiac endothelial cells [CECs], cardiac mesenchymal cells [CMCs], and bone marrow-derived cells [BMDCs]) in the heart after MI, relative to IgG2a isotype control (A and B). Pie chart radii are scaled by the number of live single cells for each treatment and time, relative to sham hearts at day 3 (denoted by dotted circles). Representative dot plots (C) show changes in expression of each population (colored gates). Separation of BMDC populations (D) revealed that SYN0012 treatment results in a significant reduction in neutrophils (light blue) and M1-like macrophages (dark green) in addition to increased bone marrow-derived proangiogenic cells (BMD-PACs, red) and nonmyeloid BMDCs (or lymphocytes, brown) at day 3 after infarct; differences in all populations between treatments were gone by day 7 (E). Representative dot plots (F) show changes in expression of each subpopulation (colored gates). Percentages of each population, relative to all live cell events, are denoted within colored gates. Data are presented as mean ± SEM, with n = 4–7 per group; dots in B and E denote individual animals. Pie charts represent average values. Significance was determined by 2-way ANOVA with a Holms-Sidak’s multiple comparison test. *P < 0.05 between treatments at the same time, ^P < 0.05 over time; color of significance marker denotes treatment group

factors *Fgf2* and *Vegfa1*, relative to IgG2a. In particular, IgG2a-treated hearts had increased *Fgf2* transcription, relative to sham, at 7 and 21 days after MI (Figure 6D). While *Vegfa1* transcription was not different from sham at any time point, SYN0012 treatment reduced transcription at 7 and 21 day after infarct, relative to IgG2a (Figure 6E); however, SYN0012-treated animals appeared to have more muscularized vessels — likely arterioles — in the infarct region at 21 days after MI (Figure 6F). Smooth muscle α -actin (α SMA) is a contractile form of actin expressed in both myofibroblasts and smooth muscle cells, which surround arteries and arterioles. Albeit not statistically significant, SYN0012 treatment resulted in an approximately 14% reduction in the expression of α SMA⁺ myofibroblasts in infarcted regions, relative to IgG2a.

Based on our findings of increased CDH11 expression in bone marrow-derived macrophages and resident CMCs (which we expect to be primarily CFs), we next wanted to determine if interactions between these cell populations might regulate the expression or transcription of proinflammatory, profibrotic, or proangiogenic factors (Figure 7). Indeed, in vitro CF-macrophage cocultures with varying CF/macrophage ratios confirmed previously reported findings that CDH11-dependent interactions between CFs and macrophages promote IL-6 secretion by CFs (ref. 18 and Figure 7A). Of note, macrophages alone expressed very low levels of IL-6, suggesting that CFs are the main source of IL-6 in CF-macrophage cocultures. Treatment with SYN0012 reduced, but did not prevent, secretion of IL-6 by CFs (Figure 7B). Gene expression analysis by qPCR further revealed that *Mmp13* transcription was increased in a manner dependent upon the CF/macrophage ratio but was not significantly affected by SYN0012 treatment, despite a slight increase relative to IgG2a in the 50:50 culture condition (Supplemental Figure 16, A and B). *Tgfb1* transcription was also increased by CF-macrophage interactions in a similar manner to *Mmp13* (Supplemental Figure 16C), but transcription of proangiogenic factors *Fgf2* and *Vegfa1* was not affected by varying CF/macrophage ratios (Supplemental Figure 16, D and E). Transcription of macrophage polarization markers *Cd14* and *Mrc1* was unaffected by SYN0012 treatment, whereas expression of *Arg1* — a marker of M2 macrophage polarization — was increased relative to IgG2a treatment in the 50:50 culture condition (Supplemental Figure 16, F and G).

Discussion

Our findings reveal that CDH11 is expressed primarily in non-CMs of the ischemic heart and suggest a functional role for CDH11 in resolving tissue breakdown and promoting myocardial remodeling. *Cdh11* transcription is nearly 10-fold higher at 7 days after MI, as compared with sham (Supplemental Figure 4, A and B), suggesting a prominent role in myofibroblasts, which are particularly active when the bulk of scar formation occurs between 2 and 3 weeks after MI (3). However, the observation that *Cdh11* is also significantly upregulated as early as 3 days after infarct suggests that other cell types — particularly those derived from infiltrating inflammatory cells, such as neutrophils, monocytes, and macrophages — may also contribute to CDH11-mediated cardiac remodeling. Flow cytometric analysis confirmed that CDH11 was expressed in the ischemic heart and further revealed that there was baseline CDH11 expression in approximately 5% of all non-CMs (Supplemental Figure 4C), distributed evenly among CECs, CMCs, and BMDCs. Three days after MI, the majority of CDH11⁺ cells were BMDCs, whereas by day 7, the majority of CDH11⁺ cells were CMCs, consistent with the time course of inflammation resolution and myofibroblast activation (Figure 1, A–C). Note that increased CDH11 expression is known to be a hallmark of myofibroblast phenotype in other cardiovascular cell types, such as aortic valve interstitial cells (19). At both 3 and 7 days after MI, the majority of CDH11⁺ BMDCs were myeloid lineage neutrophils and macrophages with either M1-like or M2-like polarization. At each time point, the highest expression of CDH11 was found in M2-like macrophages (Figure 1, D–F), consistent with prior reports of CDH11 expression in activated macrophages (20). The time-dependent expression of CDH11 in the ischemic heart suggests that targeting of CDH11 after MI has the potential to mitigate both early neutrophil- and macrophage-mediated inflammation and tissue breakdown and later myofibroblast-mediated collagen deposition and remodeling to result in substantial functional improvement in the heart after infarct.

When evaluating the effect of CDH11 on cardiac remodeling in vivo, we found that *Cdh11*^{-/-} mice did not have significantly altered EF after MI when compared with *Cdh11*^{+/+} controls (Figure 2A). While LV volume continued to increase in *Cdh11*^{+/+} and *Cdh11*^{+/-} mice between day 7 and 21, the LV dimensions of *Cdh11*^{-/-} animals did not change significantly over this period, suggesting that CDH11 contributes to the fibrotic remodeling phase of MI healing (Figure 2, B–D). A larger percentage of *Cdh11*^{+/-} and *Cdh11*^{-/-} animals survived the first week after MI than *Cdh11*^{+/+} animals, suggesting that the presence of CDH11 in the immune cells present during the initial inflammatory phase of healing may contribute to the negative remodeling that leads to cardiac rupture in mice. Transplantation of bone marrow from *Cdh11*^{-/-} donors

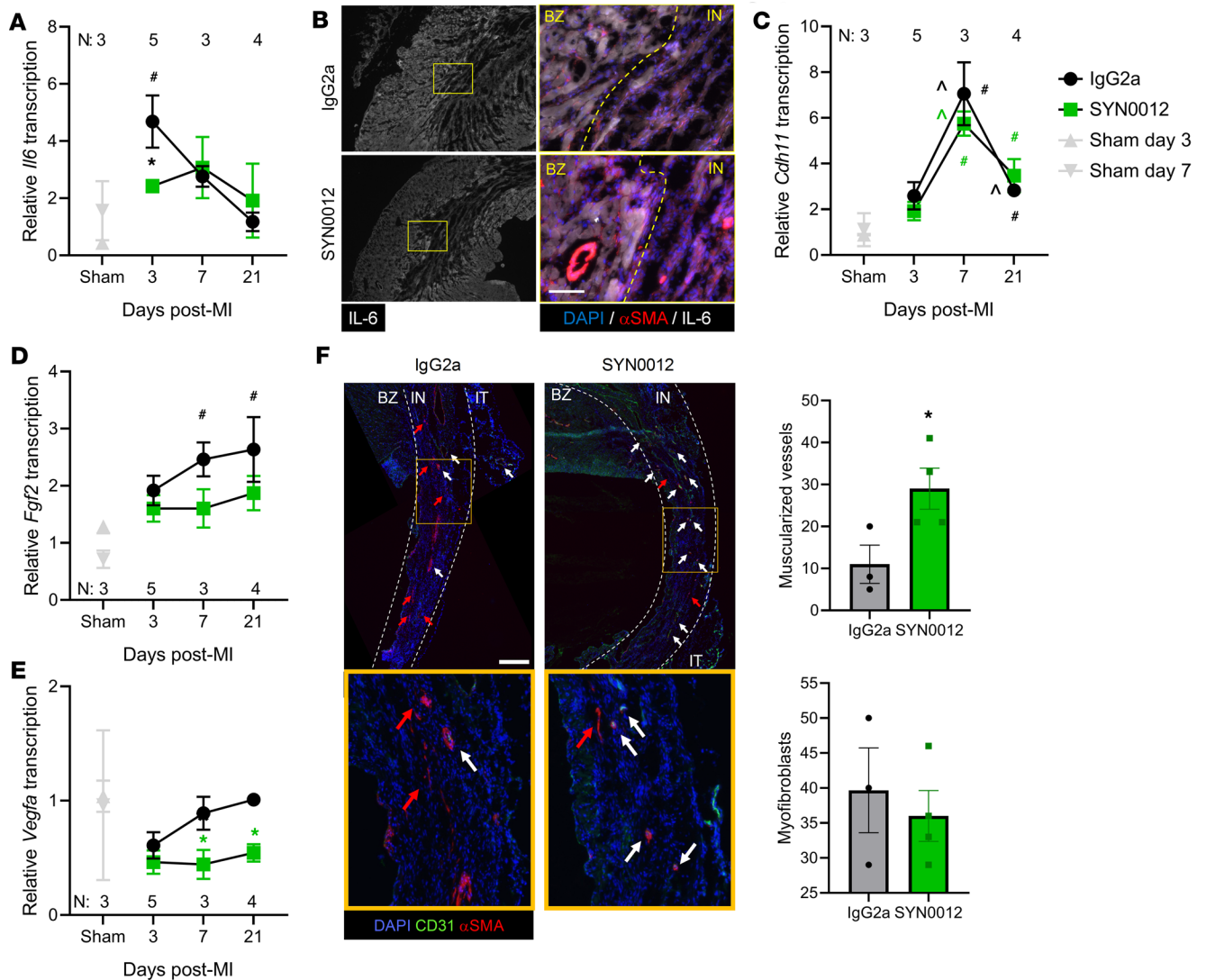


Figure 6. CDH11 blockade reduces inflammatory signaling and improves vascular maturity after MI. SYN0012 treatment significantly decreased transcription of *Il6* (A) at 3 days after MI, relative to IgG2a. Immunostaining of infarct regions of hearts 3 days after MI showed decreased IL-6 expression 3 days after MI, primarily in the non-CMs – costained with α SMA and CD45 (cf. Supplemental Figure 15) of the infarct (B). Transcription of *Cdh11* (C) was significantly increased above sham at days 7 and 21 in both treatment groups. Transcription of both *Fgf2* (D) and *Vegfa1* (E) was decreased by SYN0012, relative to IgG2a. Analysis of histological sections showed a significant increase in the number of muscularized vessels found in the infarct (IN) region of SYN0012-treated animals, but no difference in the number of myofibroblasts per field of view (F). Vessels in the border zone (BZ) and epicardial inflammatory tissue (IT) were not counted. Red arrows indicate myofibroblasts, white arrows indicate arterioles, and the yellow box is magnified below. Scale bar: 100 μ m (B); 500 μ m (F). Data are presented as mean \pm SEM; dots in F represent individual animals. Significance was determined by 2-way ANOVA analysis with a Holms-Sidak's multiple comparison test (A–E) or a 2-tailed Student's *t* test (F). **P* < 0.05 between treatments, #*P* < 0.05 relative to sham, ^*P* < 0.05 between time points; color of significance marker denotes treatment group.

was fatal to most of the WT recipients, likely due to impaired localization of hematopoietic cells to the bone marrow niche (ref. 12 and Supplemental Figure 6). However, surviving *Cdh11*^{+/-} bone marrow recipients had improved EF 3 weeks after MI and reduced LV mass, relative to *Cdh11*^{+/+} bone marrow recipients, 1 week after MI (Figure 2, F–I). It is interesting to note that the cohort that received bone marrow transplants had less severe responses to MI, which might be due to the inherent effects of irradiation and bone marrow transplantation on modulating the expression of macrophage populations and after MI remodeling (21). Overall, these data suggest that CDH11 has important functional roles in multiple resident and recruited cell types, including the migration and localization of BMDCs and the activity of myofibroblasts. Note that *Cdh11*^{-/-} aortic valve interstitial cells have reduced contractility (19), which we also observed in *Cdh11*^{-/-} CFs but notably did not observe in wild-type CFs treated acutely with SYN0012 (Supplemental Figure 11). This defect in CF contractility and other reported effects of the permanent global knockout of

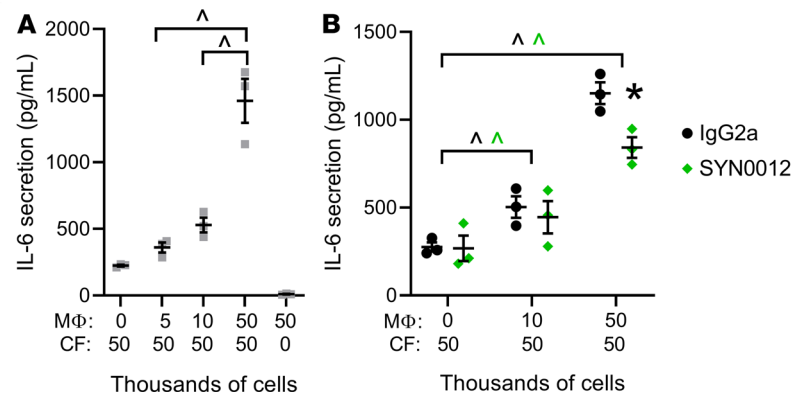


Figure 7. Coculture of macrophages and cardiac fibroblasts increases proinflammatory and profibrotic signaling.

Coculture of macrophages and cardiac fibroblasts (CFs) promotes secretion of IL-6 by CFs in a macrophage-dependent manner (A). CDH11 blockade by SYN0012 treatment significantly reduced IL-6 secretion in CF-macrophage cocultures at high macrophage concentrations (B). Secreted IL-6 was measured in media of CF-macrophage cocultures by ELISA. Data are presented as mean \pm SEM; each dot represents a biological replicate ($n = 3$). Significance was determined by 1- and 2-way ANOVA, with a Holms-Sidak's multiple comparison tests. $^{\wedge}P < 0.05$ between macrophage conditions, $^{*}P < 0.05$ relative to CF-only control, $^{*}P < 0.05$ between treatments; color of significance marker denotes treatment group.

CDH11 (22, 23) in the native cells of the heart are likely the reason we did not see the same improvement in EF and changes in LV volume after MI in the genetic model as in the bone-marrow recipient mice or acute SYN0012-treated animals.

Previous studies have shown that genetic and pharmacologic targeting of CDH11 improves functional responses in both fibrotic lung disease and aortic valve calcification (10, 11). Herein, CDH11 blockade by SYN0012 treatment appears to preserve cardiac function as early as 7 days after MI and prevents the continued functional decline observed with IgG2a treatment out to 56 days (Figure 3A). LV volume was not different at 7 days, but the dramatic increases in both diastolic and systolic volume between 7 and 56 days in IgG2a-treated animals were prevented by pharmacological inhibition of CDH11 by SYN0012 (Figure 3, C and D). This observation, combined with increased *Cdh11* transcription occurring at day 7 after MI, suggests that CDH11-expressing cells play an active role in LV remodeling and dilation during the fibrotic phase of infarct healing. Albeit not statistically significant, twice as many IgG2a-treated mice died between days 3 and 7 after MI — the highest risk time period for cardiac rupture (3) — than in the SYN0012-treated cohort (Supplemental Figure 7). Indeed, SYN0012-treated mice also showed increased survival rates relative to prior reports using the same surgical model of MI (24). This difference in mortality is likely a consequence of altered tissue breakdown and inflammation-mediated softening of the myocardial wall, consistent with the reduction in stiffness observed by AFM measurements at day 7 after MI; by day 21, and even more so at day 56, we observed high stiffness variability in IgG2a-treated infarcts, whereas SYN0012-treated infarcts had more consistent stiffness values within the range of sham animals (Figure 4).

Having identified a clear functional effect of CDH11 blockade in limiting myocardial remodeling and infarct expansion after MI, we investigated which cell types and molecular mechanisms may mediate this process. Flow cytometry-based assessment of primary non-CM populations in the ischemic heart revealed that SYN0012 treatment did not affect the overall percentages of CMCs or BMDCs at 3 or 7 days after MI (Figure 5, A–C). However, further analysis of specific BMDC subpopulations revealed that targeting CDH11 alters the early expression of myeloid lineage neutrophils and macrophages, shifting the balance from proinflammatory macrophages and neutrophils to prohealing macrophages and proangiogenic non-myeloid cell populations 3 days after MI (Figure 5, D–F). This reduction in neutrophils and M1-like macrophages may contribute to the reduced tissue remodeling observed following SYN0012 treatment. Indeed, reduced neutrophil influx has been shown to improve cardiac remodeling and prolong survival after MI by reducing proinflammatory signaling and promoting macrophage polarization toward a proreparative M2-like phenotype (25, 26). High neutrophil-to-lymphocyte ratios (NLRs) have been shown to be a reliable predictor of myocardial damage following acute coronary events (27). At 3 days after MI, we observed a slight reduction in NLR in the blood with SYN0012 treatment (0.342 ± 0.038 vs. 0.402 ± 0.121 with IgG2a; $P = 0.69$, t test) but a significant decrease in cardiac NLR (0.457 ± 0.068 vs. 1.458 ± 0.304 with IgG2a;

$P = 0.017$, t test), suggesting that CDH11 blockade alters the distribution of cardiac immune cell populations in a manner that reduces myocardial damage and leads to preserved cardiac function. Despite showing differences in the heart, the percentages of myeloid cells and proangiogenic cells circulating in the peripheral blood were not significantly different 3 days after MI (Supplemental Figure 13). In fact, the ratio of M1/M2-like macrophages in the blood was significantly increased, suggesting that the SYN0012 likely has an effect on the preferential recruitment of proangiogenic cells and M2-like macrophages to the heart. In light of these findings, future studies could test whether expression of adhesion molecules such as ICAM-1 or selectins expressed by circulating leukocytes and cardiac cells are responsible for an increase in cell recruitment. Alternatively, the unique mechanical environment within the heart may preferentially affect proliferation of recruited immune cells in a CDH11-dependent manner. Indeed, CDH11 deficiency has been shown to reduce macrophage recruitment, migration, proliferation, and expression of M2-macrophage markers — such as ARG1 and CD206 — in pulmonary fibrosis (28).

We observed a reduction in *Il6* transcription with SYN0012 treatment at 3 days after infarct, primarily in non-CMs (Figure 6A). IL-6 is a proinflammatory cytokine that has been shown to have a multifaceted role in cardiovascular disease. IL-6 signaling has been shown to promote the infiltration, migration, and polarization of macrophages as well as the activation of myofibroblasts (7, 29–31). Conversely, there is also evidence that blocking IL-6 leads to worsened outcomes after ischemic injury by reducing CM viability and angiogenesis (32–34). By leveraging CDH11 to selectively target non-CMs in the heart, we have identified a therapeutic strategy that effectively limits the negative cell activating effects of IL-6 without interfering with its function in CMs. The decrease in *Il6* transcription, and the corresponding reduction in IL-6 expression in infarcted area of representative hearts, was evident at 3 days after infarct (Figure 6, A and B). This is consistent with the time point of increased inflammatory macrophages and neutrophils in the heart (Figure 1, D–F) and the transition from the inflammatory to proliferative phases of healing. As such, there has been an increasing interest in designing treatment strategies around the role of macrophages — and the associated secreted factors and proinflammatory signaling — in the process of healing and cardiac remodeling after MI (35–38).

We hypothesized that CDH11 regulates the interactions between CFs and macrophages in the heart after MI, noting that macrophage activity has been shown to alter CF function in the ischemic heart independent of CDH11 (39). Interactions between macrophages and CFs have been reported to regulate IL-6 expression in response to TGF- β 1 signaling and fibrosis (18). CDH11-dependent CF-macrophage interactions in the lungs have also been shown to create a self-sustaining profibrotic niche via local production of latent TGF- β 1 by macrophages that can be activated by myofibroblasts (20). TGF- β 1 is a key signal to trigger the resolution of inflammation and initiation of fibrotic remodeling after MI (40, 41). We found decreased *Il6* transcription and protein expression — a hallmark of CF-macrophage interactions — in SYN0012-treated hearts, relative to IgG2a, at 3 days after MI (Figure 6, A and B). Our coculture data confirm that interactions between macrophages and CFs promote the expression of IL-6 through a partially CDH11-dependent mechanism (Figure 7, A and B). The reduction in the number of macrophages in the heart after 3 days is likely responsible for the reduction in IL-6 expression and the beneficial modulation of both inflammation and fibrosis observed with SYN0012 treatment.

Interestingly, following CDH11 blockade we observed a reduction in transcription of both *Fgf2* and *Vegfa1*, two proangiogenic genes often associated with improved revascularization and better outcomes following MI (42–45). However, we also observed an increase in muscularized vessels (i.e., arterioles) in infarcted areas of SYN0012-treated hearts at 21 days after MI; this corresponds to a time when angiogenic gene expression has run its course (46). We speculate that SYN0012 may either preserve native vasculature or hasten maturation of new vasculature, such that the hypoxic conditions that typically drive angiogenic signaling are reduced (47). Blocking CDH11 in endothelial cells could also attenuate endothelial-to-mesenchymal transitions, potentially contributing to preservation of the native vasculature (10, 48). The proportion of CECs in the heart over both time points was slightly reduced with SYN0012 treatment, but the increased recruitment of proangiogenic cells, combined with a reduction in early inflammatory cell infiltration, may contribute to a restoration or preservation of infarct vascularization (Figure 5).

Overall, our data reveal that CDH11 engagement plays important roles in the recruitment of specific BMDC populations to the heart after MI that work in concert to promote persistent collagen deposition and fibrotic remodeling by activated myofibroblasts. Importantly, targeting CDH11 with SYN0012 in mice does not prevent the acute inflammatory and reparative response, but rather it selectively acts on several

cell populations to reduce the duration of inflammation and the extent of fibrotic remodeling resulting in a smaller, more stable infarct. We believe that this effect is mediated, in part, by limiting early recruitment of myeloid lineage BMDCs — including neutrophils and M1-like macrophages — and by reducing macrophage-induced expression of IL-6 by CFs. Further, SYN0012 treatment promotes recruitment of proangiogenic immune cells to the heart and results in the preservation of arterioles in the infarct area. Taken together, this work has identified CDH11 as a potential therapeutic target to reduce inflammatory and fibrotic remodeling following MI by selectively targeting a host of active non-CMs responsible for the initiation and progression of cardiac fibrosis and heart failure.

Methods

Further information and expanded methods can be found in the Supplemental Methods.

Mice. *Cdh11*-deficient mice on a mixed C57BL/6 and C129 background were initially obtained from R. Civitelli (Washington University School of Medicine, St. Louis, Missouri, USA), and *Cdh11*^{+/+}, *Cdh11*^{+/-}, and *Cdh11*^{-/-} littermate controls were obtained from *Cdh11*^{+/-} breeding pairs. Wild-type C57BL/6J mice (for antibody treatment studies) and B6.SJL-*Ptprca*^a*Pepcb*^b/BoyJ mice expressing the CD45.1 allele (for bone marrow transplantation studies) were purchased from The Jackson Laboratory. All genotypes were maintained on their respective backgrounds for more than 10 generations.

Animal studies. MI was induced in 12- to 16-week-old male mice by permanent coronary artery ligation, as previously described (24). For antibody treatments, mice were administered either 10 mg/kg CDH11 functional blocking antibody (SYN0012; with permission from Roche) or an isotype control antibody (IgG2a) resuspended in sterile saline. Antibodies were delivered by i.p. injection every 4 days, beginning 1 day after surgery, with the last treatment given on day 17 after infarct. For bone marrow transplantation studies, 6-week-old B6.SJL-*Ptprca*^a*Pepcb*^b/BoyJ mice expressing the CD45.1 allele were lethally irradiated with a 10-Gy split dose from a Cs¹³⁷ source. Bone marrow from age- and sex-matched *Cdh11*^{+/+}, *Cdh11*^{+/-}, and *Cdh11*^{-/-} donors was isolated and transplanted into irradiated recipients by retro-orbital injection (1 × 10⁶ cells in 100 μL) within 24 hours of irradiation. Transplant efficiency was confirmed by flow cytometry of isolated bone marrow showing simultaneous expression of the donor CD45.2 allele and absence of the original CD45.1 allele (Supplemental Figure 6). To allow for reconstitution of the bone marrow, recipient mice received MI by permanent LAD ligation 6 weeks after transplantation (Figure 2E). Mice were euthanized by CO₂ inhalation in accordance with university guidelines at 3, 7, 21, and up to 56 days after infarct for further processing.

Echocardiography. EF, LV mass, and LV volume in both systole and diastole were measured from short-axis cardiac M-mode images captured on a Vevo 2100 small-animal ultrasound system (VisualSonics). A minimum of 6 independent measures of LV diameter and wall thickness were used to calculate metrics of cardiac function and geometry for each mouse at each time point. Echocardiographic measurements cardiac structure and function were made just prior to MI (baseline) and at days 7, 21, and 56 days after surgery. Mice with an EF reduced by less than 5% or greater than 70% at 7 days after MI were excluded from subsequent analyses.

Cell studies. For separation of CMs from non-CMs, slow perfusion of whole hearts with a 2% collagenase solution was used to digest the ECM and isolate cells, which were separated into CM and non-CM fractions by centrifugation for 10 minutes at 90 g (49). CFs were isolated from 8-week-old *Cdh11*^{+/+} and *Cdh11*^{-/-} mice bred onto the *Immorto* mouse line (to allow for higher passage numbers). Hearts were isolated, minced, and digested in a 2% collagenase solution supplemented with trypsin for the last 10 minutes of a 40-minute digest. Cells were then rinsed with PBS, transferred to gelatin-coated plates, and cultured in DMEM supplemented with 10% FBS, 1% penicillin/strep, and IFN-γ at 33°C to maintain the immortalized phenotype. Prior to experimental use, cells were replated in DMEM supplemented with 10% FBS and 1% penicillin/strep and grown at 37°C for 48 hours to deactivate the immortalized gene. Macrophage exfiltration was stimulated by i.p. injection of 1 mL of 4% thioglycollate media into C57BL/6 mice. After 72 hours, mice were sacrificed, and the i.p. cavity was flushed with 10 mL cold RPMI media to collect the cells. After washing in cold PBS, cells were plated in RPMI media supplemented with 10% FBS on tissue culture plastic and allowed to adhere for 1 hour. Nonadherent cells were then rinsed away, and all remaining cells were taken to be macrophages (50). For CF-macrophage coculture experiments, 50,000 CFs were plated in each well of a 12-well plate and allowed to adhere for 20 minutes prior to exposure to media containing between 0 and 50,000 macrophages. Cell suspensions were diluted to a final volume of 1.3 mL

per well. For antibody treatments, samples were incubated with antibody (10 µg/ml of either SYN0012 or IgG2a) for 15 minutes before plating. After 48 hours in culture, conditioned media were removed from each well and IL-6 secretion was measured with a DuoSet mouse IL-6 ELISA (R&D Systems), according to the manufacturer's instructions. After boiling, 100 µl of each sample was added in duplicate and compared against a provided standard (Figure 7, A and B).

Flow cytometry. Cells from the hearts and peripheral blood of sham or MI animals were isolated at 3 and 7 days after surgery and immediately placed in a solution of ice-cold FACS buffer (5% FBS in PBS). Hearts were minced and digested in 1.4 mg/mL of type II collagenase solution in HBSS for 30 minutes at 37°C. Isolated cells were filtered through a 70-µm cell strainer into room temperature red blood cell lysis buffer prior to staining with DAPI (1:100,000; Thermo Fisher Scientific) to label dead cells and conjugated antibodies for Ter-119 (1:100; violetFluor 450 clone TER-119; Tonbo Biosciences), CD45.2 (1:100; PerCP-Cy5.5 clone 104; Tonbo Biosciences), CD31 (1:100; PE-Cy7 clone MEC13.3; BioLegend), CD11b (1:100; PE clone M1/70; eBioscience), CD206 (1:100; APC clone MR6F3; eBioscience), CD86 (1:100; FITC clone GL1; eBioscience), and Gr-1 (1:100; FITC clone RB6-8C5; eBioscience). Staining for CDH11 was performed in a 2-step process with an unconjugated primary antibody (1:100; clone 23C6; from M. Brenner [Division of Rheumatology, Immunology, Allergy, Brigham and Women's Hospital and Harvard Medical School, Boston, Massachusetts, USA] [ref. 51]), followed by a PE secondary antibody (1:100; PE clone; RMG1-1; BioLegend). Using this strategy, we identified BMDCs (CD45⁺), CECs (CD45⁻CD11b⁻CD31⁺), and CMCs (CD45⁻CD11b⁻CD31⁻) — primarily myofibroblasts. Within the BMDC population, we gated for bone marrow-derived proangiogenic cells (CD45⁺CD11b⁻CD31⁺), myeloid lineage cells (CD45⁺CD11b⁺), and nonmyeloid lineage cells (CD45⁺CD11b⁻CD31⁻). Within the myeloid cell population, we identified various subpopulations, including neutrophils (CD45⁺CD11b⁺Gr-1/CD86^{hi}), eosinophils (CD45⁺CD11b⁺Gr-1/CD86^{lo}SSC^{hi}), monocytes (CD45⁺CD11b⁺Gr-1/CD86^{lo}SSC^{lo}), and macrophages (CD45⁺CD11b⁺Gr-1/CD86^{int}) (17). We further assessed macrophage polarization by gating for proinflammatory (M1-like) macrophages (CD45⁺CD11b⁺Gr-1/CD86^{int}CD206⁻) and proresolving (M2-like) macrophages (CD45⁺CD11b⁺Gr-1/CD86^{int}CD206⁺) (Supplemental Figure 1). The NLR was computed by dividing the number of positively identified neutrophils by the number of nonmyeloid BMDCs in each sample (27). Note that antibodies specific for CD45.1 (1:100; PE clone A20; BD Biosciences) and CD45.2 (1:100; FITC clone 104; BD Biosciences) were used for assessment of bone marrow engraftment efficiency (Supplemental Figure 6). More details about the gating strategy are presented in the Supplemental Methods (Supplemental Figures 1 and 2).

Histology. Following euthanasia, a subset of hearts was dissected into PBS, weighed (Supplemental Figure 10, A and B), and submerged briefly in a KCl solution to relax the CMs. Relaxed hearts were then bisected along the transverse plane (orthogonal to the long axis of the heart), embedded in OCT media, and frozen. Frozen blocks were cryosectioned into 10-µm sections, mounted onto glass slides, and stored at -20°C. Prior to staining with Masson's trichrome (MilliporeSigma) to identify regions of healthy myocardium (red/pink), collagen/ECM deposition (blue), and cell nuclei (black), slides were brought to room temperature, OCT media were dissolved in PBS, and sections were fixed in Bouin's solution. To quantify infarct morphology from Masson's trichrome-stained sections, a semiautomated image-processing pipeline was developed based on local ventricular thickness measurements and color segmentation (Supplemental Figure 9 and refs. 52, 53). Image quantification was performed on 3 sections per heart separated by at least 300 µm.

Immunohistochemistry. Frozen slides were brought to room temperature, OCT media were dissolved in PBS, and tissue sections were fixed in 4% paraformaldehyde with 0.3% Triton-X for 10 minutes followed by blocking in 1% BSA in PBS for 1 hour. Sections were then stained for αSMA (Cy3, c1A4; MilliporeSigma), CD31 (Alexa Fluor 594, c390; Biolegend), CD45 (FITC CD45.2; BD Pharmingen), or IL-6 (polyclonal ab6672; Abcam). Sections stained with nonconjugated antibodies were incubated at a 1:100 dilution in 1% BSA overnight at 4°C. Sections were then rinsed with PBS and incubated with fluorescently tagged secondary antibody (goat anti-rabbit Alexa Fluor 647, A27040; Thermo Fisher Scientific) for 1 hour at a 1:300 dilution in 1% BSA. Sections stained with directly conjugated antibodies were incubated at a 1:100 dilution in 1% BSA for 1 hour at room temperature. Stained slides were mounted in ProLong Gold with DAPI to visualize cell nuclei. Muscularized vessels smaller than approximately 100 µm in diameter and myofibroblasts (defined as αSMA⁺ cells not colocalized with endothelial cells) were manually counted, and IL-6 staining in the infarcted region was quantified by measuring the average fluorescent intensity within the infarct area (manually segmented in ImageJ [NIH]) and the myocardium as a whole (Supplemental Figure 15).

AFM. Infarct stiffness was quantified by AFM using the Biocatalyst AFM and the peak force quantitative nanomechanical mapping mode developed by Bruker. Tissue sections were brought to room temperature, and OCT media were dissolved in PBS and blocked in 10% FBS for 20 minutes prior to scanning with the AFM. All measurements were made in PBS and were acquired from at least 5 separate $10 \times 10 \mu\text{m}^2$ areas from a minimum of 2 different sections per mouse (Supplemental Figure 8).

Collagen gel contraction. CFs were diluted in a 1.28 mg/mL collagen solution derived from PureCol (Advanced Biomatrix) to a final concentration of 250,000 cells/mL and were poured into a Teflon ring in a suspension well. After polymerizing for 1 hour, DMEM supplemented with 10% FBS and 1% penicillin/strep was added to release the collagen gel. Images were acquired immediately after release and at multiple times over the next 48 hours. Gel contraction was assessed by measuring surface area using ImageJ. For comparison of IgG2a and SYN0012 treatments, antibody was added to the cell/gel mixture at a final concentration of 20 $\mu\text{g}/\text{ml}$ prior to pouring; media added to the well also contained 10 $\mu\text{g}/\text{ml}$ antibody (Supplemental Figure 11).

qPCR. Hearts from sham and MI animals were isolated under RNase-free conditions and immediately flash frozen. For isolation of mRNA and transcriptional analysis of specific profibrotic and inflammatory genes of interest, samples were subsequently thawed and lysed in TRIZOL with chloroform-induced phase separation according to the manufacturer's instructions. Similarly, cells from CF-macrophage cocultures were lysed in TRIZOL for isolation of mRNA (Figure 7, C–E, and Supplemental Figure 16). cDNA was synthesized using the Superscript IV kit (Invitrogen) using 500 ng mRNA. Real-time qPCR was used to amplify targets from the cDNA using SYBR green master mix (Bio-Rad) and specific primer sets of interest (Supplemental Table 1). The BIO-RAD CFX96 C1000 system was used to quantify gene transcription in each sample, relative to *Gapdh* (forward: ATGACAATGAATACGGCTACAG and reverse: TCTCTTGCTCAGTGCCTTG). For all in vivo transcription levels, after MI samples were normalized to the average of all 3 and 7 day sham values (Supplemental Figure 14).

Statistics. Data throughout the manuscript are presented as mean \pm SEM. Two-tailed Student's *t* tests were used to determine significant effects between 2 groups. One- or two-way ANOVAs and linear mixed-effects models with restricted maximum likelihood were used to determine statistical differences between different sample groups over multiple time points, with post hoc Holms-Sidak's tests used to account for multiple comparisons. An overall value of $P < 0.05$ was considered significant in all statistical comparisons. Specific details regarding statistical tests performed for each measured variable are outlined in the Supplemental Methods.

Study approval. All animal procedures were approved by the Institutional Animal Care and Use Committee at Vanderbilt University.

Author contributions

AKS designed experiments, performed antibody treatments, and processed qPCR, AFM, histology, immunostaining, and coculture data. MRB designed experiments, performed the flow cytometry experiments, refined the flow cytometry gating strategy, and developed the automated histological image processing codes. CRC designed experiments, collected echocardiography data from *Cdh11*-deficient animals, performed bone marrow transplantations, and performed flow cytometry experiments with antibody treatment. QZ performed MI surgeries. LHS, AKH, TLF, and HL participated in discussions regarding planning of experiments and provided expertise. SMM helped design the flow cytometry experiments and analysis. WDM designed experiments and supervised the study. AKS, MRB, and WDM wrote and revised the manuscript. All authors were involved in the analysis and interpretation of data and have read and approved the manuscript.

Acknowledgments

We thank the Vanderbilt Cardiovascular Physiology Core for performing echocardiographic assessments for this study. We thank Claire Lafferty and Joshua Bender for assisting in the collection of the AFM and histological data. We also thank Roche (Dominik Hartl and Uwe Junker, Roche Pharma Research and Early Development, Immunology, Inflammation and Infectious Diseases Discovery and Translational Area and the Cadherin-11 team, Roche Innovation Center Basel, Switzerland) for supplying the blocking antibody, SYN0012. This work was funded by the National Institutes of Health (HL135790, HL115103, HL146951, and HL007411), the National Science Foundation (1055384 and DGE-0909667), the American Heart Association (15PRE25710333), and the Leducq Foundation.

Address correspondence to: W. David Merryman, Room 9445D MRB4, 2213 Garland Avenue, Nashville, Tennessee 37212, USA. Phone: 615.322.7219; Email: david.merryman@vanderbilt.edu.

1. Benjamin EJ, et al. Heart Disease and Stroke Statistics-2018 Update: A Report From the American Heart Association. *Circulation*. 2018;137(12):e67–e492.
2. Dick SA, et al. Self-renewing resident cardiac macrophages limit adverse remodeling following myocardial infarction. *Nat Immunol*. 2019;20(1):29–39.
3. Boudoulas KD, Hatzopoulos AK. Cardiac repair and regeneration: the Rubik's cube of cell therapy for heart disease. *Dis Model Mech*. 2009;2(7-8):344–358.
4. Richardson WJ, Holmes JW. Why Is Infarct Expansion Such an Elusive Therapeutic Target? *J Cardiovasc Transl Res*. 2015;8(7):421–430.
5. Gombozhapova A, et al. Macrophage activation and polarization in post-infarction cardiac remodeling. *J Biomed Sci*. 2017;24(1):13.
6. Ikeuchi M, et al. Inhibition of TGF-beta signaling exacerbates early cardiac dysfunction but prevents late remodeling after infarction. *Cardiovasc Res*. 2004;64(3):526–535.
7. Fuchs M, et al. Role of interleukin-6 for LV remodeling and survival after experimental myocardial infarction. *FASEB J*. 2003;17(14):2118–2120.
8. Frangiannis NG. The inflammatory response in myocardial injury, repair, and remodelling. *Nat Rev Cardiol*. 2014;11(5):255–265.
9. Chang SK, et al. Cadherin-11 regulates fibroblast inflammation. *Proc Natl Acad Sci USA*. 2011;108(20):8402–8407.
10. Schneider DJ, et al. Cadherin-11 contributes to pulmonary fibrosis: potential role in TGF- β production and epithelial to mesenchymal transition. *FASEB J*. 2012;26(2):503–512.
11. Clark CR, Bowler MA, Snider JC, Merryman WD. Targeting Cadherin-11 Prevents Notch1-Mediated Calcific Aortic Valve Disease. *Circulation*. 2017;135(24):2448–2450.
12. Lee YC, et al. Inhibition of cell adhesion by a cadherin-11 antibody thwarts bone metastasis. *Mol Cancer Res*. 2013;11(11):1401–1411.
13. Cadherin-11 expression is upregulated in invasive human breast cancer. *Oncol Lett*. 2016;12(6):4393–4398.
14. Thompson SA, et al. Acute slowing of cardiac conduction in response to myofibroblast coupling to cardiomyocytes through N-cadherin. *J Mol Cell Cardiol*. 2014;68:29–37.
15. Assefnia S, et al. Cadherin-11 in poor prognosis malignancies and rheumatoid arthritis: common target, common therapies. *Oncotarget*. 2014;5(6):1458–1474.
16. Hutcheson JD, et al. Cadherin-11 regulates cell-cell tension necessary for calcific nodule formation by valvular myofibroblasts. *Arterioscler Thromb Vasc Biol*. 2013;33(1):114–120.
17. Rose S, Misharin A, Perlman H. A novel Ly6C/Ly6G-based strategy to analyze the mouse splenic myeloid compartment. *Cytometry A*. 2012;81(4):343–350.
18. Ma F, et al. Macrophage-stimulated cardiac fibroblast production of IL-6 is essential for TGF β /Smad activation and cardiac fibrosis induced by angiotensin II. *PLoS ONE*. 2012;7(5):e35144.
19. Bowler MA, Bersi MR, Ryzhova LM, Jerrell RJ, Parekh A, Merryman WD. Cadherin-11 as a regulator of valve myofibroblast mechanobiology. *Am J Physiol Heart Circ Physiol*. 2018;315(6):H1614–H1626.
20. Lodyga M, et al. Cadherin-11-mediated adhesion of macrophages to myofibroblasts establishes a profibrotic niche of active TGF- β . *Sci Signal*. 2019;12(564):eaao3469.
21. Protti A, et al. Bone marrow transplantation modulates tissue macrophage phenotype and enhances cardiac recovery after subsequent acute myocardial infarction. *J Mol Cell Cardiol*. 2016;90:120–128.
22. Horikawa K, Radice G, Takeichi M, Chisaka O. Adhesive subdivisions intrinsic to the epithelial somites. *Dev Biol*. 1999;215(2):182–189.
23. Row S, Liu Y, Alimperti S, Agarwal SK, Andreadis ST. Cadherin-11 is a novel regulator of extracellular matrix synthesis and tissue mechanics. *J Cell Sci*. 2016;129(15):2950–2961.
24. Gao E, et al. A novel and efficient model of coronary artery ligation and myocardial infarction in the mouse. *Circ Res*. 2010;107(12):1445–1453.
25. Kubota A, Suto A, Suzuki K, Kobayashi Y, Nakajima H. Matrix metalloproteinase-12 produced by Ly6C^{low} macrophages prolongs the survival after myocardial infarction by preventing neutrophil influx. *J Mol Cell Cardiol*. 2019;131:41–52.
26. Horckmans M, et al. Neutrophils orchestrate post-myocardial infarction healing by polarizing macrophages towards a reparative phenotype. *Eur Heart J*. 2017;38(3):187–197.
27. Chen C, et al. Neutrophil to lymphocyte ratio as a predictor of myocardial damage and cardiac dysfunction in acute coronary syndrome patients. *Integr Med Res*. 2018;7(2):192–199.
28. To S, Agarwal SK. Macrophages and the regulation of pulmonary fibrosis by Cadherin-11. *J Immunol*. 2018;200(Suppl 1):49.14.
29. Zhang C, Li Y, Wu Y, Wang L, Wang X, Du J. Interleukin-6/signal transducer and activator of transcription 3 (STAT3) pathway is essential for macrophage infiltration and myoblast proliferation during muscle regeneration. *J Biol Chem*. 2013;288(3):1489–1499.
30. Fernando MR, Reyes JL, Iannuzzi J, Leung G, McKay DM. The pro-inflammatory cytokine, interleukin-6, enhances the polarization of alternatively activated macrophages. *PLoS ONE*. 2014;9(4):e94188.
31. Meléndez GC, McLarty JL, Levick SP, Du Y, Janicki JS, Brower GL. Interleukin 6 mediates myocardial fibrosis, concentric hypertrophy, and diastolic dysfunction in rats. *Hypertension*. 2010;56(2):225–231.
32. Müller J, et al. Interleukin-6-dependent phenotypic modulation of cardiac fibroblasts after acute myocardial infarction. *Basic Res Cardiol*. 2014;109(6):440.
33. Huang M, Yang D, Xiang M, Wang J. Role of interleukin-6 in regulation of immune responses to remodeling after myocardial infarction. *Heart Fail Rev*. 2015;20(1):25–38.
34. Mayfield AE, et al. Interleukin-6 Mediates Post-Infarct Repair by Cardiac Explant-Derived Stem Cells. *Theranostics*. 2017;7(19):4850–4861.

35. Chen B, Frangogiannis NG. Macrophages in the Remodeling Failing Heart. *Circ Res*. 2016;119(7):776–778.
36. Frangogiannis NG. Emerging roles for macrophages in cardiac injury: cytoprotection, repair, and regeneration. *J Clin Invest*. 2015;125(8):2927–2930.
37. Ma Y, Mouton AJ, Lindsey ML. Cardiac macrophage biology in the steady-state heart, the aging heart, and following myocardial infarction. *Transl Res*. 2018;191:15–28.
38. Bajpai G, et al. The human heart contains distinct macrophage subsets with divergent origins and functions. *Nat Med*. 2018;24(8):1234–1245.
39. Shiraishi M, et al. Alternatively activated macrophages determine repair of the infarcted adult murine heart. *J Clin Invest*. 2016;126(6):2151–2166.
40. Nah DY, Rhee MY. The inflammatory response and cardiac repair after myocardial infarction. *Korean Circ J*. 2009;39(10):393–398.
41. Frantz S, et al. Transforming growth factor beta inhibition increases mortality and left ventricular dilatation after myocardial infarction. *Basic Res Cardiol*. 2008;103(5):485–492.
42. Paik DT, et al. Wnt10b Gain-of-Function Improves Cardiac Repair by Arteriole Formation and Attenuation of Fibrosis. *Circ Res*. 2015;117(9):804–816.
43. Virag JA, Rolle ML, Reece J, Hardouin S, Feigl EO, Murry CE. Fibroblast growth factor-2 regulates myocardial infarct repair: effects on cell proliferation, scar contraction, and ventricular function. *Am J Pathol*. 2007;171(5):1431–1440.
44. Yang Y, et al. Modified VEGF targets the ischemic myocardium and promotes functional recovery after myocardial infarction. *J Control Release*. 2015;213:27–35.
45. Carlsson L, et al. Biocompatible, Purified *VEGF-A* mRNA Improves Cardiac Function after Intracardiac Injection 1 Week Post-myocardial Infarction in Swine. *Mol Ther Methods Clin Dev*. 2018;9:330–346.
46. Zhao T, Zhao W, Chen Y, Ahokas RA, Sun Y. Vascular endothelial growth factor (VEGF)-A: role on cardiac angiogenesis following myocardial infarction. *Microvasc Res*. 2010;80(2):188–194.
47. Orlandini M, Oliviero S. In fibroblasts Vegf-D expression is induced by cell-cell contact mediated by cadherin-11. *J Biol Chem*. 2001;276(9):6576–6581.
48. Aisagbonhi O, Rai M, Ryzhov S, Atria N, Feoktistov I, Hatzopoulos AK. Experimental myocardial infarction triggers canonical Wnt signaling and endothelial-to-mesenchymal transition. *Dis Model Mech*. 2011;4(4):469–483.
49. O’Connell TD, Rodrigo MC, Simpson PC. Isolation and Culture of Adult Mouse Cardiac Myocytes. In: Vivanco F, ed. *Cardiovascular Proteomics*. Clifton, New Jersey: Humana Press; 2007: 271–96.
50. Zhang X, Goncalves R, Mosser DM. The isolation and characterization of murine macrophages. *Curr Protoc Immunol*. 2008;Chapter 14:Unit 14.1.
51. Chang SK, et al. Stromal cell cadherin-11 regulates adipose tissue inflammation and diabetes. *J Clin Invest*. 2017;127(9):3300–3312.
52. Yezzi AJ, Prince JL. An Eulerian PDE approach for computing tissue thickness. *IEEE Trans Med Imaging*. 2003;22(10):1332–1339.
53. Bersi MR, Khosravi R, Wujciak AJ, Harrison DG, Humphrey JD. Differential cell-matrix mechanoadaptations and inflammation drive regional propensities to aortic fibrosis, aneurysm or dissection in hypertension. *J R Soc Interface*. 2017;14(136):20170327.

Minireview

Bone morphogenetic protein signaling in inflammation

David H Wu  and Antonis K Hatzopoulos

Division of Cardiovascular Medicine, Department of Medicine and Department of Cell & Developmental Biology, Vanderbilt University Medical Center, Nashville, TN 37232, USA

Corresponding author: Antonis K Hatzopoulos. Email: antonis.hatzopoulos@vumc.org

Impact statement

By compiling findings from recent studies, this review will garner novel insight on the dynamic and complex role of BMP signaling in diseases of inflammation, highlighting the specific roles played by both individual ligands and endogenous antagonists. Ultimately, this summary will help inform the high therapeutic value of targeting this pathway for modulating diseases of inflammation.

Abstract

Bone morphogenetic protein signaling has long been established as a crucial pathway during embryonic development. In recent years, our knowledge of the function of bone morphogenetic protein signaling has expanded dramatically beyond solely its important role in development. Today, the pathway is known to have important homeostatic functions across multiple different tissues in the adult. Even more importantly, bone morphogenetic protein signaling is now known to function as a driver of diseases in the adult spanning different organ systems. In this review, we will explore the functions of bone morphogenetic protein signaling in diseases of inflammation. Through this exploration, we will highlight the

value and challenges in targeting bone morphogenetic protein signaling for therapeutic interventions.

Keywords: Atherosclerosis, myocardial infarction, vascular inflammation, anemia of inflammation, endothelial injury, inflammatory arthritis

Experimental Biology and Medicine 2019; 244: 147–156. DOI: 10.1177/1535370219828694

Introduction

Bone morphogenetic protein (BMP) ligands are part of the transforming growth factor- β (TGF- β) superfamily. As their name suggests, BMPs were first observed in the pioneering work by Urist¹ in 1965 where their activity was found to induce ectopic bone formation. Although later Urist was able to isolate the bone inducing proteins,² it was not until two decades later that these proteins were individually cloned and characterized.³ Since then, BMPs have been studied extensively outside of their established role in bone and cartilage and found to possess a multitude of functions in the embryonic development of other organ systems, including blood, heart, vasculature, brain, lung, kidney, and limbs. This review will focus on the emerging role BMPs play in inflammatory processes across organ systems in the adult.

Signaling and regulatory components in the BMP pathway

Subclassification of the more than 15 known BMPs based on phylogenetic analysis of amino acid and nucleotide

similarity creates particular subgroups of these ligands: BMP2/4, BMP5/6/7/8, BMP9/10, and BMP12/13/14.⁴ It is important to note that BMP1 does not function like the rest of the BMP family. Although able to induce bone and cartilage development, BMP1 is not part of the TGF- β superfamily of proteins. Instead, it is a procollagen C-proteinase that functions in collagen maturation.⁵ The rest of the BMP family of proteins function as signaling ligands that bind to target receptors on the cell surface.

Before being secreted into the extracellular space where they become active, BMPs are first synthesized as precursor proteins in the cytoplasm. These pre-pro-peptides consist of an N-terminal signal peptide that is required for secretion, a prodomain that plays an important regulatory role for the folding of the active protein, and a C-terminal part that contains the mature peptide that is capable of binding to and activating its receptors.⁶ BMP precursors form dimers in the cytoplasm that are subsequently cleaved by convertases to generate the mature BMP ligand that is being secreted into the extracellular space.

Once secreted, BMP ligands bind to their receptors on the surface of target cells to form a heterotetrameric complex

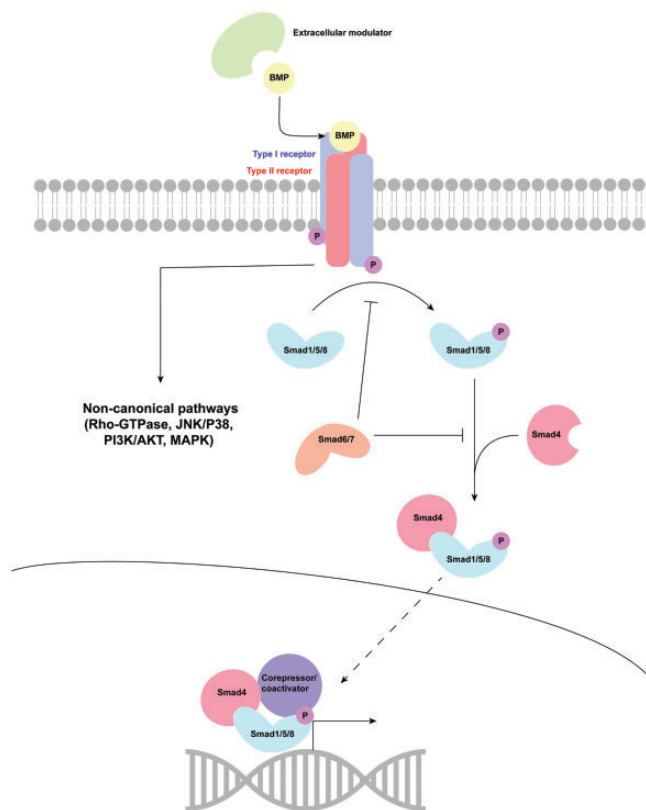


Figure 1. BMP signal transduction. Bone morphogenetic proteins transduce signals in target cells by binding to a heterotetrameric complex composed of two dimers of type I and type II receptors. This allows the constitutively active type II receptor to transphosphorylate the type I receptor, causing conformational changes that lead to activation of both canonical pathways and non-canonical pathways like the Rho-GTPase, JNK/P38, PI3K/AKT, and MAPK pathways. Through the canonical pathway, ligand-receptor complex formation leads to phosphorylation of R-Smads (Smad1/5/8), which are then able to form complexes with co-Smads (Smad4). Together, the complex translocates into the nucleus where it associates with coactivators and corepressors to regulate gene expression. BMP ligands can be regulated both by extracellular modulators including protein antagonists and by intracellular modulators like inhibitory Smads (Smad6/7). Adapted from Wang et al.⁴⁵

consisting of two dimers of type I and type II receptors⁷ (Figure 1). This complex formation allows the constitutively active type II receptor to transphosphorylate the type I receptor, and activation of the type I receptor causes conformational changes that lead to phosphorylation of downstream proteins known as R-Smads (Smad1, Smad5, and Smad8). Activated, phosphorylated R-Smads in the cytoplasm subsequently form complexes with co-Smad (Smad4), and together, they translocate into the nucleus where they associate with coactivators and corepressors to regulate gene expression.⁷ In addition to this so-called canonical signaling pathway, noncanonical BMP signaling pathways that are independent of Smads have also been identified. These include the Rho-GTPase, JNK/P38, and PI3K/AKT pathways in addition to various branches of the MAPK pathway.^{8–10}

In addition to the diversity present in downstream signaling pathways, there also exists diversity within the interactions between BMP ligands and the membrane-bound BMP receptors. Both ligand-independent

homodimerization and ligand-dependent heterodimerization of BMP type I receptors with effective signal transduction have been observed with certain type I receptor isoforms.¹¹ Moreover, certain heterodimeric complexes can only be assembled through binding with a specific BMP heterodimeric ligand.¹² Such complexities allow for an additional layer of signal regulation and coordination.

Adding to this complexity, BMP signaling is regulated by both intracellular and extracellular modulators. Extracellularly, BMP ligands are inhibited by proteins like Chordin, Noggin, and the Cerberus and Dan family of proteins, a protein family that includes Gremlin 2 (Grem2). While both Noggin and Grem2 possess a cysteine knot motif and form dimers,^{13,14} their structure and the way they inhibit BMP ligands are very different. Noggin forms a head-to-head dimer that creates a clamp-like structure to bind to BMP dimers, inhibiting ligand activity by effectively masking the type I and type II receptor binding surfaces.¹⁴ Grem2 forms a head-to-tail dimer,^{13,15} and along its convex surface, one Grem2 monomer binds to a single monomer of the BMP dimer complex, where it interferes with the type II, but not the type I, receptor binding surface.¹⁶ The other monomer of the Grem2 dimer is free to interact with another BMP dimer complex, and this second BMP dimer can then interact with another Grem2 dimer, creating a so-called “daisy chain” reaction. Grem2 demonstrates both a strong and broad inhibition of BMP ligands¹⁷ and a strong specificity for the BMP subfamily of ligands within the TGF- β superfamily.¹⁵

Intracellularly, BMP signaling is regulated by a variety of mechanisms. Specific miRNAs can regulate expression of various components of the BMP signaling pathway,⁷ whereas specific intracellular phosphatases like protein phosphatase 1 can dephosphorylate both phosphorylated R-Smads and phosphorylated type I receptors.^{18,19} Moreover, a class of inhibitory Smads or I-Smad (Smad6 and Smad7) play an important role in negative feedback inhibition of BMP signaling.²⁰ The complexity stemming from the many downstream signal transducers, both canonical and noncanonical, and the multiple layers of regulation allow BMP signaling to coordinate and precisely modulate a wide range of biological processes.

BMP signaling is crucial for development

Since their initial discovery, BMPs have been extensively studied in embryonic development utilizing primarily mouse, zebrafish, and frog models. Such studies have found that BMP signaling is indispensable for numerous developmental processes. Deletion of BMP2, BMP4, or BMP10 is embryonically lethal,^{21–23} and loss of BMP7 or BMP11 results in death shortly after birth.^{24,25} Similarly, deletion of BMP-responsive receptors, BMPRI-A, ActR1A, and BMPRII^{26–28} or knocking out of downstream transducers like Smad1, Smad5, Smad4, and the inhibitory Smad7 are also embryonically lethal.^{29–32}

In particular, BMP4 is critical during early gastrulation as its function is required for the differentiation and formation of the mesoderm,^{22,33} from which arises a number of tissues and cell types, including vascular, cardiac, skeletal,

and smooth muscles, and definitive hematopoietic stem cells (HSCs) – cells that will continue to supply blood cells into adulthood. Moreover, BMP4 is important to the function of the HSC microenvironment with deficiencies leading to reductions in both HSC function and numbers.³⁴

BMP2 is necessary for further mesoderm development and is important for the proper development of the heart and the amnion and chorion.²¹ In the heart, BMP2 is critical for endocardial cushion formation, development of the valves, and myocardial patterning,^{35,36} whereas BMP10 is essential for cardiac growth and chamber maturation.²³ BMP signaling is also important for controlling the differentiation of cardiac progenitor cells into cardiomyocytes.^{37,38} At the early stages of embryonic development, BMP signaling is critical to the proper generation of left/right axis patterning, affecting tissues including the developing heart.^{39–42} Moreover, in the central nervous system, BMP signaling is important for directing neuronal differentiation and autoregulation of neurogenesis.^{43,44} These and other studies have revealed the essential role BMPs play in normal development in these and many other biological systems, including reproductive and endocrine organs.⁴⁵

Similarly, BMP antagonists also play important roles during embryonic development. In mice, Chordin is crucial for neural induction,⁴⁶ and both Noggin and Chordin have important but overlapping roles in development of the forebrain and left-right axis patterning of the developing embryo.⁴⁷ Additionally, Noggin is necessary for the development of the axial skeleton in mice.⁴⁸ Deleting Chordin leads to stillborn mice, while Noggin knockout mice die at birth.^{47,48} In contrast, Grem2 is required for atrial development and cardiac laterality in zebrafish,⁴⁹ but it appears to be dispensable for mouse development.⁵⁰

BMP signaling in inflammatory processes

Developmental studies in genetic models have cemented the critical roles of BMP signaling throughout embryogenesis. More recent studies have investigated the role of BMP signaling in adult pathophysiological conditions, revealing a broad influence on homeostasis and disease states such as pulmonary hypertension, cancer, and anemia.^{51,52} Recent discussions about BMP involvement in other diseases have been reviewed elsewhere.^{45,53,54} Here, we will focus on the emerging roles of BMPs as key mediators of a variety of inflammatory conditions.

BMP signaling promotes the inflammatory phenotype of endothelial cells in atherosclerosis

Atherosclerosis has long been viewed as an inflammatory disease.^{55–57} Plaque formation begins with initial endothelial dysfunction that leads to accumulation of lipids in arterial intima and infiltration of immune cells. Markers of dysfunction include upregulation of cell surface molecules such as E-selectin, VCAM-1, and ICAM1, which play essential roles in the roll on, adhesion, and recruitment of immune cells.

Typically, inflammatory cytokines such as TNF- α and IL-1 induce cell adhesion receptors in endothelial cells, but they also induce expression of BMP ligands in endothelial

cells.⁵⁸ Many studies have pointed out that BMPs further promote the inflammatory phenotype of endothelial cells. In particular, BMP4 is selectively expressed in endothelial cells of atherosclerotic lesions in human coronary arteries.⁵⁹ Moreover, BMP4 is upregulated in endothelial cells in response to shear stress and increases endothelial expression of membrane adhesion molecules, leading to enhanced leukocyte adhesion.^{59,60} Likewise, BMP2 also upregulates expression of adhesion molecules and promotes leukocyte adhesion.^{50,61} Some of these pro-inflammatory effects may be further accentuated in diabetes,⁵⁸ a known risk factor for atherosclerosis. In addition to enhancing adhesion of inflammatory cells, BMP2 also induces chemotaxis of monocytes, key immune cells implicated in the pathogenesis of atherosclerotic plaques, and impairs their differentiation into anti-inflammatory M2 macrophages.⁶² The recruitment of these pathogenic inflammatory cells is further enhanced through BMP-mediated impairment of endothelial barrier function.⁶³

Consequently, inhibiting BMP signaling with extracellular protein inhibitors such as the BMP-binding endothelial regulator protein BMPER and Noggin, or with small molecule chemical inhibitors such as DMH1 suppresses vascular inflammation and lessens recruitment of leukocytes.^{63–67} Taken together, these studies suggest that BMP signaling promotes vascular inflammation through direct effects on the endothelium and infiltrating leukocytes and that blocking BMP signaling attenuates the inflammatory response. Thus, BMPs and downstream effectors of BMP ligands may be attractive therapeutic targets for managing inflammatory vessel diseases including atherosclerosis.

BMP signaling in vascular calcification

A clinically relevant consequence of chronic inflammation in atherosclerosis is vascular calcification. This results from a highly regulated process where non-osteoblastic cells, including vascular smooth muscle cells (VSMCs) and pericytes, differentiate into osteoblast-like cells that mineralize the vascular matrix in the tunica media through abnormal deposition of calcium phosphate.⁶⁸ Highlighting the similarities between calcification and bone formation, recent evidence suggests an important role for BMP signaling in this pathological process.

VSMCs typically exist in the tunica media as quiescent, differentiated cells, and function to maintain vascular tone through their contractile abilities. However, they are also able to enter a synthetic state characterized by proliferation and production of extracellular matrix,⁶⁹ and such a transition is accompanied by loss of cell markers associated with contractility.⁷⁰ Expressed in calcified human atherosclerotic plaques,⁷¹ BMP2 inhibits proliferation in VSMCs^{72,73} and induces loss of contractility markers once growth arrest has been established.⁷⁴

This suggests either a role for BMP2 in VSMCs that is dependent on proliferation status or one that facilitates along a continuum in promoting the transdifferentiation process. Moreover, BMP2 also induces expression of genes in VSMCs that are crucial for osteogenic differentiation and bone formation, including Msx-2 and Runx2.^{75–78}

Deficiency in these genes leads to defects in osteoblast differentiation and large defects in both endochondral and intramembranous ossification.^{77,79,80} Recent studies confirm the role of Runx2 and Msx-2 in the osteogenic conversion of VSMCs.^{77,81} These studies highlight the molecular similarities between the processes of vascular calcification and bone formation, and taken together, strongly posit a role for BMP signaling in vascular calcification. Moreover, studies have shown that BMP inhibition can also attenuate vascular calcification.^{67,82-84}

BMP signaling in tissue fibrosis

Another consequence of chronic vascular inflammation involves induction of processes leading to extracellular matrix (ECM) protein deposition in the adjacent tissue. Under normal conditions, this process functions to repair and preserve tissue architecture and functional integrity after injury. However, pathological dysregulation of inflammation can lead to excessive deposition and an aberrant process of tissue fibrosis that impairs normal organ function. A myriad of profibrotic cytokines released by infiltrating leukocytes act to directly activate fibroblasts, upregulate production of the fibrogenic cytokine TGF- β , increase ECM protein synthesis, and reduce degradation of matrix proteins through downregulating expression of matrix metalloproteinases.^{85,86}

Because of this intimate relationship between inflammation and fibrosis, canonical BMP signaling may initially play an indirect positive role through promoting the recruitment of infiltrating leukocytes by endothelial cells into the tissue and thus enhancing the magnitude of the profibrotic signal elicited by these cells. Interestingly, within the tissue itself however, BMP7, through a Smad-dependent antagonism of downstream TGF- β signaling,⁸⁷ exerts anti-fibrotic effects. While BMP7 is downregulated in pathological fibrosis of organs, its exogenous administration or overexpression is both anti-fibrotic and functionally protective in disease models of chronic kidney disease,⁸⁸⁻⁹⁴ liver fibrosis,⁹⁵ and pulmonary fibrosis.^{87,96-98} The differential roles of BMP signaling in tissue fibrosis, from enhancement at the endothelial level through leukocyte recruitment to regulation at the interstitial tissue level through antagonism of TGF- β signaling, reflect not only the specialized roles served by individual BMP ligands, but also points to a built-in regulatory element that modulates the overall effects of BMP signaling in promoting tissue fibrosis through inflammation.

BMP signaling in endothelial to mesenchymal transition

In addition to these molecular processes, endothelial to mesenchymal transition (EndMT) is a cellular process activated in response to inflammation that significantly contributes to the resulting consequences of vascular calcification and tissue fibrosis. In response to inflammatory cytokines, endothelial cells undergo a phenotypic conversion from a differentiated endothelial cell state to a more undifferentiated mesenchymal fibroblast-like cell state. During this process, these cells lose cell-to-cell adhesions and endothelial markers like CD31 and gain mesenchymal

characteristics, including ECM protein production and markers like α -smooth muscle actin and fibroblast specific protein 1.^{99,100} The resulting multipotent mesenchymal cell is able to differentiate and contribute to multiple different cell types to serve needed functions. Under pathological conditions, it can contribute to the fibroblast population within the tissue to help promote fibrosis in circumstances such as after acute or chronic injury,¹⁰¹⁻¹⁰⁴ or it can also contribute to an osteoprogenitor cell population that underly the pathophysiology of vascular calcification.¹⁰⁵

The process of EndMT in the adult is well known to be activated by TGF- β signaling,⁹⁹⁻¹⁰³ while signaling through the BMP subfamily of ligands, in particular BMP2 and BMP4, is well known to induce EndMT during embryonic development.^{35,106} In the adult, these ligands likely function similarly to promote this developmentally active programming. This is supported by *in vitro* evidence demonstrating treatment of cultured endothelial cells with either BMP4 or TGF- β 2 induced acquisition of mesenchymal stem cell-like features.¹⁰⁷ Moreover, inhibition of canonical BMP signaling by DMH1 a dorsomorphin analogue which specifically inhibits activation of Smad1/5/8,^{108,109} also inhibits EndMT *in vitro*. In addition, BMP6 has also been shown to pathologically promote EndMT in a disease model of cerebral cavernous malformation both *in vitro* and *in vivo*.¹¹⁰ Interestingly, BMP7 inhibits EndMT both *in vitro* and *in vivo*.^{104,111} The discrepancy can be explained by the observation that an interaction between activated Alk2 and activated Alk5 BMP receptors is necessary for EndMT.¹⁰⁷ Administration of either TGF- β 2 or BMP4 activates both receptors to allow an interaction, whereas BMP7 solely activates Alk2, preventing the necessary Alk2-Alk5 interaction. Taken together, these findings demonstrate the important and complex role BMP signaling plays in endothelial function and disease pathology beyond the initial inflammatory response.

BMP signaling regulates the inflammatory response following cardiac ischemic injury

Inflammation is a critical component of tissue repair following acute or during chronic tissue injury. For example in the heart, the systemic inflammatory response following myocardial infarction (MI) allows infiltration of immune cells into the heart to help clear cellular debris, and this acute process is essential to proper tissue healing and repair.¹¹²⁻¹¹⁶ Our group and others have measured BMP expression in the heart and found that BMP2 is upregulated following MI in mice.^{50,117} Our results show that BMP2 is transiently induced during the inflammatory phase and promotes a pro-inflammatory phenotype in endothelial cells⁵⁰ (Figure 2). This upregulates expression of adhesion molecules and increases the number of infiltrating inflammatory cells in the heart. Moreover, we found that the acute inflammatory cytokine TNF- α upregulates BMP2 expression endothelial cells and the two work synergistically to promote the inflammatory phenotype in endothelial cells.

BMP2 also upregulates the expression of its own antagonist Grem2 (Figure 2), and consequently, Grem2 expression, but not expression of other BMP antagonists, follows

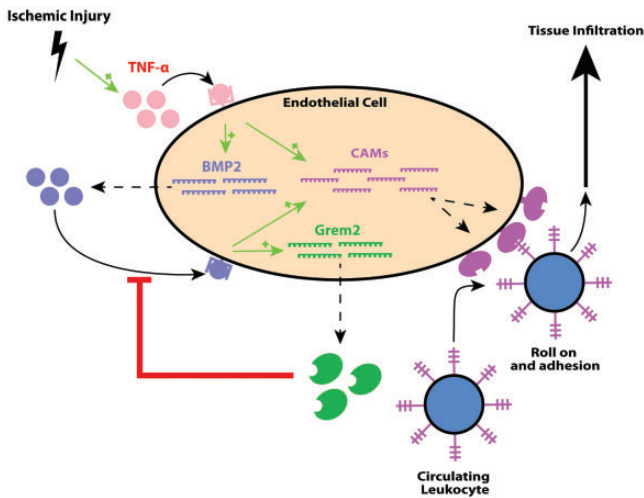


Figure 2. BMP signaling regulates the endothelial inflammatory response after ischemic injury. Ischemic injury induces local TNF- α production which promotes expression of BMP2 in endothelial cells. The two signaling proteins upregulate expression of cell adhesion molecules (CAMs), which enhances recruitment and infiltration of circulating leukocytes into the tissue. BMP2 also induces expression of its antagonist Grem2, creating a negative regulatory loop that regulates BMP activity to limit tissue inflammation.

the increasing levels of BMP2 following MI. This temporal coordination of BMP regulation is important in modulating tissue inflammation as shown by gain or loss of Grem2 function in mice. Specifically, loss of Grem2 function by homologous recombination promoted pro-inflammatory changes in endothelial cells and led to both greater levels of infiltrating inflammatory cells in the heart and worsened functional outcomes following MI.⁵⁰ Administering DMH1 rescued this pro-inflammatory phenotype. Moreover, cardiac-specific overexpression of Grem2 limited tissue inflammation and improved functional recovery.⁵⁰ These findings build upon earlier studies demonstrating the role BMPs have in promoting vascular inflammation through eliciting changes in endothelial cells that promote leukocyte recruitment. In addition, they introduce endogenous regulatory mechanisms highlighting the crucial role of endogenous BMP antagonists in limiting inflammation and the therapeutic value of regulating BMP signaling.

BMP signaling in chronic inflammatory arthritis

At the intersection of bone pathology and inflammation, studies of rheumatoid arthritis (RA) and ankylosing spondylitis (AS) offer unique opportunities to explore the role of BMPs in inflammatory processes related to a system in which they already have an established presence. The pathogenesis of both diseases involves immune-mediated inflammatory processes. RA is characterized by synovial inflammation, progressive joint damage, and bone loss, while AS is characterized by chronic enthesitis, initial bone destruction, and aberrant bone repair leading to spinal fusion and dysfunction.

BMP signaling appears to be beneficial in RA but not in AS. BMP2 and BMP6 are expressed in synovium from RA patients, and expression in patient-derived fibroblast-like synoviocytes *in vitro* becomes strongly up-regulated in

response to pro-inflammatory cytokines IL-1 β , TNF- α , or IL-17.^{118,119} However, BMP4 expression in synoviocytes decreases in response to TNF- α ,¹¹⁸ aligning with clinical studies observing lower BMP4 mRNA levels in the synovium of RA patients relative to controls.¹²⁰

The pro-inflammatory cytokines IL-17 and TNF- α induce a pro-inflammatory phenotype within synoviocytes marked by increased expression of pro-inflammatory cytokines IL-6 and GM-CSF, increased expression of the chemokine IL-8, and increased production of metalloproteinases MMP2 and MMP3. Expression and activity of these products are strongly implicated in the pathogenesis of RA.^{121,122} Blocking BMP signaling with the canonical BMP inhibitor DMH-1 further augments this response and potentiates the induction of the pro-inflammatory phenotype in synoviocytes.¹¹⁸ On the contrary, inducing BMP signaling with exogenous BMP6 reduced the expression of these products and interfered with the induction of a pro-inflammatory phenotype in synoviocytes.

In an *in vivo* model of AS, however, blocking BMP signaling through systemic gene transfer of the BMP antagonist Noggin slowed the initiation and progression of disease through regulating pathological bone remodeling.¹²³ The discrepancy in the role of BMP between these two disease states warrants further exploration and may be explained by the inherent differences between the disease pathophysiology of RA and that of AS. Moreover, it is likely that outcomes depend on cellular context, antagonistic effects of specific BMP subgroups such as BMP2/4 against BMP6/7, or differential activation of canonical versus non-canonical BMP signaling pathways. Nonetheless, these studies suggest not only an important role for BMP in well-recognized inflammatory diseases, but also in regulating inflammatory processes that drive disease.

BMP signaling in anemia of inflammation

Regulation of circulating iron is coordinated by several key proteins. As the sole exporter of intracellular iron, ferroportin functions to release intracellular iron in intestinal epithelial cells, hepatocytes, and macrophages into the circulation. An excess in circulating iron stimulates the expression of hepcidin in the liver, and releasing the protein into the circulation allows it to bind ferroportin to induce its internalization and degradation.¹²⁴ Likewise, a deficiency in iron also suppresses hepcidin expression. This negative feedback control allows for appropriate circulating iron stores, and perturbations to this system can have clinical consequences. Inflammatory cytokines such as IL-6 that are generated by a variety of diseases, including infection or autoimmune disorders, induce the hepatic expression of hepcidin, and the resulting reduction in circulating iron leads to anemia.¹²⁵

Induction of hepcidin in response to inflammatory stimuli and, thus, iron levels is dependent on BMP signaling. During homeostasis, BMP6 is the predominant BMP ligand that functions in iron homeostasis and transduces its signal through the BMP coreceptor, hemojuvelin.^{124,126,127} Expression of BMP6 in the liver is regulated by serum iron levels reflecting dietary intake,¹²⁸ and deficiency in

BMP6 leads to hepcidin deficiency and subsequent iron overload in tissues and organs.¹²⁹ It appears that other BMP ligands are unable to compensate for loss of BMP6 *in vivo* despite their ability to induce hepcidin expression in hepatocytes *in vitro*.¹³⁰ BMP2, however, may at least play a partial redundant role in inducing hepcidin expression. Hepcidin induction by either acute or chronic iron loading does not require BMP2, although hepcidin induction in either scenario is submaximal and relatively blunted.¹³¹ On the other hand, intact BMP6 function is absolutely critical to hepcidin induction by acute iron loading. Additionally, inhibition of BMP6 but not BMP2/4 significantly decreases hepcidin levels and increases serum iron.¹²⁶ Moreover, BMP2 appears to be able to induce hepcidin expression independent of hemojuvelin, though at a lower efficiency.¹²⁴

At the receptor level, the BMP type II receptors ActR2a and BMPR2 perform redundant roles in transducing signals to induce hepcidin expression. Deficiency in both receptors is required to reduce levels of hepcidin *in vivo* and is necessary to reduce BMP6-mediated induction of hepcidin expression as well as basal levels of hepcidin expression *in vitro*.¹³² In addition, both of the BMP type I receptors Alk2 and Alk3 are individually necessary for hepcidin induction by BMP2 stimulation in culture and also for hepcidin induction by iron challenge *in vivo*.¹³³ However, when compared to a liver-specific deletion of Alk2, liver-specific deletion of Alk3 results in a much more severe iron overload phenotype and near abolishment of both basal BMP signaling and hepcidin expression. This suggests differential functions of these receptors with Alk3 individually promoting basal levels of BMP signaling and hepcidin expression, and Alk2 being a necessary component in addition to Alk3 only in the context of promoting hepcidin expression in response to BMP signal transduction and iron. This may be the result of the unique ability of Alk3 receptors to homodimerize and transduce signals for inducing hepcidin expression in the absence of ligand binding.¹¹ Downstream, Smad4 is also required for mediating hepcidin expression.¹³⁴

The important roles of these BMP signaling mediators during homeostasis are also evident in response to inflammatory stimuli. Deficiencies in either BMP6 or hemojuvelin, and not in BMP2,¹³¹ lead to impaired induction of hepcidin and hypoferrremia in response to inflammation compared to normal controls,^{124,129} but inflammatory induction of hepcidin persists in isolated or combinatory deficiencies of either when compared to baseline.¹³⁵ This suggests that inflammation may induce hepcidin through pathways independent of BMP signaling. Nonetheless, inhibiting BMP signaling with BMP antagonists or LDN-193189, an inhibitor of BMP type I receptor ameliorates anemia of inflammation and iron deficiency in mice.^{135,136} These findings are consistent with observations that hepatocyte-specific deletion of BMP type I receptor, Alk3, attenuates phenotype of anemia of inflammation in mice.¹³⁷ Taken together, these studies suggest a pivotal role for BMP6 as a regulator of circulating iron both in homeostasis and chronic inflammatory conditions that warrants therapeutic considerations.

Conclusion and future directions

In the recent decade, our understanding of the role of BMP signaling has expanded beyond its initially discovered role in the skeletal system and outside its prominent and crucial roles in development. It is now well-recognized that BMPs are essential to a plethora of different processes throughout the body in the adult both during homeostasis and in disease states. Components of BMP signaling are prominently emerging as direct coordinators of inflammatory processes across various cell types from immune cells to endothelial and connective tissue cells. As the general role of inflammation in disease continues to develop and the intersection between immunology and other medical fields continues to grow, defining the multifaceted roles of BMP signaling in inflammation will allow greater insight into the molecular mechanisms that drive disease.

Already, recent studies have uncovered insight into the nonredundant roles of both specific BMP ligands and BMP antagonists that possess context-specific functions such as BMP6 in the regulation of circulating iron in response to inflammation, BMP2 and BMP4 in mediating inflammatory phenotype of endothelium in response to stress or tissue injury, and Grem2 in limiting post-injury tissue inflammation. This likely reflects the functional heterogeneity that exists among BMP ligands and their antagonists. Thus, special precautions should be taken regarding designing interventions targeting BMP signaling as broad inhibition of all BMP ligands to limit endothelial or tissue inflammation may also perturb iron homeostasis. With the increasing availability of small molecule BMP inhibitors and a recent pre-clinical study successfully utilizing such a compound,¹³⁸ it may be worth considering their pharmaceutical value and position to be clinically approved in the future. However, before moving forward into clinical applications, it will be important to design compounds to control specificity for the regulation of only certain BMP ligands to maximize efficacy while minimizing adverse off-target consequences.

Authors' contributions: DHW worked closely with AKH to compile relevant and appropriate literature and to organize ideas and discussion points. DHW wrote the manuscript draft with important suggestions and edits from AKH. Both authors contributed to the final manuscript.

DECLARATION OF CONFLICTING INTERESTS

The author(s) declared no potential conflicts of interest with respect to the research, authorship, and/or publication of this article.

FUNDING

This work was supported by grants from NIH (R01HL138519 and R01GM114640) and the Department of Defense (W81XWH-16-1-0622) to AKH and the Medical Scientist Training Program T32GM007347 to DHW.

ORCID iD

David H Wu  <http://orcid.org/0000-0003-3452-0867>

REFERENCES

- Urist MR. Bone formation by autoinduction. *Science* 1965;**150**:893–9
- Urist MR, Mikulski A, Lietze A. Solubilized and insolubilized bone morphogenetic protein. *Proc Natl Acad Sci U S A* 1979;**76**:1828–32
- Wozney JM, Rosen V, Celeste AJ, Mitsock LM, Whitters MJ, Kriz RW, Hewick RM, Wang EA. Novel regulators of bone formation: molecular clones and activities. *Science* 1988;**242**:1528–34
- Salazar VS, Gamer LW, Rosen V. BMP signaling in skeletal development, disease and repair. *Nat Rev Endocrinol* 2016;**12**:203–21
- Kessler E, Takahara K, Biniaminov L, Brusel M. Bone morphogenetic protein-1: the type I procollagen c-proteinase. *Science* 1996;**271**:360–2
- Harrison CA, Al-Musawi SL, Walton KL. Prodomains regulate the synthesis, extracellular localisation and activity of TGF- β superfamily ligands. *Growth Factors* 2011;**29**:174–86
- Rahman MS, Akhtar N, Jamil HM, Banik RS, Asaduzzaman SM. TGF- β /BMP signaling and other molecular events: regulation of osteoblastogenesis and bone formation. *Bone Res* 2015;**3**:15005
- Yamaguchi K, Shirakabe K, Shibuya H, Irie K, Oishi I, Ueno N, Taniguchi T, Nishida E, Matsumoto K. Identification of a member of the MAPKKK family as a potential mediator of TGF-beta signal transduction. *Science* 1996;**270**:2008–11
- Derynck R, Zhang YE. Smad-dependent and Smad-independent pathways in TGF- β family signaling. *Nature* 2003;**425**:577–84
- Zhang YE. Non-Smad pathways in TGF- β signaling. *Cell Res* 2009;**19**:128–39
- Traeger L, Gallitz I, Sekhri R, Bäumer N, Kuhlmann T, Kemming C, Holtkamp M, Müller JC, Karst U, Canonne-Hergaux F, Muckenthaler MU, Bloch DB, Olschewski A, Bartnikas TB, Steinbicker AU. ALK3 undergoes ligand-independent homodimerization and BMP-induced heterodimerization with ALK2. *Free Radic Biol Med* 2018;**129**:127–37
- Little SC, Mullins MC. Bone morphogenetic protein heterodimers assemble heteromeric type I receptor complexes to pattern the dorso-ventral axis. *Nat Cell Biol* 2009;**11**:637–43
- Nolan K, Kattamuri C, Luedeke DM, Deng X, Jagpal A, Zhang F, Linhardt RJ, Kenny AP, Zorn AM, Thompson TB. Structure of protein related to Dan and Cerberus: insights into the mechanism of bone morphogenetic protein antagonism. *Structure* 2013;**21**:1417–29
- Groppe J, Greenwald J, Wiater E, Rodriguez-Leon J, Economides AN, Kwiatkowski W, Affolter M, Vale WW, Izpisua Belmonte JC, Choe S. Structural basis of BMP signaling inhibition by the cystine knot protein Noggin. *Nature* 2002;**420**:636–42
- Kattamuri C, Luedeke DM, Nolan K, Rankin SA, Greis KD, Zorn AM, Thompson TB. Members of the DAN family are BMP antagonists that form highly stable noncovalent dimers. *J Mol Biol* 2012;**424**:313–27
- Nolan K, Kattamuri C, Rankin SA, Read RJ, Zorn AM, Thompson TB. Structure of Gremlin-2 in fact complex with GDF5 gives insight into DAN-family-mediated BMP antagonism. *Cell Rep* 2016;**16**:2077–86
- Sudo S, Avsian-Kretschmer O, Wang LS, Hsueh AJW. Protein related to DAN and cerberus is a bone morphogenetic protein antagonist that participates in ovarian paracrine regulation. *J Biol Chem* 2004;**279**:23134–41
- Itoh S, ten Dijke P. Negative regulation of TGF- β receptor/Smad signal transduction. *Curr Opin Cell Biol* 2007;**19**:176–84
- Knockaert M, Sapkota G, Alarcón C, Massagué J, Brivanlou AH. Unique players in the BMP pathway: small C-terminal domain phosphatases dephosphorylate Smad1 to attenuate BMP signaling. *Proc Natl Acad Sci U S A* 2006;**103**:11940–5
- Heldin CH, Moustakas A. Role of Smads in TGF β signaling. *Cell Tissue Res* 2012;**347**:21–36
- Zhang H, Bradley A. Mice deficient for BMP2 are nonviable and have defects in amnion/chorion and cardiac development. *Development* 1996;**122**:2977–86
- Winnier G, Blessing M, Labosky PA, Hogan BLM. Bone morphogenetic protein-4 is required for mesoderm formation and patterning in the mouse. *Genes Develop* 1995;**9**:2105–16
- Chen H, Shi S, Acosta L, Li W, Lu J, Bao S, Chen Z, Yang Z, Schneider MD, Chien KR, Conway SJ, Yoder MC, Haneline LS, Franco D, Shou W. BMP10 is essential for maintaining cardiac growth during murine cardiogenesis. *Development* 2004;**131**:2219–31
- Dudley AT, Lyons KM, Robertson EJ. A requirement for bone morphogenetic protein-7 during development of the mammalian kidney and eye. *Genes Develop* 1995;**9**:2795–807
- McPherron AC, Lawler AM, Lee S. Regulation of anterior/posterior patterning of the axial skeleton by growth/differentiation factor 11. *Nat Genet* 1999;**22**:260–4
- Komatsu Y, Scott G, Nagy A, Kaartinen V, Mishina Y. BMP type I receptor Alk2 is essential for proper patterning at late gastrulation during mouse embryogenesis. *Dev Dyn* 2007;**236**:512–7
- Beppu H, et al. BMP type II receptor is required for gastrulation and early development of mouse embryos. *Dev Biol* 2000;**221**:249–58
- Mishina Y, Suzuki A, Ueno N, Behringer RR. Bmpr encodes a type I bone morphogenetic protein receptor that is essential for gastrulation during mouse embryogenesis. *Genes Dev* 1995;**9**:3027–37
- Sirard C, de la Pompa JL, Elia A, Itie A, Mirtsos C, Cheung A, Hahn S, Wakeham A, Schwartz L, Kern SE, Rossant J, Mak TW. The tumor suppressor gene Smad4/Dpc4 is required for gastrulation and later for anterior development of the mouse embryo. *Genes Dev* 1998;**12**:107–19
- Chang H, Huylebroeck D, Verschuere K, Guo Q, Matzuk MM, Zwijsen A. Smad5 knockout mice die at mid-gestation due to multiple embryonic and extraembryonic defects. *Development* 1999;**126**:1631–42
- Lechleider RJ, Ryan JL, Garrett L, Eng C, Deng C, Wynshaw-Boris A, Roberts AB. Targeted mutagenesis of Smad1 reveals an essential role in chorioallantoic fusion. *Dev Biol* 2001;**240**:157–67
- Chen Q, Chen H, Zheng D, Kuang C, Fang H, Zou B, Zhu W, Bu G, Jin T, Wang Z, Zhang X, Chen J, Field LJ, Rubart M, Shou W, Chen Y. Smad7 is required for the development and function of the heart. *J Biol Chem* 2009;**284**:292–300
- Schmidt JE, Suzuki A, Ueno N, Kimelman D. Localized BMP-4 mediates dorsal/ventral patterning in the early xenopus embryo. *Dev Biol* 1995;**169**:37–50
- Goldman DC, Bailey AS, Pfaffle DL, Al Masri A, Christian JL, Fleming WH. BMP4 regulates the hematopoietic stem cell niche. *Blood* 2009;**114**:4393–401
- Ma L, Lu MF, Schwartz RJ, Martin JF. Bmp2 is essential for cardiac cushion epithelial-mesenchymal transition and myocardial patterning. *Development* 2005;**132**:5601–11
- Rivera-Feliciano J, Tabin CJ. Bmp2 instructs cardiac progenitors to form the heart-valve-inducing field. *Dev Biol* 2006;**295**:580–8
- Wang J, Greene SB, Bonilla-Claudio M, Tao Y, Zhang J, Bai Y, Huang Z, Black BL, Wang F, Martin JF. Bmp signaling regulates myocardial differentiation from cardiac progenitors through a microRNA-mediated mechanism. *Dev Cell* 2010;**19**:903–12
- de Pater E, Ciampricotti M, Priller F, Veerkamp J, Strate I, Smith K, Lagendijk AK, Schilling TF, Herzog W, Abdelilah-Seyfried S, Hammerschmidt M, Bakkers J. BMP signaling exerts opposite effects on cardiac differentiation. *Circ Res* 2012;**110**:578–87
- Kishigami S, Yoshikawa S, Castranio T, Okazaki K, Furuta Y, Mishina Y. BMP signaling through ACVRI is required for left-right patterning in the early mouse embryo. *Dev Biol* 2004;**276**:185–93
- Chocron S, Verhoeven MC, Rentzsch F, Hammerschmidt M, Bakkers J. Zebrafish Bmp4 regulates left-right asymmetry at two distinct developmental time points. *Dev Biol* 2007;**305**:577–88
- Monteiro R, van Dinter M, Bakkers J, Wilkinson R, Patient R, ten Dijke P, Mummery C. Two novel type II receptors mediate BMP signalling and are required to establish left-right asymmetry in zebrafish. *Dev Biol* 2008;**315**:55–71
- Furtado MB, Solloway MJ, Jones VJ, Costa MW, Biben C, Wolstein O, Preis JJ, Sparrow DB, Saga Y, Dunwoodie SL, Robertson EJ, Tam PP, Harvey RP. BMP/SMAD1 signaling sets a threshold for the left/right pathway in lateral plate mesoderm and limits availability of SMAD4. *Genes Dev* 2008;**22**:3037–49
- Lee KJ, Mendelsohn M, Jessell TM. Neuronal patterning by BMPs: a requirement for GDF7 in the generation of a discrete class of commissural interneurons in the mouse spinal cord. *Genes Dev* 1998;**12**:3394–407

44. Wu H-H, Ivkovic S, Murray RC, Jaramillo S. Autoregulation of neurogenesis by GDF11. *Neuron* 2003;**37**:197-207
45. Wang RN, Green J, Wang Z, Deng Y, Qiao M, Peabody M, Zhang Q, Ye J, Yan Z, Denduluri S, Idowu O, Li M, Shen C, Hu A, Haydon RC, Kang R, Mok J, Lee MJ, Luu HL, Shi LL. Bone morphogenetic protein (BMP) signaling in development and human diseases. *Genes Dis* 2014;**1**:87-105
46. Sasai Y, Lu B, Steinbeisser H, De Robertis EM. Regulation of neural induction by the Chd and Bmp-4 antagonistic patterning signals in *Xenopus*. *Nature* 1995;**376**:333-6
47. Bachiller D, Klingensmith J, Kemp C, Belo JA, Anderson RM, May SR, McMahon JA, McMahon AP, Harland RM, Rossant J, De Robertis EM. The organizer factors Chordin and Noggin are required for mouse forebrain development. *Nature* 2000;**403**:658-61
48. Wijgerde M, Karp S, McMahon J, McMahon AP. Noggin antagonism of BMP4 signaling controls development of the axial skeleton in the mouse. *Dev Biol* 2005;**286**:149-57
49. Müller II, Melville DB, Tanwar V, Rybski WM, Mukherjee A, Shoemaker MB, Wang WD, Schoenhard JA, Roden DM, Darbar D, Knapik EW, Hatzopoulos AK. Functional modeling in zebrafish demonstrates that the atrial-fibrillation-associated gene GREM2 regulates cardiac laterality, cardiomyocyte differentiation and atrial rhythm. *Dis Model Mech* 2013;**6**:332-41
50. Sanders LN, Schoenhard JA, Saleh MA, Mukherjee A, Ryzhov S, McMaster WG, Jr, Nolan K, Gumina RJ, Thompson TB, Magnuson MA, Harrison DG, Hatzopoulos AK. BMP antagonist gremlin 2 limits inflammation after myocardial infarction. *Circ Res* 2016;**119**:434-49
51. Parrow NL, Fleming RE. Bone morphogenetic proteins as regulators of iron metabolism. *Annu Rev Nutr* 2014;**34**:77-94
52. Orriols M, Gomez-Puerto MC, Ten Dijke P. BMP type II receptor as a therapeutic target in pulmonary arterial hypertension. *Cell Mol Life Sci* 2017;**74**:1-17
53. Lowery JW, de Caestecker MP. BMP signaling in vascular development and disease. *Cytokine Growth Factor Rev* 2010;**21**:287-98
54. Bandyopadhyay A, Yadav PS, Prashar P. BMP signaling in development and diseases: a pharmacological perspective. *Biochem Pharmacol* 2013;**85**:857-64
55. Ross R. Atherosclerosis - an inflammatory disease. *N Engl J Med* 1999;**340**:115-26
56. Libby P, Ridker PM, Maseri A. Inflammation and atherosclerosis. *Circulation* 2002;**105**:1135-43
57. Libby P. Inflammation in atherosclerosis. *Arterioscler Thromb Vasc Biol* 2012;**32**:2045-51
58. Csiszar A, Smith KE, Koller A, Kaley G, Edwards JG, Ungvari Z. Regulation of bone morphogenetic protein-2 expression in endothelial cells: role of nuclear factor-kappaB activation by tumor necrosis factor-alpha, H₂O₂, and high intravascular pressure. *Circulation* 2005;**111**:2364-72
59. Sorescu GP, Sykes M, Weiss D, Platt MO, Saha A, Hwang J, Boyd N, Boo YC, Vega JD, Taylor WR, Jo H. Bone morphogenetic protein 4 produced in endothelial cells by oscillatory shear stress stimulates an inflammatory response. *J Biol Chem* 2003;**278**:31128-35
60. Sucusky P, Balachandran K, Elhammali A, Jo H, Yoganathan AP. Altered shear stress stimulates upregulation of endothelial VCAM-1 and ICAM-1 in a BMP-4- and TGF- β 1-dependent pathway. *Arterioscler Thromb Vasc Biol* 2009;**29**:254-60
61. Helbing T, Rothweiler R, Ketterer E, Goetz L, Heinke J, Grundmann S, Duerschmied D, Patterson C, Bode C, Moser M. BMP activity controlled by BMPER regulates the proinflammatory phenotype of endothelium. *Blood* 2011;**118**:5040-9
62. Pardali E, Makowski L-M, Leffers M, Borgschieper A, Waltenberger J. BMP-2 induces human mononuclear cell chemotaxis and adhesion and modulates monocyte-to-macrophage differentiation. *J Cell Mol Med* 2018;**22**:5429-38
63. Helbing T, Wiltgen G, Hornstein A, et al. Bone morphogenetic protein-modulator BMPER regulates endothelial barrier function. *Inflammation* 2017;**40**:442-53
64. Chang K, Weiss D, Suo J, Vega JD, Giddens D, Taylor WR, Jo H. Bone morphogenetic protein antagonists are coexpressed with bone morphogenic protein 4 in endothelial cells exposed to unstable flow in vitro in mouse aortas and in human coronary arteries: role of bone morphogenic protein antagonists in inflammation and atherosclerosis. *Circulation* 2007;**116**:1258-66
65. Yao Y, Bennett BJ, Wang X, Rosenfeld ME, Giachelli C, Lusis AJ, Boström KI. Inhibition of bone morphogenetic proteins protects against atherosclerosis and vascular calcification. *Circ Res* 2010;**107**:485-94
66. Pi X, Lockyer P, Dyer LA, Schisler JC, Russell B, Carey S, Sweet DT, Chen Z, Tzima E, Willis MS, Homeister JW, Moser M, Patterson C. Bmper inhibits endothelial expression of inflammatory adhesion molecules and protects against atherosclerosis. *Arterioscler Thromb Vasc Biol* 2012;**32**:2214-22
67. Koga M, Engberding N, Dikalova AE, Chang KH, Seidel-Rogol B, Long JS, Lassègue B, Jo H, Griendling KK. The bone morphogenic protein inhibitor, noggin, reduces glycemia and vascular inflammation in db/db mice. *AJP Heart Circ Physiol* 2013;**305**:H747-55
68. Hruska KA, Mathew S, Saab G. Bone morphogenetic proteins in vascular calcification. *Circ Res* 2005;**97**:105-14
69. Hedin U, Roy J, Tran PK, Lundmark K, Rahman A. Control of smooth muscle cell proliferation - the role of the basement membrane. *Thromb Haemost* 1999;**82**(Suppl 1):23-6
70. Worth NF, Rolfe BE, Song J, Campbell GR. Vascular smooth muscle cell phenotypic modulation in culture is associated with reorganization of contractile and cytoskeletal proteins. *Cell Motil Cytoskeleton* 2001;**49**:130-45
71. Boström K, Watson KE, Horn S, Wortham C, Herman IM, Demer LL. Bone morphogenetic protein expression in human atherosclerotic lesions. *J Clin Invest* 1993;**91**:1800-9
72. Nakaoka T, Gonda K, Ogita T, Otawara-Hamamoto Y, Okabe F, Kira Y, Harii K, Miyazono K, Takawa Y, Fujita T. Inhibition of rat vascular smooth muscle proliferation in vitro and in vivo by bone morphogenetic protein-2. *J Clin Invest* 1997;**100**:2824-32
73. Wong GA, Tang V, El-Sabeawy F, Weiss RH. BMP-2 inhibits proliferation of human aortic smooth muscle cells via p21(Cip1/Waf1). *Am J Physiol Metab* 2003;**284**:E972-9
74. King KE, Iyemere VP, Weissberg PL, Shanahan CM. Krüppel-like factor 4 (KLF4/GKLF) is a target of bone morphogenetic proteins and transforming growth factor β 1 in the regulation of vascular smooth muscle cell phenotype. *J Biol Chem* 2003;**278**:11661-9
75. Hayashi K, Nakamura S, Nishida W, Sobue K. Bone morphogenetic protein-induced Msx1 and Msx2 inhibit myocardin-dependent smooth muscle gene transcription. *Mol Cell Biol* 2006;**26**:9456-70
76. Shao JS, Aly ZA, Lai CF, Cheng SL, Cai J, Huang E, Behrmann A, Towler DA. Vascular Bmp-Msx2-Wnt signaling and oxidative stress in arterial calcification. *Ann N Y Acad Sci* 2007;**1117**:40-50
77. Li X, Yang HY, Giachelli CM. BMP-2 promotes phosphate uptake, phenotypic modulation, and calcification of human vascular smooth muscle cells. *Atherosclerosis* 2008;**199**:271-7
78. Andrade MC, Carmo LS, Farias-Silva E, Liberman M. Msx2 is required for vascular smooth muscle cells osteoblastic differentiation but not calcification in insulin-resistant ob/ob mice. *Atherosclerosis* 2017;**265**:14-21
79. Takarada T, Nakazato R, Tsuchikane A, Fujikawa K, Iezaki T, Yoneda Y, Hinoi E. Genetic analysis of Runx2 function during intramembranous ossification. *Development* 2016;**143**:211-8
80. Komori T. Regulation of osteoblast differentiation by transcription factors. *J Cell Biochem* 2006;**99**:1233-9
81. Tanaka T, Sato H, Doi H, Yoshida CA, Shimizu T, Matsui H, Yamazaki M, Akiyama H, Kawai-Kowase K, Iso T, Komori T, Arai M, Kurabayashi M. Runx2 represses myocardin-mediated differentiation and facilitates osteogenic conversion of vascular smooth muscle cells. *Mol Cell Biol* 2008;**28**:1147-60
82. Derwall M, Malhotra R, Lai CS, Beppu Y, Aikawa E, Seehra JS, Zapol WM, Bloch KD, Yu PB. Inhibition of bone morphogenetic protein signaling reduces vascular calcification and atherosclerosis. *Arterioscler Thromb Vasc Biol* 2012;**32**:613-22

83. Yung LM, Sánchez-Duffhues G, Ten Dijke P, Yu PB. Bone morphogenetic protein 6 and oxidized low-density lipoprotein synergistically recruit osteogenic differentiation in endothelial cells. *Cardiovasc Res* 2015;**108**:278–87
84. Parra-Izquierdo I, Castaños-Mollor I, López J, Gómez C, San Román JA, Sánchez Crespo M, García-Rodríguez C. Calcification induced by type I interferon in human aortic valve interstitial cells is larger in males and blunted by a janus kinase inhibitor. *Arterioscler Thromb Vasc Biol* 2018;**38**:2148–59
85. Lee SB, Kalluri R. Mechanistic connection between inflammation and fibrosis. *Kidney Int* 2010;**78**:S22–6
86. Mack M. Inflammation and fibrosis. *Matrix Biol* 2018;**68–69**:106–21
87. Yang G, Zhu Z, Wang Y, Gao A, Niu P, Tian L. Bone morphogenetic protein-7 inhibits silica-induced pulmonary fibrosis in rats. *Toxicol Lett* 2013;**220**:103–8
88. Hruska KA, Guo G, Wozniak M, Martin D, Miller S, Liapis H, Loveday K, Klahr S, Sampath TK, Morrissey J. Osteogenic protein-1 prevents renal fibrogenesis associated with ureteral obstruction. *Am J Physiol Renal Physiol* 2000;**280**:F130–43
89. Zeisberg M, Bottiglio C, Kumar N, Maeshima Y, Strutz F, Müller GA, Kalluri R. Bone morphogenic protein-7 inhibits progression of chronic renal fibrosis associated with two genetic mouse models. *Am J Physiol Ren Physiol* 2003;**285**:1060–7
90. Zeisberg M, Hanai J, Sugimoto H, Mammoto T, Charytan D, Strutz F, Kalluri R. BMP-7 counteracts TGF- β 1-induced epithelial-to-mesenchymal transition and reverses chronic renal injury. *Nat Med* 2003;**9**:964–8
91. Zeisberg M, Shah AA, Kalluri R. Bone morphogenic protein-7 induces mesenchymal to epithelial transition in adult renal fibroblasts and facilitates regeneration of injured kidney. *J Biol Chem* 2005;**280**:8094–100
92. Wang S, de CM, Kopp J, Mitu G, Lapage J, Hirschberg R. Renal bone morphogenetic protein-7 protects against diabetic nephropathy. *J Am Soc Nephrol* 2006;**17**:2504–12
93. Sugimoto H, Grahovac G, Zeisberg M, Kalluri R. Renal fibrosis and glomerulosclerosis in a new mouse model of diabetic nephropathy and its regression by bone morphogenic protein-7 and advanced glycation end product inhibitors. *Diabetes* 2007;**56**:1825–33
94. Higgins DF, Ewart LM, Masterson E, Tennant S, Grebnev G, Prunotto M, Pomposiello S, Conde-Knape K, Martin FM, Godson C. BMP7-induced-Pten inhibits Akt and prevents renal fibrosis. *Biochim Biophys Acta Mol Basis Dis* 2017;**1863**:3095–104
95. Kinoshita K, Iimuro Y, Otagawa K, Saika S, Inagaki Y, Nakajima Y, Kawada N, Fujimoto J, Friedman SL, Ikeda K. Adenovirus-mediated expression of BMP-7 suppresses the development of liver fibrosis in rats. *Gut* 2007;**56**:706–14
96. Pegorier S, Campbell GA, Kay AB, Lloyd CM. Bone morphogenetic protein (BMP)-4 and BMP-7 regulate differentially transforming growth factor (TGF)- β 1 in normal human lung fibroblasts (NHLF). *Respir Res* 2010;**11**:85
97. Liang D, Wang Y, Zhu Z, Yang G, An G, Li X, Niu P, Chen L, Tian L. BMP-7 attenuated silica-induced pulmonary fibrosis through modulation of the balance between TGF- β /Smad and BMP-7/Smad signaling pathway. *Chem Biol Interact* 2016;**243**:72–81
98. Li X, An G, Wang Y, Liang D, Zhu Z, Lian X, Niu P, Guo C, Tian L. Anti-fibrotic effects of bone morphogenetic protein-7-modified bone marrow mesenchymal stem cells on silica-induced pulmonary fibrosis. *Exp Mol Pathol* 2017;**102**:70–7
99. Chen P, Simons M. When endothelial cells go rogue. *Embo Mol Med* 2015;**8**:1–2
100. Pérez L, Muñoz-Durango N, Riedel CA, Echeverría C, Kalergis AM, Cabello-Verrugio C, Simon F. Endothelial-to-mesenchymal transition: cytokine-mediated pathways that determine endothelial fibrosis under inflammatory conditions. *Cytokine Growth Factor Rev* 2017;**33**:41–54
101. Zeisberg EM, Tarnavski O, Zeisberg M, Dorfman AL, McMullen JR, Gustafsson E, Chandraker A, Yuan X, Pu WT, Roberts AB, Neilson EG, Sayegh MH, Izumo S, Kalluri R. Endothelial-to-mesenchymal transition contributes to cardiac fibrosis. *Nat Med* 2007;**13**:952–61
102. Aisagbonhi O, Meena R, Ryzhov S, Atria N, Feoktistov I, Hatzopoulos AK. Experimental myocardial infarction triggers canonical Wnt signaling and endothelial-to-mesenchymal transition. *Dis Model Mech* 2011;**4**:469–83
103. Dejana E, Hirschi KK, Simons M. The molecular basis of endothelial cell plasticity. *Nat Commun* 2017;**8**:14361
104. Li Y, Lui KO, Zhou B. Reassessing endothelial-to-mesenchymal transition in cardiovascular diseases. *Nat Rev Cardiol* 2018;**15**:445–56
105. Yao Y, Jumabay M, Ly A, Radparvar M, Cubberly MR, Boström KI. A role for the endothelium in vascular calcification. *Circ Res* 2013;**113**:495–504
106. McCulley DJ, Kang JO, Martin JF, Black BL. BMP4 is required in the anterior heart field and its derivatives for endocardial cushion remodeling, outflow tract septation, and semilunar valve development. *Dev Dyn* 2008;**237**:3200–9
107. Medici D, Shore EM, Lounev VY, Kaplan FS, Kalluri R, Olsen BR. Conversion of vascular endothelial cells into multipotent stem-like cells. *Nat Med* 2010;**16**:1400–6
108. Hao J, Ho JN, Lewis JA, Karim KA, Daniels RN, Gentry PR, Hopkins CR, Lindsley CW, Hong CC. In vivo structure – activity relationship study of dorsomorphin analogues identifies selective VEGF and BMP inhibitors. *ACS Chem Biol* 2010;**5**:245–53
109. Owens P, Pickup MW, Novitskiy SV, Giltman JM, Gorska AE, Hopkins CR, Hong CC, Moses HL. Inhibition of BMP signaling suppresses metastasis in mammary cancer. *Oncogene* 2015;**34**:2437–49
110. Maddaluno L, Rudini N, Cuttano R, Bravi L, Giampietro C, Corada M, Ferrarini L, Orsenigo F, Papa E, Boulday G, Tournier-Lasserre E, Chapon F, Richichi C, Retta SF, Lampugnani MG, Dejana E. EndMT contributes to the onset and progression of cerebral cavernous malformations. *Nature* 2013;**498**:492–6
111. Ribera J, Pauta M, Melgar-Lesmes P, Córdoba B, Bosch A, Calvo M, Rodrigo-Torres D, Sancho-Bru P, Mira A, Jiménez W, Morales-Ruiz M. A small population of liver endothelial cells undergoes endothelial-to-mesenchymal transition in response to chronic liver injury. *Am J Physiol Liver Physiol* 2017;**313**:G492–504
112. Dutta P, Courties G, Wei Y, Leuschner F, Gorbato R, Robbins CS, Iwamoto Y, Thompson B, Carlson AL, Heidt T, Majumdar MD, Lasitschka F, Etzrodt M, Waterman P, Waring MT, Chicoine AT, van der Laan AM, Niessen HW, Piek JJ, Rubin BB, Butany J, Stone JR, Katus HA, Murphy SA, Morrow DA, Sabatine MS, Vinegoni C, Moskowitz MA, Pittet MJ, Libby P, Lin CP, Swirski FK, Weissleder R, Nahrendorf M. Myocardial infarction accelerates atherosclerosis. *Nature* 2012;**487**:325–9
113. Zougari Y, Ait-Oufella H, Bonnin P, Simon T, Sage AP, Guérin C, Vilar J, Caligiuri G, Tsiantoulas D, Laurans L, Dumeau E, Kotti S, Bruneval P, Charo IF, Binder CJ, Danchin N, Tedgui A, Tedder TF, Silvestre JS, Mallat Z. B lymphocytes trigger monocyte mobilization and impair heart function after acute myocardial infarction. *Nat Med* 2013;**19**:1273–80
114. Frantz S, Nahrendorf M. Cardiac macrophages and their role in ischaemic heart disease. *Cardiovasc Res* 2014;**102**:240–8
115. Dutta P, Sager HB, Stengel KR, Naxerova K, Courties G, Saez B, Silberstein L, Heidt T, Sebas M, Sun Y, Wojtkiewicz G, Feruglio PF, King K, Baker JN, van der Laan AM, Borodovsky A, Fitzgerald K, Hulsmans M, Hoyer F, Iwamoto Y, Vinegoni C, Brown D, Di Carli M, Libby P, Hiebert SW, Scadden DT, Swirski FK, Weissleder R, Nahrendorf M. Myocardial infarction activates CCR2+ hematopoietic stem and progenitor cells. *Cell Stem Cell* 2015;**16**:477–87
116. Nahrendorf M, Swirski FK. Innate immune cells in ischaemic heart disease: does myocardial infarction beget myocardial infarction? *Eur Heart J* 2016;**37**:868–72
117. Chang SA, Lee EJ, Kang HJ, Zhang SY, Kim JH, Li L, Youn SW, Lee CS, Kim KH, Won JY, Sohn JW, Park KW, Cho HJ, Yang SE, Oh WI, Yang YS, Ho WK, Park YB, Kim HS. Impact of myocardial infarct proteins and oscillating pressure on the differentiation of mesenchymal stem cells: effect of acute myocardial infarction on stem cell differentiation. *Stem Cells* 2008;**26**:1901–12
118. Varas A, Valencia J, Lavocat F, Martínez VG, Thiam NN, Hidalgo L, Fernández-Sevilla LM, Sacedón R, Vicente A, Miossec P. Blockade of

- bone morphogenetic protein signaling potentiates the pro-inflammatory phenotype induced by interleukin-17 and tumor necrosis factor- α combination in rheumatoid synoviocytes. *Arthritis Res Ther* 2015;**17**:192
119. Lories RJU, Dereze I, Ceuppens JL, Luyten FP. Bone morphogenetic proteins 2 and 6, expressed in arthritic synovium, are regulated by proinflammatory cytokines and differentially modulate fibroblast-like synoviocyte apoptosis. *Arthritis Rheum* 2003;**48**:2807-18
120. Bramlage CP, Häupl T, Kaps C, Ungethüm U, Krenn V, Pruss A, Müller GA, Strutz F, Burmester GR. Decrease in expression of bone morphogenetic proteins 4 and 5 in synovial tissue of patients with osteoarthritis and rheumatoid arthritis. *Arthritis Res Ther* 2006;**8**:R58
121. Hot A, Zrioual S, Toh ML, Lenief V, Miossec P. IL-17A- versus IL-17F-induced intracellular signal transduction pathways and modulation by IL-17RA and IL-17RC RNA interference in rheumatoid synoviocytes. *Ann Rheum Dis* 2011;**70**:341-8
122. Hot A, Zrioual S, Lenief V, Miossec P. IL-17 and tumour necrosis factor α combination induces a HIF-1 α -dependent invasive phenotype in synoviocytes. *Ann Rheum Dis* 2012;**71**:1393-401
123. Lories RJU, Dereze I, Luyten FP. Modulation of bone morphogenetic protein signaling inhibits the onset and progression of ankylosing enthesitis. *J Clin Invest* 2005;**115**:1571-9
124. Fillebeen C, Wilkinson N, Charlebois E, Katsarou A, Wagner J, Pantopoulos K. Hepcidin-mediated hypoferremic response to acute inflammation requires a threshold of Bmp6/Hjv/Smad signaling. *Blood* 2018;**132**:1829-41
125. Nemeth E, Tuttle MS, Powelson J, Vaughn MB, Donovan A, Ward DM, Ganz T, Kaplan J. Hepcidin regulates cellular iron efflux by binding to ferroportin and inducing its internalization. *Science* 2004;**306**:2090-3
126. Babitt JL, Huang FW, Wrighting DM, Xia Y, Sidis Y, Samad TA, Campagna JA, Chung RT, Schneyer AL, Woolf CJ, Andrews NC, Lin HY. Bone morphogenetic protein signaling by hemojuvelin regulates hepcidin expression. *Nat Genet* 2006;**38**:531-9
127. Andriopoulos B, Jr, Corradini E, Xia Y, Faasse SA, Chen S, Grgurevic L, Knutson MD, Pietrangelo A, Vukicevic S, Lin HY, Babitt JL. BMP6 is a key endogenous regulator of hepcidin expression and iron metabolism. *Nat Genet* 2009;**41**:482-7
128. Kautz L, Meynard D, Monnier A, Darnaud V, Bouvet R, Wang RH, Deng C, Vaulont S, Mosser J, Coppin H, Roth MP. Iron regulates phosphorylation of Smad1/5/8 and gene expression of Bmp6, Smad7, Id1, and Atoh8 in the mouse liver. *Blood* 2008;**112**:1503-9
129. Meynard D, Kautz L, Darnaud V, Canonne-Hergaux F, Coppin H, Roth MP. Lack of the bone morphogenetic protein BMP6 induces massive iron overload. *Nat Genet* 2009;**41**:478-81
130. Truksa J, Peng H, Lee P, Beutler E. Bone morphogenetic proteins 2, 4, and 9 stimulate murine hepcidin 1 expression independently of Hfe, transferrin receptor 2 (Tfr2), and IL-6. *Proc Natl Acad Sci U S A* 2006;**103**:10289-93
131. Wang CY, Canali S, Bayer A, Dev S, Agarwal A, Babitt JL. Iron, erythropoietin, and inflammation regulate hepcidin in BMP2-deficient mice, but serum iron fails to induce hepcidin in BMP6-deficient mice. *Am J Hematol* 2018;**94**:240-8
132. Mayeur C, Leyton PA, Kolodziej SA, Yu B, Bloch KD. BMP type II receptors have redundant roles in the regulation of hepatic hepcidin gene expression and iron metabolism. *Blood* 2014;**124**:2116-23
133. Steinbicker AU, Bartnikas TB, Lohmeyer LK, Leyton P, Mayeur C, Kao SM, Pappas AE, Peterson RT, Bloch DB, Yu PB, Fleming MD, Bloch KD. Perturbation of hepcidin expression by BMP type I receptor deletion induces iron overload in mice. *Blood* 2011;**118**:4224-30
134. Wang RH, Li C, Xu X, Zheng Y, Xiao C, Zervas P, Cooperman S, Eckhaus M, Rouault T, Mishra L, Deng CX. A role of SMAD4 in iron metabolism through the positive regulation of hepcidin expression. *Cell Metab* 2005;**2**:399-409
135. Steinbicker AU, Sachidanandan C, Vonner AJ, Yusuf RZ, Deng DY, Lai CS, Rauwerdink KM, Winn JC, Saez B, Cook CM, Szekely BA, Roy CN, Seehra JS, Cuny GD, Scadden DT, Peterson RT, Bloch KD, Yu PB. Inhibition of bone morphogenetic protein signaling attenuates anemia associated with inflammation. *Blood* 2011;**117**:4915-23
136. Theurl I, Schroll A, Sonnweber T, Nairz M, Theurl M, Willenbacher W, Eller K, Wolf D, Seifert M, Sun CC, Babitt JL, Hong CC, Menhall T, Gearing P, Lin HY, Weiss G. Pharmacologic inhibition of hepcidin expression reverses anemia of chronic inflammation in rats. *Blood* 2011;**118**:4977-84
137. Gallitz I, Lofruthe N, Traeger L, Bäumer N, Hoerr V, Faber C, Kuhlmann T, Müller-Tidow C, Steinbicker AU. Deficiency of the BMP Type I receptor Alk3 partly protects mice from anemia of inflammation. *BMC Physiol* 2018;**18**:3
138. Carvalho D, Olaciregui NG, Ruddle R, Donovan A, Pal A, Raynaud F, Richardson PJ, Carcaboso AM, Jones C. Preclinical efficacy of combined ACVR1 and PI3K/mTOR inhibition in diffuse intrinsic pontine glioma (DIPG). *Neuro Oncol* 2018;**20**:i54-5

EDITORIAL

Disease Models & Mechanisms in the Age of Big Data

Antonis K. Hatzopoulos*

ABSTRACT

In the decade since *Disease Models & Mechanisms* was launched, the emergence of Big Data as the main foundation of biological information is having a profound effect on how we do research and it has provoked some interesting questions. Is Big Data exploration replacing hypothesis-driven basic research? And, to what extent is disease modeling in the laboratory still relevant to medical research? Recent examples of synergistic approaches utilizing animal modeling and electronic medical records mining show that combining efforts between disease models and clinical datasets can uncover not only disease etiologies, but also novel molecular and cellular mechanisms linked to gene function.

KEY WORDS: Big Data, Disease modeling, GWAS, Omics

Introduction

In a series of editorial articles in the inaugural issue of *Disease Models & Mechanisms* (DMM), Vivian Siegel, the first Editor-in-Chief, and members of The Company of Biologists and the Editorial Board laid out how the idea for the new journal was conceived, outlined its scope and expressed their hopes and expectations for the new venture (Siegel, 2008; Freeman and St Johnston, 2008). They envisioned the launch of the new publication as a forum to foster and broaden the interactions between what they considered as two poorly connected scientific silos, biological research and animal models in one, and clinical research and medicine in the other. Much has changed since the start of DMM over ten years ago, for the relationship between biological and clinical research has greatly evolved. Although this partnership faces new challenges, as the volume, complexity and heterogeneity of scientific information continues to expand, it also promises to revolutionize both basic biological knowledge and medical care. Part of this revolution stems from the emergence of Big Data as a centerpiece of scientific discovery, offering an unprecedented opportunity to determine biological and disease mechanisms (Schüssler-Fiorenza Rose et al., 2019).

Big Data come in many different forms, for example whole-genome sequencing, RNA sequencing-based transcriptomics (bulk and single cell), proteomics, metabolomics, Genome-Wide and Phenome-Wide Association Studies (GWAS, PheWAS), and Electronic Medical or Health Records (EMR/EHR). Particularly exciting as discovery tools are EHRs that contain extensive phenotype information, which is accompanied by DNA and/or tissue biobanking and genomic information, such as the Vanderbilt University Medical Center BioVU database, the Electronic Medical

Records and Genomics (eMERGE) Network, or the United Kingdom (UK) Biobank (Roden et al., 2008; Gottesman et al., 2013; Sudlow et al., 2015).

The collection, storage and mining of increasingly diverse and complex types of biological information from the general human population, or from patients with well-documented medical records – based on diagnoses organized by ICD9/10 codes and accompanied by laboratory test results, imaging and other procedures – is having a profound effect on modern-day research. This enormous data collection has thrust humans, as the ultimate experimental model, to not only understand the pathophysiology of different diseases and to develop new therapeutic approaches, but also, rather unexpectedly, to understand basic gene function and biological mechanisms.

This emerging landscape has brought new challenges in the communication and translation of information among different disciplines, demands for new skills, and a need for innovative and sophisticated research tools. It seems that the separate research silos, which the DMM founders saw as a major impediment ten years ago, have been swept away into a vast ocean of information and Big Data, an ocean we must all learn to swim in. We can now sequence all variants in a human genome from all patients and relate them to RNA and protein levels, metabolites, or functional and phenotypic traits. Yet, how to parse, analyze and, most importantly, extract meaningful information from these datasets is not always straightforward. It is evident that Big Data depend on basic biology to understand disease mechanisms. Equally, biology needs Big Data to understand the pleiotropic effects of gene function and generate knowledge that is relevant and consequential in the current scientific climate.

Why Big Data needs biology

In the last decade, GWAS have identified numerous disease-associated loci (Visscher et al., 2017). Yet, using these links to determine disease etiology or mechanisms can be challenging. In many instances, it is hard to identify the candidate gene using GWAS because single-nucleotide polymorphisms (SNPs) are frequently found outside coding sequences in genomic regions surrounded by many genes. Current experience indicates that the closest to the SNP gene is not always the disease-causing one (Smemo et al., 2014). Another limitation may stem from the fact that GWAS typically search for specific phenotypes, potentially missing additional clinical features that share the same genetic cause. Therefore, often one has to know where and how to search in order to untangle disease-causing mechanisms, especially in complex diseases. Biological evidence in animal models may help shape and guide these searches to pinpoint the gene responsible for the phenotype, reveal the full extent of gene pathogenicity, and provide functional validation and mechanistic insights in animal models using gain- or loss-of-function approaches (Unlu et al., 2019a).

From a practical point of view, GWAS and other Big Data investigations that are based on statistical associations rely on Bonferroni corrections or similar methods to improve confidence in

Department of Medicine, Division of Cardiovascular Medicine, Vanderbilt University Medical Center, Nashville, TN 37232, USA.

*Author for correspondence (antonis.hatzopoulos@vumc.org)

 A.K.H., 0000-0001-5610-0017

This is an Open Access article distributed under the terms of the Creative Commons Attribution License (<https://creativecommons.org/licenses/by/4.0/>), which permits unrestricted use, distribution and reproduction in any medium provided that the original work is properly attributed.

the results, often requiring extremely low P values to accept that an association is real. Although such strict requirements are necessary to accept statistical associations, they can also cause researchers to discard many findings, especially if the relevant cohorts are relatively small, for example in studies aiming to establish the pathogenicity of rare variants (Bastarache et al., 2018). Biological evidence in an appropriate experimental model can provide independent validation of the findings, lowering the high statistical thresholds for acceptance and opening the doors of discovery (Unlu et al., 2019).

Why biology needs Big Data

Although it might be easier to imagine why gene-disease phenotype associations, obtained by statistical means, need wet lab experimental support for validation and mechanistic insights, it is often less obvious how wet lab biology can benefit from Big Data, especially EHRs. Although the use of clinical data to assess the putative significance in human disease of a mechanism that was discovered in an animal model is expected, analyzing clinical records also has the potential to reveal new aspects of gene function that were not picked up in the laboratory.

The ‘biology of real life’ is more diverse and complex than ‘biology in the laboratory’. Animal research is often performed in genetically identical animals (an exception is outbred zebrafish), yielding results within the context of specific gene-gene interactions, and under communal environmental conditions, thus obscuring the pathogenicity of gene malfunction in a population-at-large setting. Although such strictly controlled parameters have traditionally been necessary to perform fundamental research studies, crucial aspects in a disease pathology may also include environmental influences, behavioral patterns, lifestyle, diet, interactions with microbiota or cultural influences, each dictating to various degrees to what extent aberrant gene function contributes to disease initiation, progression or severity. These aspects cannot be easily recapitulated in the laboratory and, therefore, laboratory analyses, no matter how sophisticated, may fail to capture the full phenotypic gamut and pathogenic potential of some genes. On the other hand, these features may be uncovered in large cohorts with clinical or epidemiological data.

Most of the described phenotypes in animal models are usually based on loss-of-gene-function approaches. In human subpopulations, mutations or variants can also be gain-of-function, or exert dominant-negative effects, interfering with the activities of an entire gene family or disrupting the proper function of complex genetic networks; or, certain variants might represent partial loss of function or cause variance in gene expression in specific tissues (Müller et al., 2013; Gamazon et al., 2018; Li et al., 2019). If some of these variants cause relatively mild perturbations in gene activity they likely remain benign, except in cases when the system is stressed, for example by injury, environmental factors or a co-occurring disease like diabetes. Also, most studies in a variety of injury models are more often than not performed in young and otherwise healthy animals without comorbidities. And, although things are gradually improving thanks to current NIH guidelines, most work in the past has been carried out in male animals. Conversely, the effects of sex-differences, aging or comorbidities to disease-contributing genetic alterations might be embedded in large EHR datasets, providing a more comprehensive and complete image of gene function.

Genetic animal models are usually based on alterations in the expression and/or activity levels of a single gene. On the other hand, diseases are often the result of defects in many molecular or cellular

components. Furthermore, certain genes, besides generating a recognizable phenotype in a specific organ, might also be associated with a behavioral trait or mood disorder that would likely be missed in fish or mouse models, an association that could be documented in clinical datasets. As a result, the full spectrum of clinically relevant phenotypes associated with malfunction of a gene product may not be captured in an animal model, or they may be simply overlooked because particular phenotypes are not recognized. Adding to that, as information of single-cell RNA-seq data accumulates, it appears that apparently similar cells exhibit functional and phenotypic heterogeneity that may not be evident in a controlled experimental setting, but it may be revealed in a complex population setting. It is likely some of these features will be uncovered in large human-population datasets and EHRs, which offer enormous sample sizes that are not feasible in the laboratory. Newly discovered features in humans could be then further probed for pathomechanisms, with additional tests in available animal models, or guide the generation of new models more suitable to address a specific issue.

Other important aspects of gene (mal)function that may be missed in the laboratory but can be detected in clinical datasets include long-term effects that will not manifest in animal models with short life or observational time spans. On the other hand, analyses in EHR or epidemiological studies can provide longitudinal data to complement or expand animal studies (Schüssler-Fiorenza Rose et al., 2019).

Exploring synergies

Recent elegant studies highlight the tremendous value of exploring synergies between Big Data in EHRs and biological research, especially with the advent of technologies such as CRISPR-Cas9 that have dramatically enhanced the fidelity, precision and efficacy of introducing gene variants into animal models. In one example, using BioVU and other databanks, investigators used EHR-linked genetic samples to discover gene-disease associations that were then validated in zebrafish loss-of-function models. Analysis of mutant zebrafish revealed additional phenotypes that were then verified in human patients by targeted searches among clinical phenotypes (Unlu et al., 2019). In another notable study, whole-exome sequencing in a patient with a serious lymphatic anomaly revealed a variant in *ARAF*, a gene encoding a kinase that acts upstream of the MEK/ERK signaling cascade. Modeling of the variant in human cells and zebrafish revealed overactive MEK/ERK signaling causing abnormal lymphatic morphology. The lymphatic abnormality was rescued in zebrafish with available MEK inhibitors. Treatment of the patient with a MEK inhibitor led to remodeling of the patient’s lymphatic system and a remarkable improvement in his medical condition and quality of life (Li et al., 2019).

It appears that we are entering a powerful new symbiotic relationship in which Big Data depend on biological model systems to validate statistical associations, and basic biological research needs Big Data to capture the complexity of gene function outside the well-controlled environment and genetics of the laboratory. Although Big Data cannot replace hypothesis-driven basic biological studies in animal models, taking some of the early success stories into account, it is evident that better integrating the two areas of disease models and Big Data from EHRs, at the technical and personnel level, will uncover disease mechanisms and draw us nearer to fulfilling the expectations of personalized medicine. DMM is poised to play a vital role in accomplishing this goal by nurturing the emerging synergies between clinical and biological research. Off to the next decade!

Competing interests

The author declares no competing or financial interests.

Funding

This work was supported by grants from the National Institutes of Health (R01HL138519) and the U.S. Department of Defense (W81XWH-16-1-0622).

References

- Bastarache, L., Hughey, J. J., Hebring, S., Marlo, J., Zhao, W., Ho, W. T., Van Driest, S. L., McGregor, T. L., Mosley, J. D., Wells, Q. S. et al.** (2018). Phenotype risk scores identify patients with unrecognized Mendelian disease patterns. *Science* **359**, 1233-1239. doi:10.1126/science.aal4043
- Freeman, M. and St Johnston, D.** (2008). Wherefore DMM? *Dis. Model Mech.* **1**, 6-7. doi:10.1242/dmm.000760
- Gamazon, E. R., Segrè, A. V., van de Bunt, M., Wen, X., Xi, H. S., Hormozdiari, F., Ongen, H., Konkashbaev, A., Derks, E. M., Aguet, F. et al.** (2018). Using an atlas of gene regulation across 44 human tissues to inform complex disease- and trait-associated variation. *Nat. Genet.* **50**, 956-967. doi:10.1038/s41588-018-0154-4
- Gottesman, O., Kuivaniemi, H., Tromp, G., Faucett, W. A., Li, R., Manolio, T. A., Sanderson, S. C., Kannry, J., Zinberg, R., Basford, M. A. et al.** (2013). The electronic medical records and genomics (eMERGE) network: past, present, and future. *Genet. Med.* **15**, 761-771. doi:10.1038/gim.2013.72
- Li, D., March, M. E., Gutierrez-Uzquiza, A., Kao, C., Seiler, C., Pinto, E., Matsuoka, L. S., Battig, M. R., Bhoj, E. J., Wenger, T. L. et al.** (2019). ARAF recurrent mutation causes central conducting lymphatic anomaly treatable with a MEK inhibitor. *Nat. Med.* **25**, 1116-1122. doi:10.1038/s41591-019-0479-2
- Müller, I. I., Melville, D. B., Tanwar, V., Rybski, W., Mukherjee, A., Shoemaker, B. M., Wang, W.-D., Schoenhard, J. A., Roden, D. M., Darbar, D. et al.** (2013). Functional modeling in zebrafish demonstrates that the atrial-fibrillation-associated gene *GREM2* regulates cardiac laterality, cardiomyocyte differentiation and atrial rhythm. *Dis. Model Mech.* **6**, 332-341. doi:10.1242/dmm.010488
- Roden, D. M., Pulley, J. M., Basford, M. A., Bernard, G. R., Clayton, E. W., Balsler, J. R. and Masys, D. R.** (2008). Development of a large-scale de-identified DNA biobank to enable personalized medicine. *Clin. Pharmacol. Ther.* **84**, 362-369. doi:10.1038/clpt.2008.89
- Schüssler-Fiorenza Rose, S. M., Contrepolis, K., Moneghetti, K. J., Zhou, W., Mishra, T., Mataraso, S., Dagan-Rosenfeld, O., Ganz, A. B., Dunn, J., Hornburg, D. et al.** (2019). A longitudinal Big Data approach for precision health. *Nat. Med.* **25**, 792-804. doi:10.1038/s41591-019-0414-6
- Siegel, V.** (2008). Provoking progress. *Dis. Model Mech.* **1**, 3-5. doi:10.1242/dmm.000778
- Smemo, S., Tena, J. J., Kim, K.-H., Gamazon, E. R., Sakabe, N. J., Gómez-Marín, C., Aneas, I., Credidio, F. L., Sobreira, D. R., Wasserman, N. F. et al.** (2014). Obesity-associated variants within *FTO* form long-range functional connections with *IRX3*. *Nature* **507**, 371-375. doi:10.1038/nature13138
- Sudlow, C., Gallacher, J., Allen, N., Beral, V., Burton, P., Danesh, J., Downey, P., Elliott, P., Green, J., Landray, M. et al.** (2015). UK Biobank: an open access resource for identifying the causes of a wide range of complex diseases of middle and old age. *PLoS Med.* **12**, e1001779. doi:10.1371/journal.pmed.1001779
- Unlu, G., Gamazon, E. R., Qi, X., Levic, D. S., Bastarache, L., Denny, J. C., Roden, D. M., Mayzus, I., Breyer, M., Zhong, X. et al.** (2019). *GRIK5* genetically regulated expression associated with eye and vascular phenomes: discovery through iteration among biobanks, electronic health records, and zebrafish. *Am. J. Hum. Genet.* **104**, 503-519. doi:10.1016/j.ajhg.2019.01.017
- Visscher, P. M., Wray, N. R., Zhang, Q., Sklar, P., McCarthy, M. I., Brown, M. A. and Yang, J.** (2017). 10 Years of GWAS discovery: biology, function, and translation. *Am. J. Hum. Genet.* **101**, 5-22. doi:10.1016/j.ajhg.2017.06.005

1 **Balanced Wnt/Dickkopf1 signaling by mesenchymal vascular progenitor cells in**
2 **the microvascular niche maintains distal lung structure and function**

3
4 Megan E. Summers¹, Bradley W. Richmond², Jonathan A. Kropski², Sarah A. Majka¹,
5 Julie A. Bastarache², Antonis K. Hatzopoulos², Jeffery Bylund², Moumita Ghosh¹, Irina
6 Petrache¹, Robert F. Foronjy³, Patrick Geraghty³ and Susan M. Majka^{*1,4,5}

7
8 **Affiliations:** ¹Department of Medicine, Division of Pulmonary, Critical Care & Sleep
9 Medicine, National Jewish Health, Denver CO, 80206, USA; ²Department of Medicine,
10 Division of Allergy, Pulmonary and Critical Care Medicine or Cardiology, Vanderbilt
11 University Medical Center or Department of Veterans' Affairs, Nashville TN, 37232,
12 USA; ³Division of Pulmonary and Critical Care Medicine, SUNY Downstate Medical
13 Center, Brooklyn, NY, 11203, USA; ⁴Department of Medicine, Pulmonary & Critical Care
14 Medicine, ⁵Gates Center for Regenerative Medicine and Stem Cell Biology, University of
15 Colorado, Aurora, CO, 80045, USA.

16
17
18 **Figures 6; Tables 0**

19
20 **Corresponding Author:**

21 Susan M. Majka, Ph.D.
22 Professor of Medicine
23 National Jewish Health; Division of Allergy, Pulmonary and Critical Care Medicine
24 1400 Jackson St; K810; Denver, CO 80206
25 susanmajka@mac.com
26 Ph (303) 883-8786

27
28
29 **Sources of support:** This work was funded by grants to S.M. Majka from the NIH
30 R01HL116597 and NIH R01HL136449. Additional funding includes: B.R. VA 5 IK2 BX
31 003841-02 and P.G. FAMRI CIA160005 and the Alpha-1 Foundation 614218.

32
33 **Running head:** DKK1 regulates Microvascular Niche

34
35 **Key words:** Mesenchymal vascular progenitor cell, Wnt signaling, emphysema,
36 microvascular niche, microvascular endothelial cells, vascular smooth muscle cells,
37 Dkkopf1, DKK1, CKAP4

39 **ABSTRACT**

40

41 The well described Wnt inhibitor Dickkopf-1 (DKK1) plays a role in angiogenesis

42 as well as regulation of growth factor signaling cascades in pulmonary remodeling

43 associated with chronic lung diseases including emphysema and fibrosis. However, the

44 specific mechanisms by which DKK1 influences mesenchymal vascular progenitor

45 (MVPC), endothelial and smooth muscle cells within the microvascular niche have not

46 been elucidated. In this study, we show that knock down of DKK1 in *Abcg2*^{pos} lung

47 mouse adult tissue resident MVPC alters lung stiffness, parenchymal collagen

48 deposition, microvessel muscularization and density as well as loss of tissue structure in

49 response to hypoxia exposure. To complement the *in vivo* mouse modeling, we also

50 identified cell or disease specific responses to DKK1, in primary lung COPD MVPC,

51 COPD MVEC and SMC, supporting a paradoxical disease specific response of cells to

52 well-characterized factors. Cell responses to DKK1 were dose dependent and

53 correlated with varying expression of the DKK1 receptor, *CKAP4*. These data

54 demonstrate that DKK1 expression is necessary to maintain the microvascular niche

55 while its effects are context specific. They also highlight DKK1 as a regulatory candidate

56 to understand the role of Wnt and DKK1 signaling between cells of the microvascular

57 niche during tissue homeostasis and during the development of chronic lung diseases.

58

59

60

61 **INTRODUCTION**

62

63 The tightly controlled formation of the alveolar-capillary network, and complex
64 signaling between vasculature, mesenchyme and epithelium that occurs during lung
65 development provides some insight into how vasculopathy may influence loss of lung
66 structure and function during the development of chronic lung diseases (CLDs) (2, 13,
67 14, 24, 41, 59, 63, 70). The etiology of microvascular remodeling and mechanisms
68 through which it contributes to the development and severity of various CLDs remain
69 unknown, due in part to a lack of adult rodent models evaluating early stage
70 vasculopathy. The relevance of vasculopathy to the pathophysiology of CLDs has not
71 been resolved as conflicting evidence depicts angiogenesis as both, reparative or
72 pathologic (10, 12, 25, 33, 35, 36, 46, 51, 57, 61, 65, 68), highlighting the need to
73 identify the early mechanisms underlying the initiation of disease.

74 Our previous work has demonstrated that ABCG2-expressing adult
75 mesenchymal vascular progenitor cells (MVPCs) are a key component of lung
76 microvascular homeostasis, angiogenesis in response to injury and are necessary to
77 maintain distal lung tissue structure (30, 62). MVPC function is dependent on canonical
78 Wnt signaling, with β -catenin as a central mediator (30, 62). The Wnt signaling pathway
79 controls a variety of developmental and biological processes including cell fate,
80 proliferation, and migration, and recent studies have also linked the Wnt signaling
81 pathways to proper vascular growth in humans (21, 23, 27, 32, 40, 69). Aberrant Wnt/ β -
82 catenin signaling has also been implicated in most CLDs, highlighting its importance in
83 the study of COPD and idiopathic pulmonary fibrosis (IPF)(4-7, 38, 43, 56). To date,
84 Dickkopf-1 (DKK1) is widely accepted as an antagonist of the canonical Wnt signaling

85 pathway as DKK1 inhibits formation of a ternary complex involving LRP5/6, frizzled,
86 and Wnt ligands which results in inhibition of the canonical Wnt signaling (49, 58). It
87 also regulates epithelial proliferation, mesenchymal transition and migration in a dose
88 dependent manner through Kremens (Krm) 1 and 2 or cytoskeleton-associated protein
89 4 (CKAP4) (37, 54). Dkk-1 binding of Krm 1 and 2 triggers the internalization and
90 degradation of the LRP receptor (8, 19). Furthermore, DKK1 induces angiogenesis
91 through Wnt/ β -catenin dependent and independent mechanisms in endothelial and
92 progenitor cells (16, 17, 53, 60). It also regulates lung smooth muscle cell differentiation
93 and proliferation (22, 31, 66). To date, the role DKK1 plays in regulating pulmonary
94 microvascular homeostasis is unknown.

95 Our previous studies demonstrated that DKK1 expression by MVPC varies
96 depending on the CLD. DKK1 protein levels are increased in primary MVPC isolated
97 from pulmonary arterial hypertension (PAH) patients (both familial FPAH and idiopathic
98 IPAH), IPF and COPD (29, 30, 62). In lung tissue corresponding to these CLDs, DKK1
99 localized to the endothelial and smooth muscle cell layers of the remodeled vasculature,
100 relative to normal lung tissue. Exposure of primary MVPC from normal and FPAH
101 patients induced a profibrotic phenotype with increased expression of smooth muscle
102 alpha actin, collagens and extracellular matrix. Treatment with the DKK1 inhibitor,
103 gallocyanin decreased the expression of these genes and in some instances reduced
104 the expression to that of the normal MVPC (29). As DKK1 is a target of β -catenin (50),
105 we recently demonstrated that transgenic mice with stabilized β -catenin and Wnt
106 activation in MVPC express increased levels of DKK1, which correlated with enhanced
107 adaptive angiogenesis by the microvascular endothelium as well as MVPC (62). This

108 shows the complex interactions between β -catenin and its upstream inhibitor Dkk-1.
109 However, the cell specific mechanisms by which DKK1 may influence the microvascular
110 niche have not been elucidated.

111 To address the afore mentioned gaps in knowledge we designed studies to test
112 the hypothesis that DKK1 was a modulator of three cell types comprising a pulmonary
113 microvascular niche, microvascular endothelium (MVEC), MVPC and smooth muscle
114 (SMC). *In vitro*, DKK1 expression differentially affected sprouting and migration of
115 murine and human MVEC and MVPC and well as the SMC contractile phenotype,
116 correlated to level of Wnt signaling, dose and CKAP4 receptor expression. *In vivo*,
117 genetic depletion of lung MVPC *DKK1* compared to wild-type demonstrated tissue
118 stiffening, parenchymal collagen deposition and increased muscularization. DKK1KO
119 responded to hypoxia exposure with loss of tissue structure and increased MLI. Taken
120 together the data demonstrate that DKK1 expression is necessary to maintain the
121 microvascular niche while its effects are context specific.

122

123

124

125 **METHODS**

126

127

128 **Study approval.** The Institutional Animal Care and Use Committee at National Jewish
129 Health approved all animal procedures and protocols. These studies utilized banked
130 patient cell lines obtained using IRB #9401 approved by the Vanderbilt University
131 Medical Center IRB Committee, Nashville, TN, USA. Patients were consented under
132 this IRB for the generation and storage of human cell lines. Primary cells were obtained
133 from advanced COPD patients with severe physiological impairment requiring lung
134 transplantation as previously described (29, 30). Isolated human and murine MVPC and
135 murine *in vivo* age matched models were utilized. Endpoint analysis was performed in a
136 blinded fashion. Primary human MVPC and MVEC were isolated and characterized as
137 previously described (28, 30, 62), or purchased from LONZA (Lonza, Walkersville).
138 Human pulmonary artery smooth muscle cells were purchased from LONZA (Lonza,
139 Walkersville).

140

141 **Genetic manipulation of murine ABCG2^{pos} mesenchymal progenitor cells**
142 **(MVPCs).** ABCG2-Cre^{ERT2} mice, a generous gift of Dr. B. Sorrentino (St. Jude Children's
143 Research Hospital, Memphis, TN) (26), were crossed to a fluorescent eGFP reporter
144 (Cg)-Gt(ROSA)26Sortm4(ACTB-tdTomato,-EGFP) JAX stock# 007676; designated
145 mT/mG) strain to facilitate lineage analysis and quantitation via eGFP expression. A
146 third gene was crossed into the mice to stabilize β catenin(Catnb^{loxP}(Δ ex3) a generous
147 gift of Dr. M.M. Taketo (Kyoto University, Kyoto, Japan) (34), designated β OE. A third
148 gene was crossed into the mice to knockdown DKK1 (Dkk1^{tm1.1Svo}(55); fl DKK1;
149 MGI:5013423), designated DKK1 knockdown (DKK1^{+/-} or DKK1^{-/-}).

150 To knock down MVPC *in vivo*, we crossed the *Abcg2* driver/reporter strain to a mouse
151 containing a floxp stop allele regulating the expression of Diphtheria toxin A (42, 64)
152 (JAX stock# 009669). Mice were injected intraperitoneally at 10-12 weeks of age with a
153 single low dose (0.5mg) tamoxifen (T-5648; SIGMA, St. Louis MO) in sesame oil, or
154 sesame oil alone (vehicle control) (18, 46). The mice were randomized and distributed
155 as 3-5 mice per cage for studies (both male and female). These model systems, as well
156 as isolated MVPC, were validated as previously described (30, 62) and label the cells
157 with the highest expression of *Abcg2*.

158

159 **Phenotyping of pulmonary vascular dysfunction and airway physiology.**

160 Pulmonary artery pressure was documented indirectly by the measurement of right
161 ventricular systolic pressure (RVSP) coupled with quasi-static mechanical properties of
162 the lung we measured using the flexiVent invasive plethysmography system (SciREQ,
163 Inc.) as previously described (39). Histologic endpoints included muscularization and
164 microvessel density of the distal microvessels by immunostaining to detect smooth
165 muscle actin (SMA; Dako clone 1A4) or Factor 8 (A0082 DAKO) on 6-8 mice per group
166 (15). To analyze changes in distal lung structure, images of H&E stained lung sections
167 were taken on a Nikon Eclipse 80i microscope using NIS Elements AR software
168 (version 4.13). A minimum of 6-10 non-overlapping images were taken blinded at 20x
169 excluding images containing large vessels or airways. Images were then loaded into a
170 macro within Metamorph Software (version 7.5.0.0) for analysis (47). MLI was
171 calculated from the average of all the images.

172

173 **Quantitation of collagen.** 10 fields of view per two sections, four sections per mouse of
174 trichrome stained mouse lungs were photographed at 40x mag. Resulting color images
175 were scanned to quantitate the number and intensity of blue (collagen) positive pixels
176 relative to red. Images were scanned using Fiji (Image J; version 2.0.0-rc-43/1.51a)
177 using a custom plug in written by M. Majka (Denver,CO). The tool was written in the
178 ImageJ macro language to detect pixels with a blue intensity over a desired threshold.
179 This macro set all pixels that had the desired blue intensity to the color yellow and
180 outputs a count of the number of yellow pixels. The specified threshold limit was based
181 on a positive and negative control image.

182

183 **Imaging.** Epifluorescent and brightfield images were captured with Nikon Eclipse 90i
184 upright epifluorescence or Nikon Eclipse TS100 using the Nikon DS-Fi1 camera with
185 NIS elements AR 4.11.00 acquisition software. The BZ-X800 KEYENCE system, with
186 capture and analysis software, was also used. Fluorochromes used included DAPI (to
187 label nuclei), secondary antibodies conjugated to Alexa 488 or Alexa 594
188 (ThermoFisher, Hampton, NH).

189

190 **RNA Isolation and qPCR.** qRT-PCR was performed in triplicate or with an n of three or
191 greater independent patient samples. Briefly, total RNA was prepared with Qiagen RNA
192 Isolation Kit reagents (Qiagen, Valencia, CA) for total RNA isolation and analysis of
193 gene expression. Complimentary DNA generated from amplified RNA was hybridized to
194 duplicate Affymetrix (Santa Clara, CA) Human Gene 1.0 ST arrays. To determine the
195 cellular response to the DKK1, cells were plated at a concentration of 60,000 cells per

196 well in medium containing 20% serum. The cells were allowed to remain in 20% serum
197 medium for 24 hours. After 24 hours, the medium was changed to 20% serum
198 treatment medium containing 50, 100, or 150 ng/mL DKK1 (Origene, Rockville, MD).
199 SMC were treated with 100ng/mL of Wnt5A. RNA lysates were collected at 48 hours
200 and protein lysates were collected at 72 hours for analyses of gene and protein
201 expression. qRT-PCR assays were performed in triplicate (for each of the wells
202 collected) and levels of analyzed genes were normalized to hypoxanthine
203 phosphoribosyltransferase abundance (GAPDH or HPRT) using available TaqMan
204 primer sets.

205

206 **ECIS.** Human lung MVECs (Lonza, Walkersville) were plated at a concentration of
207 112,500 cells per well on gelatin coated 8W1E PET ECIS culture ware arrays (Applied
208 Biophysics, Troy) overnight to achieve confluence. The following day, MVPCs were
209 added at a concentration of 37,500 cells per well. Prior to experiments the optimal
210 concentration of MVEC and ratio of MVPC was determined. MVPC lines were
211 normalized by cell number. Controls for these experiments included untreated MVEC
212 and MVEC with wounding. On the third day, the arrays were put on the ECIS ZTheta,
213 Applied Biophysics (Troy, NY). Resistance recordings were performed at 4 kHz every
214 10 minutes over 24 hours. At 2-3 hours, an electrical wound was created by
215 administering a 20 second pulse at 60,000 Hz. In some cases, the pulse was
216 immediately repeated to ensure cell death. In other experiments not including MVPC, a
217 total 150,000 MVEC were applied per well and allowed to adhere overnight. A
218 concentration of 100ng/mL of DKK1 was applied to the MVEC monolayer the next day,

219 6 hours prior to wounding. Recovery from wounding in all experiments was normalized
220 to the first resistance value data collected subsequent to wounding. These experiments
221 were performed with two sample replicates and repeated twice.

222

223 **Spheroid assays and quantitation.** Confluent WT and β OE MVPCs were passaged
224 for spheroid formation. A micro-mold (MicroTissues Inc. #24-906) was used to create a
225 2% agarose three-dimensional petri dish containing 96 individual recesses which allow
226 cells to self-assemble into spheroids. 3D petri dishes were pre-treated with 1 mL of
227 culture medium for 45 minutes (3 treatments of 15 minutes each) prior to cell seeding in
228 a 24 well plate. MVPCs were seeded into the 3D dish at a density of 500 cells per well
229 in 75 μ L total volume per the manufacturer's recommendation. Cells were allowed to
230 settle for 30 minutes before adding 1 mL of endothelial medium to the area surrounding
231 the 3D dish. Cells were allowed to form spheroids for 24 hours, at which point the
232 endothelial medium was aspirated and replaced with fresh medium containing either
233 100 ng/mL DKK1 or no DKK1. Cells were then cultured overnight with or without DKK1.
234 Spheroids were collected by aspirating the medium surrounding the 3D petri dish and
235 pipetting 500 μ L of pre-warmed medium into the mold to dislodge spheroids. Spheroid-
236 containing medium was collected into a 15 mL conical tube and centrifuged for 5
237 minutes at 110 x g. Supernatant was aspirated, and spheroids were resuspended in a
238 solution of 2 mg/mL rat tail collagen (Gibco A10483-01) combined with an equal volume
239 of 0.5% 4,000 cP methylcellulose solution (Sigma M0512) in endothelial medium.
240 Spheroids were then pipetted in 1 mL volumes to a new 24 well plate and incubated for
241 30 minutes to polymerize the collagen before adding 500 μ L of culture medium with or

242 without DKK1 to each well. After 24 hours, spheroids were imaged on a Keyence BZ-
243 X810 digital fluorescent microscope. Keyence BZ-X800 software was used to measure
244 the migration radius of cells from the center of the spheroid.

245

246 **Statistical analysis.** Data were analyzed by one-way ANOVA followed by Tukey's HSD
247 post-hoc analysis. Murine qPCR and patient samples were analyzed using
248 nonparametric Wilcoxon/Kruskal Wallis and a chi square approximation. All analyses
249 used JMP version 9.0.2. Data presented as +/- standard error from the mean (+/-SEM).
250 Significance was defined as p-value <0.05*, p-value <0.01** or p-value <0.001***.

251

252

253 **Results**

254 Vascular localization and altered expression of DKK1 is apparent in a variety of
255 CLD, including PAH, COPD/emphysema and IPF (29, 30, 62). While initially described
256 as an inhibitor of canonical Wnt signaling, the functions of DKK1 are concentration and
257 cell type specific (16, 17, 37, 53, 54, 60). Because MVPC are a central component of
258 the microvascular niche and participate in de novo angiogenesis in response to injury
259 (30), we evaluated the effects of DKK1 on sprouting angiogenesis using a three-
260 dimensional spheroid assay, comparing wild-type (WT) to Wnt activated (β OE) murine
261 MVPC. We found that DKK1 administration did not affect sprouting or migration of the
262 WT MVPC at 24 hours (**Figure 1**). In contrast, the Wnt activated β OE MVPC
263 demonstrated significant increases in sprouting and migration upon treatment (**Figure**
264 **1A**). DKK1 differentially affected the sprouting and migration of murine MVPC based on
265 their Wnt/ β -catenin signaling status.

266 To analyze the effects of DKK1 on the microvascular niche *in vivo*, we genetically
267 depleted the expression of lung MVPC DKK1 via knock down (KD) of one or both alleles
268 ($\text{DKK1}^{+/-}$ & $^{-/-}$) *in vivo*. DKK1^{KD} decreased the number of MVPC identified by lineage
269 tracing, confirmed by flow cytometry to detect CD45^{neg} GFP^{pos} cells in single cell
270 suspensions of lung tissue (**Figure 1C&D**). Cell lines were isolated and cultured from
271 each strain as previously described (30, 62). Spheroid analysis of cell sprouting
272 suggested that DKK1^{KD} cells exhibit decreased migration (**Figure 1E&F**). Decreased
273 expression of DKK1 was confirmed by immunostaining of cytopins from WT or DKK1^{KD}
274 primary cell lines (**Figure 1G**).

275 We next compared the resulting lung function and structure from mice with
276 activated Wnt signaling (β OE) or DKK1 KD in MVPC or WT. Both DKK1^{KD} (DKK1^{+/-} & ^{-/-})
277 and Wnt activation (β OE) in MVPC resulted in a statistically significant trend of altered
278 lung mechanics characterized by decreased compliance (Crs), increased elastance
279 (Ers), and a downward shift in pressure volume loops (**Figure 2A-E**). Changes in airway
280 physiology were independent of significant alterations to the right ventricular systolic
281 pressure (RVSP) or Fulton's index (RV/LV+S; **Figure 3A&B**), indications of significant
282 vascular remodeling or the development of pulmonary hypertension (PAH). Subtle
283 alterations in lung mechanics is typically associated with changes in matrix and fibrosis,
284 so we next evaluated the lung parenchyma. Lineage tracing of lung MVPC revealed
285 that they did not express smooth muscle alpha actin (SMA; **Figure 2F-H**). However,
286 enhanced SMA expression was localized to the interstitium in both β OE and DKK1^{KD}
287 lung tissue alluding to the presence of myofibroblasts. Trichrome staining to detect
288 collagen deposition and blinded quantitation using Fiji analysis revealed increased
289 collagen in the interstitium of β OE and DKK1^{+/-} lung tissue relative to WT (**Figure 2I-O**).
290 The increased collagen and tissue mechanics correlated to decreased MLI in the
291 DKK1^{KD} tissue (**Figure 3J**). Interestingly, DKK1^{KD} lungs also exhibited increased fully
292 muscularized and total microvessels relative to WT and β OE (**Figure 2P-R**).

293 Congruous to these findings, we have previously reported that Wnt activated
294 β OE MVPC express increased DKK1 while lungs exhibited decreased muscularization,
295 SMA expression as well as contractility (30, 62). Therefore, we next evaluated the effect
296 of Dkk1 depletion in a murine model of hypoxia induced pulmonary hypertension (PAH),
297 which is characterized by changes in microvascular structure and function. The mouse

298 strains all responded to hypoxia exposure (10% Denver altitude) with increased Fulton's
299 index, RVSP and hematocrit (**Figure 3A-C**). In terms of airway physiology, the most
300 significant changes were in the hypoxia exposed DKK1^{KD} mice, relative to the room air
301 (RA) DKK1^{KD} mice (**Figures 2A-D and 3D-G**). The hypoxia exposed DKK1^{KD} mice
302 exhibited increased IC ($p < 0.0001^{***}$), Crs ($p < 0.0002^{***}$), Ers ($p < 0.0013^{**}$) and a
303 downward shift in pressure volume loops relative to RA (**Figure 3H**). This relative
304 "normalization" in function and levels approaching WT were related to a loss of distal
305 lung tissue structure indicated by increased mean linear intercept (MLI; **Figure 3I**).

306 Our data suggest that MVPC expression of DKK1 influences the
307 microvasculature as well as tissue structure. Therefore, it is reasonable to speculate
308 that the function of MVPC is regulated by the disease microenvironment, to influence
309 the microvasculature. DKK1 expression by MVPC varies depending on the CLD (29,
310 30). *DKK1* transcript expression is increased in Wnt activated murine MVPC which
311 correlates with increased levels in COPD MVPC (62). DKK1 is known to have varying
312 effects on Wnt activation as well as angiogenesis, in a concentration and receptor
313 dependent fashion (17, 19, 53). Thus, we sought to evaluate the effects of DKK1 on the
314 angiogenic phenotypes of normal compared to COPD lung MVEC, COPD lung MVPC
315 as well as normal lung vascular SMC (**Figures 4&5**).

316 We first examined the expression of DKK1 receptors by normal and COPD
317 MVEC. Individual MVEC isolates from COPD lung explants varied in their expression of
318 *CKAP4* (**Figure 4A**), facilitating the comparison between lines with low or high levels of
319 receptor expression. In addition to *CKAP4* expression, there were additional baseline
320 differences between the CKAP4^{low} and CKAP4^{high} COPD MVEC lines, including their

321 expression of *AXIN2*, *ACTA2*, *TAGLN* and *ROR2*. We next tested the effect of DKK1 on
322 primary human lung MVEC phenotype and function based on their expression of
323 CKAP4. The CKAP4^{low} and CKAP4^{high} COPD MVEC responded to DKK1 with opposite
324 trends in the expression of *ACTA2*, *TAGLN* and *SLIT2* (**Figure 4A**). In the CKAP4^{high}
325 COPD MVEC, DKK1 treatment decreased both *CKAP4* and *ROR2* receptor expression.
326 The ability of MVEC to form a functional barrier was next evaluated following electrical
327 wounding, in the absence or presence of DKK1 (**Figure 4B-E**). Following wounding,
328 normal and CKAP4^{low} MVEC recovered their barrier function at a faster rate than the
329 CKAP4^{high} COPD MVEC (**Figure 4B**). However, both the CKAP4^{low} and CKAP4^{high}
330 COPD MVEC plateaued at a much lower resistance than MVEC from healthy donors,
331 suggesting that COPD MVEC either migrate more slowly or do not form a stable barrier.
332 The presence of DKK1 decreased the rate at which barrier function was regained
333 following injury in normal and CKAP4^{high} COPD MVEC (**Figure 4C&E**). DKK1 had no
334 measurable effect on the CKAP4^{low} COPD MVEC (**Figure 4D**). Since DKK1 had no
335 effect on MVEC proliferation (not shown), these data suggest DKK1 impacted the
336 MVEC migration and barrier formation. Thus, elevated levels of DKK1 in COPD and
337 emphysema may decrease vascular integrity, both important in angiogenesis as well as
338 overall tissue repair.

339 Similar to MVEC, DKK1 affected MVPC in a dose dependent and cell specific
340 manner. Exogenous DKK1 had no effect on the canonical Wnt targets *AXIN2* and
341 *PROX1* in MVPC from healthy individuals, however it increased the expression of both
342 targets in COPD MVPC at the lower dose (**Figure 5A**). While counterintuitive, we
343 hypothesized that this effect was likely receptor dependent. Indeed, we found that

344 COPD MVPC had significantly increased levels of *CKAP4* and *ROR2*, the receptors for
345 *DKK1* and *WNT5A*, respectively (11, 37, 48). The expression of both receptors,
346 however, was downregulated by *DKK1* (**Figure 5A**).

347 Since *DKK1* and Wnt signaling play a major role in vSMC developmental
348 specification, and since MVPC likely impact vascular SMC remodeling function in the
349 microvascular niche, we next defined the effect of *DKK1* on isolated human lung SMC
350 (22). *DKK1* did not increase the canonical Wnt targets *AXIN2* and *PROX1* (**Figure 5B**).
351 SMC expressed both *CKAP4* and *ROR2* and responded to *DKK1* with significant
352 decreases in the contractile cytoskeletal transcripts *ACTA2* and *TAGLN* (**Figure 5B**).
353 These data further support findings in our murine model in which Wnt activation in
354 MVPC resulted in a loss of microvascular associated smooth muscle alpha actin
355 expression. Additionally, we analyzed the effect of *WNT5A* on SMC phenotype
356 because, first, *DKK1* and *WNT5A* reciprocally regulate each other's activity, secondly,
357 both COPD MVPC and murine Wnt activated MVPC express increased levels of
358 *WNT5A* (62) and lastly, COPD MVPC expressed increased level of the *WNT5A*
359 receptor, *ROR2* (**Figure 5A**). Similar to *DKK1*, *WNT5A* decreased expression of the
360 cytoskeletal proteins *ACTA2* and *TAGLN* while not affecting *AXIN2* (**Figure 5B**). Taken
361 together these data illustrate cell specific effects of the MVPC production of the Wnt
362 modulator *DKK1* within the microvascular niche (**Figure 6**).

363

364 **Discussion**

365 The differential expression of DKK1 by human and murine Wnt activated MVPC
366 suggested a potential mechanism for paracrine regulation of the microvascular niche
367 during the development of CLDs (28-30, 62). In this study, we show that depletion of
368 DKK1 in *Abcg2*^{pos} lung mouse adult tissue resident vascular precursors (MVPC) alters
369 lung mechanics, parenchymal collagen deposition as well as of microvessel
370 muscularization and density. To complement the *in vivo* mouse modeling, we have
371 identified cell or disease specific responses to DKK1, in primary COPD MVPC as well
372 as COPD MVEC, supporting a paradoxical disease specific response of cells to well-
373 characterized factors. DKK1 also regulated the expression of contractile determinants
374 by lung vascular SMC. Responses to DKK1 were dose dependent and correlated with
375 varying expression of the DKK1 receptor, *CKAP4*.

376 While DKK1 is known to regulate lung branching morphogenesis (17, 22, 31), our
377 results suggest that DKK1 exerts effects on the angiogenic potential of lung MVPC
378 depending on their level of active canonical Wnt signaling. Wnt activated MVPC
379 respond to DKK1 stimulation with enhanced sprouting and migration, relative to wild-
380 type MVPC. Our previous work also demonstrated that primary lung MVPC from normal
381 versus Wnt activated-pulmonary hypertension patients respond differently to DKK1, with
382 the disease cells expressing increased levels of collagen and fibronectin as well as
383 smooth muscle alpha actin (29). Thus, the proangiogenic effects of DKK1 with activated
384 Wnt signaling may be dependent on MVPC expression of Wnt target genes, matrix or
385 integrins.

386 Selective depletion of DKK1 expression by MVPC in adult mice resulted in
387 decreased lung function indicative of altered lung mechanics in the absence of
388 detectable changes in cardiovascular physiology. The detrimental changes in
389 physiology were correlated to increased appearance of myofibroblasts and parenchymal
390 collagen in the lung tissue as well as decreased MLI and number of MVPC. Previous
391 studies also link decreased MVPC with increased MLI and the development of
392 emphysema(62). Interestingly, Wnt activation in MVPC yielded a similar effect on the
393 lungs, to a lesser degree. In the presence of vascular injury induced by the exposure of
394 the strains to hypoxia driven PAH, resulted in loss of tissue structure in the DKK1^{+/-}
395 strain. Both results indicating the significance of spatiotemporal regulation of Wnt
396 signaling and DKK1 expression by MVPC. Our current studies are directed toward
397 understanding how DKK1 regulated parenchymal mechanics may result in loss of tissue
398 structure and whether DKK1 or receptor distribution determine whether fibrosis or
399 emphysema develop. We speculate that regional changes in DKK1 or CKAP4
400 expression could explain why one patient develops both fibrosis and emphysema in
401 combined pulmonary fibrosis and emphysema (CPFE), which is distinct from fibrosis or
402 emphysema alone (3, 44).

403 The activation, migration or proliferation of myofibroblasts as well as subsequent
404 collagen deposition is attenuated by DKK1 expression likely via reciprocal inhibition of
405 canonical Wnt signaling (1, 56). DKK1 also regulates the profibrogenic TGF- β , platelet
406 derived growth factor (PDGF) and connective tissue growth factor (CTGF) signaling
407 pathways in myofibroblasts and vascular cells by inhibiting activated MAPK and JNK
408 signaling cascades (56). In addition, TGF- β stimulates canonical Wnt signaling in a p38-

409 dependent manner by decreasing the expression of the Wnt antagonist Dickkopf-1,
410 conversely increased DKK1 expression attenuates TGF driven fibrosis (1). Increased
411 expression of DKK1 with subsequent inhibition of Wnt signaling following treatment may
412 be used as a prognostic marker of improvement in SSC (20, 67). Thus, it is not
413 surprising that differential expression of DKK1 has been demonstrated in tissue from
414 IPF and systemic sclerosis patients (1, 54).

415 An additional characteristic of CLDs is abnormal microvascular remodeling and
416 angiogenesis (41, 65). We found that with decreased MVPC DKK1 expression, there
417 was both increased microvessel muscularization and density, absent in the other
418 groups. DKK1 appears to direct lung vSMC homeostasis by regulating smooth muscle
419 alpha actin expression (22, 31, 66). Converse to the *in vivo* result, *in vitro*, exogenous
420 DKK1 also decreased the expression of contractile proteins in vSMC. These data also
421 support the hypothesis that the increased levels of DKK1 produced by both β OE MVPC
422 and COPD MVPC decrease the SMA^{POS} vSMC in Wnt activated MVPC lungs (30, 62),
423 influencing SMC phenotype as well as function. During microvessel regression, vascular
424 SMC may also express lower levels of SMA, exhibiting loss of the contractile phenotype
425 as opposed to apoptosis (45). Taken together these results support that MVPC
426 production of DKK1 likely influences vascular SMC phenotype and function.

427 The role for DKK1 in angiogenesis is well supported (16, 17, 53, 60), however
428 the mechanisms are not well defined. These studies show a cell specific effect of DKK1
429 on primary human lung MVEC from normal and COPD patients. The cells expressed
430 heterogenous levels of the DKK1 receptor, CKAP4 and exhibited significant differences
431 in the ability to migrate and repair barrier function. Decreased barrier repair in the

432 presence of DKK1 correlated to increased expression of CKAP4. Previous studies have
433 linked DKK1 dependent endothelial cell migration in collagen to the expression of β 1
434 integrin and level of canonical Wnt signaling (9). More recently, CKAP4 was shown to
435 interact with β 1 integrin and coordinate integrin recycling and subsequent cell adhesion
436 and migration (52). COPD MVPC express increased levels of CKAP4 as well as the
437 Wnt5A receptor, ROR2. They respond to DKK1 in a concentration specific manner, at
438 low concentrations Wnt signaling is enhanced. Together these data suggest a role for
439 Wnt-DKK1-CKAP4 signaling in microvascular angiostasis as well as angiogenesis.

440 In conclusion, our results provide new insight into MVPC expression of DKK1 in
441 the microvascular niche during lung homeostasis. Ongoing studies in our lab are
442 designed to better understand the complexity of this niche and interactions at a single
443 cell level, DKK1 regulation of the inflammatory repertoire in lung as well as impacts on
444 epithelial cells in the distal lung. Because CKAP4 was differentially expressed in COPD
445 MVPC versus normal as well as heterogeneously in COPD MVEC, it appeared a
446 reasonable regulatory candidate to further evaluate to understand the role of Wnt and
447 DKK1 signaling in the microvascular niche during tissue homeostasis, adaptive
448 angiogenesis and during the development of CLDs.

449

450

451

452 **Acknowledgments:**

453 The authors would like to thank Dr. Jennifer Matsuda, Director, Genetics Core Facility at
454 NJH for her insight in to development, analysis and use of transgenic mouse models.
455 The authors would like to extend our greatest appreciation for the expert technical
456 assistance provided by Heather Waters, Ruth Francheschi, Desiree Garcia, Katie Kopf,
457 C. Gaskill and N. Putz.

458

459 **Conflicts of interest:**

460 J. Kropski: Although not directly related to this work, I report advisory board fees for
461 Boehringer Ingelheim, study support from Genentech, and grants from Boehringer
462 Ingelheim.

463

464

465 **FIGURE LEGENDS**

466

467 **Figure 1. DKK1 differentially affected MVPC numbers and angiogenic sprouting**

468 **depending on their Wnt signaling status.** WT or Wnt activated (β OE) MVPC

469 spheroids were plated in collagen and methylcellulose in the absence or presence of

470 DKK1 [100ng/ml] for 24 hours. The radius of sprouts and migrating cells was

471 quantitated. The experiment was repeated twice independently and a total of

472 21,21,23,24 spheroids was quantitated per group. The cell line was isolated from 10

473 pooled female mice. Scale bar = 50 μ M. **C&D.** Lungs from WT and DKK1KD MVPC

474 mice were collected 8 weeks following low dose tamoxifen induction and GFP

475 expression analyzed via **C.** lineage tracing or **D.** flow cytometry. n=4,5; Scale bar =

476 100 μ M. **E&F.** Isolated WT or DKK1 knockdown (DKK1_{KD}) MVPC spheroids were plated

477 and the radius of sprouts and migrating cells was quantitated after 48 hours. The

478 experiment was repeated twice independently and a total of 11,11 spheroids was

479 quantitated per group. The cell lines were isolated from 5 pooled female mice. Scale bar

480 = 50 μ M. Data presented as mean (+/-SEM). **G.** Cytospins were immunostained to

481 detect expression of DKK1. Scale bar = 50 μ M.

482

483 **Figure 2. Airway function in DKK1 knockdown (KD) MVPC mice demonstrated**

484 **increased lung stiffening and parenchymal collagen deposition.** FlexiVent analysis

485 measurement in WT, Wnt activated (β OE) or DKK1^{KD} MVPC mice 8 weeks following

486 low dose tamoxifen induction. FlexiVent analysis of **A.** inspiratory capacity (IC), **B.** total

487 resistance (Rrs), **C.** system compliance (Crs) and **D.** elastance (Ers). n= 10, 4, 12 mice

488 per group. **E.** Pressure volume curves and quantitation of the area under the curve. **F-H.**

489 Lineage labeling of WT, Wnt activated (β OE) or DKK1^{KD} GFP^{pos} MVPC in lung tissue. 8
490 weeks following low dose tamoxifen induction mice were sacrificed, and lungs agarose
491 inflated using constant pressure, to obtain lung tissue for histological and
492 immunofluorescent analyses. Scale bar = 100 μ M. Smooth muscle alpha actin (SMA)
493 was also localized by immunodetection. n= 5, 4, 4. **I-N.** Representative bright field
494 images of trichrome stained lung tissue (**L-N.** enlarged panels); collagen deposition is
495 visible in blue. **O.** Quantitation of parenchymal collagen via Fiji/ImageJ v2.0 2018. n= 5,
496 4, 4 mice per group. Immunostaining was performed on lung tissue sections to detect
497 smooth muscle alpha actin (SMA) and Factor 8 (F8) positive microvessels ranging from
498 0-50 micrometers in diameter. Scale bar = 100 μ M. **P.** Degree of muscularization was
499 analyzed as < 50% SMA positive being partial and >50% SMA positive, fully
500 muscularized. **Q.** Total numbers of SMA positive microvessels. **R.** F8 positive
501 microvessels per field of view (f.o.v.). Immune-positive microvessels were counted in 20
502 f.o.v. per mouse at 20x magnification. Data presented as mean (+/-SEM). n= 5, 4, 4
503 mice per group.

504

505 **Figure 3. Hypoxia exposure drives loss of lung structure in DKK1 knockdown**
506 **(KD) MVPC mice.** 2 weeks following low dose tamoxifen induction, WT, Wnt activated
507 (β OE) or DKK1^{KD} mice were randomized and exposed to relative hypoxia (10%
508 oxygen) or room air (RA) at Denver altitude for 6 weeks to induce pulmonary
509 hypertension (PAH). At 8 weeks, lungs were agarose inflated using constant pressure,
510 to obtain lung tissue for histological analyses. RVSP and FlexiVent analysis was
511 performed. Indices of PAH were analyzed including **A.** Fulton's index (RV/LV+S) and **B.**

512 RVSP measured by a pressure transducer placed in the right ventricle. **C.** Hematocrit
513 increased with hypoxia. Data presented as mean (+/-SEM). The mean is indicated by +.
514 n=10,4,12,9,5,14 mice/group. FlexiVent analysis of **D.** inspiratory capacity (IC), **E.** total
515 resistance (Rrs), **F.** system compliance (Crs) and **G.** elastance (Ers). **H.** Pressure
516 volume curves and quantitation of the area under the curve. Loss of tissue structure
517 was quantitated by **I.** analysis of MLI. Data presented as mean (+/-SEM). n= 9,5,14
518 mice per group.

519

520 **Figure 4. Effect of DKK1 on the recovery of endothelial barrier function following**
521 **injury is dependent on CKAP4.** The effects of exogenous DKK1 on human lung
522 MVEC were analyzed. **A.** Human lung MVEC, normal and COPD, were treated with 0 or
523 100 ng/ml of DKK1. qPCR analysis was performed to compare selected differences in
524 gene expression. Selected genes included the DKK1 receptor, *CKAP4*, the WNT5A
525 receptor, *ROR2*, Wnt target, *AXIN2*, the cytoskeletal elements *ACTA2*, *TAGLN* and the
526 migratory receptor ligand complex, *ROBO2*, *SLIT2*. Analysis was performed in triplicate
527 for each sample. * indicates difference from vehicle control. **B-E.** The electrical
528 wounding injury on recovery of barrier function of normal or COPD MVEC (with low or
529 high expression of *CKAP4*) in the absence or presence of DKK1 (0 or 100ng/ml) was
530 measured by ECIS. Resistance was measured (Ohms) over time. Groups were color
531 coded and are indicated in the legend. Quantitation of normalized resistance at
532 indicated time points (Δ) was presented in bar graph format. **B.** Three time points
533 indicated by Δ presented in bar graph format. * indicates difference from normal unless
534 indicated by a line. **C-E.** One time point indicated by Δ presented in bar graph format

535 Analysis was performed in duplicate or triplicate for each sample and repeated twice
536 independently. Data presented as the mean (+/-SEM). * indicates difference from
537 vehicle control.

538

539 **Figure 5. DKK1 regulates the phenotype of MVPC and SMC in a cell and dose**
540 **dependent manner.** The effects of exogenous DKK1 on human lung MVPC and SMC
541 were analyzed. qPCR analysis was performed to compare selected differences in gene
542 expression. Selected genes included the DKK1 receptor, *CKAP4*, the WNT5A receptor,
543 *ROR2*, Wnt targets, *AXIN2* and *PROX1*, and the cytoskeletal elements *ACTA2*, *TAGLN*.
544 **A.** Human lung MVPC, normal and COPD, were treated with 0 or 50 ng/ml of DKK1. *
545 indicates difference from vehicle control. **B.** Pulmonary vascular SMC were treated with
546 0 or 50 ng/ml of DKK1. Analysis was performed in triplicate for each sample. Data
547 presented as mean (+/-SEM).

548

549 **Figure 6. DKK1 regulates the individual functions of and paracrine effects**
550 **between cells of the microvascular niche, including MVPC, MVEC and SMC.** DKK1
551 regulates MVPC function depending on their Wnt/ β -catenin activation status. MVPC
552 production of DKK1 regulates lung tissue function, structure and parenchymal collagen
553 deposition which correlates to DKK1 dependent effects on microvascular
554 muscularization and density. In vitro, DKK1 regulates MVEC barrier function and
555 migration in likely through a CKAP4 dependent mechanism. It also regulates Wnt/ β -
556 catenin signaling by MVPC in a dose dependent manner. Lastly, DKK1 decreases the
557 expression of contractile proteins by vascular SMC, similar to Wnt5A.

558

559

560 **LITERATURE CITED**

- 561
- 562 1. **Akhmetshina A, Palumbo K, Dees C, Bergmann C, Venalis P, Zerr P, Horn A,**
563 **Kireva T, Beyer C, Zwerina J, Schneider H, Sadowski A, Riener M-O, MacDougald OA,**
564 **Distler O, Schett G, and Distler JHW.** Activation of canonical Wnt signalling is required for
565 TGF- β -mediated fibrosis. *Nature Communications* 3: 735, 2012.
- 566 2. **Almeida FM, Saraiva-Romanholo BM, Vieira RP, Moriya HT, Ligeiro-de-Oliveira**
567 **AP, Lopes FD, Castro-Faria-Neto HC, Mauad T, Martins MA, and Pazetti R.**
568 Compensatory lung growth after bilobectomy in emphysematous rats. *PLOS ONE* 12: e0181819,
569 2017.
- 570 3. **Antoniou KM, Margaritopoulos GA, Goh NS, Karagiannis K, Desai SR, Nicholson**
571 **AG, Siafakas NM, Coghlan JG, Denton CP, Hansell DM, and Wells AU.** Combined
572 Pulmonary Fibrosis and Emphysema in Scleroderma-Related Lung Disease Has a Major
573 Confounding Effect on Lung Physiology and Screening for Pulmonary Hypertension. *Arthritis &*
574 *Rheumatology* 68: 1004-1012, 2016.
- 575 4. **Baarsma HA, Boczkowski J, Yildirim AO, and Konigshoff M.** Fibroblast-derived
576 non-canonical WNT ligands contribute to attenuated alveolar epithelial repair in COPD.
577 *European Respiratory Journal* 44: 2014.
- 578 5. **Baarsma HA, and Königshoff M.** 'WNT-er is coming': WNT signalling in chronic lung
579 diseases. *Thorax* 72: 746-759, 2017.
- 580 6. **Baarsma HA, Skronska-Wasek W, Mutze K, Ciolek F, Wagner DE, John-Schuster**
581 **G, Heinzelmann K, Gunther A, Bracke KR, Dagouassat M, Boczkowski J, Brusselle GG,**
582 **Smits R, Eickelberg O, Yildirim A, and Konigshoff M.** Noncanonical WNT-5A signaling
583 impairs endogenous lung repair in COPD. *The Journal of Experimental Medicine* 214: 143,
584 2017.
- 585 7. **Baarsma HA, Spanjer AIR, Haitsma G, Engelbertink LHJM, Meurs H, Jonker MR,**
586 **Timens W, Postma DS, Kerstjens HAM, and Gosens R.** Activation of WNT / β -Catenin
587 Signaling in Pulmonary Fibroblasts by TGF- β 1 Is Increased in Chronic Obstructive Pulmonary
588 Disease. *PLoS ONE* 6: e25450, 2011.
- 589 8. **Baetta R, and Banfi C.** Dkk (Dickkopf) Proteins. *Arteriosclerosis, Thrombosis, and*
590 *Vascular Biology* 39: 1330-1342, 2019.
- 591 9. **Barbolina MV, Liu Y, Gurler H, Kim M, Kajdacsy-Balla AA, Rooper L, Shepard J,**
592 **Weiss M, Shea LD, Penzes P, Ravosa MJ, and Stack MS.** Matrix rigidity activates Wnt
593 signaling through down-regulation of Dickkopf-1 protein. *The Journal of biological chemistry*
594 288: 141-151, 2013.
- 595 10. **Barratt S, and Millar A.** Vascular remodelling in the pathogenesis of idiopathic
596 pulmonary fibrosis. *QJM: An International Journal of Medicine* 107: 515-519, 2014.
- 597 11. **Bhavanasi D, Speer KF, and Klein PS.** CKAP4 is identified as a receptor for Dickkopf
598 in cancer cells. *The Journal of Clinical Investigation* 126: 2419-2421, 2016.
- 599 12. **Birbrair A, Zhang T, Files D, Mannava S, Smith T, Wang Z-M, Messi M, Mintz A,**
600 **and Delbono O.** Type-1 pericytes accumulate after tissue injury and produce collagen in an
601 organ-dependent manner. *Stem Cell Research & Therapy* 5: 122, 2014.
- 602 13. **Carmeliet P.** Mechanisms of angiogenesis and arteriogenesis. *Nat Med* 6: 389-395.,
603 2000.
- 604 14. **Carmeliet P, and Jain RK.** Molecular mechanisms and clinical applications of
605 angiogenesis. *Nature* 473: 298-307, 2011.

- 606 15. **Case D, Irwin D, Ivester C, Harral J, Morris K, Imamura M, Roedersheimer M,**
607 **Patterson A, Carr M, Hagen M, Saavedra M, Crossno J, Jr., Young KA, Dempsey EC,**
608 **Poirier F, West J, and Majka S.** Mice deficient in galectin-1 exhibit attenuated physiological
609 responses to chronic hypoxia-induced pulmonary hypertension. *Am J Physiol Lung Cell Mol*
610 *Physiol* 292: L154-164, 2007.
- 611 16. **Cheng S-L, Shao J-S, Behrmann A, Krczma K, and Towler DA.** Dkk1 and Msx2-
612 Wnt7b Signaling Reciprocally Regulate The Endothelial-Mesenchymal Transition In Aortic
613 Endothelial Cells. *Arteriosclerosis, thrombosis, and vascular biology* 33:
614 10.1161/ATVBAHA.1113.300647, 2013.
- 615 17. **Choi H-J, Park H, Lee H-W, and Kwon Y-G.** The Wnt pathway and the roles for its
616 antagonists, DKKS, in angiogenesis. *IUBMB Life* 64: 724-731, 2012.
- 617 18. **Chow K, Fessel JP, KaoriIhida S, Schmidt EP, Gaskill C, Alvarez D, Graham B,**
618 **Harrison DG, Wagner DH, Nozik-Grayck E, West JD, Klemm DJ, and Majka SM.**
619 Dysfunctional resident lung mesenchymal stem cells contribute to pulmonary microvascular
620 remodeling. *Pulmonary Circulation* 3: 31-49, 2013.
- 621 19. **Cselenyi CS, and Lee E.** Context-Dependent Activation or Inhibition of Wnt-B-Catenin
622 Signaling by Kremen. *Science Signaling* 1: pe10, 2008.
- 623 20. **Daoussis D, Tsamandas A, Antonopoulos I, Filippopoulou A, Papachristou DJ,**
624 **Papachristou NI, Andonopoulos AP, and Liossis S-N.** B cell depletion therapy upregulates
625 Dkk-1 skin expression in patients with systemic sclerosis: association with enhanced resolution
626 of skin fibrosis. *Arthritis Research & Therapy* 18: 118, 2016.
- 627 21. **de Jesus Perez VA, Alastalo TP, Wu JC, Axelrod JD, Cooke JP, Amieva M, and**
628 **Rabinovitch M.** Bone morphogenetic protein 2 induces pulmonary angiogenesis via Wnt-beta-
629 catenin and Wnt-RhoA-Rac1 pathways. *J Cell Biol* 184: 83-99, 2009.
- 630 22. **De Langhe SP, Sala FG, Del Moral P-M, Fairbanks TJ, Yamada KM, Warburton**
631 **D, Burns RC, and Bellusci S.** Dickkopf-1 (DKK1) reveals that fibronectin is a major target of
632 Wnt signaling in branching morphogenesis of the mouse embryonic lung. *Developmental*
633 *Biology* 277: 316-331, 2005.
- 634 23. **Dejana E.** The Role of Wnt Signaling in Physiological and Pathological Angiogenesis.
635 *Circulation Research* 107: 943-952, 2010.
- 636 24. **deMello DE, and Reid LM.** Embryonic and Early Fetal Development of Human Lung
637 Vasculature and Its Functional Implications. *Pediatric and Developmental Pathology* 3: 439-449,
638 2000.
- 639 25. **Duffield JS.** The elusive source of myofibroblasts: problem solved? *Nat Med* 18: 1178-
640 1180, 2012.
- 641 26. **Fatima S, Zhou S, and Sorrentino BP.** Abcg2 Expression Marks Tissue-Specific Stem
642 Cells in Multiple Organs in a Mouse Progeny Tracking Model. *STEM CELLS* 30: 210-221, 2012.
- 643 27. **Franco CA, Liebner S, and Gerhardt H.** Vascular morphogenesis: a Wnt for every
644 vessel? *Current Opinion in Genetics & Development* 19: 476-483, 2009.
- 645 28. **Gaskill C, and Majka SM.** A high-yield isolation and enrichment strategy for human
646 lung microvascular endothelial cells. *Pulmonary Circulation* 7: 108-116, 2017.
- 647 29. **Gaskill C, Marriott S, Pratap S, Menon S, Hedges LK, Fessel JP, Kropski JA, Ames**
648 **D, Wheeler L, Loyd JE, Hemnes AR, Roop DR, Klemm DJ, Austin ED, and Majka SM.**
649 Shared gene expression patterns in mesenchymal progenitors derived from lung and epidermis in
650 pulmonary arterial hypertension: identifying key pathways in pulmonary vascular disease.
651 *Pulmonary Circulation* 6: 483-497, 2016.

- 652 30. **Gaskill CF, Carrier EJ, Kropski JA, Bloodworth NC, Menon S, Foronjy RF, Taketo**
653 **MM, Hong CC, Austin ED, West JD, Means AL, Loyd JE, Merryman WD, Hennes AR,**
654 **De Langhe S, Blackwell TS, Klemm DJ, and Majka SM.** Disruption of lineage specification
655 in adult pulmonary mesenchymal progenitor cells promotes microvascular dysfunction. *The*
656 *Journal of Clinical Investigation* 127: 2262-2276, 2017.
- 657 31. **Glaw JT, Skalak TC, and Peirce SM.** Inhibition of Canonical Wnt Signaling Increases
658 Microvascular Hemorrhaging and Venular Remodeling in Adult Rats. *Microcirculation (New*
659 *York, NY : 1994)* 17: 348-357, 2010.
- 660 32. **Gore AV, Swift MR, Cha YR, Lo B, McKinney MC, Li W, Castranova D, Davis A,**
661 **Mukouyama Y-s, and Weinstein BM.** Rspo1/Wnt signaling promotes angiogenesis via
662 Vegfc/Vegfr3. *Development* 138: 4875, 2011.
- 663 33. **Hanumegowda C, Farkas L, and Kolb M.** Angiogenesis in pulmonary fibrosis: Too
664 much or not enough? *Chest* 142: 200-207, 2012.
- 665 34. **Harada N, Tamai Y, Ishikawa T, Sauer B, Takaku K, Oshima M, and Taketo MM.**
666 Intestinal polyposis in mice with a dominant stable mutation of the beta-catenin gene. *Embo J*
667 18: 5931-5942, 1999.
- 668 35. **Hung C, Linn G, Chow Y-H, Kobayashi A, Mittelsteadt K, Altemeier WA, Gharib**
669 **SA, Schnapp LM, and Duffield JS.** Role of Lung Pericytes and Resident Fibroblasts in the
670 Pathogenesis of Pulmonary Fibrosis. *American Journal of Respiratory and Critical Care*
671 *Medicine* 188: 820-830, 2013.
- 672 36. **Keane MP.** Angiogenesis and Pulmonary Fibrosis. *American Journal of Respiratory and*
673 *Critical Care Medicine* 170: 207-209, 2004.
- 674 37. **Kimura H, Fumoto K, Shojima K, Nojima S, Osugi Y, Tomihara H, Eguchi H,**
675 **Shintani Y, Endo H, Inoue M, Doki Y, Okumura M, Morii E, and Kikuchi A.** CKAP4 is a
676 Dickkopf1 receptor and is involved in tumor progression. *The Journal of Clinical Investigation*
677 126: 2689-2705, 2016.
- 678 38. **Königshoff M, and Eickelberg O.** WNT Signaling in Lung Disease. *American Journal*
679 *of Respiratory Cell and Molecular Biology* 42: 21-31, 2010.
- 680 39. **Kopf KW, Harral JW, Staker EA, Summers ME, Petrache I, Kheifets V, Irwin DC,**
681 **and Majka SM.** Optimization of combined measures of airway physiology and cardiovascular
682 hemodynamics in mice. *Pulmonary Circulation* 10: 2045894020912937, 2020.
- 683 40. **Korn C, Scholz B, Hu J, Srivastava K, Wojtarowicz J, Arnsperger T, Adams RH,**
684 **Boutros M, Augustin HG, and Augustin I.** Endothelial cell-derived non-canonical Wnt ligands
685 control vascular pruning in angiogenesis. *Development* 141: 1757-1766, 2014.
- 686 41. **Kropski JA, Richmond BW, Gaskill CF, Foronjy RF, and Majka SM.** Deregulated
687 angiogenesis in chronic lung diseases: a possible role for lung mesenchymal progenitor cells
688 (2017 Grover Conference Series). *Pulmonary circulation* 8: 2045893217739807-
689 2045893217739807, 2017.
- 690 42. **Lee CG, Ma B, Takyar S, Ahangari F, DelaCruz C, He CH, and Elias JA.** Studies of
691 Vascular Endothelial Growth Factor in Asthma and Chronic Obstructive Pulmonary Disease.
692 *Proceedings of the American Thoracic Society* 8: 512-515, 2011.
- 693 43. **Lehmann M, Baarsma HA, and Königshoff M.** WNT Signaling in Lung Aging and
694 Disease. *Annals of the American Thoracic Society* 13: S411-S416, 2016.
- 695 44. **Lin H, and Jiang S.** Combined pulmonary fibrosis and emphysema (CPFE): an entity
696 different from emphysema or pulmonary fibrosis alone. *Journal of Thoracic Disease* 7: 767-779,
697 2015.

- 698 45. **Mancuso MR, Davis R, Norberg SM, O'Brien S, Sennino B, Nakahara T, Yao VJ,**
699 **Inai T, Brooks P, Freimark B, Shalinsky DR, Hu-Lowe DD, and McDonald DM.** Rapid
700 vascular regrowth in tumors after reversal of VEGF inhibition. *Journal of Clinical Investigation*
701 116: 2610-2621, 2006.
- 702 46. **Marriott S, Baskir RS, Gaskill C, Menon S, Carrier EJ, Williams J, Talati M, Helm**
703 **K, Alford CE, Kropski JA, Loyd J, Wheeler L, Johnson J, Austin E, Nozik-Grayck E,**
704 **Meyrick B, West JD, Klemm DJ, and Majka SM.** ABCG2(pos) lung mesenchymal stem cells
705 are a novel pericyte subpopulation that contributes to fibrotic remodeling. *American Journal of*
706 *Physiology - Cell Physiology* 307: C684-C698, 2014.
- 707 47. **McGrath-Morrow SA, Cho C, Soutiere S, Mitzner W, and Tuder R.** The Effect of
708 Neonatal Hyperoxia on the Lung of p21Waf1/Cip1/Sdi1-Deficient Mice. *American Journal of*
709 *Respiratory Cell and Molecular Biology* 30: 635-640, 2004.
- 710 48. **Minami Y, Oishi I, Endo M, and Nishita M.** Ror-family receptor tyrosine kinases in
711 noncanonical Wnt signaling: Their implications in developmental morphogenesis and human
712 diseases. *Developmental Dynamics* 239: 1-15, 2009.
- 713 49. **Niehrs C.** Function and biological roles of the Dickkopf family of Wnt modulators.
714 *Oncogene* 25: 7469-7481, 0000.
- 715 50. **Niida A, Hiroko T, Kasai M, Furukawa Y, Nakamura Y, Suzuki Y, Sugano S, and**
716 **Akiyama T.** DKK1, a negative regulator of Wnt signaling, is a target of the β -catenin/TCF
717 pathway. *Oncogene* 23: 8520-8526, 2004.
- 718 51. **Noble PW, Barkauskas CE, and Jiang D.** Pulmonary fibrosis: patterns and
719 perpetrators. *The Journal of Clinical Investigation* 122: 2756-2762, 2012.
- 720 52. **Osugi Y, Fumoto K, and Kikuchi A.** CKAP4 Regulates Cell Migration via the
721 Interaction with and Recycling of Integrin. *Mol Cell Biol* 39: 2019.
- 722 53. **Park H, Jung HY, Choi H-J, Kim DY, Yoo J-Y, Yun C-O, Min J-K, Kim Y-M, and**
723 **Kwon Y-G.** Distinct roles of DKK1 and DKK2 in tumor angiogenesis. *Angiogenesis* 17: 221-
724 234, 2014.
- 725 54. **Pfaff EM, Becker S, Gunther A, and Konigshoff M.** Dickkopf proteins influence lung
726 epithelial cell proliferation in idiopathic pulmonary fibrosis. *European Respiratory Journal* 37:
727 79, 2010.
- 728 55. **Pietilä I, Ellwanger K, Railo A, Jokela T, Barrantes IdB, Shan J, Niehrs C, and**
729 **Vainio SJ.** Secreted Wnt antagonist Dickkopf-1 controls kidney papilla development
730 coordinated by Wnt-7b signalling. *Developmental Biology* 353: 50-60, 2011.
- 731 56. **Ren S, Johnson BG, Kida Y, Ip C, Davidson KC, Lin S-L, Kobayashi A, Lang RA,**
732 **Hadjantonakis A-K, Moon RT, and Duffield JS.** LRP-6 is a coreceptor for multiple fibrogenic
733 signaling pathways in pericytes and myofibroblasts that are inhibited by DKK-1. *Proceedings of*
734 *the National Academy of Sciences of the United States of America* 110: 1440-1445, 2013.
- 735 57. **Rock JR, Barkauskas CE, Cronic MJ, Xue Y, Harris JR, Liang J, Noble PW, and**
736 **Hogan BLM.** Multiple stromal populations contribute to pulmonary fibrosis without evidence
737 for epithelial to mesenchymal transition. *Proceedings of the National Academy of Sciences* 108:
738 1475-1483, 2011.
- 739 58. **Semenov MV, Zhang X, and He X.** DKK1 Antagonizes Wnt Signaling without
740 Promotion of LRP6 Internalization and Degradation. *The Journal of Biological Chemistry* 283:
741 21427-21432, 2008.

- 742 59. **Shalaby F, Rossant J, Yamaguchi TP, Gertsenstein M, Wu XF, Breitman ML, and**
743 **Schuh AC.** Failure of blood-island formation and vasculogenesis in Flk-1-deficient mice. *Nature*
744 376: 62-66, 1995.
- 745 60. **Smadja David M, d'Audigier C, Weiswald L-B, Badoual C, Dangles-Marie V,**
746 **Mauge L, Evrard S, Laurendeau I, Lallemand F, Germain S, Grelac F, Dizier B, Vidaud**
747 **M, Bièche I, and Gaussem P.** The Wnt Antagonist Dickkopf-1 Increases Endothelial Progenitor
748 Cell Angiogenic Potential. *Arteriosclerosis, Thrombosis, and Vascular Biology* 30: 2544-2552,
749 2010.
- 750 61. **Steinhauser ML, and Lee RT.** Pericyte Progenitors at the Crossroads Between Fibrosis
751 and Regeneration. *Circulation Research* 112: 230-232, 2013.
- 752 62. **Summers ME, Richmond BW, Menon S, Sheridan RM, Kropski JA, Majka SA,**
753 **Takeito MM, Bastarache JA, West JD, De Langhe S, Geraghty P, Klemm DJ, Chu HW,**
754 **Friedman RS, Tao YK, Foronjy RF, and Majka SM.** Resident mesenchymal vascular
755 progenitors modulate adaptive angiogenesis and pulmonary remodeling via regulation of
756 canonical Wnt signaling. *The FASEB Journal* n/a: 2020.
- 757 63. **Vila Ellis L, Cain MP, Hutchison V, Flodby P, Crandall ED, Borok Z, Zhou B,**
758 **Ostrin EJ, Wythe JD, and Chen J.** Epithelial Vegfa Specifies a Distinct Endothelial Population
759 in the Mouse Lung. *Developmental Cell* 52: 617-630.e616, 2020.
- 760 64. **Voehringer D, Liang H-E, and Locksley RM.** Homeostasis and Effector Function of
761 Lymphopenia-Induced Memory-Like T Cells in Constitutively T Cell-Depleted Mice. *The*
762 *Journal of Immunology* 180: 4742-4753, 2008.
- 763 65. **Voelkel NF, Douglas IS, and Nicolls M.** Angiogenesis in Chronic Lung Disease. *Chest*
764 131: 874-879, 2007.
- 765 66. **Wang X, Adhikari N, Li Q, and Hall JL.** LDL receptor-related protein LRP6 regulates
766 proliferation and survival through the Wnt cascade in vascular smooth muscle cells. *American*
767 *Journal of Physiology - Heart and Circulatory Physiology* 287: H2376, 2004.
- 768 67. **Wei J, Fang F, Lam AP, Sargent JL, Hamburg E, Hinchcliff ME, Gottardi CJ, Atit**
769 **R, Whitfield ML, and Varga J.** Wnt/B-catenin signaling is hyperactivated in systemic sclerosis
770 and induces Smad-dependent fibrotic responses in mesenchymal cells. *Arthritis and rheumatism*
771 64: 2734-2745, 2012.
- 772 68. **Xie T, Liang J, Liu N, Huan C, Zhang Y, Liu W, Kumar M, Xiao R, DArmiento J,**
773 **Metzger D, Chambon P, Papaioannou VE, Stripp BR, Jiang D, and Noble PW.**
774 Transcription factor TBX4 regulates myofibroblast accumulation and lung fibrosis. *The Journal*
775 *of Clinical Investigation* 126: 3063-3079, 2016.
- 776 69. **Yuan K, Orcholski ME, Panaroni C, Shuffle EM, Huang NF, Jiang X, Tian W,**
777 **Vladar EK, Wang L, Nicolls MR, Wu JY, and de Jesus Perez VA.** Activation of the
778 Wnt/Planar Cell Polarity Pathway Is Required for Pericyte Recruitment during Pulmonary
779 Angiogenesis. *The American Journal of Pathology* 185: 69-84, 2015.
- 780 70. **Zeng X, Wert SE, Federici R, Peters KG, and Whitsett JA.** VEGF enhances
781 pulmonary vasculogenesis and disrupts lung morphogenesis in vivo. *Dev Dyn* 211: 215-227,
782 1998.
- 783

Figure 1

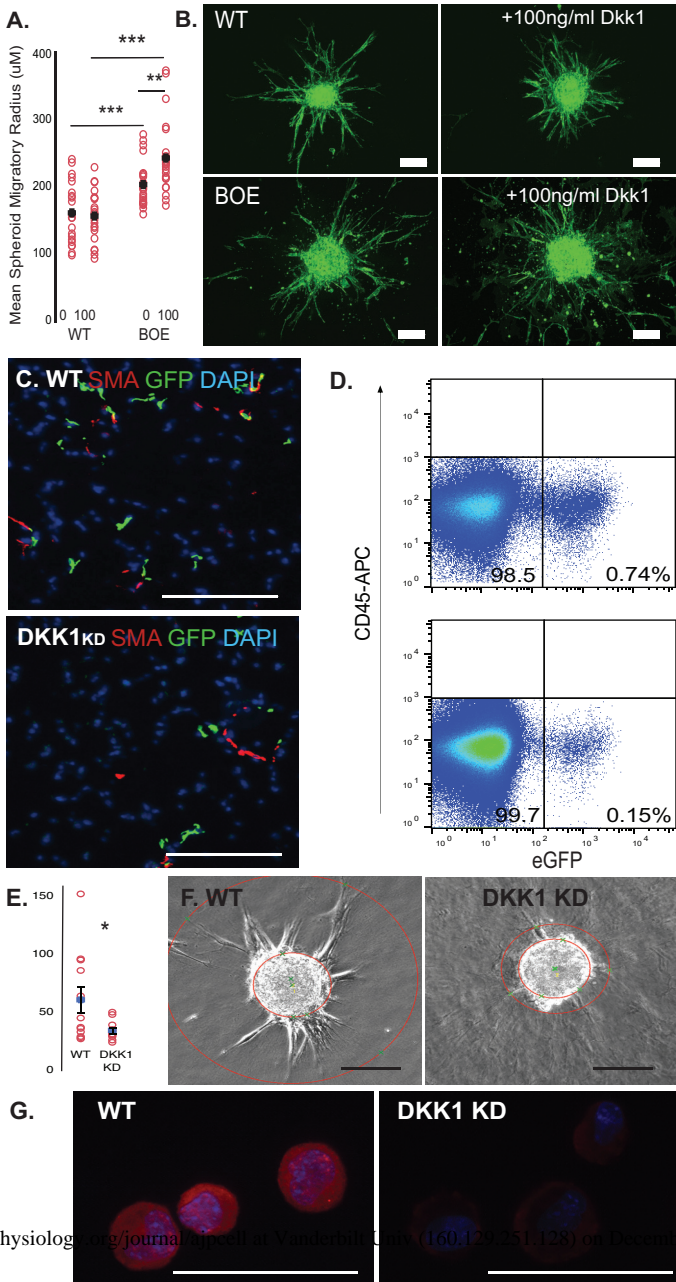


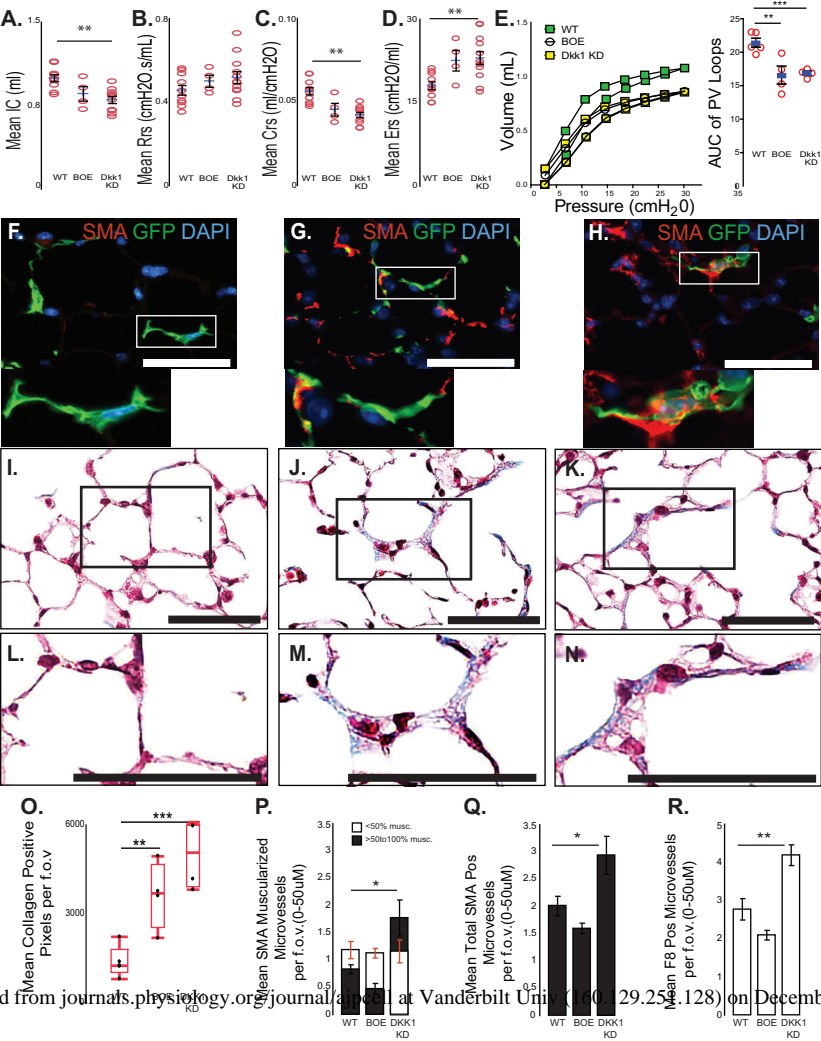
Figure 2.

Figure 3.

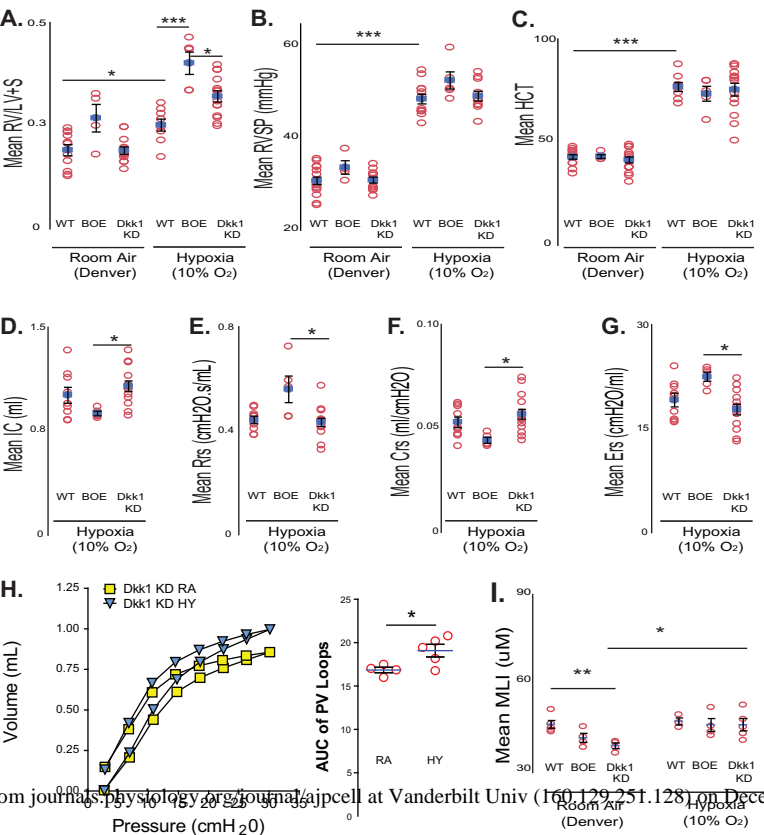
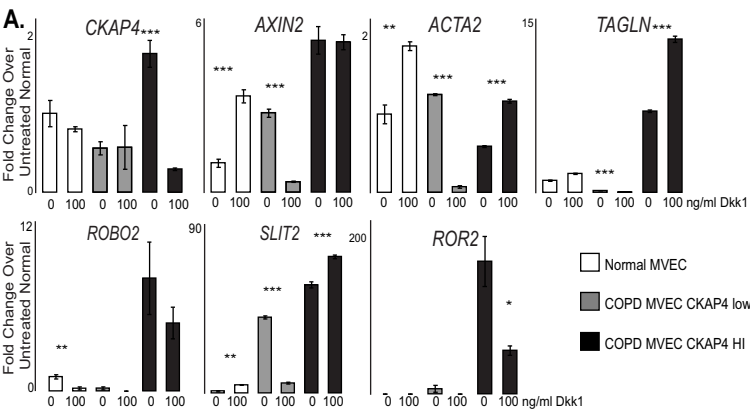
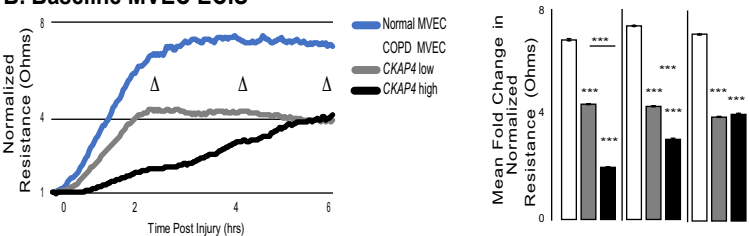


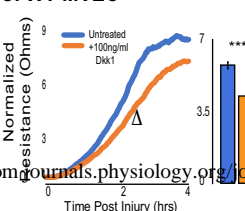
Figure 4.



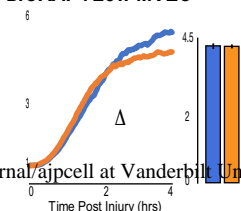
B. Baseline MVEC ECIS



C. WT MVEC



D. CKAP4 Low MVEC



E. CKAP4 High MVEC

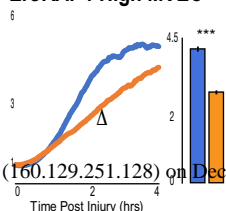
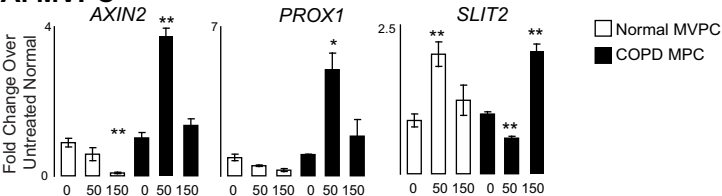


Figure 5.

A. MVPC



B. SMC

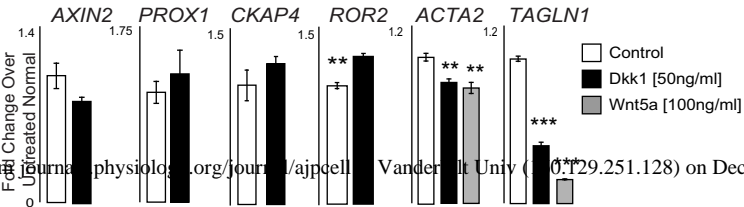
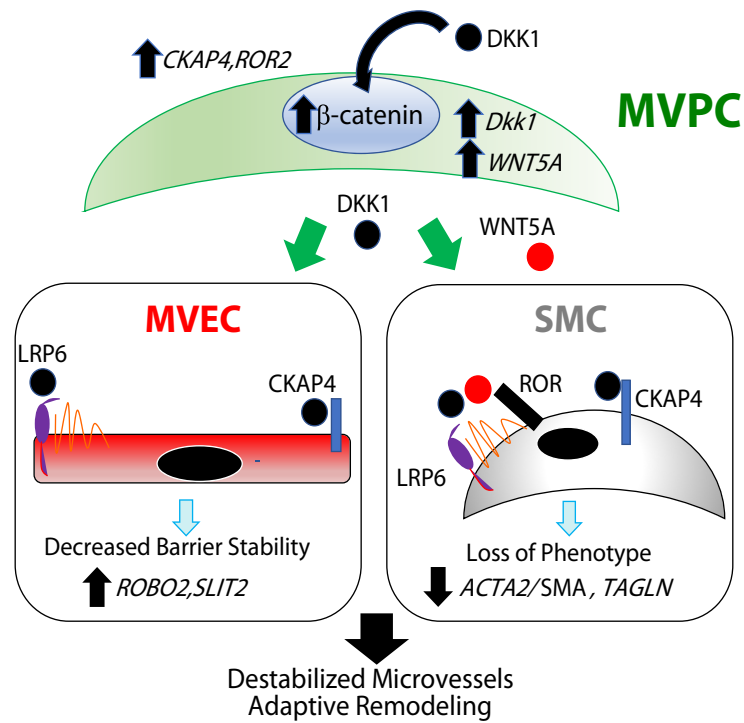


Figure 6.





Article

The BDNF rs6265 Polymorphism is a Modifier of Cardiomyocyte Contractility and Dilated Cardiomyopathy

Frank J. Raucci Jr. ^{1,2,†}, Anand Prakash Singh ^{3,†}, Jonathan Soslow ¹, Larry W. Markham ⁴, Lin Zhong ⁵, Wejdan Aljafar ⁵, Natasja Lessiohadi ⁵, Cassandra P. Awgulewitsch ⁵, Prachi Umbarkar ³, Qinkun Zhang ³, Presley L. Cannon ⁵, Maciej Buchowski ⁶, Joseph T. Roland ⁵, Erica J. Carrier ⁵, William B. Burnette ⁷, Antonis K. Hatzopoulos ⁵, Hind Lal ³ and Cristi L. Galindo ^{5,8,*}

- ¹ Thomas P. Graham Division of Pediatric Cardiology, Vanderbilt University Medical Center, Nashville, TN 37232, USA; frank.raucci@vumc.org (F.J.R.J.); jonathan.h.soslow@vumc.org (J.S.)
 - ² Division of Pediatric Cardiology, Department of Pediatrics, Children's Hospital of Richmond at Virginia Commonwealth University, Richmond, VA 23219, USA
 - ³ Division of Cardiovascular Disease, Department of Medicine, University of Alabama Birmingham School of Medicine, Birmingham, AL 35233, USA; apsingh@uabmc.edu (A.P.S.); pumbarkar@uabmc.edu (P.U.); qzhang@uabmc.edu (Q.Z.); hindlal@uabmc.edu (H.L.)
 - ⁴ Division of Cardiology, Department of Pediatrics, Riley Hospital for Children at Indiana University Health, Indianapolis, IN 46202, USA; lwmarkha@iu.edu
 - ⁵ Division of Cardiovascular Medicine, Vanderbilt University Medical Center, Nashville, TN 37232, USA; lin.zhong@vumc.org (L.Z.); wejdanaljafar@gmail.com (W.A.); Natasjalessiohadi@gmail.com (N.L.); cassandra.p.awgulewitsch@vanderbilt.edu (C.P.A.); pcannon18@outlook.com (P.L.C.); joseph.t.roland@vumc.org (J.T.R.); erica.carrier@vumc.org (E.J.C.); antonis.hatzopoulos@vumc.org (A.K.H.)
 - ⁶ Division of Clinical Pharmacology, Vanderbilt University Medical Center, Nashville, TN 37232, USA; maciej.buchowski@vumc.org
 - ⁷ Division of Pediatric Neurology, Department of Pediatrics, Vanderbilt University Medical Center, Nashville, TN 37232, USA; william.b.burnette@vumc.org
 - ⁸ Department of Biology, Western Kentucky University, Bowling Green, KY 42101, USA
- * Correspondence: cristi.galindo@wku.edu; Tel.: +1-270-745-3696
- † Equal contribution and joint first authors.

Received: 3 September 2020; Accepted: 8 October 2020; Published: 10 October 2020



Abstract: Brain-derived neurotrophic factor (BDNF) is a neuronal growth and survival factor that harbors cardioprotective qualities that may attenuate dilated cardiomyopathy. In ~30% of the population, BDNF has a common, nonsynonymous single nucleotide polymorphism rs6265 (Val66Met), which might be correlated with increased risk of cardiovascular events. We previously showed that BDNF correlates with better cardiac function in Duchenne muscular dystrophy (DMD) patients. However, the effect of the Val66Met polymorphism on cardiac function has not been determined. The goal of the current study was to determine the effects of rs6265 on BDNF biomarker suitability and DMD cardiac functions more generally. We assessed cardiovascular and skeletal muscle function in human DMD patients segregated by polymorphic allele. We also compared echocardiographic, electrophysiologic, and cardiomyocyte contractility in C57/BL-6 wild-type mice with rs6265 polymorphism and in *mdx*/mTR (mDMD) mouse model of DMD. In human DMD patients, plasma BDNF levels had a positive correlation with left ventricular function, opposite to that seen in rs6265 carriers. There was also a substantial decrease in skeletal muscle function in carriers compared to the Val homozygotes. Surprisingly, the opposite was true when cardiac function of DMD carriers and non-carriers were compared. On the other hand, Val66Met wild-type mice had only subtle functional differences at baseline but significantly decreased cardiomyocyte contractility. Our results indicate that the Val66Met polymorphism alters myocyte contractility, conferring worse

skeletal muscle function but better cardiac function in DMD patients. Moreover, these results suggest a mechanism for the relative preservation of cardiac tissues compared to skeletal muscle in DMD patients and underscores the complexity of BDNF signaling in response to mechanical workload.

Keywords: brain-derived neurotrophic growth factor; dilated cardiomyopathy; rs6365 polymorphism; Duchenne muscular dystrophy; Val66Met

1. Introduction

Brain-derived neurotrophic growth factor (BDNF) is an essential mediator of neuronal growth, differentiation, and survival and plasticity [1]. BDNF is also important for development of the cardiac microvasculature, basal cardiac contractility in the postnatal heart, and response to cardiac injury [2]. BDNF is produced as a proprotein (proBDNF), which upon cleavage releases an N-terminal fragment (prodomain) and C terminus that represents mature BDNF (mBDNF) [3]. Processed mBDNF binds to tyrosine kinase receptor B (TrkB), which transduces BDNF's mitogenic, pro-survival, and cardioprotective benefits. Proteolytic cleavage of proBDNF releases a functional N-terminal prodomain along with BDNF. Once liberated, the BDNF prodomain binds to and regulates trafficking and secretion of mBDNF [3,4].

In approximately 30% of the general population, the prodomain of BDNF has a nonsynonymous (G→A) single nucleotide polymorphism (SNP) at codon position 66 (rs6265), resulting in replacement of valine (Val) with methionine (Met) [5]. The Val66→Met substitution substantially increases the binding stability of the prodomain to mature BDNF, consequently reducing BDNF's trafficking and secretion [6,7]. Val→Met may additionally alter receptor binding and signaling of proBDNF [8], as well as confer biological activity on the secreted prodomain itself [4]. The rs6265 polymorphism has been implicated in the risk of cardiovascular disease, although results from different clinical studies are conflicting. In one study [9], the Met allele was associated with obesity in patients with coronary artery disease ($n = 206$) but not in otherwise healthy individuals ($n = 498$), whereas the Met allele was apparently protective compared to the Val/Val genotype in a separate cohort of 5510 patients assessed for severity of coronary artery disease and incidence of clinical cardiovascular disease events [10]. The potential contribution of rs6265 to human disease is further complicated by substantive variability in allelic frequency among different populations (e.g., <1% in Sub-Saharan Africans, ~7–35% in Europeans, and ~44% in Asians) [5,11,12].

We previously demonstrated an association of circulating BDNF with better heart function in a small cohort of Duchenne muscular dystrophy (DMD) patients [13]. However, when we added additional patients to our analysis, this positive relationship between BDNF levels and left ventricular ejection fraction (LVEF) was no longer significant, prompting us to investigate whether or not the BDNF rs6265 polymorphism might contribute to these extemporaneously negative findings. In this study, we tested the hypothesis that the Val→Met conversion reduces bioavailability of functional BDNF in DMD patients, thereby leading to reduced function compared to non-carriers. Although we confirmed our original findings that circulating BDNF correlates positively with cardiac function in DMD patients who express normal BDNF [13], here we show that DMD patients who are carriers of the rs6265 allele exhibit better (rather than worse) cardiac function, when compared to age-matched non-carriers. Using a knock-in mouse model (Val66Met mice), which harbors the BDNF G→A substitution, we discovered a role for the Val66Met polymorphism in modulating cardiomyocyte contractility as a possible mechanism contributing to altered heart function in the context of dilated cardiomyopathy. This is the first study implicating the rs6265 polymorphism in DMD or in skeletal muscle function in a progressively destructive neuromuscular disease.

2. Results

2.1. BDNF rs6265 (Val66Met) in DMD Patients

In a cohort of 61 DMD patients genotyped for the rs6265 allele, 61.7% (37/61) were non-carriers (GG) and 36.7% (23/61) were single allelic carriers (GA). Only one person (1/61 or 1.7%) had the Val66Met conversion for both alleles (AA) (Table 1). In a subset of patients for whom cardiac magnetic resonance (CMR) was performed and circulating BDNF levels measured, there was a modest but insignificant association ($n = 43$, $r = 0.28$, $p = 0.06$) between BDNF and LVEF (Figure 1A). This positive correlation increased substantially ($r = 0.58$) and reached significance ($p = 0.002$) for non-carriers only ($n = 25$) (Figure 1B). For carriers ($n = 18$), BDNF levels were negatively correlated with LVEF ($r = 0.28$) (Figure 1C), but this association was not statistically significant. Overall, carriers had lower mean plasma BDNF levels compared to non-carriers ($16,957 \pm 2066$ pg/mL, $n = 18$ vs. $23,217 \pm 1894$ pg/mL, $n = 25$, $p = 0.032$, Figure 1D). Carriers also had modestly higher but significant mean LVEF compared to non-carriers ($56.0 \pm 1.6\%$, $n = 23$, vs. $51.5 \pm 1.5\%$, $n = 37$, $p = 0.044$, Figure 1E) and better global circumferential strain ($-30.7 \pm 1.3\%$, $n = 23$ vs. $-26.5 \pm 1.2\%$, $n = 34$, $p = 0.017$, Figure 1F). There was not a significant difference in angiotensin converting enzyme inhibitor (ACEI)/angiotensin receptor blocker (ARB) or beta-blocker use between carriers and non-carriers, although steroid use was more common in carriers (Table 1). Interestingly, carriers had significantly lower indexed left ventricular (LV) mass (44.5 ± 1.5 g/m², $n = 23$, vs. 50.5 ± 2.0 g/m², $n = 37$, $p = 0.032$, Figure 1G) and indexed end-diastolic volumes (61.0 ± 2.5 mL/m², $n = 23$, vs. 71.1 ± 3.7 mL/m², $n = 37$, $p = 0.05$).

Table 1. Demographics by genotype. Late gadolinium enhancement (LGE) global severity score is ranked from zero (no LGE) to four (extensive involvement of septum and free wall). Group means compared with unpaired t-test for continuous variables or Mann–Whitney rank sum for non-parametric variables. Abbreviations: BSA: Body surface area, LVEF: Left ventricular ejection fraction, LVEDV: Left ventricular end diastolic volume, GCS: Global circumferential strain, GLS: Global longitudinal strain, ACEI: Angiotensin converting enzyme inhibitor, ARB: Angiotensin receptor blocker.

	GG (<i>n</i> = 37)	GA/AA (<i>n</i> = 24)	<i>p</i>
Age (years)	14.9 ± 0.7	14.9 ± 0.9	0.99
Height (cm)	150.6 ± 3.1	146.7 ± 3.0	0.39
Weight (kg)	54.3 ± 3.5	52.6 ± 3.5	0.74
BSA (m ²)	1.5 ± 0.1	1.5 ± 0.1	0.67
LVEF (%)	51.5 ± 1.5	56.1 ± 1.5	0.044
Heart Rate (bpm)	94.7 ± 2.8	101.8 ± 3.1	0.099
Indexed LV Mass (g/m ²)	50.6 ± 2.0	44.5 ± 1.5	0.032
Indexed LVEDV (mL/m ²)	71.1 ± 3.7	61.0 ± 2.5	0.05
GCS	−25.3 ± 1.8 (<i>n</i> = 34)	−30.7 ± 1.3 (<i>n</i> = 23)	0.03
GLS	−19.6 ± 0.7 (<i>n</i> = 30)	−20.4 ± 0.6 (<i>n</i> = 20)	0.39
LGE Global Severity Score	2.0 ± 0.2	1.7 ± 0.3	0.26
ACEI or ARB	32 (87%)	19 (79%)	0.49
Beta Blocker	23 (62%)	10 (42%)	0.19
Steroids	22 (60%)	21 (89%)	0.023

In order to assess differences in functional status between allelic groups, we assessed skeletal muscle strength and activity level. Skeletal muscle function was more significantly impaired in carriers, based on quantitative muscle testing (QMT) (Figure 2A), accelerometer (Figure 2C) and percentage of patients who were ambulatory (Figure 2D) relative to non-carriers of similar age (Figure 2B).

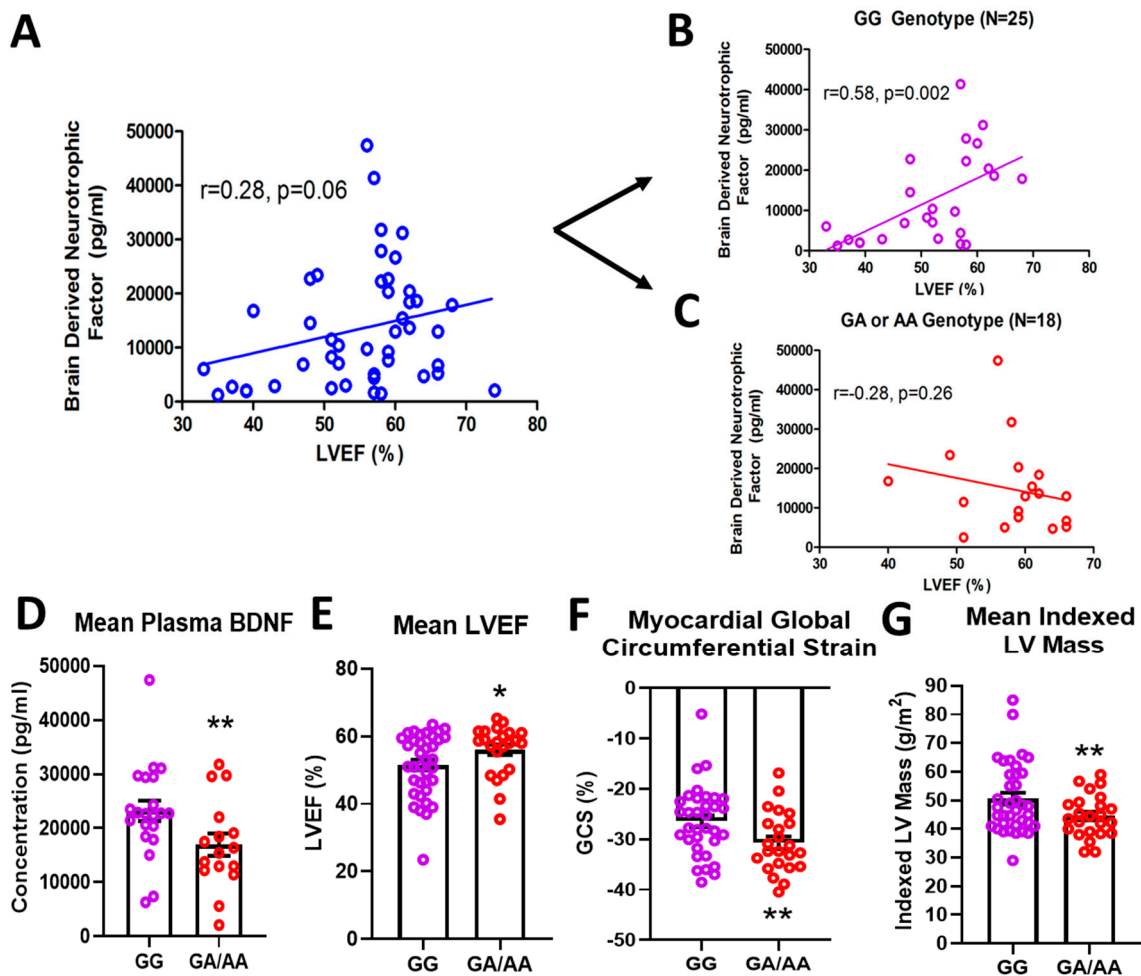


Figure 1. Effects of rs6265 polymorphism on cardiac phenotype. There is a disparate relationship between brain-derived neurotrophic factor (BDNF) levels and left ventricular ejection fraction (LVEF) for Duchenne muscular dystrophy (DMD) patients segregated by rs6265 polymorphism. (A) plot for the entire DMD subset cohort ($n = 43$) demonstrating positive correlation of plasma BDNF concentration (pg/mL) vs. LVEF (%) by cardiac magnetic resonance (CMR) ($r = 0.28$, $p = 0.06$). When segregated by rs6265 polymorphism, a similar positive correlation ($r = 0.58$, $p = 0.002$) was seen for GG (Val/Val) DMD patients (B) but a negative correlation was observed ($r = -0.28$, $p = 0.26$) for GA (Val/Met) and AA (Met/Met) DMD patients (C). GA/AA carriers had lower plasma levels of BDNF (D), higher mean LVEF ($n = 37$ vs. 24) (E), better global circumferential strain (GCS) ($n = 37$ vs. 24) (F), and lower indexed LV mass ($n = 37$ vs. 24) (G). Comparisons by two-way ANOVA or Welch's t-test. Asterisk represents statistical significance for GG versus GA/AA, * $p < 0.05$, ** $p < 0.03$. Individual patients (unsegregated) are indicated by blue circles. Purple circles indicate patients without (GG) the BDNF polymorphism. Red circles denote those patients with one (GA) or both (AA) BDNF rs6265 alleles.

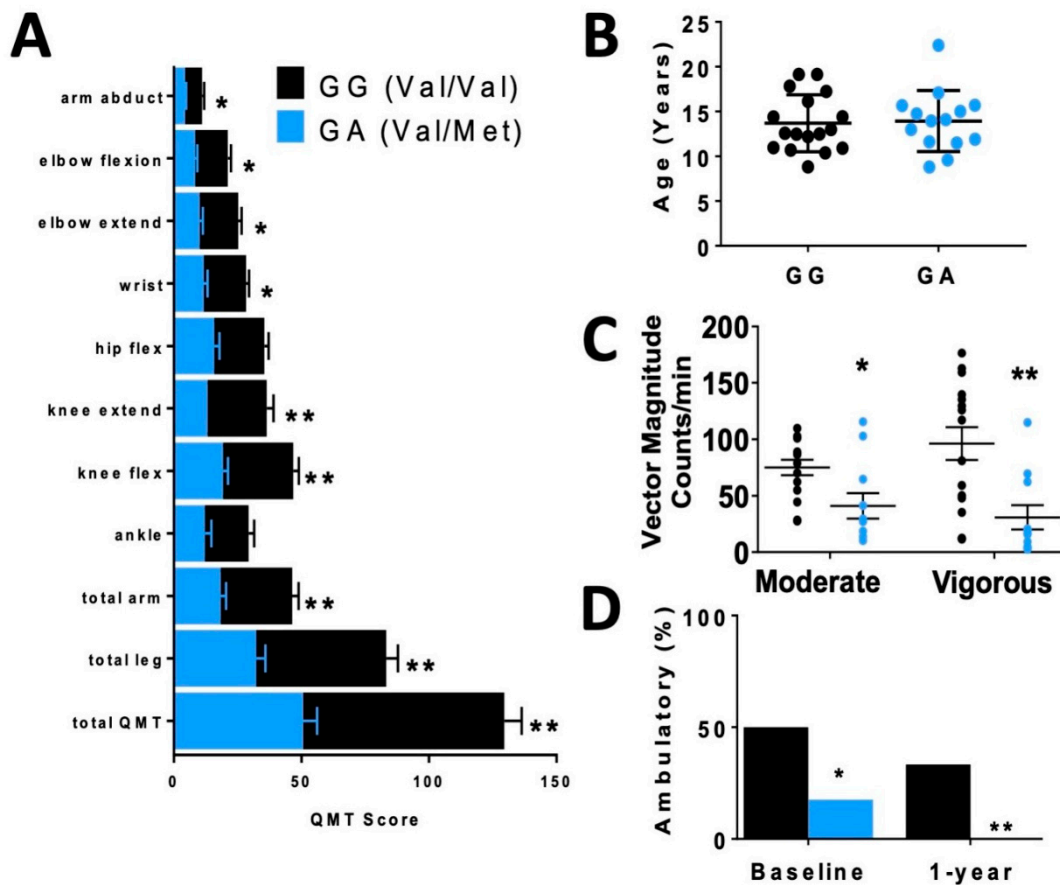


Figure 2. Disparate skeletal muscle performance in DMD patients when compared by rs6265 polymorphism. (A) Comparative bar graphs of quantitative muscle testing (QMT) scores for several muscle groups compared by rs6265 phenotype for GG (Val/Val) and GA (Val/Met). All muscle groups in the Val/Met patients showed significantly lower scores. (B) There was no difference in mean age between the phenotype groups. (C) Accelerometry data demonstrated Val/Met patients had significantly lower performance with moderate and vigorous exercise compared to Val/Val patients (41 ± 11 counts/min, $n = 11$, vs. 75 ± 7 counts/min, $n = 15$, * $p = 0.031$, and 31 ± 11 , $n = 11$, vs. 96 ± 15 , $n = 15$, ** $p = 0.003$, respectively). Comparisons by two-way ANOVA. (D) Age-similar Val/Met DMD patients were less likely to be ambulatory at baseline assessment and at 1 year follow-up.

2.2. Cardiac Characterization of Val66Met Mice

Cardiac BDNF (27kDa) was significantly higher in whole heart lysates of mice with the BDNF rs6265 (Val/Met, VM) polymorphic allele compared to non-carrier (Val/Val, V) littermate controls (Figure 3A,B). There was no significant difference in cleaved BDNF (14 kDa) between VM and V (Figure 3C). Although this finding is counter intuitive to lower circulating blood plasma levels in DMD patients (Figure 1D), the results are consistent with the reported role of the rs6265 SNP in processing and trafficking of mature BDNF in neuronal cell cultures [7]. There could be lower bioavailability of BDNF, which is suggested by a lower ratio of mature BDNF (mBDNF) to unprocessed proBDNF (Figure 3C) and histological assessment of whole heart slices (Figure 3D).

Consistent with what was observed in human DMD patients, Val/Met mice exhibited increased left ventricular (LV) ejection fraction (EF, Figure 3C) and lower LV mass (Figure 3D), as measured by echocardiography. Asterisks indicate * $p < 0.01$ or ** $p < 0.001$.

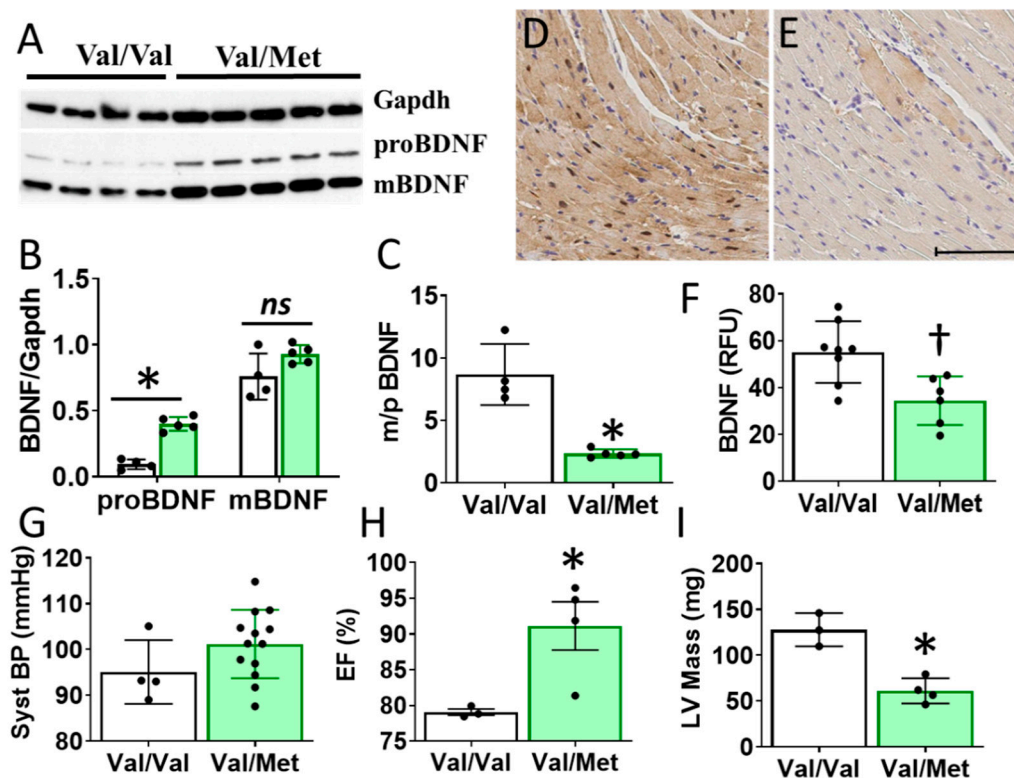


Figure 3. Val66Met mice have increased BDNF in tissue lysates and altered cardiac function as measured by echocardiography. (A) Western blot of left ventricular cardiac tissues from Val66Met mouse for proprotein brain-derived neurotrophic factor (proBDNF) (~27 kDa, middle) and mature BDNF (mBDNF) cleavage product (~14 kDa, bottom). (B) Bar graph of densitometry analysis of pBDNF and mBDNF normalized to gapdh (y axis) for Val/Val (white bars, $n = 4$) and Val/Met (green bars) ($n = 5$). (C) Bar graph showing processed BDNF as a ratio of mBDNF/proBDNF (m/p). (D,E) Anti-BDNF-DAB stained hearts from Val/Val (D) and Val/Met (E) mice at 20X magnification, scale bar = 100 μm . (F) Bar graph showing quantification of whole hearts from V ($n = 8$) and Val/Met ($n = 6$) mice relative to total tissue area. (G) Plot showing systolic blood pressure (mmHg) as measured by tail cuff for Val/Val ($n = 4$) and Val/Met ($n = 13$). (H,I) Results of echocardiography assessment of Val/Val (white bars, $n = 3$) and Val/Met (green bars, $n = 4$) mice are shown. Parameters shown (y axis) are (H) percent (%), ejection fraction (EF); (I) LV mass (corrected). Asterisks represent statistical significance for V versus VM * $p < 0.0001$ (B), * $p < 0.0006$ (C), † $p = 0.0079$ (F), * $p = 0.0302$ (H), * $p = 0.0026$ (I).

2.3. Cardiomyocyte Contractility in Val66Met Mice

To identify possible mechanisms that could account for altered cardiac functions in mice with the human BDNF rs6265 polymorphism, we performed transcriptome sequencing of whole hearts from Val66Met mice. Differentially expressed genes included myosin heavy chains, ion channels, and calcium regulators. Gene enrichment analysis revealed two notable cardiac-specific functions: heart contraction ($p = 0.0148$, see Supplementary Table S1 for additional categories) and regulation of calcium ion transport into the cytosol ($p = 2.45 \times 10^{-4}$) (Figure 4A). Consistent with sequencing results, we noted differences, although insignificant, in cardiomyocyte sarcomere shortening between Val/Met and Val/Val genotypes (Figure 4B). Peak fractional shortening and re-lengthening were significantly reduced in Val/Met cardiomyocytes, compared to those from Val/Val littermate controls (Figure 4C,D).

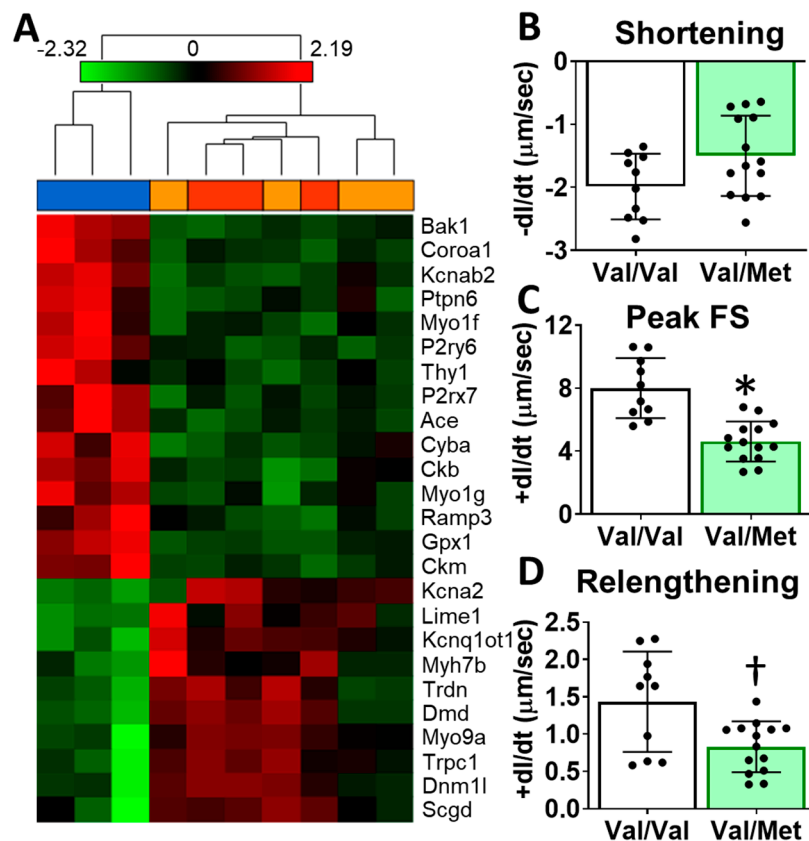


Figure 4. Val66Met mice have altered cardiac tissue gene expression of contractile proteins and reduced cardiomyocyte contractility. **(A)** Hierarchical cluster of cardiac-associated genes identified as significantly differential (FDR-corrected $p < 0.01$, fold-difference > 1.5) using deep sequencing. Vertical dendrograms and columns represent individual samples from whole hearts of Val/Val (blue), Val/Met (orange), and Met/Met (red) mice. Rows represent individual transcripts, indicated by official gene symbol. Heat map colors represent the highest (bright red), lowest (bright green) and median (black) expression levels. **(B–D)**, Contractility measurements of isolated cardiomyocytes from Val/Val (V, white bars, $n = 10$) and Val/Met (VM, green bars, $n = 14$) mice showing the change in length (dl) over time (dt). Comparisons by two-way ANOVA. Asterisk represents statistical significance for V versus VM * $p < 0.0001$, † $p = 0.0084$.

2.4. Val66Met in a Model of Dilated Cardiomyopathy

To assess the effects of the Val66Met allele in a model of progressive cardiac contractile dysfunction and dilated cardiomyopathy and Duchenne muscular dystrophy (DMD), we crossed Val66Met mice with mdx/mTR (mDMD) mice, which develop cardiac fibrosis and dilated cardiomyopathy that is pathophysiologically comparable to the human disease. Observationally, Val66Met mice on the C57BL/6J background produce offspring with a phenotypic Mendelian ratio of 1:2:1 as expected. However, homozygous carriers of the rs6265 allele (Met/Met mice) were rarely observed on the mDMD background due in part to death shortly after birth (Figure 5A). Cardiomyocyte contraction (peak fractional shortening (FS)) was also significantly reduced in mDMD Val/Met mice compared with Val/Met on the C57BL/6 background (Figure 5B). Cardiac electrophysiology was significantly altered in Val/Met on the mDMD background (Figure 5C,D), with significantly elongated RR interval in mDMD mice with the rs6265 allele, compared to littermate controls (Figure 5E). In contrast to what was observed on the BL6 background, the rs6265 allele reduced cardiac function, as demonstrated by increased systolic diameter and volume and reduced ejection fraction and fractional shortening in mDMD; Val/Met mice (Figure 6).

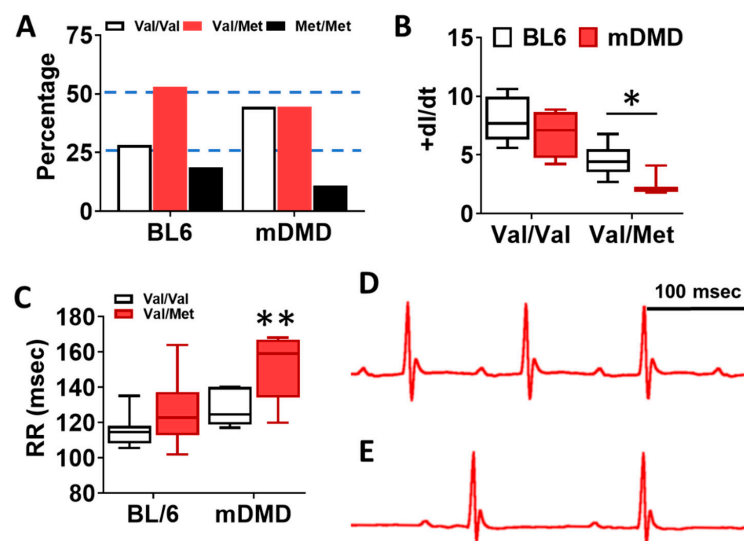


Figure 5. Dystrophic mice have altered distribution of rs6265 polymorphisms, altered cardiomyocyte contractility, and bradycardia. (A) Plot showing genotypic distribution of offspring from Val/Met breeding pairs on a normal C57BL/6 (BL6) or mdx/mTR dystrophic (mDMD) background. Percentage of offspring for each of the three possible genotypes are shown on the y axis, with the expected Mendelian ratio of 1:2:1 (or 25%, 50%, 25%) indicated by dashed lines. Val/Val (white), Val/Met (red), and Met/Met (black). (B) Box and whisker plot showing peak fractional shortening as the change in the length over time (+dl/dt) of cardiomyocytes isolated from Val/Val or Val/Met mice on a BL6 ($n = 10$, $n = 14$) or mDMD ($n = 4$, $n = 3$) background. (C) Plot showing the RR interval as measured by electrocardiography of Val/Val (white) and Val/Met (red) mice on the C57BL/6 (BL6, $n = 8$, 18) or mdx/mTR (mDMD, $n = 6$, 3) background. Example electrocardiograms are also shown for Val/Val (D) and Val/Met (E) mice on the mDMD background. * Asterisk represents statistical significance (* $p = 0.0282$, Student's t -test, $p = 0.0032$, two-way ANOVA), ** $p = 0.0025$ (two-way ANOVA).

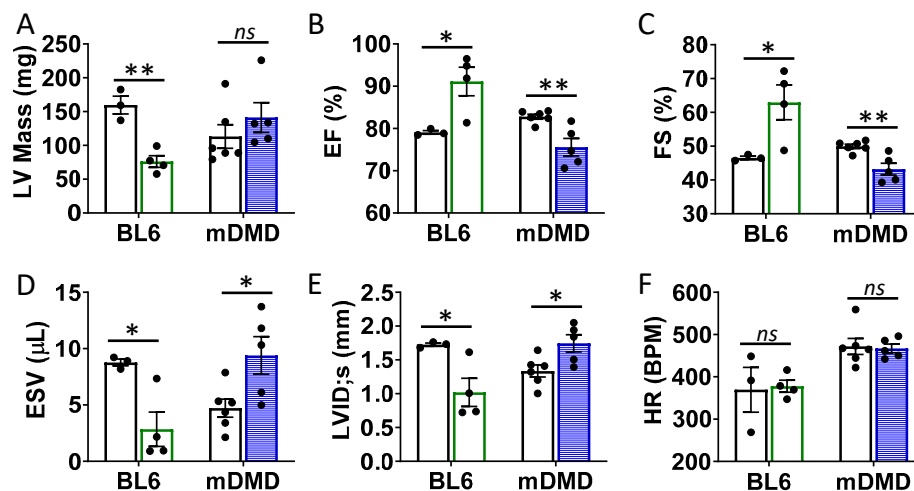


Figure 6. Val66Met leads to decreased ventricular function and increased end diastolic volumes in dystrophic mice. (A) Plot showing results of echocardiography assessment of mice with the rs6265 Val/Met polymorphism on a normal C57BL/6 (BL6, green bars) or mdx/mTR dystrophic (mDMD, blue bars) background relative to non-carrier controls (white bars). Parameters shown (y axis) are (A) left ventricular (LV) mass, (B) percent (%) ejection fraction (EF), (C) fractional shortening (FS), (D) end systolic volume (ESV), (E) left ventricular internal dimension at end systole (LVID;s) and (F) heart rate (HR). $n = 4$ (BL6), $n = 5$ (mDMD). Asterisks represent statistical significance. * $p < 0.05$, ** $p < 0.01$, ns = not significant.

2.5. Acute Cardiovascular Functions in Response to BDNF Receptor Inhibition

To determine the acute effects of systemic inhibition of BDNF signaling, we intraperitoneally injected wild-type (WT) mice with 500 ng/kg N-[2-[[[Hexahydro-2-oxo-1H-azepin-3-yl]amino]carbonyl]phenyl]benzo[b]thiophene-2-carboxamide (ANA-12) [14,15], a specific, small molecule inhibitor of the BDNF tyrosine kinase receptor (TrkB), and monitored mice by echocardiography at baseline (Figure 7A) and every five minutes for 30 total minutes. ANA-12 acutely reduced cardiac function, with a peak response at 15 min (Figure 7B) and essentially normalized function by 30 min (Figure 7C), as demonstrated by a slight decrease in heart rate (Figure 7D), decreased left ventricular (LV) ejection fraction (Figure 7E), increased diastolic diameter (Figure 7F) and end-systolic volume (Figure 7G) in WT mice. Cardiac electrophysiology was also significantly altered in response to ANA-12 injection (Figure 7H–J), with significantly elongated RR interval (Figure 7H) within three minutes that lasted for the duration of monitoring time (~12 min). This was accompanied by a slight decrease in heart rate (Figure 7I) with clear bradycardia as shown in representative electrocardiography traces (Figure 7J).

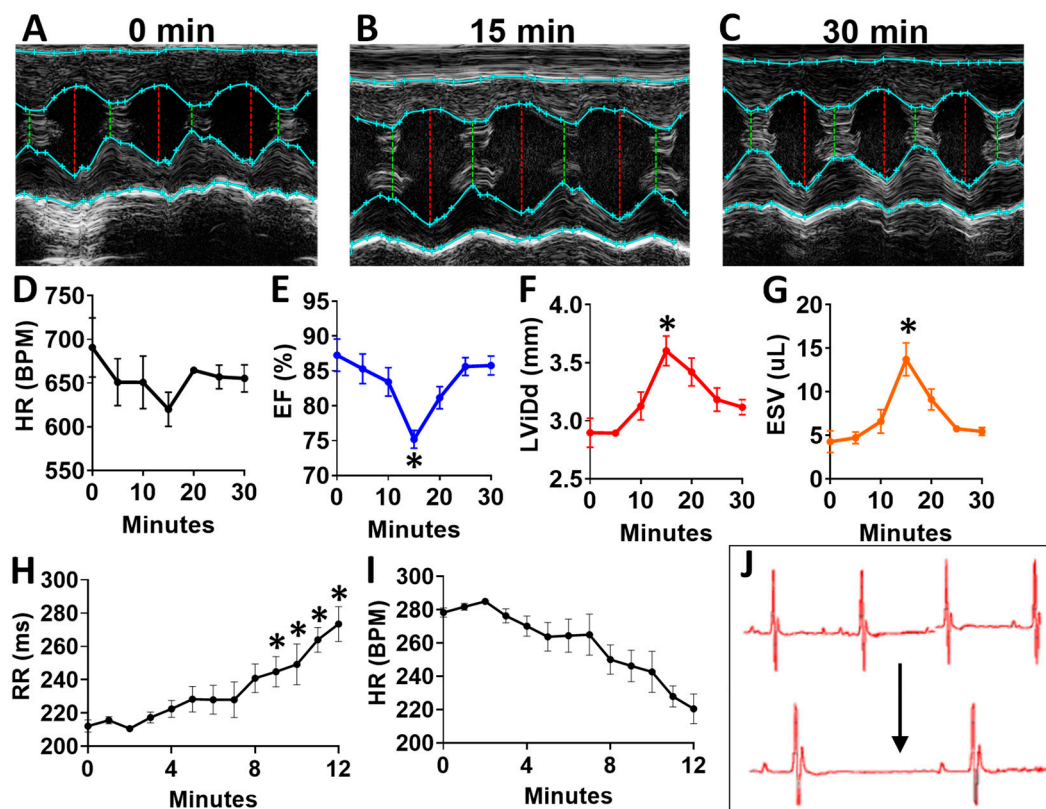


Figure 7. N-[2-[[[Hexahydro-2-oxo-1H-azepin-3-yl]amino]carbonyl]phenyl]benzo[b]thiophene-2-carboxamide (ANA12) injection leads to acutely altered ventricular function and bradycardia in wild-type animals (A) Example M-mode echocardiographic traces at baseline (A) and at 15 min (B) and 30 min (C) after a single injection of ANA-12. Plot showing results of echocardiography assessment in mice ($n = 4$) at baseline and at 5 min intervals, including the following echocardiographic parameters (y axis) (D) heart rate, (E) percent (%) ejection fraction (EF) and (F) end systolic volume (ESV) and left ventricular internal dimension at G, diastole (LVID;d); $n = 4$. Asterisks represent statistical significance. For EF ($* p = 0.0183$, $n = 4$), LVID; d ($* p = 0.0169$, $n = 4$), and ESV ($* p = 0.0190$, $n = 4$). Plots showing the RR interval (H) and heart rate (HR, I) as measured by electrocardiography in ANA-12 injected wild-type mice ($n = 4$). Example electrocardiograms are also shown (J) at baseline (top) and at 12 min after ANA-12 treatment (bottom). Asterisks represents statistical significance ($* p < 0.01$, $n = 4$). Colors are for emphasis as follows: blue = EF%, red = LViDd, orange = ESV.

3. Discussion

There is controversy over the importance of circulating BDNF and the utility in correlating with cardiovascular function [10,16–18]. Our data provide strong evidence that circulating BDNF levels are correlative with functional markers when segregated by the rs6265 polymorphism. The Val66→Met polymorphism is human-specific [19]. To study the molecular mechanisms underlying differences in cardiac function, Dr. Francis Lee generated the polymorphism in mice [20]. These mice are more prone to anxiety [20] and have been used extensively to study a variety of neurological and psychiatric disorders [21]. However, the cardiac phenotype of these mice has not been examined. In Val66Met mice, we observed significant changes in LV function with a decrease in LV mass that mirrored findings in humans. One major discrepancy, however, was increased BDNF in murine tissues (Figure 2A,B) but decreased BDNF levels in blood plasma of humans with DMD (Figure 1E). Unfortunately, these disparate findings cannot be easily addressed experimentally, as circulating BDNF is essentially undetectable in mice, larger Val66Met animals in which plasma BDNF can be measured have yet to be produced and obtaining biopsies from genotyped patients for measuring BDNF tissue levels is highly problematic, especially in the DMD population.

Despite having higher cardiac levels of BDNF and an increase in LVEF at baseline, Val66Met mice had abnormal cardiomyocyte contractility, which is consistent with gene expression alterations in contractile and calcium handling domains. Thus, this polymorphism appears to predispose cardiac muscle to abnormal contraction, and while there may be compensatory mechanisms under basal conditions, there may be less contractile reserve and a higher risk of developing functional decline under pathological conditions. This finding was consistent with CMR data from DMD patients demonstrating decreased LV mass but increased LVEF and better GCS. While this may at first appear counterintuitive, recent evidence in young adult cancer survivors showed heart failure symptoms correlated with decline in LV mass and not necessarily with LVEF [22]. In DMD patients, the lower LV mass and worse skeletal muscle function may represent higher myocyte turnover leading to ultimately faster disease progression. It should also be noted that significantly more carriers were on steroids (89% vs. 60%), which is most likely due to the poorer skeletal muscle function. It is known that steroids have cardioprotective effects [23,24]; therefore, some of the improved parameters of LV function could be secondary to earlier and more consistent steroid use and may delay the decreased function seen in the murine studies.

Given the correlation of BDNF levels with cardiovascular risk in the general population and the fact that BDNF is produced by and acts upon cardiomyocytes to directly impact contractility [25], it is possible that lower expression of BDNF in the heart is associated more generally with dilated cardiomyopathy (DCM). A meta-analysis of the Gene Expression Omnibus (GEO) [26,27] repository gene expression data of cardiomyocytes derived from human induced pluripotent stem cells (GSE13834, GSE35108) and cardiac tissues of various etiologies of end-stage human heart failure, including DCM (GSE42955) [28] supports this contention (Supplementary Figure S1A). Further, the gene encoding the receptor for BDNF is significantly up-regulated ($n = 27$, $p = 0.002$) in explants from patients with end-stage human heart failure, compared to unused donor healthy heart controls ($n = 16$) (Supplementary Figure S1B), perhaps as a compensatory response to reduced BDNF levels. To determine the effect of the rs6265 polymorphic alleles in such a disease state, we chose to use the mDMD mouse as a model for progressive dilated cardiomyopathy DCM. This highlights an important possible mechanism for BDNF effects in DMD specifically and DCM more generally. TrkB-T1 receptors have been demonstrated to be critical for normal contractility in both skeletal [29] and cardiac [25] myocytes. Selective cardiac deletion of TrkB-T1 results in decreased contractile force generation and the development of cardiomyopathy [25]. Altered active BDNF excretion or altered BDNF-induced receptor activation are possible mechanisms that will need further exploration in future studies. It will also be important to assess the effects of the rs6265 polymorphism over an extended time frame to assess disease progression and determine whether disparate results are due to compensatory effects that in older mice would be progressive and more closely resemble what is seen in humans.

DMD cardiomyopathy is characterized by muscle fibrosis, loss of contractility, and progressive development of DCM. The apparent disparate correlations between plasma BDNF levels and LVEF observed when segregating by polymorphic allele in DMD patients may help to partially explain the controversial effects of BDNF in human disease. Another universal feature of DMD muscle cells is that the absence of dystrophin leads to altered calcium handling through multiple mechanisms [30]. This has also been demonstrated in dystrophic murine skeletal and cardiac muscle cells [31], providing the opportunity to ascertain whether reduced contractility was due to altered calcium handling alone or other contributing mechanisms. Expression of the polymorphic alleles in the murine mDMD model led to substantial functional differences in addition to heart rate reduction, including decreased LVEF and FS, as well as increased end diastolic volumes. If this effect were primarily due to alteration in calcium handling, such a profound difference between Val/Val mDMD cardiomyocytes and the Val/Met and Met/Met groups would not be expected, as all of the groups would have abnormal calcium regulation. This suggests that altered BDNF metabolism and trafficking and/or altered regulation of contractility genes plays a significant role in the phenotype and may represent a novel role for this polymorphism as a modulator of cardiovascular disease. We suspect that the seemingly contradictory findings in LV function on DMD patients and in mDMD animals may represent a period of relative compensation as cardiomyocyte turnover increases while abnormally contractile cells undergo apoptosis. We would predict that as DMD boys are followed over time we would see LVEF ultimately segregate by rs6265 polymorphism.

The striking difference seen in skeletal muscle performance in DMD patients segregated by the Val66Met polymorphism was not entirely surprising, given BDNF's known role as a mitokine and in promoting exercise-induced skeletal muscle regeneration [32]. As DMD affects both cardiac and skeletal muscle, leading to the abnormal calcium handling and muscle weakness that is characteristic of the disease, it is unclear if rs6265 would have a similar, detectible effect in the general population. It is more likely that this functions in a "two hit" mechanism, where the abnormal contractility of myocytes can be compensated for during normal conditions, however in diseased states, such as DMD or other forms such as DCM, this fragile balance is disrupted leading to a worse clinical phenotype.

For the first time, we have shown that a polymorphism in the BDNF gene leads to functional changes in both mouse models and humans with DCM and in skeletal muscle function in DMD patients. This will allow for further investigation into the mechanisms of altered cardiomyocyte contractility and may provide a novel component of risk assessment in patients with cardiomyopathy or other cardiovascular diseases.

4. Materials and Methods

4.1. Animals

This study was carried out in accordance with the National Institutes of Health's Public Health Service Policy of Humane Care and Use of Laboratory Animals and the Animal Welfare Act. Transgenic BDNF_{Met} knock-in allele (Val66Met) mice [20] were crossed with first generation mdx/mTR KO (B6.Cg-Terc^{tm1Rdp}/Dmd^{mdx-4Cv}/Blau), Jackson #023535 [33], which develop progressive cardiac fibrosis and dilated cardiomyopathy [34]. Litter mates (8–12 weeks old) were used wherever possible. For all experiments, animals were euthanized with either isoflurane followed by tissue isolation or via carbon dioxide asphyxiation. For treatments with the TrkB receptor antagonist N-[2-[[[Hexahydro-2-oxo-1H-azepin-3-yl)amino]carbonyl]phenyl]benzo[b]thiophene-2-carboxamide (ANA-12) (Tocris Bioscience, Minneapolis, MN, USA), mice were injected with a conservative dose (500 ng/kg), diluted in saline solution made from a 1mg/mL stock solution in DMSO (Sigma-Aldrich, St. Louis, MO, USA [14,15]).

4.2. Echocardiography

Transthoracic M-mode echocardiography was performed with a 12-mHz probe (VisualSonics, Toronto, ON, Canada) on conscious mice and on mice anesthetized by inhalation of isoflurane (1–1.5%). LV end-systolic interior dimension (LVID;s), LV end diastolic interior dimension (LVID;d), ejection fraction (EF) and fractional shortening (FS) values were obtained by analyzing data using the Vevo 2100 program (VisualSonics, Toronto, ON, Canada).

4.3. Electrocardiography

ECG leads were recorded with surface electrodes (ADInstruments, Colorado Springs CO, USA) on anesthetized mice by constant inhalation of isoflurane (1–1.5%). The mean value for each mouse was obtained from four values consisting of four consecutive cardiac cycles using LabChart software (ADInstruments, Colorado Springs CO, USA).

4.4. Cardiomyocyte Contractility

Adult mouse cardiomyocytes were isolated as described previously [35]. For recordings, myocytes were paced at 1 Hz with a MyoPacer field stimulator (IonOptix, Westwood, MA, USA). Contractility measurements were made using sarcomere length (SarLen) parameters and processed with IonWizard 6.0 software (IonOptix, Westwood, MA, USA).

4.5. Patients

The Vanderbilt Institutional Review Board approved this prospective study, and this investigation conforms with the principles outlined in the Declaration of Helsinki (IRB Protocol numbers 120929, 140049, and 161524). Appropriate consents and assents were obtained as part of study enrollment. Sixty-one DMD subjects were enrolled from the Neuromuscular Cardiology Clinic. Inclusion criteria were: (1) diagnosis of DMD with clinical phenotype and confirmation with either genetic testing or muscle biopsy, (2) blood obtained at time of cardiac MRI (CMR), (3) able to tolerate CMR without sedation or anesthesia. Exclusion criteria were: (1) additional cardiac diagnoses that could affect biomarkers, (2) inadequate volume of blood. Enrolled DMD subjects underwent blood draw, CMR, skeletal muscle strength assessment, and assessment of physical activity levels using accelerometry.

4.6. ELISA

BDNF was measured using the Quantikine BDNF enzyme linked immunosorbent assay (ELISA) kit (R&D systems, Minneapolis, MN, USA, cat no. DBD00), as previously described [13].

4.7. Cardiac Magnetic Resonance

CMR was performed using a 1.5 Tesla Siemens Avanto (Siemens Healthcare Sector, Erlangen, Germany) and calculations performed as previously described [36]. A peripheral intravenous line was used to administer Gd-DTPA contrast (gadopentate dimeglumine, Magnevist[®], Bayer Healthcare Pharmaceuticals, Wayne, NJ, USA or gadobutrol, Gadovist[®], Bayer Healthcare Pharmaceuticals, Wayne, NJ, USA) at a dose of 0.2 mmol/kg.

4.8. Skeletal Muscle Assessment

Quantitative muscle testing (QMT) was performed on DMD subjects using a handheld myometer—an objective, reproducible method for upper and lower extremity strength evaluation in DMD. QMT score was calculated as previously described [37]. QMT was performed in 33 of 35 DMD subjects. Physical activity was assessed using triaxial accelerometers (GT3X+, ActiGraph, Pensacola, FL, USA) that recorded raw accelerometry data at a sampling frequency of 30 Hz (30 observations per second for each axis) for 7 consecutive days and 24 h per day (one monitor on the ankle of the dominant leg and one on the wrist of the dominant hand). Raw accelerometry data were integrated into 15-s

epochs and expressed as vector magnitude (VM) counts using Actilife software (ActiGraph, Pensacola, FL, USA). Accelerometer non-wear and wear periods were assessed as previously described [38]. A recording was considered valid if it included ≥ 3 valid days with ≥ 2 weekdays and ≥ 1 weekend night with ≥ 6 h of monitor wearing from 7:00am to 10:00pm.

4.9. Transcriptome Sequencing

RNA sequencing (RNA-seq) was performed by Vanderbilt Technologies for Advanced Genomics (VANTAGE) core as previously described [39], using Illumina TruSeq and HiSeq 3000 (Illumina San Diego, CA, USA) on paired-end-150 flow cell runs at ~ 32 M PF reads per sample. Raw reads (fastq files) were aligned to the mm10 assembly using STAR 2.5.3a and analyzed as previously described using Partek Flow server and Genomics Suite (Partek, Inc, Chesterfield, MO, USA [39]).

4.10. Immunoblotting

Gel electrophoresis was performed as previously described [39] and probed with rabbit anti-BDNF (cat. #ARP41970, Aviva Systems Biology Corporation, San Diego, CA, USA) and rabbit anti-GAPDH (cat. #5174, Cell Signaling Technology, Inc, Danvers, MA, USA).

4.11. Statistical Analysis

All data are expressed as means \pm SEM. Statistical comparisons made between two variables were performed using the Student's t test. Comparisons between more than two variables were performed using one-way ANOVA with a Tukey's post hoc test. Human demographic variables were compared using either a Wilcoxon rank-sum (continuous variables) or a chi-square or Fisher's exact test (categorical variables). Patient data were collected and managed using research electronic data capture (REDCap) at Vanderbilt [40].

5. Limitations

This study is limited by the relatively small population of the study cohort of DMD patients. The number of patients could be potentially increased in future studies using multicenter collaborative data collection. CMR analysis was done separately from BDNF analysis in order to minimize potential bias.

6. Translational Perspective

The rs6265 polymorphism alters cardiomyocyte contractility in mice without overt cardiovascular disease and is augmented in a mouse model of progressive dilated cardiomyopathy; thus, it may represent a novel risk factor for worse outcomes in cardiovascular disease. In patients with Duchenne muscular dystrophy, the rs6265 polymorphism is associated with altered relationship between plasma BDNF levels and LVEF and worse skeletal muscle performance.

Supplementary Materials: Supplementary materials can be found at <http://www.mdpi.com/1422-0067/21/20/7466/s1>.

Author Contributions: Author contributions to the study and manuscript are as follows: "conceptualization, C.L.G. and F.J.R.J.; methodology, L.Z., M.B. and W.B.B.; software, J.T.R. and P.U.; validation, L.W.M., J.S., H.L. and A.K.H.; formal analysis, L.Z.; investigation, C.L.G., A.P.S., F.J.R.J., W.A., N.L., C.P.A., P.U., Q.Z. and P.L.C.; resources, E.J.C.; data curation, J.S.; writing—original draft preparation, C.L.G., F.J.R.J. and A.P.S.; writing—review and editing, C.L.G., F.J.R.J., A.P.S. and H.L.; visualization, A.P.S.; supervision, C.L.G.; project administration, C.L.G. and J.S.; funding acquisition, C.L.G., H.L., and A.K.H. All authors have read and agreed to the published version of the manuscript.

Funding: This work was supported by the American Heart Association (18IPA34170062), National Institutes of Health (K01HL121045, F32HL137394, K23HL123938, R01HL138519, R01HL133290, R01HL143074, K12HD087023, and R01HL119234), Department of Defense (W81XWH-16-1-0622), and Ogden College of Science and Engineering of Western Kentucky University.

Acknowledgments: This study complies with the Declaration of Helsinki. Local approvals (IRB, IACUC) and informed consent from subjects were obtained. We acknowledge the Translational Pathology Shared Resource supported by NCI/NIH Cancer Center Support Grant 5P30 CA68485-19 and Vanderbilt Mouse Metabolic Phenotyping Center Grant 2 U24 DK059637-16.

Conflicts of Interest: The authors declare no conflict of interest. The funders had no role in the design of the study; in the collection, analyses, or interpretation of data; in the writing of the manuscript, or in the decision to publish the results.

References

1. Allen, S.J.; Watson, J.J.; Shoemark, D.K.; Barua, N.U.; Patel, N.K. GDNF, NGF and BDNF as therapeutic options for neurodegeneration. *Pharmacol. Ther.* **2013**, *138*, 155–175. [[CrossRef](#)] [[PubMed](#)]
2. Kermani, P.; Hempstead, B. BDNF Actions in the Cardiovascular System: Roles in Development, Adulthood and Response to Injury. *Front. Physiol.* **2019**, *10*, 455. [[CrossRef](#)] [[PubMed](#)]
3. Mowla, S.J.; Farhadi, H.F.; Pareek, S.; Atwal, J.K.; Morris, S.J.; Seidah, N.G.; Murphy, R.A. Biosynthesis and post-translational processing of the precursor to brain-derived neurotrophic factor. *J. Biol. Chem.* **2001**, *276*, 12660–12666. [[CrossRef](#)]
4. Zanin, J.P.; Unsain, N.; Anastasia, A. Growth factors and hormones pro-peptides: The unexpected adventures of the BDNF prodomain. *J. Neurochem.* **2017**, *141*, 330–340. [[CrossRef](#)] [[PubMed](#)]
5. Petryshen, T.L.; Sabeti, P.C.; Aldinger, K.A.; Fry, B.; Fan, J.B.; Schaffner, S.F.; Waggoner, S.G.; Tahl, A.R.; Sklar, P. Population genetic study of the brain-derived neurotrophic factor (BDNF) gene. *Mol. Psychiatry* **2010**, *15*, 810–815. [[CrossRef](#)]
6. Uegaki, K.; Kumanogoh, H.; Mizui, T.; Hirokawa, T.; Ishikawa, Y.; Kojima, M. BDNF Binds Its Pro-Peptide with High Affinity and the Common Val66Met Polymorphism Attenuates the Interaction. *Int. J. Mol. Sci.* **2017**, *18*, 1042. [[CrossRef](#)]
7. Egan, M.F.; Kojima, M.; Callicott, J.H.; Goldberg, T.E.; Kolachana, B.S.; Bertolino, A.; Zaitsev, E.; Gold, B.; Goldman, D.; Dean, M.; et al. The BDNF val66met polymorphism affects activity-dependent secretion of BDNF and human memory and hippocampal function. *Cell* **2003**, *112*, 257–269. [[CrossRef](#)]
8. Kailainathan, S.; Piers, T.M.; Yi, J.H.; Choi, S.; Fahey, M.S.; Borger, E.; Gunn-Moore, F.J.; O'Neill, L.; Lever, M.; Whitcomb, D.J.; et al. Activation of a synapse weakening pathway by human Val66 but not Met66 pro-brain-derived neurotrophic factor (proBDNF). *Pharmacol. Res.* **2016**, *104*, 97–107. [[CrossRef](#)]
9. Sustar, A.; Nikolic Perkovic, M.; Nedic Erjavec, G.; Svob Strac, D.; Pivac, N. A protective effect of the BDNF Met/Met genotype in obesity in healthy Caucasian subjects but not in patients with coronary heart disease. *Eur. Rev. Med. Pharmacol. Sci.* **2016**, *20*, 3417–3426.
10. Jiang, R.; Babyak, M.A.; Brummett, B.H.; Hauser, E.R.; Shah, S.H.; Becker, R.C.; Siegler, I.C.; Singh, A.; Haynes, C.; Chryst-Ladd, M.; et al. Brain-derived neurotrophic factor rs6265 (Val66Met) polymorphism is associated with disease severity and incidence of cardiovascular events in a patient cohort. *Am. Heart J.* **2017**, *190*, 40–45. [[CrossRef](#)]
11. Pivac, N.; Kim, B.; Nedic, G.; Joo, Y.H.; Kozaric-Kovacic, D.; Hong, J.P.; Muck-Seler, D. Ethnic differences in brain-derived neurotrophic factor Val66Met polymorphism in Croatian and Korean healthy participants. *Croat. Med. J.* **2009**, *50*, 43–48. [[CrossRef](#)] [[PubMed](#)]
12. Yeebo, M.F. Ethnic differences in BDNF Val66Met polymorphism. *Br. J. Psychiatry* **2015**, *207*, 363. [[CrossRef](#)] [[PubMed](#)]
13. Galindo, C.L.; Soslow, J.H.; Brinkmeyer-Langford, C.L.; Gupte, M.; Smith, H.M.; Sengsayadeth, S.; Sawyer, D.B.; Benson, D.W.; Kornegay, J.N.; Markham, L.W. Translating golden retriever muscular dystrophy microarray findings to novel biomarkers for cardiac/skeletal muscle function in Duchenne muscular dystrophy. *Pediatr. Res.* **2016**, *79*, 629–636. [[CrossRef](#)] [[PubMed](#)]
14. Mazzaro, N.; Barini, E.; Spillantini, M.G.; Goedert, M.; Medini, P.; Gasparini, L. Tau-Driven Neuronal and Neurotrophic Dysfunction in a Mouse Model of Early Tauopathy. *J. Neurosci.* **2016**, *36*, 2086–2100. [[CrossRef](#)]
15. Nishihara, T.; Ochi, M.; Sugimoto, K.; Takahashi, H.; Yano, H.; Kumon, Y.; Ohnishi, T.; Tanaka, J. Subcutaneous injection containing IL-3 and GM-CSF ameliorates stab wound-induced brain injury in rats. *Exp. Neurol.* **2011**, *229*, 507–516. [[CrossRef](#)]

16. Krabbe, K.S.; Mortensen, E.L.; Avlund, K.; Pedersen, A.N.; Pedersen, B.K.; Jorgensen, T.; Bruunsgaard, H. Brain-derived neurotrophic factor predicts mortality risk in older women. *J. Am. Geriatr. Soc.* **2009**, *57*, 1447–1452. [[CrossRef](#)]
17. Ejiri, J.; Inoue, N.; Kobayashi, S.; Shiraki, R.; Otsui, K.; Honjo, T.; Takahashi, M.; Ohashi, Y.; Ichikawa, S.; Terashima, M.; et al. Possible role of brain-derived neurotrophic factor in the pathogenesis of coronary artery disease. *Circulation* **2005**, *112*, 2114–2120. [[CrossRef](#)]
18. Kaess, B.M.; Preis, S.R.; Lieb, W.; Beiser, A.S.; Yang, Q.; Chen, T.C.; Hengstenberg, C.; Erdmann, J.; Schunkert, H.; Seshadri, S.; et al. Circulating brain-derived neurotrophic factor concentrations and the risk of cardiovascular disease in the community. *J. Am. Heart Assoc.* **2015**, *4*, e001544. [[CrossRef](#)]
19. Bath, K.G.; Lee, F.S. Variant BDNF (Val66Met) impact on brain structure and function. *Cogn. Affect. Behav. Neurosci.* **2006**, *6*, 79–85. [[CrossRef](#)]
20. Chen, Z.Y.; Jing, D.; Bath, K.G.; Ieraci, A.; Khan, T.; Siao, C.J.; Herrera, D.G.; Toth, M.; Yang, C.; McEwen, B.S.; et al. Genetic variant BDNF (Val66Met) polymorphism alters anxiety-related behavior. *Science* **2006**, *314*, 140–143. [[CrossRef](#)]
21. Notaras, M.; Hill, R.; van den Buuse, M. The BDNF gene Val66Met polymorphism as a modifier of psychiatric disorder susceptibility: Progress and controversy. *Mol. Psychiatry* **2015**, *20*, 916–930. [[CrossRef](#)] [[PubMed](#)]
22. Jordan, J.H.; Melendez, G.; Suerken, C.; D’Agostino, R.; Hundley, W. Decreases in left ventricular mass and not left ventricular ejection fraction are associated with heart failure symptoms in cancer patients six months after potentially cardiotoxic chemotherapy. *J. Am. Coll. Cardiol.* **2017**, *69*, 1410. [[CrossRef](#)]
23. Barber, B.J.; Andrews, J.G.; Lu, Z.; West, N.A.; Meaney, F.J.; Price, E.T.; Gray, A.; Sheehan, D.W.; Pandya, S.; Yang, M.; et al. Oral corticosteroids and onset of cardiomyopathy in Duchenne muscular dystrophy. *J. Pediatr.* **2013**, *163*, 1080–1084.e1081. [[CrossRef](#)]
24. Silversides, C.K.; Webb, G.D.; Harris, V.A.; Biggar, D.W. Effects of deflazacort on left ventricular function in patients with Duchenne muscular dystrophy. *Am. J. Cardiol.* **2003**, *91*, 769–772. [[CrossRef](#)]
25. Fulgenzi, G.; Tomassoni-Ardori, F.; Babini, L.; Becker, J.; Barrick, C.; Puverel, S.; Tessarollo, L. BDNF modulates heart contraction force and long-term homeostasis through truncated TrkB.T1 receptor activation. *J. Cell Biol.* **2015**, *210*, 1003–1012. [[CrossRef](#)]
26. Cao, F.; Wagner, R.A.; Wilson, K.D.; Xie, X.; Fu, J.D.; Drukker, M.; Lee, A.; Li, R.A.; Gambhir, S.S.; Weissman, I.L.; et al. Transcriptional and functional profiling of human embryonic stem cell-derived cardiomyocytes. *PLoS ONE* **2008**, *3*, e3474. [[CrossRef](#)]
27. Sun, N.; Yazawa, M.; Liu, J.; Han, L.; Sanchez-Freire, V.; Abilez, O.J.; Navarrete, E.G.; Hu, S.; Wang, L.; Lee, A.; et al. Patient-specific induced pluripotent stem cells as a model for familial dilated cardiomyopathy. *Sci. Transl. Med.* **2012**, *4*, 130ra147. [[CrossRef](#)] [[PubMed](#)]
28. Molina-Navarro, M.M.; Roselló-Lletí, E.; Ortega, A.; Tarazón, E.; Otero, M.; Martínez-Dolz, L.; Lago, F.; González-Juanatey, J.R.; España, F.; García-Pavía, P.; et al. Differential gene expression of cardiac ion channels in human dilated cardiomyopathy. *PLoS ONE* **2013**, *8*, e79792. [[CrossRef](#)]
29. Dorsey, S.G.; Lovering, R.M.; Renn, C.L.; Leitch, C.C.; Liu, X.; Tallon, L.J.; Sadzewicz, L.D.; Pratap, A.; Ott, S.; Sengamalay, N.; et al. Genetic deletion of trkB.T1 increases neuromuscular function. *Am. J. Physiol. Cell Physiol.* **2012**, *302*, C141–C153. [[CrossRef](#)]
30. van Westering, T.L.; Betts, C.A.; Wood, M.J. Current understanding of molecular pathology and treatment of cardiomyopathy in duchenne muscular dystrophy. *Molecules* **2015**, *20*, 8823–8855. [[CrossRef](#)]
31. Hopf, F.W.; Turner, P.R.; Denetclaw, W.F., Jr.; Reddy, P.; Steinhardt, R.A. A critical evaluation of resting intracellular free calcium regulation in dystrophic mdx muscle. *Am. J. Physiol.* **1996**, *271*, C1325–C1339. [[CrossRef](#)] [[PubMed](#)]
32. Yu, T.; Chang, Y.; Gao, X.L.; Li, H.; Zhao, P. Dynamic Expression and the Role of BDNF in Exercise-induced Skeletal Muscle Regeneration. *Int. J. Sports Med.* **2017**, *38*, 959–966. [[CrossRef](#)] [[PubMed](#)]
33. Sacco, A.; Mourkioti, F.; Tran, R.; Choi, J.; Llewellyn, M.; Kraft, P.; Shkreli, M.; Delp, S.; Pomerantz, J.H.; Artandi, S.E.; et al. Short telomeres and stem cell exhaustion model Duchenne muscular dystrophy in mdx/mTR mice. *Cell* **2010**, *143*, 1059–1071. [[CrossRef](#)] [[PubMed](#)]
34. Mourkioti, F.; Kustan, J.; Kraft, P.; Day, J.W.; Zhao, M.M.; Kost-Alimova, M.; Protopopov, A.; DePinho, R.A.; Bernstein, D.; Meeker, A.K.; et al. Role of telomere dysfunction in cardiac failure in Duchenne muscular dystrophy. *Nat. Cell Biol.* **2013**, *15*, 895–904. [[CrossRef](#)]

35. O'Connell, T.D.; Rodrigo, M.C.; Simpson, P.C. Isolation and culture of adult mouse cardiac myocytes. *Methods Mol. Biol.* **2007**, *357*, 271–296. [[CrossRef](#)]
36. Doust, J.A.; Pietrzak, E.; Dobson, A.; Glasziou, P. How well does B-type natriuretic peptide predict death and cardiac events in patients with heart failure: Systematic review. *BMJ* **2005**, *330*, 625. [[CrossRef](#)]
37. Posner, A.D.; Soslow, J.H.; Burnette, W.B.; Bian, A.; Shintani, A.; Sawyer, D.B.; Markham, L.W. The Correlation of Skeletal and Cardiac Muscle Dysfunction in Duchenne Muscular Dystrophy. *J. Neuromuscul. Dis.* **2016**, *3*, 91–99. [[CrossRef](#)]
38. Choi, L.; Liu, Z.; Matthews, C.E.; Buchowski, M.S. Validation of accelerometer wear and nonwear time classification algorithm. *Med. Sci. Sports Exerc.* **2011**, *43*, 357–364. [[CrossRef](#)]
39. Kirabo, A.; Ryzhov, S.; Gupte, M.; Sengsayadeth, S.; Gumina, R.J.; Sawyer, D.B.; Galindo, C.L. Neuregulin-1beta induces proliferation, survival and paracrine signaling in normal human cardiac ventricular fibroblasts. *J. Mol. Cell. Cardiol.* **2017**, *105*, 59–69. [[CrossRef](#)]
40. Harris, P.A.; Taylor, R.; Thielke, R.; Payne, J.; Gonzalez, N.; Conde, J.G. Research electronic data capture (REDCap)—A metadata-driven methodology and workflow process for providing translational research informatics support. *J. Biomed. Inform.* **2009**, *42*, 377–381. [[CrossRef](#)]



© 2020 by the authors. Licensee MDPI, Basel, Switzerland. This article is an open access article distributed under the terms and conditions of the Creative Commons Attribution (CC BY) license (<http://creativecommons.org/licenses/by/4.0/>).